531

Chemical Modification of Activated Carbon Adsorbents

A Thesis submitted for the degree of Doctor of Philosophy Brunel.

by

Richard James Holmes

Chemical and Biological Defence Establishment, Porton Down

October 1991

To Susan

Abstract

Activated carbons have been modified using reactive chemicals to produce adsorbents of enhanced hydrophobic character which will also be resistant to surface oxidation that results from exposure to humid air ("ageing"). The intention was that modification would not disrupt the carbon pore structure. The adsorptive properties of the modified carbons have been investigated using probe molecules including nitrogen, water, hexane, and chloropicrin, and the ageing characteristics of the carbons, and the factors controlling the adsorption of a model hydrophobic vapour from high humidity air have been studied. Directly fluorinated carbons were unstable, probably due to weakly adsorbed fluorine. Treatment of these adsorbents with other chemicals indicated the potential of the technique for introducing specific functional groups onto the carbon surface. Carbons modified using selective fluorinating reagents (hexafluoropropene and 1,1-difluoroethene) were more hydrophobic, and adsorbed hydrophobic vapours more efficiently from humid air in comparison to controls. These adsorbents aged, but at a reduced rate in comparison to control carbon. Carbons modified using chlorinating reagents (carbonyl chloride and chlorine) and treated with solvents to remove adsorbed reagent and/ or reaction products were of improved hydrophobic character, and adsorbed hydrophobic vapours from humid air at least as efficiently as the control samples. More importantly, these carbons offered resistance to ageing effects. A study of the factors controlling the efficiency with which hydrophobic vapours are adsorbed from humid air revealed that the surface chemistry of the carbon is important, but that under typical conditions of use, filter performance was limited by the rate at which water displaced by the organic vapour could be carried away by the airstream. The results illustrate that filters containing chemically modified activated carbon offer advantages when volatile hydrophobic contaminant vapours are present, and where ageing effects are an important mechanism by which filtration efficiency is degraded.

Contents

Abbreviations

Symbol	Meaning
α_s	Alpha-s value
BET	Brunauer-Emmett-Teller
^oC	Temperature in degrees Centigrade
CO	Carbon Monoxide
CO_2	Carbon Dioxide
DFE	1,1-difluoroethene
DPA	Dipropylamine
DSC	Differential Scanning Calorimetry
EDX	Energy Dispersive X ray analysis
HFP	Hexafluoropropene
NO_2	Dinitrogen Tetroxide
Pa	Pascal (101,325 Pa=1 atmosphere pressure at 0^oC)
p^o	Saturated vapour pressure
p/p^o	Relative pressure
Phosgene	Carbonyl Chloride
PS	Chloropicrin (trichloronitromethane)
RH	Relative Humidity
STP	Standard Temperature and Pressure
TDMS	Thermal Desorption Mass Spectrometry
TFE	Trifluoroethene
TG	Thermal Gravimetric Analysis
XPS	X ray Photoelectron Spectroscopy

Tables

Table Page

Chapter 6

Table Page

Chapter 7

Table Page

Chapter 8

Table Page

Chapter 9

Figures

Figure Page

Chapter 7

Figure Page

Chapter 8

Figure Page

Figure Page

CHAPTER 1

Introduction

Activated carbon adsorbents have found many and varied applications in recent times. This is a consequence of both a well developed polydisperse porous structure, which is of a size distribution favourable for molecular sorption, and a large internal surface area.

Important activated carbon applications include waste water treatment, as catalysts and catalyst supports, and in precious metal and solvent recovery. Their use in air purification is the basis of this present study.

Carbon adsorbents have proved to be uniquely applicable to air filtration when contaminants of varying molecular size and shape are present. Other adsorbents, such as those based upon zeolites, have thus far proved to be of finite use, owing to cost, the presence of monodisperse porosity, and a high affinity for moisture.

Structure and Preparation of Activated Carbon.

Activated carbons are highly porous. The pore structure may be viewed as the interstices and openings between folded and stacked aromatic carbon sheets linked in three dimensions: these sheets will contain structural defects and heteroatoms. The aromatic regions (or crystallites) are separated by disorganised carbonaceous structures, which also contribute to the porosity. Any impurity is probably distributed throughout the structure, although surface localisation is possible. Pores are generally classified according to size (width). The IUPAC classification[1] is shown below.

Maximum Width (nm)	Description
<2	Micropores, forming the majority of the available surface area. May be classified as primary and secondary (inferred from adsorption data[2]).
2-50	Mesopores, or transitional pores. These pores are part of the transport pore structure, enabling adsorbate molecules to reach the micropore structure.
>50	Macropores. The largest pores, which include pore openings. The meso- and macropores typically account for approximately 10% of the total pore volume.

An alternative pore classification is one according to shape: assessment of pore shape is somewhat difficult, although evidence for the presence of slit shaped pores in some activated carbons is strong[3]. Inferences with respect to shape may also be drawn from adsorption data, although direct measurements are difficult[4].

Preparation

The presence of porosity of a certain size distribution depends on the nature of the base material (eg. coal, wood, nutshell) and the manufacturing method. Thus to some extent, the adsorptive properties of the carbon (which are

dependent upon such factors as pore shape, size and volume) may be tailored during preparation.

Manufacture involves two distinct stages, carbonisation and activation: often, both are combined into a single process. Carbonisation involves heating the raw material in the absence of oxygen, typically at temperatures in the region of 800°C. During this stage, some oxygen and moisture, and the bulk of any other volatile matter is lost. Aromatic character increases, and large condensed ring systems develop. The yield of the carbonised product depends on such factors as the heating rate and duration, and the ultimate temperature. The material is essentially non- porous, consisting of aromatic sheets separated by residues which are largely carbonaceous in nature, and must be activated to develop the porous structure. In addition to removal of residues, activation results in the development of porosity by partial gasification ("burnoff") of the folded aromatic carbon sheets.

Activation is carried out by means of a chemical process. Two different processes are employed, and are termed chemical or physical activation. Chemical activation usually involves impregnation of (normally cellulosic) base material with an agent to promote dehydration. The agent is typically phosphoric acid, or zinc chloride, and on calcination at temperatures below ca. 800°C, carbonisation and activation take place. The products may be of high activity (high surface area and pore volume), although they may contain some of the activating agent as a residual impurity. Potassium hydroxide is also used in chemical activation, but it does not behave as a dehydrating agent, and although the exact mechanism of action is not known, it can be used to produce carbons of very high activity from a range of precursor materials.

Physical activation is usually carried out at high temperature (above 800°C), and is essentially an oxidative process. Carbon is strongly reducing, and is readily oxidised by agents such as air, steam, or carbon dioxide under

appropriate conditions. Pore development takes place by carbon gasification (burnoff), the rate of which varies locally within the structure. For example, less organised carbon material is more susceptible to gasification than organised graphitic-like regions. It is this preferential gasification mechanism which gives rise to the porosity. The products of gasification include carbon monoxide and dioxide. The extent of pore development is dependent upon the activating gas, the temperature, and the length of time for which activation is continued. The product contains chemically adsorbed oxygen, which may vary between 1 and 7% by weight, depending on whether any post activation treatments, such as annealing, are employed. The majority of carbons used in vapour adsorption applications are prepared using this process.

Activated carbons are generally impure, and the quantity of non carbon material is dependent on the carbon source, and method of manufacture. The principal impurities are oxygen, nitrogen, hydrogen and ash. The ash is composed mainly of alkali and heavy metal complexes, and typically represents between one and twenty five percent by weight of the adsorbent. Coal based carbons generally contain a more exotic mixture of impurities than products derived from nutshells. These impurities can have a major impact on the adsorptive properties of the carbon.

Considerable effort has been expended in attempts to modify the structural characteristics of activated carbon to optimise the adsorptive properties.

In addition to these structural parameters, the influence of the chemical composition of the surface (surface chemistry) on the adsorptive properties of the carbon is often significant. Less attention has been given to this aspect,

however. Some research has been carried out into the manipulation of carbon surface chemistry[eg. 5-10], but the majority of studies have not considered the utility of the modified adsorbents for vapour adsorption applications, or their stability in the presence of humid air. These aspects form one of the principal aims of this present research, which are detailed below.

Research Aims

[1] To chemically modify the surface of activated carbon without significantly altering structural parameters.

One of the most demanding vapour adsorption applications is the removal of low concentrations of volatile hydrophobic chemicals from airstreams containing high concentrations of water vapour. Manipulation of the surface chemical composition of the carbon, as a means of enhancing vapour adsorption under such conditions, is one of the important aims of this research. In addition, activated carbon surfaces are known to oxidise ("age") in the presence of humid air, a process which further reduces the efficiency with which volatile hydrophobic vapours are adsorbed. Thus, this research will also address the stability of the modified carbons under these conditions, with the aim of reducing the propensity of the surface to "age" during storage and use in a humid environment. The introduction of reactive functional groups onto the carbon surface, and the ageing characteristics of control (unmodified) carbon, will also form part of this aim.

[2] A study of activated carbon filters used in vapour adsorption applications.

This aspect of the research is intended to enable a better understanding of the mechanism of vapour adsorption in the presence of adsorbed water, including the effect of using surface modified carbons. The influence of the relative humidity (RH) and temperature of the air, and the structure (porosity) of the carbon, on filter efficiency will also be considered.

In the following chapter, theoretical aspects relevant to this research will be considered. The preparation and adsorptive properties of chemically modified carbons will be reviewed in chapter three: factors affecting the use of activated carbon filters are considered at chapter four, and the experimental techniques employed in this present study will be described at chapter five, and in more detail in the Appendix.

The experimental studies of surface chemical modification are presented at chapters six to eight. The results will be considered in each chapter, and will form part of a general discussion at chapter ten.

Chapter nine contains the results of a study of the vapour adsorption properties of activated carbon filters. The conclusions of this study will be considered at chapter ten.

REFERENCES

1] "IUPAC Manual of Symbols and Terminology, Appendix 2, Pt 1. Colloid and Surface Chemistry"; Pure Appl. Chem. 31 1972 578.

2] Sing, K.S.W., eg. Carbon 25 1987. 155.

3] Bansal, R.C., Donnet, J-B, Stoeckli, H. F. Active Carbon, Marcel Dekker, New York, 1988.

4] Kenny, M.B. and Sing K.S.W, Chem. and Ind. January 1990 39.

5] Puri, B.R., Surface Complexes on Carbon, Chemistry and Physics of Carbon, Marcel Dekker, 6 1970 191.

6] Boehm, H.P., Chemical Identification of Surface Groups, in Advances in Catalysis, D.D. Eley, H. Pines, and P.B. Weisz (Eds.), 16 1966 179.

7] Loskutov, A.I. and Khlopotov, M.N., Adsorbenty 10 1982.

8] Kuzin, I.A., Loskutov, A.I., Palfitov, V.F., Koemets, L.A., Zh. Prikl. Khim. 45 1972 760.

9] Fedotov, V.A. and Loskutov, I.A., Akad. Sci. USSR, J. App. Chem., Leningrad, 1984. UDK 661.183:546.162.

10] Karpinski, K. and Wojcik, G., Chem. Stosow. 24 1980 141.

CHAPTER 2

Theoretical Aspects

Characterisation of Activated Carbon Adsorbents-Adsorption

Adsorption at the gas- solid interface is the process whereby the concentration of one or more components (the adsorbate) from the gas phase (the adsorptive) is enhanced at the surface of the solid phase (the adsorbent)[1]. The adsorption process can involve either chemical or physical forces.

Chemical adsorption is the formation of chemical bonds between the adsorbate and the adsorbent (or the adsorbent which has been modified by impregnation with, for example metal complexes). This process is important in the removal of toxic gases such as hydrogen sulphide, sulphur dioxide, hydrogen cyanide and cyanogen chloride from an airstream using activated carbon filters. In this present research, the adsorption properties of control and chemically modified activated carbon toward nitrogen, and vapours such as water, methanol, hexane and chloropicrin (trichloronitromethane (CCl_3NO_2), designated here as PS) are considered. These adsorbates will be used as a method of characterising the structural and adsorptive properties of the carbons. In these examples, adsorption is physical in nature (but see chapter 3,4).

2.1 Physical Adsorption (Physisorption)

Physical adsorption can result from one or more effects; non specific interactions between the adsorbate and the adsorbent surface (such as the adsorption of vapours which do not possess a permanent dipole moment (London forces)) and/ or specific interactions (eg. where both the adsorbate and adsorbent are polar in nature). The interaction between the adsorbent and the adsorbate will therefore depend to some extent upon the electronic characteristics of both, but also upon structural properties: that is, the

molecular size and shape of the adsorbate, and the characteristics of the pore structure of the adsorbent (pore volume, shape, and width (chapter 1)).

Adsorption at the gas- solid interface is usually temperature dependent: thus, adsorption isotherms are often determined to characterise a particular system.

2.2 Adsorption Isotherms

The volume (f) of gas adsorbed per unit mass of adsorbent at a constant temperature T (which is below the critical temperature of the gas) is concentration dependent, and is usually expressed in terms of the relative pressure (where p^0 is the saturated pressure of the adsorbate).

$$f = C.\left(\frac{p}{p^0}\right)\ (gas, solid, T)$$

{C is a constant}

Adsorption isotherms are classified according to the recommendations of IUPAC[1]. Six isotherm types are identified using this classification (figure 2.1), although some may not be classified accurately using this approach due to the presence of characteristics of more than one type.

Type I isotherms are identified by a steep initial rise in the amount adsorbed, followed by a plateau region extending to high relative pressures (eg. figure 2.2, which shows a nitrogen adsorption/ desorption isotherm measured for Chemviron BPL activated carbon at -196°C).

The adsorption mechanism in the steep region of the isotherm is considered to be one of volume filling[2], by the formation of a liquid-like phase, rather than surface coverage. Because the width of a micropore is of molecular

dimensions, the adsorption forces of opposite pore walls will overlap, leading to an enhancement in the adsorption potential[3] (primary micropores). This effect is strongly dependent on micropore width, being rapidly lost as the pore width is increased[4]. The mechanism of adsorption in wider micropores is somewhat different, and is probably the result of a cooperative process[2], whereby the presence of an adsorbed monolayer on both sides of the pore wall will promote the adsorption of further molecules into the pore space. This mechanism is not believed to result in the formation of a liquid meniscus. Primary micropore filling is usually complete upon reaching a relative pressure of 0.01. The mechanism of micropore filling cannot, however, result in the formation of an adsorbed phase within the pores that is of normal liquid density. Considerations of the packing constraints within such pores has demonstrated that this must be the case[5].

Micropore filling (primary and secondary) is usually complete at a relative pressure of approximately 0.4. Above this value, the larger (meso) pores become important, and the adsorption mechanism consists of a gradual and multilayer process as described by the BET theory (2.2.1.1[6]). Filling of these pores with nitrogen is usually complete at a relative pressure of about 0.95.

Type II isotherms are obtained for non porous adsorbents, or those materials possessing only a macroporous structure (eg. the adsorption of nitrogen on (non porous) carbon black). The position at the beginning of the linear portion of the isotherm signifies the stage at which the statistical monolayer (point "B") is complete. Type III isotherms result from weak adsorbate- adsorbent interactions, where isotherm shape is controlled largely by the strength of adsorbate- adsorbate interactions (eg. the adsorption of water vapour on carbon black). For mesoporous adsorbents, type IV and type V characteristics are obtained instead of type II and type III characteristics respectively. These isotherms exhibit adsorption hysteresis, which is associated with capillary condensation in the mesopores. Type VI characteristics are exhibited by energetically uniform non porous surfaces.

CLASSIFICATION OF ADSORPTION ISOTHERMS
(IUPAC)

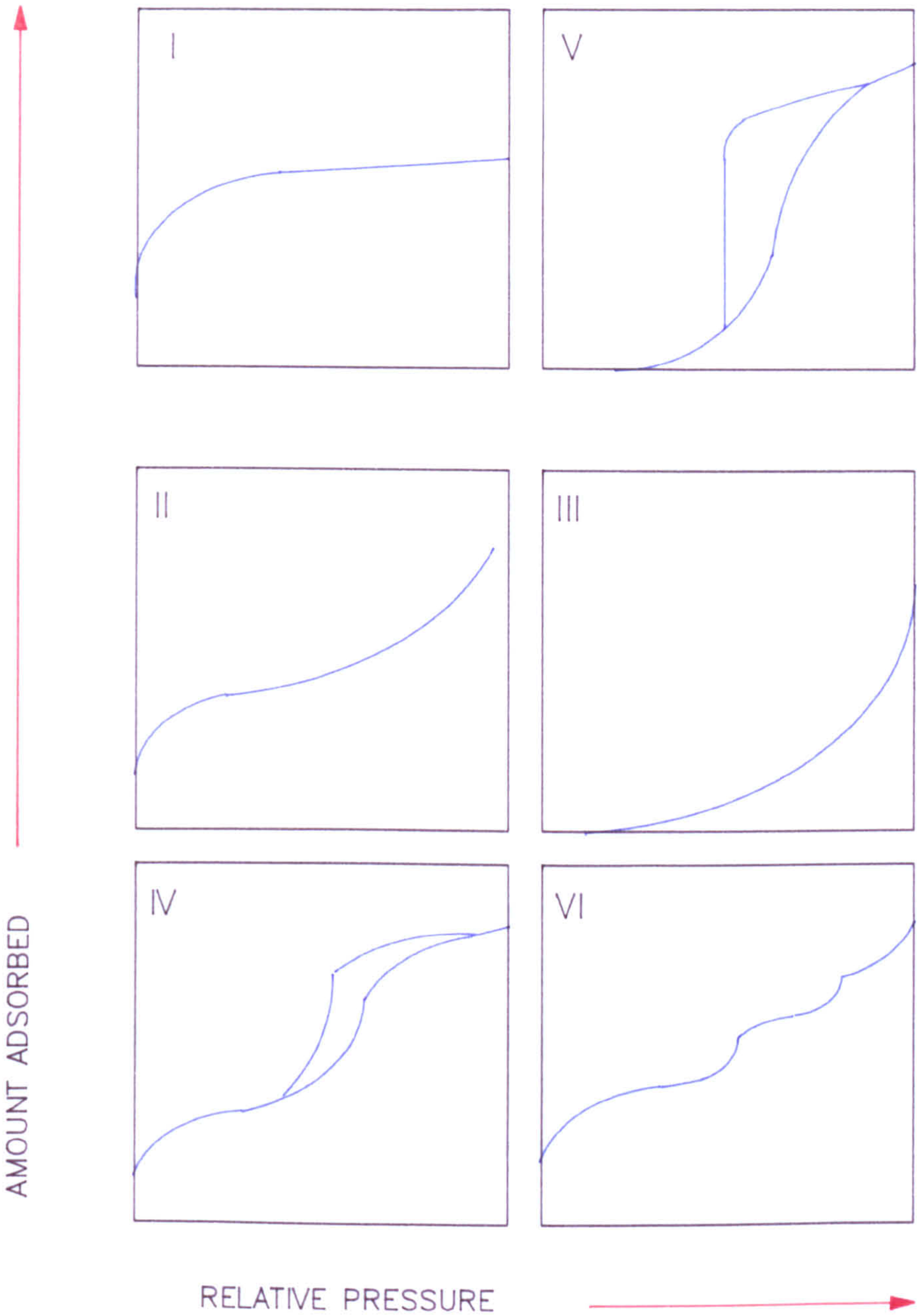

FIGURE 2.1.

NITROGEN ISOTHERM FOR BPL CARBON

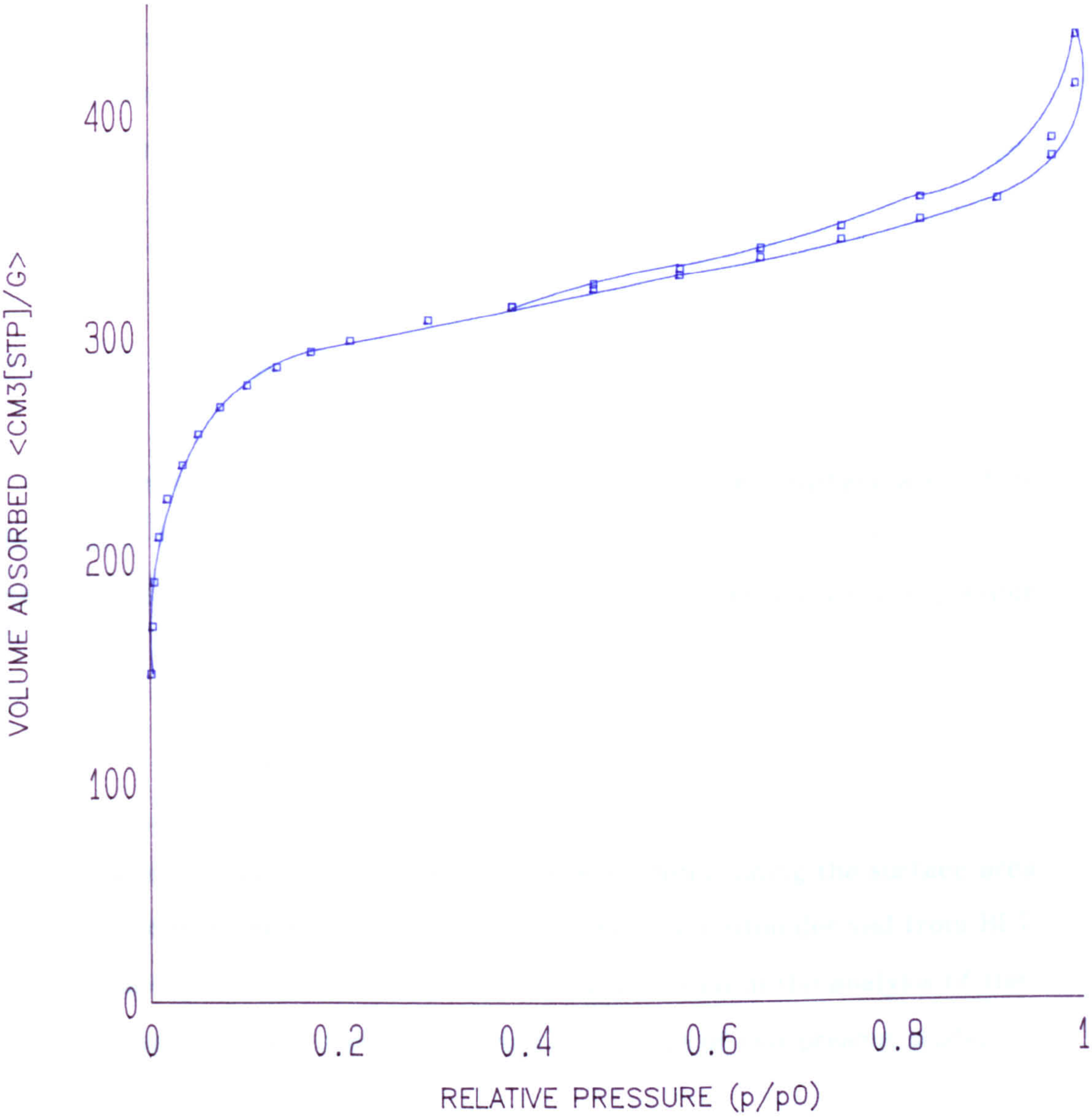

FIGURE 2.2.

In the context of this present research, it is the isotherms of type I and V that are of relevance. Type I characteristics are normally observed for the activated carbon- nitrogen system. Nitrogen adsorption is used as a means of characterising the structure of control and modified adsorbents (chapter 5, Appendix). Common organic compounds also exhibit type I characteristics. The adsorption mechanism is adequately described above. Type V characteristics are found for the activated carbon- water vapour systems (2.2.2). The water adsorption properties of control and modified adsorbents is an important aspect of this study (chapter 5, Appendix).

2.2.1 Analysis of Type I Isotherms

Isotherm analysis enables an assessment of the total surface area of the adsorbent to be made: in addition, estimates of pore volume, and the contributions arising from any meso- and/ or macro- porosity are also possible.

2.2.1.1 BET Theory

Analysis of adsorption data as a means of determining the surface area of an adsorbent is commonly achieved using the calculation derived from BET theory (Brunauer, Emmett, Teller[6]). BET theory is used in the analysis of the nitrogen adsorption data measured during the course of this present study.

The theory, developed in the late 1930's, assumes that dynamic equilibrium exists within the adsorbed layers, that the rates of condensation and evaporation are the same in all layers subsequent to the first, and that the heat of adsorption is equal to the heat of condensation (liquefaction) in all layers but the first. The theory accounts for multilayer adsorption, but suffers from a number of limitations. The more important of these are that the adsorbent surface is assumed to be homogenous, that interactions between adsorbed

molecules are neglected, and that molecules in all layers other than the first are equivalent. It is quite evident that, for activated carbon, these assumptions cannot be entirely valid[7]. The BET equation is shown below:

$$\frac{p}{v(p^0-p)} = \frac{1}{V_m C} + \frac{(C-1)}{V_m C} \cdot \frac{P}{p^0}$$

V_m = monolayer capacity (cm^3<STP>g^{-1}); C = constant (related to the enthalpy and entropy of adsorption); V is the volume of gas adsorbed at a given relative pressure (cm^3<STP>g^{-1})

V_m and C are obtained from a plot of p/p^0 against $p/V(p^0-p)$, which, over a limited range of relative pressure, is linear. From this linear region (slope L), and the axis intercept (I) the monolayer capacity, V_m, and the C constant may be calculated.

$$V_m = \frac{1}{L+I} \qquad C = L + \frac{1}{I}$$

For type I isotherms, the range of relative pressures over which the plot is linear for activated carbon adsorbents is usually 0.01 - 0.1.

BET theory is routinely applied to the analysis of nitrogen adsorption data, even though it is apparent that limitations as to the validity of the theory exist. Probably the most important limitation is that type I characteristics are believed to be due to micropore filling, rather than surface coverage by mono- and multi-layer adsorption. In addition, arguments for, and against, the use of nitrogen as the adsorbate have been made[8].

Because, in the present case, the data is used as a technique for comparing the structural characteristics of activated carbons before and after surface chemical modification, the above limitations are believed unimportant.

Nitrogen Adsorption

Nitrogen isotherms for activated carbons often exhibit adsorption-desorption hysteresis (figure 2.2), which is believed to result from capillary condensation in the larger pores at high relative pressures. The shape of the hysteresis loop, which is observed at relative pressures above 0.4 p/p^0, may in some examples reflect activated diffusion of the nitrogen molecule through narrower, or constricted pores. Due to the speculative nature of their interpretation, an analysis of the shape of the hysteresis loops for activated carbon was not useful in the context of this present research.

2.2.1.2 Analysis of Nitrogen Adsorption Isotherms using the α_s Method

Further analysis of nitrogen adsorption data can, however, reveal subtle differences between the structural characteristics of control and modified carbons. The α_s[9,10] technique is used in this study, which is an empirical approach for the assessment of the microporosity of an adsorbent. It involves measurement of the slope and intercept from the linear region of a plot of the amount adsorbed at a particular relative pressure against α_s, which is the ratio of the amount adsorbed by a reference adsorbent at the same value of the relative pressure, to the amount adsorbed at a standard value. The standard value is somewhat arbitrary, and, for activated carbon, is set at unity at a relative pressure of 0.4. Below this value, micropore filling is important: above 0.4 p/p^0, adsorption in larger pores (the external surface) takes place. The linear region of the plot corresponds to the range of relative pressures where the adsorption mechanism is the same for both solids (sooty silica is used as the

reference adsorbent in this study, and is a non porous solid: the linear region of the plot therefore corresponds to the non microporous surface area (or external surface area) of activated carbon).

The external surface area (S_{ext}) of the adsorbent is given by:

$$S_{ext} = \frac{(S_{reference} \cdot L)}{V}$$

Where $S_{reference}$ is the total surface area of the reference adsorbent, L is the slope of the linear portion of the plot, and V is the amount adsorbed by the reference at the standard value of the pressure.

The volume of the micropores (V_m) is given by:

$$V_m = \frac{(M_w \cdot I)}{(22414 \cdot \varrho)}$$

Where I is the intercept of the linear region; M_w is the molecular weight of the adsorbate; 22414 $cm^3\ mol^{-1}$ is the ideal gas volume (STP) and ϱ is the liquid density of the adsorbate. For nitrogen at -196°C, this expression simplifies to:

$$V_m = 0.00156 \cdot I$$

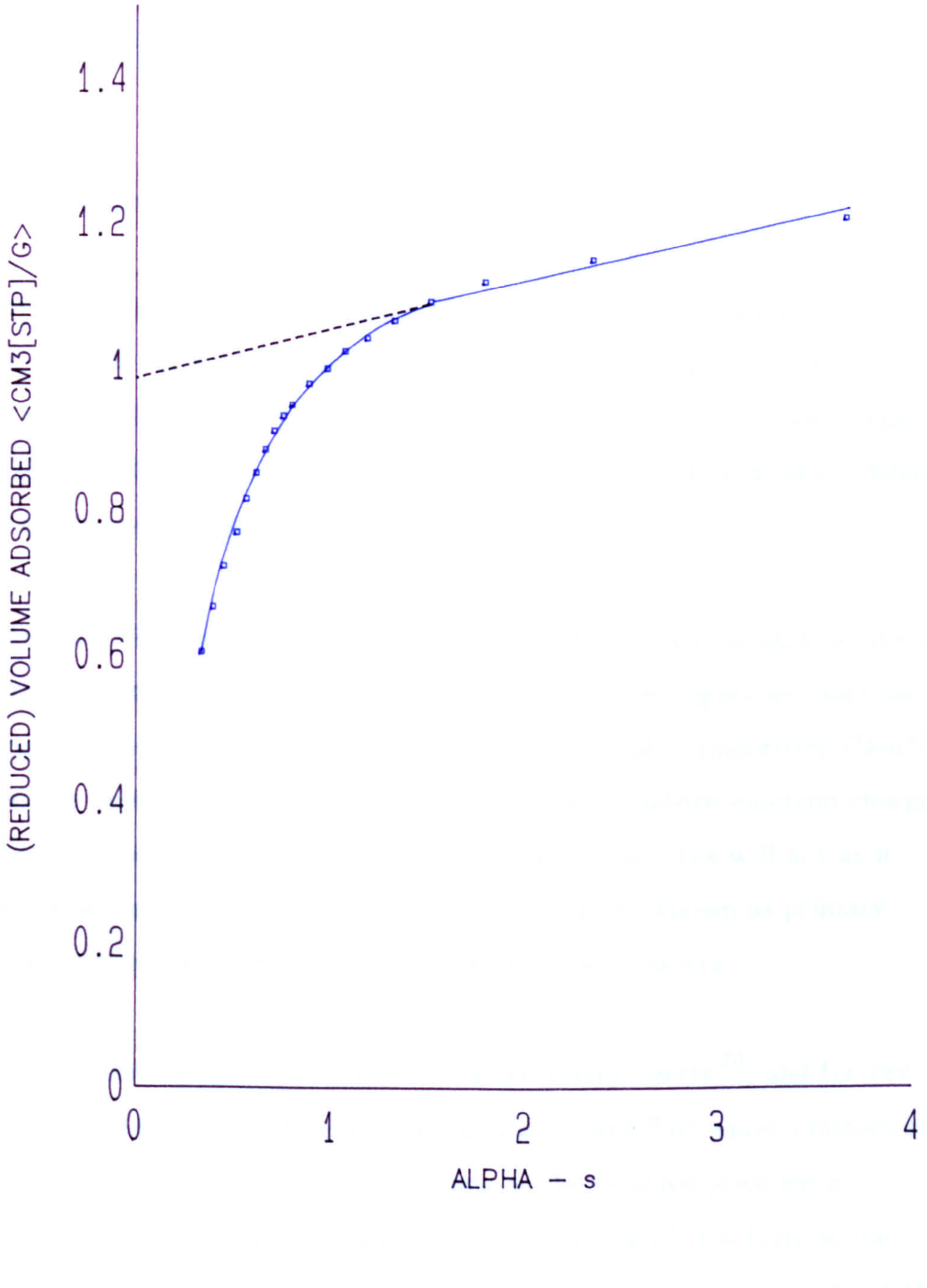
ALPHA – s PLOT FOR BPL CARBON
(REDUCED) VOLUME ADSORBED <CM3[STP]/G>
1.4
1.2
1
0.8
0.6
0.4
0.2
0
0
1
2
3
4
ALPHA – s

FIGURE 2.3.

This approach can therefore be used to separate the contributions to the total surface area resulting from adsorption (of nitrogen) into the microporous and non microporous regions. For this reason, it is a useful in the analysis of modified carbons. A typical example of an α_s plot (obtained for Chemviron BPL activated carbon) is at figure 2.3.

2.2.2 Water Adsorption Properties of Activated Carbon

Figure 2.4 shows a typical water adsorption-desorption isotherm, measured at 22°C for BPL (Chemviron; Brussels, Belgium) carbon[11]. The isotherm (type V^2) is typical for activated carbon, and consists of two distinct regions, above and below a relative pressure of approximately 0.4. Much debate exists as to the reasons for the observed shape[eg.7].

The most plausible explanation[12-18] is that adsorption initially occurs on active sites present on the surface, which may be surface impurities, such as nitrogen or oxygen containing functional groups, or metallic impurities ("ash") present in the base carbon material. Structural defects, where electron charge localisation can take place may also be important. These sites will act as a focus for the adsorption of water molecules[19,20] and are known as primary adsorption centres: they are occupied at low relative pressures.

The adsorbed water will then act as a secondary centre[20], and further adsorption occurs through hydrogen bonding. The "islands" of water clusters so formed enlarge and spread across the surface as the relative pressure is increased, until a continuous film develops. The merging of this film on the walls within the micropores corresponds to the steep (pore filling) region of the isotherm. The hysteresis loop results from the presence of menisci at the pore entrances which are of a different shape to those formed during adsorption. Desorption will only then take place if the relative pressure is reduced sufficiently[21].

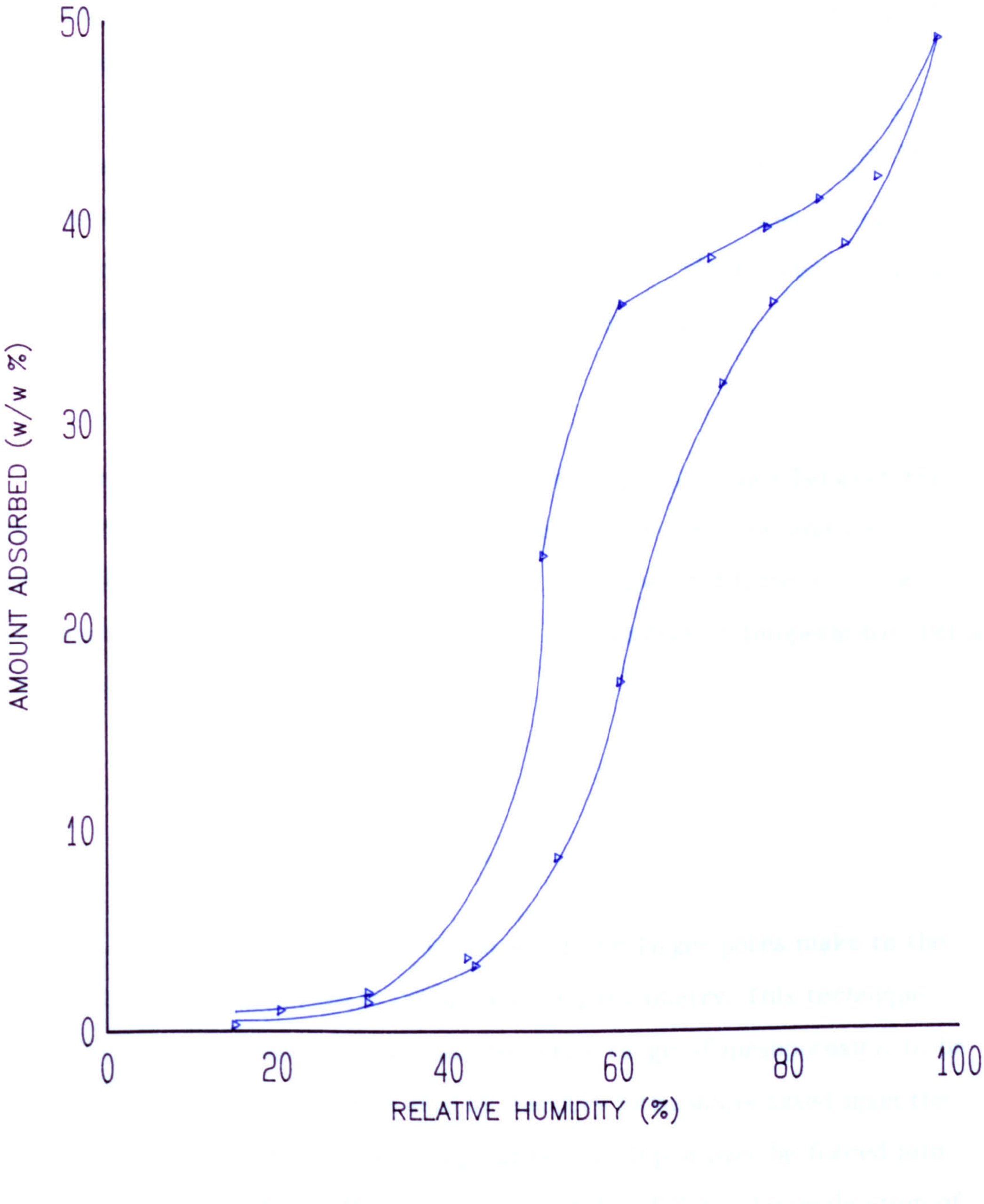
WATER ISOTHERM FOR BPL CARBON
AMOUNT ADSORBED (w/w %)
0
10
20
30
40
50
0
20
40
60
80
100
RELATIVE HUMIDITY (%)

FIGURE 2.4.

An alternative view[22-25] is that only capillary condensation governs the water adsorption process, which occurs initially in narrow pore entrances or constrictions where the adsorption potential is greatest. Further adsorption occurs through hydrogen bonding until the thickness of the layer is such that pore filling results. Hysteresis is then a result of the unfavourable desorption of water through the narrow pore constrictions. The failure of the desorption branch of the isotherm to close completely is a consequence of the strong association of water molecules with active sites in the capillary pores[26-28]. Such sites do not necessarily promote adsorption, but they inhibit desorption. Doubt as to the validity of this argument is apparent[13,29]: the mechanism may be plausible for carbons which may possess "ink bottle" pores.

For organic compounds, there exists a strong dependency between the amount adsorbed (at a particular value of the relative pressure) and the temperature. The behaviour of water vapour is somewhat different, in that adsorption by activated carbon is essentially independent of temperature over a wide range[30].

2.3 Mercury Porosimetry

An assessment of the contribution which the larger pores make to the total surface area may be made using mercury porosimetry. This technique enables the macroporosity, and almost the entire range of mesoporosity, to be measured. Determination of pore size by mercury intrusion is based upon the behaviour of non wetting liquids in capillaries. The liquid may be forced into small pores which have a wetting angle greater than 90^{o} by the application of external pressure, which is a function of the pore size. It is a simple technique, and involves submerging a known quantity of porous sample under a confined quantity of mercury and then increasing the applied pressure. With the aid of a pore model, the dimensional distribution of pore sizes may be calculated.

For cylindrical pores:

$$R_p = -2\left(\frac{\zeta}{\rho}\right)\cos\theta$$

ζ=*surface tension of mercury* (480mN/m^2)
R_p=*pore radius* (*nm*)
ρ=*applied pressure* (N/m^2)
θ=*contact* $\angle$(°)

The above equation, due to Washburn[2] is normally written in the form:

$$R_p = \frac{7300}{\rho}$$

A θ value of 141.3° is used.

The use of mercury intrusion relies on assumed values of the mercury-carbon contact angle. In addition, the technique is applied to activated carbon, even though these adsorbents are not believed to contain cylindrical pores. Thus the above equation is used to calculate the pore size distribution (macroporosity, and a proportion of the mesopore volume (technical limitations prevent the complete range of mesopores to be determined)).

As before, the approach enables comparison between different carbons to be made: knowledge of the precise theoretical interpretation of the data in the context of this present study is therefore deemed unnecessary.

REFERENCES

1] Sing, K.S.W, Everett, D.H., Haul, R.A.W., Moscou, L., Pierotti, R.A., Rouquerol, J., and Siemieniewska, T., Pure and Appl. Chem. 57 1985 603.

2] Gregg, S.J. and Sing, K.S.W., in Adsorption, Surface Area and Porosity, second edition, Academic Press, London 1982.

3] Everett, D.H. and Powl, J.C., J. Chem. Soc. Farad. Trans. 1 72 1976 619.

4] Stoeckli, H.F., Helv. Chim. Acta. 57 1974 2195.

5] Carrott, P.J.M., Roberts, R.A., and Sing, K.S.W., Chem. and Ind. 24 1987 829.

6] Brunauer, S., Emmett, P.H., Teller, E., J. Am. Chem. Soc. 60 1938 309.

7] Bansal, R.C., Donnet, J-B., Stoeckli, H.F., Active Carbon, Marcel Dekker, New York, 1988.

8] Roberts, R.A., Ph.D. thesis, Brunel University, 1988.

9] Sing, K.S.W., in D.H. Everett and R.H. Ottewill (Eds.) Surface Area Determination, Butterworths, London 1970 25.

10] Carrott, P.J.M., Roberts, R.A., and Sing, K.S.W., Carbon 25 1987 769.

11] Yates, M., Unpublished data, Brunel University.

12] Barton, S.S., Evans, M.J.B., Holland, J., Koresh, J.E., Carbon 22 1984 265.

13] Studebaker, M.L., Rubber Chem. Technol., 30 1957 1400: Studebaker, M.L., Proc. Third Biennial Conf. Carbon, Pergamon Press, New York 1957 289.

14] Pierce, C. and Smith, R.N., J. Phys. Colloid Chem., 54 1950.

15] Pierce, C., Smith, R.N., Wiley, J.K., Corder, H.J., J. Am. Chem. Soc., 73 1951 4551.

16] Dubinin, M.M., Zaverina, E.D., Serpinski, V.V., J. Chem. Soc., 1955 1760.

17] Evans, M.J.B., Carbon 25 1987.

18] Dubinin, M.M., Carbon 18 1980 355.

19] Swiatkowski, A. and Gowerek, J., Carbon 25 3 1987 333.

20] Malenkov, G.G. and Dubinin, M.M., Izv. Akad. Nauk. SSSR, Ser. Khim., 6 1984 1217.

21] Cohan, L.H., J. Am. Chem. Soc., 60 1938.

22] Puri, B.R., Singh, D.D., Sharma, C.R., J. Phys. Chem., 62 1958 756.

23] Kiselev, A.V. and Kovaleva, N.V., Zh. Fiz. Chem., 30 1956 2775.

24] Avgul, N.N., Dzhigit, O.M., Kiselev, A.V., Scherbakova, K.D., Dokl. Akad. Nauk. SSSR 92 1953 105.

25] Avgul, N.N., Dzhigit, O.M., Kiselev, A.V., Scherbakova, K.D., Dokl. Akad. Nauk. SSSR 101 1955 285.

26] Wiig, E.O. and Juhola, A.J., J. Am. Chem. Soc., 71 1949 561.

27] Wiig, E.O. and Juhola, A.J., J. Am. Chem. Soc., 71 1949 2069.

28] Juhola, A.J. and Smith, S.B., J. Am. Chem. Soc., 74 1952 61.

29] Karpinski, K. and Willmann, G., Chem. Stosow. 21 1977 2.

30] Emmett, P.H., Chem. Rev. 43 1948 69.

CHAPTER 3

INDEX

The Preparation and Properties of Chemically Modified Activated Carbon

3.1 Reaction with oxygen and oxidising reagents

3.1.1 The Surface of Carbon Modified with Oxygen

Irrespective of the method of oxidation, carbons (activated carbon, carbon black, graphite, and diamond) eliminate carbon dioxide and monoxide during thermal desorption, due to the decomposition of surface oxygen containing functional groups (surface oxides).

Attempts have been made to identify and quantify the surface oxides[1-5], and many structures have been suggested, including the common organo-oxygen containing functional groups. Unambiguous assignments are difficult: conjugated organic structures may exist, and attempts to identify groups may cause further surface modification. It is of some significance that studies to date have not accounted for the entire quantity of chemisorbed oxygen[2,6].

The pore structure of active carbon complicates these studies, and techniques such as XPS (X Ray Photoelectron Spectroscopy; or ESCA (Electron Spectroscopy for Chemical Analysis)) only enable analysis of the external surface. Additionally, chemical reagents may not fully penetrate the porous network: the kinetics of adsorption may be slow, such that analyses will be difficult[4,7]. Long equilibration times in solution, or heating under reflux, may promote modification.

The absence of significant porosity enables carbon blacks and graphites to be studied with some confidence, although steric, kinetic effects, and the carbon source may affect reproducibility [8-10].

In addition to carbon dioxide and monoxide, methane, water vapour and hydrogen have been identified during thermal desorption analysis[11], but oxygen has not. Water vapour desorption generally occurs between 200-500°C [1,11].

The desorption profiles of the carbon oxides from carbon blacks[2,12] and graphites[13,14] exhibit distinct maxima, similar to those for active carbon. The presence of more than one maxima for each species suggests that the surface oxides are not chemically identical[1-3,14,15]. They are also not present in sufficient number to give rise to monolayer coverage[16,17].

The surface oxides are generally stable at 115°C, temperatures above 150-200°C being necessary to cause significant decomposition[1,11,18].

At 200-300°C, the principal desorption product is CO_2. This desorption continues until temperatures of approximately 600°C are attained[3,11,19]. The presence of two maxima during desorption is common[1-4,16,20-23], although some of the desorbed carbon dioxide may react to yield carbon monoxide and surface oxides[13]: care interpreting data may be necessary.

Desorption of CO is observed to begin at 300-400°C and is the major product above 600-700°C, usually present as a single broad peak. This desorption is complete at 900-1000°C[2,19]. During desorption, the ratio of the two carbon oxides changes continuously[1,18,20].

Above 700-800°C, hydrogen desorption may occur[11], and can continue to approximately 1200°C[2,18]. At higher temperatures, graphitisation leads to the closure of smaller pores[3,24].

Carbons are acidic or basic in solution. This effect is dependent on the temperature at which preparation is carried out[2,3,14,25]. Thus, acidic carbons are prepared by oxidation above ca. 200°C, whereas basic carbons are formed below 200°C, or above ca. 700°C (the limiting temperature for the formation of acidic carbons).

3.1.2 Surface Oxygen Complexes on Acidic Carbons

Surface structures have been proposed[3] (figure 3.1), which would behave chemically in a manner similar to the "f-lactone" (fluorescein lactone)[26] (figure 3.2). The "f-lactone" and carboxyl groups[2,14] are believed to be responsible for the carbon dioxide emissions and the acidity[27]. Carboxyl, carbonyl and phenol groups have been identified, by use of such techniques as selective neutralisation[10], although it is not possible to account for all the oxygen: steric effects, oxide impurities and/ or the presence of ethers cannot be ruled out.

Carbon monoxide is believed to arise through the decomposition of quinones, hydroquinones (figure 3.3) phenols, or anhydrides[2,28]. The stability of anhydrides in the presence of even trace quantities of moisture is questionable.

Desorbed water may originate from hydroquinone and phenol groups: other structures have also been proposed[2] (figure 3.4).

Studies with carbon blacks[14,29,30] suggest that lactones are responsible for the low and high temperature CO_2 emissions[2,14]. A direct correlation between carbon dioxide desorption and acidity was found[1], consistent with the presence of monobasic (simple lactone) and dibasic (f-lactone) species. Groups desorbing carbon monoxide did not contribute significantly to the acidity. Graphite possessed a single carbon dioxide emission maxima, due to the

decomposition of f-type lactones. Evidence for phenolic groups on graphites and blacks was also strong[31,32]. Carboxyl groups may also occur on the surface of oxidised blacks[32,33], although this is doubtful[2,26]. Conjugated quinones may also be present[34]. Quinones, carboxyl groups and acid anhydrides may occur on carbon films oxidised with nitric acid[35,36], although carbon nitrogen complexes could also be formed[4,35].

Activated carbons exposed to humid air possess acidic surface oxides[2], which liberate carbon monoxide and dioxide during thermal desorption[11,20]. Examination of the desorption profiles[20] suggests they are similar to those present on carbons oxidised at elevated temperature[1,6].

Surface oxides are also present on diamond exposed to humid air[8,21,37], or to oxygen at elevated temperature[10].

IR spectral data is often employed for the identification of surface oxide structures, but is poorly resolved[35,38]: the evidence is used to propose the presence of specific oxygen containing functional groups without supporting data[35,36,39]. Few have combined IR and chemical techniques[40]. FTIR PDS (photothermal beam deflection) spectroscopy[41], and XPS have been applied, although XPS cannot resolve the carbon-oxygen surface structures, and so in isolation does not enable functional groups to be identified[6], although classes may be identified[42-44]. Fast atom bombardment indicates that groups containing carbonyl, carboxyl and hydroxy, are present[45].

3.1.3 Surface Complexes on Basic Carbons

The functional groups imparting basic characteristics to carbon are poorly understood. Physical forces[6] or specific functional groups,[2,3,6] such as the "chromene" (figure 3.5)[46] or "pyrone" (figure 3.6)[3] groups are probably responsible. PDS suggested that the IR band at 1600 cm^{-1} may be due to

olefinic bonds. It was believed that ether-like oxidised layers caused the carbon double bonds to be active in the region normally occupied by simple carbonyl groups[41].

Some effort has been directed toward establishing the structure of surface oxides on carbon: further contributions are difficult. The presence of certain classes of oxygen containing surface functional groups has been recognised, however.

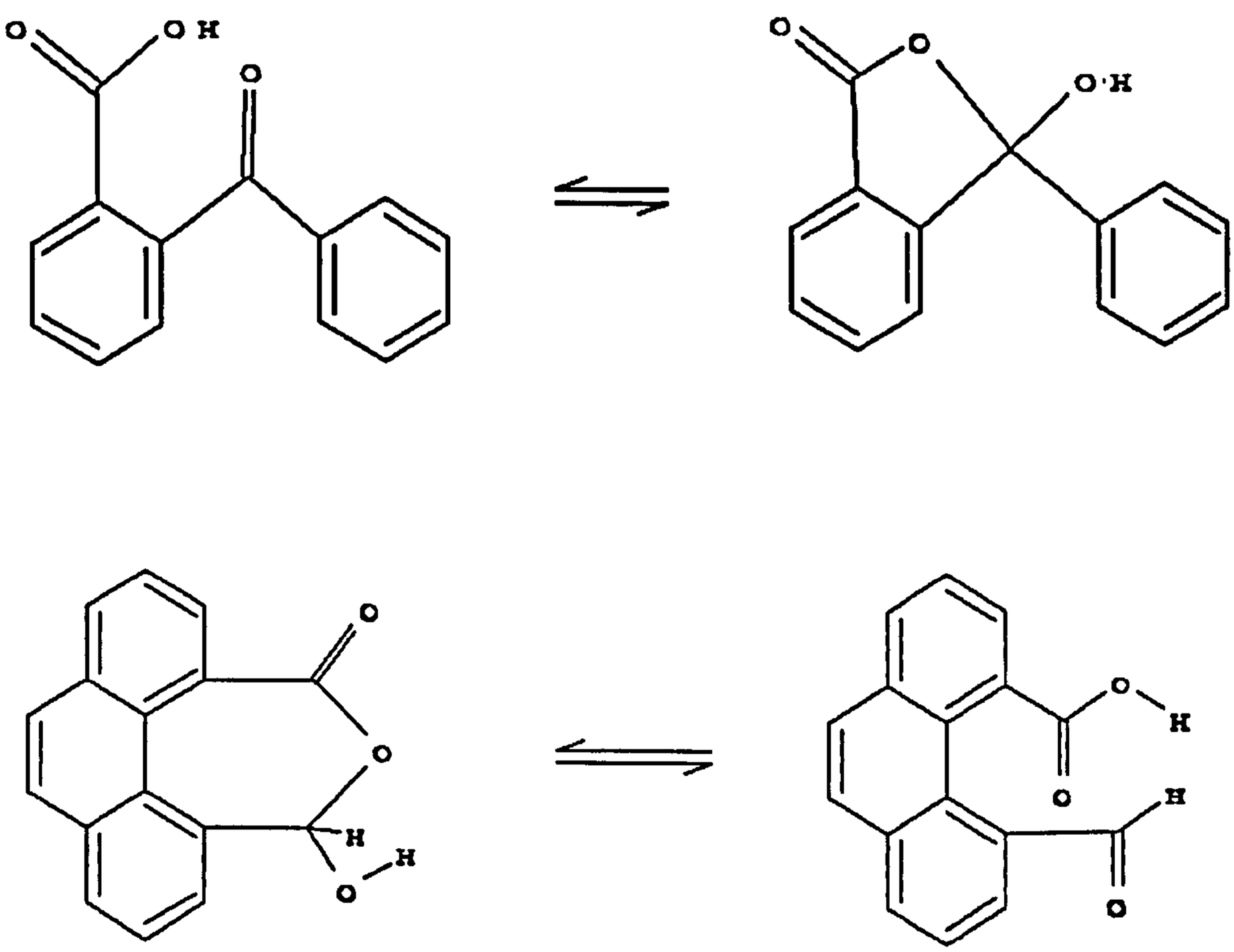

Figure 3.1.

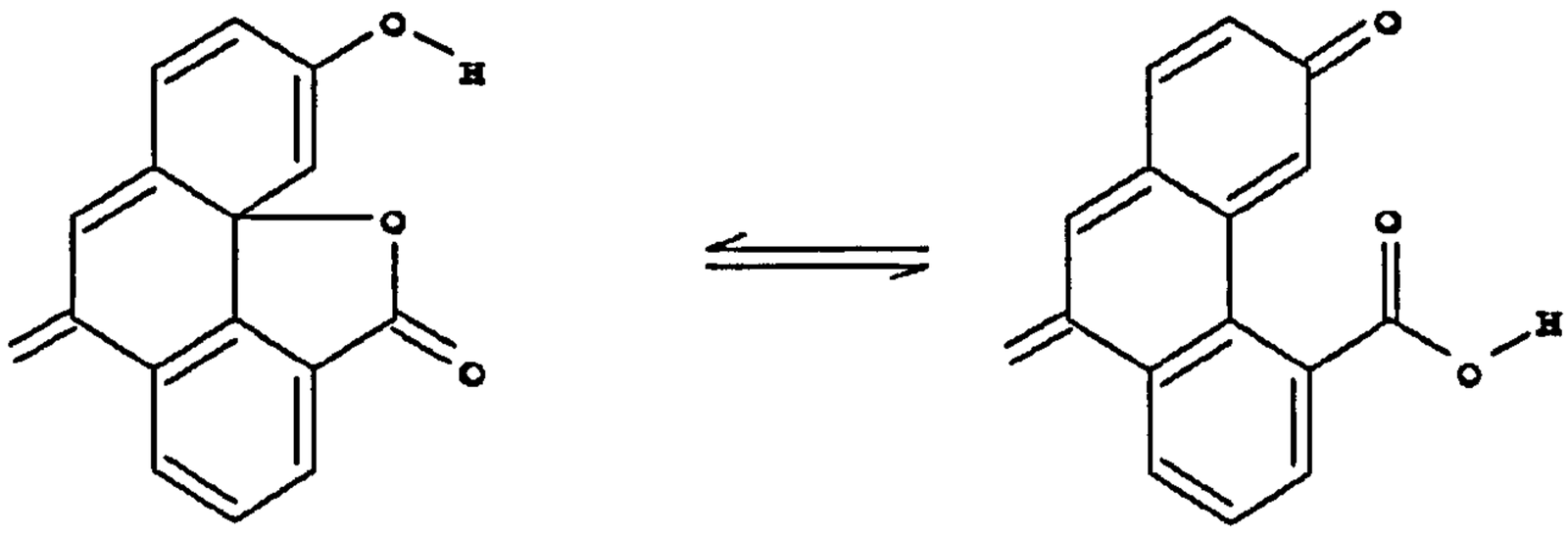

Figure 3.2.

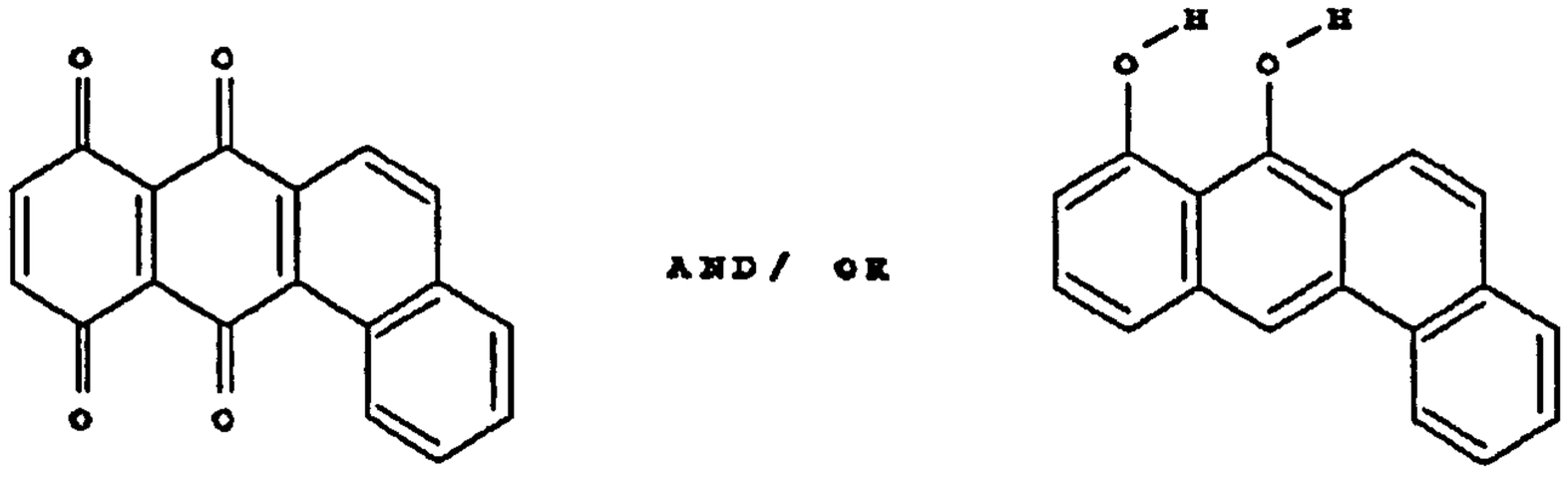

Figure 3.3.

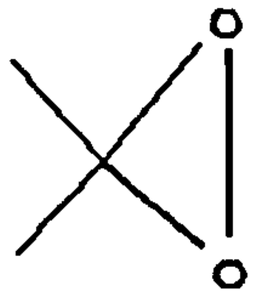

Figure 3.4.

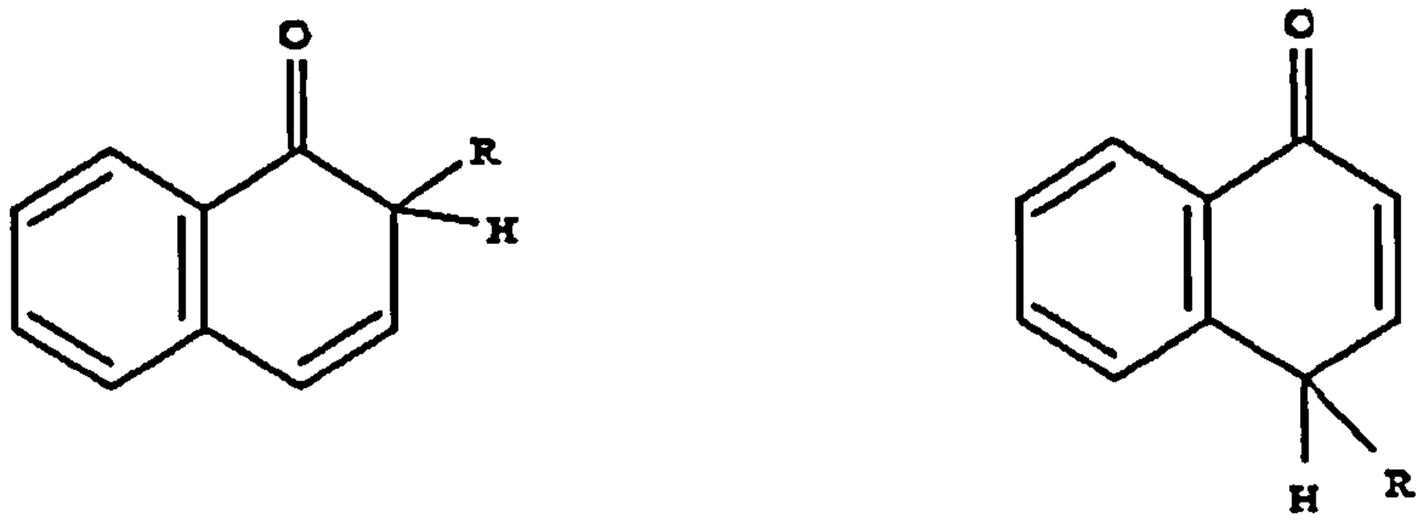

Figure 3.5.

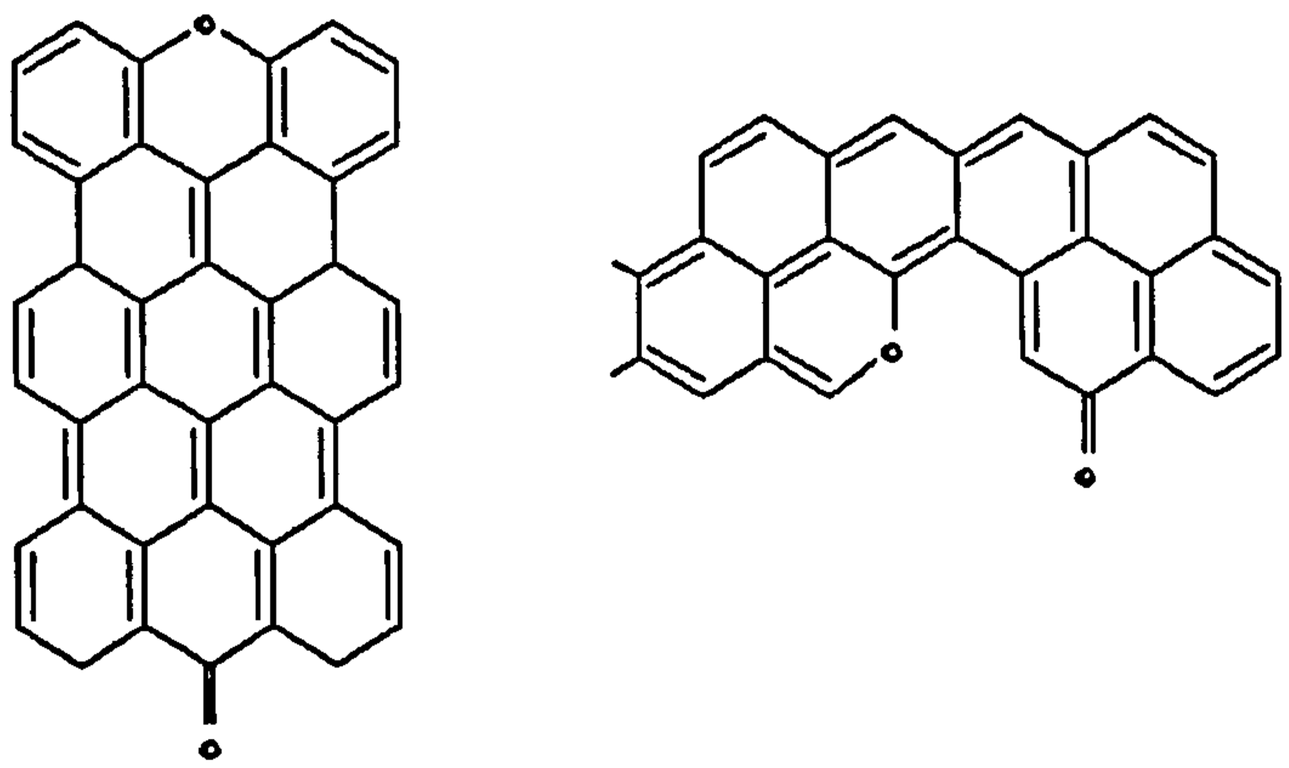

Figure 3.6.

3.2 Preparation of Oxidised Carbons

3.2.1 Reaction with Oxygen

At -78°C or lower, oxygen is physisorbed[18]: chemisorption is observed at -40°C[8]. Grinding in air results in chemisorption[19,34,47], due to the exposure of active sites (free valencies/defects). Reaction with atomic oxygen in a discharge tube at room temperature has also been observed[42,48], and[42] resulted in increased surface roughness. XPS evidence indicated that the more than one surface complex had been generated.

High temperature combination with molecular oxygen is most common[18], and up to 20% by weight may be fixed under optimum conditions: at 1000°C, gasification predominates and few surface oxides form.

For activated carbon and blacks[2,49], oxygen pressures of 0.7-0.8 atmospheres at 400-450°C result in maximum oxygen fixation[2]: for graphitized carbon black, a temperature of 500°C is necessary to maximise reaction without causing significant burnoff[23].

Oxidation of active carbon can result in further activation, an effect that will complicate interpretation of experimental data due to structural modification[23,50,51]. The rate of oxidation is enhanced in the presence of surface oxides, indicating a participation in the reaction[52].

Studies of carbon oxidation often include the concept of the active surface area (ASA) as a means of classifying reactivity. The ASA is a small percentage (ca. 3% [53,54]) of the total surface area that is "active" toward oxygen chemisorption. Doubt as to the usefulness of the concept[51,55-57] is apparent, especially at high reaction temperatures[50].

3.2.2 Reaction with Oxidising Gases

A relatively large (ca. 5-10% weight) amount of oxygen may be fixed using dinitrogen tetroxide (NO_2)[5,58] or ozone[2,5,18]. Carbons of lower oxygen content may be prepared by reaction with nitrous oxide or carbon dioxide[59,60]. Oxidation with nitrous oxide is fast at 300°C, resulting in nitrogen liberation and the fixation of oxygen[61].

Nitrogen monoxide (nitric oxide) will oxidise carbons[62], and activated carbon has been used for its removal from gas streams[63]: at temperatures of

ca. 375°C, the products were found to be N_2O and CO_2. Sample regeneration with hydrogen was possible, but the presence of carbon oxides at all reaction temperatures suggested that burn off was occurring. Nitric oxide will also oxidise over carbon at ambient temperature to yield dinitrogen tetroxide, which will react at the surface[64]. The reduction of nitric oxide to molecular nitrogen was insignificant, however. In the presence of moisture nitric acid formed.

At low temperatures (less than ca. 100°C), oxidising gases are unlikely to cause significant structural modification of activated carbon[34], although the fixation of non oxygen species is likely at elevated temperatures.

3.2.3 Reaction with Water

Exposure of carbon to water[4,5,65-67], water vapour[24] or steam[6] results in oxygen (and/or) hydrogen[68] fixation. Reaction may also proceed with water vapour at temperatures as high as 1200°C[69].

Activated carbon, black, and diamond, chemisorb significant quantities of oxygen during exposure to humidified air at ambient temperatures[1,15,16,70]. The extent of oxidation of activated carbon ("ageing")[20,71] increases with the relative humidity (RH)[20], indicating a dependence upon the adsorption characteristics (adsorption isotherm), rather than on the water vapour concentration. Experimental results[72] using high purity nitrogen suggest that reaction with water was most important, a contention supported by the lack of reactivity between activated carbons and dry air[20,71].

3.2.4 Oxidation in Solution

Nitric acid is a common oxidant[2,35], often used under forcing conditions[73]. Mixtures of nitric and sulphuric acid have been used to prepare oxidised carbon black[4,5], and nitration of the carbon was probable, although supporting evidence was lacking[35]. Severe conditions can cause structural modification, and may complicate data interpretation[50]. This problem is recognised[74], although some disagreement as to the effect of acid treatment on the carbon structure persists[75,76]. Other oxidants have been used, including hydrogen peroxide, sodium hypochlorite[4], and potassium permanganate, which lead to significant structural modification[77,78]. This may be due to deposition of residual reagent within the pore structure[2].

3.2.5 The Effect of Impurities upon Oxidation

The nature and amounts of any impurity (non- carbon elements and ash) depend upon the carbon source and the techniques used for carbonisation and activation. Coal carbons often contain more impurity than those derived from nutshells or fruit stones. The "ash" content of production coal based carbons is often as high as 10% weight[6,79]; for nutshell carbons, values between 2-5% weight are typical[79].

Non carbon impurities influence significantly the rate and extent of oxygen chemisorption[80]: de ashed active carbon chemisorbed less oxygen, and at a reduced rate. The original carbons contained many impurities (eg. alumina, silica, magnesium calcium iron and sodium oxides) although only sodium or potassium[53] appeared to promote reaction. The influence of these impurities upon reactivity has been recognised[5,23,81], and shown to affect the thermal desorption characteristics[11], and the course of pore development[82,83].

3.3 Modification of the Surface of Carbon using Chemicals other than Oxygen

Activated carbon filters will degrade during use as a result of two principal processes: surface oxidation (ageing), and a loss of working capacity through the adsorption of environmental pollutants[84].

3.3.1 Regeneration of Aged Carbons

One approach is to outgas the carbon (ca.900-1000°C) to decompose the surface oxides[eg. 1,18,20]. The principal objection to this is that the carbon will re oxidise. Hydrogenation at 1000°C[66,85,86] is an alternative, although an increase in surface area may result due to gasification[87]. Hydrogen treated activated carbons oxidised more slowly, suggesting that chemisorbed hydrogen blocks a proportion of the active sites[62]. This observation may not be consistent with the reduction in the hydrogen content of the carbon resulting from the treatment[88].

An alternative, and more attractive, approach is to chemically transform the surface oxides, because a "fully oxidised" and modified carbon could offer resistance to further oxidation. Attempts to identify surface oxides have utilised various reagents[2,3,6]. In some instances[eg. 89-92], the adsorptive properties of the modified products would be of interest, but were not reported.

3.4 Carbon Modifications using Sulphur and Sulphur Compounds

Sulphur is an impurity in activated carbons and blacks; nutshell-based carbons generally contain only trace quantities[93]. The chemical form of the sulphur is not understood, but its reactivity was shown by the liberation of hydrogen sulphide in the presence of moisture[65].

3.4.1 Sulphur

The combination of sulphur with carbon is temperature dependent, passing through a maximum at approximately 600°C[94-98], which depended on the carbon[94-96] but could be up to 40 weight %[97]. Hydrogen sulphide[94,98-100] and carbon disulphide[94] were formed, and reactivity increased with carbon hydrogen and oxygen content[98]. The sites occupied by sulphur and oxygen may be the same[101], although proof is difficult due to the reactivity of surface oxides with sulphurising agents[98].

The bulk of the sulphur may be removed by solvent extraction[94,96,98], in elemental form (S_8)[95]. Evacuation (1100°C) removes most as elemental sulphur and carbon disulphide[102]: hydrogen sulphide and carbon disulphide were detected at lower temperatures (600°C)[98]. Complete removal of sulphur was achieved by hydrogenation at 700°C. That the carbon-sulphur complexes are stable was evidenced by the lack of significant reactivity with hot nitric acid[103].

Adsorption of sulphur into the micropores in activated carbon[95], as well as the formation of a carbon-sulphur solid solution (intercalate) appears important[104], although intercalate formation is unproven[105]: chemisorption accounts for only a small fraction[95,104]. A proportion of the chemisorbed sulphur is believed to occupy unsaturated surface sites, and may be present in aromatic ring structures[98] (figure 3.7). Thio-ether "bridge" structures may also be present[105,106].

Nitrogen adsorption indicated that small quantities of sulphur (2 weight %) markedly reduced the micropore volume. Adsorption in the mesopores also resulted in a significant loss of porosity[95].

Water adsorption was fundamentally different compared to control carbon, in that type V characteristics were lost. Small quantities produced

type I characteristics, commonly observed with organic vapours. Uptake of water vapour at saturation was reduced significantly[98], and high uptake at low relative pressure indicated that polar functional groups are formed. In addition[98], these carbons adsorbed essentially no benzene vapour even at saturation: a marked reduction in methanol adsorption was probably due to pore occlusion. An increase in hydrophilic character due to sulphur chemisorption is unproven[24,107].

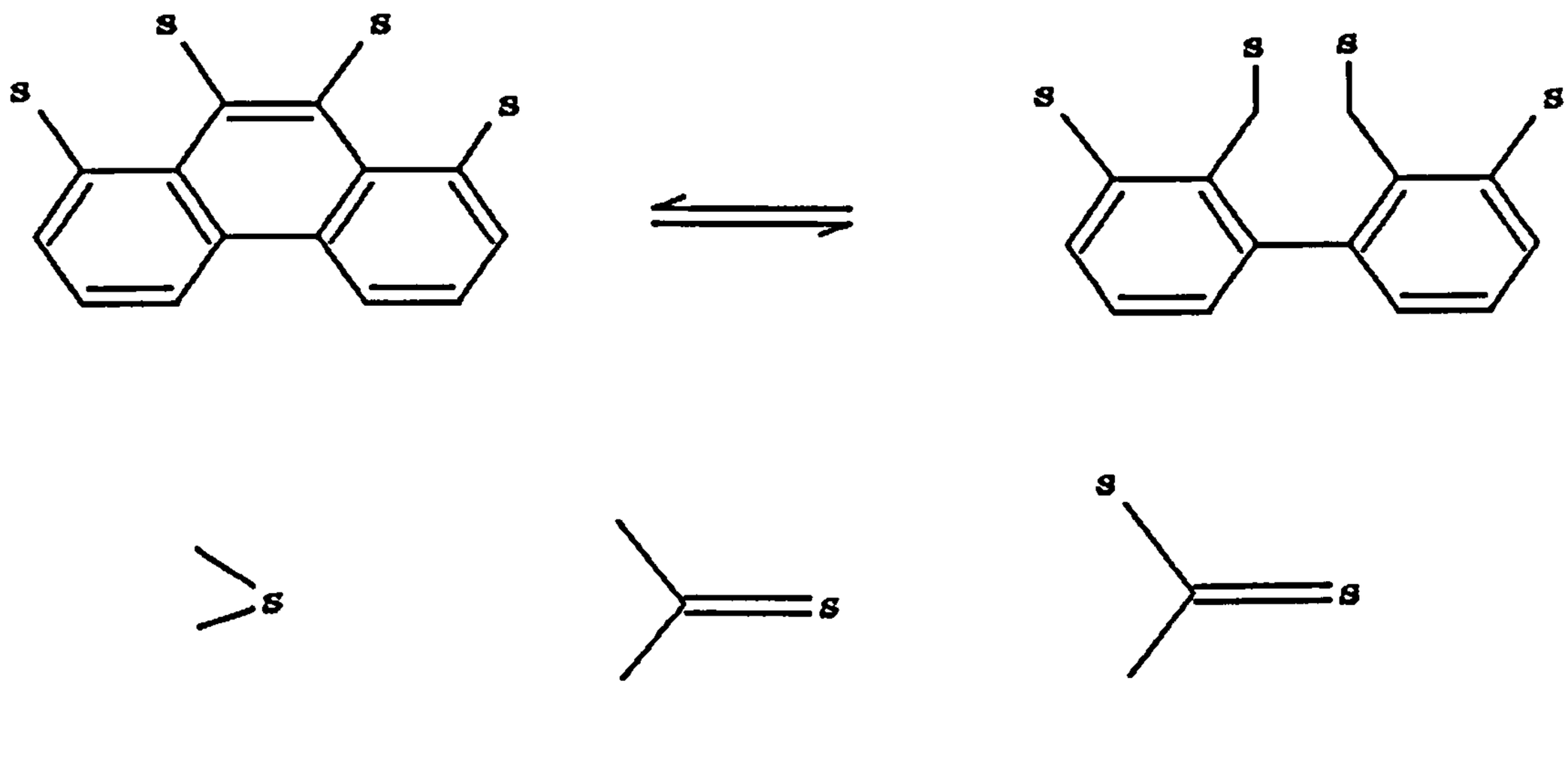

Figure 3.7.

3.4.2 Carbon Disulphide

Activated carbon reacts with carbon disulphide at elevated temperature[98,105,106]: the products are stable in acid, but not base, solution. Carbons modified between 475 and 600°C were stable to 700°C[105]. The complexes produced by treatment with carbon disulphide or elemental sulphur are believed similar[107] (eg. figure 3.7), and direct analogues of surface oxygen species may exist[98,105]. The sorptive properties of the modified carbons can be controlled through selective hydrogenation[108].

3.4.3 Hydrogen Sulphide

Active carbons and blacks react readily with hydrogen sulphide at ambient temperature[3,99]. Above 700°C, significant quantities of carbon disulphide form[109]. In each case, appreciable fixation of sulphur occurred, in two stages[99]. The first stage occurs by oxygen substitution of surface quinones, whilst a slower sequence involved hydrogen substitution. Addition of sulphur at unsaturated sites may also be important[110]. The functional groups produced by treatment with sulphur, carbon disulphide or hydrogen sulphide may be similar (eg. figure 3.7[98,105]), and the vapour adsorption properties were analogous. Both gas and liquid phase treatments yield similar products[111].

3.4.4 Sulphur Dioxide

Sulphur dioxide combines readily with carbon[98,105,112] to yield sulphoxide and sulphone groups. At ca. 650°C CO and COS were detected, and elemental sulphur was deposited. Almost all of the sulphur could be recovered[103] during desorption, and sulphur dioxide and carbon oxides were detected[2]. Fixation of sulphur at unsaturated sites and reaction with surface oxides was probable[98,113].

The vapour adsorption properties of carbons modified in this manner have received little attention, although water[114] and air purification[115] applications have been considered.

Other reagents, including thionyl chloride[105], have been studied to lesser degrees. Carbon modified with sulphur would appear to have limited vapour adsorption applications, although further studies could be revealing: their stability in humid air, and the adsorptive properties at high humidities may be of interest, given the discontinuities between the observations of different research groups.

3.5 Carbon Modifications using Nitrogen Compounds

Carbons contain fixed nitrogen (<~0.5% weight, BPL activated carbon), although the chemical form is unknown. No evidence is available to suggest that molecular nitrogen combines directly with carbon under normal conditions[116], but modification using plasma deposition[116] may produce surface groups amenable to further transformations[117,118].

3.5.1 Carbon Modifications using Ammonia

Ammonia may be used as an activating[eg. 87,119] or hydrogenating agent[95]. In the former role, amine groups were probably not formed[120], although nitrogen and hydrogen fixation was observed. Thermal desorption indicated that chemically distinct complexes were present. Ammonia treated carbon was found to exhibit catalytic activity[121], probably due to groups at the peripheral carbon layers (figure 3.8).

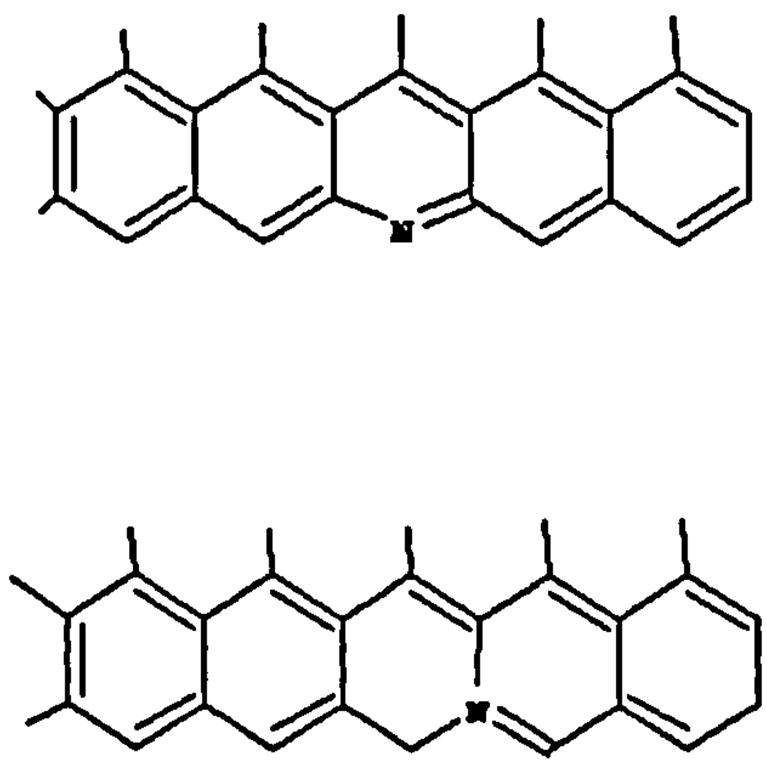

Figure 3.8.

Treatment with hydrogen cyanide or cyanogen at elevated temperature gave rise to similar products, but without gasification. The surface complex may be a simple nitrile[122]. Water adsorption measurements indicate ammonia

treated carbons are polar compared with control samples[123]. An XPS study of ammonia plasma treated carbon fibres[124] revealed that amine functional groups may be present.

Surface oxides adsorb ammonia at ambient temperature[eg. 2,87,125] because ammonia uptake by oxidised carbon was enhanced. Only weak sorption took place, and the ammonia could be pumped off at 100°C[87]. Ammonium salt or amide formation with carboxyl groups may have occurred[eg. 125], and the product was of reduced surface polarity compared with the oxidised sample. Imides may be formed[126], and nitrile groups were probably present after treatment of chlorinated carbon with ammonia at 300°C[125]. Others believe that surface amines are generated by treatment with ammonia[127]: further study is thought necessary[2].

3.5.2 Modification using other Nitrogen Containing Reagents

Sodium and Potassium cyanide react with chlorinated carbon, and the product is believed to be a surface nitrile[125]. The carbon was resistant to alkaline hydrolysis, and may be suitable for further modification. A study of the interaction of amines with oxidised carbon[128] indicated hydrogen bonding was important, but no evidence of chemisorption was found: in the absence of surface oxides, little reaction was observed[2,128]. A study of the interaction of dimethyl- benzylalkylammonium chloride with oxidised carbon suggested that chemisorption took place[129]. The modified product appeared more hydrophobic, although significant pore occlusion was apparent. Other vapour adsorption measurements were not reported.

3.6 Carbon Modifications using the Halogens and Halogen Compounds

3.6.1 Carbon Modifications using Chlorine and Chlorine Containing Compounds

Chlorine reacts readily with activated carbons and blacks[130,131]. Activated carbons adsorb large quantities of chlorine at ambient temperature[87,131], and outgassing (400°C[87]; 600°C[131]) does not result in complete desorption (ca. 9% weight chemisorbed[87]). Higher temperatures (ca. 200°C) result in greater fixation (ca. 18 weight)[87]. Similar amounts were fixed at 450°C[95], and optimum reaction occurs between 400-500°C[131]. High temperature reaction with activated carbon[87] yields, for example, carbon tetrachloride, tetrachloroethene[132] and hydrogen chloride[95,131]. The hydrogen originates from the carbon, and elemental analysis revealed significant decreases in hydrogen content[131]. The modified carbons were not found to be acidic in solution.

The reaction may proceed by the formation of atomic chlorine, a view substantiated by attempts to chlorinate toluene[133]. The extent of reaction also depends upon textural properties[125,133].

The complexes were chemically[87] and thermally[eg.2,134] stable. In vacuo, little chlorine could be desorbed even at 1200°C[2], whereas it could be entirely removed at 600°C in a current of ammonia or hydrogen[eg. 2,95,135]. The hydrogen exchange behaviour suggests that simple carbon-chlorine species exist[125], although addition across olefinic bonds may be important[133]. Attempts to distinguish between different surface carbon- chlorine complexes produced on carbon cloth and black[136] were unsuccessful due to interference from physisorbed chlorine, at temperatures as high as 400°C. The study also supported the exchange mechanism[eg.133]. The reaction may involve three steps: saturation of olefinic bonds, hydrogen exchange, and dehydrogenation to yield

hydrogen chloride and olefinic bonds[137]. A study of the simultaneous chemisorption of chlorine and oxygen at 400°C[138] suggested both reagents largely competed for similar active sites, although some chemisorption of oxygen took place on sites inactive toward chlorine. This implies that the carbons would "age" even if the surface chlorine complexes were hydrolytically stable. This may not be the case[132].

The complexes are chemically active, since substitution with cyanide ions is possible[125]. The chlorinating reagent is probably unimportant[139]: grinding under an atmosphere of carbon tetrachloride caused measurable chlorine chemisorption[140].

Adsorptive Properties of Chlorinated Carbons

Large (> ca. 10 weight %) quantities of adsorbed chlorine do not result in any major change in surface area[87,95]. The small decrease suggested that chemisorption took place predominantly in the mesopores[95], although α_s analysis[141] may have been revealing. After treatment with ammonia at 600°C, the nitrogen isotherm resembled closely that of the control, indicating that the chlorination process did not measurably disrupt the carbon structure. Reduced benzene adsorption, observed for chlorinated carbon fibres[139], may reflect a smaller average pore size, and a narrower pore size distribution however[142].

In general, increased water sorption at low partial pressures, and a small reduction at high relative pressures, is observed[123,127,134,143]. The effect of chlorination was compared with oxidation[123], suggesting that the number of primary adsorption centres[144] formed using chlorine was less. A small increase in the immersional heat was observed[127], although it was believed too small to indicate that chemisorption of water was occurring at the modified adsorption centres. Others[143] believe specific interactions lead to enhancement in adsorption at low relative pressures, since the immersion heat almost doubled

after chlorination: strongly physisorbed chlorine may be at least partly responsible.

3.6.2 Carbon Modifications using Bromine and Bromine Containing Compounds

Treatment of activated carbon and black with bromine vapour[145], formed a carbon-bromine complex. A temperature dependence on bromine fixation was observed, with a maxima at ca. 500°C. Hydrogen bromide was eliminated, indicating substitution of surface carbon- hydrogen bonds. Addition across olefinic bonds may also be important. The bromine complex was less stable than the chlorine analogue, although high temperature evacuation did not result in complete elimination[146,147]. Considerable bromine could be removed by pumping: similar effects were observed when hydrogen bromide was used.

Modification by exposure of activated carbon to bromine vapour at room temperature has also been studied[148,149]: no mass loss was observed at 100°C, which appears inconsistent with the observation that the bulk of the bromine could be removed either by gentle warming or pumping[150].

Bromination of graphitised carbon fibre did not improve oxidation resistance[151-153]. Intercalation was believed to cause structural damage and promote the rate of oxidation.

Vinyl bromide and similar reagents may react at olefinic centres on the carbon to yield useful adducts for further modification[154]. This was demonstrated for chlorine containing reagents.

Adsorptive Properties of Brominated Carbons

Nitrogen adsorption[148] indicates that little reduction in pore volume occurs, even at high bromine loadings (ca. 40 weight %). This surprising observation was rationalised on the basis that the adsorbed bromine coated, but did not fill, the micropores.

Water vapour adsorption was enhanced at all relative pressures[155], and it was proposed that one molecule of water was adsorbed at each surface bromine complex. The heat of immersion in water was also significantly greater. Activated carbon, prepared by reaction with bromine water[156] was of reduced porosity and enhanced surface polarity.

The relative ease with which bromine may be substituted by other reagents suggests that these materials may be amenable to further modifications.

3.6.3 Carbon Modifications using Iodine

At low temperatures iodine adsorption may be fully reversible and has been used as a technique for determining the surface area of carbon blacks[157]. At ca. 300°C chemisorption takes place[2]. Hydrogen exchange was also observed. Iodine treatment of carbon fibres at 100°C resulted in fixation of as much as 60 weight %[139], although all of this could be removed by alkali treatment and solvent extraction. The adsorbed iodine decreased benzene adsorption, suggesting that pore occlusion was significant. The utility of iodine modified carbon as a precursor for further modification has not been established: chlorinated or brominated derivatives may be more useful.

3.6.4 Carbon Modifications using Fluorine and Fluorine Compounds

Direct fluorination is in principle a promising approach, because fluorinated surfaces are hydrophobic and relatively inert. At -78°C fluorine is reversibly physically adsorbed[158]. Chemical reaction proceeds above this temperature.

Early studies involved reaction of activated carbons and blacks with molecular fluorine[159], often at elevated temperatures[160] and explosively, although smooth reaction between fluorine and activated carbon or graphite was observed below 300°C, when sufficient fluorine could be sorbed such that the activated carbon granules turned white or grey[161,162]. This colouration was believed to be graphite fluoride, "CF".

Higher reaction temperatures (ca. 400°C) proceeded explosively, with the formation of low molecular weight fluorocarbons. At ca. 700°C, the reaction once again proceeded smoothly.

Low temperature products were acidic in solution, and liberated iodine from potassium iodide solution. High temperature products were not found to be acidic.

Others[163] believe that graphite fluoride is formed at room temperature, as evidenced by the presence of white filaments at the surface. These could be seen with the aid of an optical microscope. No fluorocarbons were detected under these conditions.

Attempts have been made[164] to optimise the reaction, such that only surface modification results. 25°C was the optimum temperature, although outgassing at 150°C to remove hydrogen fluoride generated during reaction was necessary, indicating a hydrogen exchange mechanism.

Activated carbons and blacks fluorinated at ambient temperature were oxidising in solution[165]. The eventual loss of oxidising power may be due to desorption of weakly bound "F"[166]. No evidence for the formation of intercalation compounds was found, however[158]. Graphite fluoride was only formed at high temperatures, and the process almost always resulted in carbon gasification[161,164,167,168].

Graphite[169] formed moisture sensitive intercalation compounds, and hydrogen fluoride enhanced the rate of intercalation, yielding more complex products[170]. Fluorinated graphite exhibited low heats of wetting in water, and was of a lower surface energy compared with teflon® or graphon[171].

Adsorptive Properties of Fluorinated Carbons

A progressive decrease in nitrogen BET surface area took place as the amount of fixed fluorine increased[163], and the products were vacuum stable. Benzene adsorption was also sequentially reduced[164,172].

Water adsorption indicated that the carbons were of reduced surface polarity, and of lower porosity[164,172]. The carbons[158] were unstable in humid air, although this was not observed in all cases[164,172]. One group[168] believe that such carbons may be useful in vapour adsorption applications.

3.6.5 Carbon Modifications using Fluorine Containing Compounds

Less attention has been given to the use of fluorine compounds. Graphite[173] or diamond[174], modified using atomic fluorine generated by microwave discharge, contained surface fluorides: CF, CF_2 and CF_3 groups were identified using XPS. The products decomposed at ca. 800°C, suggesting

that strong carbon- fluorine bonds were present: no measurement of the adsorptive properties were made.

PTFE deposition by spraying has been studied[175]. It was proposed that the particulate PTFE blocked a proportion of the macropores. A similar process has been patented in the UK[176] as a means of producing hydrophobic carbons for vapour adsorption applications. It is not anticipated that such adsorbents would be particularly efficient.

A more selective approach has been attempted[177], whereby active carbon was modified with tetrafluoroethene, to produce adsorbents containing 9-34 weight % of the modifier. An inverse relationship between fluorine content and the decrease in pore volume due to blocking effects was found, and the products were of reduced surface polarity. Gas chromatography revealed that the adsorbents were water repellant.

3.7 Miscellaneous Techniques

Activated carbon has been modified using phosphorous trichloride at 700-800°C[123]. The nature of the surface functional groups formed is unclear. Treatment resulted in little change to the water adsorption properties at low partial pressures, but resulted in burn off, and significant pore blocking/ narrowing effects.

Carbons have been modified using hydrocarbons at elevated temperature[178], or at ambient temperatures using plasma techniques[eg.179]: an adequate analysis of the adsorptive properties has not been undertaken, however. The pyrolysis of propylene over carbon black suggested that carbon deposition took place initially on active surface sites[178]. Thereafter, a unsaturated (probably polymeric) deposit was formed. For activated carbon, significant pore narrowing and blocking effects would probably result.

The reaction between surface oxides on activated carbon and silating reagents has received minor consideration, but would appear selective[180,181]. Carbons modified using trimethylchlorosilane vapour at 200°C were more hydrophobic compared to control samples[180,181]. The products were thermally stable, and the quantity of water adsorbed at low partial pressures was reduced.

Application of Techniques Applied During Modification of Non-Carbonaceous Surfaces

Aluminas may be modified using fluorinating reagents such as ammonium fluoride[182] and trichlorofluoromethane[183] at 400-500°C. In these examples, only fluorine is present at the surface after treatment. Silicas may also be fluorinated, although the use of reagents such as carbon tetrafluoride, sulphur tetrafluoride, nitrogen trifluoride, and chlorofluorocarbons have been more successful[184]. The modified surfaces were hydrophobic, and the optimum reagent was trichlorofluoromethane: sulphur tetrafluoride and carbon tetrafluoride required high reaction temperatures (ca. 1500°C).

Hexafluoropropene has also been used to fluorinate silicas[185], and zeolites have successfully been fluorinated using trichlorofluoromethane[186,187]. Modification with disilane yielded products which were shown to possess a degree of shape selectivity[188,189].

The modification of composite adsorbents, such as those derived from silicon carbide[190], may offer interesting future possibilities.

It is apparent that the majority of research into the preparation and properties of chemically modified carbons has not, to date, included an adequate consideration of the vapour adsorption properties of the products, nor of the stability of the modified adsorbents in humid air. It is also clear that the practical applications of such carbons has received little attention in recent years.

REFERENCES

1] Barton, S.S., Gillespie, D., Harrison, B.H., Carbon 11 1973 649.

2] Puri, B.R., Surface Complexes on Carbon, Chemistry and Physics of Carbon, Marcel Dekker, 6 1970 191.

3] Boehm, H.P., Chemical Identification of Surface Groups, in Advances in Catalysis, D.D Eley, H. Pines, and P.B. Weisz (Eds.), 16 1966 179.

4] Kiselev, A.V., Kovaleva, N.V., Korolev, A.Y., Kolloidnyl Zhurnal 23 1961 485.

5] Puri, B.R., Singh, D.D., Sharma, C.R., J. Phys. Chem. 62 1958 756.

6] Bansal, R.C., Donnet, J-B, Stoeckli, H. F. Active Carbon, Marcel Dekker, New York, 1988.

7] Argawal, R.K., Noh, J.S., Schwarz, J.A., Davini, P., Carbon 25 1987 219.

8] Donnet, J-B., Carbon 6 1968 161.

9] Zarif'yants, Yu. A., Kiselev, V.F., Lezhnel, N.N., Novikova, I.S., Fedorov, G.G., Dokl. Akad. Nauk. SSSR 143 1962 1358.

10] Boehm, H.P., Heck, W., Sappok, R., Agnew. Chem. Int. Edit. 3 1964.

11] Anderson, R.B. and Emmett, P.H., Symposium on Adsorption of Gases. 110th meeting of the American Chemical Society, Illinois, September 1946 1308.

12] Barton, S.S., and Harrison, B.H., Carbon 10 1972 245.

13] Barton, S.S. and Harrison, B.H., Dollimore, J., J. Phys. Chem. 82 1978 290.

14] Barton, S.S. and Harrison, B.H., Carbon 13 1975 87.

15] Tremblay, G., Vastola, F.J., Walker P.L. Jr., Carbon 16 1978 35.

16] Dollimore, J., Freedman, C.M., Harrison, B.H., Quinn, D.F., Carbon 8 1970 587.

17] Laine, N.R., Vastola, F.J., Walker, P.L. Jr., J. Phys. Chem. 67 1963 2030.

18] Nelson Smith, R., Quarterly Reviews 13 1959 287.

19] Caltharp, M.T., Hackerman, N., J. Phys. Chem. 72 1968 1171.

20] Billinge, B.H.M., Evans, M.G., J. Chim. Phys. 81 1984 779.

21] Matsumoto, S. and Sekata, N., Carbon 17 1979 303.

22] Anderson, R.B. and Emmett, P.H., J. Am. Chem. Soc. 52, 1952 753.

23] Philips, R., Vastola, F.J., Walker, P.L. Jr., Carbon 8 1970 197-210.

24] Everett, D.H. and Ward, R.J, J. Chem. Soc. Farad. Trans. 1 82 1986 2915.

25] Sing, K.S.W., eg. Carbon 25 1987 155.

26] Garten, V.A. and Weiss, D.E., Proc. third Biennial Conf. Carbon, Pergamon Press, New York, 1957 295.

27] Studebaker, M.L., Proc. fifth Conf. Carbon, Penn State, 1961 vol 2, Pergamon Press, New York 1963 189.

28] Boehm, H.P., Diehl, E., Heck, W., Sappok, R., Agnew. Chem. 3 1964 669.

29] Vastola, F.J., and Walker, P.L. Jr., J. Chim. Phys. 58 1961 20.

30] Laine, N.R., Vastola, F.J., Walker, P.L. Jr., Proc. fifth Conf. Carbon, Penn State, 1961 vol 2, Pergamon Press, New York 1963 211.

31] Barton, S.S., Gillespie, D.J., Harrison, B.H., Kemp, W., Carbon 16 1978 363.

32] Studebaker, M.L., Hoffman, E.W.D., Wolfe, A.C., Nabors, L.G., Ind. Eng. Chem. 48 1956 162.

33] Hoffman, U. and Ohlerich, G., Agnew. Chem. 16 1963 62.

34] Studebaker, M.L. and Rinehart, R.W., Rubber Chem. Technol. 45 1972 106.

35] Zawadzki, J., Carbon 18 1980 281.

36] Zawadzki, J., Carbon 16 1978 491.

37] Plaskin, I.N. and Alekseev, V.S., Chem. Abstr.59 2194 (1963)

38] Kavan, L., Dousek, F.P., Kubelkova, L., Carbon 24 1986.

39] Ishizaki, C. and Marti, I., Carbon 19 1981 409.

40] Sellitti, C., Koenig, J.L., Ishida, H., Carbon 28 1990.

41] Monterra, C. and Low, M.J.D., Spec. Lett. 15 1982 9.

42] Evans, J.F. and Kuwana, T., Anal. Chem. 49 1977 11.

43] Schlogl, R., Proc. Int. Conf. Carbon (Carbon 90) Paris, France, 1990 542. GFEC Paris.

44] Marchon, B., Carrazza, J., Heinemann, H., Somorjai, G.A., Carbon 26 1988 507.

45] Smith, R.W. and Schaeffer, W.D., Rubber Chem. and Technol. 23 1950 625.

46] Garten, V.A. and Weiss, D.E., Aust. J. Chem. 10 1957 309.

47] Brown, J.G., Dollimore, J., Freedman, C.M., Harrison, B.H., Thermochimica Acta 1 1970 449.

48] Streznewski, J., Turkevich, J., Proc. third Biennial Conf. Carbon, Pergamon Press, New York 1957 273.

49] Snow, C.W., Wallace, D.R., Lyon, L.L., Crocker, G.R., Proc. third Biennial Conf. Carbon, Pergamon Press, NY, 1957 279.

50] Van Driel, J., in Activated Carbon, a Fascinating Material, Norit (pub.), 1983 40.

51] Philips, R., Vastola, F.J., Walker, P.L. Jr., Carbon 8 1970 205.

52] Ahmed, S. and Back, M.H., Carbon 23 1985 513.

53] Cheng, P. and Harriot, P., Carbon 24 1986 143.

54] Leroy, J., Bastick, M., Bastick, J., Proc. Int. Conf. Carbon (Carbon 90), Paris, France 1990 574. GFEC Paris.

55] Laine, N.R., Vastola, F.J., Walker, P.L. Jr., J. Phys. Chem. 67 1963 2030.

56] Huttinger, K.J., Proc. Int. Conf. Carbon (Carbon 90), Paris France 1990 536. GFEC Paris.

57] Lizzio, A.A., Jiang, H., Radovic, L.R., Carbon 28 1990.

58] Monterra, C. and Low, M.J.D., Carbon 23 1985 301-335.

59] Shah, M.S., J. Chem. Soc. 1929 2676.

60] Strickland-Constable, R.F., Trans. Faraday Soc. 34 1938.

61] Madley, G.G. and Strickland-Constable, R.F., Trans. Faraday Soc. 49 1953.

62] Smith, R.N., Swinehart, J., Lesnini, D., J. Phys. Chem. 60 1956 1063; 63 1959 544.

63] Bedjai, G., Orbach, H.K., Riesenfeld, F.C., Ind. and Eng. Chem. 50 1958 8.

64] Richter, E., Kleinschmidt, R., Pilarczyk, E., Knoblauch, K., Jontgen, H., Thermochim. Acta. 85 1985 311.

65] Smith, R.N., Pierce, G, Joel, C.D., J. Phys. Chem. 58 1954 298.

66] Mc.Dermot, H.L. and Arnell, J.C., J. Phys. Chem. 58 1954 492.

67] Pierce, G. and Smith, R.N., J. Phys. Colloid Chem. 54 1950 784.

68] Studebaker, M.L., Rubber Chem. Technol. 30 1957 1400.
Studebaker, M.L., Proc. Third Biennial Conf. Carbon, Pergamon Press, New York 1957 289.

69] Singh, D.D., Parkash, S., Puri, B.R., Chem. and Ind. 18 1959.

70] Sappok, R. and Boehm, H.P., Carbon 6 1968 283.

71] Collins, R.D., Hillary, J.J., Taylor, L.R., Abbey, F., Int. Symp. on Management of Gaseous Wastes from Nuclear Facilities, Vienna, 1980.

72] Adams, L.B., Unpublished Data, CDE Porton Down.

73] Ogata, Y., Matsumura, Y., Takahashi, H., J. Colloid and Polym. Sci. 11 1979 257.

74] Karpinski, K. and Willmann, G., Chem. Stosow 21 1977 2.

75] Jankouska, H. and Swiatowski, A., Oscik, J., Kusak, R., Carbon 21 1983 117.

76] Puri, B.R., Singh, S., Mahajan, O.P., J. Ind. Chem. Soc. Int. News Ed. 13 1950.

77] Youssef, A.M., Ghazy, T.M., El-Nabarawy, Th., Carbon 20 1982 113.

78] Hippo, E.J., Murdie, N., Hyjazie, A., Carbon 27 1989 689.

79] Product Data Sheets, Chemviron Carbon, Brussels, Belgium.

80] Walker, P.L. Jr., Cariaso, O.C., Ismail, I.M.K., Carbon 18 1980 375.

81] Billinge, B.H.M., Docherty, J.B., Bevan, M.J., Carbon 22 1984 83.

82] Munoz-Guillena, J., Illan-Gomez, J., Martin-Martinez, J.M., Linares-Solano, A., Salinas-Martinez de Lecea, C., Proc. Int. Conf. Carbon (Carbon 90) Paris, France, 1990 4. GFEC Paris.

83] Cazorla-Amoros, D., Linares-Solano, A., Salinas-Martinez de Lecea, C., Joly, J.P., Proc. Int. Conf. Carbon (Carbon 90) Paris, France, 1990 36. GFEC Paris.

84] Lamontagne, R.A., Isaacson, L., Matuszko, R.A., Proc. Third Int. Symp. Protection Against Chemical Warfare Agents, Umea, Sweden, 11-16 June 1989 247.

85] Gao, S., Yamabe, K., Takahashi, H., Saito, Y., Tanso 119 1984 207.

86] Smith, R.N., Duffield, J., Pierotti, R.A., Mooi, J., J. Phys. Chem. 60 1956 495.

87] Emmett, P.H., Chem. Rev. 43 1948 69.

88] Puri, B.R., Kumar, B., Singh, D.D., J. Sci. Ind. Res. 200 1961 366.

89] Papirer, E. and Guyon, E., Carbon 16 1978 127.

90] Bastick, M., Dupuper, G., Morlot, M., Perrot, J.M., Weber, J., Carbon 15 1977 25.

91] Meldrum, B. and Rochester, C.H., J. Chem. Soc. Farad. Trans. 1 86 1990 1881.

92] Strashko, B.K., Kuzin, I.A., Loskutov, A.I., Zh. Prikl. Khim. 39 1966 2018.

93] DQA/TS Chorley, Laboratory Report No. 750, January 1990.

94] Wilbaut, J.P. and La Bastide, G., Rec. Trav. Chim. Pays-Bas 43 1924 731.

95] Boehm, H.P., Tereczki, B., Schanz, K., in J. Rouquerol and K.S.W. Sing (Eds.) Adsorption at the Gas-Solid and Liquid-Solid Interface, Studies in Surface Science and Catalysis, Elsevier, Amsterdam, 1982 395.

96] Wilbaut, J.P., J. Appl. Chem. 40 1927 1136.

97] Mixter, W.G., Amer. J. Sci. 45 1893 363.

98] Puri, B.R. and Hazra, R.S., Carbon 9 1971 123.

99] Studebaker, M.L. and Nabors, L.G., Rubber Age 80 1957 661.

100] Loskutov, A.I. and Khlopotov, M.N., Adsorbenty 9 1981 86.

101] Hofmann, U. and Ohlerich, G., Agnew. Chem. 62 1950 16.

102] Wilbaut, J.P. and Van der Kam, E.J., Rec. Trav. Chim.,49 1930 121.

103] Puri, B.R., Kaistha, B.C., Hazra, R.S., J. Ind. Chem. Soc. 45 1968 1001.

104] Juza, R. and Blanke, W., Z. Anorg. Allgem. Chem. 210 1933 81.

105] Chang, C.H., Carbon 19 1981 175.

106] Blayden, H.E. and Patrick, J.W., Carbon 5 1967 533.

107] Sykes, K.W. and White, P., Trans. Farad. Soc. 1 52 1956 660.

108] Bansal, R.C., Proc. Int. Conf. Carbon (Carbon 90), Paris, France, 1990 22. GFEC Paris.

109] Owen, A.J., Sykes, K.W., Thomas, D.J.D., White, P., Trans. Farad. Soc. 1 49 1953 1198.

110] Puri, B.R., Jain, C.M., Hazra, R.S., J. Ind. Chem. Soc. 43 1966 67.

111] Loskutov, A.I. and Khlopotov, M.N., Adsorbenty 10 1982 28.

112] Stacy, W.O., Vastola, F.J., Walker Jnr., P.L., Carbon 6 1968 917.

113] Loskutov, A.I. and Khlopotov, M.N., Adsorbenty 10 1982 14.

114] Chang, C.H., Savage, D.W., Longo, J.M., J. Colloid and Int. Sci. 79 1981 178.

115] Davini, P., Fuel 68 1989 145.

116] Ricci, M., Trinquecoste, M., Garrigou-Lagrange, C., Amiell, J., Clin, B., Delhaes, P., Proc. Int. Conf. Carbon (Carbon 90), Paris, France 1990 584. GFEC Paris.

117] Hollahan, J.R., Stafford, B.B., Falb, R.D., Payne, S.T., J. Appl. Polym. Sci. 13 1969 807.

118] Tither, D., Matthews, A., Fitzgerald, A.G., Storey, B.E., Henderson, A.E., Moir, P.A., Dines, T.J., Bower, D.I., Lewis, E.L.V., Doughty, G., Foster, W., Carbon 27 1989 899.

119] Karpinsli, K. and Wojcik, G., Chem. Stosow. 24 1980 141.

120] Boehm, H.P., Clauss, A., Hofmann, U., Proc. third Biennial Conf. Carbon, Pergamon Press, Oxford, England 1962 Vol. 1, 16.

121] Boehm, H.P., Mair, G., Stoehr, T., de Rincon, A., Tereczki, B., Fuel 63 1984 1061.

122] Wilbaut, J., Proc. Third Int. Conf. on Bituminous Coal, 1932 657.

123] Kuzin, I.A., Loskutov, A.I., Palfitov, V.F., Koemets, L.A., Zh. Prikl. Khim 45 1972 760.

124] Jones, C. and Sammann, E., Carbon 28 1990 509.

125] Boehm, H.P., Hofmann, U., Claus, A., Proc. third Biennial Conf. Carbon, Pergamon Press, Oxford, England 1962 241.

126] Zawadski, J., Carbon 19 1981 19.

127] Puri, B.R. and Bansal, R.C., J. Ind. Chem. Soc. 5 1967 566.

128] Anderson, R.B. and Emmett, P.H., J. Phys. Chem. 56 1952 756.

129] Dushchenko, V.P., Kravtsov, A.N., Kulandina, A.N., Issled. Po. Molekulyar. Fiz. i Fiz. Tverdogo Tela. 1976 114-118.

130] Kloepfer, H., Patent (German) 1953. 893 241.

131] Puri, B.R., Malhotra, S.L., Bansal, R.C., J. Ind. Chem. Soc. 40 1963 179.

132] Nikitina, O.V., Kiselev, V.F., Lejnev, N.N., Carbon 8 1970 402.

133] Puri, B.R. and Bansal, R.C., Ind. J. Chem. 5 1967 381.

134] Puri, B.R. and Bansal, R.C., Carbon 5 1967 189.

135] Reyerson, L.H. and Wishart, A.W., J. Phys. Chem. 42 1938 679.

136] Tobias, H. and Soffer, A., Carbon 23 1985 291.

137] Tobias, H. and Soffer, A., Carbon 23 1985 281.

138] Puri, B.R. and Sandle, N.K., Ind. J. Chem. 6 1968 267.

139] Morozov, A.A., Ermolenko, I.N., Fedorov, A.A., Vesti. Akad. Navuk. B. SSR Ser. Khim. Navuk. Cone. VBSKA. 76 1976 16.

140] Boehm, H.P., in Structure and Reactivity of Surfaces, C. Monterra, A. Zecchina and G. Costa (Eds.), Elsevier, Amsterdam, 1989 145.

141] Sing, K.S.W., in D.H. Everett and R.H. Ottewill (Eds.), Surface Area Determination, Butterworths, London, 1970 25.

142] Dribinskii, A.V. and Shteinberg, A.V., Elektrochimiya 21 1985 1182 (CA: 103:201389).

143] Barton, S.S., Evans, M.J.B., Koresh, J.E., Tobias, H., Carbon 25 1987 663.

144] Dubinin, M.M., Zaverina, E.D., Serpinsky, V.V., J. Chem. Soc. 1955 1760.

145] Puri, B.R. and Sehgal, K.C., Ind. J. Chem. 4 1966 206.

146] Puri, B.R., and Sehgal, K.C., Ind. J. Chem. 5 1967 379.

147] Puri, B.R., Mahajan, O.P., Singh, D.D., J. Ind. Chem. Soc. 38 1961 943.

148] Baksh, M.S.A., Yang, R.T., Chung, D.D.L., Carbon 27 1989 931.

149] Ho, C.T. and Chung, D.D.L., Carbon 28 1990 815.

150] Hooley, J.G. and Dietz, V.R., Carbon 16 1978 251.

151] Zubkova, Yu.N. and Lopanov, A.N., Soviet Progr. Chem. 46 1980 23.

152] Chiou, J.M., Ho, C.T., Chung, D.D.L., Carbon 27 1988 227.

153] Ho, C.T. and Chung, D.D.L., Carbon 27 1989 603.

154] Mazur, S., Matusinovic, T., Cammann, K., J. Am. Chem. Soc. 99 1977 3888.

155] Puri, B.R. and Bansal, R.C., Carbon 3 1966 533.

156] Puri, B.R., Sandle, N.K., Mahajan, O.P., J. Chem. Soc. 1963 4880.

157] Puri, B.R. and Bansal, R.C., Carbon 3 1965 227.

158] Watanabe, N., Nakajima, T., Touhara, H., Graphite Fluorides, Elsevier, Amsterdam, 1988.

159] Ruff, Von O. and Keim. R., Z. Anorg. U. Allgem. Chemie. 1930 192.

160] Simons, J.H. and Block, L.P., J. Am. Chem. Soc. 61 1939 2962.

161] Ruff, Von O. and Bretschneider, O., Z. Anorg. U. Allgem. Chemie. 1934 217.

162] Flalkov, A.S., Polyakova, N.V., Yurkovskiy, N.M., Sevast'yanova, Na., Zaychikov, S.G., 5th All Union Symp. on the Chemistry of Inorganic Fluorides, Dnepropetrovsk, 27-30 June 1978. Moscow Nauka 1978 103.

163] Bernard, M.C., Hardy, A., Hobbes, P., Lucas, R., Roux, M., Bull. Soc. Chim. France 6 1972 2192.

164] Fedotov, V.A. and Loskutov, I.A., Akad. Sci. USSR, J. App. Chem., Leningrad, 1984. UDK 661.183:546.162.

165] Watanabe, N., Kawaguchi, T., Kita, Y., Nippon Kagaku Kaishi, J. Chem. Soc. Jpn., Chem. and Ind. Chem. 8 1978.

166] Dubinin, M.M., in Chemistry and Physics of Carbon, Volume 2, New York, 1966 51-120.

167] Serushkin, I.L. and Kutsenok, Yu. B., 4th All Union Symp. on the Chemistry of Inorganic Fluorides, Dushanbe, 27-30 September, 1975. Moscow Nauka 1975 177.

168] Loskutov, A.I. and Fedotov, V.A., Interactions in the Carbon-Fluorine System. Deposited Document, Available SPSTL 1981.

169] Nakajima, T., Ino, T., Watanabe, N., Carbon 26 1988.

170] Takashima, M., Watanabe, N., Nippon Kagaku Kaishi, J. Chem. Soc. Jpn., Chem. and Ind. Chem. 6 1976.

171] Watanabe, N., Takenaka, H., Kimura, S., Nippon Kagaku Kaishi., J. Chem. Soc. Jpn., Chem. and Ind. Chem. 1975 10.

172] Horita, K., Hashimoto, Y., Watanabe, N., Nippon Kagaku Kaishi, J. Chem. Soc. Jpn., Chem. and Ind. Chem. 1979 9.

173] Cadman, P., Scott, J.D., Thomas, J.M., Carbon 15 1977 75.

174] Cadman, P., Scott, J.D., Thomas, J.M., J. Chem. Soc., Chem. Comm. 1975 654.

175] Goto, S. and Morita, M., Chem. Eng. Comm. 60 1987 253.

176] Maggs, F.A.P., GB Patent 2,137,608 1985. CA:102:48187.

177] Loskutov, A.I., Bityugov, A.Yu., Palfitov, V.F., Zh. Prikl. Khim., Leningrad 51 1978 2485.

178] Hoffman, W.P., Vastola, F.J., Walker, P.L. Jnr., Carbon 26 1988 485.

179] Proc. Int. Conf. Carbon (Carbon 90), Paris, France 1990 584. GFEC Paris.

180] Wojcik, G. and Karpinski, K., Chem. Stosow. 22 1978 351.

181] Karpinski, K. and Wojcik, G., Chem. Stosow. 24 1980 141.

182] Matulewicz, E.R.A., Kerkhof, F.P.J.M., Moulijn, J.A., Reitsma, H.J., J. Colloid and Int. Sci. 77 1980 110.

183] Kurosaki, A. and Okazaki, S., Chem. Lett. 1983 1741.

184] Okazaki, A. and Kurosaki, A., Bull. Chem. Soc. Jpn. 60 1987 2833.

185] Dahl, I.M., Ellestad, O.H., Karlsen, B., Appl. Surface Sci., 28 1987 302.

186] Okazaki, S. and Jouhouji, H., Bull. Chem. Soc. Jpn. 59 1986 1931.

187] Kowalak, S., J. Chem. Soc., Farad. Trans. 1 84 1988 2035.

188] Yan, Y., Verbiest, J., De Hulsters, P., Vansant, E.F., J. Chem. Soc., Farad. Trans. 1 85 1989 3087.

189] Yan, Y., Verbiest, J., De Hulsters, P., Vansant, E.F., J. Chem. Soc., Farad. Trans. 1 85 10 1989 3095.

190] Fedorov, N.F., Ivakhnyuk, G.K., Tetenov, V.V., Matyukhin, G.V., Zh. Prikl. Khim. 54 1981 1464.

CHAPTER 4

The Vapour Adsorption Properties of Activated Carbon

Many vapour filtration processes utilise activated carbon as the adsorbent. The efficiency with which impurities are removed from an airstream such that their concentration in the filter effluent is of a safe or desired value (the filter performance) is dependent upon a number of factors. These include the structure (porosity) of the adsorbent, the nature of any functional groups present at the surface, the temperature, and the properties of any competing adsorbates.

Often, the impurity is present in low concentration, in air containing a high concentration of water vapour, and although pure carbon surfaces are hydrophobic, activated carbon will adsorb moisture as a result of the presence of surface impurities/defects, and the pore structure (chapter 2).

In this chapter, the influence of surface oxygen containing functional groups (surface oxides) on the adsorption of water and chemical vapours by activated carbon are considered. The vapour adsorption properties of control and oxidised carbon in the presence of water vapour are also reviewed.

4.0 Water Vapour Adsorption Properties of Oxidised Activated Carbon

Activated carbon will react with a range of oxidants (chapter 3), the more important of which in the context of this present research is moist air.

Figure 4.1 shows typical water adsorption desorption isotherms measured for a sample of control BPL carbon (Chemviron, Brussels, Belgium), and BPL carbon which had been aged (oxidised) in humid air for approximately 900 days[1]. The isotherms were measured gravimetrically using a quartz spring balance of

the McBain-Bakr type[2]. Such results could, however, be obtained equally well gravimetrically using an airflow of controlled temperature and relative humidity (RH) (Appendix). This system could be used for p/p^0 values up to a maximum of 0.95.

When surface oxides are present on the carbon, water adsorption is enhanced at low pressures (figure 4.1;[1,3-9]). This promotes pore filling. The adsorption capacity of the carbon at saturation is largely unchanged, unless oxidation has resulted in pore modification[8,9].

The theory of "island formation" on active sites accounts most adequately for the observed effects[10-14] (chapter 2). Indeed, calculations indicate[8,15] that the concentration of primary adsorption sites (the sites on the carbon surface at which water adsorption initially takes place) controls both adsorption at low relative pressure, and the position of the steep rise in the isotherm (the underlying porosity of the carbon will also influence, to some extent, the steep rise in the isotherm). These sites become less important at higher relative pressures (ca. >0.8 p/p^0), where adsorption is limited by the volume of the micropores, and adsorbate-adsorbate interactions. That the isotherms should cross (figure 4.1;[8]) is due to the relationship between the pore width and the concentration of primary adsorption centres which determine which pores fill at a particular relative pressure. Others, using a static adsorption technique and the same carbon (BPL) have not found the isotherms to cross[15].

This behaviour upon oxidation is exhibited by other carbon forms, including carbon black[16].

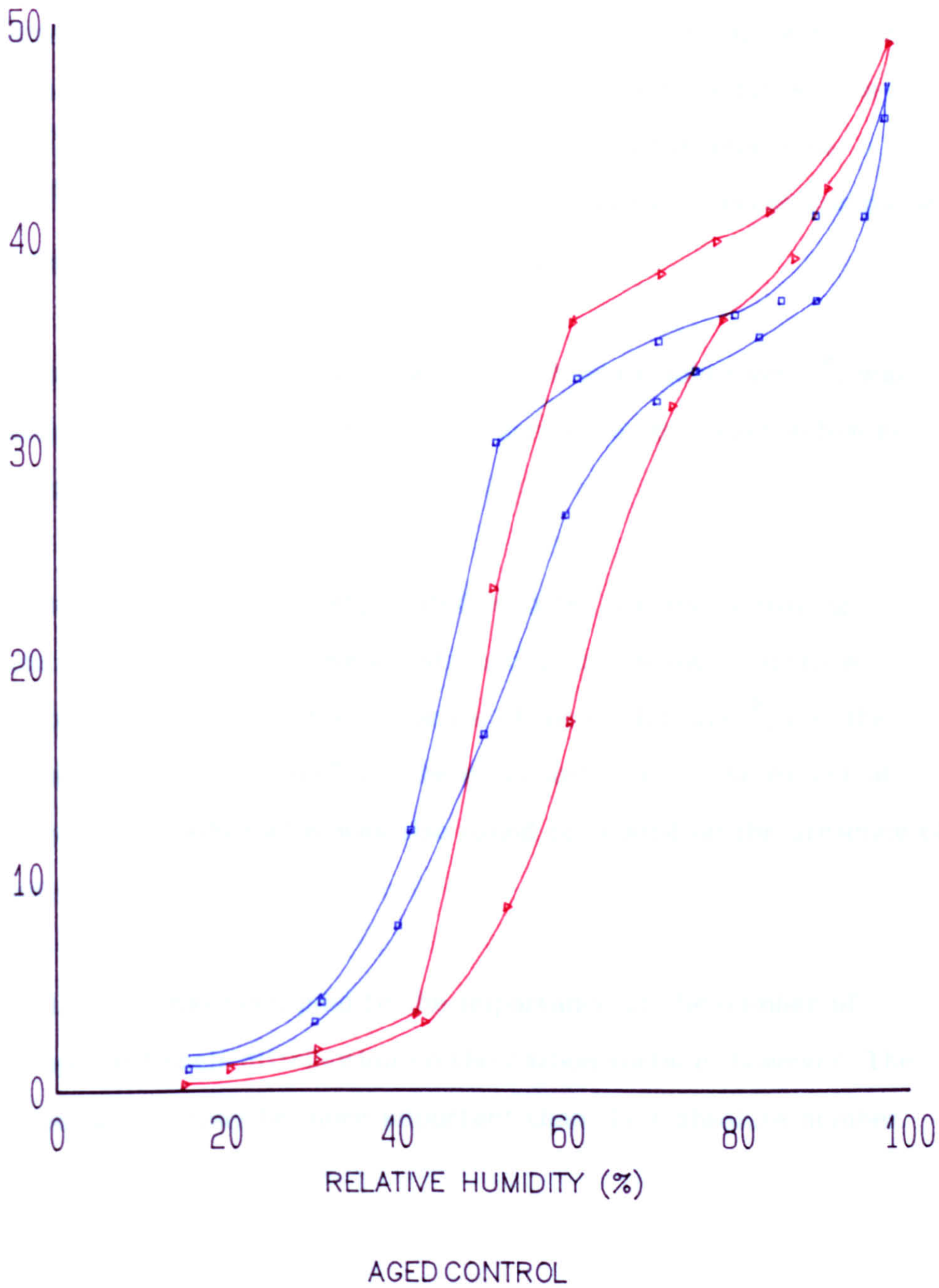
WATER ISOTHERMS FOR BPL CARBON
AMOUNT ADSORBED (w/w %)
0
10
20
30
40
50
0
20
40
60
80
100
RELATIVE HUMIDITY (%)
AGED CONTROL

FIGURE 4.1.

4.1 Vapour Adsorption Properties of Oxidised Activated Carbon (in the Absence of Water Vapour)

At low relative pressures, and in comparison with un oxidised (control) carbons, oxidised carbons adsorb a greater quantity of a polar vapour such as methanol, from an airstream[17-19]. Classical measurement techniques (quartz spring balance[2]) using simple alcohols also indicated an enhancement in adsorption (p/p^0= 0->1)[7,20], although the influence of surface oxygen complexes was believed less important at high relative pressures[21,22].

The adsorption of a non polar adsorbate, such as cyclohexane[3,18], was not significantly influenced by the presence of surface oxides: carbon blacks behaved in a similar manner[23].

Such observations may be complicated by other processes: hydrogen adsorption was enhanced in the presence of acidic, but not basic, surface oxides[24] (chapter 3). In addition, the influence of molecular size[18], and the formation of adsorbate "complexes" may be of importance[25]. The extent of phenol[26] and pyridine[27] adsorption was also found to depend on the presence of surface oxides.

Little attention has been paid to the importance of the number of functional groups, and their distribution on the carbon surface, however. The location of these groups may be more important than their absolute number.

4.1.1 The Behaviour of Oxidised Carbons in Solution

Some similarities exists between the properties of oxidised carbons in vapour and solution applications.

Oxidised carbon black adsorbs polar organic compounds preferentially from solution[28]. The degree of selectivity of simple alcohol adsorption reduced with increasing molecular weight, suggesting that specific dipole-dipole interactions with surface oxides were significant. Specific interactions were also believed to be responsible for the behaviour of benzene[28-30], water[31], and methanol[31]. Oxidised samples outgassed at elevated temperature subsequently behaved in a similar manner to unoxidised carbon[32] because the complexes decomposed to yield carbon oxides. It was unclear, however, from what complex the adsorption phenomenon originated[33-35].

Oxidised activated carbons exhibited similar properties, but attempts to determine the location of the oxygen containing complexes within the pore structure were unsuccessful[36,37]. Ethanol or methanol adsorption from benzene increased with the carbon oxygen content, demonstrating a relationship between selectivity and surface oxide concentration[38-41]. Some chemisorption on defects and unsaturated sites generated during oxidation of the carbon cannot be ruled out[36].

Measurement of heats of immersion for oxidised carbon indicated that an enhancement in adsorption occurred when the wetting liquid was polar[3,40]: no enhancement was observed when the wetting liquid was non polar, however[3,42,43].

Pre adsorbed water, and/ or airflows containing high concentrations of water vapour, can have a major impact upon the chemical vapour adsorption properties of activated carbon.

4.2 The Effect of Pre Adsorbed Water and the RH of the Air on the Vapour Adsorption Properties of Activated Carbon

In general, the performance (or vapour breakthrough time) of an activated carbon filter for removing contaminants from an airstream decreases as the relative humidity (RH), (and hence the quantity of water adsorbed by the carbon, figure 4.1) is increased[eg. 44-46]. The adsorbate is important, and performance is generally reduced as the volatility and hydrophobicity of the vapour increases[47]: molecular size and shape may be critical.

Competitive vapour adsorption will depend on the relative adsorption energies of the adsorbates (the ease with which one adsorbate may displace another from the surface[48]), and kinetic aspects. When the adsorbates are organic, the lower boiling component will normally be displaced[48]. If the carbon has been exposed to humid air, it may contain a substantial quantity of pre adsorbed water (figure 4.1): if a vapour is then to be efficiently adsorbed, some displacement of water must take place. The ease with which the water is displaced, and the efficiency of transportation from the pore structure will influence filter performance[46,49].

When the competing vapour is polar, and water miscible, adsorbed water may not result in reduced efficiency; for example, the methanol adsorption capacity of humidified filter beds was greater compared with that of dry beds[17,18]. Water vapour enhanced adsorption over the concentration range studied, indicating that the transfer coefficient of methanol (pore diffusion rate) was greater[50]. This was probably a result of methanol absorption into the sorbed water phase.

Conversely, others[47] have observed that polar vapours were less efficiently adsorbed from a humid airstream. It was found that the quantity of

moisture on the filter bed at the end of the experiment was greater; hence the reduction in the breakthrough time of the filter may be a result of coadsorption.

The carbon equilibration RH had little impact on filter performance when it was below approximately 50%[47] (probably because the quantity of water adsorbed by the carbon was small). Above ca. 65%, marked decreases in filter breakthrough time were observed. Difficulties in predicting filter behaviour were apparent when the vapour was volatile, and/or polar. Others[51] also observed reduced performance with an increasing RH, and that the polarity, and solubility, of the challenge vapour was of little consequence. Static (quartz spring balance) adsorption studies supported these observations[52].

Methyl iodide is a volatile hydrophobic vapour and is removed using activated carbon filters impregnated with potassium iodide or triethylenediamine (TEDA)[53]. Increasing the carbon equilibration RH from 50% to 90% resulted in an approximately seven fold loss of efficiency[54], the relationship between the equilibration RH and penetration time being approximately linear[54,55]. RH values below ca. 40% had little effect. At high values of the RH, it was believed that pre adsorbed water behaved as a barrier film, thus inhibiting the adsorption process. Significant differences were also observed between the behaviour of dry filters challenged in humid air, and filters which had been first pre equilibrated[56]. Adsorption by dry filter beds challenged in humid air was independent of the RH (within the experimental limits)[56,57], whereas identical filters which had first been pre equilibrated with moisture performed less well, by an extent which increased with the equilibration RH. The behaviour of dry filters challenged in humid air probably reflects the relatively slow rate with which moisture is adsorbed in comparison to organic vapours[58]. Such an observation may not be general[59], but appears true of vapours such as benzene[60] and chlorohydrocarbons[56,61] which are strongly physisorbed, and are able to displace water adsorbed during the filter challenge. Other observations support the view that filter performance is more

dependent upon the quantity of pre adsorbed water than on the RH of the airstream[49,56,62].

Water displacement was related to the concentration of the challenge vapour and, as anticipated, decreased at low vapour concentrations[48,60]. That the filter performed proportionally less well at lower vapour concentrations suggests that localised heating of the filter bed may aid the displacement of water.

Within a class of vapours the relationship between boiling point and filter breakthrough time passed through a maximum, with the highest boiling point materials being less efficiently adsorbed[47]. This may be related to the molecular size of the adsorbate, and the consequent reduction in the rate of pore diffusion.

Challenging filters at humidities close to saturation can, however, result in an almost total loss of performance[62]. If the same humidified carbon was challenged in dry air, sufficient water was displaced such that vapour adsorption proceeded to some extent[62].

In addition to the equilibration and challenge RH, textural properties of the carbon may be important[46,59,63], and carbons containing pores with constricted entrances (eg. "ink bottle pores") performed less well[46].

The adsorption process may be controlled by two rate determining steps[63]: bulk diffusional transport of the vapour, controlling the initial stages of adsorption until filter breakthrough, which occurred when the external surface area of the carbon granules were at capacity, and then micropore diffusion, which resulted in the breakthrough curve exhibiting a biphasic behaviour at high breakthrough concentrations. It was demonstrated[64] that filter efficiency could be improved by the addition of material which adsorbed the displaced water (but not the vapour).

Because high values of the RH of the challenge airstream and the presence of significant quantities of adsorbed water on the carbon generally result in a reduction in filter performance, filter testing under these conditions is often employed either to evaluate performance, or as part of a quality control regime for batch testing. Such testing normally involves the use of volatile hydrophobic vapours, because it is the adsorption these materials that is most affected by the combination of the effects described above. In many countries, Chloropicrin (PS, trichloronitromethane) is employed as the test vapour[65-67].

In addition to the effects of the RH of the air and the carbon water content, the presence of oxygen containing functional groups are also an important factor affecting the vapour adsorption properties of activated carbons in the presence of water vapour.

4.5 The Influence of Surface Oxides on the Vapour Adsorption Properties of Activated Carbon in the Presence of Water Vapour

The presence of oxygen containing functional groups on the surface of activated carbon further complicates the vapour adsorption properties: methanol adsorption by oxidised carbon was enhanced compared with unoxidised (control) samples[17,18]. Presumably, the surface oxides promote the formation of hydrogen bonded methanol- water "complexes". The adsorption of hydrophobic vapours (such as benzene[18]) from flowing airstreams was reduced at high humidity (80%), probably reflecting the difficulty with which the adsorbed water was displaced from the polar surface sites. Surface oxides affect the ease with which physisorption (and hence water displacement) takes place, and will

therefore indirectly reduce any chemical reactivity of the filter bed (that is, the extent, but probably not the rate, of reaction is affected). This was shown to be the case for perfluoroisobutene, a toxic volatile hydrophobic chemical which reacts on the carbon surface to yield harmless products[68].

The adsorption of methyl iodide by oxidised carbons was also significantly worse compared to control carbons[43,53]. The oxidation mechanism in humid air may also involve reaction with any impregnants on the carbon surface. For example, cyanogen adsorption by carbons impregnated with chromium is degraded as a result of the reduction of chromium (VI) species to chromium (III)[69,70]. Presumably the carbon support, in the presence of moisture, is reducing, although direct reaction between the impregnants and surface oxides cannot be ruled out.

Although some disagreement as to the precise influence exerted by surface oxides and/ or adsorbed water vapour on the performance of activated carbon filters persists, it is apparent that these factors can severely limit the efficiency of many air purification processes. Some effort to systematically investigate the importance of these effects (and that of the surface chemistry in general) is necessary if the behaviour of carbon filters under a range of conditions is to be understood, and, ultimately, predicted.

In the longer term, research into the preparation and properties of alternative adsorbents may, at least in part, address the problems associated with the use of activated carbon filters in humid air. One approach would involve investigating the possibilities of modifying pore shape, since it has been demonstrated that adsorbents based on Silicalite have only a small adsorptive capacity for water vapour, yet adsorb significant quantities of nitrogen[71]. This selectivity is attributed to pore shape, and the consequent unfavourable packing constraints placed upon the water molecules within the narrow (tubular) pore structure[71].

References

1] Yates, M., unpublished data, Brunel University.

2] McBain, J.W. and Bakr, A.M., J. Am. Chem. Soc. 48 1926 690.

3] Barton, S.S., Evans, M.J.B., Holland, J., Koresh, J.E., Carbon 22 1984 265.

4] Studebaker, M.L., Rubber Chem. Technol., 30 1957 1400: Studebaker, M.L., Proc. Third Biennial Conf. Carbon, Pergamon Press, New York 1957 289.

5] Karpinski, K. and Willmann, G., Chem. Stosow. 21 1977 2.

6] Puri, B.R., Murari, K., Singh, D.D., J. Phys. Chem. 65 1961 37.

7] Puri, B.R., Carbon 4 1966 391.

8] Bansal, R.C., Dhami, T.L., Parkash, S., Carbon 16 1978 389.

9] Barton, S.S. and Koresh, J.E., J. Chem. Soc. Farad. Trans. 1 79 1983 1147.

10] Pierce, C. and Smith, R.N., J. Phys. Colloid Chem. 54 1950.

11] Pierce, C., Smith, R.N., Wiley, J.K., Corder, H.J., J. Am. Chem. Soc. 73 1951 4551.

12] Dubinin, M.M., Zaverina, E.D., Serpinski, V.V., J. Chem. Soc. 1955 1760.

13] Evans, M.J.B., Carbon 25 1987.

14] Dubinin, M.M., Carbon 18 1980 355.

15] Stoeckli, H.F., Kraehenbuhl, F., Morel, D., Carbon 21 1983 589.

16] Everett, D.H. and Ward, R.J., J. Chem. Soc. Farad. Trans. 1 82 1986 2915.

17] Matsumara, Y., Yamabe, K., Takahashi, H., Carbon 23 1985.

18] Gao, S., Yamabe, K., Takahashi, H., Tanso 120 1985 2.

19] Lahaye, J. and Ehrburger, P., Pure and Applied Chem. 61 1989 1853.

20] Bansal, R.C. and Dhami, T.L., Carbon 18 1980 137.

21] Rozwadowski, M. and Wojsz, R., Carbon 19 1981 383.

22] Rozwadowski, M., Siedlewski, J., Wosjz, R., Carbon 17 1979 411.

23] Puri, B.R., Kaistha, B.C., Vardhan, Y., Mahajan, O.P., Carbon 11 1973 329.

24] Sing, K.S.W., eg. Carbon 25 1987 155.

25] Rozwadowski, M., Kazimierz, E., Wisniewski, E, Wojsz, R., Carbon 22 1984 273.

26] Costa, E., Calleja, G., Marijuan, L., Ads. Sci. and Technol. 6 1989 213.

27] Zawadski, J., Carbon 26 1988 627.

28] Gasser, C.G. and Kipling, J.J., Proc. fourth Biennial Conf. Carbon, Buffalo, 1959. Pergamon Press, Oxford, England, 1960 55.

29] Bhacca, N.S., Tet. Lett. 41 1969 3127.

30] Puri, B.R., Singh, D.D., Kaistha, B.C., Carbon 10 1972 481.

31] Kiselev, A.V., Kovaleva, N.V., Korolev, A.Y., Kolloidnyl Zhurnal 23 1961 485.

32] Graham, D., J. Phys. Chem. 59 1955 896.

33] Barton, S.S. and Harrison, B.H., Carbon 11 1973 649.

34] Dollimore, J., Freedman, C.M., Harrison, B.H., Third Conf. Ind. Graphite, Society of Chemical Industry, London 1969.

35] Kraus, G., J. Phys. Chem. 59 1955 343.

36] Jankouska, H., Swiatkowski, A., Oscik, J., Kusak, R., Carbon 21 1983 117.

37] Barton, S.S., Evans, M.J.B., Harrison, B.H., J. Colloid and Int. Sci. 45 1973 3.

38] Oscik, J., Gowerek, J., Kusak, R., J. Colloid and Int. Sci. 79 1981 308.

39] Bansal, R.C. and Dhami, T.L., Carbon 15 1977 153.

40] Van Driel, J., in Activated Carbon, a Fascinating Material, Norit (pub.), 1983 40.

41] Gowerek, J., Kazmierczak, J., Swiatkowski, A., Proc. Int. Conf. Carbon (Carbon 90), Paris, France 1990 70. GFEC Paris.

42] Nelson Smith, R., Quarterly Reviews 13 1959 287.

43] Puri, B.R., Singh, D.D., Sharma, C.R., J. Phys. Chem. 62 1958 756.

44] Nelson, G.O., Correia, A.M., Harder, C.A., Am. Ind. Hyg. Assoc. J. 9 1976 514.

45] Balieu, E., J. Intern. Soc. Resp. Protect. 1 1983.

46] Bailey, A., Lawrie, G.A., Williams, M.R., Proc. Int. Conf. Carbon (Carbon 90), Paris, France, 1990 14. GFEC Paris.

47] Nelson, G.O. and Harder, C.A., Am. Ind. Hyg. Assoc. J. 35 1974.

48] Grant, R.J., Joyce, R.S., Urbanic, J.E., Engineering Foundation Conference, Fundamentals of Adsorption, Bavaria, West Germany, May 1983 219.

49] Dubinin, M.M., Kut'kov, V.S., Larin, A.V., Nikolaev, K.M., Polyakov, N.S., Izv. Akad. Nauk. SSR Ser. Khim., 83 1983 1111.
CA 99:94176.

50] Nemeth, J., Baticz, S., Peter-Horanyi, M., J. Hungarian Ind. Chem. 11 1983 357.

51] Walker, B.E. and Thompson, J.K., Hughes Associates Inc., Wheaton, MD 20902. Available DTIC, May 23 1986. AD-A167 982.

52] Okazaki, M., Tamon, H., Toei, R., J. Chem. Eng. Japan 11 1978 209.

53] Collins, R.D., Hillary, J.J., Taylor, L.R., Abbey, F., The Ageing of Charcoals used to Trap Radioiodine. Int. Symp. on Management of Gaseous Wastes from Nuclear Facilities, Vienna 1980.

54] Wood, G.O., Am. Ind. Hyg. Assoc. J. 46 1985 251.

55] May, F.G. and Polson, H.J., "Methyl Iodide Penetration of Charcoal Beds: Variation with Relative Humidity and Face Velocity". Australian Atomic Energy Commision 1974. ISBN 0 642 99653 9

56] Jonas, L.A., Sansone, E.B., Farris, T.S., Am. Ind. Hyg. Assoc. J. 46 1985 20.

57] Swearengen, P.M. and Weaver, S.C., Am. Ind. Hyg. Assoc. J. 49 1988 70.

58] Plokhov, Yu.M., Musakin, G.A., Plachenov, T.G., Zhur. Prikl. Khim. 62 1989 1238.

59] Nelson, G.O., Correia, A.N., Harder, C.A., Am. Ind. Hyg. Assoc. J. 37 1976 280.

60] Potorzhinskii, I.V. and Serpionova, E.N., Tr. Mosk. Khim. Tekhnol. Inst. 65 1970 79.

61] Petrova, N.I. and Nikolaev, K.M., Zh. Prikl. Khim. 55 1982 2089.

62] Nikolaev, K.M. and Petrova, N.I., Zh. Prikl. Khim. 54 1981 1071.

63] Ackerman, F.J. and Grens, J.Z.. Lawrence Radiation Laboratory, University of California, Livermore. 1966 (Conf-660904-6). Available NTIS.

64] Bailey, A., Woodward, G.A., Williams, M.R., Proc. Int. Conf. Carbon (Carbon 88), Newcastle Upon Tyne, September 1988. Ed. B. McEnaney and T.J. Mays 137.

65] Shali, U., and Aharoni, C., Am. Ind. Hyg. Assoc. J. 35 1974 552.

66] NATO Army Armaments Group NBC Defense Panel. Document AC/196-D/103. Combined Operational Characteristics, Technical Specifications and Evaluation Criteria for the Protective Mask (Triptych). Unclassified version, 1967.

67] Specification TS50605. Charcoal Activated Coal-Based Type 1101. Issued by the Director of Quality Assurance/ Materials Centre, E135/1, Royal Arsenal East, Woolwich, London SE18 6TD UK, 1985.

68] Hall, C.R., Lawston, I.W., Tinsley, A.M., Chem. and Ind. 5 1989 145.

69] Brown, P.N., Jayson, G.G., Thompson, G., Wilkinson, M.C., Carbon 27 1989 821.

70] Ehrburger, P., Dentzer, J., Lahaye, J., Dziedzinl, P., Fangeat, R., Carbon 28 1990 113.

71] Carrott, P.J.M, Kenny, M.B., Roberts, R.A., Sing, K.S.W., and Theocharis, C.R., in F. Rodriguez-Reinoso et. al. (Eds.), Characterisation of Porous Solids II, Studies in Surface Science and Catalysis 62 Elsevier 1991 685-692.

CHAPTER 5

Experimental

5.1 Carbons

Unimpregnated activated carbons (control carbons) derived from coal (BPL; Chemviron Ltd., Brussels, Belgium) or coconut shell (SCII; Chemviron Ltd., Brussels, Belgium and AC35; CECA SA, Paris, France) were used in this study, and were of a similar particle size (12 x 30 ASTM (particle size measured according to the American Standard Test Method)). They were stored as received in sealed containers, and dried prior to use (3 hours, 120°C, 3mbar).

5.2 Carbon Ageing, and the Preparation of Chemically Modified Carbons

The propensity of control carbons to oxidise (age) as a result of exposure to humid air was studied as a function of the relative humidity (RH) of the air. Aged samples were prepared using climatic chambers maintained at 22°C and 45°C. The RH of the air within the chambers could be varied between 40 and 80%.

Carbon modifications were achieved using a number of reactive chemicals. The apparatus and precise experimental technique utilised for each modification are noted in the relevant chapter (6-9), and the design of the apparatus employed, and its mode of operation, is discussed in detail at the Appendix. The apparatus used for chemically modifying the carbon samples is described in brief.

Low temperature (<200°C) reactions were carried out using a purpose designed stainless steel vessel, which was fitted to a gas handling system to enable the introduction of reagent, sampling of the vessel atmosphere, pressure monitoring, and pumping.

High temperature reactions were performed using an Inconel (nickel alloy) lined stainless steel tube. The tube was held in a vertical furnace, and was attached to pressure and temperature sensors. Gaseous reagent was introduced using a stopcock arrangement. The quantity of gas within the reactor vessel was monitored using a pressure transducer. Evacuation of the tube was achieved using a stopcock arrangement.

5.3 Analysis of Control, Modified, and Aged Carbons

The analytical equipment, its design, and mode of operation, is detailed at the Appendix.

An analytical regime was developed to establish the effect of modification upon the adsorptive properties of the carbon. The principal techniques employed were those of nitrogen, methanol, water, and chloropicrin (trichloronitromethane, designated here as PS) adsorption. Control and aged carbons were also studied using these techniques.

It was the intention that modification would not disrupt or alter the porous structure of the carbon. To determine whether structural modification resulted, nitrogen adsorption and desorption isotherms were measured at -196^{o}C using a Carlo Erba Sorptomatic instrument. To analyse the data, isotherms for the carbon before and after treatment were compared: that is, the quantity of nitrogen adsorbed was corrected using the gravimetric change recorded after reaction. This enabled the amounts of nitrogen adsorbed by the samples to be compared on the basis of equal quantities of carbon. It was assumed that modification did not result in significant carbon gasification: where possible, measurements to establish if this was important were made, by analysis of any gaseous reaction products using either a VG Instruments PETRA quadrupole mass spectrometer, or a Varian model 3400 GC linked to a Finnegan MAT ITD (Ion Trap Detector mass spectrometer).

Structural modification was also studied by measurement of vapour adsorption from a dry airstream using dry carbon. Thus, chloropicrin (PS-CCl_3NO_2) and n-hexane sorption was used for some samples. Because both of these vapours are non polar, the extent of adsorption from a dry airstream is governed by the porosity of the carbon, and not by the presence of polar surface functional groups.

Conversely, the adsorption of methanol by activated carbon depends upon the quantity of hydrophilic sites at the adsorbent surface (chapter 6). Thus, measurement of methanol breakthrough curves for dry samples was used to determine whether the modified carbons were of increased, or reduced, hydrophobic character. This technique allowed a rapid assessment of any changes to the nature of the surface to be made, and was used in conjunction with nitrogen and water adsorption data.

Water adsorption, measured in flowing air, was used to establish whether the modified sample was more or less hydrophobic compared to control carbon, but the measurement occupies approximately three to four weeks, and so was not a rapid technique. The data was also used to determine whether pore occlusion occurred, and as a measure of the stability of the carbon surface to humid air. Recycling samples enabled the carbon ageing characteristics to be investigated.

The adsorption of PS vapour from air of high RH was used as a measure of the filtration efficiency of the modified carbon. PS is hydrophobic, and relatively low boiling: the efficiency of adsorption in the presence of water vapour is therefore sensitive to the nature of the carbon surface, and provides the best measure as to the effect of a particular chemical modification. This technique was also applied to studies of the ageing characteristics of the modified carbons.

Other techniques employed included TG (Stanton Redcroft TG770 thermal gravimetric analyser), DSC (Stanton Redcroft DSC 1500 differential scanning calorimeter), XPS (Kratos Analytical XSAM800 X ray photoelectron spectrometer), EDX (Hitachi S800 SEM (field emission system) fitted with a Link analytical thin window/ windowless energy dispersive X ray analyser), X ray diffraction, mercury porosimetry (Carlo Erba Porosimeter 2000), and elemental analysis (Carlo Erba 1106 analyser).

TG and DSC were used as a comparative measure of the stability of the modified carbons; XPS and EDX provide information with regard to the chemical composition of the modified surface. X ray diffraction and mercury porosimetry reveal carbon structural information.

The ageing characteristics of selected modified samples were studied in more detail by exposing carbons to 80%RH air at 45^{o}C for 45 days. This exposure regime is arbitrary, but was sufficient to provide measurable ageing.

5.4 Vapour Adsorption at high Relative Humidity (RH)

The second aspect of this research is intended to address the mechanism of vapour adsorption by carbon filters in equilibrium with air of high RH. These studies were performed using the water and PS vapour adsorption apparatus detailed at the Appendix. The effect of using modified carbons was also considered.

CHAPTER 6

The Effect of Storage Conditions on the Properties of Activated Carbon Adsorbents

Results and Discussion

Section | Page

6.1 Introduction

Carbons used in vapour adsorption applications are normally activated using steam or carbon dioxide at elevated temperature (chapter 1). As a result, they contain chemisorbed oxygen, in an amount which is dependent upon such factors as whether any post activation treatments are employed (for example, high temperature annealing to decompose surface oxygen containing functional groups (surface oxides)). Any remaining surface oxides are likely to result from a reaction at the active sites (surface defects, centres of unsaturation, and the edges of graphitic layers). The temperature and relative humidity (RH) at which the adsorbent is subsequently stored can then result in a further increase in the amount of chemisorbed oxygen, a process which is known to permanently change some of the adsorptive properties of the carbon (chapter 3,4). For example, this is known to occur during storage in the presence of high RH air, and results in a degradation in the efficiency with which filters adsorb volatile hydrophobic contaminants. Specific examples are found in the nuclear industry and in individual respiratory protection (chapter 4).

The change in adsorptive properties described above is commonly referred to as ageing (chapter 3,4). The ageing process has received attention because of its consequence upon the performance of carbon filters in critical processing applications and in hazardous operations. In this chapter, some parameters affecting the rate and extent to which ageing takes place for BPL activated carbon are described. In addition, the effect of ageing upon some of the adsorptive properties of activated carbon will be discussed, and a comparison made between the properties of aged carbons, and carbons oxidised using dinitrogen tetroxide (N_2O_4, abbreviated hereafter to NO_2). The techniques used for the analysis of the carbons are described below.

The introduction of oxygen containing functional groups onto the surface of activated carbon results in an increase in the number of polar adsorption

centres (chapter 3,4). To monitor these changes, a test procedure was developed using an adsorbate with which polar surface sites can interact specifically. Methanol was selected as the test vapour because it is a relatively small polar molecule which, like water, will interact through hydrogen bonding. As a result, it is probable that a small number of polar adsorption centres will act as a focus for the adsorption of a number of methanol molecules. On this basis, relatively small changes in the number of polar sites can be monitored because the change in the quantity of methanol adsorbed will be more significant.

The test procedure involved passing a constant concentration of methanol vapour in dry air and at a known flow velocity and temperature through a fixed quantity of dry carbon until the concentration in the influent and effluent airstream was the same. On the presumption that ageing does not significantly alter the porosity of the carbon (see below), a comparison of the results (eg. using the weight increase due to the amount of methanol adsorbed per gramme of adsorbent) should then enable any changes in surface polarity to be directly monitored. The extent of any observed change will also depend upon the methanol vapour concentration: at high values, the test will be less sensitive because adsorbate- adsorbate interactions will predominate. At lower concentrations, however, specific adsorbate- adsorbent interactions will be more important. Thus a low vapour concentration was used (1300±25mg m^{-3}), which equated to a relative pressure (p/p^o) of 0.01. At this concentration, and using an FID detector (flame ionisation detector), complete breakthrough curves could be monitored within a relatively short timescale (the duration of the test was typically 90-120 minutes).

The use of water breakthrough curves was investigated, but was found to be of less value, because of difficulties associated with the routine measurement of the very low water vapour concentrations where adsorbate-adsorbent interactions are important. However, because the equilibrium water adsorption properties of the carbons are relevant to this present study, water adsorption- desorption isotherms were determined (which did not require the

measurement of very low water vapour concentrations). As before, adsorbate-adsorbent interactions are more important at low relative pressures. Thus the amount of water adsorbed below ca. RH60% is controlled mainly by the number of polar adsorption centres, and so (for a constant distribution of pore widths) increases with the adsorbent polarity (chapter 4). Water adsorption at high RH (ca. RH80% and greater) is controlled mainly by the available pore volume, and so does not change markedly unless the oxidative process involves significant structural modification.

Interpretation of such measurements will depend on whether ageing results in significant structural modification (an increase or decrease in porosity). Thus nitrogen adsorption at -196^{o}C, and measurement of hexane breakthrough curves for dry carbon samples, was used. The technique for measuring hexane adsorption was the same as that used for methanol adsorption (Appendix). The vapour concentration employed (6470 ±30 mg m^{-3}) equated to the same partial pressure used for the methanol tests.

It is probable that ageing results in the introduction of relatively few surface oxides. If this is so, then the amount of hexane adsorbed by a dry carbon should be largely independent of the polarity of the surface because of the absence of specific adsorbate- adsorbent interactions. On this basis, comparison of the amounts adsorbed by aged and control samples will allow an assessment of structural modification to be made. Any dissimilarity in the profiles of the breakthrough curves may indicate a change in the adsorption kinetics, which may be due to pore narrowing. Mercury porosimetry was not found to be a useful technique for the analysis of aged carbons, because the instrument employed only enabled an assessment of meso- and macroporosity to be made.

Thermal gravimetric (TG) analysis of the samples as a method for monitoring changes in the amount of chemisorbed oxygen was also found to be unsuitable, because the weight losses observed were small. This precluded a

meaningful comparison to be made between samples stored for different time periods at a particular value of the RH.

To determine the effect that ageing has upon the efficiency of activated carbon filters in the presence of humid air, PS (trichloronitromethane; chloropicrin) and hexane adsorption at high RH (80%) has been used. Unless otherwise indicated, the carbon was pre-equilibrated with RH80% air prior to commencement of the test (Appendix). Both PS and hexane are volatile and hydrophobic. The adsorption of these vapours in the presence of water vapour will therefore be sensitive to the surface chemistry of the carbon, because any polar surface centres will act as a focus for the adsorption of (polar) water molecules in preference to hydrophobic adsorbates.

The techniques used for the measurements described are detailed at the Appendix.

6.2 The Effect of the Relative Humidity and Temperature on the Rate and Extent of Ageing

6.2.1 The Effect of the RH

Assessment of the vapour adsorption properties of activated carbons used in air filtration applications are not usually carried out under environmental conditions similar to those that would be encountered during use (chapter 4). In practice, filter efficiency is measured using either "as received" carbon, or carbon which has been equilibrated with air of low RH (ca. 50%). However, because the average RH is above approximately 60%, it is probable that such measurements will not be a true reflection of "in service" filter performance. In some cases, however, vapour filter specifications require that performance is measured under more representative conditions: that is, after equilibrating the adsorbent with high humidity air (usually RH80%; eg. references 65-67, chapter 4). Equilibration is normally achieved by passing a stream of air of the appropriate RH, temperature, and flow rate through the filter until constant weight is attained. Whilst for high RH values this technique usually results in consistent values of moisture uptake (on the basis of the weight of adsorbed moisture/ weight of dry carbon), it has been found that the subsequent vapour test results can vary considerably. This has been shown to be a consequence of the way in which the carbon had been stored prior to testing.

To determine the precise influence that the storage conditions have upon the rate and extent to which ageing takes place, BPL activated carbon was stored in shallow trays (ca. 1cm depth) in static air at RH60 and 80% at 22°C for extended time periods. During storage, samples were periodically removed, and dried under reduced pressure (120°C; 3 hours; 3 mbar). The properties of the aged carbons were examined using the techniques described above.

Figure 6.2.1 shows a series of methanol breakthrough curves measured for (dry) carbon samples aged at RH80%. As storage time is increased, it is

apparent that the amount of methanol adsorbed by the sample is also increased, an observation consistent with there being a greater number of polar adsorption centres on the carbon surface. That the shapes of the breakthrough curves are essentially the same suggests that the kinetics of adsorption are not markedly affected by the modification. Figure 6.2.2 shows the adsorption data in terms of the 50% filter breakthrough time (in minutes) as a function of the storage time (in days). It is apparent that the rate of change is most rapid during the first 50-100 days of storage. After this time, only small increases in the amount of methanol adsorbed were found.

Examination of the water adsorption isotherms for these samples revealed similar effects (eg. figure 6.2.3- control, and 860 days aged carbon), in that it was found that the water uptake at low values of the RH (below ca. 60%) was enhanced. This enhancement is explained on the same basis as the methanol adsorption data, and results in a displacement of the pore filling region of the isotherm to lower RH (or partial pressure) values (chapters 2,4). Measurement of water adsorption using the technique employed in this present study was not as sensitive a test as methanol adsorption in revealing small changes, however. The changes in the adsorptive characteristics of the carbons revealed by water and methanol adsorption are both due to their being specific adsorbent- adsorbate interactions (dipole-dipole), since ageing did not result in a major change to the nitrogen BET surface area (table 6.2.1. A small reduction was observed after ageing the carbon, but at least part of this difference may be attributed to the unknown weight of oxygen chemisorbed by the carbon- ie., one gramme of aged and control materials contain different amounts of carbon). The elemental analysis data (table 6.2.2) revealed that ageing is associated with an increase in the oxygen content of the carbon.

Figure 6.2.4 shows hexane breakthrough curves measured under dry conditions for a sample of control carbon, and a sample aged at RH80%. The similarity of the curves reflects the absence of specific adsorbent- adsorbate interactions, and the fact that little change in porosity has taken place. Similar

measurements, but under humid conditions (RH80%, figure 6.2.5) reveal that substantial differences in filter performance result from pre-equilibrating the carbons with RH80% air, and that the performance of the aged carbon is comparatively poor. The efficiency of PS adsorption by the aged carbon was also found to be reduced (figure 6.2.6). Because the polar surface groups act as a focus for the adsorption of water, it is probable that the reduced rate of hexane and PS adsorption is a consequence of the difficulty with which water displacement from the surface takes place. Both PS and hexane are poorly soluble in water: the adsorption of these vapours at high RH must involve displacement of at least some of the preadsorbed water.

Analysis of the aged carbons using thermal desorption- mass spectrometry (TDMS; Appendix) revealed that the principal desorption products were carbon dioxide and carbon monoxide (table 6.2.3). The size and shapes of the desorption profiles were found to be similar to previously reported data (chapter 3), but the technique was not found to be straightforward- because of the difficulties associated with calibrating the mass spectrometer, quantification of the desorbed species was not possible. However, as a means of comparing samples aged under different conditions, integration of the peak areas for m/e 28 and m/e 44 (assigned to CO and CO_2 respectively) provides a direct measure of the effect of the RH on the relative amounts of chemisorbed oxygen (table 6.2.3). Analysis of the desorption spectra also showed the presence of sulphur dioxide (table 6.2.3): since BPL carbon contains approximately 1% w/w sulphur, it is likely that ageing also involves the oxidation of surface sulphur species.

Methanol breakthrough times (50% penetration) as a function of the number of days storage are shown at figure 6.2.7 for samples of BPL carbon aged at RH60%. The data suggest that the rate and extent of ageing is similar to that at RH80%. However, measurement of PS adsorption for samples aged at both RH values for the same time period (170 days) suggests that the sample

stored at RH60% contains fewer surface oxygen containing functional groups than the sample stored at RH80% because the loss in filter performance was not as significant (table 6.2.4). That this was also apparent from the TDMS analysis suggests that methanol adsorption does not provide the best measure of the effect of ageing on filter performance at high RH.

One explanation for the apparent anomaly is that because there are more polar functional groups present on the surface of the sample aged at RH80%, they are in closer proximity than those on the sample aged at RH60%. On this basis, it is probable that a number of these groups act as a single focus for the adsorption of methanol. The difference in the PS adsorption properties is then, as before, a consequence of the greater number of polar adsorption centres present on the RH80% aged sample, which limit more effectively the ease with which adsorbed water is displaced.

Although limitations on the use of methanol vapour adsorption as a technique for monitoring surface polarity are apparent, the test is useful as a means of revealing such changes.

As before, ageing at RH60% was not found to result in any significant structural modification (nitrogen and hexane adsorption), but lead to an enhancement in the amount of water adsorbed at low values of the RH (below ca. 60%).

Exposure of carbon to RH40% air at 34^{o}C was also carried out. The rationale for using 34^{o}C was that RH40% air at this temperature contains the same absolute concentration of water vapour as RH80% air at 22^{o}C. This approach therefore allows the RH to be varied whilst maintaining a constant water vapour concentration.

Methanol adsorption as a function of storage time at RH40% is shown at figure 6.2.8, which also shows the data for samples aged at RH60 and 80% (22°C). It is apparent that at RH40%, no increase in surface polarity takes place after 200 days storage, whereas at RH60 and 80%, ageing is most rapid during this period. Support for the contention that ageing does not occur to any measurable extent under these conditions was obtained from measurement of PS adsorption at high RH, where it was found that filter performance was unchanged after 170 days storage (table 6.2.4). In addition, the water adsorption isotherm for the aged sample was essentially the same as that for the control.

TDMS analysis did, however, suggest that exposure resulted in a small increase in the number of surface oxygen containing functional groups (table 6.2.3): in comparison to the control sample, the differences were small, indicating that ageing did not proceed to as significant an extent at RH40% as at RH60 or 80%. The results also highlight the importance of the RH, rather than the absolute water vapour concentration, on the ageing characteristics of activated carbon.

One possible explanation for the absence of significant ageing effects at RH40% is that during exposure, water adsorption occurs primarily on any polar surface sites that are present on the carbon after manufacture (eg., surface defects, ash impurities, surface oxygen containing functional groups). Such sites would act as a focus for the adsorption of water vapour, and, as a result, the surface of the carbon might be visualised as possessing a surface covered with discrete clusters or "islands" of adsorbed water. That some ageing does take place presumably reflects a small degree of island growth, whereby water spreads across the surface and is adsorbed onto less favourable surface sites which are amenable to chemical change (oxidation).

As the RH of the air is raised to 60%, the islands will then cover more of the carbon surface, exposing a greater number of reactive sites to water: more

extensive surface oxidation would then result. Similarly, at RH80%, where most of the surface is presumed to be covered by the islands of adsorbed water (chapter 2, section 2.2.2) further oxidation will be promoted. The quantity of water adsorbed by (control) BPL carbon at RH40, 60, and 80% is ca. 2.5, 16.2, and 35.2 w/w% respectively (based on the weight of dry carbon).

The mechanism of surface oxidation presumably involves both water and oxygen, although preliminary results obtained during measurement of water isotherms using high purity nitrogen carrier gas, rather than air (chapter 3, reference 72), suggest that water is most important in promoting ageing. Further support for this contention is that (dry) samples stored in dry air showed no measurable change in adsorptive properties over a period of at least five years. This observation has also been made by other workers (eg. chapter 3, reference 71).

The main conclusion from this part of the study is that ageing results in a major decrement in filter performance against volatile hydrophobic chemicals, but that the level of filtration efficiency can be maintained by controlling the RH of the airstream to the filter at a low value (ie. RH40% or below). It is also likely that environmental contaminants (eg. fuel vapours) will also affect filter performance to an extent which will depend on the location of the filter, the rate of air throughput, and the length of time for which it has been in service. This aspect is, however, beyond the scope of this present research.

The adsorption of PS by control and aged carbons is considered in more detail at chapter 9, where some of the factors controlling filter performance are discussed.

6.2.2 The Effect of Temperature

One intention of this part of the research was to develop a rapid, but realistic, test to enable the ageing characteristics of chemically modified carbons (chapters 7,8) to be evaluated. At RH80% and 22°C, storage of samples for approximately 60 days would be required if unambiguous conclusions were to be made with regard to the stability of the modified samples in the presence of high humidity air. Raising the temperature was considered to be the most appropriate approach, because accurate control of the RH at above ca. 80% for extended time periods is technically difficult. A temperature of 45°C was selected on the basis that this represents a realistic maximum air temperature to which filters might be exposed (it is appreciated, however, that in some circumstances, higher operational temperatures might be encountered).

Thus BPL carbon was stored at RH80% at 22°C and 45°C. Figures 6.2.9 shows the methanol and PS adsorption data as a function of storage time for these samples.

It is apparent that ageing occurs more rapidly at the higher temperature. More importantly, the data suggest that the extent of ageing is slightly greater at 45°C, because the data plots do not converge after 200 days storage. Comparison of the water adsorption isotherms for these samples illustrates that at both temperatures, the enhancement in surface polarity is most noticeable after the first few weeks of storage (figure 6.2.10-6.2.11). Thereafter, little difference is apparent between samples stored at the same temperature (figures 6.2.12-13), supporting the view that water adsorption is not the most sensitive test. The technique is, however, useful for revealing the gross changes which are observed after the first few weeks of exposure.

Comparison of the isotherms at figure 6.2.14 suggests that samples aged at 22 and 45°C are different, an observation consistent with the PS and methanol adsorption data. It may be that the ultimate performance of the

carbons will be the same, but it is equally likely that they will not, because at 45°C, it is probable that more extensive surface oxidation occurs. That is, the active sites at the surface do not possess a discrete activation energy. As before, nitrogen adsorption revealed that a small decrease in surface area resulted from exposure.

That the degree of surface oxidation is probably temperature dependent is apparent from the fact that at high temperatures (ca. 800°C), contact with water vapour results in carbon burn off (activation, chapter 1).

Because of the need to employ an accelerated ageing technique, and because exposure of carbons to RH80% air at 45°C represents a more severe test, chemically modified samples were routinely aged under these conditions for a period of 45 days. The exposure time is arbitrary, but was sufficient to produce significant ageing effects for control carbons.

Table 6.2.1 Nitrogen Adsorption for Control and Aged Carbons

	Sample					
	Control	Ageing Period (days at RH80%)				
		400	860	1220	150	150*
Surface Area ($m^2\ g^{-1}$)	1182	1124	1100	1110	1115	1120
Total Pore Volume (ml g^{-1})	0.60	0.55	0.55	0.57	0.57	0.57
Primary Micropore Volume	0.35	0.34	0.32	0.32	0.34	0.33
Secondary Micropore Volume	0.15	0.14	0.15	0.15	0.13	0.14
Mesopore Volume	0.09	0.08	0.08	0.09	0.09	0.09

The results are for single determinations. Typical error on measurement of surface area is ± $12m^2g^{-1}$, and ± 0.01 cm^3<STP>g^{-1} for the total pore volume (per gramme of carbon). *Sample aged at 45°C.

Table 6.2.2 Elemental Analysis of Control and Aged Carbons

Sample	Element (w/w%)					
	C	H	N	O	S	ASH
BPL Control	86.6	0.2	0.5	2.0	1.2	7.5
BPL Aged (400 days; RH80%; 22°C)	84.3	0.2	0.5	3.4	1.0	7.6
BPL Aged (860 days; RH80%; 22°C)	85.2	0.3	0.5	4.1	1.0	7.3

The results are an average of at least two determinations

Table 6.2.3 Thermal Desorption Mass Spectrometry for Control and Aged Carbons

Ageing Conditions (170 days @ %RH @ 22°C)	Integrated Peak Areas ($x10^{-3}$ counts)		Counts at Peak Maxima	
	m/e= 28	m/e= 44	m/e= 48	m/e= 64
0	50	43	235	450
40	146	521	335	732
60	295	1046	626	1394
80	1722	2216	1970	4240

{Peaks are attributed as follows: m/e 28= CO+; m/e 44= CO_2+; m/e 48=SO+; m/e 64= SO_2+}

Table 6.2.4 Chloropicrin (PS) Adsorption for Control and Aged Carbons

Sample	Time to Initial Filter Breakthrough (min) {Samples stored above RH0% tested after 170 days}			
	RH0%	RH40%	RH60%	RH80%
BPL	81	81	69	62

FIGURE 6.2.1 METHANOL BREAKTHROUGH CURVES

L-R: CONTROL BPL; BPL AGED (RH80%, 22°C) FOR 7, 35, AND 250 DAYS

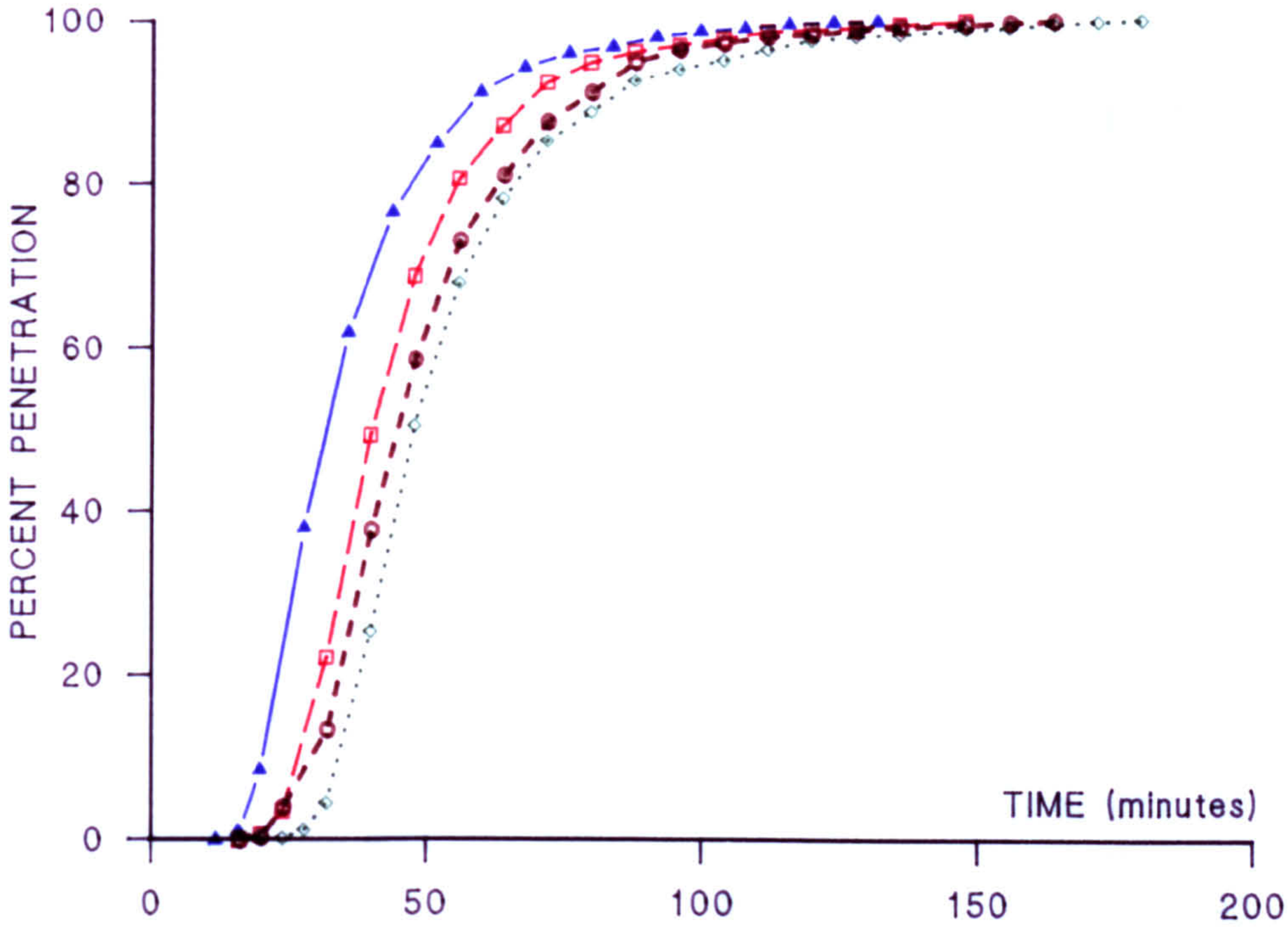

FIGURE 6.2.2 METHANOL ADSORPTION

(BPL CARBON, AGED AT RH80% AND 22°C)

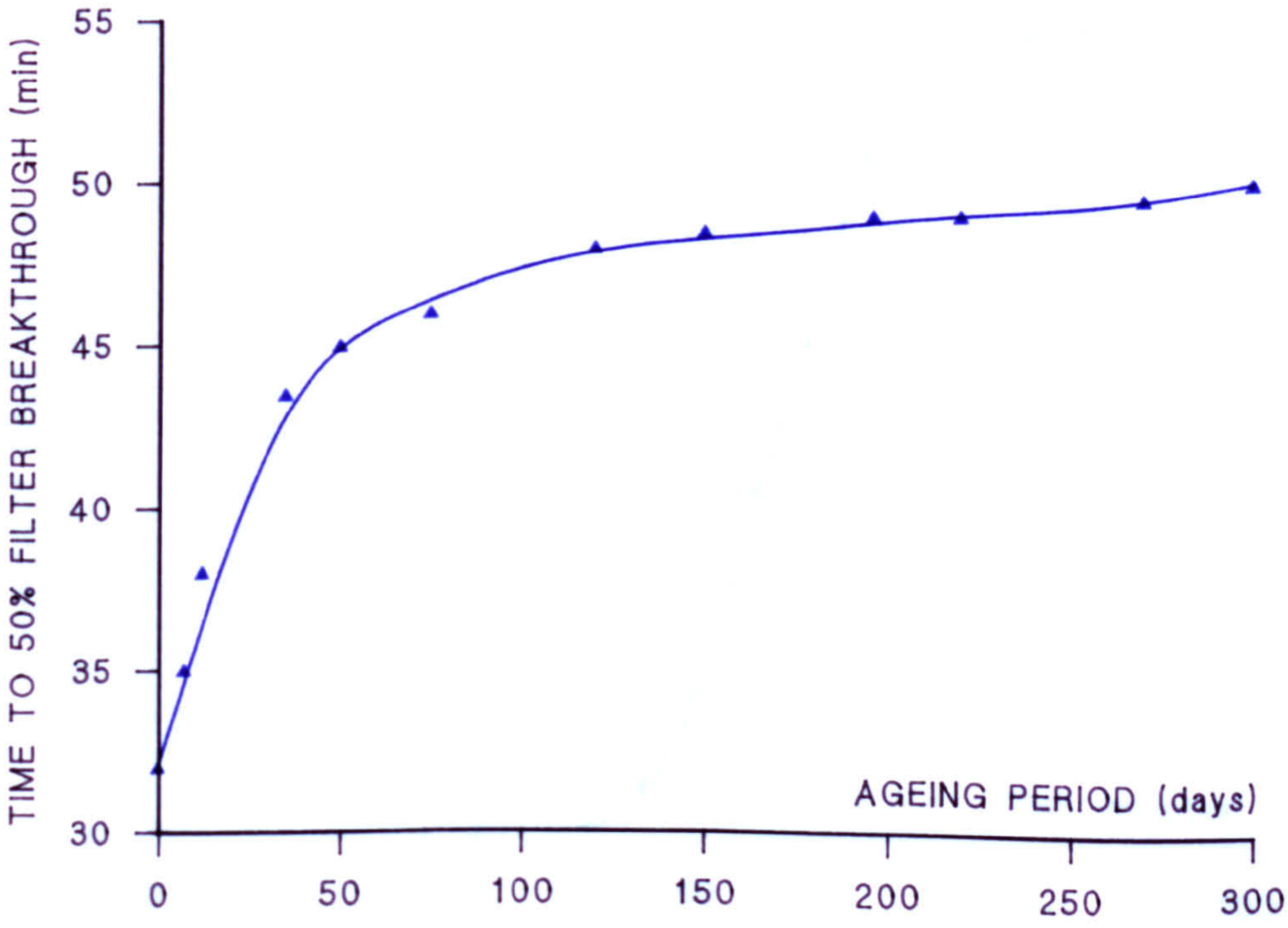

FIGURE 6.2.3 WATER ADSORPTION

● CONTROL BPL ▲ AGED BPL (RH80%, 22°C, 860 DAYS)

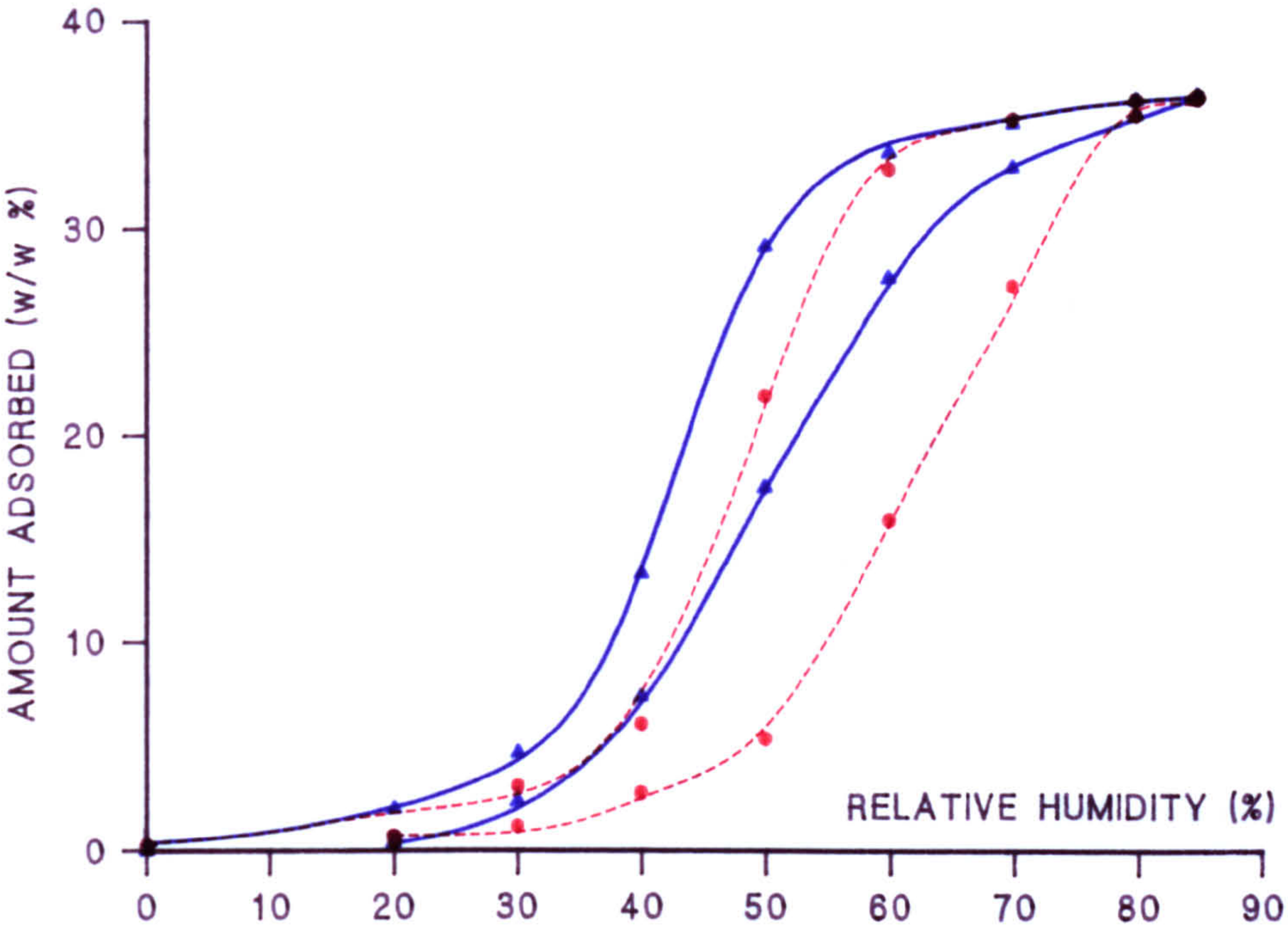

FIGURE 6.2.4 HEXANE BREAKTHROUGH CURVES

L–R: BPL AGED (RH80%, 22°C, 400 DAYS); BPL CONTROL

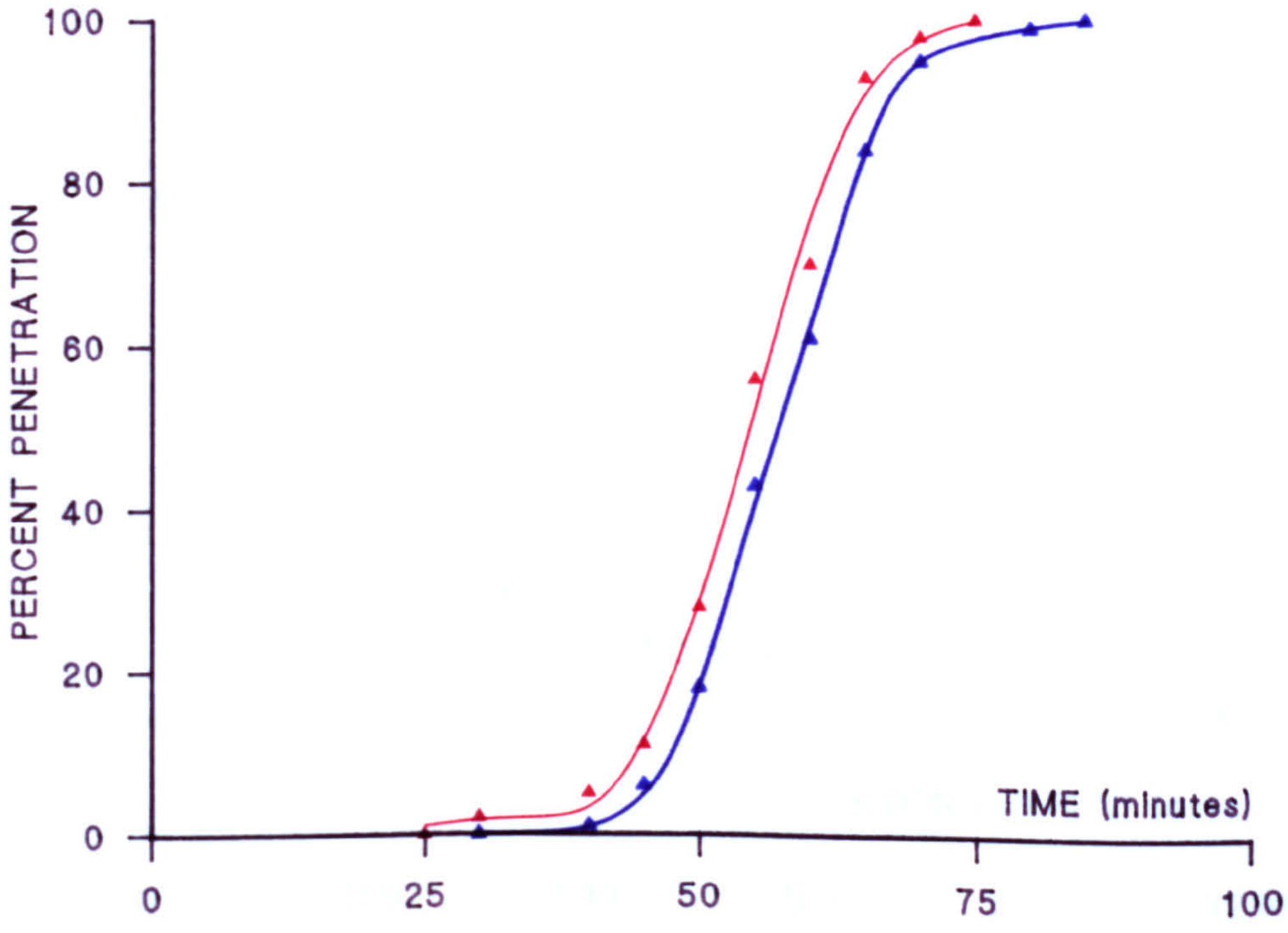

FIGURE 6.2.5 HEXANE BREAKTHROUGH AT RH80% AND 22°C

L–R: AGED BPL (RH80%, 22°C FOR 250 DAYS); CONTROL BPL CARBON

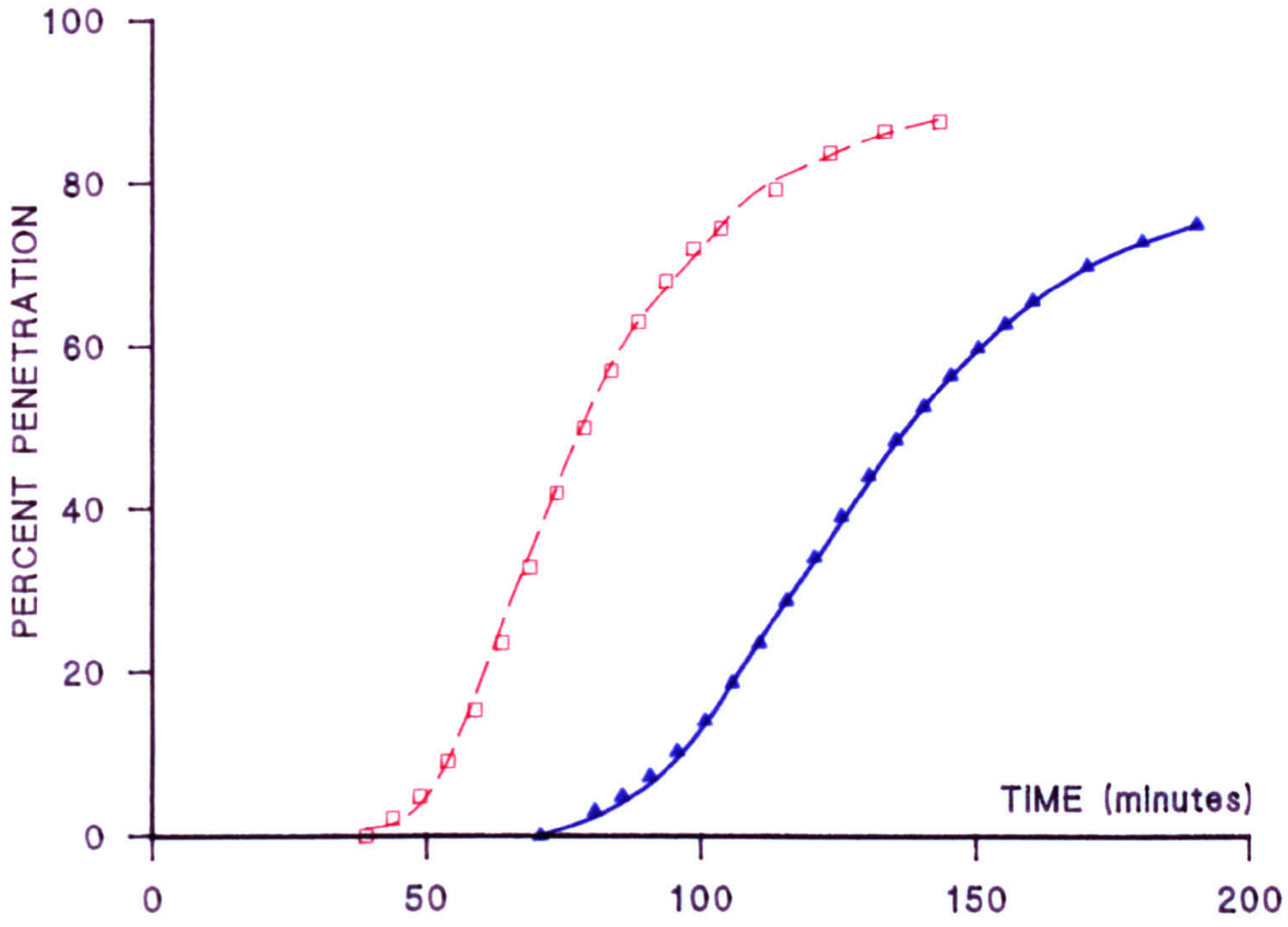

FIGURE 6.2.6 PS BREAKTHROUGH

(BPL CARBON, AGED AT RH80% AND 22°C)

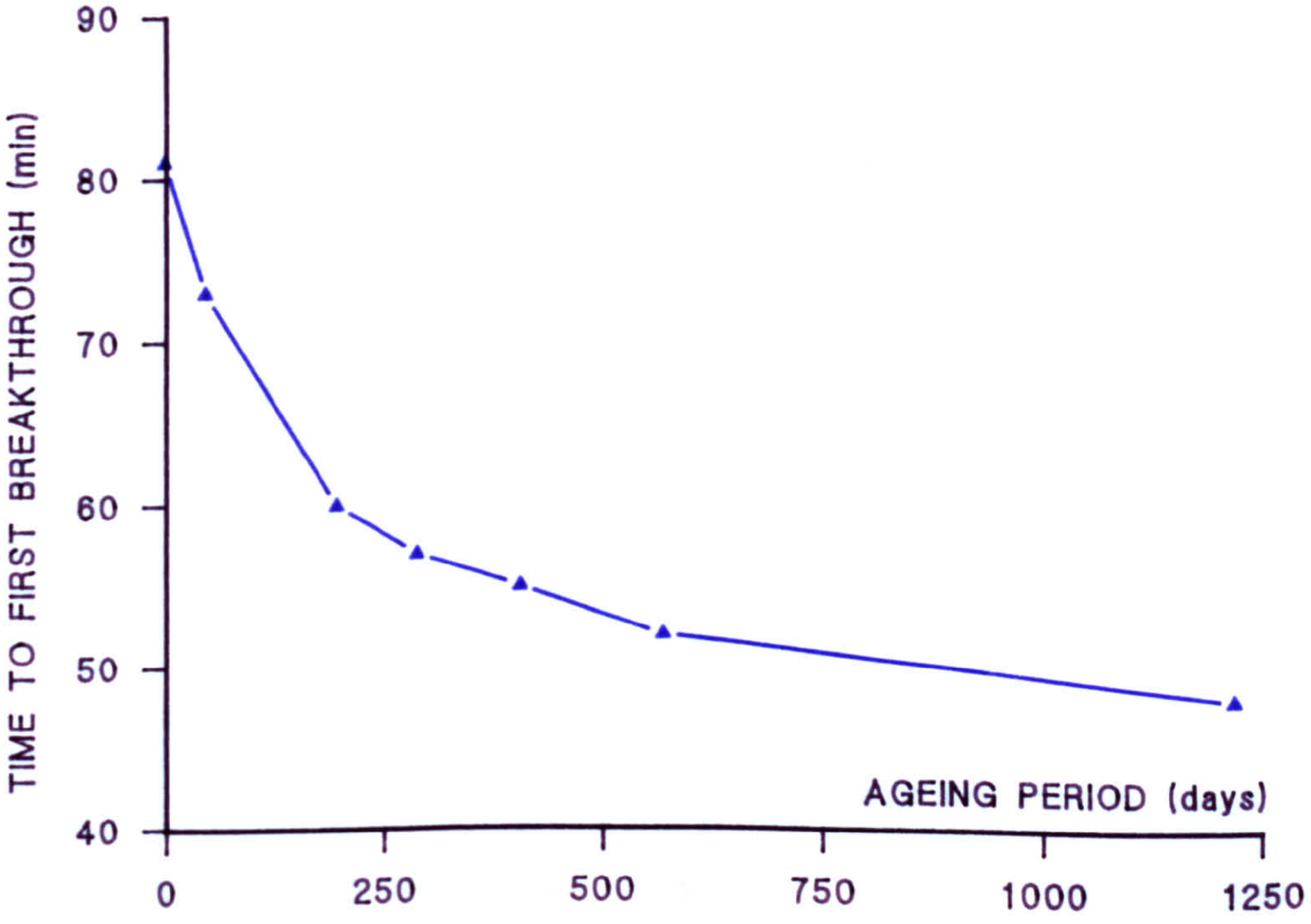

FIGURE 6.2.7 METHANOL ADSORPTION

(BPL CARBON AGED AT RH60% AND 22°C)

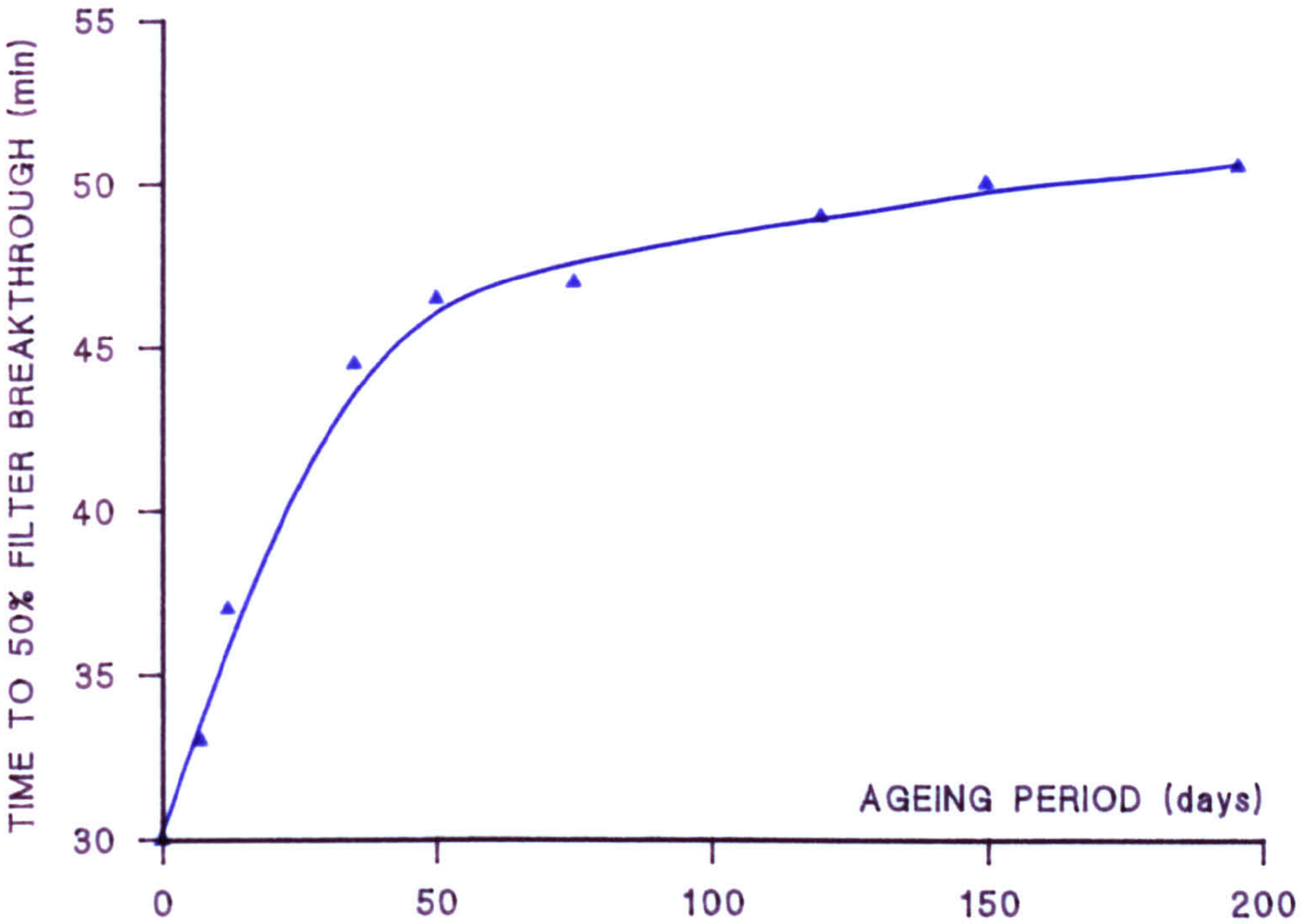

FIGURE 6.2.8 METHANOL ADSORPTION

(BPL CARBON AGED AT △ RH80%, ○ RH60% AND □ RH40%)

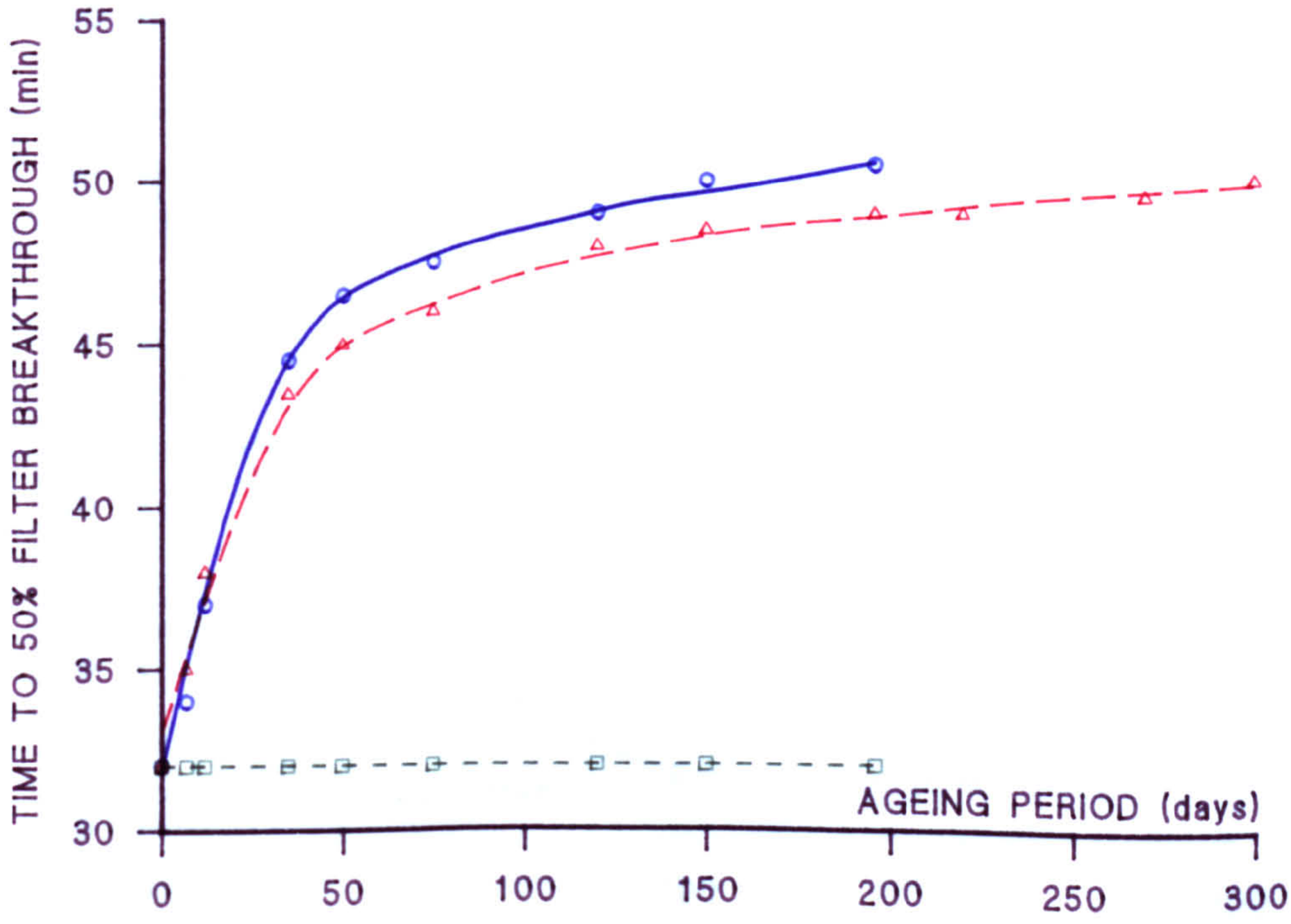

FIGURES 6.2.9 METHANOL AND PS ADSORPTION

UPPER CURVES: METHANOL ADSORPTION; LOWER CURVES: PS ADSORPTION
(BPL CARBON AGED AT RH80%, □ 22 AND ▲ 45°C)

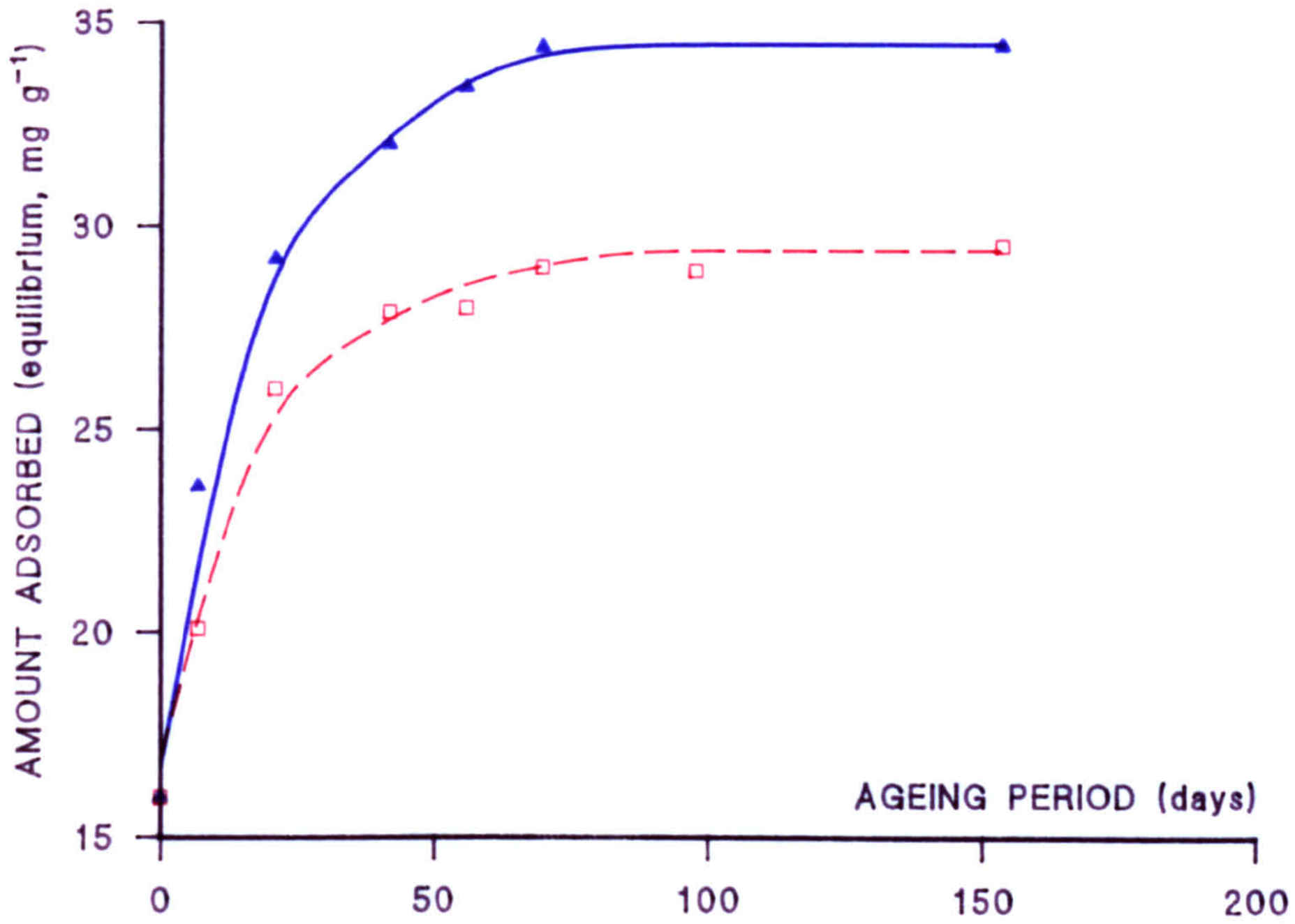

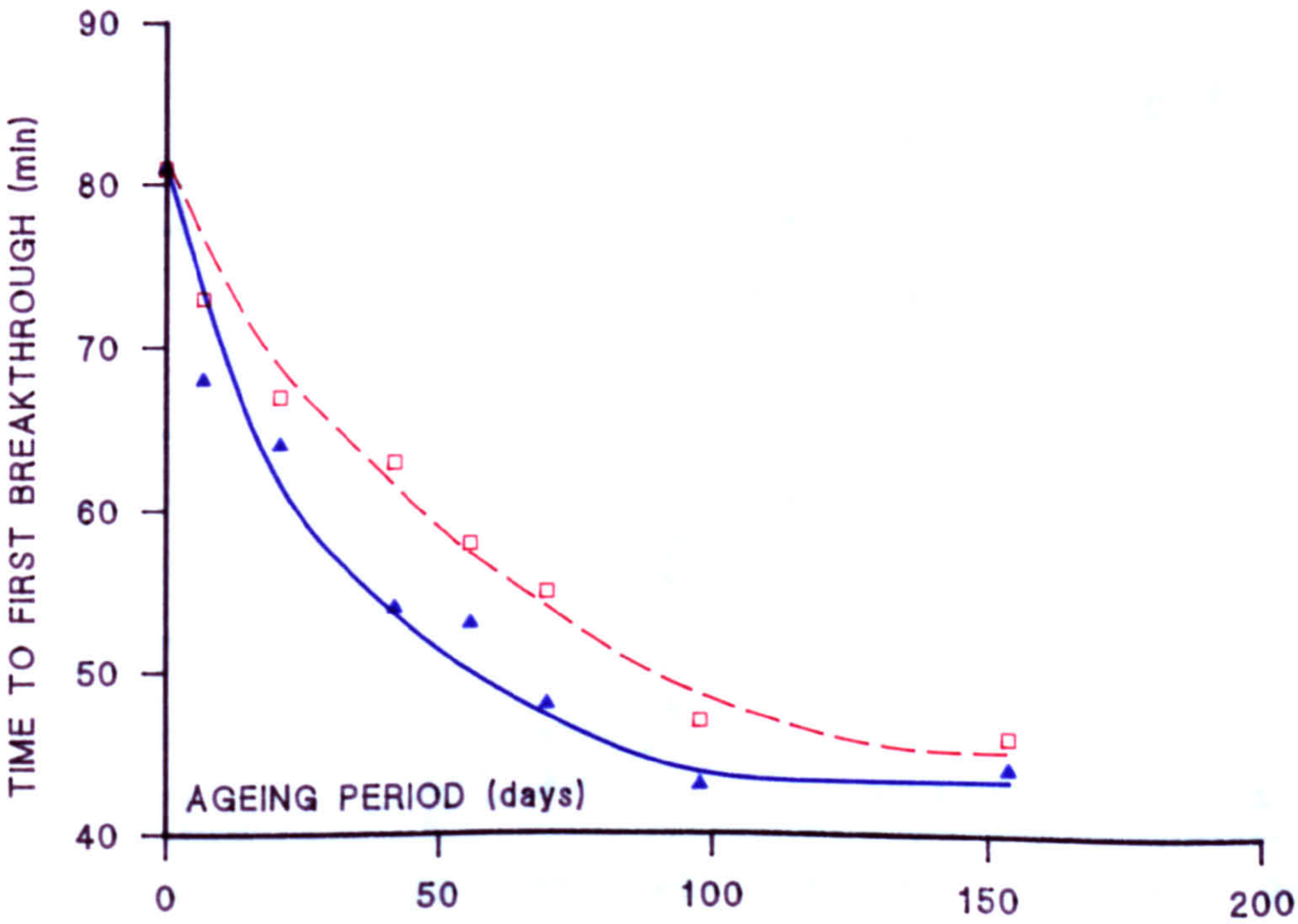

FIGURE 6.2.10 WATER ADSORPTION

● CONTROL BPL ▲ AGED BPL (RH80%, 22°C, 56 DAYS)

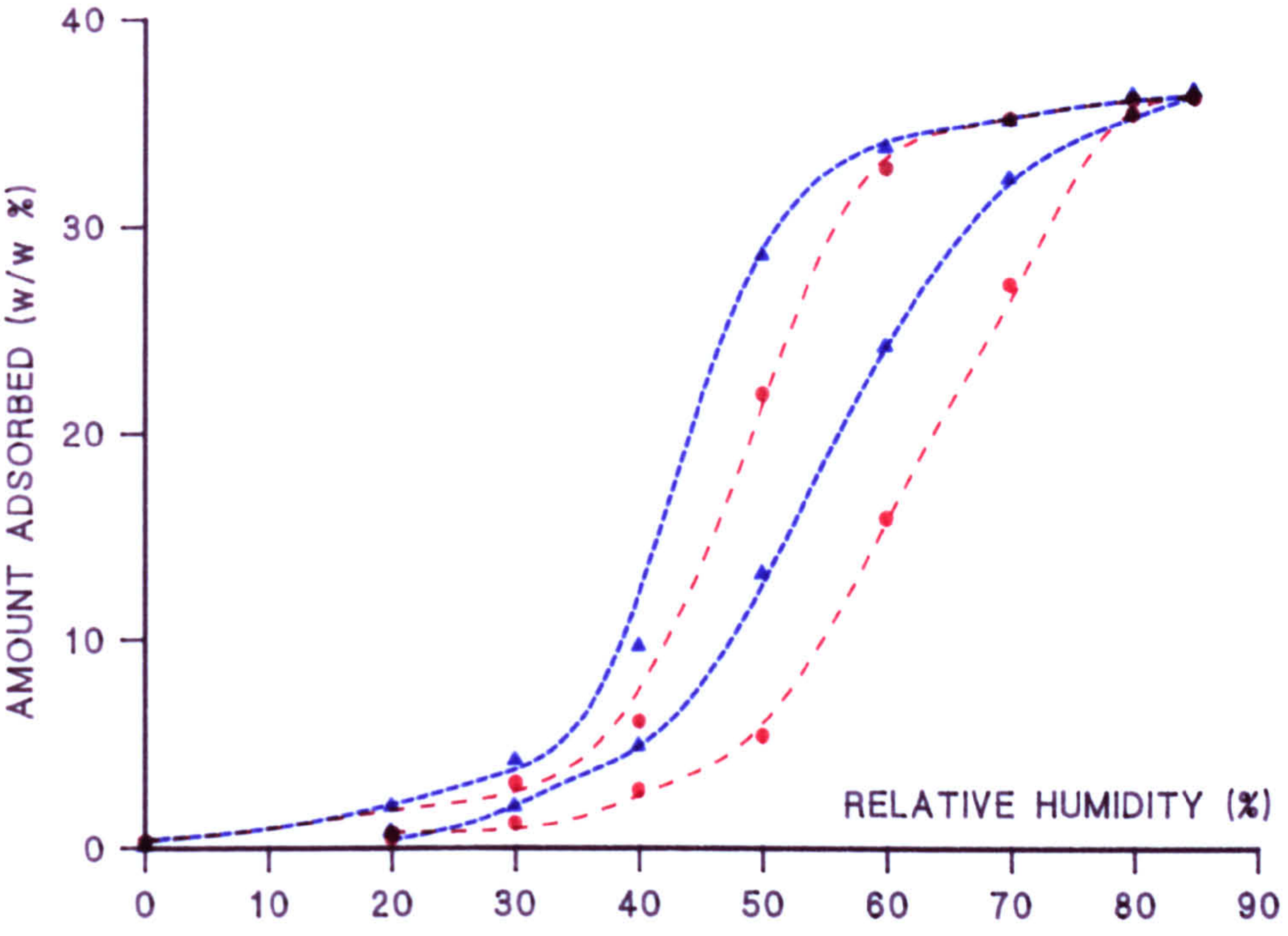

FIGURE 6.2.11 WATER ADSORPTION

● CONTROL BPL ▲ AGED BPL (RH80%, 45°C, 56 DAYS)

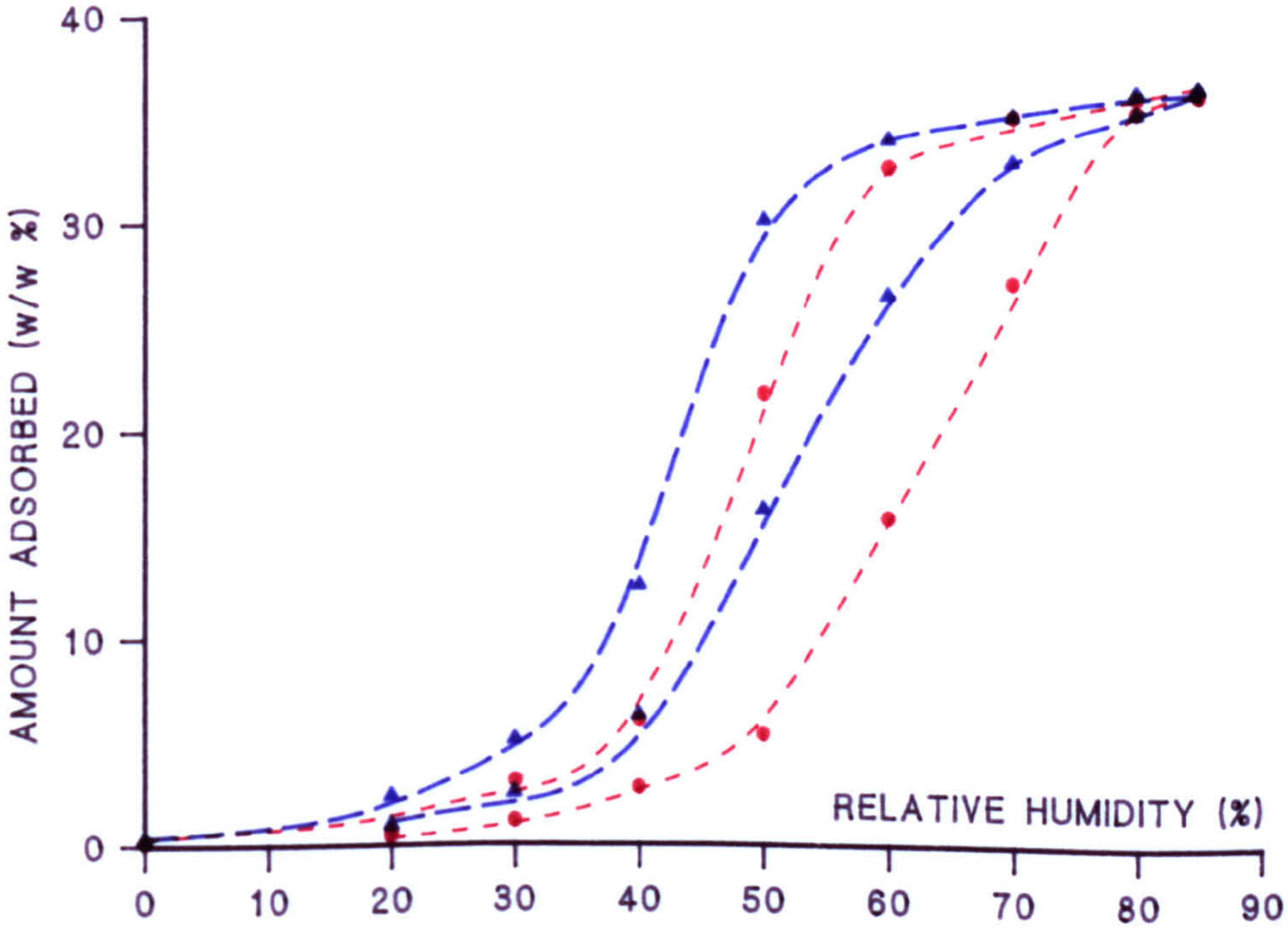

FIGURE 6.2.12 WATER ADSORPTION
AGED BPL (RH80%, 22°C, ▲ 56 AND ● 100 DAYS)

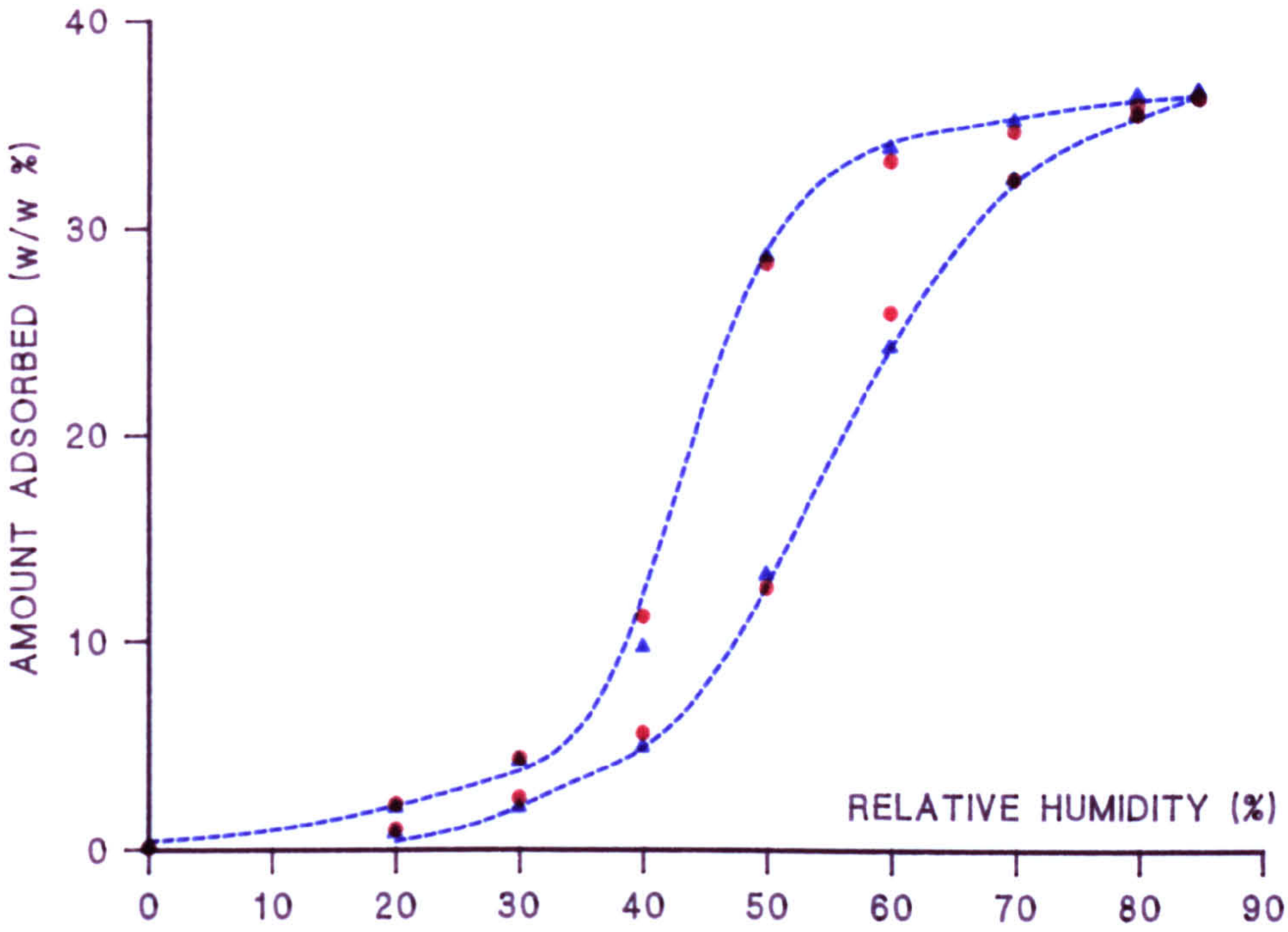

FIGURE 6.2.13 WATER ADSORPTION
AGED BPL (RH80%, 45°C, ▲ 56 AND ● 100 DAYS)

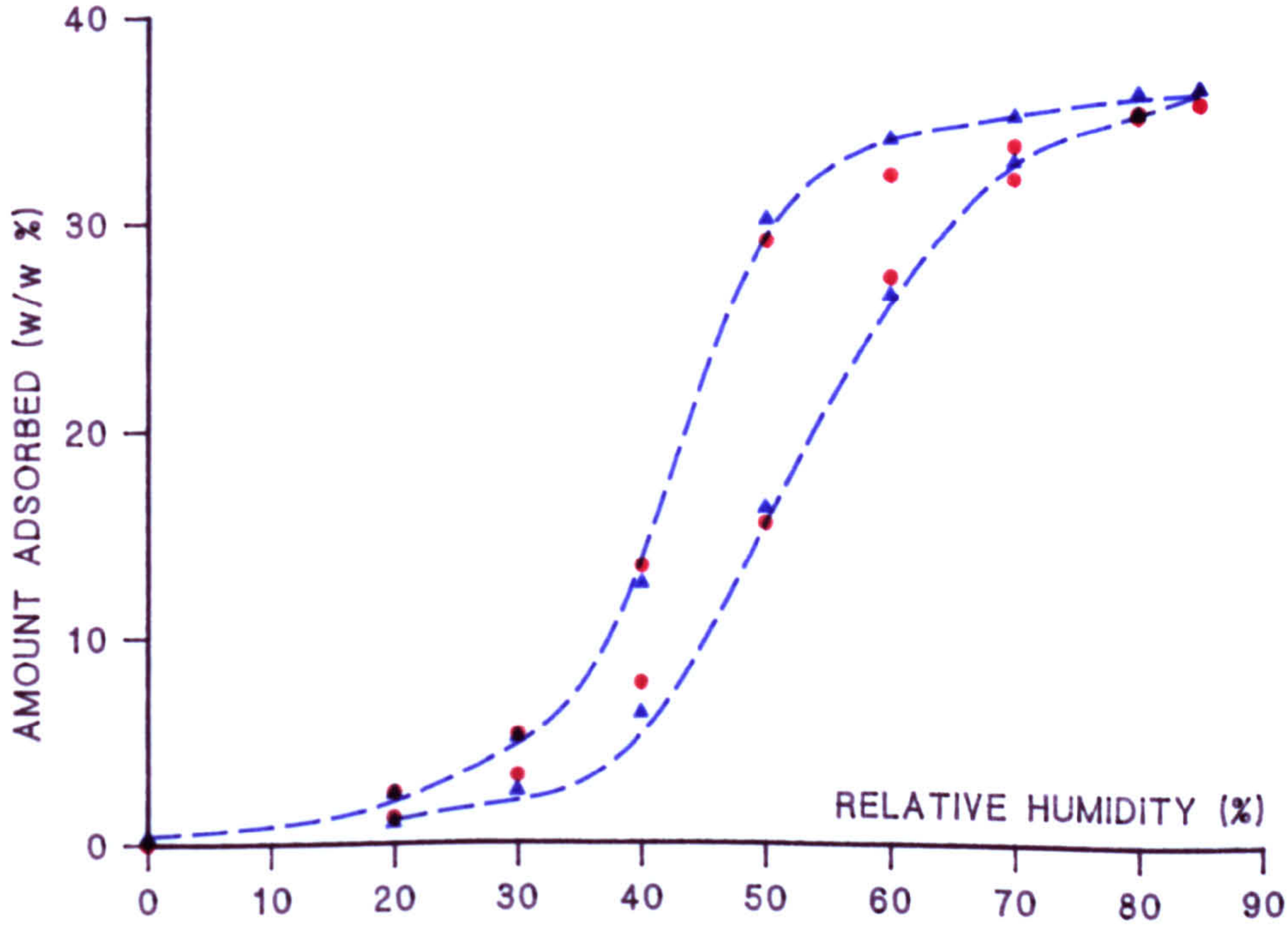

FIGURE 6.2.14 WATER ADSORPTION

AGED BPL (RH80%, ▲ 22°C, 56 DAYS AND ● 45°C, 56 DAYS)

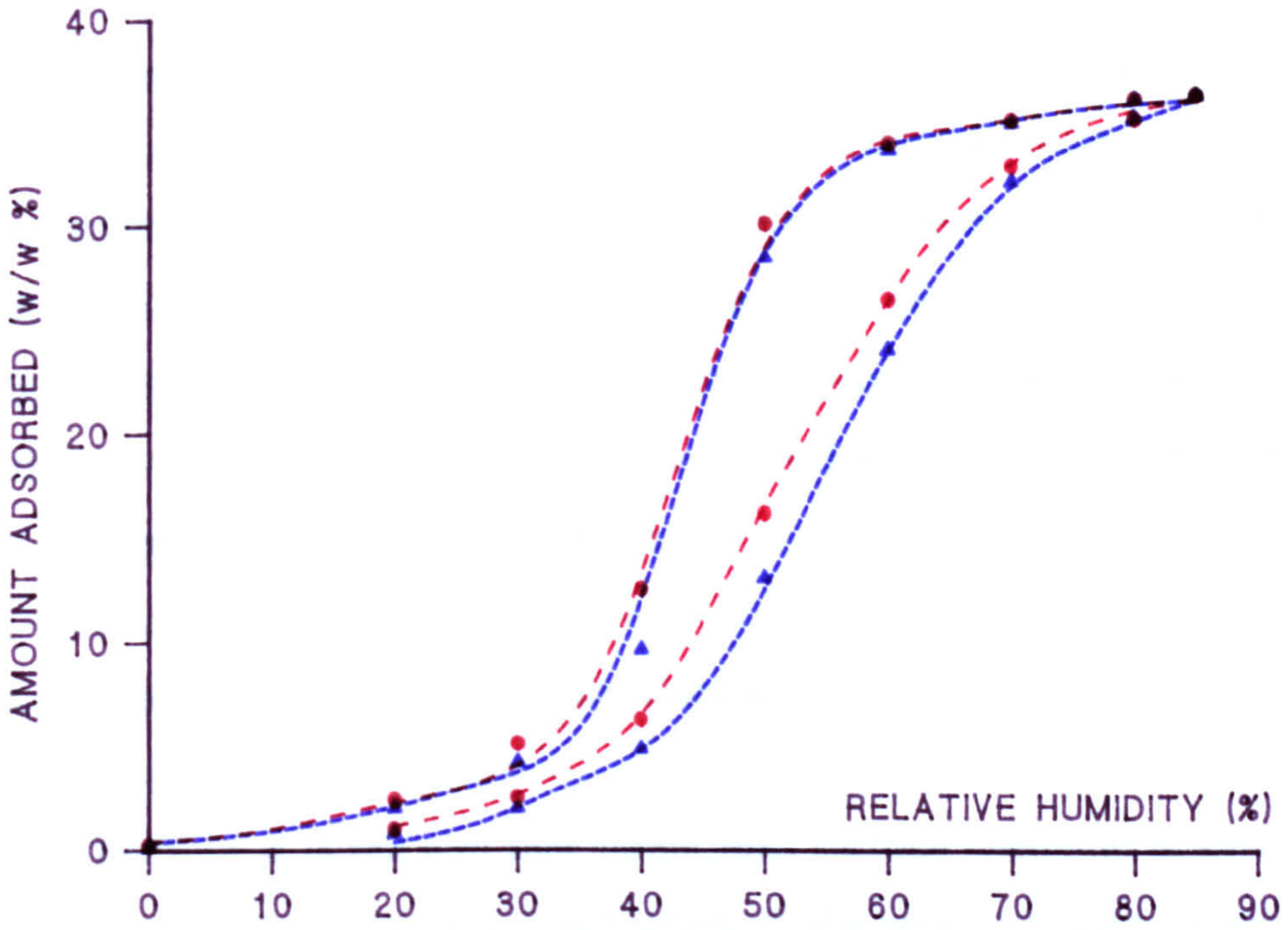

6.3 The Preparation and Properties of NO_2 Oxidised Carbons

The changes in the adsorptive properties of activated carbon brought about by exposure to high humidity air demonstrate well the importance of surface chemistry. Because the changes described above take place over relatively long time periods, an attempt to identify a suitable oxidant which would produce the same effect more rapidly was undertaken.

Nitric acid solution is often used to produce oxidised carbons, but this technique can result in significant structural modification (chapter 3). Oxidation in solution was also avoided because deposition of reagent or reaction products within the pore structure may occur (chapter 3). Thus dinitrogen tetroxide (NO_2), which is a gaseous oxidant at ambient temperature, and which is readily available, was selected. The reagent was obtained from BDH Ltd (>99.5%) and was used without further purification.

6.3.1 Preparation of Modified Adsorbents

Because it is the aim that intentional surface chemical modification should not result in significant disruption of the pore structure, reactions were carried out at 25°C by exposing approximately 20g of dry (120°C; 3 hours; 3 mbar) BPL carbon to a known pressure of NO_2. A layer of carbon (ca. 0.5cm depth) was placed in a glass dish within a desiccator, which was evacuated prior to the introduction of reagent. Aliquots of NO_2 were introduced until the pressure stabilised (ca. 25 minutes) at either 120, 500, 700 or 900 mbar. Samples were then stored overnight (22 hours) prior to outgassing in situ. After removal, the modified carbons were outgassed to constant weight (120°C; 3 hours; 3 mbar). Both aged (400 days at RH80% and 22°C) and control carbons were modified using this technique. Typical weight gains after treatment are shown in table 6.3.1. It is notable that samples aged prior to modification exhibited

consistently lower weight increases compared to control samples. This difference is presumably due to the fact that a proportion of the active sites are occupied by oxygen containing functional groups as a result of ageing, and suggests that both ageing and exposure to NO_2 result in the oxidation of the same sites on the carbon surface.

6.3.2 The Reaction of NO_2 with Activated Carbon

To determine whether the reaction involved significant carbon gasification, gas analysis was performed, and carbon dioxide, nitric oxide (NO) and nitrogen dioxide were detected. Both carbon dioxide and nitric oxide were present in small amounts, but quantification was not possible due to on- column decomposition of NO_2. Some of the NO appeared to result from the reduction of NO_2 on the carbon surface. That the amounts of CO_2 found were small indicates that carbon gasification was not extensive.

Further experimentation revealed that the reaction with NO_2 was rapid, and was essentially complete within ca. 60 minutes, since the adsorptive properties of the modified and outgassed samples (6.3.3) prepared by contact with the reagent for 60 minutes or 22 hours were the same.

The elemental analysis data (table 6.3.2) suggest that reaction primarily results in the incorporation of oxygen, but also in the chemisorption of a small quantity of nitrogen. The nature of any surface nitrogen containing functional groups is unknown, but it is possible that surface nitroso groups might be present. That the oxidation technique is relatively mild is supported by the observation that the ash content of the modified carbon is essentially the same as that of the control.

TDMS analysis did not reveal the presence of any nitrogen containing decomposition products, but in each case, carbon dioxide and monoxide were detected in significant amounts.

6.3.3 Adsorptive Properties

Nitrogen Adsorption

Nitrogen isotherms for samples of NO_2 modified carbons are at figures 6.3.1-6.3.3. Values derived from these measurements are at table 6.3.3. In each case, the data have been corrected using the weight change observed as a result of treatment such that comparison is made on the basis of equal weights of carbon. This approach relies on their being no significant gasification of the carbon, and so in the present case appears to be justified.

Treatment of both control and aged carbons resulted in a small increase in the total pore volume. It must be the case, however, that incorporation of functional groups within the pore structure must, if there is no loss of carbon, result in a decrease in total pore volume when expressed on the basis of unit weights of carbon. That the total pore volume is slightly increased must reflect loss of carbon due to gasification. This implies that the use of gravimetric changes in these examples leads to an overestimate of the carbon content of the adsorbent, and an underestimate of pore volume. That the hysteresis loops on the isotherms do not close completely may indicate that the generation of surface functional groups has introduced a degree of restriction toward nitrogen adsorption and desorption for some of the pores. The small difference in the quantities of hexane adsorbed supports the contention that NO_2 modification does not result in a major disruption of the pore structure (table 6.3.4).

Water Adsorption

Figures 6.3.4-6.3.8 show water isotherms for samples of modified carbons. As before, the data has been corrected using the gravimetric changes resulting from modification.

The enhancement in the quantity of water adsorbed at low RH values (below ca. RH60%) in comparison to control samples is consistent with a significant increase in surface polarity (6.2). The similarity of the isotherms for the control and aged samples treated with NO_2 at 900 mbar (figure 6.3.6) may indicate that these samples are "fully aged". It is also notable that the hysteresis loops on the isotherms are tighter in comparison to the respective controls, and that they almost close at low values of the RH. It is probable that the reason for the failure of the hysteresis loops for the control carbons to close (figures 6.3.4-5) is that ageing is occurring during measurement of the isotherm, and that the adsorbent is, at the end of the measurement, a different material. This implies that the carbons exposed to NO_2 (900 mbar) do not age during exposure to humid air, supporting the view that the samples may be "fully aged". Figure 6.3.7 compares the isotherms for samples of aged BPL (400 days), and control BPL exposed to 120 mbar of NO_2. That they are very similar suggests that the oxidation technique may be a convenient way of producing aged carbon for further experimental study. The functional groups present on both samples may not be identical, however.

Figure 6.3.8 shows the isotherms (adsorption branches only) for control samples oxidised using increasingly greater treatment pressures. The data illustrate well the dependence of treatment pressure on the extent of oxidation.

Methanol Adsorption

As before, methanol adsorption has been used to follow the changes in surface polarity that result from treatment. Figure 6.3.9 shows a family of methanol breakthrough curves measured for control and aged carbon, and aged carbon modified using NO_2 pressures of 500 and 900 mbar. Treatment of the aged carbon at 500 mbar results in a large increase in the delay of methanol breakthrough (and therefore a significantly greater amount of methanol is

adsorbed). Increasing the treatment pressure to 900 mbar only results in a comparatively small shift in the breakthrough curve. That treatment at the higher pressure only causes a small increase in methanol adsorption may be due to the fact that the lower pressure is sufficient to oxidise the majority of the active sites. It may be the case, however, that the change to both the methanol adsorption profile, and the water isotherm, is only dependent on the presence of polar groups up to a certain degree of surface coverage. The methanol adsorption characteristics are consistent with the water adsorption properties of the samples (6.2). Methanol adsorption data for the controls, and some of the modified carbons are at table 6.3.5.

Chloropicrin (PS) Adsorption

Ageing carbons in humid air was shown to result in a major decrement in the efficiency of PS adsorption from humid air. Similarly, the performance of the NO_2 modified carbons was found to be poor, presumably for the same reason (table 6.3.6). In fact, the decrement in performance becomes greater with increasing NO_2 treatment pressure, illustrating that a direct relationship exists between the extent of oxidation (increasing surface polarity) and the performance of carbon filters against volatile hydrophobic chemicals in the presence of humid air. Under the most severe treatment conditions, an almost 60% loss of performance results. Comparison of the PS adsorption data with that for carbon aged at RH80% (figure 6.2.6) may indicate that carbons modified using these techniques might not contain the same types of functional groups: that is, the adsorption efficiency of the aged carbon after more than 3 years storage is significantly greater in comparison to the carbon exposed to 900 mbar of NO_2.

The mechanism of PS adsorption by NO_2 modified carbon is considered in more detail at chapter 9. The use of such carbons as precursors for further chemical transformations is considered at chapter 8 (section 8.5).

Table 6.3.1 Increase in Carbon Weight after NO_2 Modification

Treatment Pressure (mbar)	Weight Gain (w/w%; dry carbon) Control	Aged
120	1.9	1.2[a]
500	3.4	2.8
700	3.8	3.2
900	4.0	3.3

[a]This sample was aged for 200 days at RH80% and 22°C prior to modification: the remaining samples were aged for 400 days under these conditions.

Table 6.3.2 Elemental Analysis of Control, Aged, and NO_2 Modified Carbons

Sample	Element (w/w%)					
	C	H	N	O	S	ASH
BPL Control	86.6	0.2	0.5	2.0	1.2	7.5
BPL Aged (860 days; RH80%; 22°C)	85.2	0.3	0.5	4.1	1.0	7.3
BPL Control, NO_2 Modified (900 mbar)	85.0	0.2	0.9	7.4	1.0	7.4
BPL Aged (as above), NO_2 Modified (900 mbar)	83.2	0.2	0.9	8.3	1.1	7.4

The results are an average of at least two determinations

Table 6.3.3 Nitrogen Adsorption

	Sample					
	Control	Control 500 mbar	Control 900 mbar	Aged*	Aged 500 mbar	Aged 900 mbar
Surface Area ($m^2\ g^{-1}$)	1182	1122	1094	1124	1096	1101
Total Pore Volume ($ml\ g^{-1}$)	0.60	0.65	0.64	0.55	0.62	0.58
Primary Micropore Volume	0.35	0.35	0.38	0.34	0.33	0.35
Secondary Micropore Volume	0.15	0.18	0.15	0.14	0.17	0.15
Mesopore Volume	0.09	0.12	0.11	0.08	0.12	0.09

The results are for single determinations. Typical error on measurement of surface area is ± $12m^2g^{-1}$, and ± 0.01 cm^3<STP>g^{-1} for the total pore volume (per gramme of carbon).*Samples were aged for 400 days prior to modification.

Table 6.3.4 Hexane Adsorption

Treatment Pressure (mbar)	Control Total Uptake mg g^{-1}	Control TT50% (min)	Aged Total Uptake mg g^{-1}	Aged TT50% (min)
None	254	56	250	57
120	-	-	230	52
500	224	50	225	51
700	233	54	229	52
900	-	-	220	53

TT50% is the time in minutes to 50% hexane filter breakthrough.

Table 6.3.5 Methanol Adsorption

Treatment Pressure (mbar)	Control Total Uptake mg g^{-1}	Control TT50% (min)	Aged Total Uptake mg g^{-1}	Aged TT50% (min)
None	19	36	28	53
120	30	60	30	58
500	38	77	38	79
700	40	79	39	79
900	-	-	41	84

TT50% is the time in minutes to 50% methanol filter breakthrough.

Table 6.3.6 Chloropicrin (PS) Adsorption

Treatment	Control		Aged	
Pressure (mbar)	TTB (min)	TT1% (min)	TTB (min)	TT1% (min)
None	81	96	54	66
120	69	83	50	64
500	40	45	32	39
700	36	41	30	36
900	31	37	29	35

TTB is the time in minutes at which PS was first detected in the filter effluent (10-15 mg m^{-3}). TT1% is the time to 1% filter penetration (50 mg m^{-3} PS)

{2cm diameter, 2cm bed depth filters, challenged with PS at 5000 mg m^{-3} in equilibrium with RH80% air at 22°C. The flow velocity was 382 cm min^{-1}.}

FIGURE 6.3.1 NITROGEN ISOTHERMS FOR BPL CARBON

● CONTROL AND ■ NO_2 (500 mbar) MODIFIED BPL

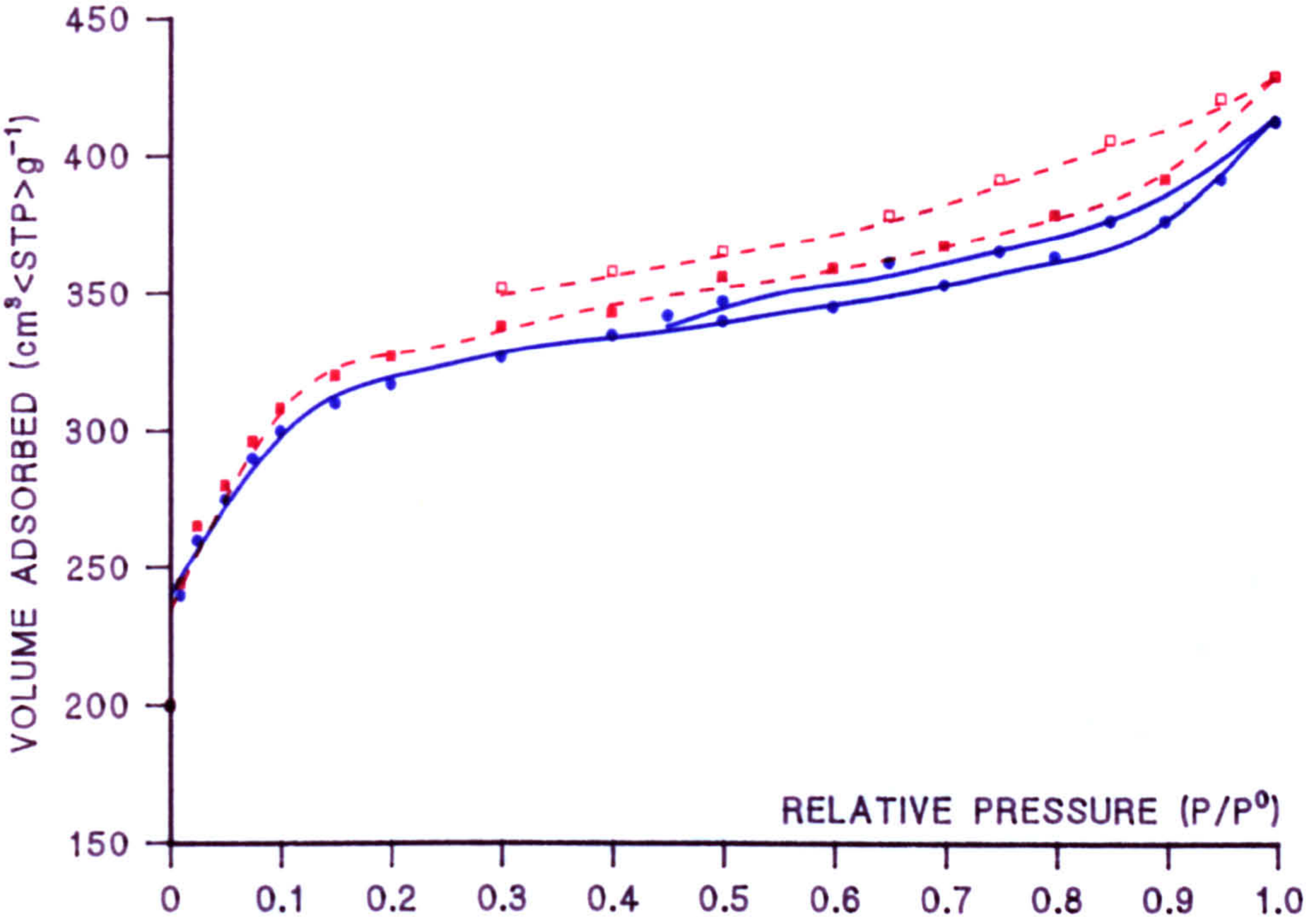

FIGURE 6.3.2 NITROGEN ISOTHERMS FOR BPL CARBONS

● AGED CONTROL ■ AGED, NO_2 (500 mbar) MODIFIED

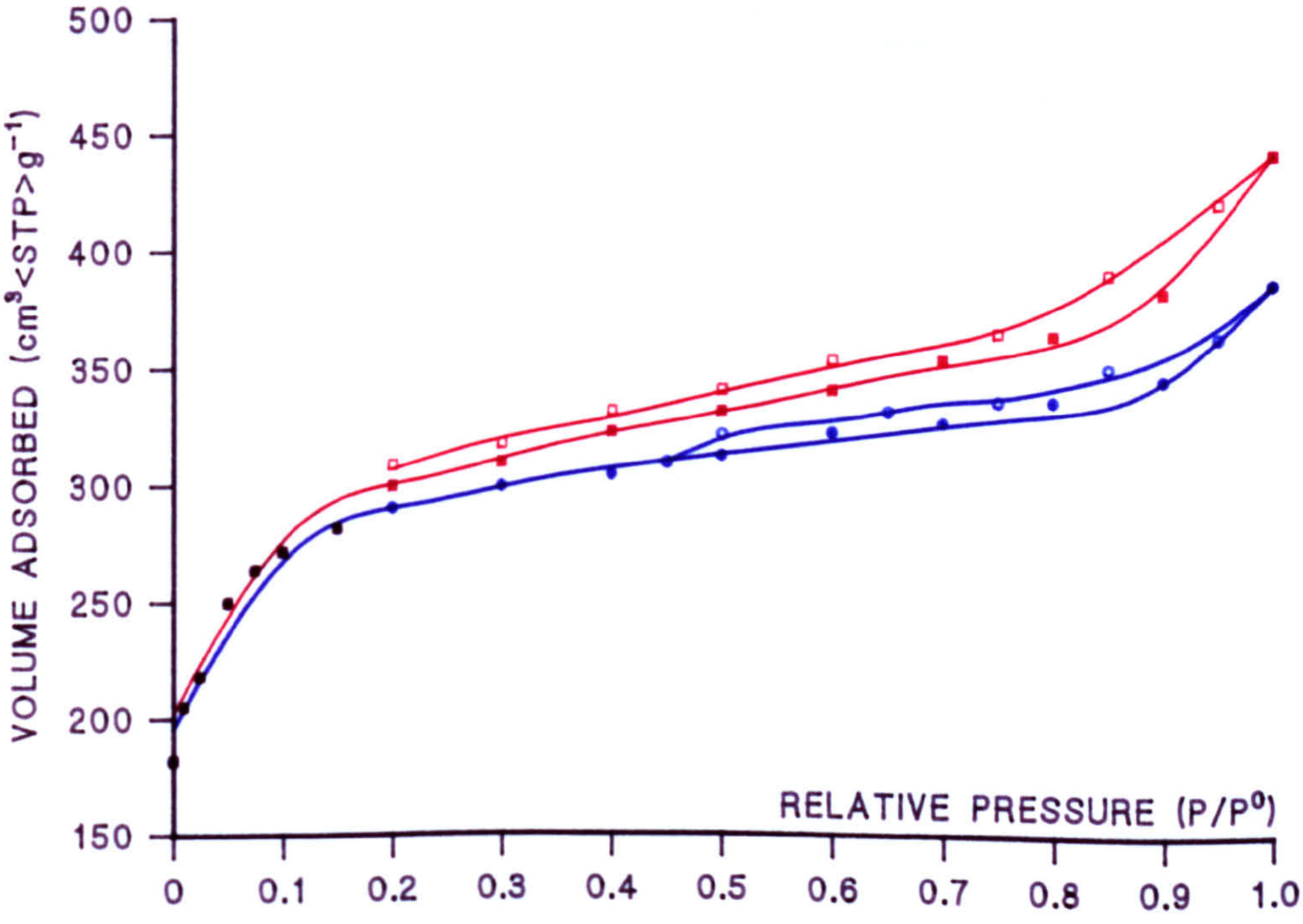

FIGURE 6.3.3 NITROGEN ISOTHERMS FOR BPL CARBON

NO_2 ● 700 mbar AND ■ 900 mbar MODIFIED BPL

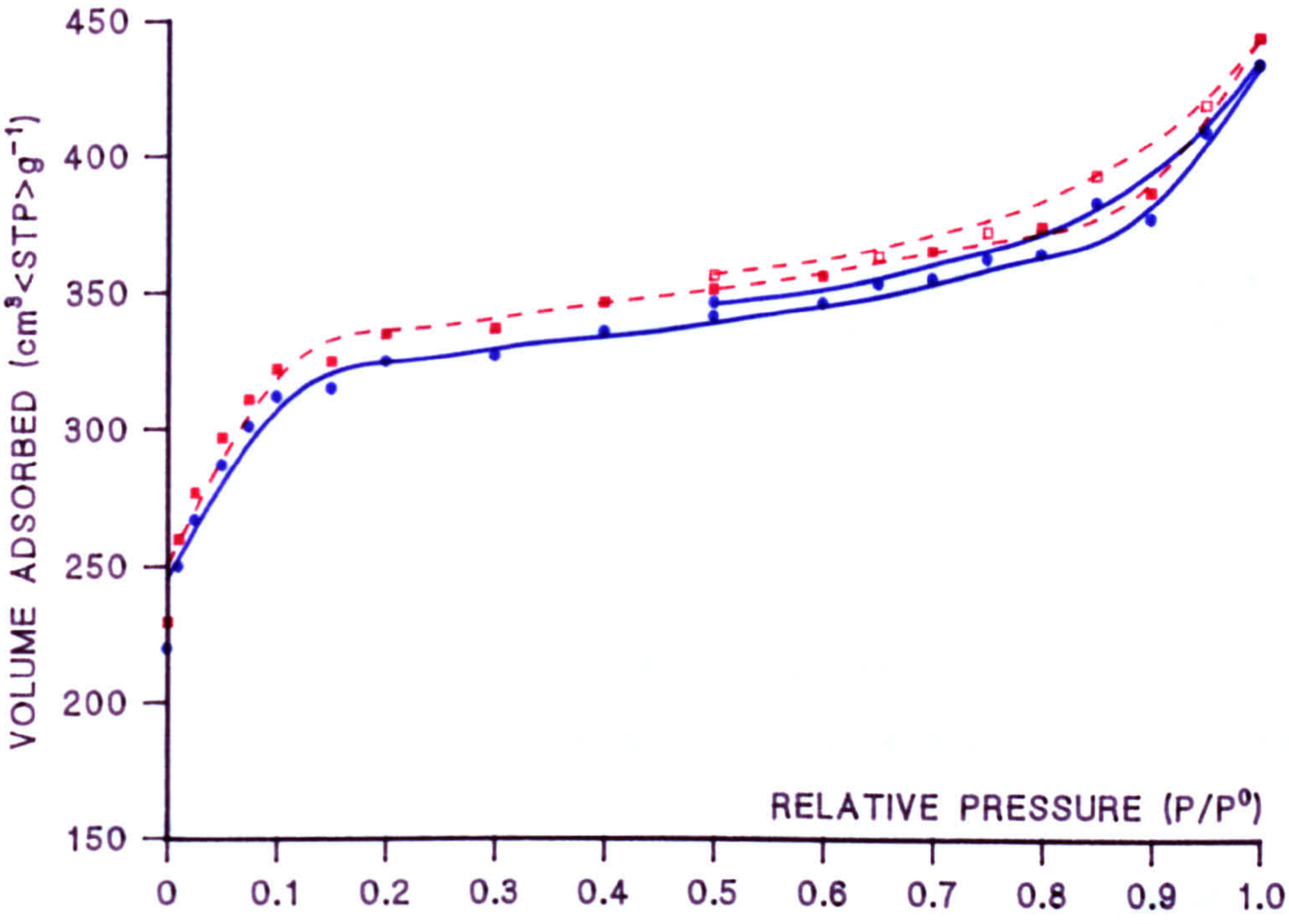

FIGURE 6.3.4 WATER ADSORPTION

● CONTROL BPL ▲ NO_2 MODIFIED (900 mbar) BPL

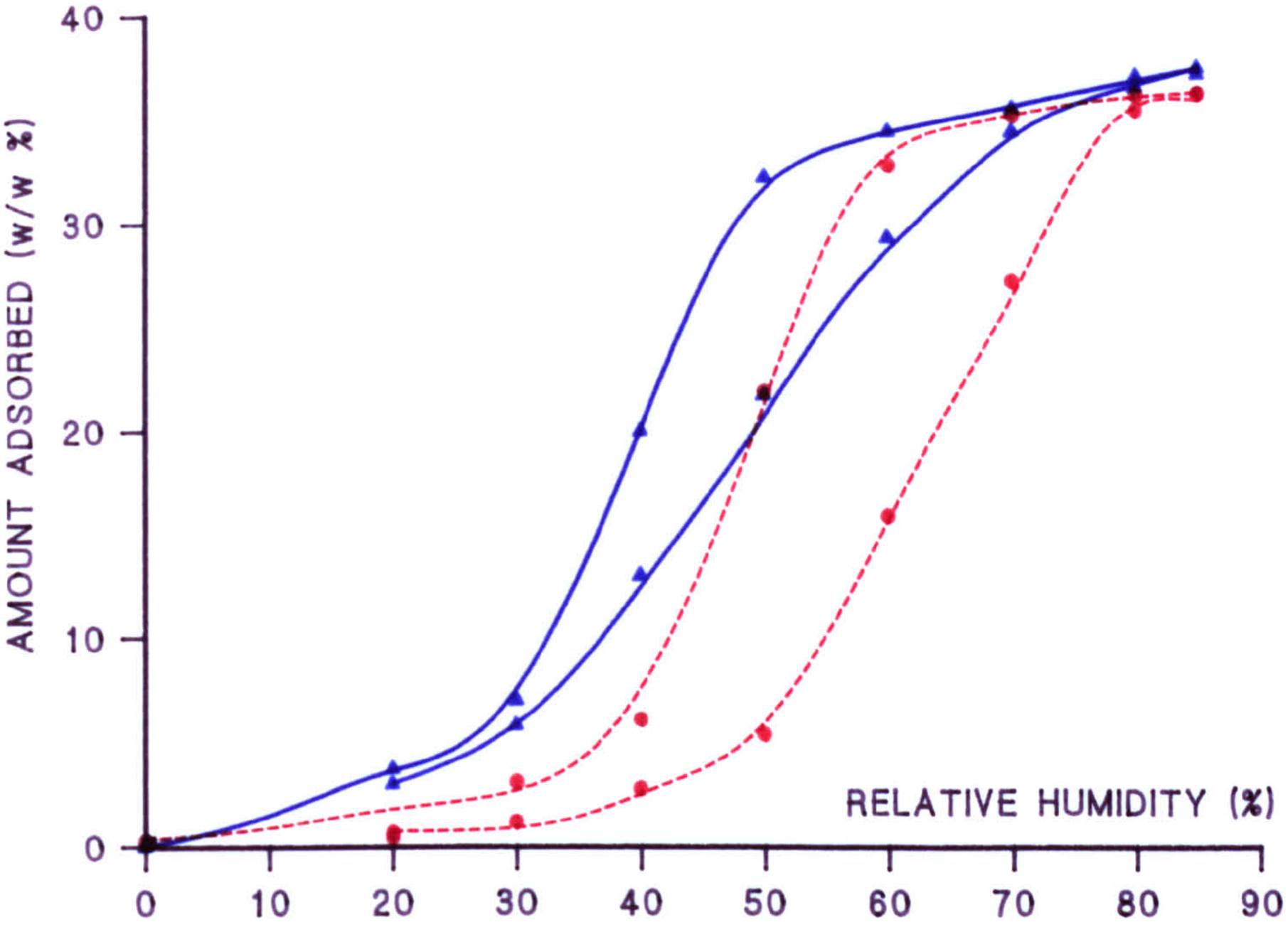

FIGURE 6.3.5 WATER ADSORPTION

▲ BPL AGED (400 DAYS, RH80%, 22°C) AND ● AGED NO_2 (900 mbar) MODIFIED

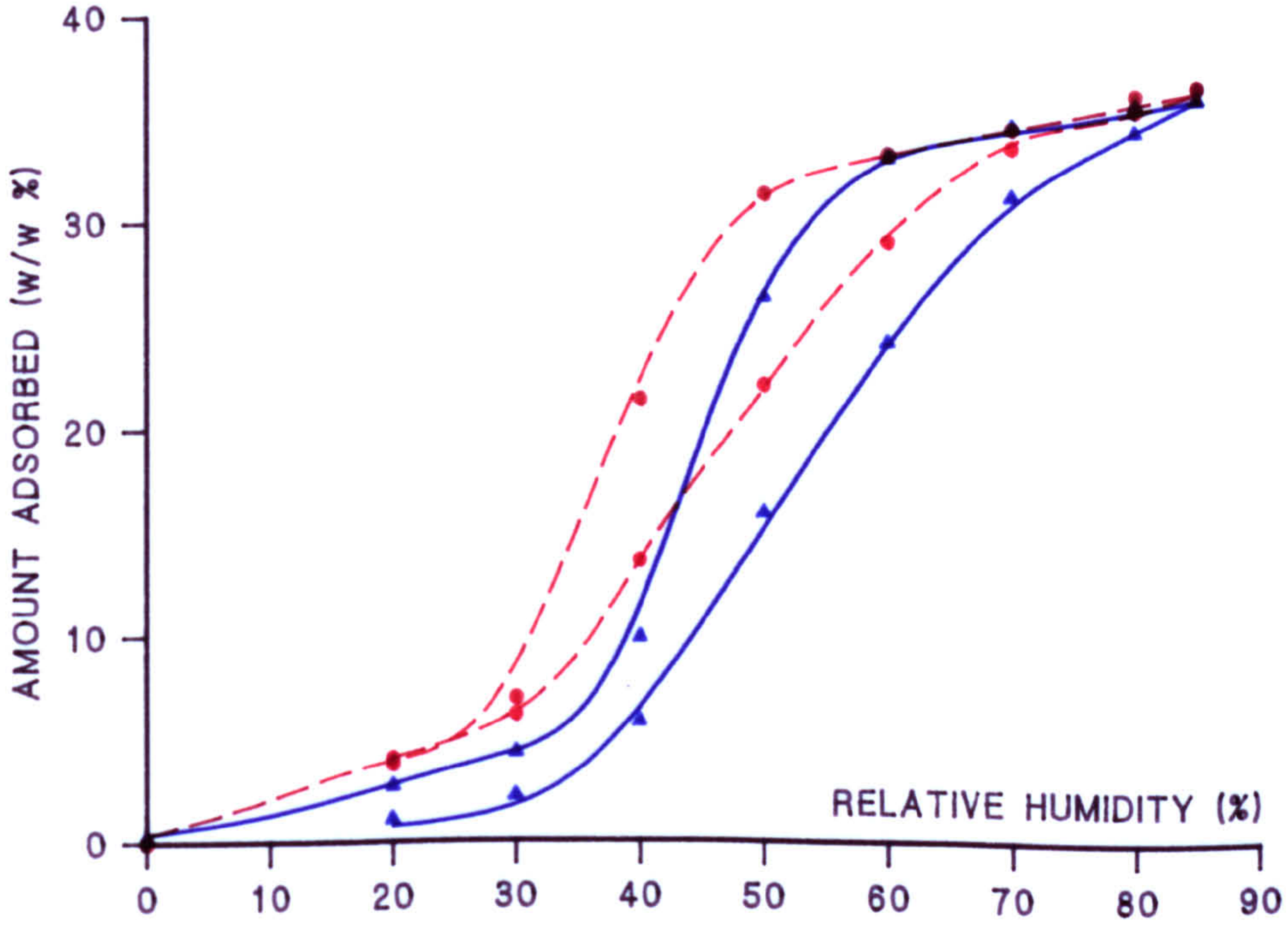

FIGURE 6.3.6 WATER ADSORPTION

▲ CONTROL AND ● AGED BPL, NO_2 MODIFIED (900 mbar)

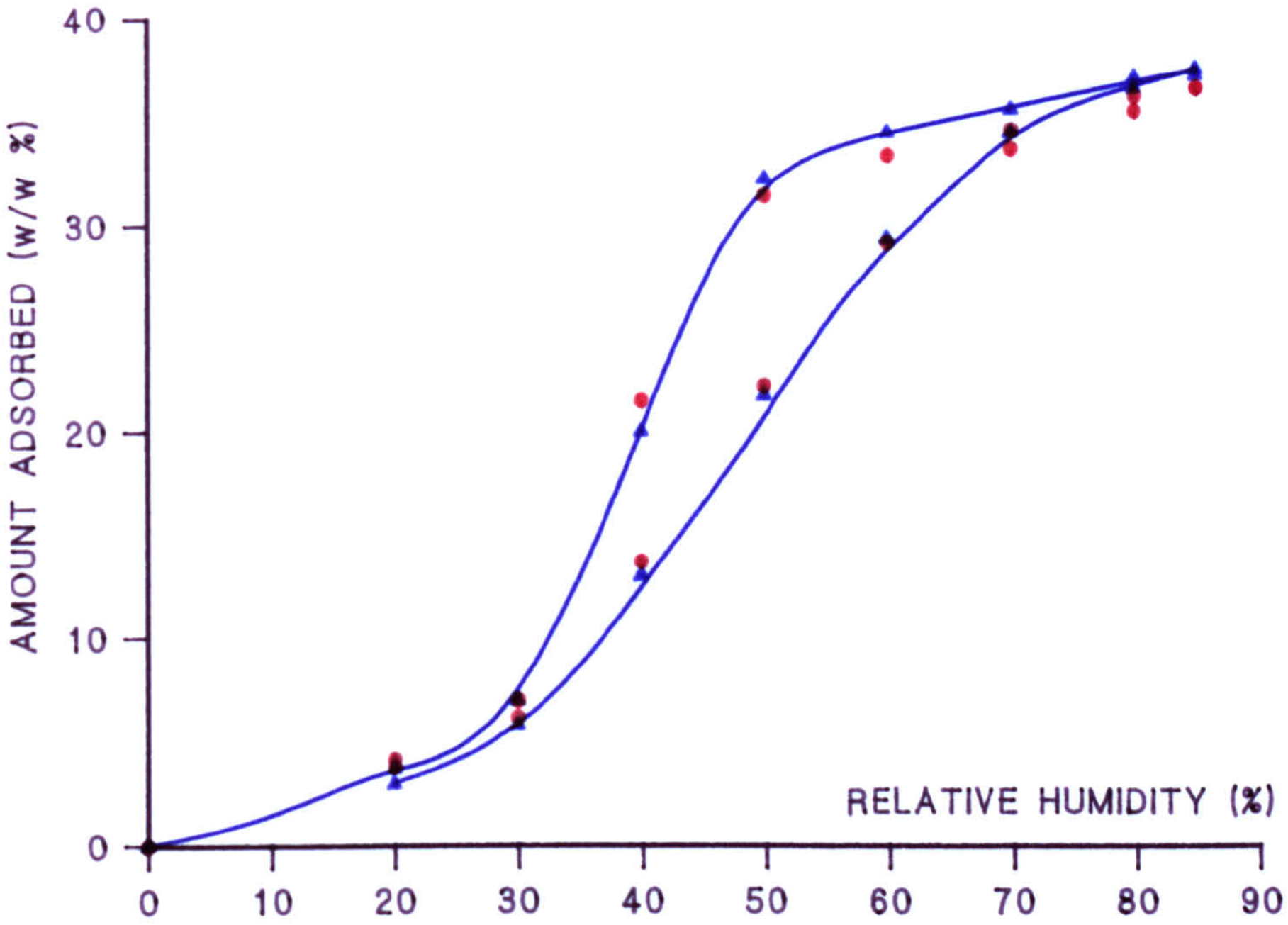

FIGURE 6.3.7 WATER ADSORPTION

▲ BPL (AGED 400 DAYS, RH80%, 22°C) AND ● NO_2 (120 mbar) MODIFIED

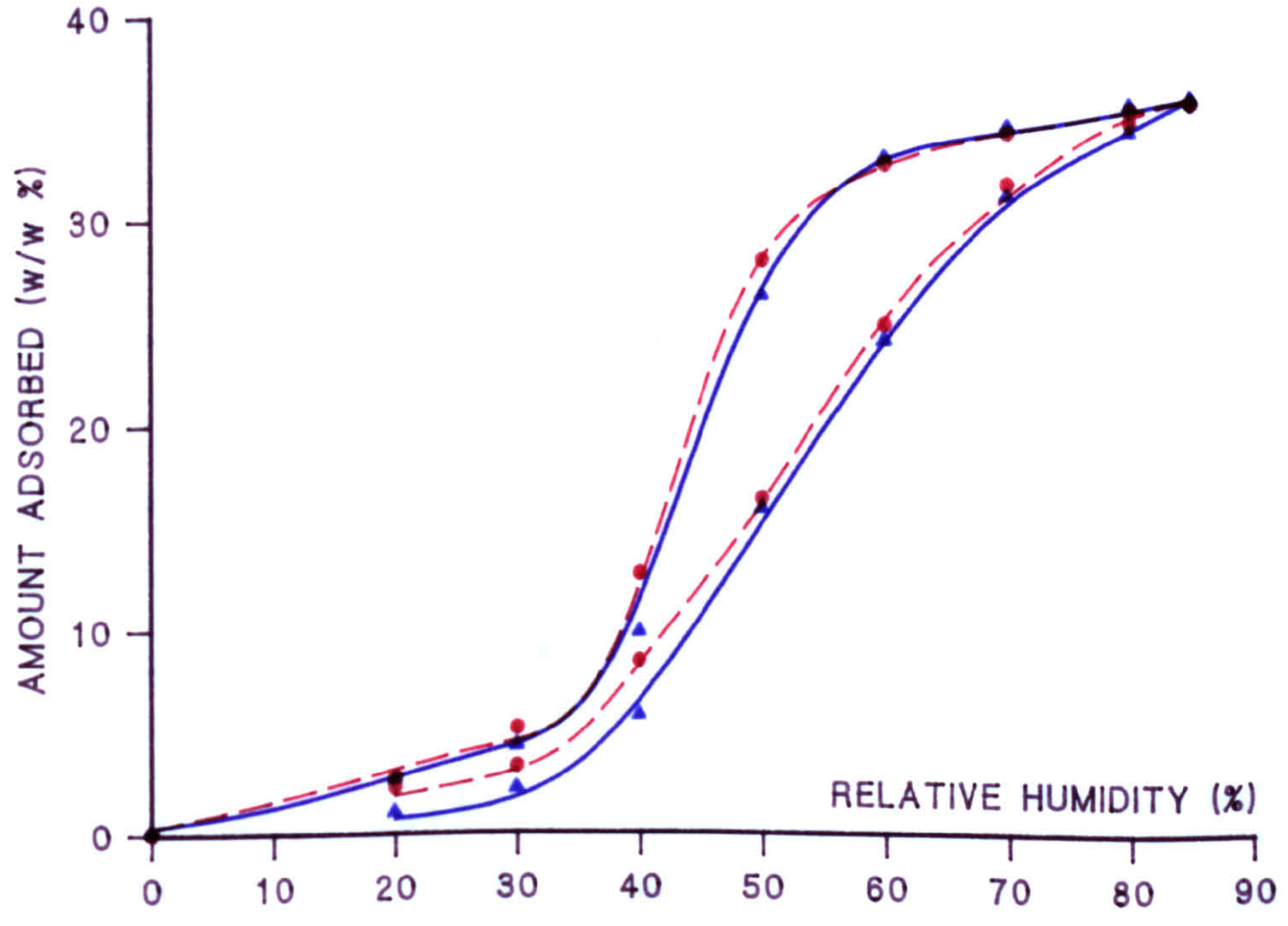

FIGURE 6.3.8 WATER ADSORPTION

▲ CONTROL, NO_2 MODIFIED (■ 120, ● 500, ◆ 700, ▬ 900 mbar) BPL

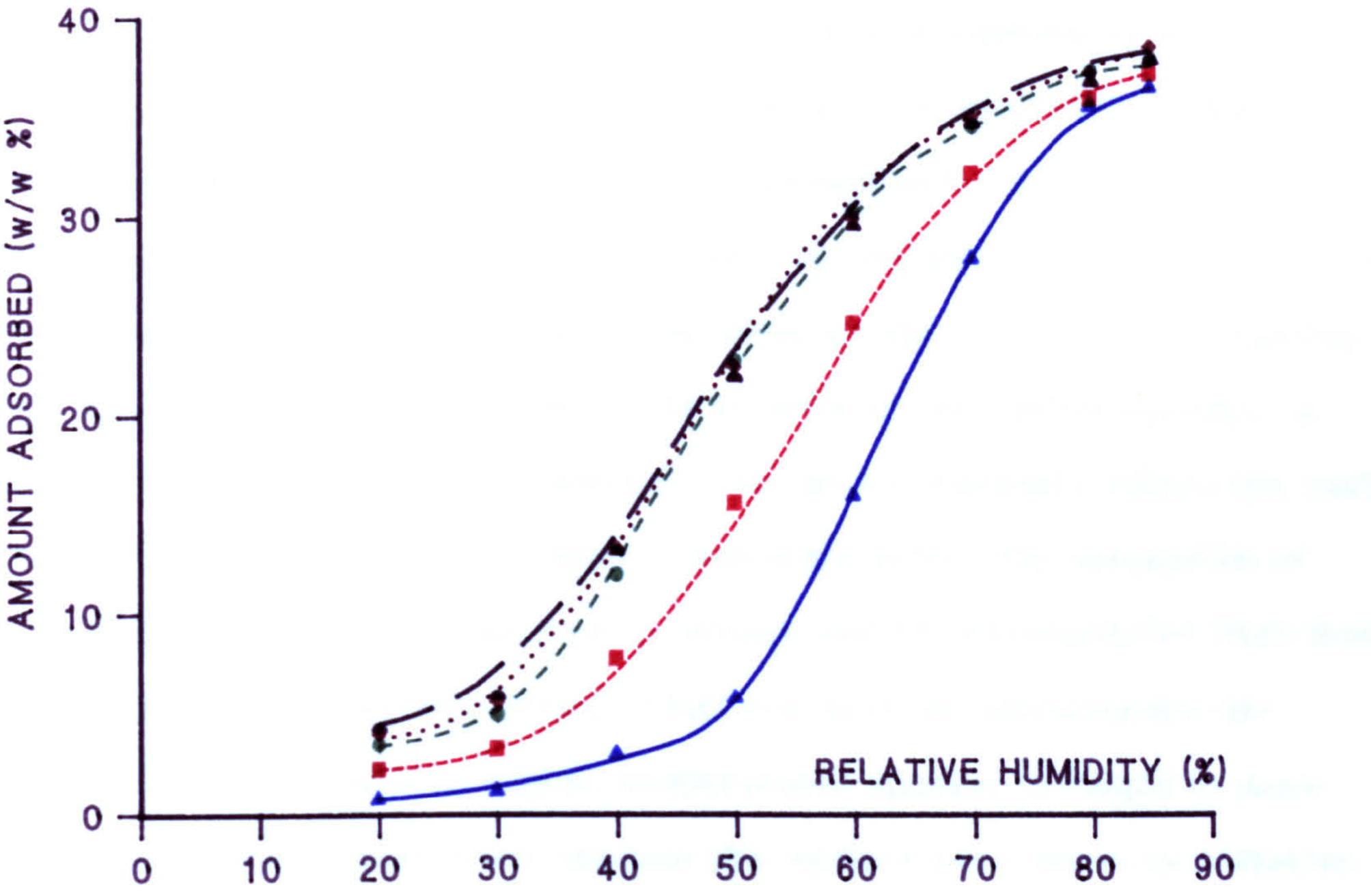

FIGURE 6.3.9 METHANOL BREAKTHROUGH CURVES

L-R: (BPL) CONTROL; AGED (400 DAYS); AGED AND NO_2 MODIFIED– 500, 900 mbar

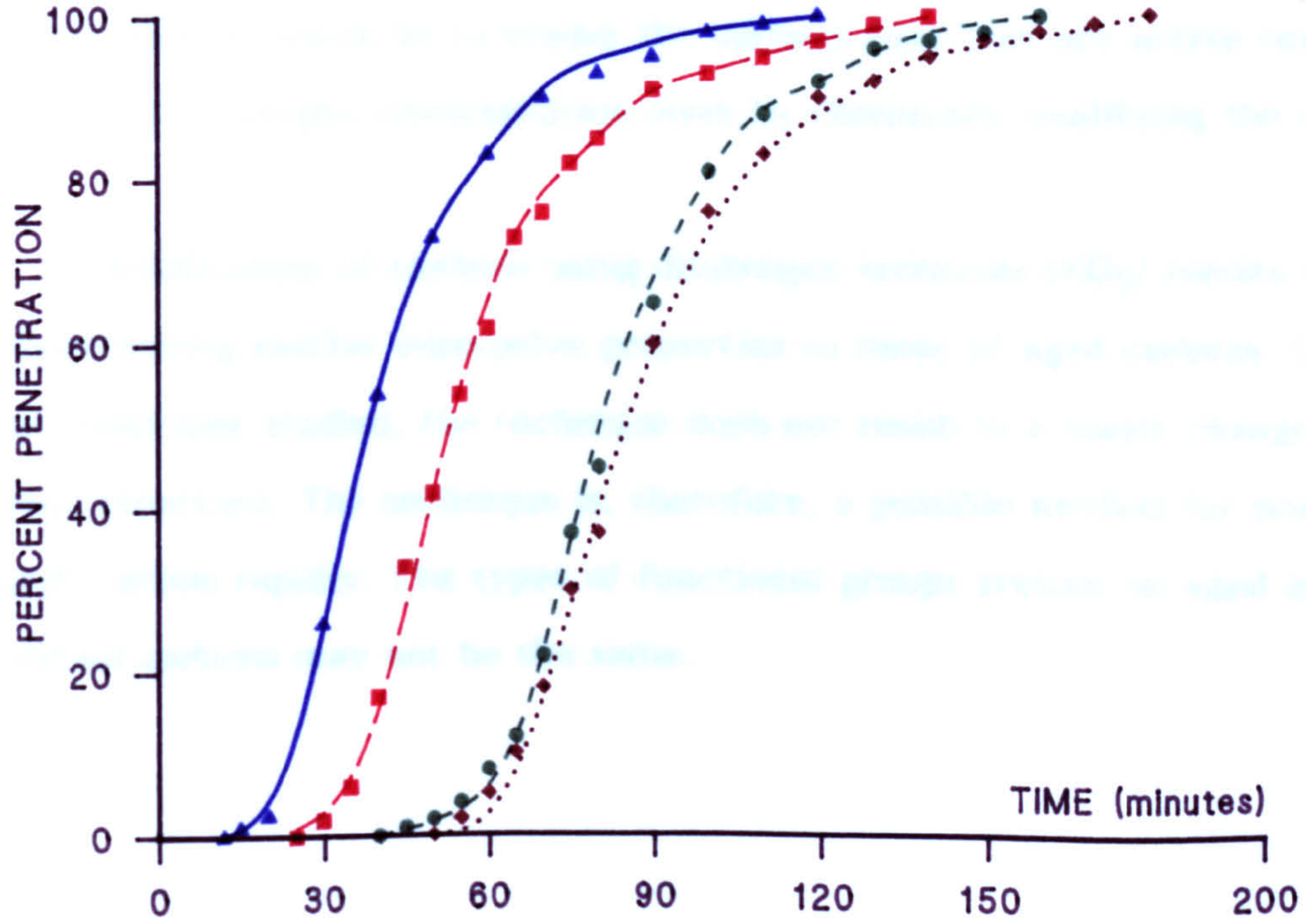

6.4 Summary

The adsorptive properties of activated carbons exposed to dry air, or to air of low relative humidity (RH), do not change after extended storage periods. Storage of carbons under conditions more representative of use (ie. high RH; >60%) results in a permanent change in some of the adsorptive properties due to the generation of oxygen containing functional groups at the surface (ageing). These groups result in an increase in the polarity of the carbon surface, as shown by methanol and water adsorption, but do not markedly affect the carbon structure (porosity). They do, however, indirectly affect the adsorption of volatile hydrophobic chemicals such as hexane and PS (chloropicrin) from humid air, with the result that substantial reductions in filter performance are observed. Ageing carbons at higher temperatures appears to result in more extensive oxidation, presumably because the surface sites prone to oxidation possess a broad range of activation energies.

One way in which ageing can be limited is to maintain the RH of the airflow passing through filter beds at or below RH40%: such a solution is not practical in some cases, however (eg. individual protective respirators). A more elegant solution would be to render the surface sites that are active toward water and/ or oxygen chemisorption inert by chemically modifying the carbon.

Modification of carbons using dinitrogen tetroxide (NO_2) results in carbons having similar adsorptive properties to those of aged carbons. Under mild conditions studied, the technique does not result in a major change in carbon structure. The technique is, therefore, a possible method for producing "aged" carbon rapidly. The types of functional groups present on aged and NO_2 modified carbons may not be the same.

CHAPTER 7

Chemical Modification of Activated Carbon using Fluorinating Reagents

Results and Discussion

The Interaction of Carbon with Molecular Fluorine

7.1 Introduction

The results of chemically modifying activated carbon using fluorine are presented in this section. The preparative techniques and the adsorptive properties of the modified carbons will be described.

The results are discussed in the context of the aims of the present research, which are the effect of the modification upon the carbon structure, the carbon vapour adsorption characteristics, and the stability of the modified adsorbents in the presence of humid air. Consideration to a possible reaction mechanism will also be given.

Direct fluorination has been reported prior to this study (chapter 3), although little attention has been given to the adsorptive properties of the modified products in the context of this present research. It is also apparent that some disagreement persists with regard to the stability of the modified carbons, and their vapour adsorption properties.

Carbon modification using fluorine may offer some advantages because fully fluorinated surfaces are relatively inert, and are hydrophobic. Such carbons may therefore prove to be useful for the adsorption of volatile hydrophobic vapours in the presence of humid air. In addition, they may afford resistance to carbon ageing effects.

7.1.1 The Preparation of Modified Adsorbents

The three activated carbons described at chapter 5 have been used in this part of the study. The carbons were used as received, and were not aged prior to modification.

Because of the reactivity and toxicity of molecular fluorine, a survey was carried out to identify a suitable system within which the reagent could be handled. Nickel is most suitable, but is costly. An alternative medium, stainless steel 316 grade, was identified, and a reactor vessel and gas handling system was designed and constructed. This could be used at a maximum temperature of 200°C, and is detailed at the Appendix (the low temperature modification apparatus).

No attempts were made to modify carbons using pure fluorine; thus low gas concentrations (5 and 10% volume in nitrogen or helium) were obtained from Gas and Equipment Ltd., Stratford, London, and were used without further purification.

The purity of the mixture was greater than 99.5%, and the principle impurities were air and hydrogen fluoride (0.05% and 0.02% volume respectively- manufacturers data). Analysis of the gas mixture using GC-MS (Finnegan Ion Trap Detector; 2mm x 2m glass column, Poropak QS, 80°C, 18 $cm^3\ min^{-1}$ helium carrier gas) revealed that trace quantities of nitrogen trifluoride were also present.

Prior to reaction, the system was passivated by introducing reagent into the empty vessel and storing overnight. High concentrations of fluorine remained after passivation, as shown by the use of a simple detector (filter paper soaked in methyl iodide solution- approximately 25ppm detection limit).

Carbon samples (approximately 30g) were outgassed in situ at 120°C for 3 hours (1 mbar or better), and were then cooled to ca. 25°C. Fluorine gas was introduced to a pressure of about 1700 mbar, and left until the fluorine was consumed. Typically, this took one hour. The vessel was re-evacuated, prior to the introduction of further reagent (second treatment cycle), or was purged with high purity nitrogen before removal of the modified carbons. After removal, samples were outgassed at the reaction temperature or 120°C (3 mbar) (which ever was the greater) until constant weight was attained. Some of the samples prepared below 120°C were outgassed at 150°C.

It was found that the quantity of fluorine adsorbed was dependent on the number of treatment cycles, and that substantial quantities were fixed at 25°C (table 7.1.1). Carrying out the reaction at higher temperature (190°C) had no measurable influence upon the amount adsorbed. In addition, it was observed that small quantities of carbon dust were formed: presumably, this was due to the fracture of some of the granules caused by fluorine adsorption (or absorption).

7.1.2 The Reaction of Fluorine with Activated Carbon

To determine whether reaction resulted in significant carbon gasification, gas analysis was performed. Thus, after consumption of the fluorine, aliquots of gas were removed from the vessel into a Lamofoil M12/12/75 bag fitted with an inlet valve and septum. Samples were analysed using a GC-MS (7.1.1).

A number of gaseous products were detected, including saturated fluorocarbon homologues. For BPL, sulphur fluorides (sulphuryl fluoride, sulphur hexafluoride) were also found. Components were identified by analysing the mass spectrum of each peak in the ion chromatogram (a typical chromatogram of the gases formed during fluorination of BPL at 25°C is at figure 7.1.1).

Quantification was achieved by reference to gas standards of known concentration. This involved determining the extent of adsorption of the gaseous products by the carbon. Thus, known amounts of the pure components were injected into the empty vessel, and into the vessel containing carbon. This approach enabled the quantities of gaseous product generated per gram of carbon to be established. Table 7.1.2 shows the compounds identified, and the amounts of adsorbent gasified during reaction. It is apparent from these data that the extent of carbon gasification was small even at 190°C. This is supported by elemental and gravimetric analysis of the modified carbons, because the quantities of fluorine found were in good agreement (table 7.1.1). It was observed, however, that the ash content of the carbons (by analysis) was reduced by approximately 50% as a result of fluorination. Since no inorganic gaseous fluorides (eg. SiF_4) were detected during GC-MS analysis, the most likely explanation is that ash-fluorides were formed, which were relatively stable except under the ashing conditions employed (combustion in air at 800°C- see Appendix). Control BPL carbon contained approximately 7.5 w/w% ash, and CECA carbon about 3%.

Comparing the elemental analysis data on the basis of the molar ratio of each element to that for carbon (that is, calculating the number of moles of each element on the basis of the amount per gram of adsorbent, and normalising these values to that for carbon) revealed that reaction results in the fixation of fluorine and a reduction in the hydrogen content of the carbon (table 7.1.3).

EDX analysis revealed that high concentrations of fluorine were present at the surface (figure 7.1.2, BPL carbon). XPS analysis indicated that simple surface fluorides were formed (carbon bound to single fluorine atoms), an observation consistent with the most plausible reaction sequence. The XPS data are considered in more detail in the section describing the interaction of 1,1-difluoroethene with activated carbon.

It was apparent, however, that some, or all, of the fluorine adsorbed at 25°C and 190°C was chemically reactive, since the carbons formed highly acidic aqueous suspensions (pH 2), and rapidly liberated iodine from potassium iodide solution. The oxidising power and acidity presumably result from the availability of "F" liberated from weak carbon fluorine complexes. This observation, and the fact that the quantity of fluorine adsorbed by each carbon was dependent upon the number of treatment cycles, suggests that some fluorine may be weakly absorbed (ie. physically adsorbed, weakly chemisorbed, or intercalated) by the carbon. This would be expected to cause structural modification of the carbon, which may be revealed by X ray diffraction analysis. Thus, a sample of control and fluorinated (30% F) BPL was analysed using this technique (Appendix).

Figure 7.1.3 shows the X ray diffraction patterns for a sample of control and modified BPL carbon. Little difference was observed, and both samples were almost entirely amorphous. In both cases, the average crystallite size is of the order of 10nm. It may be that the sorbed fluorine does result in structural modification, but that the small crystallite size precludes any change being observed using this technique.

Further information regarding the stability of the modified products was obtained from TG and DSC analysis. The example TG traces, shown at figures 7.1.4 (BPL control carbon, BPL fluorinated 16.7% F), indicate that the fluorinated carbon is of low thermal stability. In comparison to the control, a continuous and considerable loss of weight was observed above the temperature used for outgassing the fluorinated carbon, suggesting that there is a broad carbon fluorine bond energy distribution. Examination of the differential trace indicates that the rate of weight loss is greatest at relatively low temperatures (ca. 200-400°C). The behaviour of the nutshell carbons was essentially the same, except that the temperature range over which the rate of weight loss was a maximum was approximately 50°C higher (CECA carbon, table 7.1.4). This difference may be due to the presence of a greater number of ash-fluorine complexes on BPL carbon which influence the thermal stability. Alternatively,

the nature of the desorption profiles may reflect a combination of differences in the number and stability of ash fluorine complexes, and the loss of intercalated and/ or weakly chemisorbed reactive fluorine from within the carbon structure. This contention is supported by the results of DSC analysis (fluorinated BPL (10.7% F) and SCII (9.5% F) carbons; figures 7.1.5). In both cases, a broad and significant exotherm was observed, indicating that a temperature dependent chemical reaction was taking place (probably between adsorbed/ absorbed "F" and the carbon- the net heat change was found to be ca. -48 kJ mol^{-1} (of fluorine), and the maximum heat liberation found for BPL was at a lower temperature compared to the nutshell carbon. The appropriate non-fluorinated control carbons were used as the reference samples, and a linear trace was observed when the sample and reference pans contained control carbon). Further support for this contention was obtained from the results of thermal desorption- mass spectrometry (section 7.3.3, table 7.3.7), where it was found that the principal desorption of gaseous species took place over the temperature range for which the exotherm in the DSC profile was observed (table 7.3.7). That is, the gaseous species detected over this temperature range are the reaction products formed between the desorbed "F" and the constituents of the carbon.

The weight losses observed during desorption did not, however, suggest that the adsorbed fluorine promoted substantial carbon gasification (eg. the weight loss observed for BPL control carbon was 12.2%: that for the fluorinated sample was 31.8%, which exhibited a 16.7% increase in weight after modification. The percentage weight changes are based upon the initial dry weight of carbon prior to modification).

7.1.3 Adsorptive Properties of Fluorine Modified Carbons

7.1.3.1 Nitrogen

Nitrogen adsorption has been used to determine the extent of any carbon structural modification. To compare the data for the control and modified carbons, it is necessary to correct the isotherms. Thus, comparison has been made on the basis of equal carbon weights by use of the weight changes observed after modification. This approach relies on there being no significant carbon gasification, and so is justified in the present case (7.1.2).

Nitrogen isotherms for samples of control and fluorinated BPL and CECA carbons are at figures 7.1.6 and 7.1.7 respectively. Values of the BET surface area, micropore volume and external surface area (α_s analysis) for selected samples are at table 7.1.5.

The isotherms illustrate that when the amount of fixed fluorine is below approximately 10% of the initial dry carbon weight, the amount of nitrogen adsorbed is very similar to that for the control samples. A small reduction in the amount adsorbed below a relative pressure of approximately 0.1 suggests that some loss of microporosity results from modification. When the quantity of adsorbed fluorine is greater than ca. 10% weight, a more marked reduction in microporosity is observed. In fact, α_s analysis (table 7.1.5) suggests that fluorination results in a progressive reduction in both the micropore volume and external surface area, indicating that reaction occurs throughout the pore structure. This is unsurprising, given the reactivity of the modifier.

7.1.3.2 Methanol Adsorption

Measurement of methanol breakthrough curves for samples of control and modified nutshell carbons suggests that the number of polar adsorption centres

decreases as the fluorine content is increased (CECA carbon, figure 7.1.8). The results for BPL carbon (figure 7.1.9) indicate that modification has not resulted in any significant change, although a small increase in the number of polar adsorption centres appears probable.

On the basis that nitrogen adsorption indicates that fluorination results in a loss of porosity, an equally valid interpretation of the results for CECA carbon is that they do not accurately reflect any change in the hydrophobic character of the surface: rather, they reflect the loss of porosity.

7.1.3.3 Water Adsorption

Typical examples of water adsorption isotherms for samples of control and modified carbon, measured in flowing air (chapter 5, Appendix), are shown at figures 7.1.10-7.1.12. Information derived from the data are at table 7.1.6.

For modified BPL (10% F, figure 7.1.10), the amount of water adsorbed below approximately RH50% is noticeably higher in comparison to the control, indicating that the number of polar adsorption centres is greater. This results in the promotion of pore filling at lower values of the RH in comparison to the control. The uptake of water at high RH (85%) is similar for both samples, supporting the view that structural modification in not significant unless the carbons contain more than ca. 10% weight fluorine. More importantly, a net weight loss was observed after completion of the isotherm. This was probably associated with the formation of hydrogen fluoride, since the glass through which the effluent air passed rapidly became etched. The HF presumably resulted from the hydrolysis of carbon-fluorine bonds. Measurement of a second isotherm using the same sample (after first outgassing at 120°C for 3 hours (3 mbar)) indicated that the number of polar adsorption centres was further increased, an observation consistent with a greater number of oxygen containing surface functional groups. The process of surface hydrolysis is clearly slow,

since a further significant net weight loss was recorded (table 7.1.6) after completing the measurement.

These results indicate that the chemistry of the modified carbons is complex, since hydrolysis of, for example, simple C-F bonds (XPS analysis) to yield C-OH, would not account for the observed changes in weight. It is probable, therefore, that these observations arise from the desorption of weakly bound (possibly absorbed) fluorine. Indeed, storage of dry samples in glass airtight containers suggests that this is a plausible mechanism, because in each case, a heavy etching of the wall of the container was noticeable within a few weeks.

The water adsorption properties of the fluorinated nutshell carbons were found to be similar to those of BPL, except that the polarity of the modified surface was initially comparable with, but not less than, that of the control. This is illustrated at figure 7.1.11 for a sample of control and fluorinated (6% F) CECA carbon. This difference may be related to the nature of the ash impurities present in the carbons, and their interaction with fluorine.

Figure 7.1.12 shows the first and second isotherms for a sample of fluorinated CECA carbon (18.8% F). The quantity of water adsorbed is, as before, expressed as a percentage of the dry carbon weights measured before commencement of each isotherm. As previously noted, the increase in the amount adsorbed below ca. RH50% is consistent with the presence of a greater number of polar adsorption centres: the observed increase in water adsorption at high RH during measurement of the second isotherm may be a result of surface hydrolysis, whereby restrictions to some of the micropores are removed during determination of the first isotherm.

7.1.3.4 Chloropicrin (PS) Adsorption

PS adsorption data for samples of control and modified carbons are at table 7.1.7.

Although the modified carbons were found to be unstable in the presence of humid air, an assessment of their vapour adsorption characteristics was made.

In each case, it was observed that fluorination resulted in a marked loss of filter performance in comparison to samples of control carbon. In addition, this loss of performance was found to be essentially independent of fluorine content. This effect is probably due to a combination of the presence of pore restrictions, which inhibit the adsorption of PS molecules, and the unstable nature of the surface.

To test the hypothesis that pore restrictions are at least partly responsible for the poor PS adsorption characteristics, samples of fluorinated carbon were challenged in dry air (< RH2%). In each case, a reduction in both the filter breakthrough time, and the equilibrium adsorption capacity, was apparent.

The observed change in both the adsorption kinetics, and the equilibrium adsorption capacity, are consistent with the presence of pore restrictions. This is illustrated at figure 7.1.13 for a sample of control and fluorinated (6% F) CECA carbon.

This observation may also explain, at least in part, the methanol adsorption data.

7.1.4 High Temperature Modification Reactions

Because carbons fluorinated below approximately 200°C were found to be unstable, and unsuitable for vapour adsorption applications, exploratory studies were carried out above 200°C using the high temperature modification apparatus described at chapter 5, and in more detail at the Appendix. The intention of this approach was to produce stable surface fluorides. The method used for preparing the carbons was essentially the same as that described above (7.1).

Treatments were carried out at 330, 450, and 600°C. In each case, carbon burnoff was found to be the predominant mechanism, and was important at all of the temperatures studied. Fluorine gas clearly behaves as an activating agent, since significant changes in the BET surface area and micropore volume were observed (table 7.1.8). An investigation of the relationship between the reaction temperature and the extent of activation was not carried out, however. The amount of gasification probably also depends upon the number of treatment cycles.

Samples fluorinated at 300 and 450°C contained small amounts of fluorine (ca. 1-2%; elemental analysis), and formed acidic aqueous suspensions (pH 4.5), but were not found to oxidise iodide. Samples modified at 600°C appeared to be stable. The significant structural modification brought about by these treatments appeared to have little effect on the adsorption of PS in comparison to control samples (table 7.1.8). The improvement in the PS breakthrough time for the fluorinated CECA carbon probably reflects the increased micropore volume, rather than any effects due to surface modification.

In addition, the small quantities of adsorbed fluorine did not significantly affect the water adsorption properties of the carbon below ca. RH50%- the uptake at RH80-85% was similar to that for the control.

Since high temperature reaction had little impact upon the water adsorption properties at high values of the RH, it is probable that gasification occurred predominantly on the external parts of the granules: that is, burnoff may have taken place at the periphery of the carbon layers. No significant weight changes were observed after outgassing control carbon at 600°C.

Because of the difficulty of correlating the effects associated with simultaneous carbon gasification and surface modification, and because this approach does not appear to offer any significant advantages in terms of the aims of this part of the research, further studies were not carried out.

Interesting effects were, however, observed for these samples, in that a proportion of the granules were whitened after modification. This behaviour appeared to be random, since non uniform colouration of some granules was observed: for others, complete portions were white after treatment.

EDX examination revealed that the concentration of fluorine was exceptionally high in these instances (figure 7.1.14). This effect may be due to the formation of graphite fluoride ("CF" ;chapter 3). SEM examination of these granules revealed that significant textural modification resulted: the white regions bore no resemblance to similar regions on samples of control carbons, or carbons fluorinated below 200°C (figures 7.1.15). Carbons modified below 200°C were visually similar to the controls.

Figures 7.1.15 also show SEM micrographs for samples of CECA carbon modified at 600°C. The unusual surface features support the view that carbon burnoff has taken place.

7.1.5 The Effect of Post Treatment on the Properties of Fluorine Modified Carbons

On the basis of the above results, further attempts were made to stabilise carbons fluorinated below 200°C.

One approach involved outgassing the modified carbons at temperatures up to 350°C. Carbons outgassed at 300°C or below contained less fluorine, but formed acidic aqueous suspensions, and also liberated iodine from potassium iodide. However, the PS breakthrough time, the quantity of methanol adsorbed, and the BET surface area, were increased suggesting that outgassing results in the removal of thermally unstable surface fluorides which constrict some of the pores.

Outgassing at 350°C resulted in a further increase in PS filter life and BET surface area. In addition, the carbons no longer formed acidic suspensions, nor did they oxidise iodide. The extended time required for the samples to reach constant weight (ca. 100 hours) suggests that a slow desorption of fluorine containing species was taking place, supporting the idea that some of the fluorine is intercalated. The ultimate fluorine content of these carbons was low (table 7.1.9).

The technique was not found to be useful because the PS adsorption characteristics remained relatively poor in comparison to those for control samples. In addition, water adsorption measurements indicated that the carbons were still unstable in the presence of humid air.

An alternative approach was adopted, whereby samples of modified carbon were washed with, and refluxed in, water or methanol until the pH of the mother liquor was neutral (6-7). The principal aim of this was to remove adsorbed reagent and/ or reaction products which may give rise to the observed instability of these carbons.

In addition, these solvents may react to yield, for example, surface methoxy (methanolysis) or surface hydroxyl groups. Any changes in the surface chemistry brought about by these treatments can then be studied using the techniques described above.

The weight changes associated with the treatments are at table 7.1.10. In each case, significant weight losses were observed, indicating that solvolysis must effect the removal of at least some of the adsorbed "F" (eg., if reaction with water only involved formation of surface hydroxyl groups and the formation of HF, only a small reduction in weight would be observed). BPL carbon, after treatment with water, exhibited a substantial weight loss, of greater magnitude than the initial quantity of fluorine adsorbed. This effect may be due to the solvation of ash fluorides. The adsorption of PS at high RH by the methanol treated sample compared to that for the water treated carbon suggested that methanolysis resulted in the generation of bulky surface functional groups which hinder PS adsorption (table 7.1.10). Outgassing the carbons at 250^{o}C resulted in improved filter performance, but the methanol treated sample remained comparatively poor supporting the view that bulky functional groups may be present. Alternatively, it may be that methanolysis did not result in complete removal of absorbed "F", a contention supported by DSC analysis (figure 7.1.16). That is, the DSC curve for the methanol treated carbon exhibits an exotherm similar to that for the fluorinated but untreated sample. The exotherm is somewhat smaller, however (241 J g^{-1} cf. 65 J g^{-1}) suggesting that the bulk of the absorbed fluorine has been removed. The exotherm is absent in the case of the water treated sample, indicating that this approach is more successful in removing reactive fluorine species (figure 7.1.16). Analysis of the water adsorption properties of the treated samples suggests that some surface reaction has resulted. Figure 7.1.17 shows the water adsorption isotherms for samples of fluorinated SCII carbon treated with water or methanol and outgassed at 250^{o}C. The differences between the isotherms below ca. RH60% (adsorption) are consistent with the presence of surface hydroxy (water) and methoxy (methanol) groups (ie., the polarity of the

methanol treated carbon is, as would be anticipated, lower than that of the water treated sample). Recycling the samples indicated that the surface of the water treated sample was stable (ie. the isotherm was unchanged), but that the methanol treated sample was not (it aged). This difference is probably due to the presence of absorbed "F" in the case of the methanol treated sample (elemental analysis revealed that the water treated sample contained a residual fluorine content of ca. 1 w/w%: the methanol treated sample contained ca. 4 w/w% - the initial fluorine content prior to treatment was 9.9 w/w%).

The results therefore suggest that fluorinated carbons may be suitable precursors for the introduction of different functional groups. To further test this hypothesis, fluorinated SCII carbon was modified using dipropylamine (DPA) vapour at 200°C. After treatment, samples were outgassed to constant weight, and washed with dilute acid, base and water prior to further outgassing, which was continued until constant weight was attained. The weight changes associated with the treatment are at table 7.1.11. Two endotherms were observed in the DSC trace, which may be due to the decomposition or desorption of chemisorbed amine (figure 7.1.18). No exotherm was observed, suggesting that essentially complete removal of absorbed "F" was brought about by the treatment. Examination of the DSC profile for a sample of SCII carbon onto which DPA had been preadsorbed (physically adsorbed) at 25°C supports the contention that DPA is chemisorbed onto the surface of the fluorinated carbon. In this case (figure 7.1.18), only a single endotherm was observed, and at a lower temperature in comparison to those found for the DPA treated fluorinated carbon. Examination of the TG traces for these samples supports the view that the amine is more strongly bound in the case of the fluorinated carbon (figure 7.1.19). Water adsorption by the fluorinated and DPA modified sample below RH60% was similar to that for the control, but was reduced at high RH, suggesting that modification and treatment resulted in some pore blocking. This was also apparent from measurement of PS adsorption from air of high RH (table 7.1.11). Fluorinated BPL carbon was found to exhibit the same behaviour as SCII carbon.

Table 7.1.1 The Fluorine Content of the Modified Activated Carbons

Sample	Fluorination Temperature (°C)	Outgassing Temperature (°C)	Amount of Fluorine (%)	
			Gravimetric	Analysis
BPL				
Control	-	150	-	0.0
A	25	150	6.1	6.0
B	25	150	10.0	-
C	25	150	16.7	-
D	190	190	10.0	-
CECA				
Control	-	150	-	0.0
A	25	150	6.0	-
B	25	150	18.8	18.6
C	25	150	30.0	29.1
D	190	190	7.7	-

{The letters serve to identify particular samples for which other results are shown in this section}

Table 7.1.2 Gaseous Reaction Products. Analysis and Quantification

Fluorination Temperature (^{o}C)	25^{o}C		190^{o}C	
Carbon	BPL	CECA	BPL	CECA
Compounds Detected (mg)				
CF_4	9.5	11.2	41.0	47.6
C_2F_6	0.7	0.9	12.0	10.1
C_3F_8	0.2	0.1	6.6	5.1
SF_6	3.4	-	29.2	-
SO_2F_2	2.5	-	64.3	-
Total Carbon Gasified (mg)	1.5	2.6	8.9	10.6
Total Sulphur Gasified (mg)	1.5	-	26.6	-
Amount Gasified (w/w %) as Sulphur and/ or Carbon Fluorides	<0.01	<0.02	<0.05	<0.07

Table 7.1.3 Elemental Analysis

Sample	Element (%)					
	C	H	N	O	S	F
BPL Control	86.6	0.2	0.6	2.0	1.1	0.0
BPL A	81.2	0.1	0.6	-	0.8	6.0
Element Molar Ratio (To C = 100)						
BPL Control	100	3.2	0.5	1.7	0.4	0.0
BPL A	100	2.3	0.6	-	0.4	4.7
CECA Control	91.2	0.3	0.7	3.1	0.0	0.0
CECA B	78.2	0.1	0.7	-	0.0	18.6
CECA C	73.6	0.1	1.0	-	0.0	29.1
Element Molar Ratio (To C = 100)						
CECA Control	100	3.7	0.3	2.1	0.0	0.0
CECA B	100	1.5	0.7	-	0.0	15.0
CECA C	100	1.3	0.8	-	0.0	24.9

Oxygen analysis for the fluorinated carbons was not possible using the elemental analyser. The values are an average of at least two determinations, and are corrected for moisture content.

Table 7.1.4 Thermal Analysis

Sample	Total Weight Loss (%)	Principal Region of Weight Loss	
		Temperature Range (°C)	Weight Loss (w/w %)
BPL Control	12.2	>900	9.5
BPL C	31.8	200-450	12.0
CECA Control	24.6	>800	20.5
CECA C	41.6	250-500	17.0

Table 7.1.5 Nitrogen Adsorption and α_s Analysis

Sample	BET Surface Area (m^2g^{-1})	Micropore Volume (cm^3<STP>g^{-1})	External Surface Area (m^2g^{-1})
BPL Control	1208	0.53	53
BPL A	1172	0.51	48
BPL E	1071	0.48	45
BPL C	974	0.44	41
CECA Control	1460	0.61	51
CECA A	1440	0.60	43
CECA B	1405	0.58	39
CECA C	1230	0.51	38

The results are for single determinations. Typical error on measurement of surface area is ±12 m^2g^{-1}; and ±0.01 cm^3<STP>g^{-1} for the total pore volume (per gram of carbon).

Table 7.1.6 Water Adsorption. Weight Changes Observed during Measurements

Sample	Fluorine Content (w/w %)	First Isotherm Weight Change (w/w%)	Second Isotherm Weight Change (w/w%)
BPL Control	-	+0.3	-
BPL A*	10.0	-3.6	-0.6
CECA Control	-	+0.1	-
CECA A	6.0	-3.1	-0.6
CECA B	18.8	-4.6	-2.0
CECA C	30.0	-5.1	-2.1

*Outgassed at 120°C

Table 7.1.7 Chloropicrin (PS) Adsorption

Sample	Water Content (RH80%; 22°C: Corrected)	Breakthrough Time (minutes)	
		1st Break	1% Break
BPL Control	35.4	81	96
BPL A	33.3	24	36
BPL E	30.6	21	30
CECA Control	46.9	58	75
CECA A	46.8	22	34
CECA B	43.6	19	26
CECA C	39.0	19	27

All values are an average of at least two determinations. 1st Break is the time to first measured filter breakthrough (5-10 mg m^{-3}): 1% Break is 50 mg m^{-3}.

{2cm diameter, 2cm bed depth filters: flow velocity 382 cm min^{-1}. Challenged in equilibrium with RH80% air at 22°C. PS concentration 5000 mg m^{-3}}

Table 7.1.8 High Temperature Modification

	Sample					
	CECA	CECA	CECA	CECA	BPL	BPL
Reaction Temperature (^{o}C)	-	330	450	600	-	450
Number of Treatment Cycles	0	3	4	6	0	6
Calculated Weight Change*	0	5.9	8.8	6.9	0	12.1
Observed Weight Change	-	0	-1.2	-2.3	-	-2.4
Fluorine Content (w/w %, Analysis)	0.0	1.8	1.3	0.9	0.0	1.6
BET Surface Area (m^2g^{-1})	1460	1563	1488	1435	1208	-
Micropore Volume (cm^3<STP>g^{-1}; α_s)	0.61	0.74	0.68	0.66	0.53	-
Water Content (RH80%; 22^{o}C)	46.9	48.3	47.9	47.0	35.2	35.4
PS Adsorption						
1st Break	58	72	68	-	81	78
1% Break	75	85	83	-	96	92

*From the reactor volume, amount of fluorine, temperature and pressure.

Table 7.1.9 The Effect of Post Treatment (High Temperature Outgassing)

	BPL					CECA			
Fluorination Temperature (°C)	25 (E)	25 (E2)	25 (E3)	25 (F)	25 (F2)	25 (E)	25 (E2)	25 (E3)	25 (E4)
Outgassing Temperature (°C)	120	250	300	120	350	120	250	300	350
Fluorine (Gravimetric, w/w %)	13.7	7.9	4.2	15.4	1.5	14.1	13.7	5.8	3.7
Fluorine (Analysis, w/w %)	-	-	3.7	-	-	-	-	6.2	4.1
BET Surface Area (m^2g^{-1})	1071	1092	1110	-	-	-	1410	1450	1496
Water Content RH80%, 22°C	30.6	33.7	-	29.8	36.8	43.6	42.5	-	41.9
PS Breakthrough (minutes)									
1st Break	21	26	-	19	53	23	24	-	41
1% Break	30	41	-	24	67	29	35	-	52

Table 7.1.10 The Effect of Post Treatment (Solvolysis)

		Carbon	
		SCII	BPL
Fluorine Content, Initial (gravimetric, w/w%)		9.9	8.7
Net Weight Change (cf. initial carbon weight: solvolysis, outgassing 250°C)			
Methanol		4.3	1.1
Water		0.9	-3.0
PS Adsorption			
Outgassed 120°C			
Water Content (% w/w); TT1%	Methanol	35.1; 57	-
	Water	45.1; 68	-
Outgassed 250°C			
Water Content (% w/w); TT1%	Methanol	39.0; 77	34.0; 84
	Water	44.8; 85	35.5; 70

PS: all values are an average of at least two determinations.

TT1% is the time to 1% PS filter breakthrough (50 mg m^{-3}).

{2cm diameter, 2cm bed depth filters: flow velocity 382 cm min^{-1}.
Challenged in equilibrium with RH80% air at 22°C. PS
concentration 5000 mg m^{-3}}

Table 7.1.11 The Effect of Post Treatment (Dipropylamine)

	Carbon	
	SCII	BPL
Fluorine Content, Initial (gravimetric, w/w%)	11.5	10.7
Net Weight Change (cf. initial carbon weight: dipropylamine treated, acid/base/water washed)	15.4	15.0
PS Adsorption Outgassed 120°C Water Content (% w/w); TT1%	17.9; 23	16.6; 26
Net Weight Change (cf. initial carbon weight: dipropylamine preadsorbed)	13.1	10.8
PS Adsorption Outgassed 120°C Water Content (% w/w); TT1%	23.0; 52	19.8; 65

PS: all values are an average of at least two determinations. TT1% is the time to 1% PS filter breakthrough (50 mg m^{-3}).

{2cm diameter, 2cm bed depth filters: flow velocity 382 cm min^{-1}. Challenged in equilibrium with RH80% air at 22°C. PS concentration 5000 mg m^{-3}}

FIGURE 7.1.1 ION CHROMATOGRAM FOR THE GASES FORMED DURING FLUORINATION OF BPL CARBON

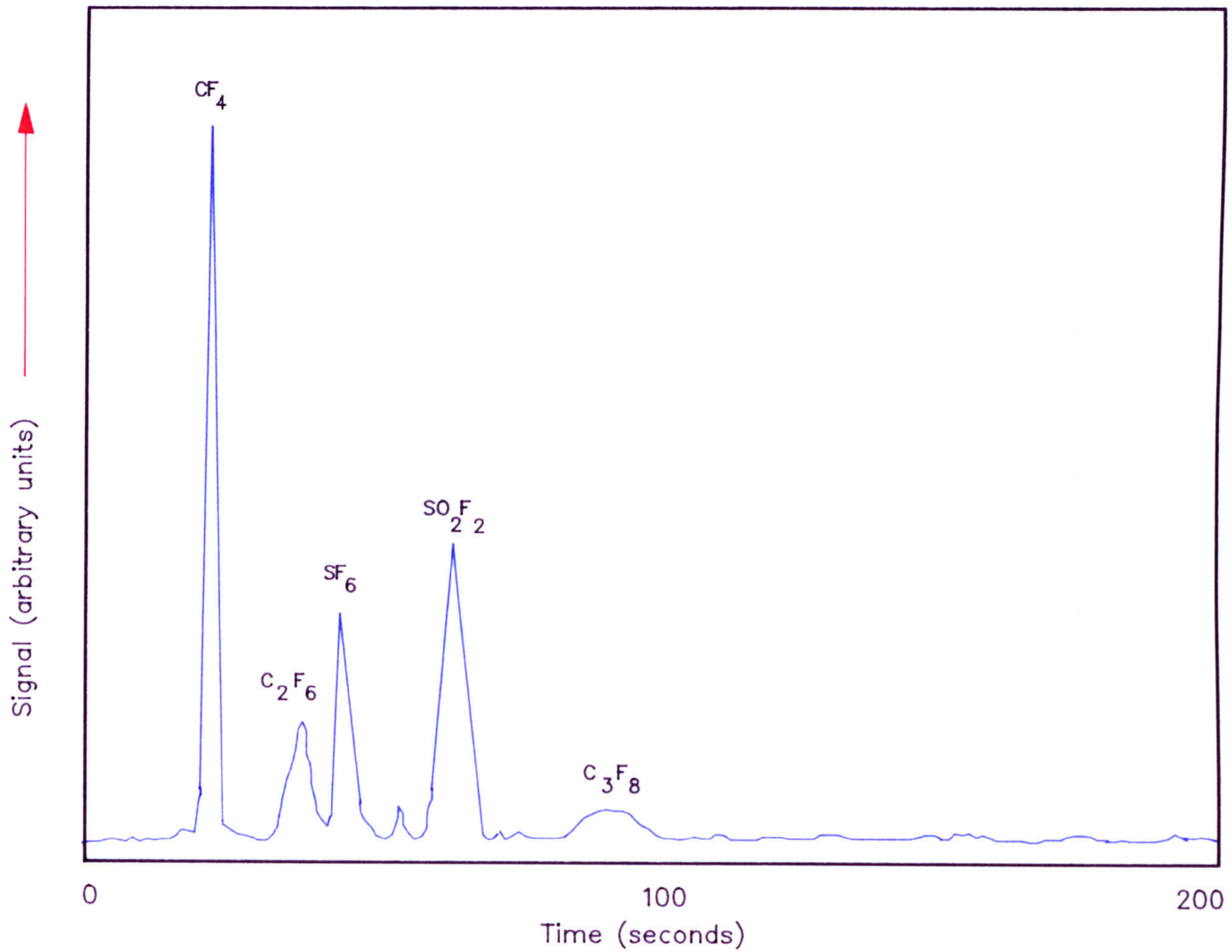

FIGURE 7.1.2 EDX SPECTRUM FOR FLUORINATED BPL CARBON

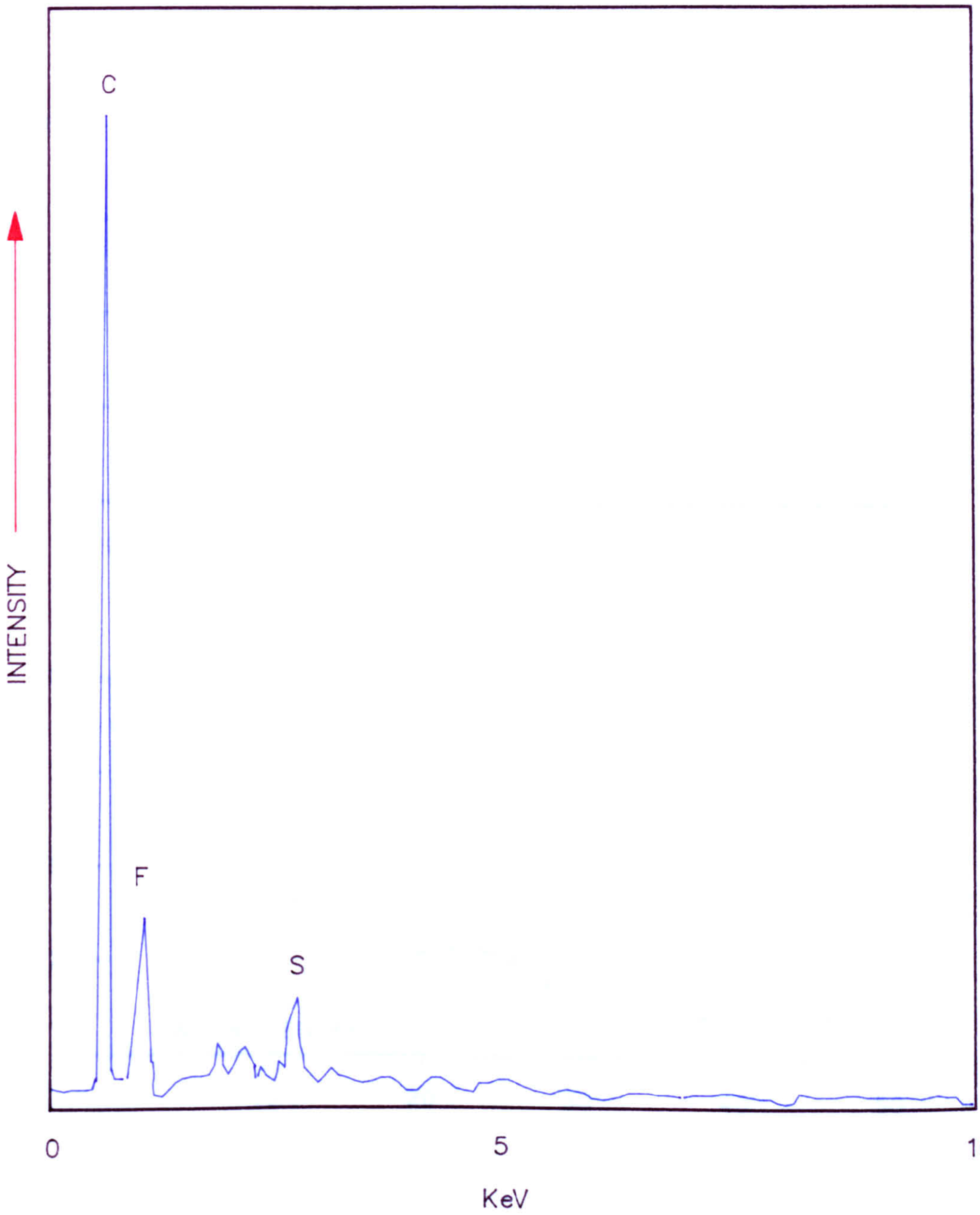

FIGURE 7.1.3 X RAY DIFFRACTION ANALYSIS

UPPER: CONTROL BPL
LOWER: FLUORINATED BPL (30 w/w%)

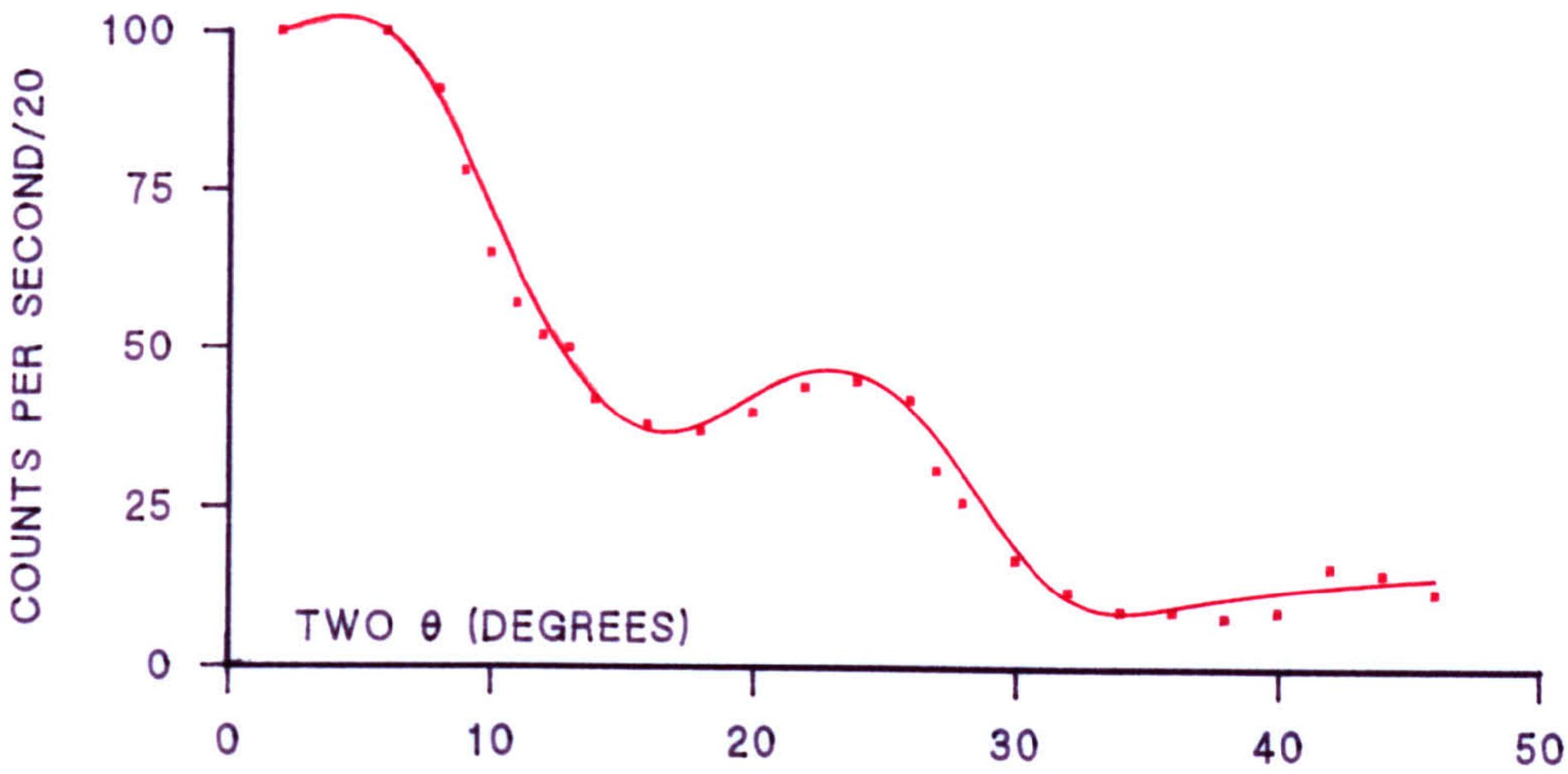

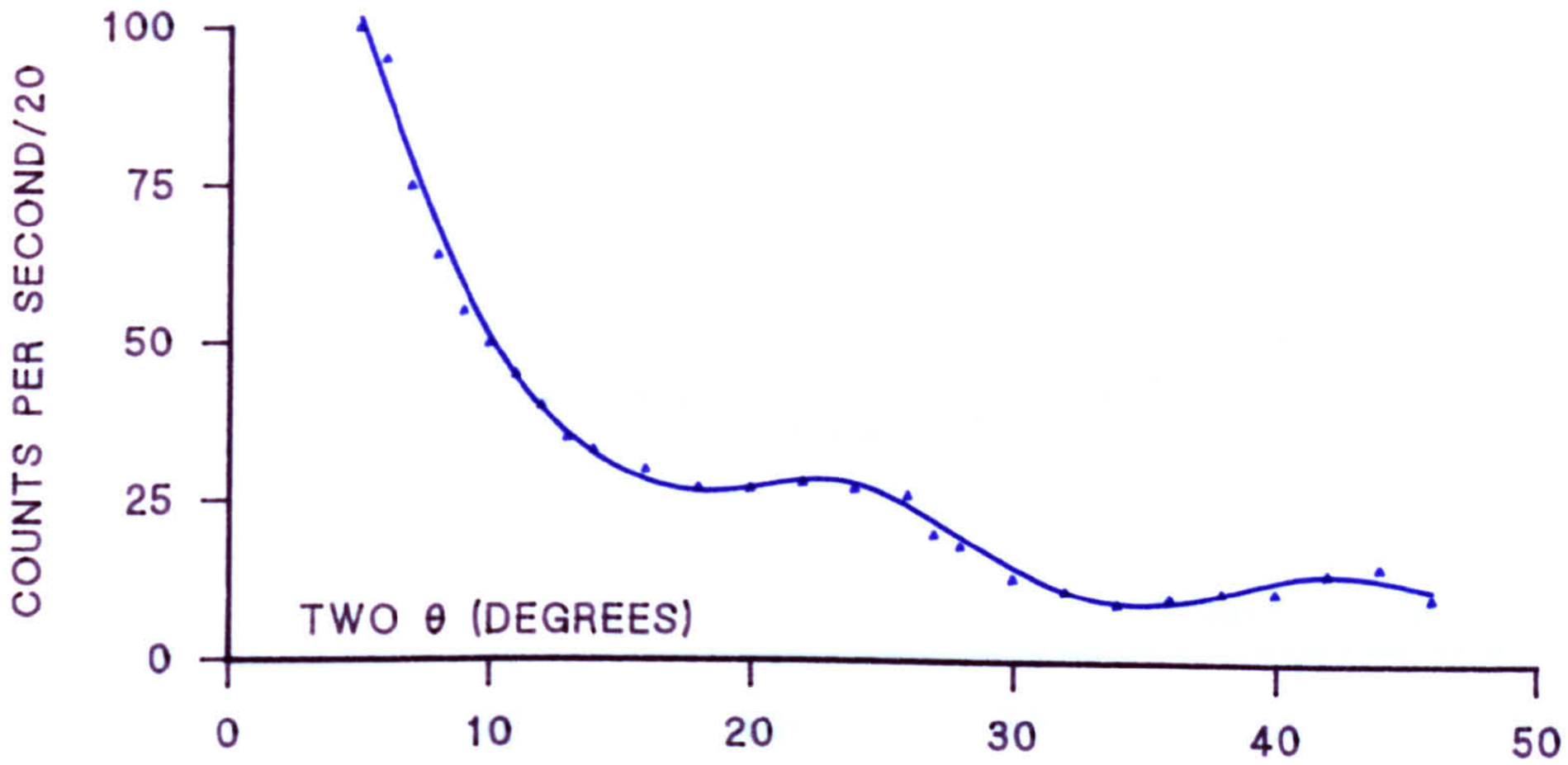

FIGURES 7.1.4 THERMAL ANALYSIS FOR BPL CARBONS

UPPER: TG CURVE FOR CONTROL BPL

LOWER: DIFFERENTIAL TRACE FOR CONTROL BPL

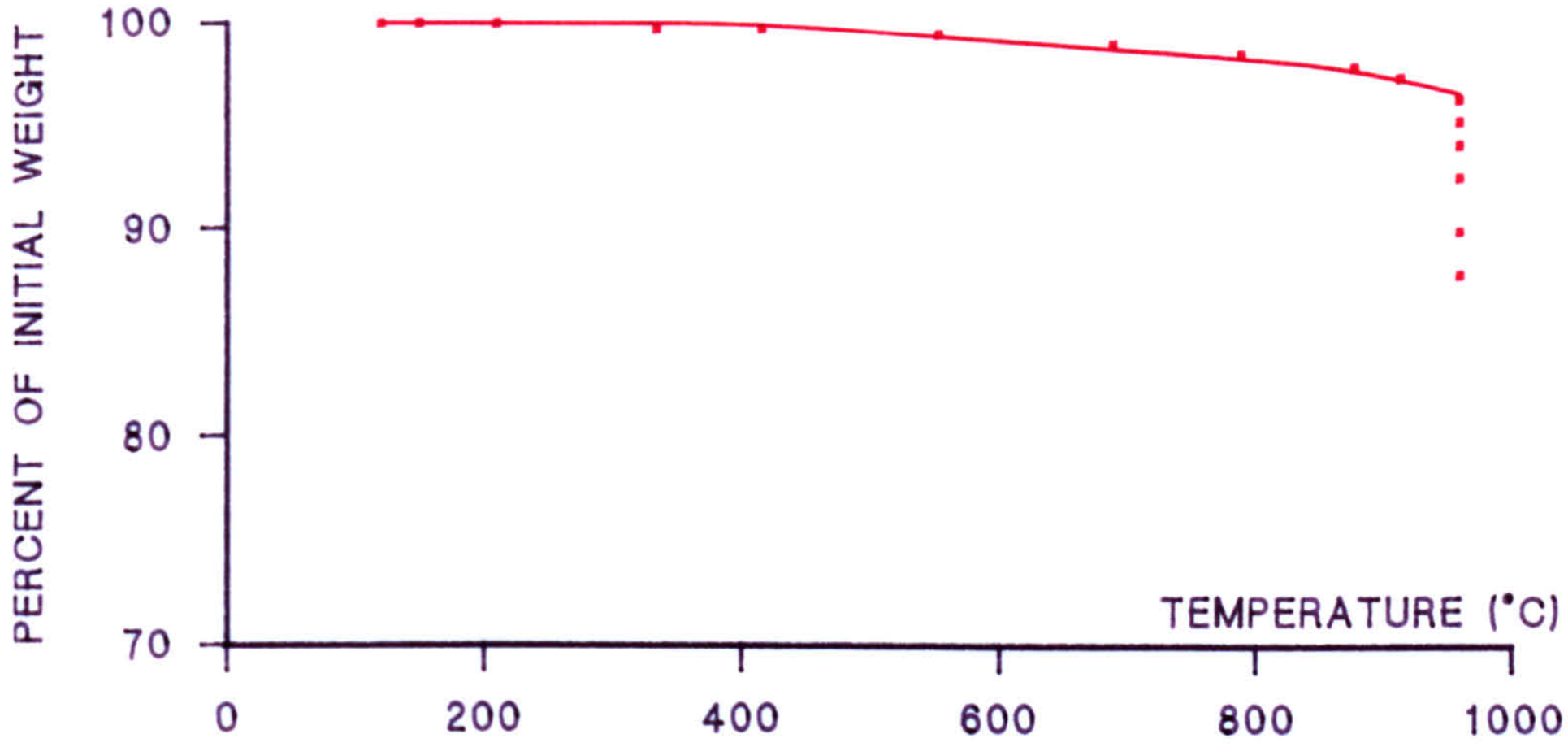

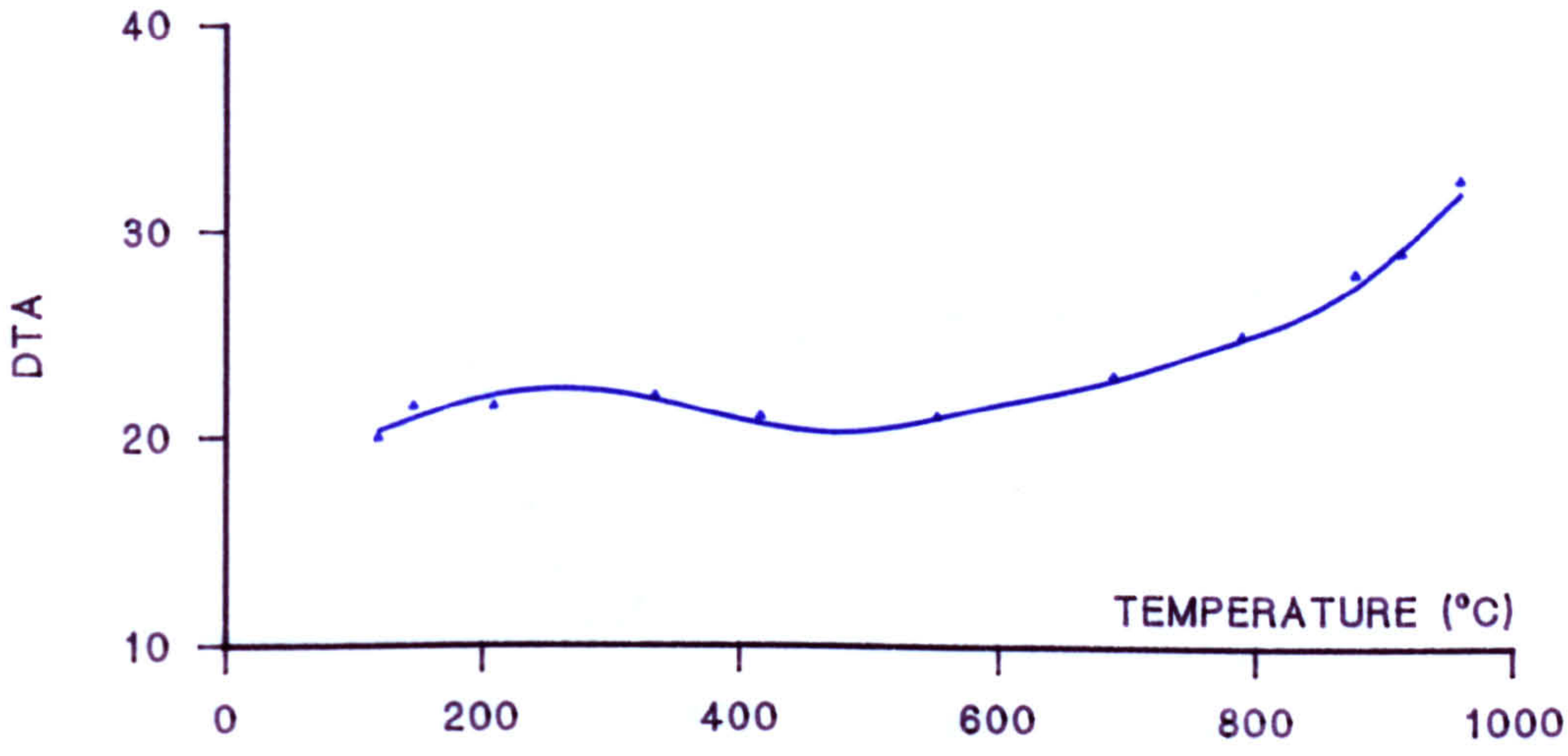

FIGURES 7.1.4 THERMAL ANALYSIS FOR BPL CARBONS

UPPER: TG CURVE FOR FLUORINATED BPL (16.7% F)

LOWER: DIFFERENTIAL TRACE FOR FLUORINATED BPL (16.7% F)

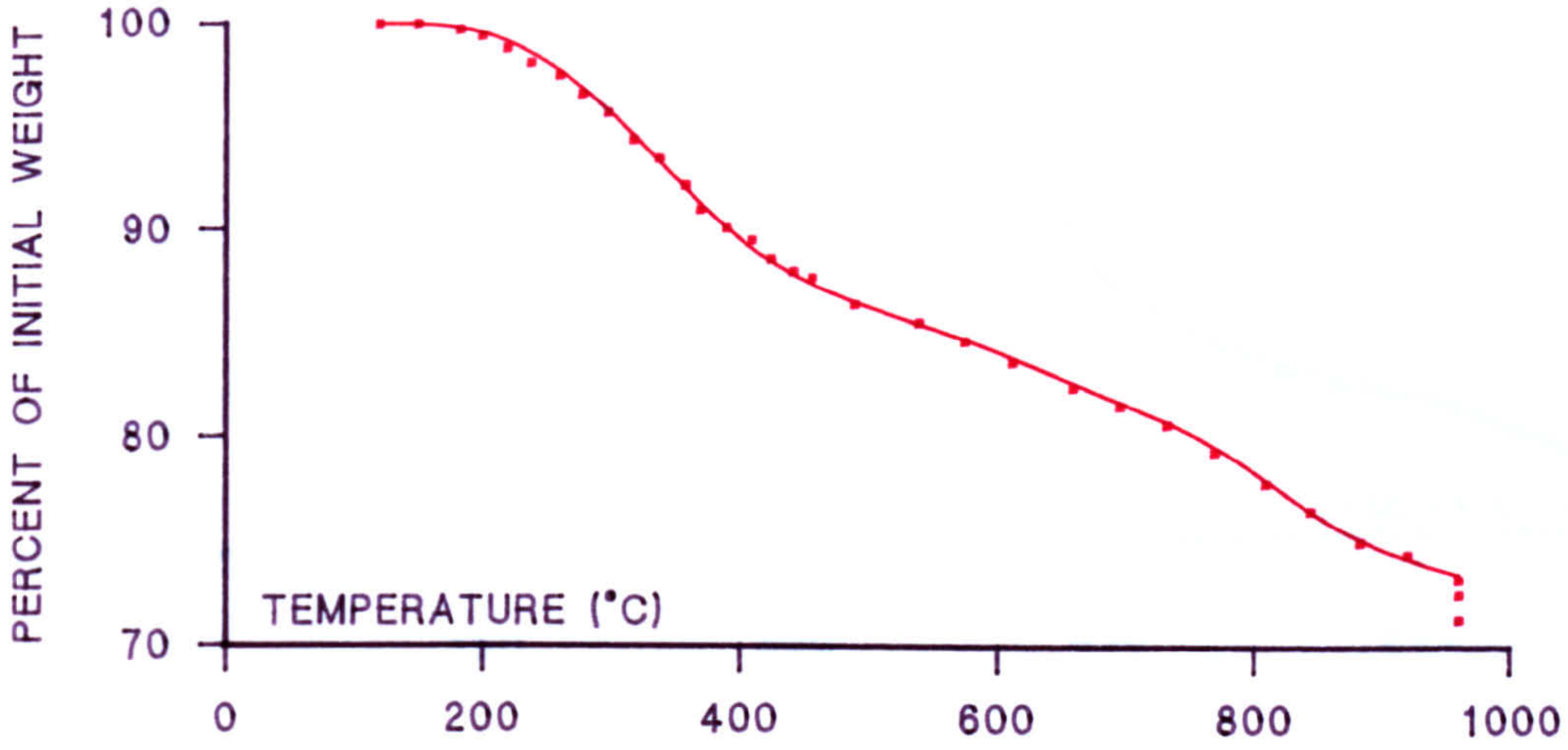

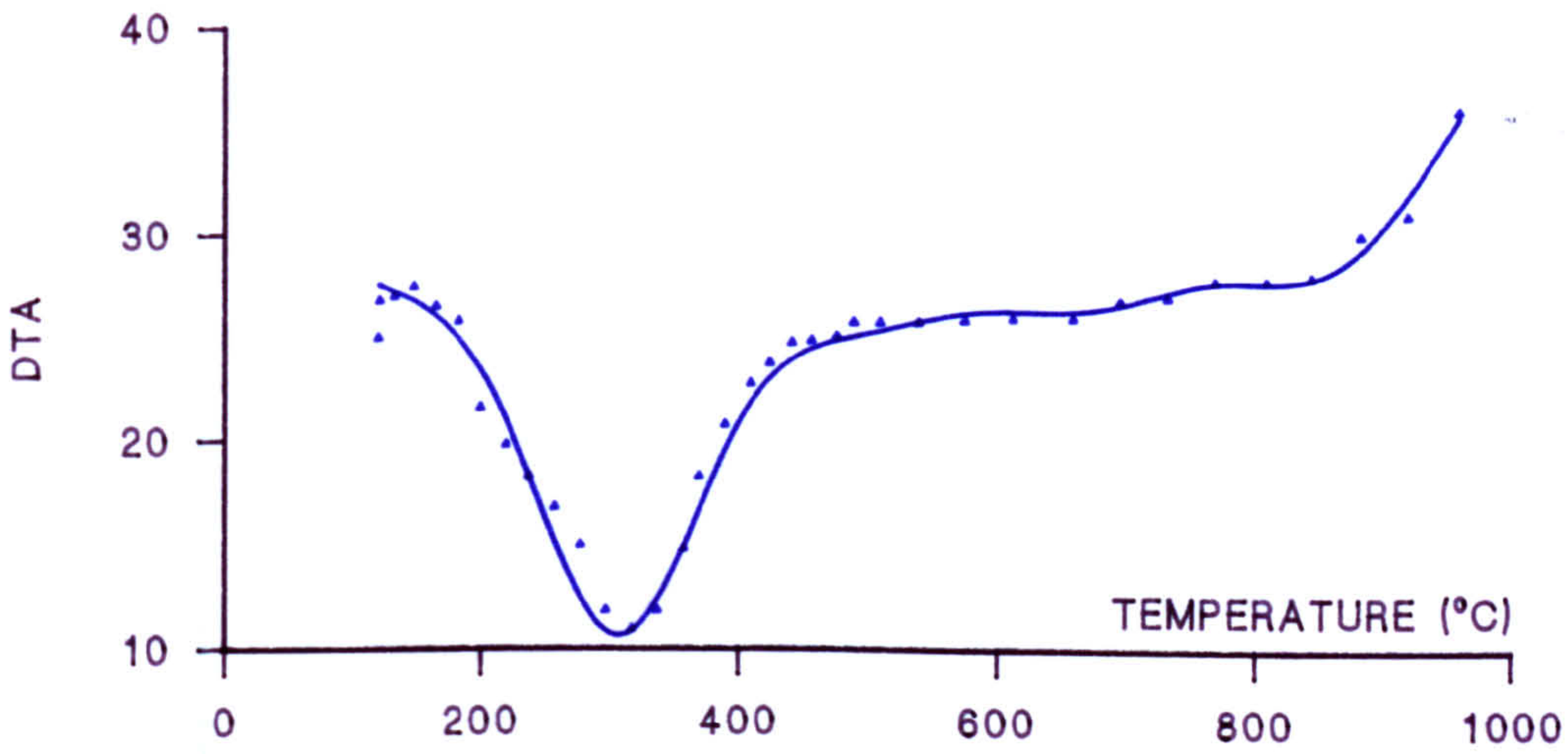

FIGURE 7.1.5 DSC CURVES FOR SCII AND BPL CARBON

(UPPER) FLUORINATED BPL; (LOWER) FLUORINATED SCII

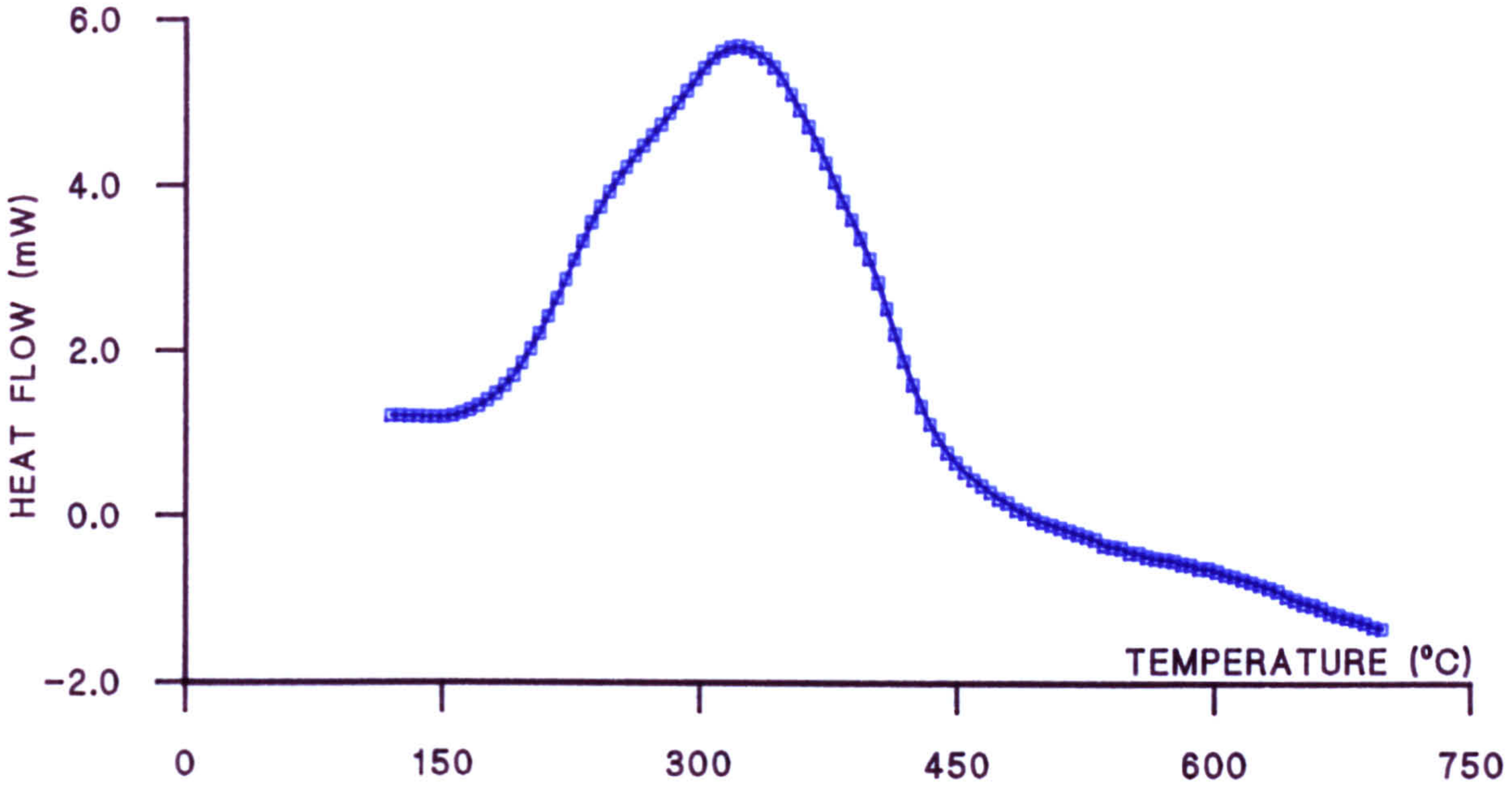

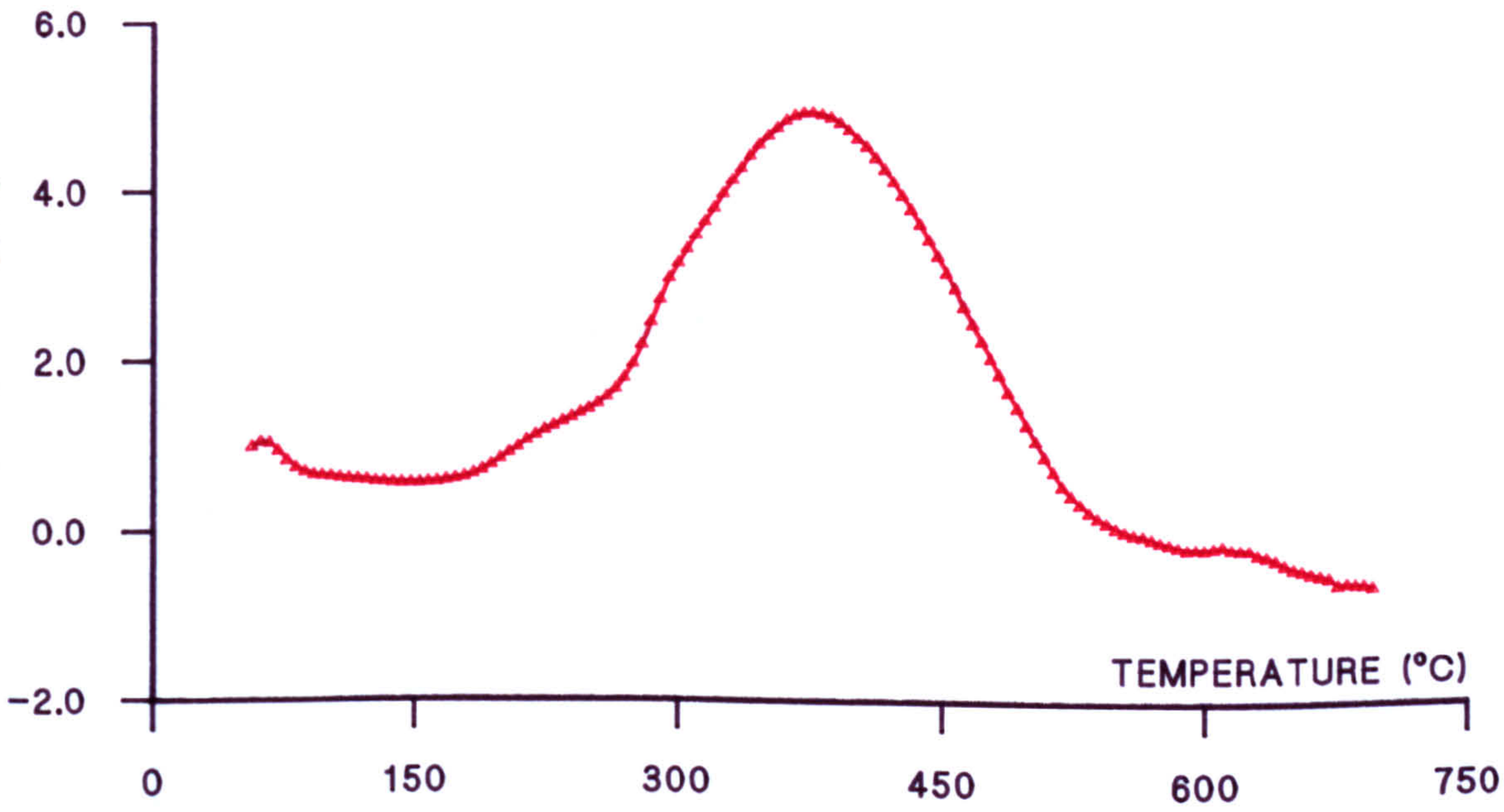

FIGURE 7.1.6 NITROGEN ISOTHERMS FOR BPL CARBON

● CONTROL FLUORINATED ■ 13.7% F, ▲ 16.7% F

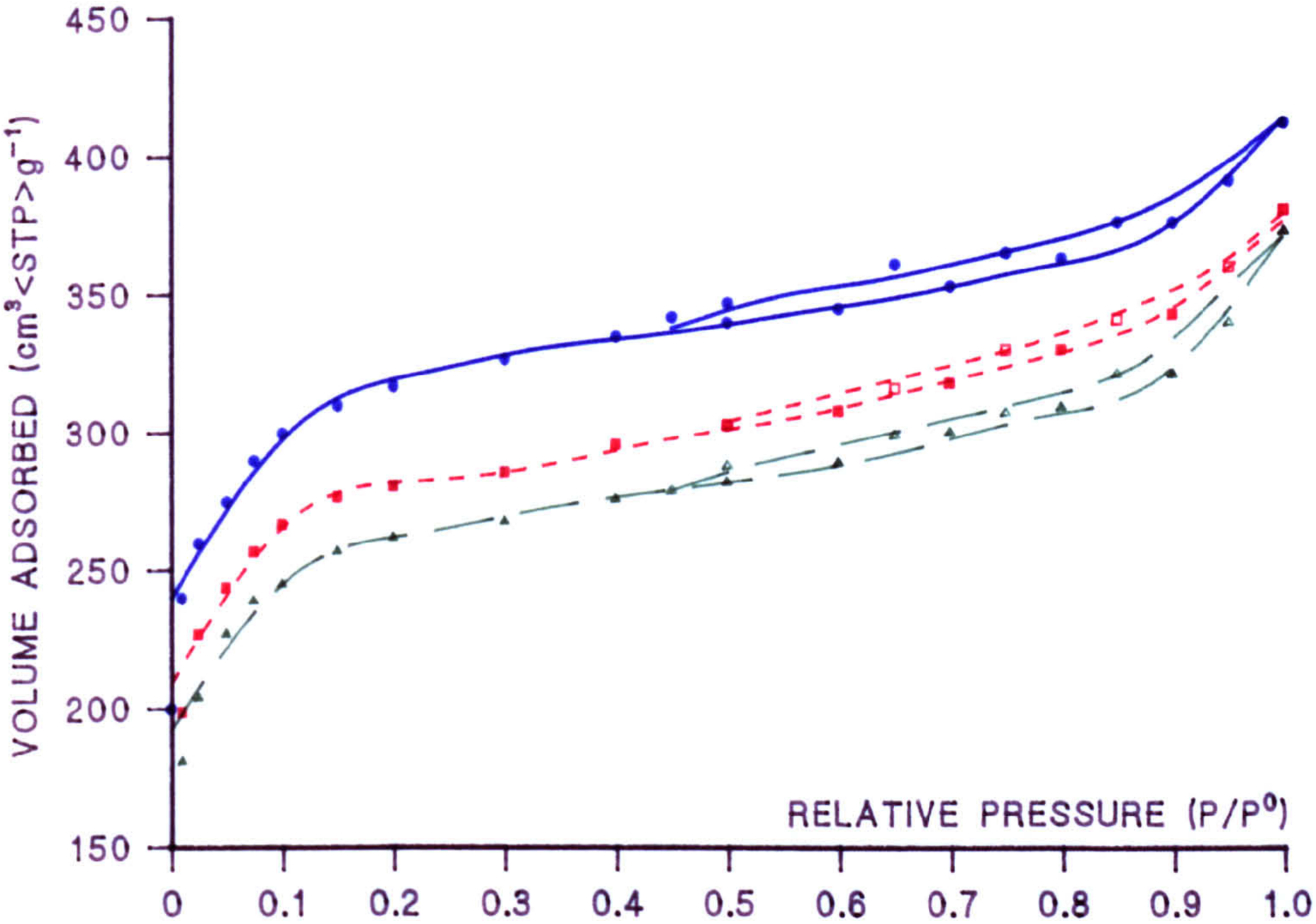

FIGURE 7.1.7 NITROGEN ISOTHERMS FOR CECA CARBONS

● CONTROL FLUORINATED ■ 6% F, ▲ 30% F

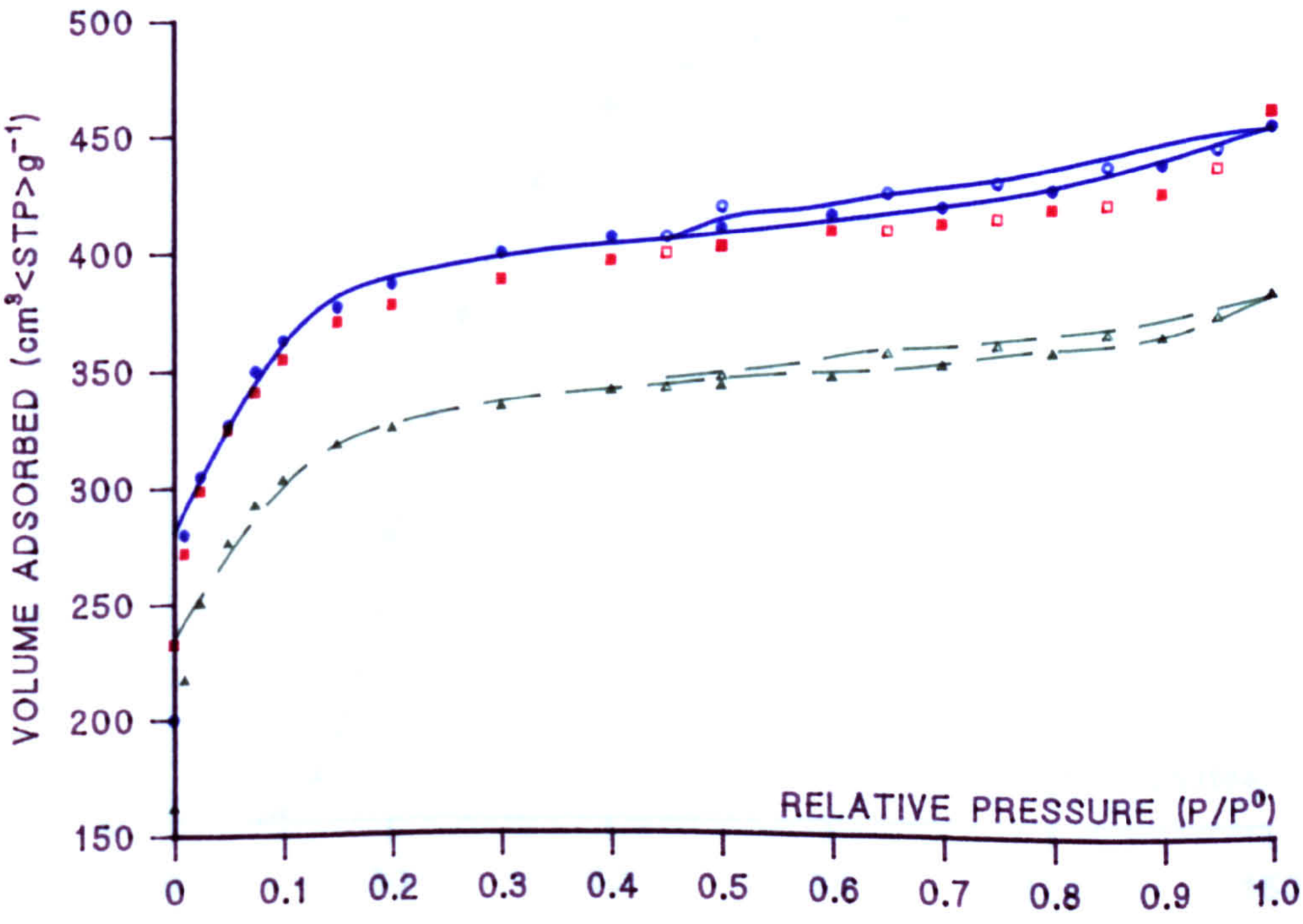

FIGURE 7.1.8 METHANOL BREAKTHROUGH CURVES

L–R: CECA FLUORINATED 30%, 18.8%, 6% F; CECA CONTROL

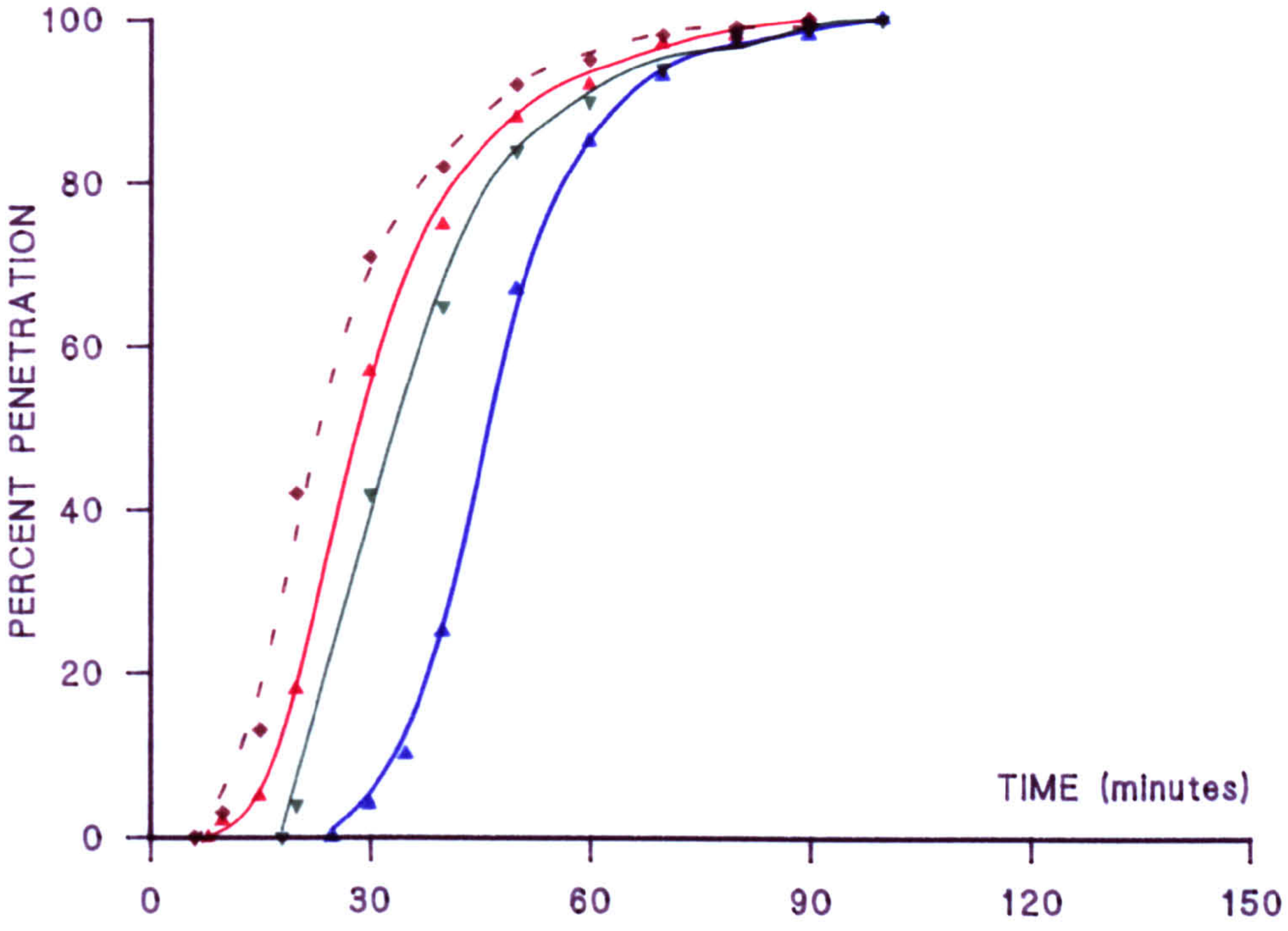

FIGURE 7.1.9 METHANOL BREAKTHROUGH CURVES

L–R: BPL CONTROL, FLUORINATED (6% F)

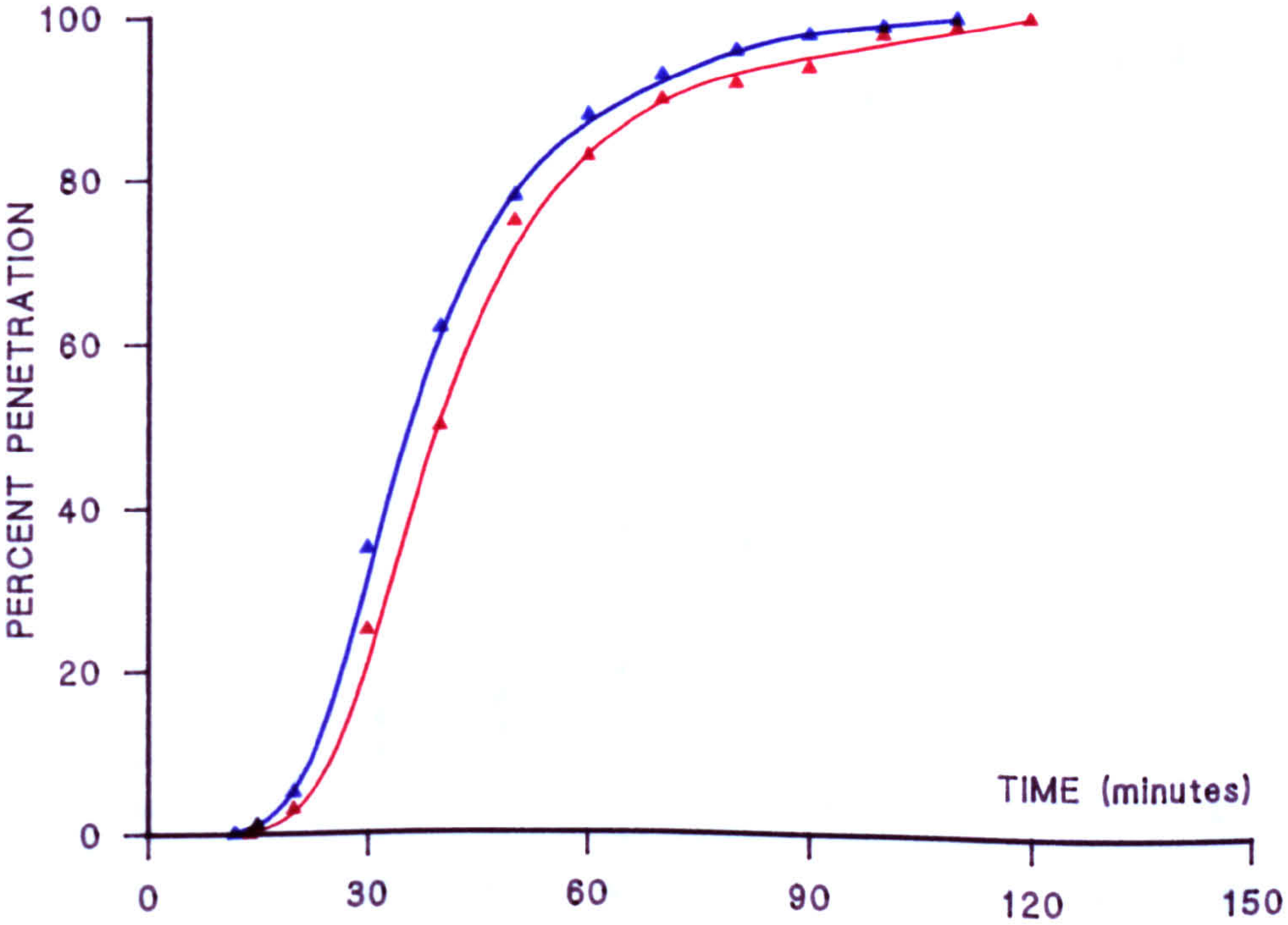

FIGURE 7.1.10 WATER ADSORPTION

▲ BPL CONTROL ● FLUORINATED (10% F)

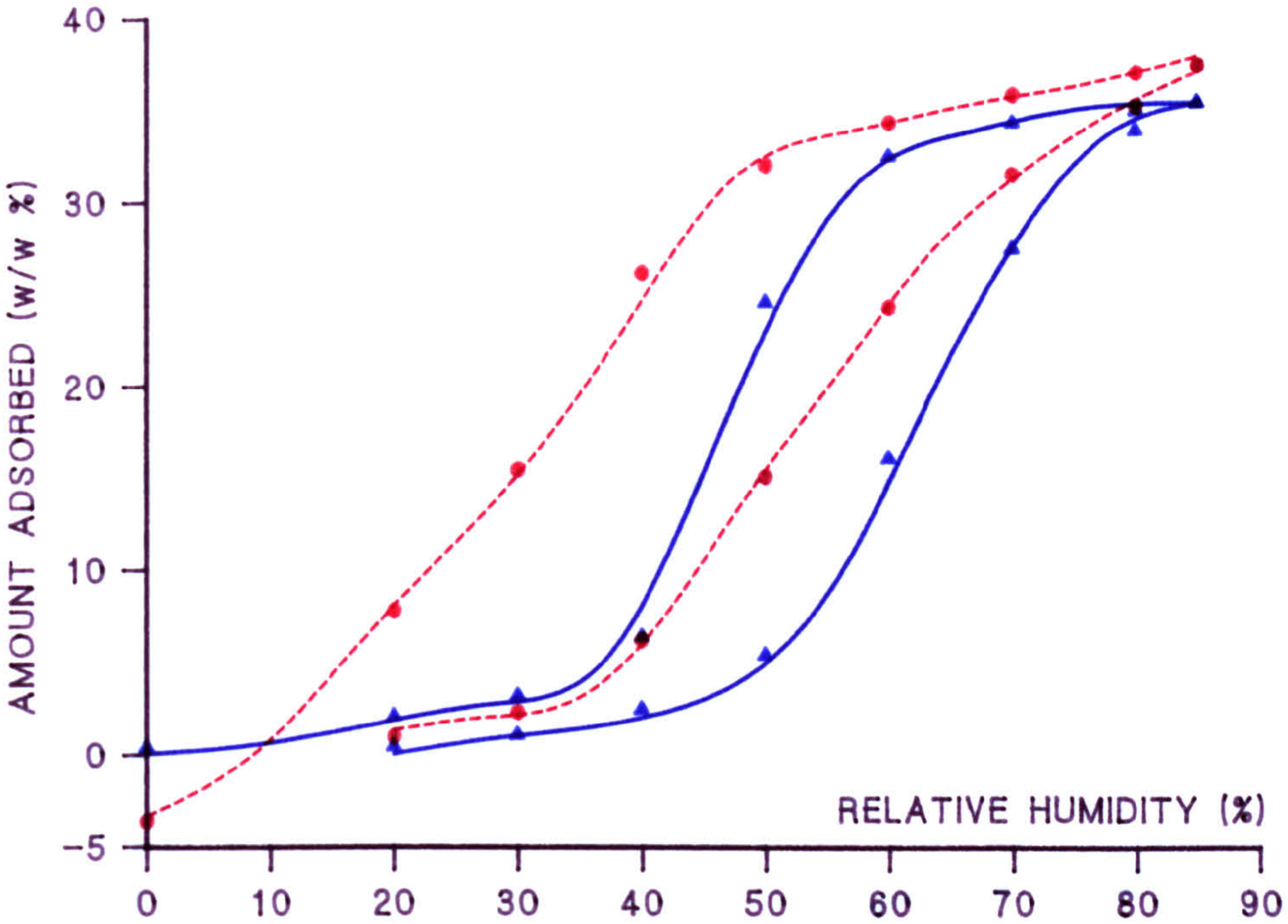

FIGURE 7.1.11 WATER ADSORPTION

▲ CECA CONTROL ● CECA FLUORINATED (6% F)

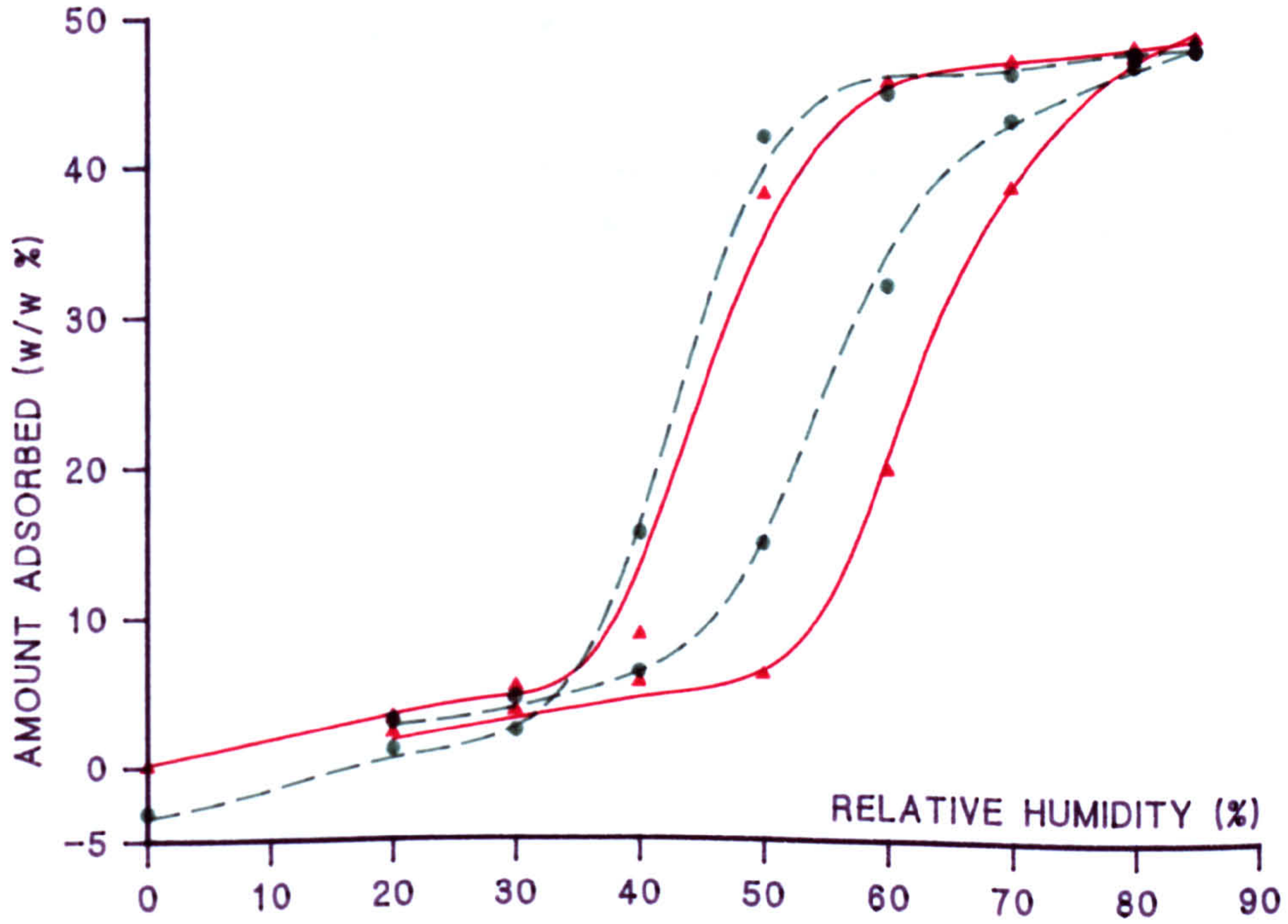

FIGURE 7.1.12 WATER ADSORPTION

FLUORINATED CECA (18.8% F): ▲ FIRST AND ● SECOND ISOTHERMS

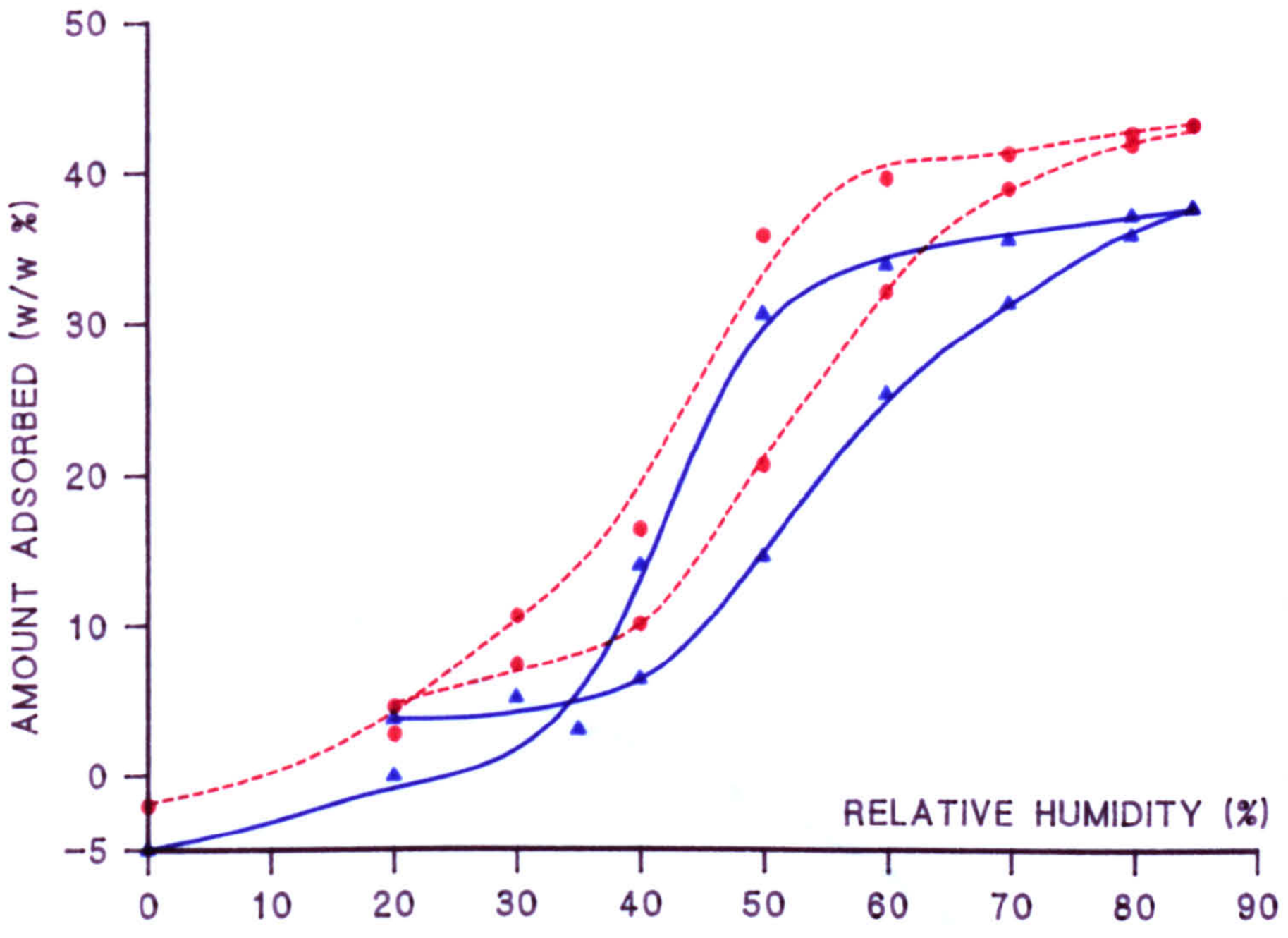

FIGURE 7.1.13 CHLOROPICRIN BREAKTHROUGH CURVES MEASURED IN DRY AIR

▲ CONTROL CECA CARBON ● FLUORINATED CECA (6% F)

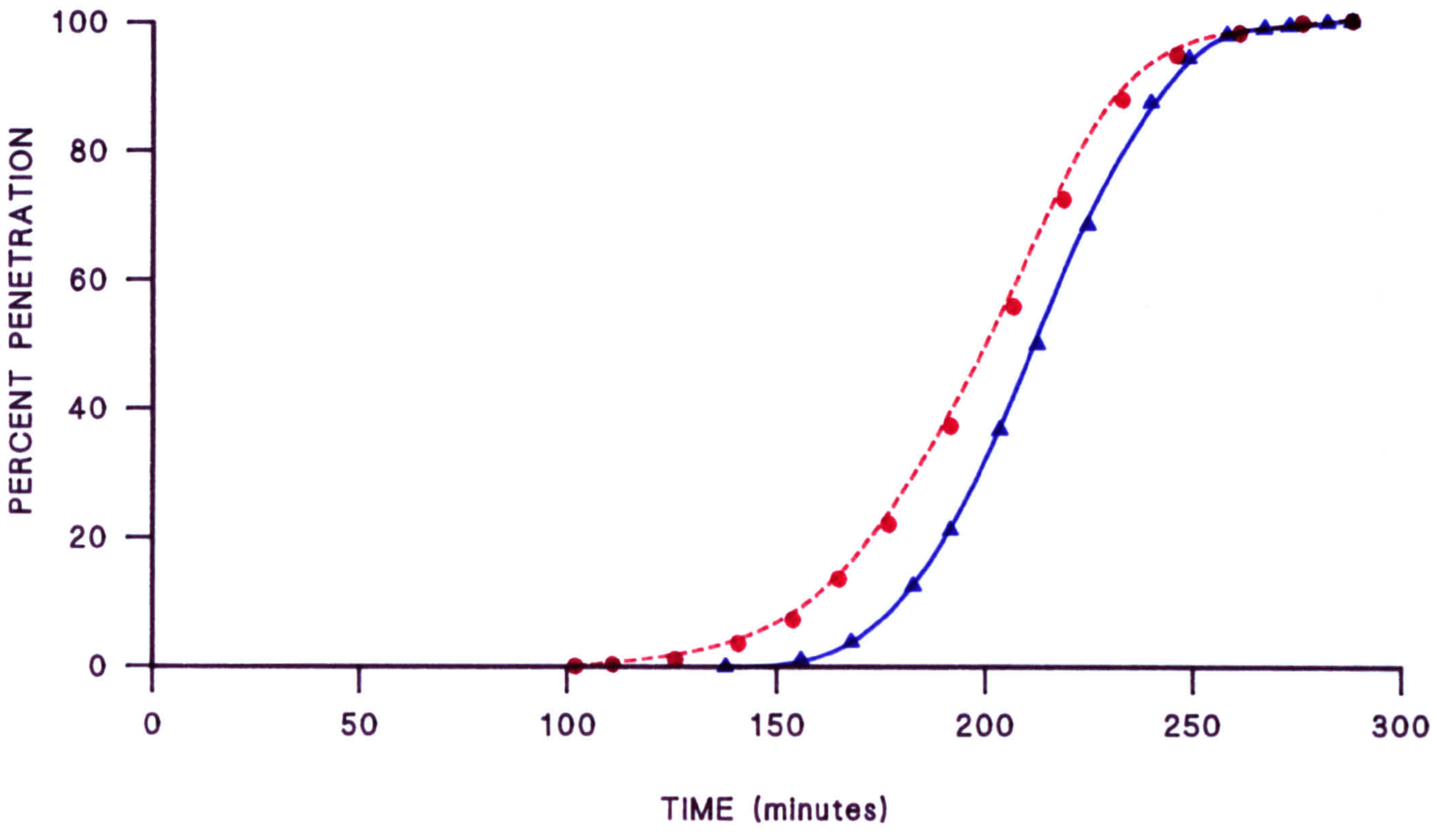

FIGURE 7.1.14 EDX SPECTRUM BPL CARBON FLUORINATED AT HIGH TEMPERATURE

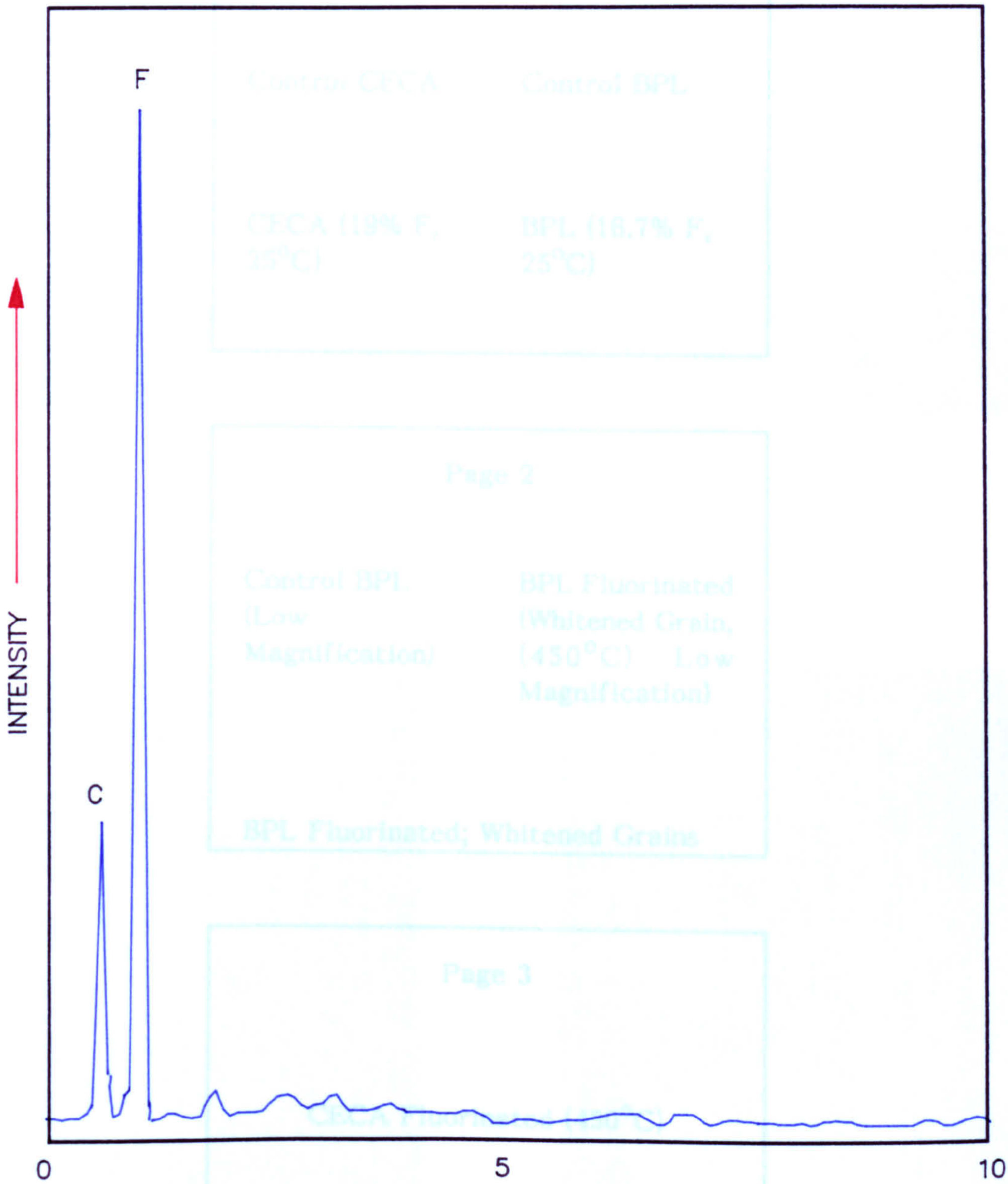

Figures 7.1.15

KEY

Page 1

Control CECA

Control BPL

CECA (19% F, 25°C)

BPL (16.7% F, 25°C)

Page 2

Control BPL (Low Magnification)

BPL Fluorinated (Whitened Grain, (450°C) Low Magnification)

BPL Fluorinated; Whitened Grains

Page 3

CECA Fluorinated (450°C)

CECA Fluorinated (450°C)

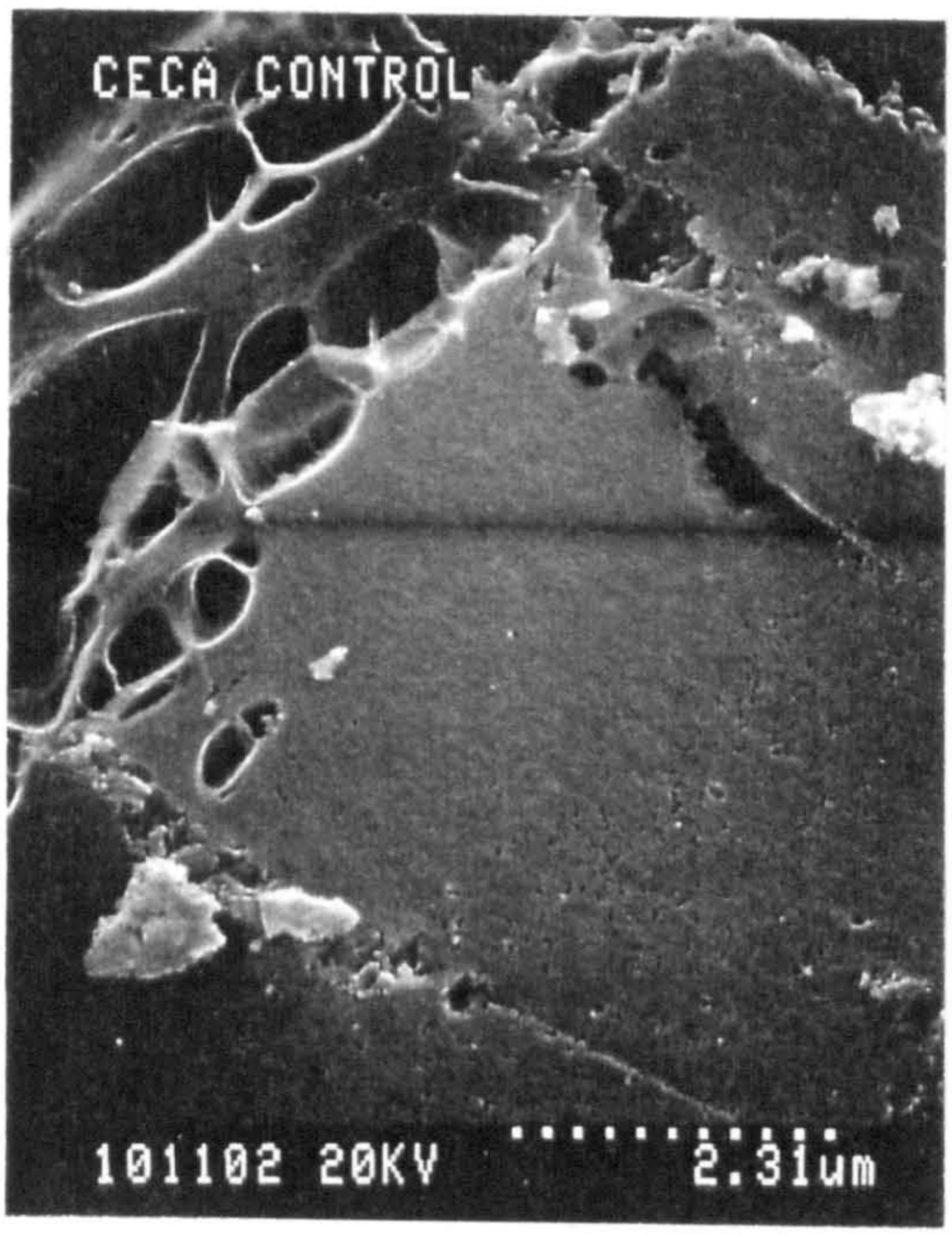
CECA CONTROL
101102 20KV
2.31um


BPL CONTROL
101100 20KV
2.31um

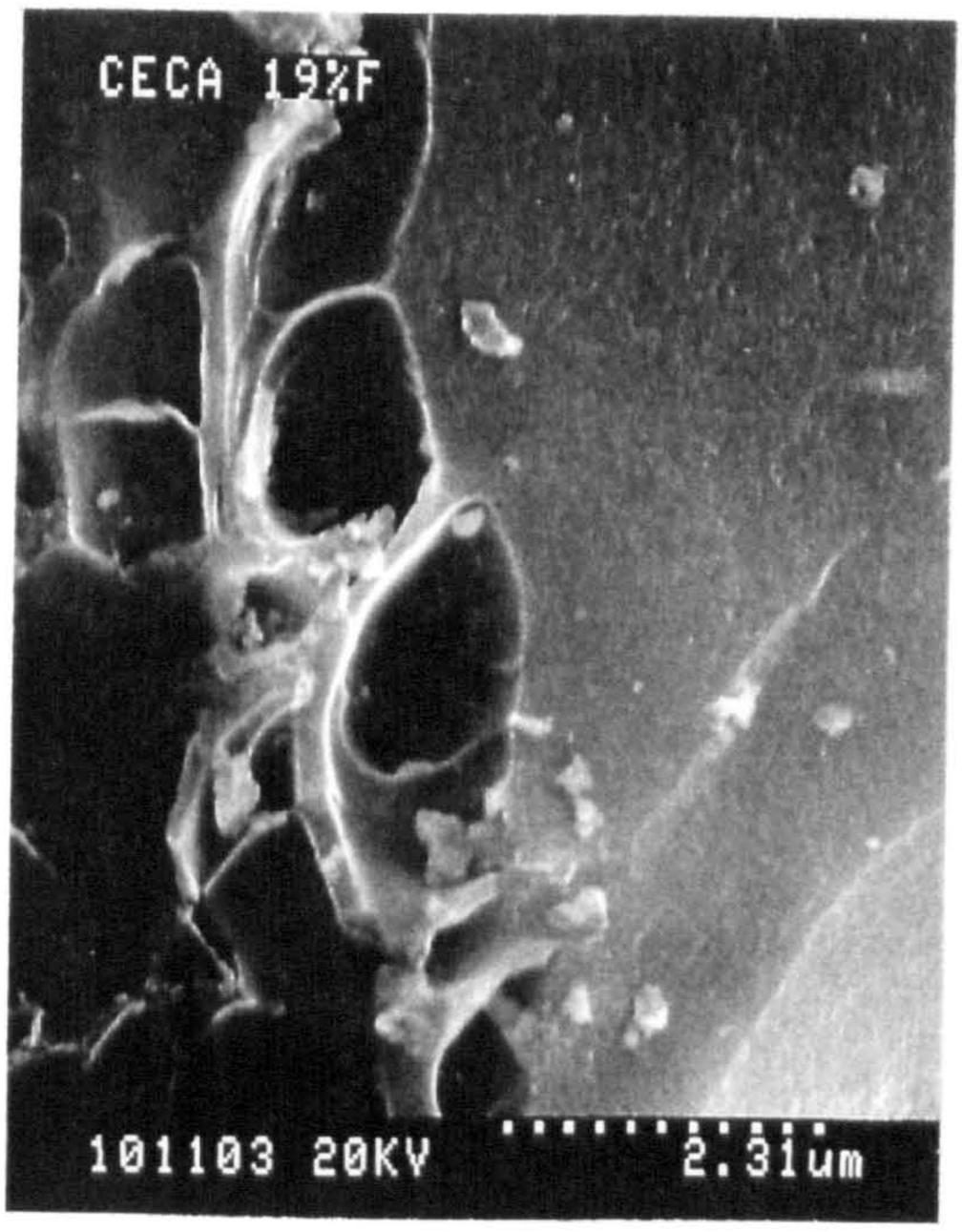
CECA 19%F
101103 20KV
2.31um

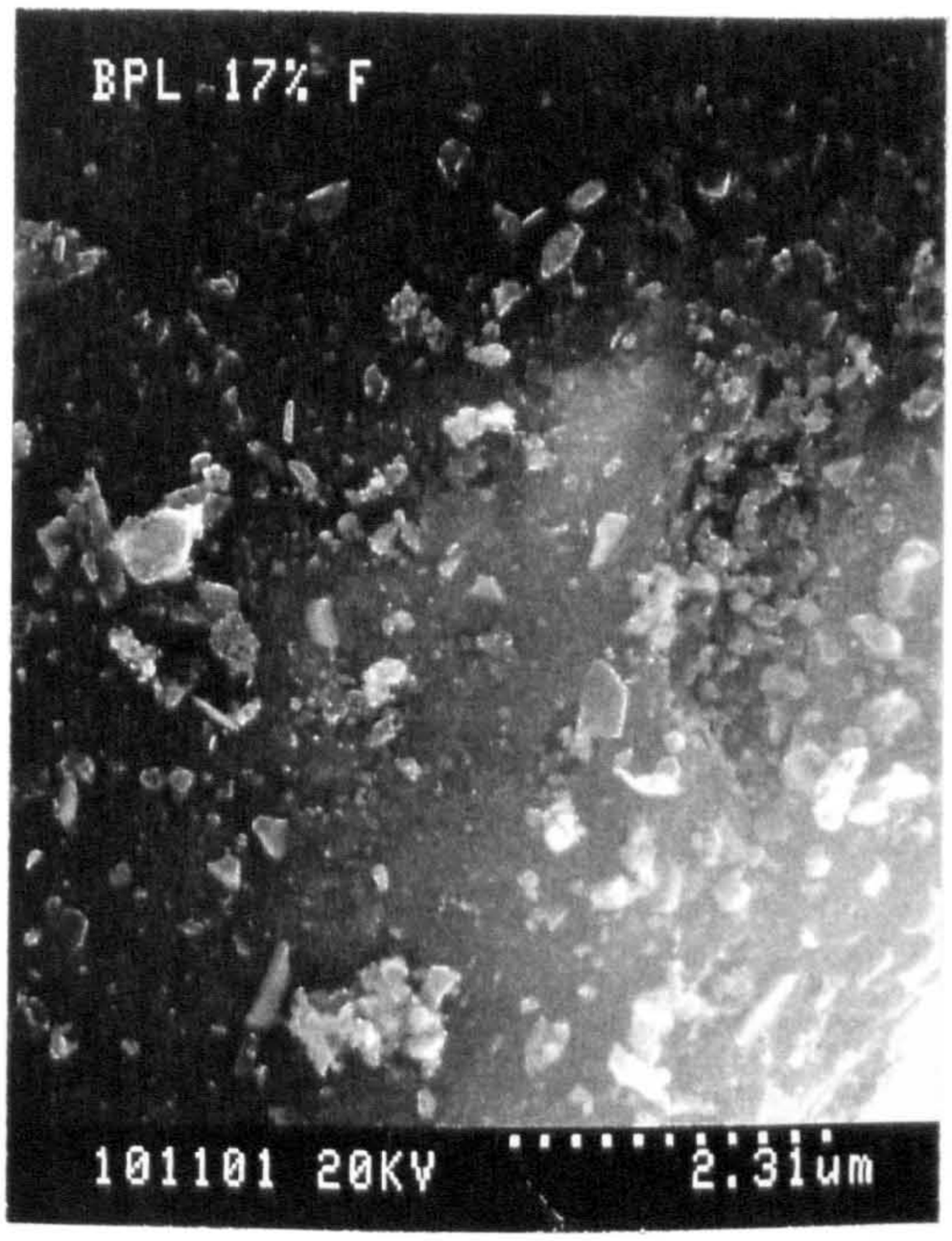
BPL-17% F
101101 20KV
2.31um

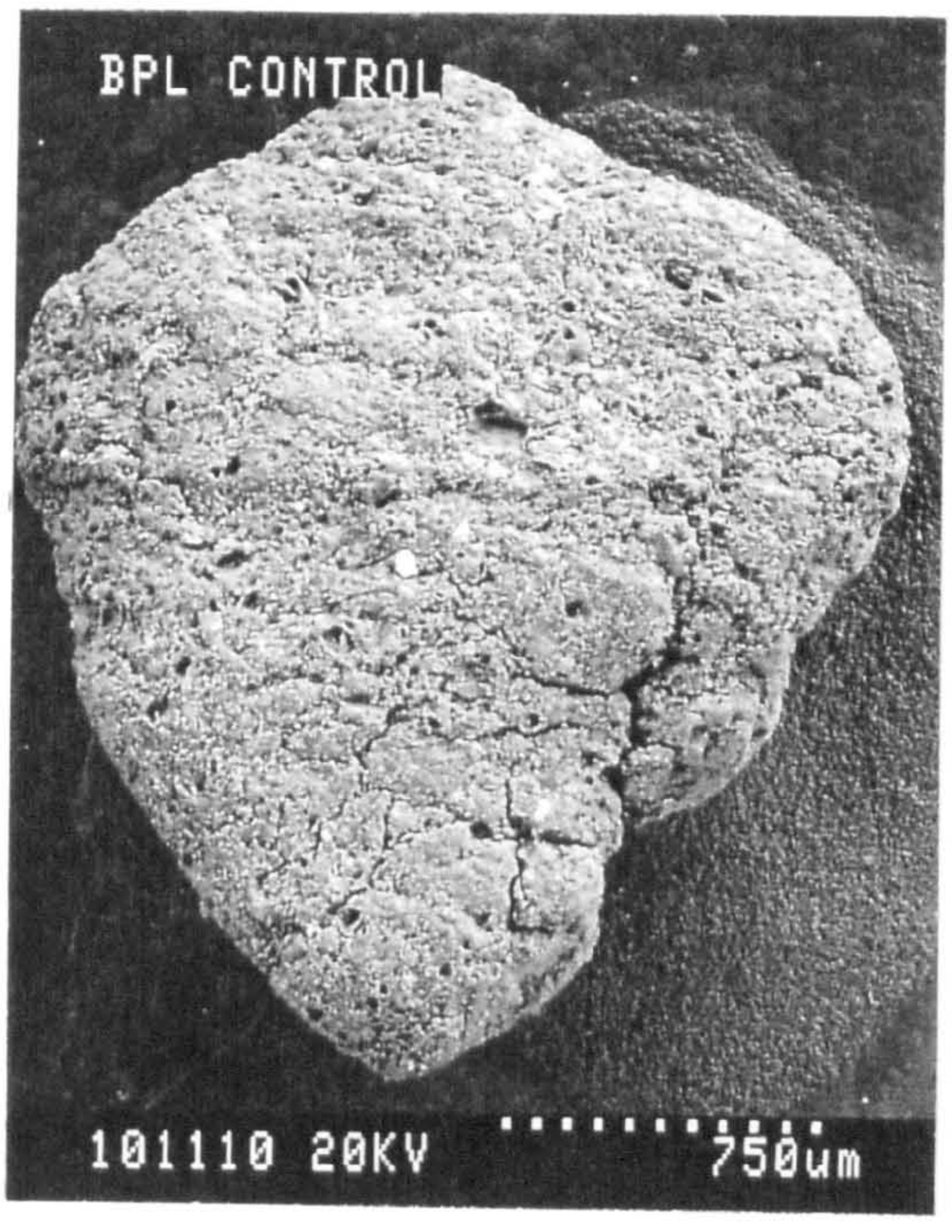
BPL CONTROL
101110 20KV
750um

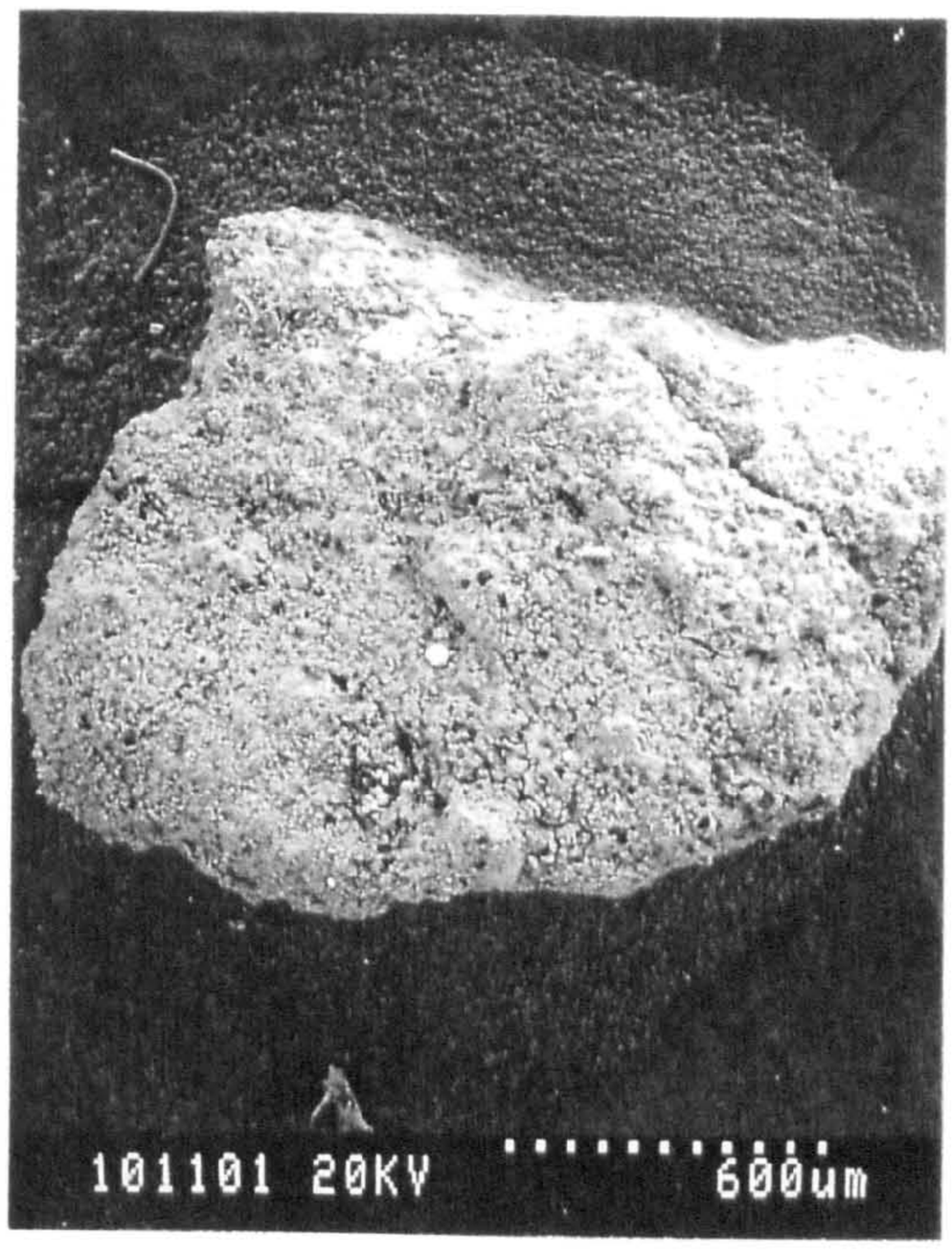
101101 20KV
600um

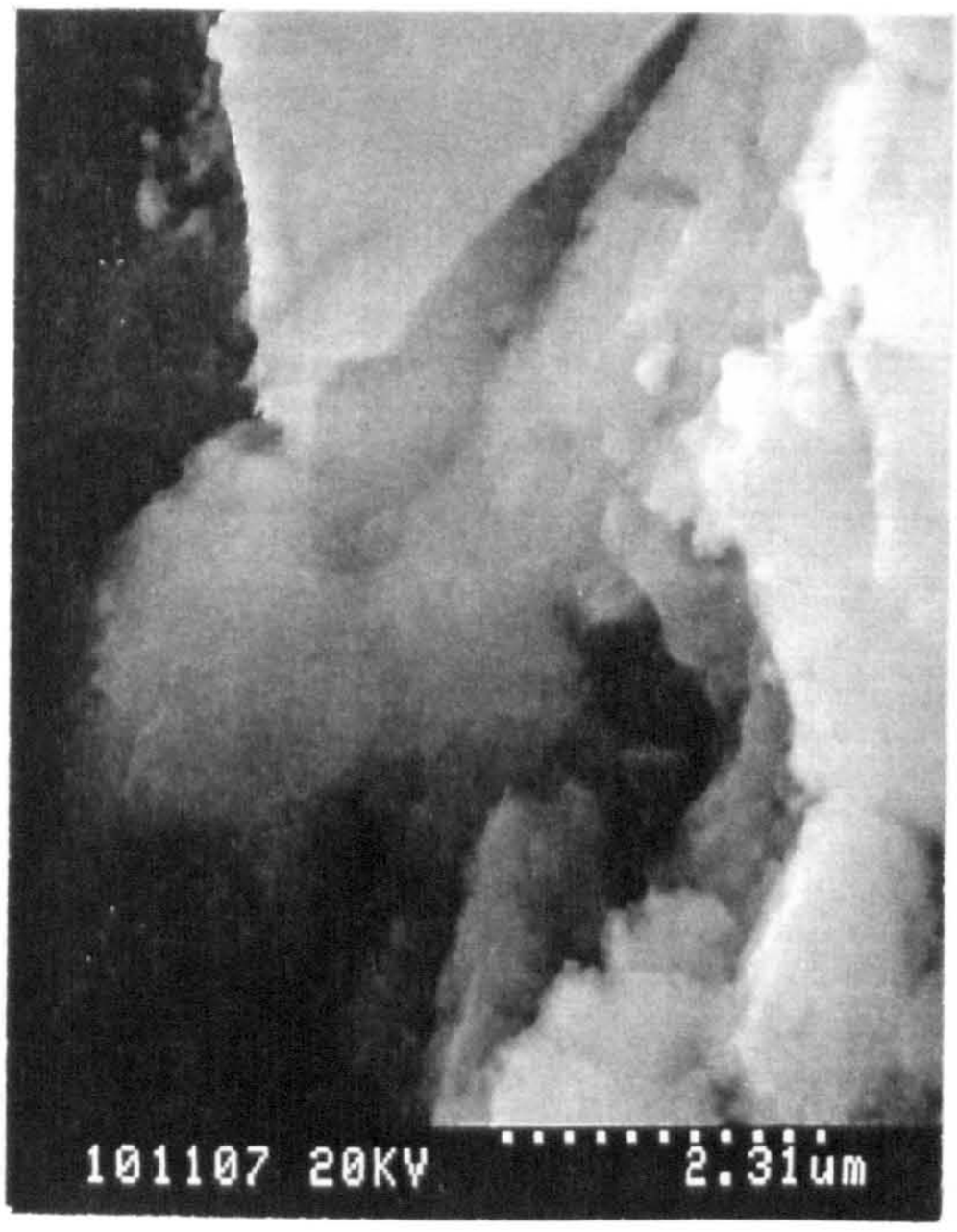
101107 20KV
2.31um

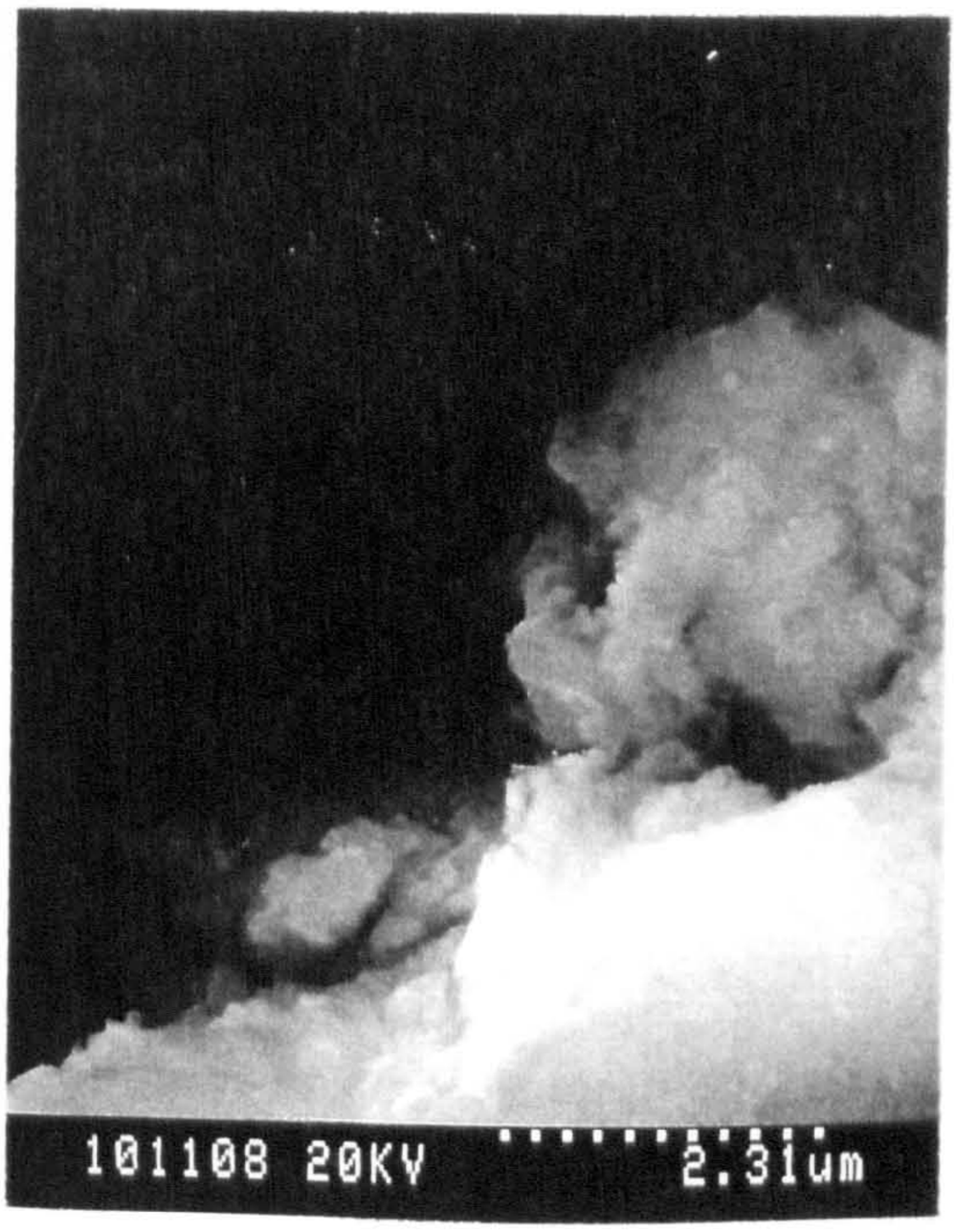
101108 20KV
2.31um

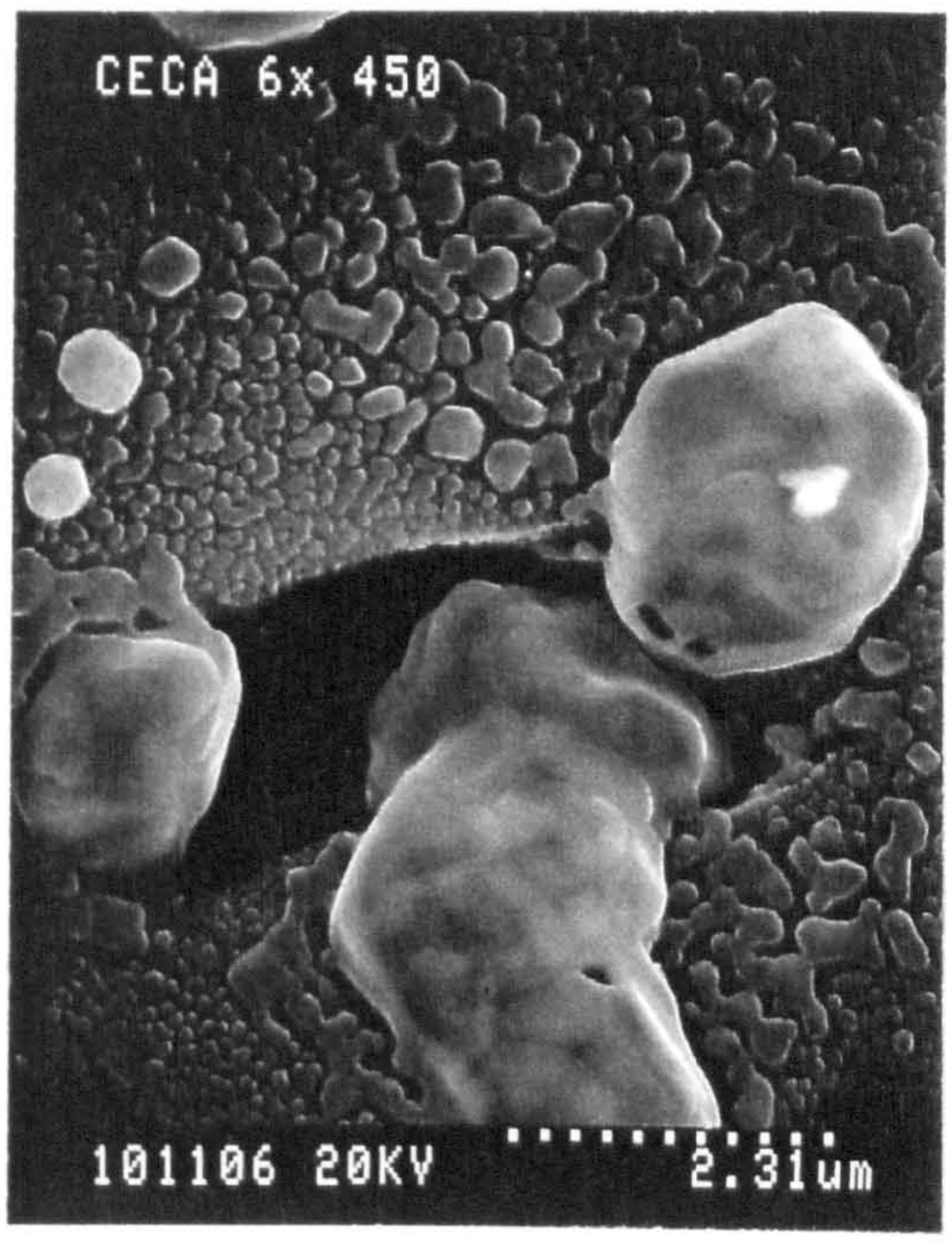
CECA 6x 450
101106 20KV
2.31um

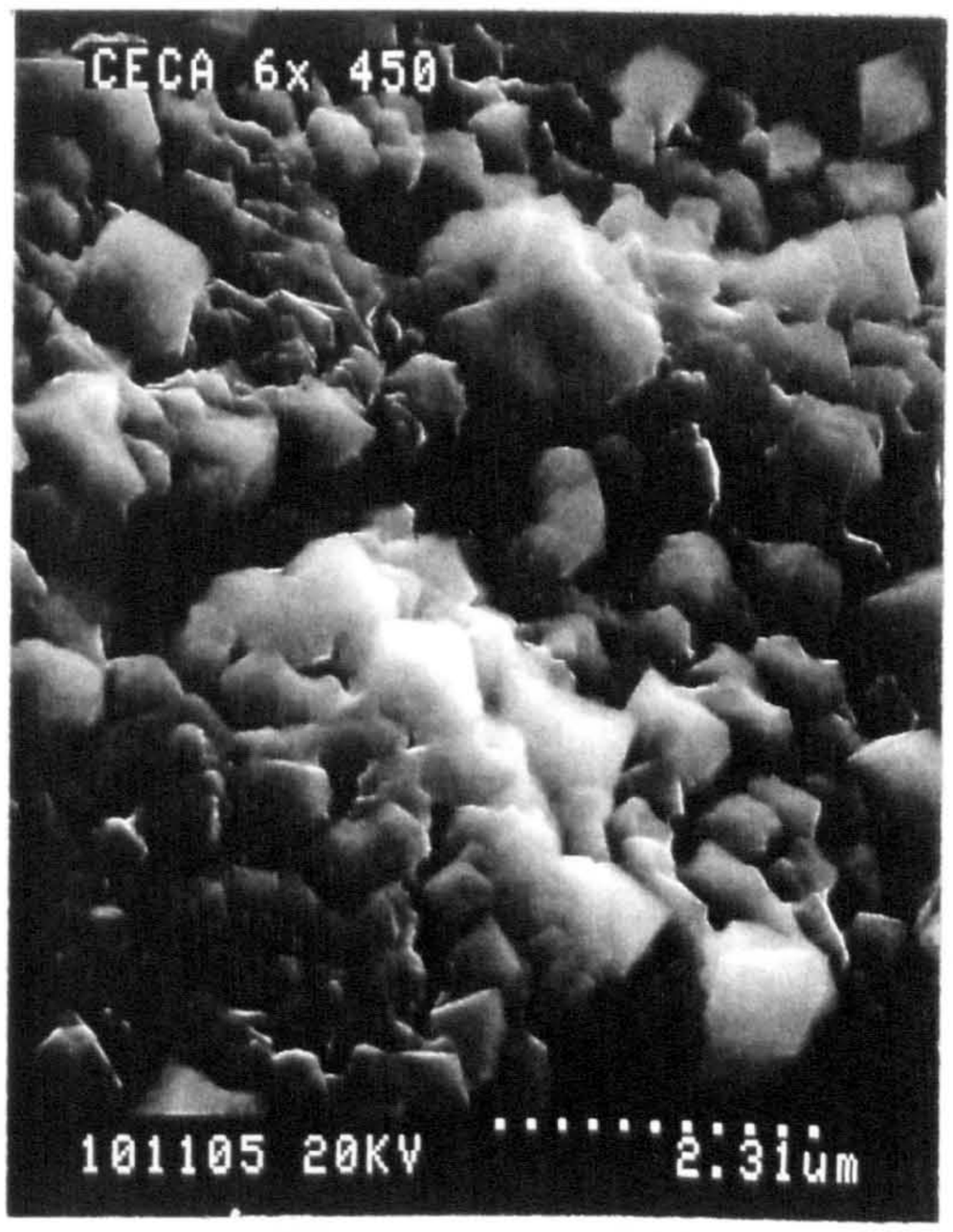
CECA 6x 450
101105 20KV
2.31um

FIGURE 7.1.16 DSC CURVES FOR SCII CARBON

□ FLUORINATED METHANOL TREATED; ▲ FLUORINATED
● FLUORINATED WATER TREATED

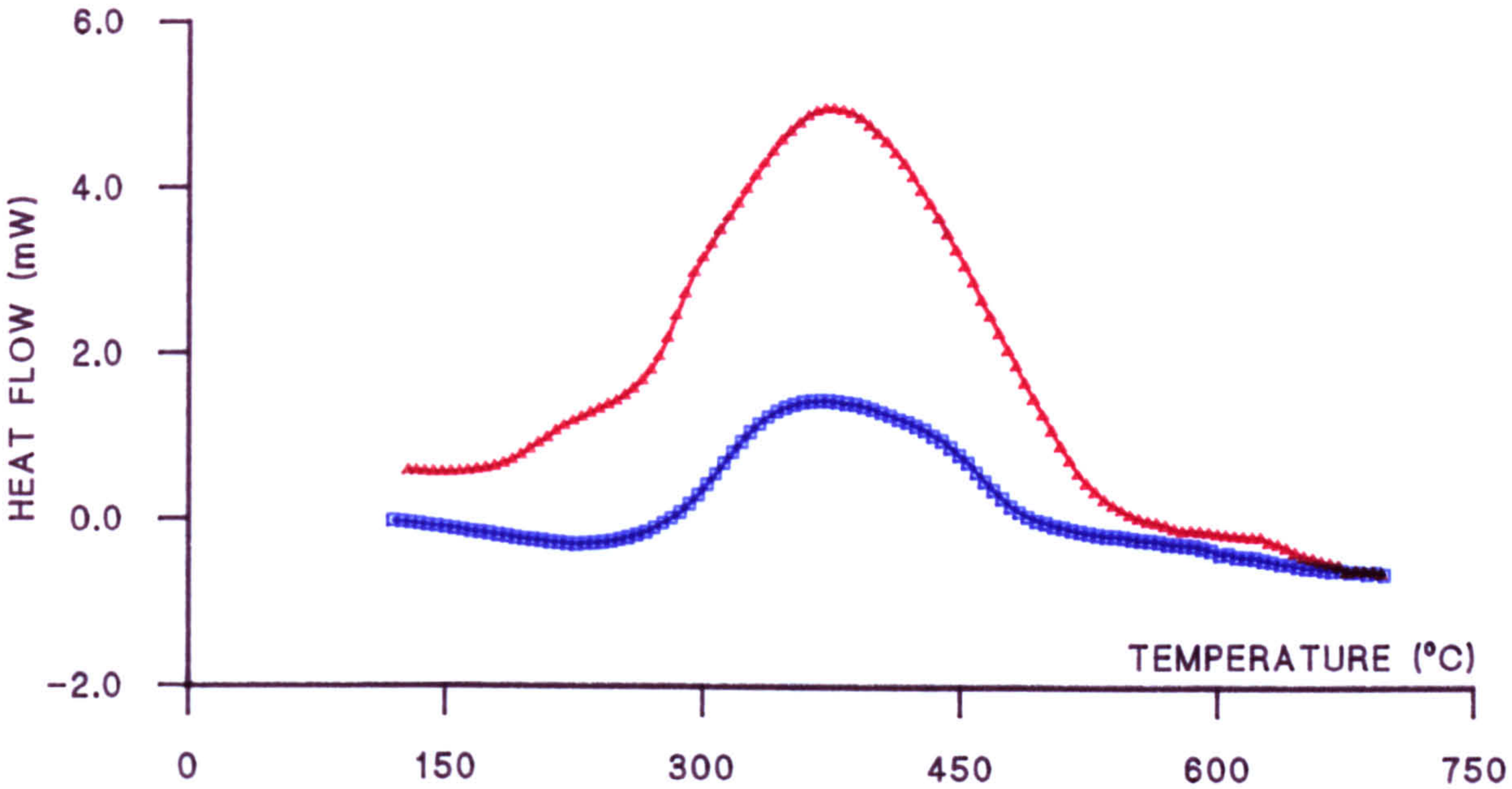

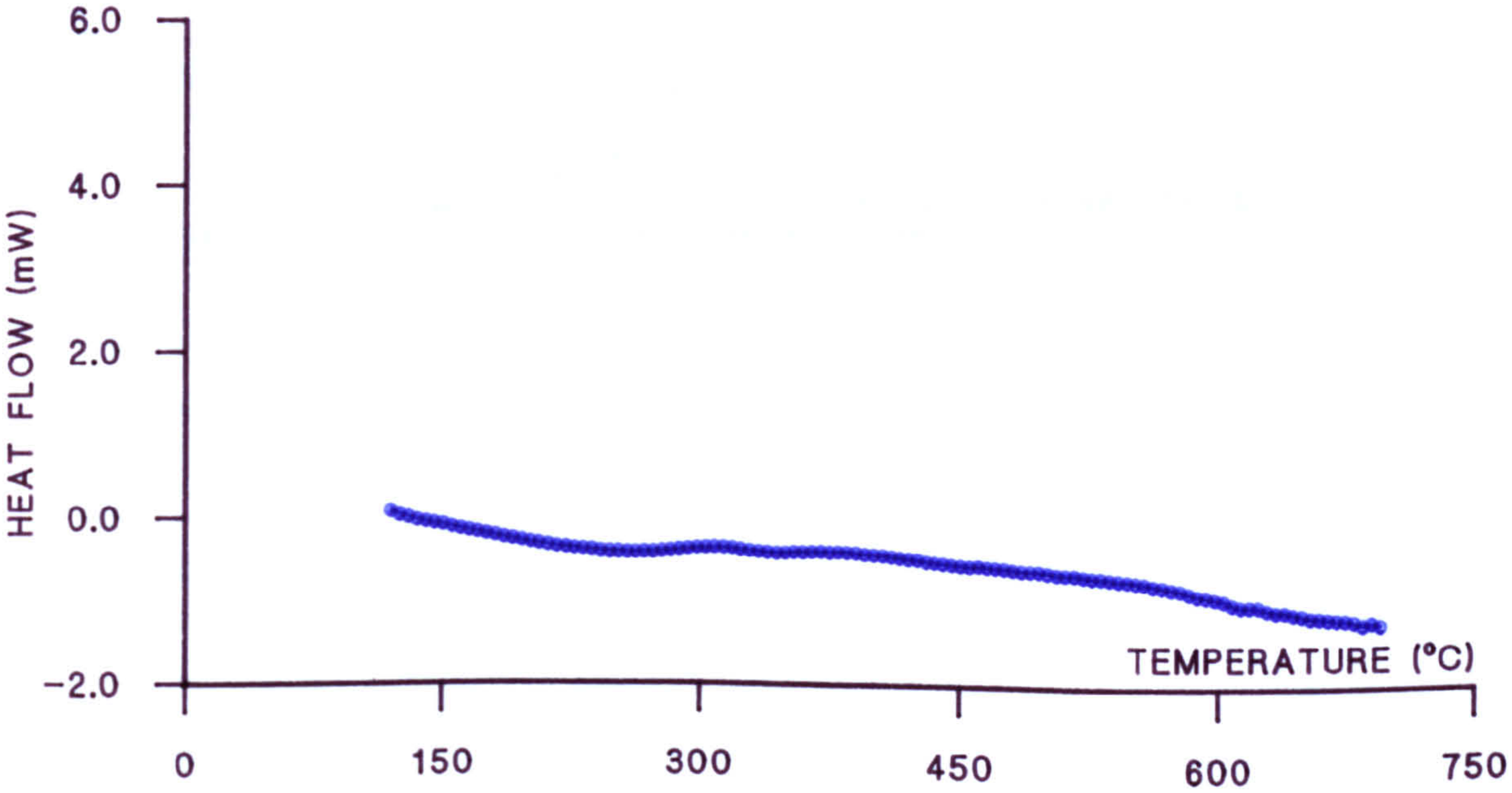

FIGURE 7.1.17 WATER ADSORPTION

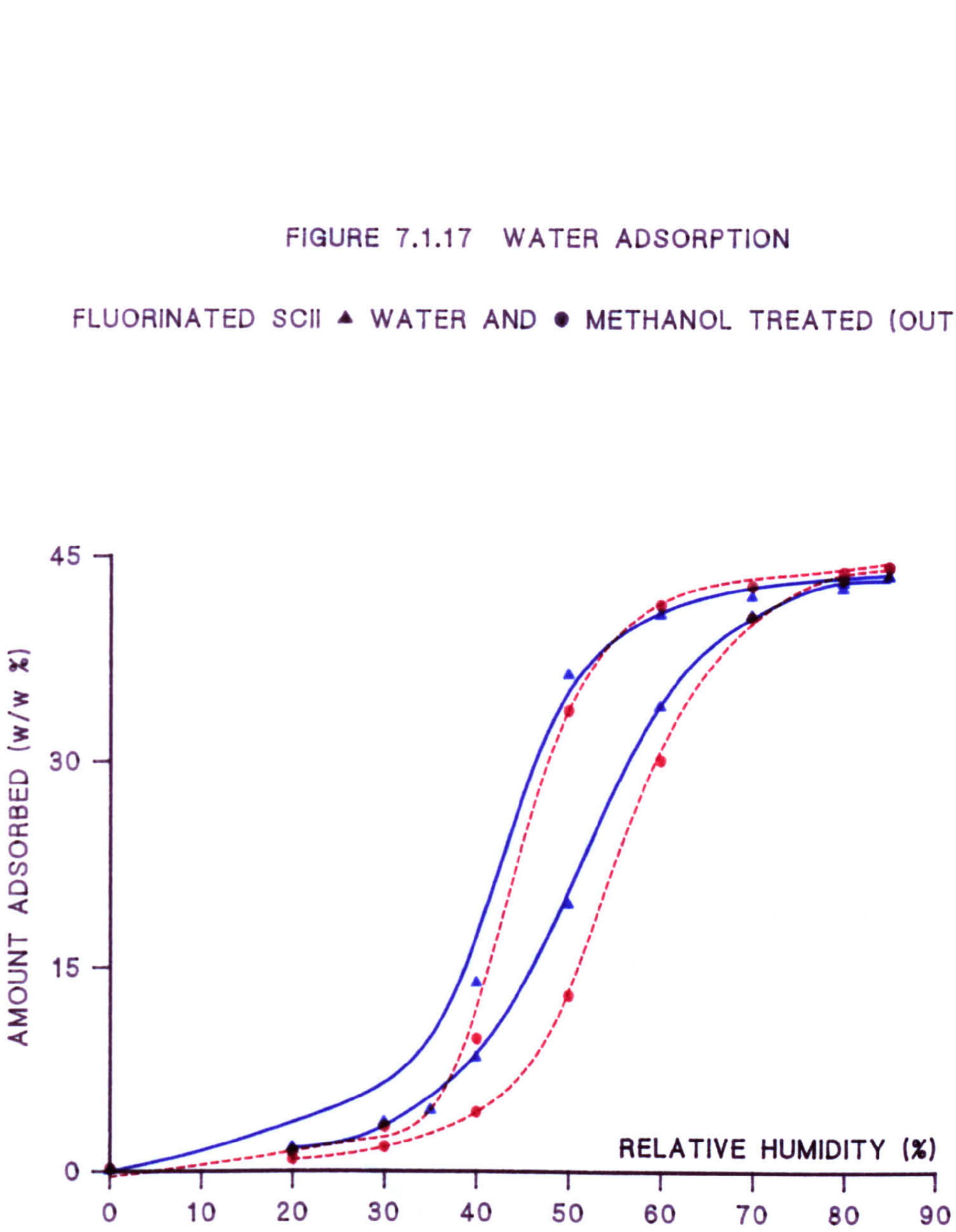

FIGURES 7.1.18 DSC AND TG CURVES FOR SCII CARBON

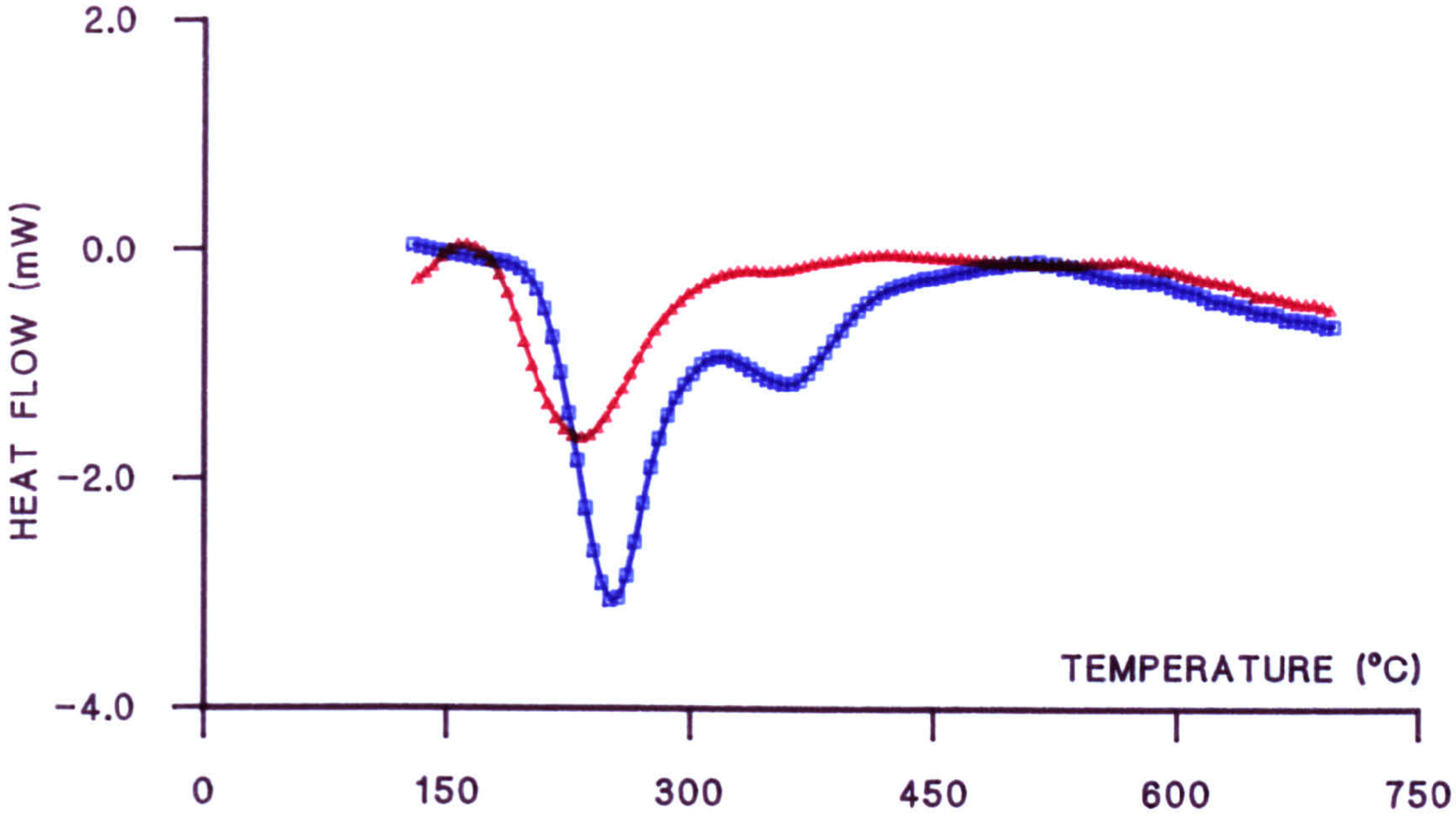

TG CURVES FOR SCII CARBON

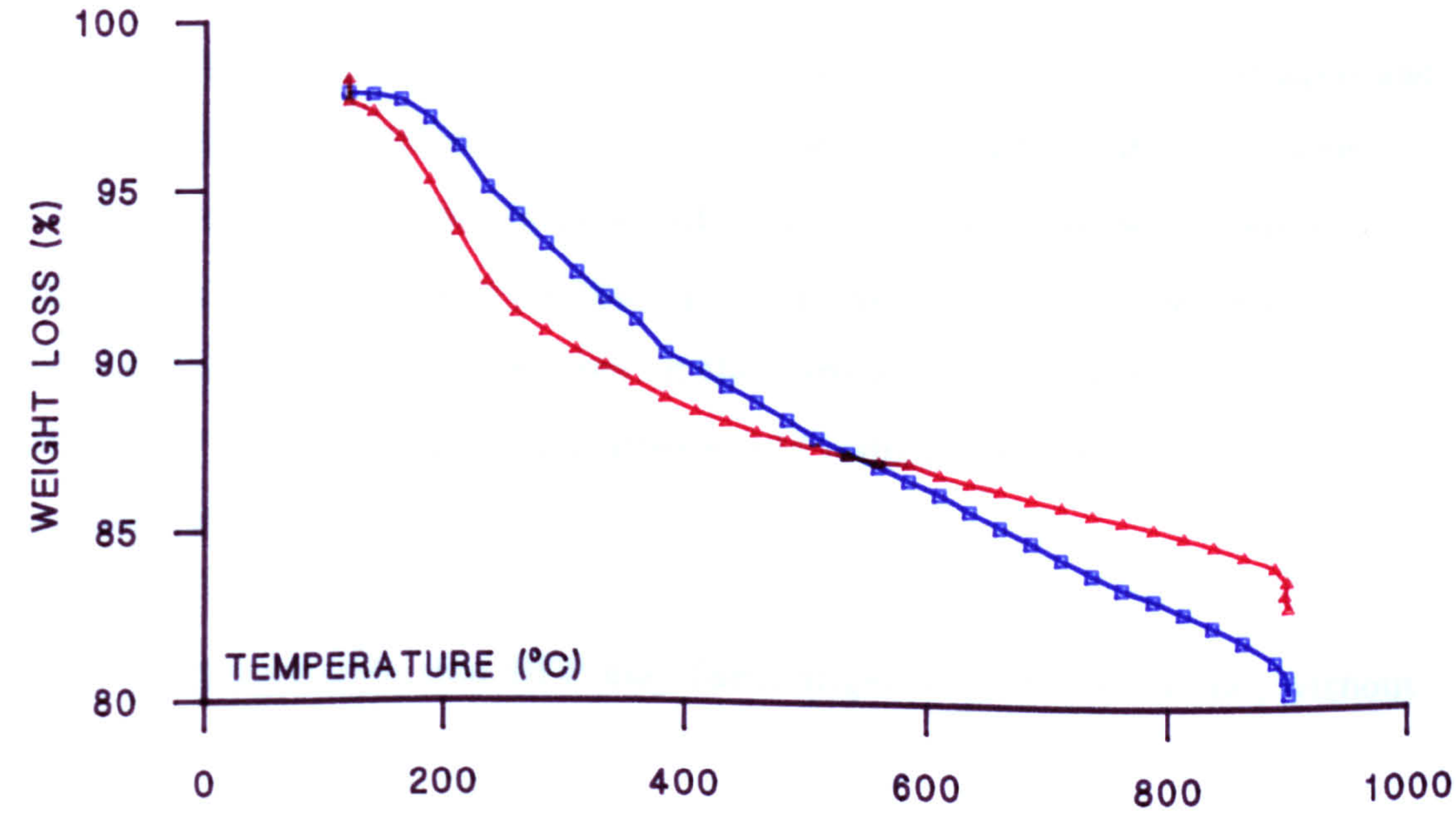

The Interaction of Carbon with Hexafluoropropene

7.2 Introduction

The results of chemically modifying activated carbon using hexafluoropropene are discussed in this section.

Direct fluorination was found to yield an unstable product, probably due to fluorine absorption into the carbon granules. Because this behaviour may be anomalous, a more selective fluorinating reagent was identified which would be more likely to react only at the carbon surface.

No reports of the use of hexafluoropropene (HFP) to modify carbon surfaces prior to this present study have been found, although silicas have successfully been fluorinated using this reagent (chapter 3).

HFP may undergo specific chemical reactions at the surface of aged and control carbons, to produce an adsorbent of improved hydrophobic character. Any reduction in the number of polar adsorption centres may be due either to reaction with surface oxygen containing functional groups, or as a result of direct combination with active sites on the carbon, such as centres of unsaturation. The masking of such sites would reduce the number of polar adsorption centres.

It is also possible that HFP may form oligermers on the carbon, without reaction.

7.2.1 The Preparation of Modified Adsorbents

BPL activated carbon was used in this part of the study. Both control and aged control samples were used. HFP (>98% purity) was obtained from Fluorochem Ltd., Old Glossop.

Exploratory studies performed using a 16 litre vacuum vessel revealed that significant reaction did not take place at temperatures below ca. 180°C. Thus, approximately 20g samples were modified by exposure to HFP at 180°C and at a pressure of approximately one atmosphere. After storing overnight, the samples were outgassed in situ, cooled, and removed. The samples were further outgassed at 180°C until constant weight was attained.

7.2.2 Adsorptive Properties of HFP Modified Carbons

Adsorption data has been corrected as described previously: gas analysis (GC) did not reveal the presence of any reaction products (the reagent was readily detected), suggesting that carbon gasification did not take place to any significant extent.

HFP modified carbon was found to be of reduced surface area compared to the control. This was due to a loss of microporosity (nitrogen adsorption, table 7.2.1). This contention was supported by measurement of hexane breakthrough curves, in that the modified samples adsorbed less hexane in comparison to the controls (table 7.2.1, figure 7.2.1).

Methanol adsorption revealed that the modified carbons contained fewer polar adsorption centres compared to the control (figure 7.2.2).

Because nitrogen and hexane adsorption indicate that modification only results in a small loss of porosity, the methanol adsorption characteristics of

the modified carbon probably reflect a genuine change in the hydrophobic character of the surface, rather than pore occlusion.

This contention is supported by measurement of the water isotherm for the modified sample, where it was found that the uptake of water below RH values of approximately 50% was reduced (figure 7.2.3). The reduction in the amount adsorbed at high RH values probably reflects a combination of the change in the hydrophobic character of the surface, and the small degree of pore occlusion. In comparison to carbons modified with fluorine, the HFP treated carbons were found to be relatively stable: at the end of the measurement (outgassing the sample at 120^{o}C for 3 hours (3 mbar)), a small increase in sample weight was observed, consistent with sample ageing effects (chapter 6).

PS adsorption (table 7.2.1) was slightly improved in comparison to samples of control carbon, indicating that the rationale for selecting HFP for surface modification was correct.

Attempts to use this approach for modifying the surface of aged carbons were less successful, in that the PS adsorption properties were largely unchanged (table 7.2.1). Water (figure 7.2.4) and methanol adsorption indicated that the modified aged sample contained few polar adsorption centres: the relatively poor PS adsorption characteristics may therefore result from a combination of the reduction in the micropore volume, and the presence of bulky oxygen and fluorine containing functional groups at the surface, which hinder vapour adsorption from humid air.

Examination of the thermal desorption profiles suggested that the surface species were relatively stable (no significant weight loss was observed until ca. 350^{o}C).

Although it is probable that HFP undergoes a chemisorption reaction at the surface, an equally valid explanation is that the reagent oligermerised on the carbon without reaction.

On the basis of the exploratory results, it is evident that the use of fluoroolefins for carbon modification offers some promise, but that the molecular size of the modifier is equally important. Thus the use of another, less bulky, reagent has been investigated (7.3).

Table 7.2.1 HFP Modified Carbons

	Sample			
	Control	Control- HFP	Aged Control	Aged Control- HFP
Weight Increase After Modification (w/w %)	-	8.0	-	6.5
BET Surface Area (m^2g^{-1})	1195	1089	1100	1047
Micropore Volume ($cm^3<STP>g^{-1}$; α_s)	0.55	0.57	0.53	0.52
Hexane Adsorption Amount Adsorbed ($mg\ g^{-1}$)	247	201	238	194
50% Break time (minutes)	55	46	57	45
Methanol Adsorption Amount Adsorbed ($mg\ g^{-1}$)	18	12	24	13
Chloropicrin Adsorption				
1st Break	93	99	81	84
1% Break	105	108	90	93

{Control samples were outgassed at 180°C}

FIGURE 7.2.1 HEXANE BREAKTHROUGH CURVES

L-R: HFP MODIFIED BPL; CONTROL BPL

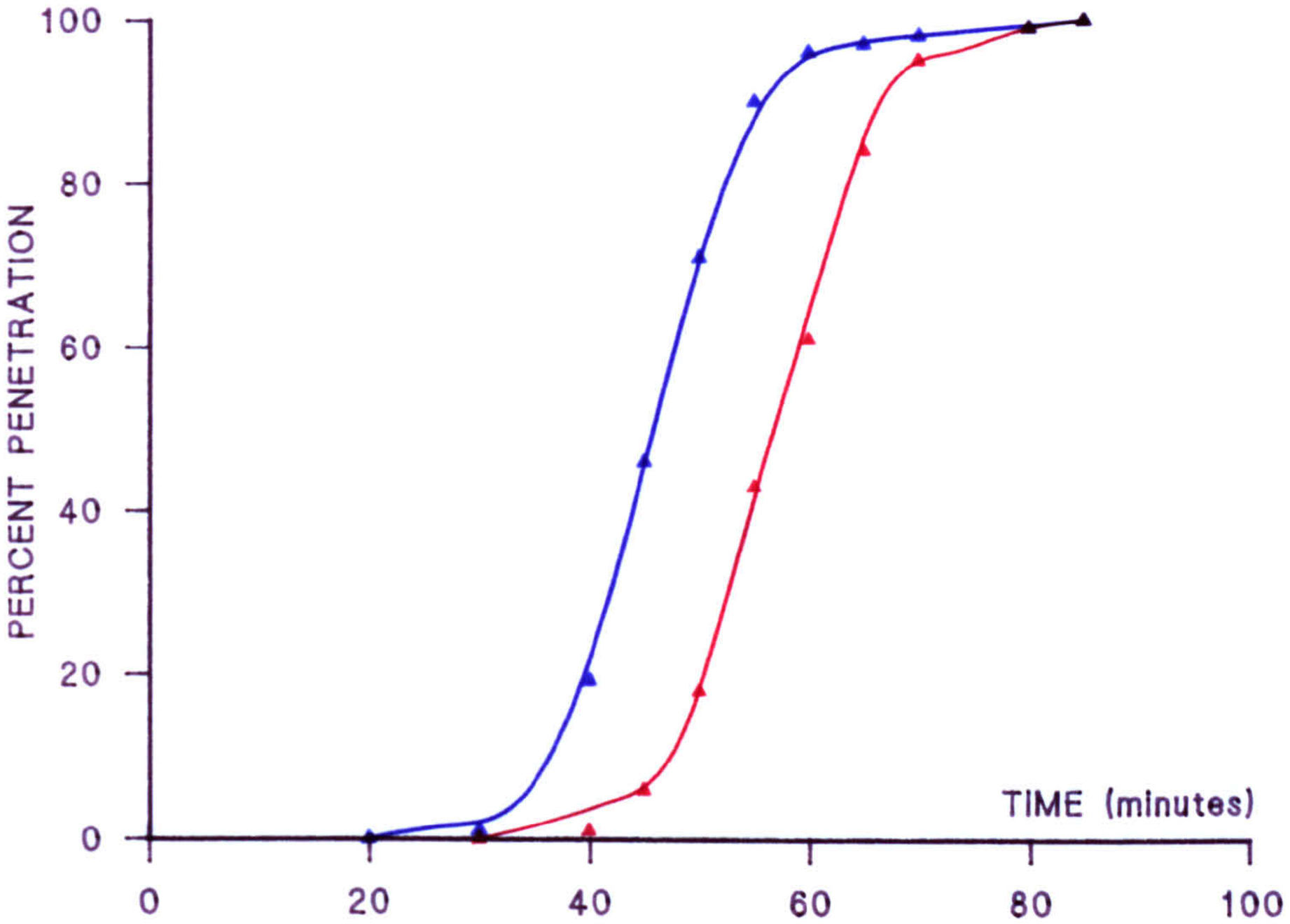

FIGURE 7.2.2 METHANOL BREAKTHROUGH CURVES

L-R: BPL HFP; BPL (AGED) HFP; BPL CONTROL

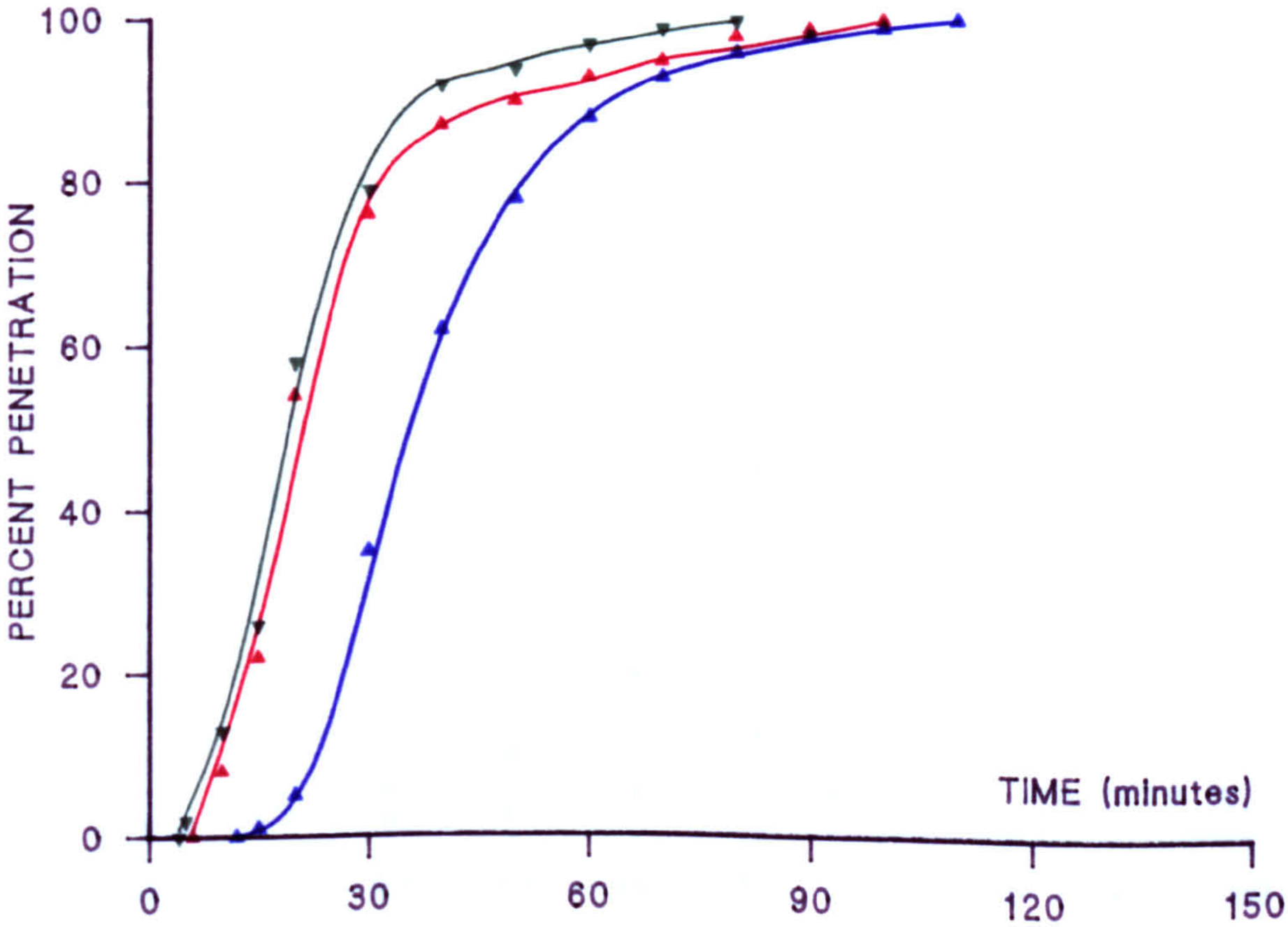

FIGURE 7.2.3 WATER ADSORPTION

● CONTROL BPL ▲ HFP MODIFIED CONTROL CARBON

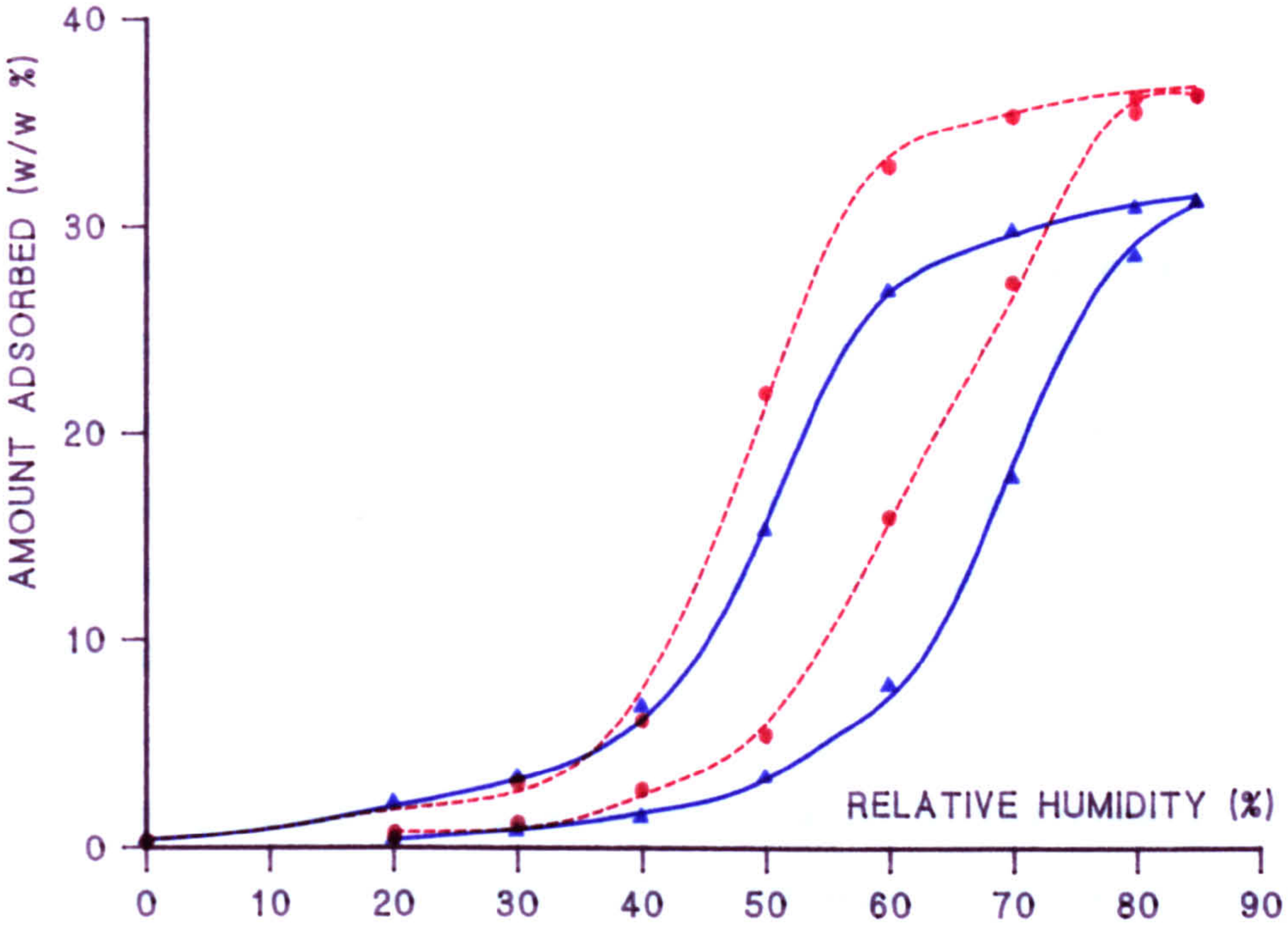

FIGURE 7.2.4 WATER ADSORPTION

▲ CONTROL (AGED) BPL ● HFP MODIFIED (AGED) BPL

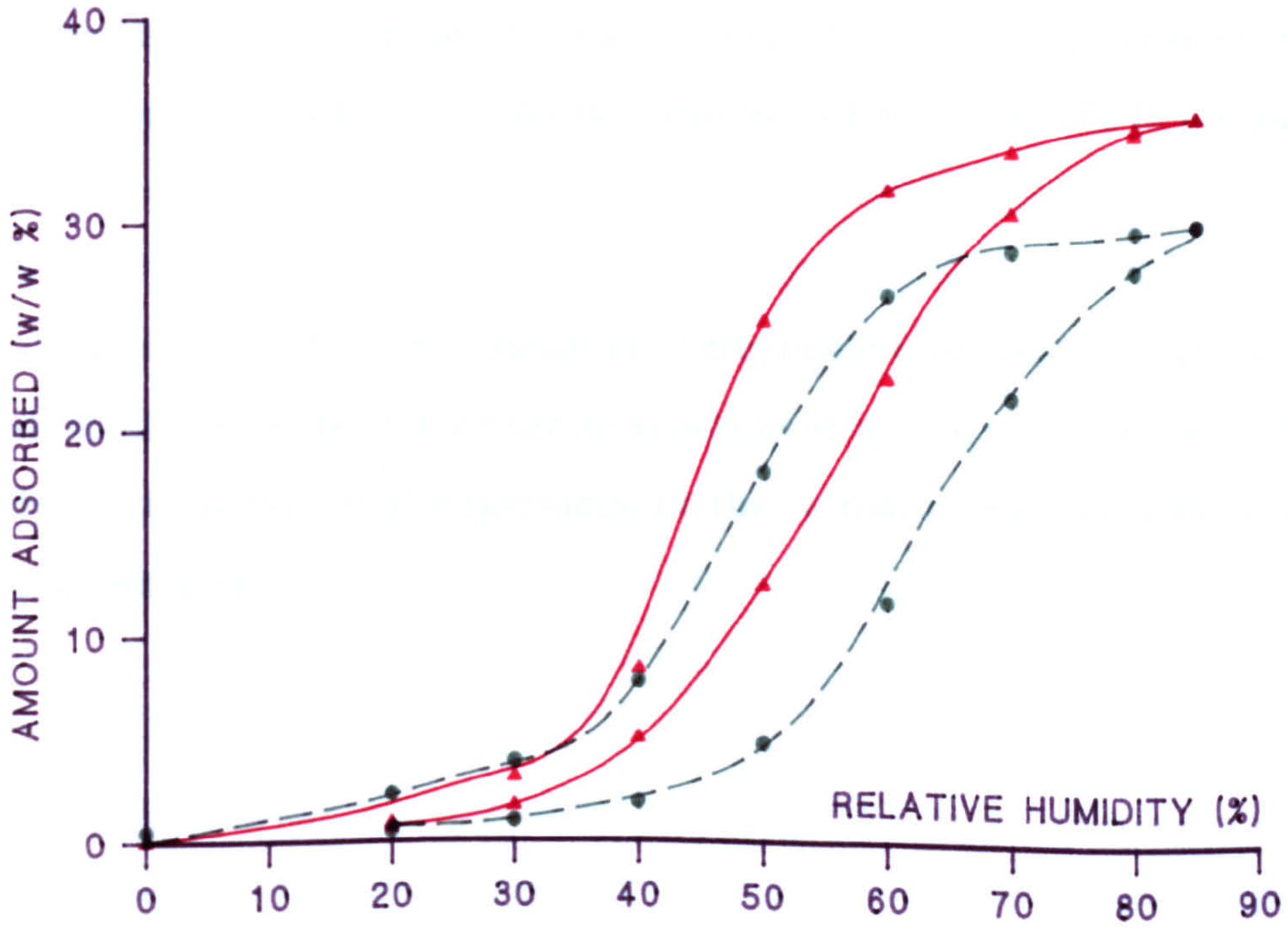

The Interaction of Carbon with 1,1-Difluoroethene

7.3 Introduction

Activated carbon has been modified using tetrafluoroethene (chapter 3). The results indicated that significant pore occlusion resulted, although the products were found to be more hydrophobic in comparison to control samples. It is very probable that the predominant reaction mechanism was that of polymerisation at the carbon surface, since substantial quantities of reagent were fixed.

A reagent of similar bulk, but which would be less prone to polymerisation, would be a more appropriate selection in the context of the aims of the present research.

1,1-difluoroethene (DFE) may undergo similar reactions to those of HFP. DFE will, however, polymerise more readily than HFP, but the molecule is comparatively small. If specific surface reactions are the predominant mechanism, then pore occlusion is likely to be less important in comparison to HFP.

As before (7.2) any change in hydrophobic character brought about by modification must be due either to reaction at active sites on the carbon surface, the presence of oligermers, or the formation of functional groups with surface oxygen.

7.3.1 The Preparation of Modified Adsorbents

BPL carbon was used in this part of the study. The DFE was obtained from Fluorochem Ltd., Old Glossop.

Exploratory studies revealed that little or no reaction occurred at temperatures up to 300°C. At 450°C, significant weight changes were observed.

No attempts were made to modify samples of aged carbon because the high reaction temperatures employed were sufficient to decompose a significant proportion of the surface oxygen containing functional groups.

On the basis of the preliminary results, carbon modifications were carried out at 450°C. Thus, approximately 20g of dry carbon was placed into the high temperature modification apparatus described at chapter 5, and in more detail at the Appendix. The vessel was heated to the reaction temperature under vacuum (1 mbar). After approximately 1 hour, DFE was introduced into the reactor until the pressure stabilised at ca. 1 atmosphere. After a further hour, the samples were outgassed, and either cooled to room temperature, or treated with a further aliquot of reagent. At the end of treatment, samples were removed and weighed.

It was found that the change in sample weight was sensitive to the number of treatment cycles (table 7.3.1): that is, the sample weight increased with the number of cycles, reaching a maxima after the introduction of about six aliquots. Increasing the number of cycles to twelve did not result in a further substantial weight change. Gas analysis (GC) only revealed the presence of unreacted DFE, suggesting that carbon gasification was unimportant.

It is probable that the observed dependence of the change in sample weight upon the number of treatment cycles was a result of the destruction of

the reagent within the reactor vessel before reaction at the carbon surface was complete. It is likely that the DFE molecules decomposed or polymerised at the vessel wall (a grey- white film was deposited on the cooled part of the reactor).

If the DFE- carbon reaction involved polymerisation at the surface, it might be predicted that a much stronger dependence between the weight change resulting from treatment and the number of treatment cycles would be observed.

This hypothesis was tested by carrying out DFE modifications at temperatures (600 and 700°C) where polymerisation reactions would be expected to be more important. Table 7.3.1 shows the weight changes associated with these higher temperature treatments.

In each case, large quantities of DFE could be fixed. That the pressure in the reactor reduced rapidly after the introduction of reagent suggests that polymerisation was probably taking place: at 450°C, the pressure in the reactor fell only slowly. On the basis of these observations, surface polymerisation would appear less likely at the lower temperature.

That DFE is suitable for surface modification was apparent from a study of the interaction of 1,1,2-trifluoroethene (TFE) with BPL carbon. Exploratory experiments revealed that at 450°C, polymerisation of the reagent within the pore structure was probably taking place, since large weight increases were observed (ca. 20%). Similar behaviour was observed at lower temperatures (ca. 300°C) suggesting that TFE is not suitable for surface modification due to the propensity of the reagent to polymerise, rather than react more specifically at the surface. Samples modified using this reagent were of very low nitrogen BET surface area, and did not adsorb PS efficiently compared with control carbon.

7.3.2 The Adsorptive Properties of DFE Modified Carbon

The nitrogen and water adsorption data has been corrected as described previously.

7.3.2.1 Nitrogen and Hexane

Nitrogen adsorption isotherms for samples of carbons modified with DFE at 450°C are at figure 7.3.1. Values of the BET surface area and micropore volume (α_s analysis) for these samples, and for those carbons modified at higher temperatures, are at table 7.3.2.

The similarity between the nitrogen isotherms for samples of control and DFE modified carbons suggests that little structural modification results (outgassing the control carbon at 450 or 600°C did not measurably change the isotherm).

It is apparent, however, that increasing the number of treatment cycles results in a small reduction in the micropore volume. In addition, a reduction in the external surface area (α_s analysis) was observed when the number of treatment cycles at 450°C was increased from six to twelve. These effects are probably the result of pore narrowing, although an equally valid interpretation is that pore blocking has taken place. It is probably the case that pore blocking has resulted from exposing the carbon to 12 treatment cycles.

Comparison of the data at table 7.3.2 indicates that at higher temperature, a substantial loss of porosity occurs. It is most likely in these examples that deposition of polymerised DFE within the micropore structure and on the external surface of the granules has resulted. Analysis of the sample modified at 600°C indicated that an almost total loss of microporosity resulted (the α_s plot was almost completely linear). The surface of these samples (SEM analysis) was noticeably different compared to the control, and carbons

modified at 450°C. In each case, a powdery material, of high fluorine content (EDX analysis) was deposited non- uniformly on the granules. Carbons modified at 450°C were similar to the control, but contained high local concentrations of fluorine (EDX), suggesting that specific reactions at surface active sites is an important mechanism at this temperature.

Hexane adsorption, measured for samples of (dry) carbon modified using up to six treatment cycles at 450°C, supports the view that little structural change has resulted (figure 7.3.2 and table 7.3.3): in addition, the shape of the breakthrough curve indicates that the adsorption kinetics, and the equilibrium adsorption capacity, are essentially the same as those of the control.

7.3.2.2 Water Adsorption

Water adsorption isotherms for samples of control (450°C outgassed) and DFE modified carbons are at figure 7.3.3. For both DFE modified samples, it is apparent that modification results in a carbon whose surface is significantly more hydrophobic compared to the control. It is also clear that increasing the number of treatment cycles (three to six) leads to a further improvement in hydrophobic character. Increasing the number of treatment cycles to twelve has little further effect on the number of polar adsorption centres: it is evident, however, that the addition of further aliquots of reagent results in a more significant reduction in the micropore volume, an observation consistent with the reduced uptake at high values of the RH (figure 7.3.4).

Thus, the reduced uptake of water vapour at high values of the RH in each case is a consequence of the presence of pore constrictions, but more importantly, because of the displacement of the pore filling region of the isotherm to higher values of the relative pressure due to the presence of fewer polar adsorption centres.

That the isotherm for the control is essentially the same after outgassing at 450°C (figure 7.3.5) suggests that few surface oxygen containing functional groups are present at the surface, and indicates that the change brought about by modification is due to reaction with DFE, rather than a simple thermal effect.

Nitrogen adsorption indicates that samples modified at 600 or 700°C are essentially non porous. The water isotherm for the 600°C modified carbon indicates otherwise, suggesting that this technique could be useful for preparing molecular sieve carbons (figure 7.3.6).

The propensity of the modified carbons to resist ageing effects was investigated (chapter 5). Figure 7.3.7 compares the isotherms for the 450°C modified (six treatment cycles) and for the same modified sample which had been aged prior to measurement of the isotherm. It is apparent that ageing has taken place, and that the aged sample contains a similar number of polar adsorption centres compared to the unaged control sample. This observation suggests that modification has not successfully masked all of the active sites on the surface. Alternatively, it may be that the functional groups present on the modified carbon are not hydrolytically stable.

7.3.2.3 Methanol Adsorption

Measurement of methanol breakthrough curves supports the view that the DFE modified carbons are of improved hydrophobic character in comparison to the control. The measurements also showed that the modified carbons are susceptible to ageing effects.

Carbons modified at 600 or 700°C adsorbed only small quantities of methanol, probably reflecting the low pore volume remaining after treatment.

7.3.2.4 PS Adsorption

PS adsorption data for the control and modified carbons are at table 7.3.4.

Modification at 450°C results in a carbon which adsorbs PS from a humid airstream more efficiently than the control. This observation, which is consistent with the water and methanol data, must be due to the improvement in the hydrophobic character of the surface. It is probable that the PS displaces pre- adsorbed water from the carbon more readily: that is, the control carbon contains significantly more polar adsorption centres from which water displacement is less energetically favourable.

The PS adsorption performance of the carbons modified at 600 or 700°C is poor, presumably due to the substantially reduced pore volume. The samples do, however, adsorb significant amounts of PS, indicating that nitrogen adsorption is not, in these examples, providing a meaningful measure of porosity.

PS adsorption data also indicates that the modified carbons are susceptible to ageing, although their use is advantageous in comparison to the control.

7.3.2.5 Hexane Adsorption at High RH

Carbons modified with DFE at 450°C were found to adsorb PS more efficiently compared with the control. To further investigate the improvement in hydrophobic character brought about by modification, a more severe test was applied, whereby samples of control, aged-control, and DFE modified carbons were challenged with a short duration, high concentration pulse of hexane vapour (arbitrary concentration/ time of 15000 mg m^{-3} for 2 minutes). Each

carbon was challenged in equilibrium with RH80% air, and the filter effluent was monitored using a VG PETRA mass spectrometer.

The challenge conditions employed are purely arbitrary, but they demonstrate well the improvement in filter performance brought about by using the modified carbon (figure 7.3.8; table 7.3.3). They also illustrate the severe effect that ageing can have upon the adsorptive properties of activated carbon (chapter 6).

Because the properties of the modified carbons were of importance in terms of the aims of this research, the interaction between DFE and BPL carbon was studied in more detail.

7.3.3 The Reaction of DFE with Activated Carbon

Examination of the elemental analysis data (table 7.3.5) revealed that reaction at 450°C resulted in an increase in carbon, hydrogen and fluorine content. The decrease in the oxygen content may be due to the decomposition of surface oxygen containing functional groups: however, it is equally possible that no change in the absolute amount of oxygen resulted from modification; rather that the amount found on a percentage basis is lower due to the increases in carbon, hydrogen, and fluorine content. This would seem most likely because of the similarity between the water adsorption isotherms for the control carbon, and the control which had first been outgassed at 450°C.

The data also confirms that fluorine incorporation results from modification. EDX analysis indicated that a significant quantity of the adsorbed fluorine was at the surface (7.3.2).

On the basis of the EDX analyses, XPS measurements were carried out. These analyses were extended to include directly fluorinated carbon in an attempt to establish a relationship between the fluorinating reagent and the chemical state of the adsorbed fluorine.

Figures 7.3.9-7.3.10 compare the wide scan spectra for control and directly fluorinated carbon. Prominent peaks in the spectra for control carbon are due to C (1S), O (1S) and OKLL Auger transitions. There are no peaks in the 680-700ev region, indicating that no fluorine is present at the surface. This was confirmed by elemental analysis. The presence of fluorine at the surface of the directly fluorinated carbon (6% w/w F, figure 7.3.10) is apparent (F (1S) and FKLL Auger transitions).

The spectrum for DFE modified carbon is not included, although it was similar to that for the directly fluorinated carbon (the only difference being the size of the fluorine signal). The use of carbons containing higher fluorine contents resulted in a more intense fluorine signal compared with that due to carbon C (1S).

Figures 7.3.11-7.3.12 show comparative narrow scan C (1S) spectra for control and directly fluorinated carbon respectively. The C (1S) peak at 285ev is due to C-H and C-C interactions, and the inflexion to higher binding energy values is attributed to C-O bonds.

In contrast to the spectrum for control carbon, the directly fluorinated sample exhibits a well resolved peak at a binding energy of 288.6ev. This is attributed to surface carbon- fluorine bonds, indicating that chemical reaction, rather than physical adsorption, has taken place. This peak cannot be due to carbon-oxygen species for a number of reasons. The most important is that the wide scan spectrum shows that the oxygen level is largely unchanged as a result of modification (figures 7.3.9 and 7.3.10). In addition, care was taken to ensure

that oxygen was excluded during the modification process. Comparison of this binding energy shift with that found for fluorinated graphite (chapter 3, references 173 and 174) suggests that this peak is due to C-F single bonds (table 7.3.6).

The spectrum for the DFE modified carbon is not included, although it resembles closely the spectrum for control carbon. The wide scan spectrum indicates that significant quantities of fluorine are fixed using either technique: that a sidepeak in the C (1S) spectra for the DFE carbon was not observed suggests that the C-F bonds are present in a low concentration, or are unstable in Ultra High Vacuum (UHV), or to the X ray beam. In addition, this part of the spectrum is recorded where the baseline is sloping steeply, suggesting that a small signal would be less readily detected. Peak deconvolution techniques were not found to be helpful.

The narrow scan F (1S) spectra for directly fluorinated carbon and DFE modified carbon are at figures 7.3.13 and 7.3.14 respectively. These show distinct peaks, of considerably different binding energies (sharp peak centred at 687.8 ev for the directly fluorinated carbon, and a smaller, broader peak at 692.1 ev for the DFE carbon). The shape of the peak for the DFE carbon suggests that a small proportion of the surface fluorides may be common to both modified samples.

The fluorine containing species at the surface of the DFE modified, or directly fluorinated, carbons are stable since no time- dependent degradation was observed in UHV conditions. Varying the X ray beam energy from 50 to 250W did not alter the observed spectra. In addition, heating the samples in UHV to approximately 300^{o}C (maximum temperature) did not result in any measurable change to the spectra. Trace quantities of carbon oxides (CO, CO_2), HF and moisture were, however, detected using a quadrupole mass analyser.

The most probable explanation for the absence of a signal attributable to the presence of C-F bonding in the C (1S) spectra for the DFE modified carbon is that the surface species are present in relatively low concentrations, and are not detected due to the characteristics of the baseline.

Figure 7.3.15 shows the relationship between the F (1S) binding energy and the kinetic energy of the Auger electrons due to FKLL transitions for a number of fluorine containing materials. It is apparent that the binding energy values found in this present study are consistent with there being predominantly C-F single bonds at the surface of the directly fluorinated carbon, and predominantly CF_2 species at the surface of the DFE modified carbon. The difference in the binding energy values compared with those found for fluorinated graphite, which is the substrate most similar to active carbon, are significant. It is probable that these differences arise through the major dissimilarity of the electronic structures of these two carbon allotropes, and not through instrumental effects.

Based upon the XPS data, a possible reaction mechanism of each fluorinating reagent with the carbon may be proposed.

For the directly fluorinated carbon, such a mechanism might be:

$$C(H) + F_2 \longrightarrow \text{"CF"} + \text{C-F} + \text{H-F}$$

Thus surface carbon- fluorine complexes are generated, by a mechanism which includes hydrogen exchange (7.1). "CF" is representative of carbon fluorine species which have not been generated by a hydrogen exchange mechanism.

It is, however, hard to reconcile C-F covalent bonds being responsible for the observed instability of the directly fluorinated carbon. Rather, it is probable

that adsorbed fluorine, held relatively weakly within the carbon structure (which cannot be detected using this technique), is responsible for this effect.

For the DFE modified carbon, it is plausible that at 450°C, the initial stage of reaction involves fission of the DFE molecule across the double bond:

$$CH_2\text{-}CF_2 \text{ ----heat----> } CF_2\text{:} + CH_2\text{:}$$

The reactive carbene species would then combine with the active carbon:

$$C + CH_2\text{:} + CF_2\text{: ---------> } C\text{-}CH_2 + C\text{-}CF_2$$

This sequence is consistent both with the observation that bulk polymerisation did not take place, and that the products were of greater Carbon and Hydrogen, as well as of Fluorine, content.

It is, however, appreciated that the surface species may not be simple C-F and CF_2. The presence of more complex species cannot be ruled out, and XPS would not enable their unambiguous identification.

A further study of DFE modified and directly fluorinated carbon was carried out using thermal desorption- mass spectroscopy (Appendix) in an attempt to identify any gaseous products specific to either reagent. For example, the presence of tetrafluoroethene would support the idea that the DFE reacted at the carbon surface via the formation of difluorocarbene. These analyses indicated that carbons modified with DFE or fluorine liberated HF, COF_2, and SiF_4, which was not observed during study of control carbon. SiF_4 was observed using either quartz or stainless steel sample holders, and so was not a consequence of the reaction of thermally desorbed "F" with the quartz holder. Other products included SO_2 and CO_2, which were found during analysis of control carbon. Elemental analysis revealed that silicon was present in control carbon.

The temperatures at which the desorption maxima for each species were observed (table 7.3.7) was dependent upon the fluorination technique: that is, carbon modified with DFE generally contained the most thermally stable fluorides. No fluorocarbons were observed during study of the DFE carbons, although trace amounts were found for the directly fluorinated samples. It is probable that the absence of fluorocarbons in the case of the DFE modified carbon is a consequence of a higher thermal stability (maximum desorption temperature ca. 700°C). TG analysis indicated that the carbons were stable to at least 500°C: thereafter, only a small weight loss was observed (ca. 1% at a temperature of 910°C)

Although the (qualitative) technique revealed that similar species were desorbed by both the modified carbons, no obvious differences were evident that would go some way toward rationalising the differences between the carbons modified using these techniques.

Table 7.3.1 Weight Changes Resulting from DFE Modification (BPL Carbon)

	Number of Treatment Cycles (450°C)					
	0	1	3	5	6	12
Weight Gain (w/w %)	0.0	2.0	2.3	2.9	3.4	3.8

Sample	Treatment Temperature (°C)	Number of Treatment Cycles	Weight Gain (w/w %)
A	600	6	11.4
B	700	4	13.8

Table 7.3.2 Nitrogen Adsorption and α_s Analysis

Sample	BET Surface Area (m^2g^{-1})	Micropore Volume (cm^3<STP>g^{-1})	External Surface Area (m^2g^{-1})
BPL Carbon			
Control	1208	0.53	53
Control (Outgassed 450°C)	1190	0.53	61
Control (Outgassed 600°C)	1200	0.53	52
DFE (3 Treatment Cycles, 450°C)	1120	0.50	52
DFE (6 Treatment Cycles, 450°C)	1125	0.51	55
DFE (12 Treatment Cycles, 450°C)	1020	0.47	45
DFE (6 Treatment Cycles, 600°C)	93	0.04	33

Table 7.3.3 Hexane Adsorption for Dry (< RH2%) and Humidified (RH80%) Carbons

Sample	Hexane Adsorption (RH80%[1]) Penetrating Ct (mg min m^{-3})	Hexane Adsorption (<RH2%[2]) 50% Filter Break Time (minutes)	Hexane Adsorption (<RH2%[2]) Amount Adsorbed (Equilibrium, mg g^{-1})
Control	3100	56	255
Aged-Control*	23400	57	250
DFE (1 Cycle, 450°C)	-	53	232
DFE (2 Cycles, 450°C)	-	52	220
DFE (6 Cycles, 450°C)	300	50	216

[1] Samples were challenged in equilibrium with RH80% air at 22°C. A two minute pulse of hexane vapour (15000 mg m^{-3} (Ct=30000 mg min m^{-3})) was used. The flow velocity was 382 cm min^{-1} (2cm bed depth, 2cm diameter filters).

[2] Samples were challenged in dry air at a flow velocity of 382 cm min^{-1}. A continuous challenge of hexane vapour of concentration 6470 ±30 mg m^{-3} was used. Filters (2 cm bed, 2 cm diameter) were challenged to 100% breakthrough.

Table 7.3.4 Chloropicrin (PS) Adsorption

Sample	Carbon Water Content (RH80%; 22°C: Corrected)	Filter Breakthrough Time (minutes)	
		1st Break	1% Break
Control	34.9	93	104
Aged*-Control	35.2	62	78
DFE (2 Cycles, 450°C)	30.7	107	119
DFE (6 Cycles, 450°C)	28.6	114	125
DFE (6 Cycles, 450°C, Aged*)	28.8	88	106
DFE (6 Cycles, 600°C)	21.2	33	42
DFE (6 Cycles, 600°C, Aged*)	21.3	29	38

*Samples were aged at RH80%, 22°C, for 60 days prior to the measurement.

All values are an average of at least two determinations. 1st Break is the time to first measured filter breakthrough (5-10 mg m^{-3}): 1% Break is 50 mg m^{-3}.

{2cm diameter, 2cm bed depth filters: flow velocity 382 cm min^{-1}. Challenged in equilibrium with RH80% air at 22°C. PS concentration 5000 mg m^{-3}}

Table 7.3.5 Elemental Analysis

Sample	Element (%)					
	C	H	N	O	S	F
BPL Control	86.6	0.2	0.6	2.0	1.1	0.0
BPL DFE (5 Cycles, 450°C)	91.1	0.35	0.5	1.0	0.8	3.0
Element Molar Ratio (To C = 100)						
BPL Control	100	3.2	0.5	1.7	0.4	0.0
BPL DFE (5 Cycles, 450°C)	100	4.6	0.5	0.9	0.4	2.1

Table 7.3.6 X ray Photoelectron Spectroscopy

Substrate	Binding Energy Shift of Carbon (1S) Satellite (eV)	Surface Functional Group
Graphite	4.5 - 5.0	CF
Graphite	6.5 - 7.0	CF_2
Graphite	8.7 - 9.3	CF_3
BPL Carbon (present study)	3.7 - 4.0	CF
Fluoropolymers	2.0 - 5.5	CF
Fluoropolymers	5.5 - 8.0	CF_2
Fluoropolymers	8.0 - 10.0	CF_3

Table 7.3.7 Thermal Desorption Mass Spectrometry

Desorbed Species	Number of Peaks	Desorption Maxima (°C)	Peak Width (°C)
Directly Fluorinated BPL Carbon			
HF	1	450	180 - 680
COF_2	1	520	270 - 710
SiF_4	2	180 690	90 - 310 540 - 720
SO_2	1	440	170 - 680
CO_2	1	620	150 - 700
DFE Modified BPL Carbon			
HF	1	720	600 - 750
COF_2	2	200 670	150 - 290 590 - 700
SiF_4	2	210 670	140 - 300 590 - 700
SO_2	1	680	170 - 720
CO_2	1	300	170 - 700

*Fluorocarbon species were detected during analysis of the directly fluorinated carbon above ca. 500°C. The maxima was at approximately 630°C. The principal ions are shown below.

m/e	69	100	119	169
Ion	CF_3	C_2F_4	C_2F_5	C_3F_7
Major/minor	M	m	m	m

{Weaker signals were also detected, to an m/e maximum of 343}

FIGURE 7.3.1 NITROGEN ISOTHERMS FOR BPL CARBON

● CONTROL DFE MODIFIED ■ 3 AND ▲ 6 TREATMENT CYCLES

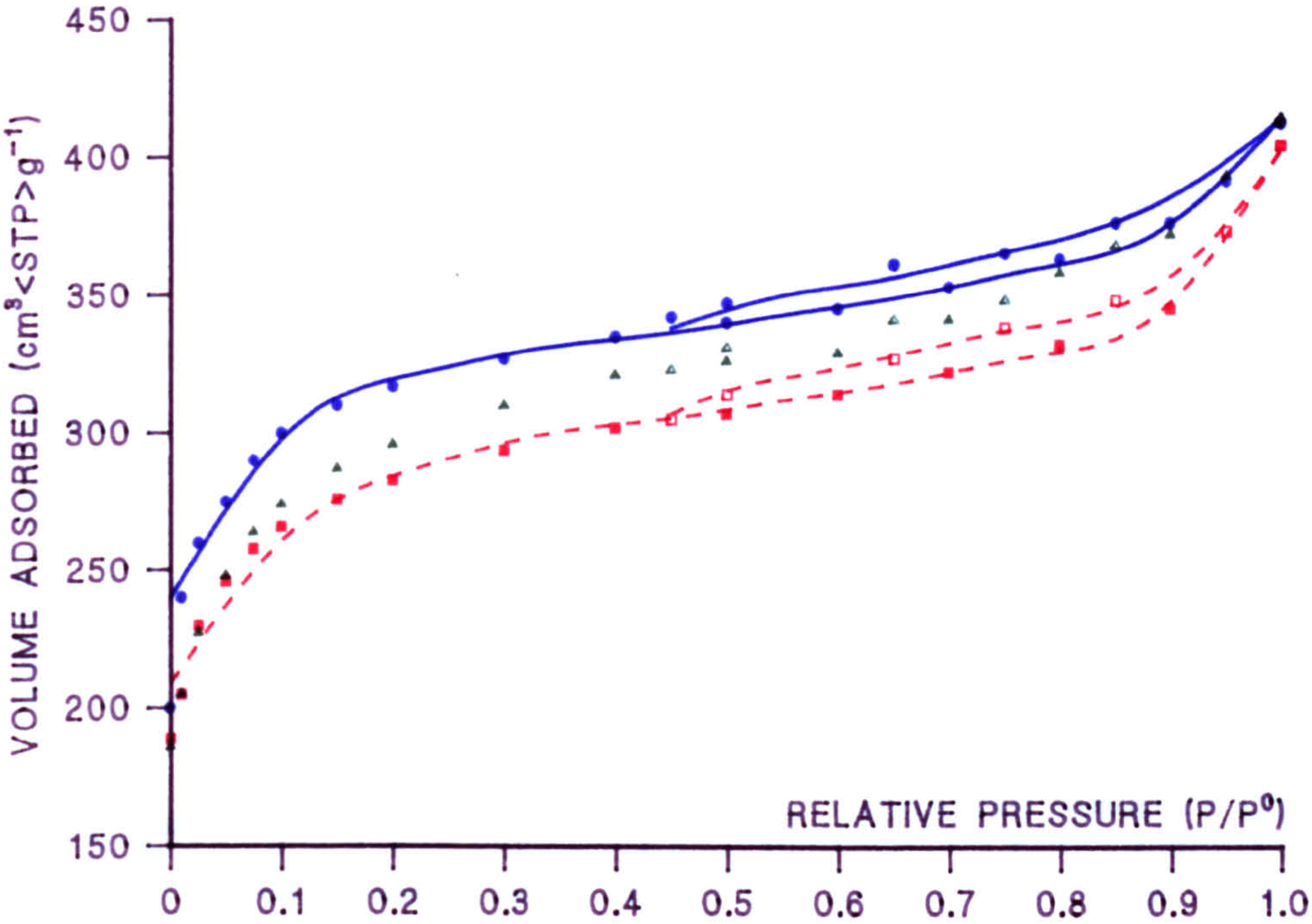

FIGURE 7.3.2 HEXANE BREAKTHROUGH CURVES

L-R: BPL DFE 6, 3, TREATMENT CYCLES; BPL CONTROL

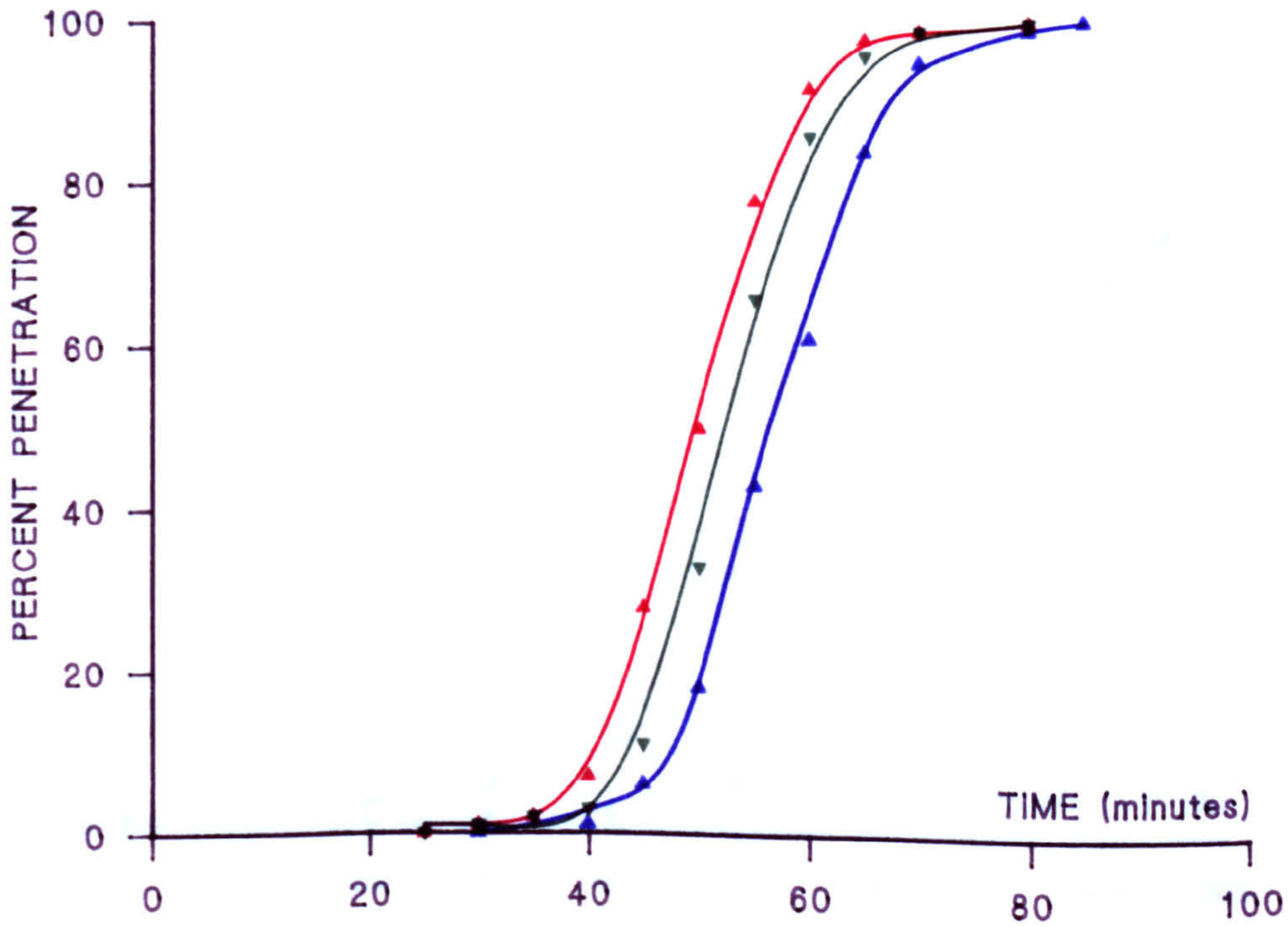

FIGURE 7.3.3 WATER ADSORPTION

▲ CONTROL BPL; DFE ● 3 AND ■ 6 TREATMENT CYCLES

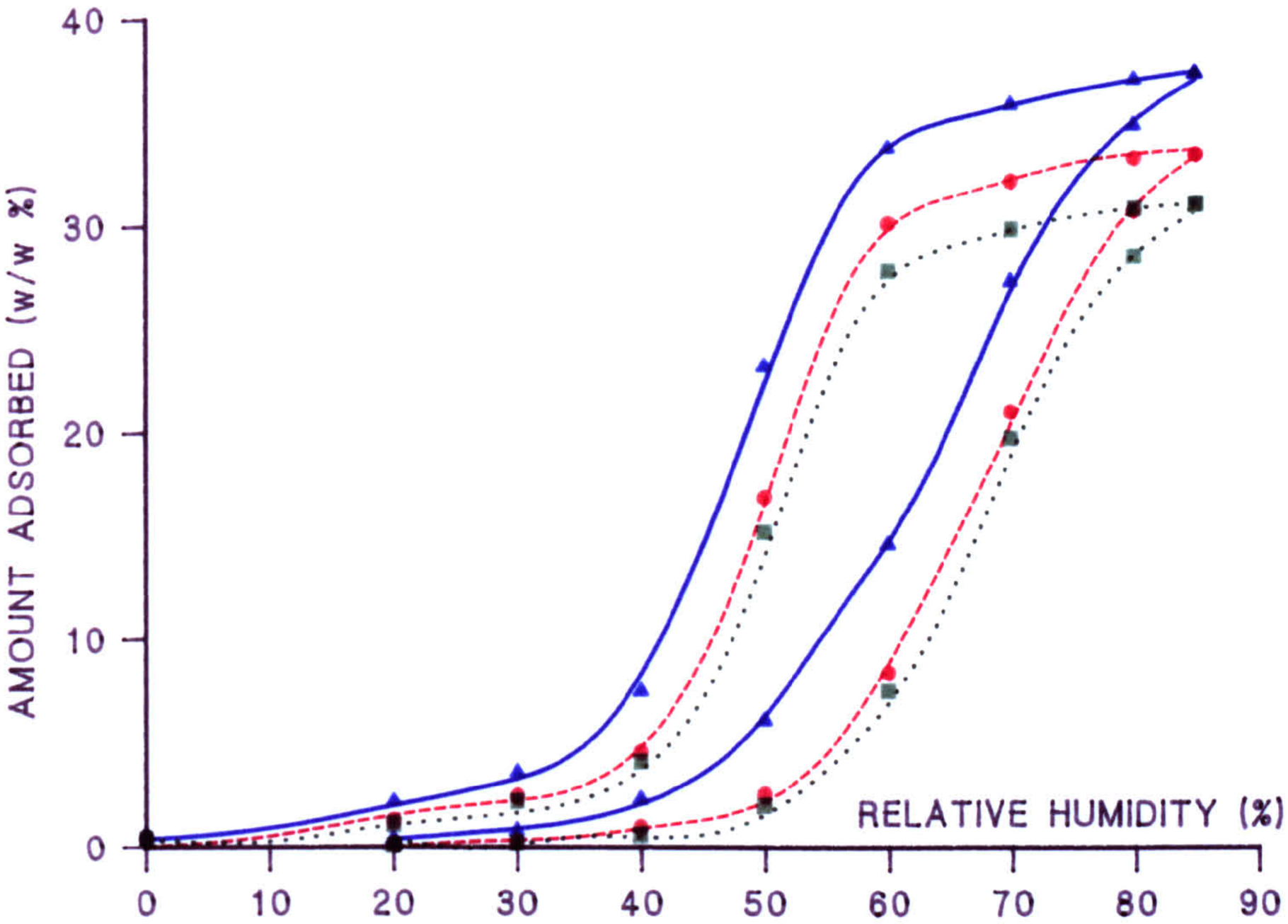

FIGURE 7.3.4 WATER ADSORPTION

DFE ▲ 6 AND ● 12 TREATMENT CYCLES

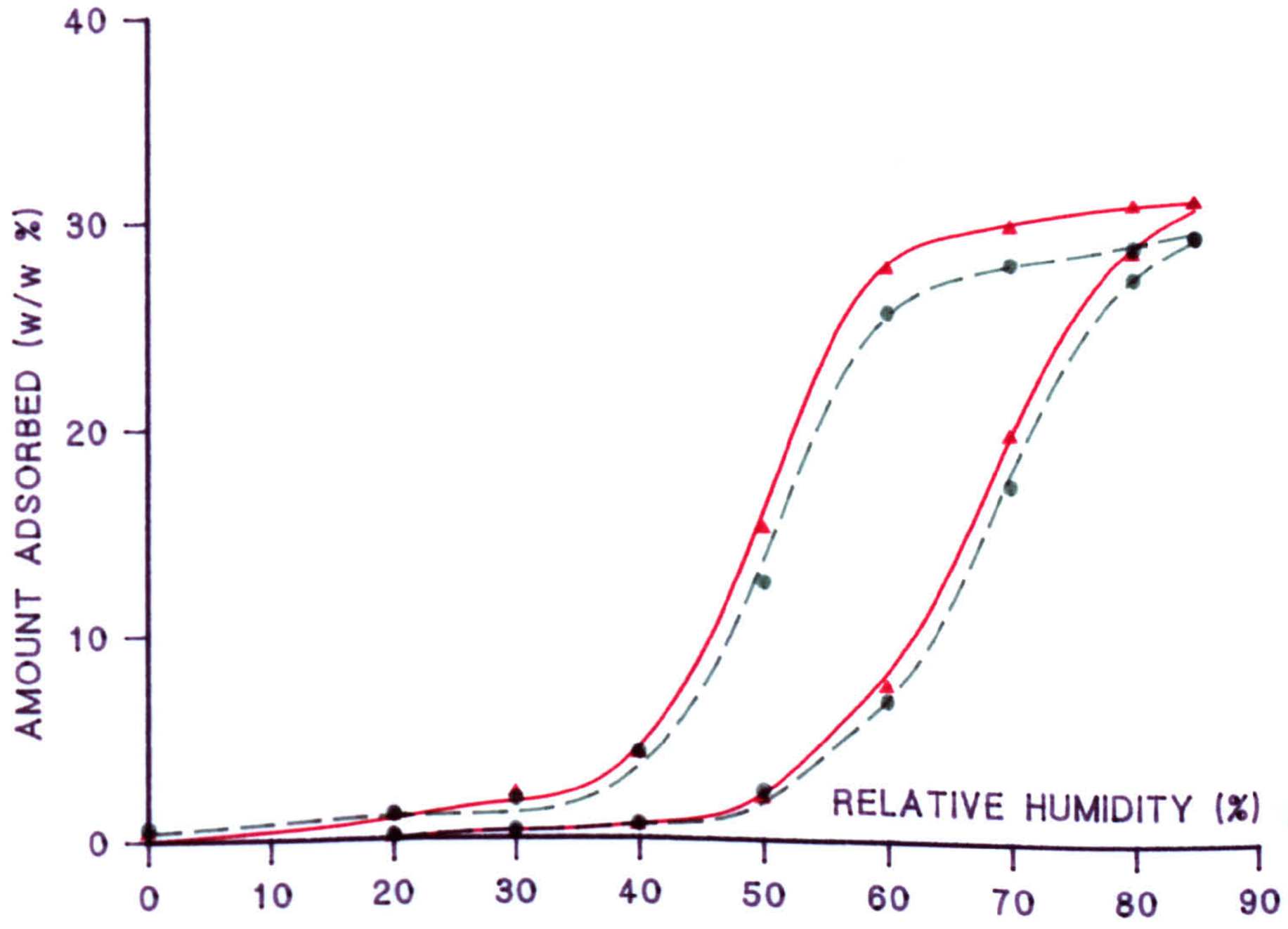

FIGURE 7.3.5 WATER ADSORPTION
CONTROL BPL OUTGASSED AT ▲ 450°C AND ● 120°C

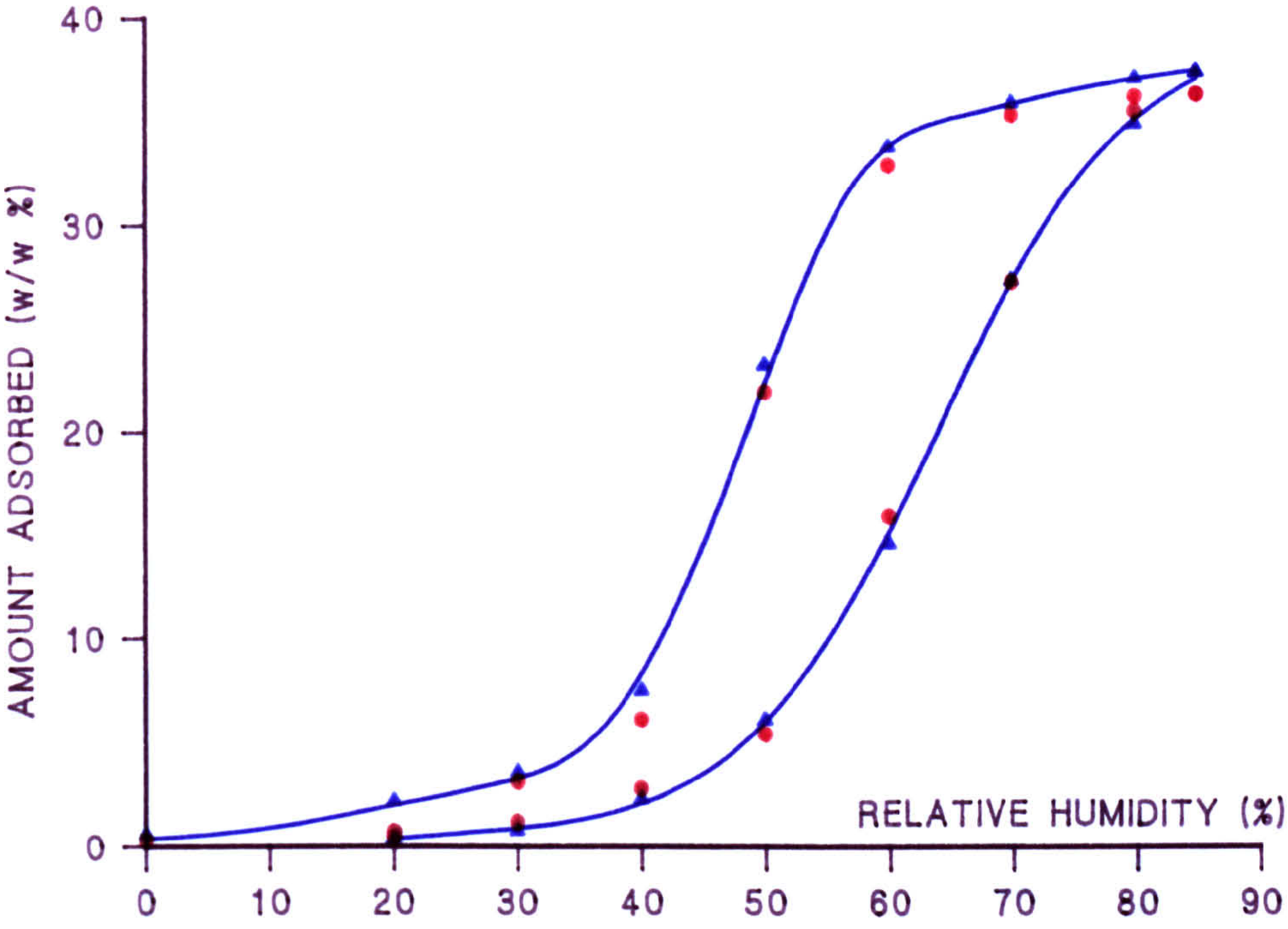

FIGURE 7.3.6 WATER ADSORPTION
DFE MODIFIED BPL: 6 TREATMENT CYCLES, 600°C

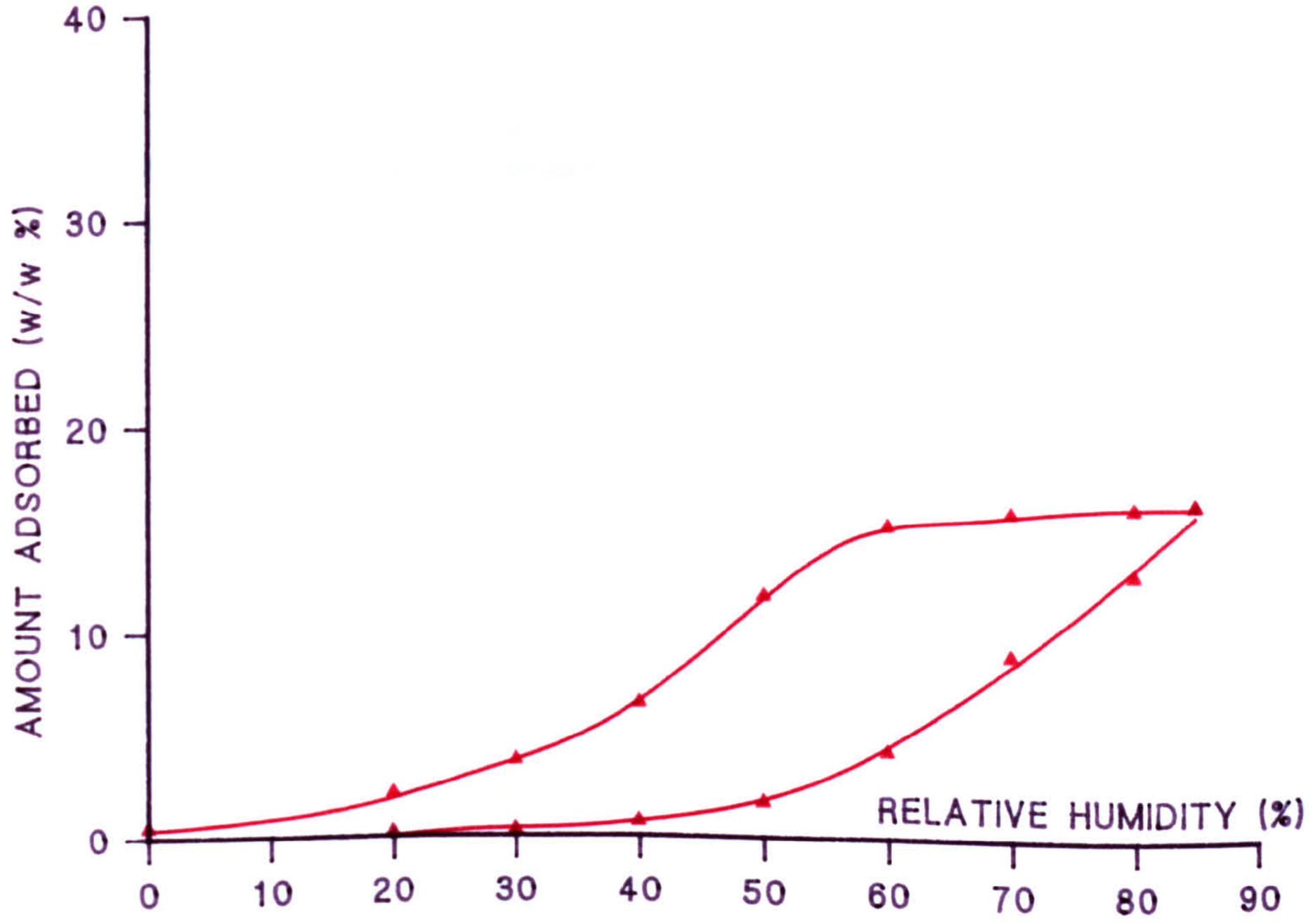

FIGURE 7.3.7 WATER ADSORPTION

DFE MODIFIED BPL ▲ 6 CYCLES, ● 6 CYCLES (AGED)

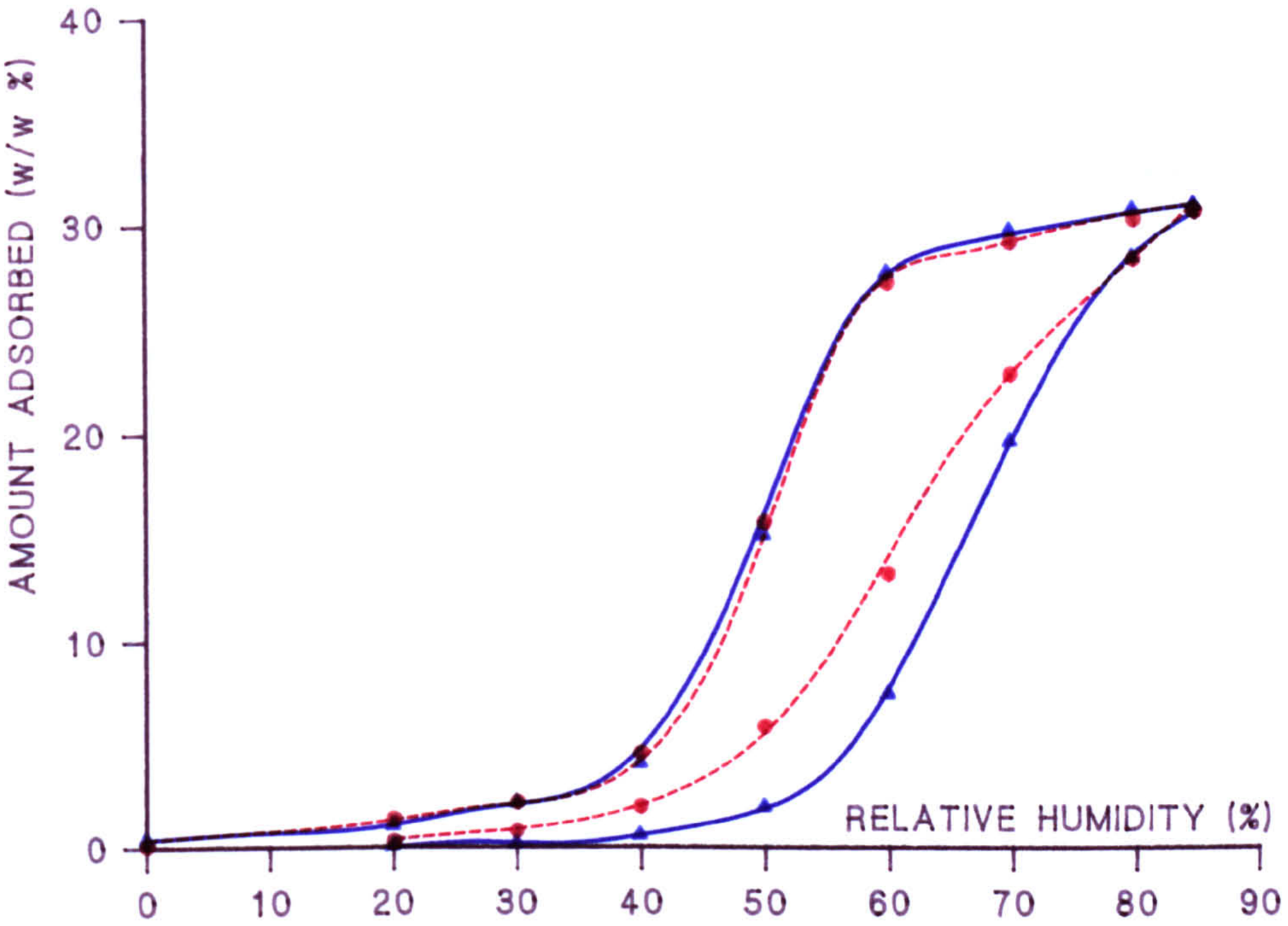

FIGURES 7.3.8 HEXANE BREAKTHROUGH MEASURED AT RH80%

▲ CONTROL BPL CARBON ● DFE MODIFIED BPL (6 TREATMENT CYCLES, 450°C)

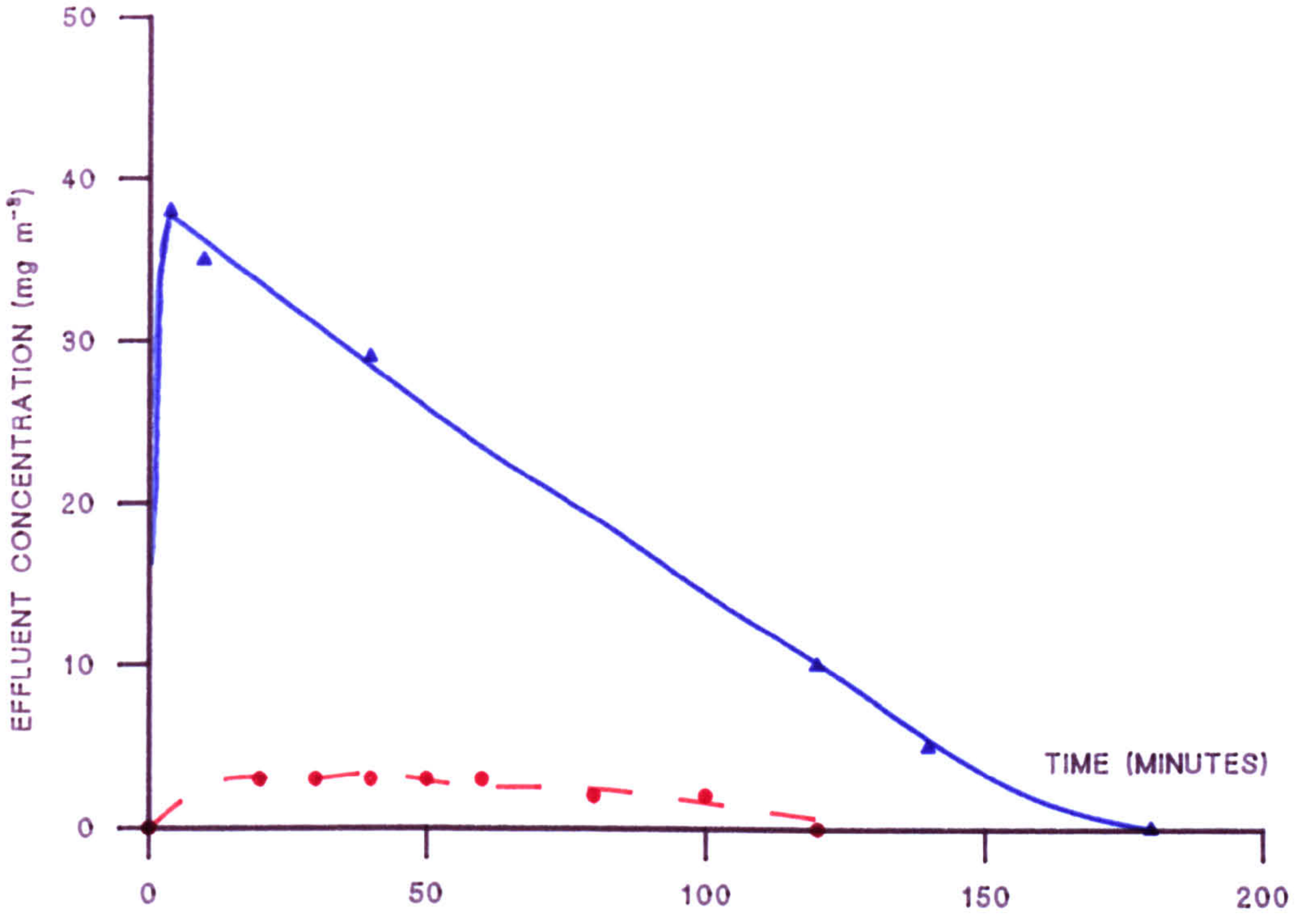

▲ CONTROL BPL CARBON ● AGED BPL CARBON

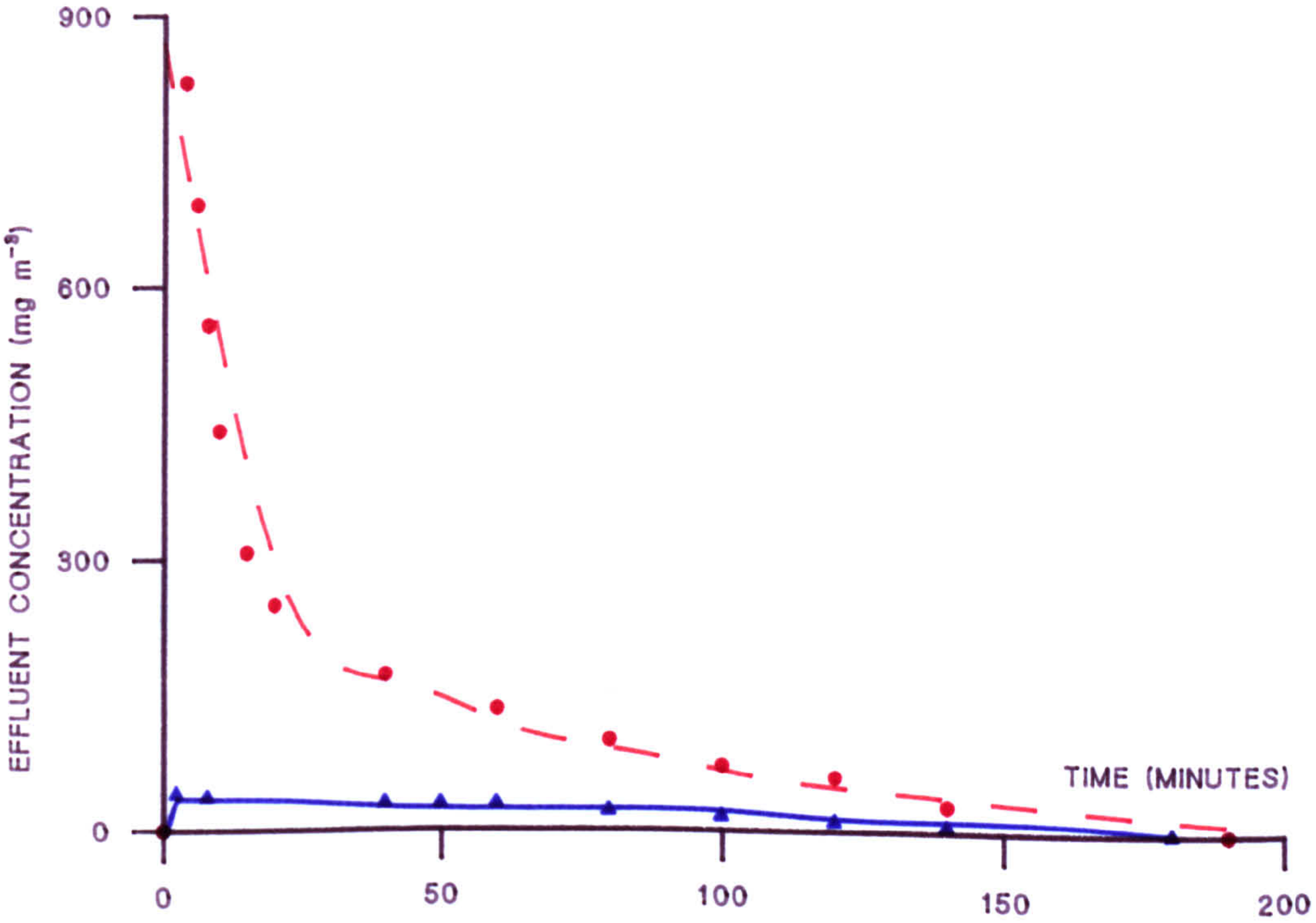

FIGURE 7.3.9 WIDE SCAN XPS SPECTRUM FOR CONTROL BPL CARBON

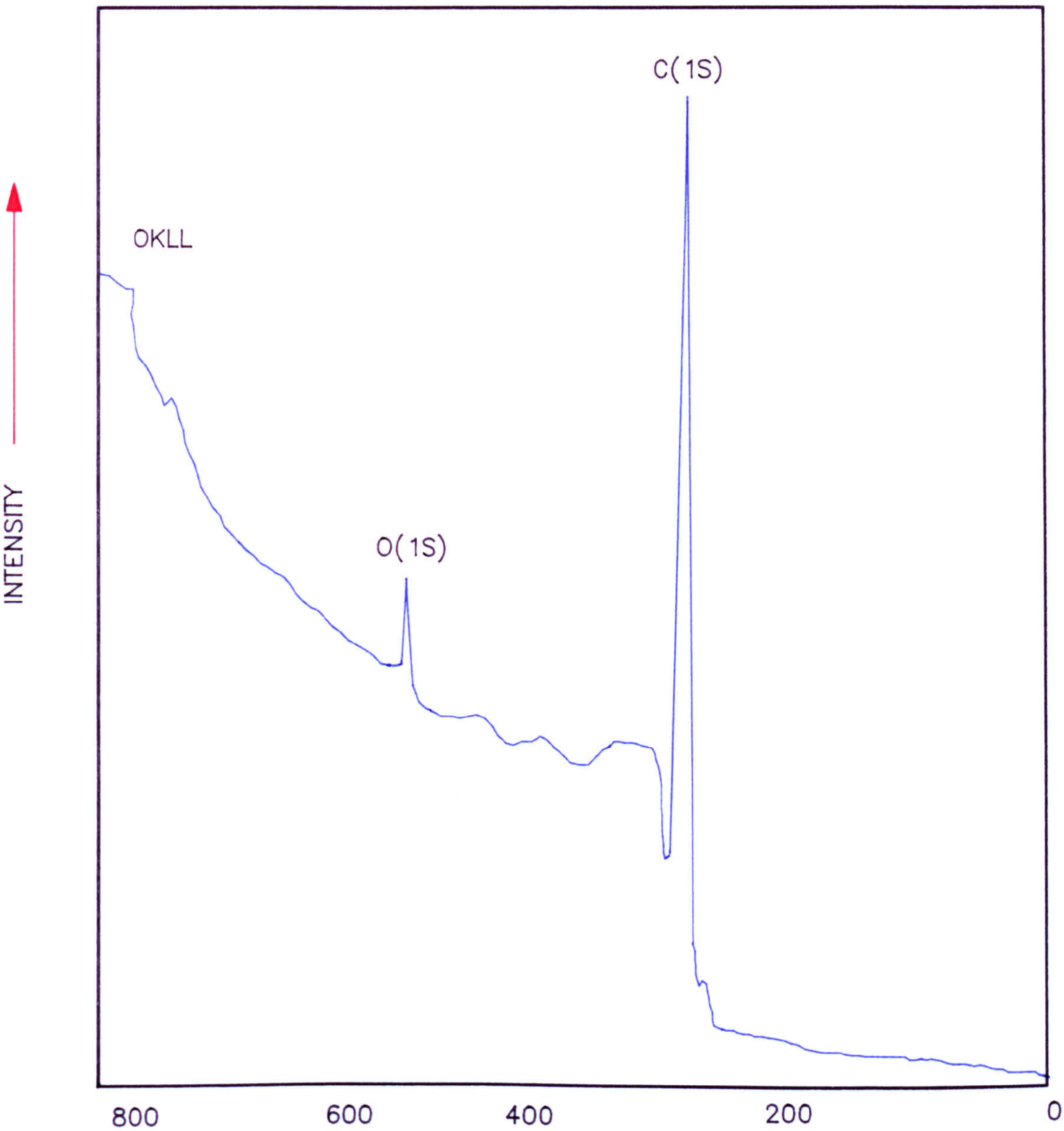

FIGURE 7.3.10 WIDE SCAN XPS SPECTRUM FOR CONTROL BPL CARBON FLUORINATED (17 w/w%)

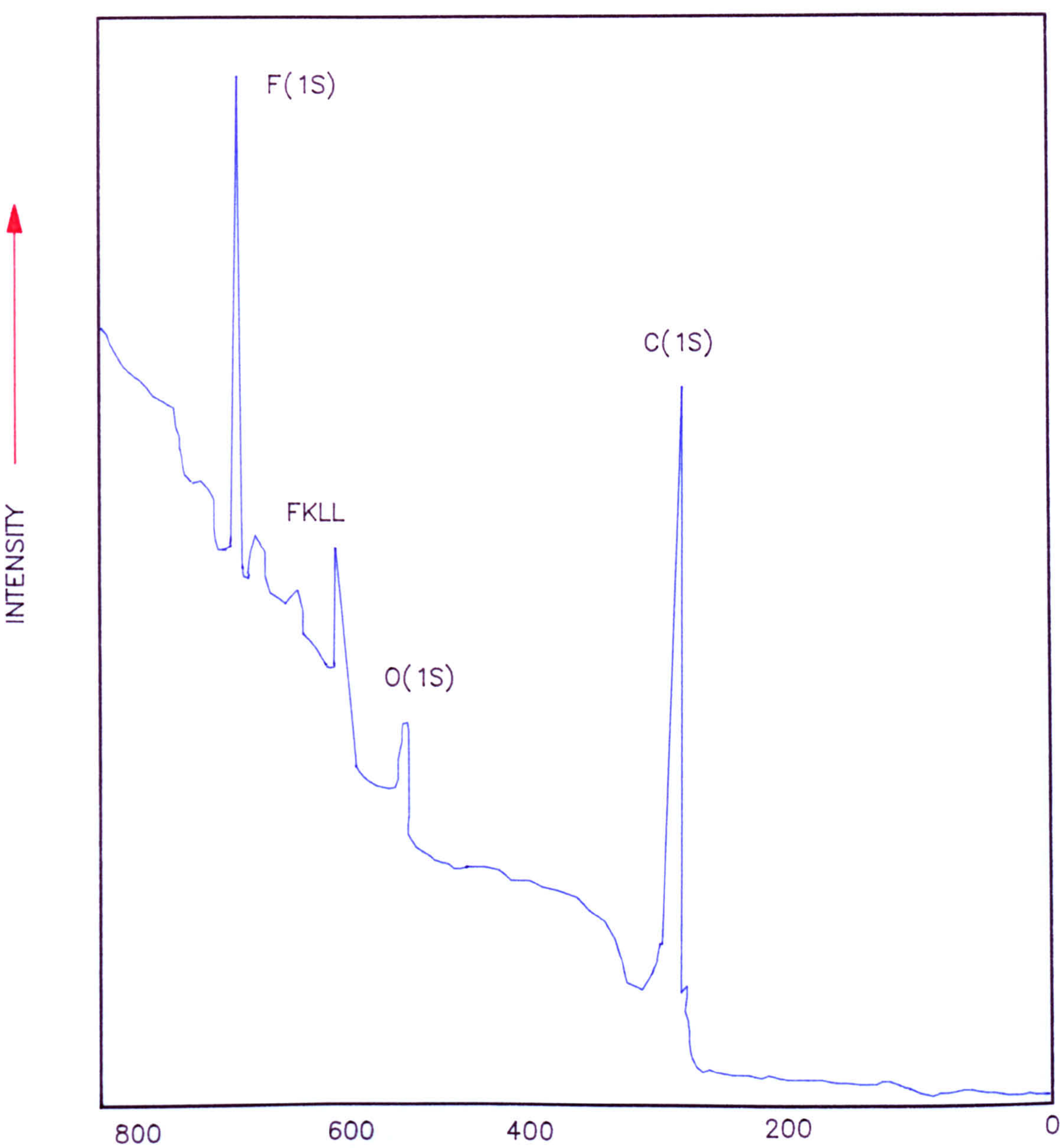

FIGURE 7.3.11 NARROW SCAN C(1S) XPS SPECTRUM FOR CONTROL BPL CARBON

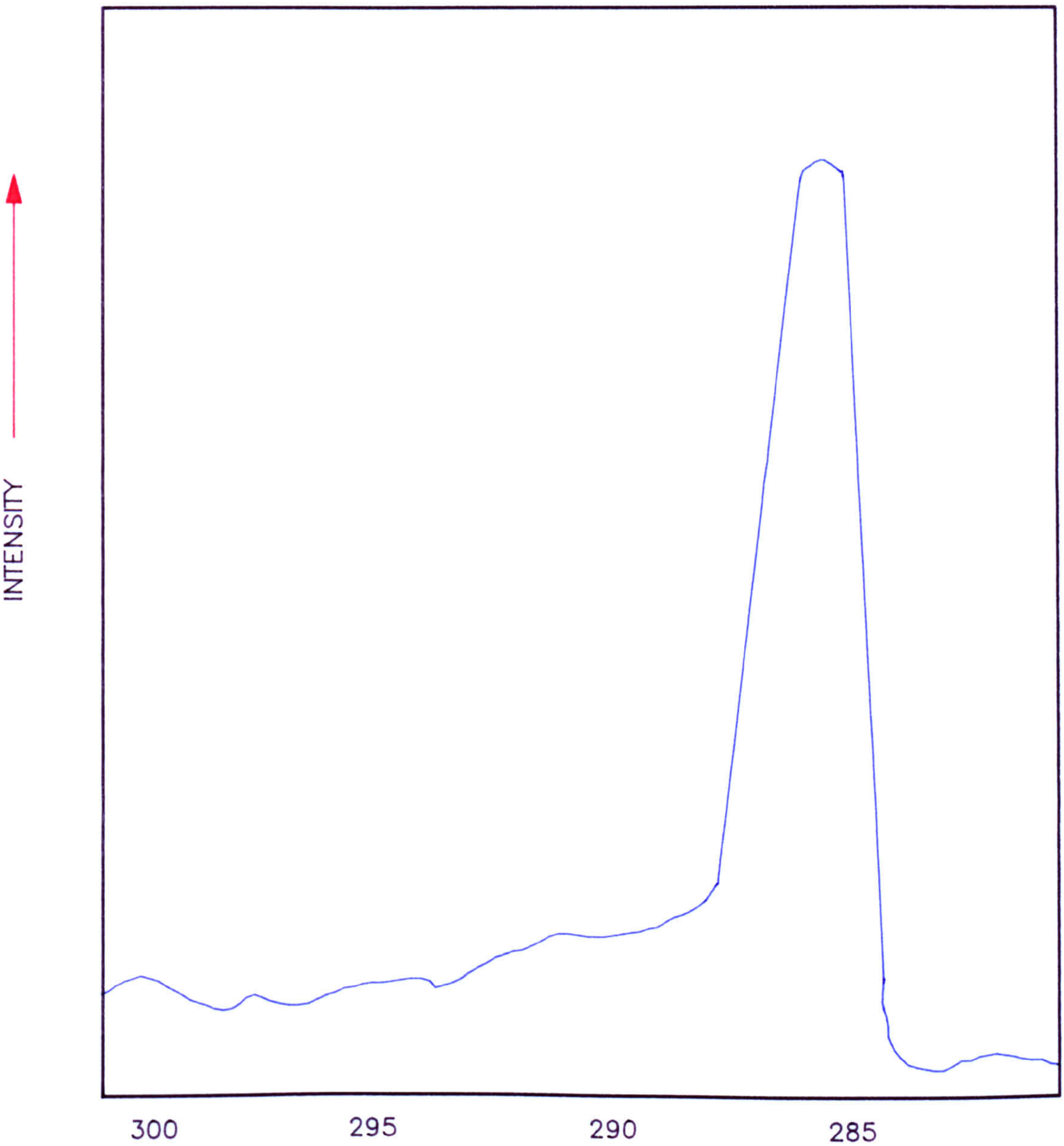

FIGURE 7.3.12 NARROW SCAN C(1S) XPS SPECTRUM FOR CONTROL BPL CARBON FLUORINATED (17 w/w%)

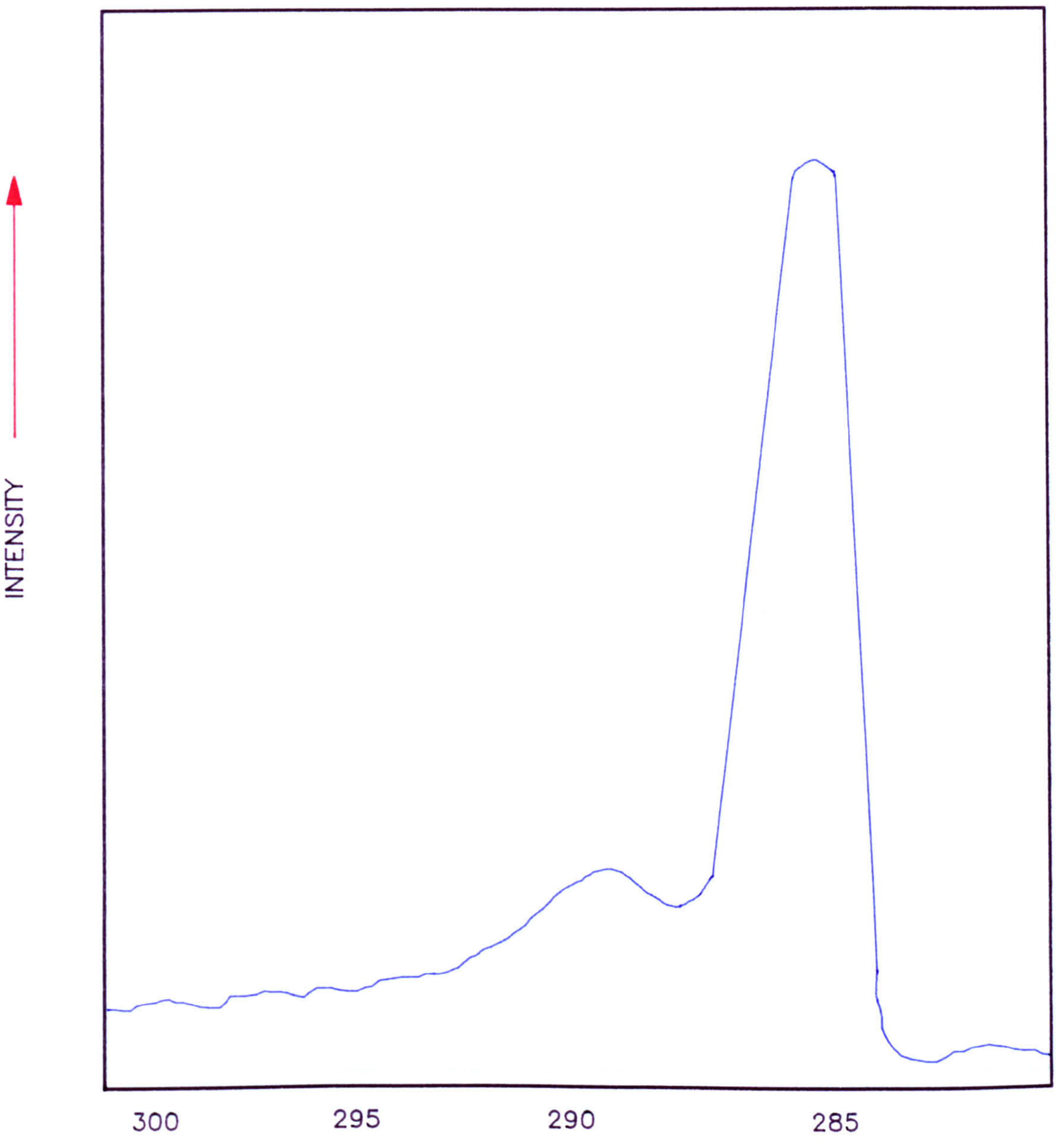

FIGURE 7.3.13 NARROW SCAN F(1S) XPS SPECTRUM FOR CONTROL BPL CARBON (FLUORINATED; 17 w/w%)

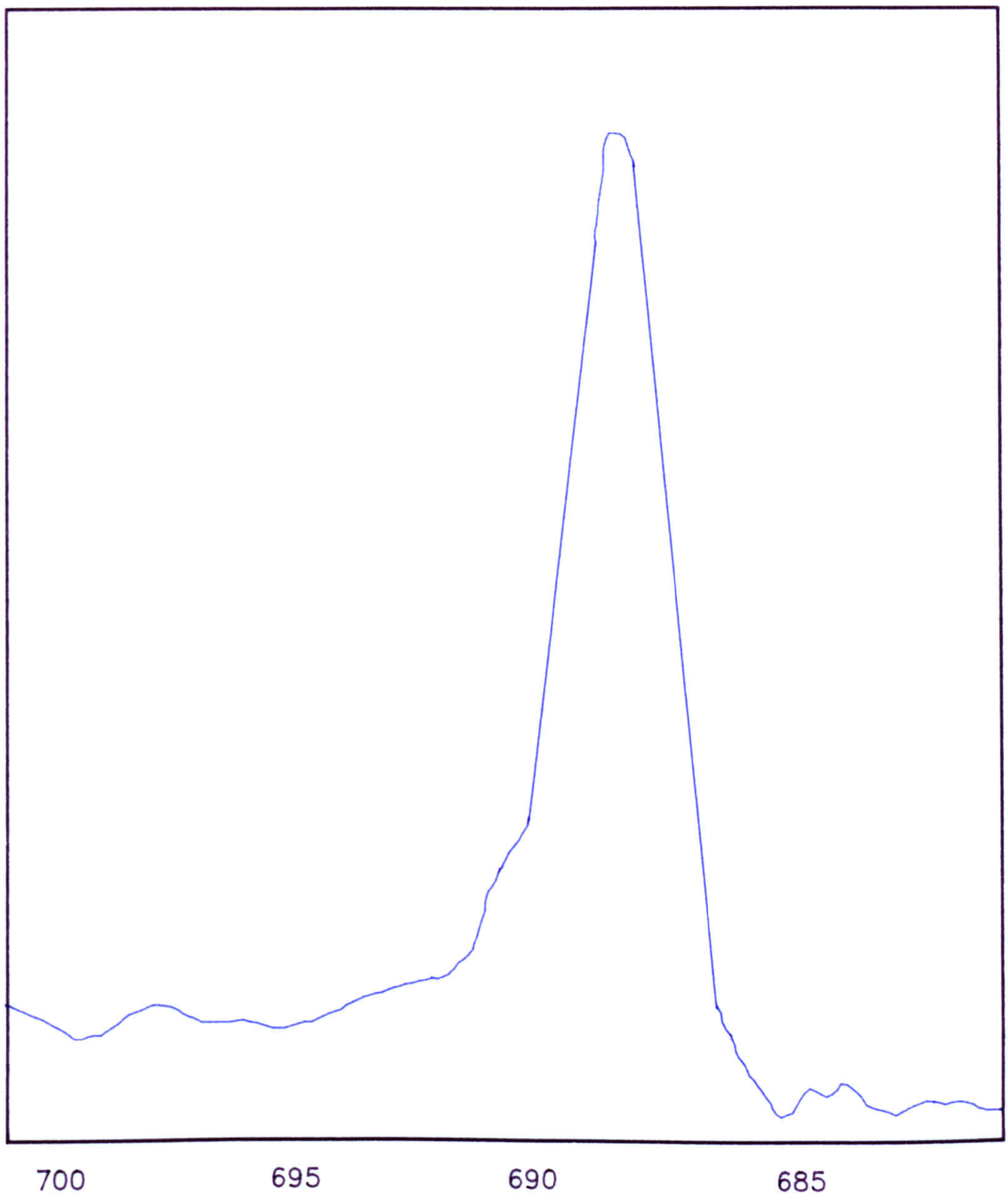

FIGURE 7.3.14 NARROW SCAN F(1S) XPS SPECTRUM FOR CONTROL BPL CARBON (DIFLUOROETHENE MODIFIED)

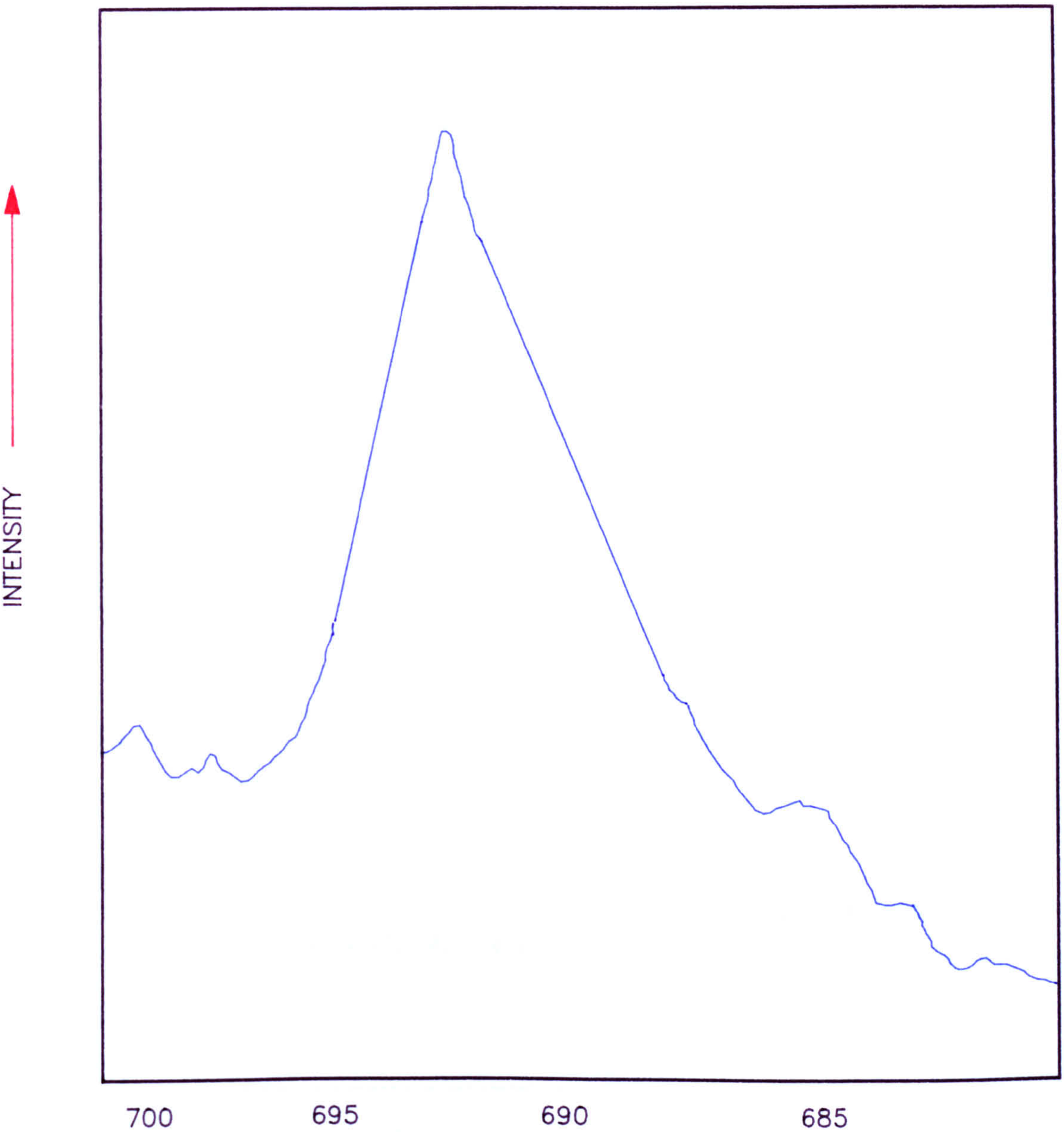

FIGURE 7.3.15 RELATIONSHIP BETWEEN F(1S) BINDING ENERGY AND THE KINETIC ENERGY OF THE FKLL AUGER ELECTRONS FOR FLUORINE CONTAINING MATERIALS

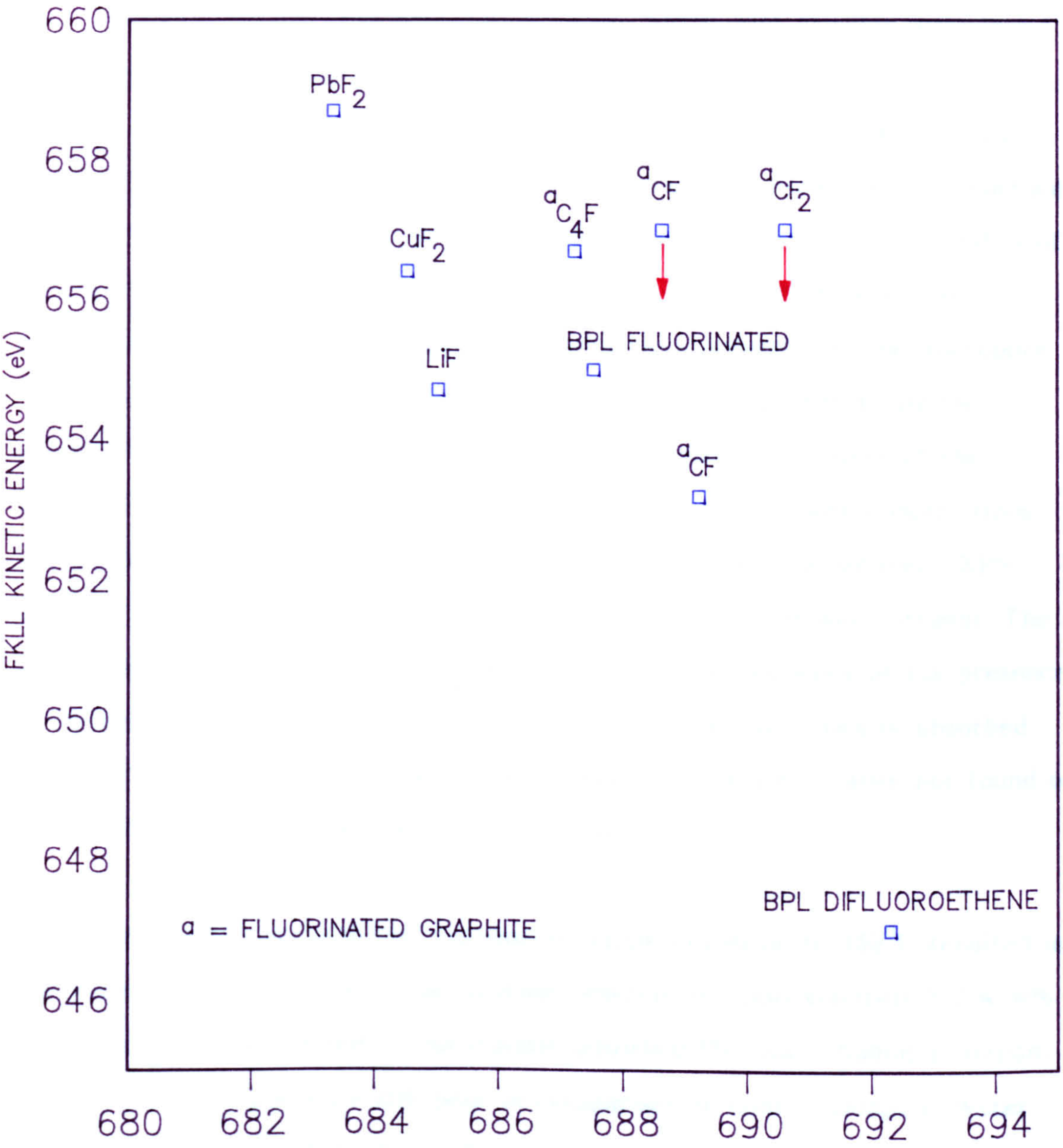

7.4 Summary

7.4.1 Direct Fluorination

Activated carbons modified at or below 200°C with fluorine were found to be unstable, as shown by water adsorption measurements and thermal analysis. Large quantities of fluorine could be adsorbed, the majority of which appeared to be weakly bound, and possibly absorbed within the carbon structure. The presence of adsorbed (or absorbed) fluorine was confirmed by the ability of the modified carbons to oxidise iodide. Nitrogen adsorption showed that increasing fluorine content resulted in a successive reduction in the micropore volume and external surface area. PS adsorption from high RH air by the modified carbons was poor, an effect that was largely independent of the fluorine content. PS adsorption from dry air indicated that pore constrictions were present, which degraded both the rate, and extent, of adsorption. XPS analysis indicated that surface carbon- fluorine single bonds were present. The instability of the modified adsorbents is probably a consequence of the presence of hydrolytically unstable surface fluorides, and weakly adsorbed or absorbed fluorine ("F"). Carbons fluorinated and outgassed below 200°C were not found to be suitable for vapour adsorption applications.

Outgassing the modified carbons at temperatures up to 350°C resulted in the desorption of the bulk of the fluorine, whereafter approximately 1-2 w/w% remained. Carbons treated in this manner adsorbed PS from a humid airstream more efficiently, but were still poor in comparison to control samples. Water adsorption measurements indicated that the carbons remained unstable in the presence of humid air.

Modification with fluorine at temperatures between 330 and 600°C resulted in carbon gasification, and the fixation of only small quantities of

fluorine. Because of the difficulty associated with correlating the effects associated with simultaneous carbon gasification and surface modification, and because this approach does not appear to offer any significant advantages in terms of the aims of this part of the research, further studies at elevated temperature were not carried out.

Treatment of directly fluorinated carbon using methanol or water was investigated as a method for stabilising the carbons. It was anticipated that this technique would remove weakly adsorbed reagent or reaction products to leave stable surface fluorides, or that the solvents would react with unstable surface fluorides to yield stable surface functional groups.

The results suggest that the treatments do serve to remove adsorbed reagent and/or reaction products, but also that some surface reaction takes place, probably yielding surface methoxy (methanol) or hydroxy (water) functional groups. Treatment with water appeared to be most effective in producing a stable carbon, whereas treatment with methanol did not result in complete removal of the absorbed/ adsorbed fluorine. Modification of fluorinated carbon with dipropylamine appears to result in the generation of surface amine functional groups, but also in significant pore blocking as revealed by water and PS adsorption.

Directly fluorinated carbons are not suitable for vapour adsorption applications, but they offer potential as reactive substrates which may be amenable to further chemical transformations.

7.4.2 Reaction with Hexafluoropropene (HFP) or 1,1-difluoroethene (DFE)

Samples of BPL carbon modified with HFP were found to be of improved hydrophobic character in comparison to the control. Measurement of hexane and nitrogen adsorption indicated that treatment did not result in significant

structural modification. The PS adsorption efficiency of the modified carbons was slightly improved in comparison to the controls, suggesting that the use of fluoroolefins to modify activated carbon is a useful approach. Modification of aged carbons using this approach was less successful.

Because HFP is a relatively bulky molecule, an alternative reagent was selected for further study, since it was anticipated that pore blocking effects would be less important.

BPL carbon did not react with DFE to a significant extent until the temperature exceeded ca. 300°C. Carbon Modified at 450°C was structurally very similar to the control, and was found to be more hydrophobic compared with both the control, and carbon modified with HFP. In addition, the samples adsorbed PS from humid air with a greater efficiency than either control or HFP modified carbon. DFE modified carbons were found to age on exposure to air of high relative humidity, but the rate of ageing appeared to be slower in comparison to control samples, suggesting that a proportion of the surface sites which are susceptible to this effect were masked by the DFE treatment. XPS analysis indicated that CF_2 groups were present on the modified surface, indicating that the reaction may proceed via the formation of difluorocarbene.

That the reaction at 450°C was selective was apparent from a study carried out at 600 and 700°C, where it was probable that polymerisation of the reagent within the pore structure was taking place.

Carbons modified with fluoroolefins were found to be of greater stability and hydrophobicity compared to directly fluorinated samples, and were found to adsorb PS from a humid airstream more efficiently. The behaviour of fluorine therefore appears to be anomalous.

CHAPTER 8

Chemical Modification of Activated Carbon using Phosgene and Chlorine

Results and Discussion

8.0 Introduction

The results of chemically modifying activated carbon using phosgene (carbonyl chloride) or chlorine are presented in this chapter. As before (chapter 7), the results and discussion primarily address the impact of modification upon the adsorptive properties of the carbons, with emphasis upon their vapour adsorption characteristics, and their stability in the presence of air of high relative humidity.

The preparation and some of the properties of chlorinated activated carbon reported prior to this present study have been discussed in chapter 3. This research principally addressed carbons modified by direct chlorination: the use of phosgene in this respect has received little attention.

These studies did not include an adequate consideration of the properties of the modified carbons in the context of this present research (chapter 1). It is also apparent that some confusion persists with regard to the adsorptive properties of carbons modified using chlorinating reagents.

Direct chlorination has been addressed because this may enable carbons of improved hydrophobic character to be prepared. In addition, surface carbon chlorine species may be hydrolytically stable. Thus, carbons modified in this manner could offer advantages in vapour adsorption applications, and may also afford some resistance to ageing effects.

Phosgene has been selected on the basis that specific classes of oxygen containing functional groups are present on the surface of activated carbon prior to, and as a result of, ageing (chapter 3,6), and that such groups are, in principle, reactive.

Thus selective and specific chemical reactions may be possible, such as the transformation of carboxylic acids to acid chlorides, and hydroxyl groups to surface carbon chlorine species. The acid chloride functions can then be chemically transformed to stable esters, by treatment with, for example, methanol. Carbons modified in this manner may be of improved hydrophobic character.

8.1 The Preparation of Modified Adsorbents

The three activated carbons described at chapter 5 were used in this part of the study. Both control and aged- control (chapter 5) samples were used.

Initial exploratory experiments using phosgene or chlorine were performed using 1 litre glass flasks maintained within an air oven at constant temperature (30°C to 200°C). Dry carbon samples (120°C; 3 hours; 3 mbar) were exposed to undiluted phosgene (> 99% purity, Gas and Equipment Ltd., Stratford, London) or chlorine (> 99%, BDH Ltd., Poole) until the pressure stabilised (1 atmosphere). Both gases were used without further purification (>99%). The carbons were, after modification, outgassed at the reaction temperature, (or at 120°C for the samples modified below this temperature) cooled where necessary, removed and weighed.

8.1.1 Phosgene

The reaction between activated carbon and phosgene was found to be temperature dependent, with little or no change in sample weight taking place at 30°C for both the control and aged- control samples. The effect of the modification temperature upon the quantity of phosgene adsorbed by BPL carbon is shown in table 8.1.

Based upon these initial studies, carbon modifications were subsequently carried out at a temperature of 180°C using the low temperature modification apparatus described at chapter 5, and in more detail at chapter 12. This temperature reflects a need to chemically modify the carbon surface, but without causing significant structural disruption (that is, a significant loss of porosity as revealed by, for example, nitrogen adsorption at -196°C). In addition, the use of relatively low temperatures simplifies sample handling procedures.

Carbon samples were maintained at the reaction temperature and under a pressure of approximately 1200 mbar of reagent until the system pressure was constant. In practice, the pressure stabilised within 30 - 60 minutes, but the samples were stored overnight (ca. 22 hours) because of the time required to heat and cool the reactor vessel. After cooling under vacuum, the carbons were removed and outgassed at 120°C (3 mbar) until constant weight was attained.

The increase in sample weight was found to be independent of the number of treatment cycles (that is, the introduction of a second aliquot of phosgene after first evacuating the reactor vessel did not result in a further significant increase in carbon weight).

8.1.2 Chlorine

The initial exploratory studies revealed that the quantity of chlorine fixed by the carbons was also temperature dependent, and significant quantities were adsorbed by all three carbons at 30°C (eg. BPL, table 8.1). It was not possible to remove the entire quantity of chlorine adsorbed at 30°C by pumping (3mbar; 300°C).

Subsequently, the carbons were modified at 180°C using the apparatus and procedures described above.

The quantity of chlorine adsorbed was found to increase with the number of treatment cycles, which suggests that chlorine is a less selective chlorinating reagent in comparison to phosgene. It is probable that this dependence was due to a build-up of reaction products within the pore structure which limited the extent of the reaction: outgassing the sample in situ resulted in some desorption of these products, such that further reaction took place on introducing further aliquots of gas. Alternatively, it may be that the carbon "absorbed" the chlorine

in a manner similar to fluorine, where it was observed that the amount adsorbed was also dependent upon the number of treatment cycles (chapter 7).

During the course of the reaction, gaseous samples were removed and analysed using a Finnegan MAT ITD mass spectrometer. Attempts to identify and quantify any reaction products were unsuccessful. Hydrogen chloride was, however, detected after modifying the carbons with either of the chlorinating reagents described above. No chlorinated hydrocarbons (eg. carbon tetrachloride) were found.

8.2 The Reaction of Phosgene and Chlorine with Activated Carbon

Modification using phosgene resulted in significant increases in sample weight (table 8.2). This increase was probably independent of the carbon source, since the ratios of the quantities of reagent adsorbed to the values of the BET surface area were not substantially different (8.3.1). This was also true of chlorine modified carbons which exhibited less than an approximately 10% weight increase (table 8.2).

Examination of the elemental analysis data (table 8.3) reveals that the weight changes associated with modification using phosgene or chlorine were due to chlorine adsorption. Indeed, EDX analysis of the modified carbons revealed that high concentrations of chlorine were present at the surface (the control carbons did not contain chlorine). This is illustrated at figure 8.0 for a sample of chlorinated SCII carbon.

The elemental analysis data are also compared on the basis of the molar ratio of each element to that of carbon. This comparison also suggests that the reaction with either chlorinating reagent primarily leads to chlorine fixation, but also to a reduction in the hydrogen content of the carbon.

Measurement of the acidity of aqueous suspensions (pH 2) indicated, however, that the surface of the modified carbons may be unstable. Thermal analysis (Figure 8.1, control and modified SCII carbon) illustrates a similarity between the carbons modified with phosgene and chlorine, and also that significant weight losses occurred above a temperature of ca. 400 - 450°C. This behaviour was observed for the three carbons used in this study. Below this value, the carbons were found to be of similar character to the control.

Gas analysis of the desorbed species was not possible using the TG apparatus, but it is probable that a number of products were generated, including chlorine and hydrogen chloride.

In addition, the weight decreases observed during thermal desorption did not suggest that the adsorbed chlorinating reagent or its reaction products promoted significant carbon gasification: that is, the weight losses observed during thermal analysis of the modified samples were very similar to the original weight increases resulting from modification (note, however, that the control carbons lost weight during analysis: eg., for SCII carbon, the weight decrease for the control sample was 14.4%: that for the chlorinated sample was 27.8%, which exhibited a 13.1% increase in weight after chlorination).

8.3 Adsorptive Properties of Phosgene and Chlorine modified Carbons

8.3.1 Nitrogen

To study the effect of modification upon the structural properties of the carbon, nitrogen adsorption has been used. The data has been corrected as described previously (chapter 7). In the present case, this has been done so on the presumption that no significant carbon gasification resulted.

The data at table 8.2 illustrate typical gravimetric changes resulting from modification. Comparison of this data with the results of elemental analysis (table 8.3) suggests that it is reasonable to assume that gasification of the carbon was not significant when using either reagent.

Typical examples of nitrogen adsorption isotherms for samples of control carbons, and carbons modified with phosgene or chlorine are at figures 8.2- 8.5.

Values of the BET surface area and micropore volume (α_s analysis) for some of these samples are at table 8.4.

Phosgene

Nitrogen isotherms for samples of phosgene modified carbons are at figures 8.2 (BPL) and 8.3 (CECA). These indicate that processing does not result in significant structural changes, although the amount of nitrogen adsorbed is reduced. This reduction, below a relative pressure of approximately 0.1-0.15, indicates that reaction primarily leads to a loss of primary and secondary microporosity. This contention is supported by the results of α_s analysis. No obvious trends are apparent from values of the external surface areas of the modified carbons in comparison to control samples, however, but they do suggest that reaction has occurred throughout the pore structure.

Chlorine

Nitrogen isotherms for samples of control and chlorinated CECA and SCII carbons are at figures 8.4 and 8.5. In these examples, the adsorption of more than 10% w/w chlorine (16.6%, CECA; 12.5%, SCII) results in a marked reduction in the micropore volume (table 8.4): as before, no obvious trends were observed between values of the external surface area. Isotherms for chlorinated carbons containing less than approximately 10% chlorine were similar to those for samples modified with phosgene.

8.3.2 Water Adsorption

Water adsorption isotherms were measured in flowing air at 22°C (chapter 5, Appendix), and the quantities of adsorbed moisture have been calculated on the basis that carbon gasification was not significant. The isotherms presented are representative: the effects described were reproduced at least twice.

The isotherms for a sample of control SCII (nutshell) carbon, and SCII carbon modified with phosgene are at figure 8.6. The uptake of water by the modified carbon is marginally reduced across the width of the adsorption branch of the isotherm, suggesting that the surface contains fewer polar adsorption centres in comparison to the control. The reduced capacity of the carbon at RH85% may be a consequence of the small reduction in the micropore volume that resulted from modification. The broad hysteresis loop observed below ca. RH50%, which was also observed for the directly fluorinated carbons (chapter 7), may be a result of a reactive surface whose chemistry is changing during the measurement. That this is so is evidenced from the fact that after outgassing the carbon (120°C; 3 hours; 3 mbar) on completion of the isotherm, the weight of the sample was greater (ca. 0.8-1.0%).

This increase in weight may be due to the formation of oxygen containing functional groups at the surface (ageing, chapter 6). That this weight change is associated with surface chemical changes is evidenced from a comparison of the first and second isotherms for the modified sample (the second isotherm was determined using the same sample after first outgassing as described above). In this case, (figure 8.7) the amount of water adsorbed is increased below RH values of approximately 60%, which is consistent with the presence of a greater number of polar adsorption centres. In addition, the weight of the sample was further increased, suggesting that the process was incomplete. Similar observations were made during studies of the water adsorption properties of carbons prepared by direct chlorination (< ca. 10% weight chlorine). Carbons

containing above ca. 10% weight of chlorine were found to be of higher surface polarity in comparison to control samples, but adsorbed essentially the same quantity of water vapour at high values of the RH (figure 8.8; SCII carbon: 12.5% chlorine).

8.3.3 Chloropicrin (PS) Adsorption

PS adsorption data for samples of control and modified carbons are at table 8.5.

Phosgene

Modification of the three carbons with phosgene did not result in any substantial change in the efficiency of PS adsorption compared to control samples. In addition, the modified carbons afforded no resistance to ageing effects. The efficiency of PS adsorption after ageing the modified samples was similar to that of the aged- control carbons.

Water adsorption measurements indicated that the samples were reactive (unstable in the presence of moisture): the PS adsorption data for the aged samples may reflect this. This reactivity may be due to the presence of, for example, acid chlorides, or weakly bound surface carbon- chlorine complexes.

Chlorine

In comparison to samples of control, the adsorption of PS from humid air by the chlorinated carbons was poor. Outgassing at elevated temperature resulted in an increase in filter breakthrough time, which was (ultimately) improved in comparison to the control sample. However, carbons modified with chlorine and outgassed at elevated temperature formed acidic aqueous

suspensions, and did not afford resistance to ageing effects.

Nitrogen adsorption suggests that the loss of performance may be associated with a loss of porosity, and water adsorption indicates that it is probably a combination of this, and an increase in the number of polar adsorption centres. The unstable nature of these samples may be due to the presence of weak (reactive) carbon- chlorine bonds, which may be amenable to further transformation.

8.4 The Effect of Post Treatment on the Properties of Phosgene or Chlorine Modified Carbons

Phosgene

Because carbons modified with phosgene may contain reactive functional groups which should be amenable to further chemical transformation, derivitisation using methanol was attempted. Thus, the modified carbons were refluxed with methanol, after first outgassing the carbon to constant weight and ensuring that contact with air was minimised (during outgassing, only small weight losses were observed- ca. 1-2%).

Treatment of the modified samples with methanol resulted in significant reductions in mass (table 8.6), an observation inconsistent with the presumption that functional groups such as acid chloride, or reactive carbon - chlorine surface species were present. Indeed, calculations based upon the results of elemental analysis (by comparing the data on the basis of the molar ratio of each element to that of carbon; table 8.7) indicate that insufficient oxygen is present on the carbon for there to be predominantly acid chloride functions at the surface of the modified carbon and, more importantly, that methanolysis does not result in an increase in the carbon oxygen content.

It is more likely, therefore, that the weight decreases associated with treatment of the modified carbons with methanol were due to loss of the adsorbed reagent or its reaction products. This contention is supported by the observation that samples of control carbon treated with methanol exhibited only marginal weight changes (table 8.6).

If methanol treatment merely results in the removal of reaction products, then carbons treated with other polar solvents should behave in a similar manner. Thus, to test this hypothesis, samples were treated with water. This was carried out by washing (typically 6-8 times) until the pH of the mother liquor was neutral, and then refluxing in water for approximately 8 hours. Methanol treatments were subsequently carried out using this approach.

Because elemental analysis (table 8.3) indicates that both chlorine and phosgene react with the carbons to the same effect, samples modified using chlorine were treated as described above. The weight changes associated with modification and treatment are at table 8.6: elemental analyses are at table 8.8.

Treatment of the phosgene or chlorine modified carbons with either methanol or water results in significant weight losses, but the use of water resulted in the greatest change. Elemental analysis reveals that this involves a reduction in both the chlorine and the hydrogen content. The residual hydrogen content was also dependent on the amount of chlorine adsorbed, since it was observed to decrease as the chlorine content increased.

These observations suggest, therefore, that both chlorinating reagents react at the carbon surface by addition of chlorine, and by substitution of hydrogen, and that subsequent treatment with methanol or water merely serves to remove adsorbed reagent and/ or reaction products which give rise to the measured acidity of the carbons in aqueous suspension. The addition of chlorine probably takes place at any active sites on the surface (8.4.2).

Thermal analyses data for some of the modified and treated (SCII) carbons are shown at figures 8.9-8.11.

The data at figures 8.9 and 8.10 indicate that treatment of phosgene or chlorine modified carbons with water (or methanol) results in a substantial change in thermal stability. The differences, observed above ca. 400-450^{o}C, indicate that the material removed during treatment is either very strongly physically adsorbed, or is weakly chemisorbed.

After modification and treatment, the carbons were of similar thermal stability to the control (figure 8.11). EDX spectra for the modified and treated carbons were similar, resembling that shown at figure 8.0 for chlorinated SCII carbon.

Both BPL and CECA carbons were found to exhibit similar thermal desorption characteristics to those of SCII carbon after modification and treatment.

Based upon these results, XPS analysis of the modified and modified/ treated carbons was undertaken, with the aim of substantiating the above observations. Some of the spectra are shown at figures 8.12A-K.

Examination of the narrow scan C (1S) spectra for phosgene and phosgene/ methanol modified BPL carbon samples (figure 8.12A) suggests that little or no change is brought about by treating the phosgene modified carbon with methanol. In both spectra, the inflexion to higher binding energy values is attributed to carbon-oxygen bonds: that the spectrum for the control carbon was the same supports the view that modification and treatment does not result in an increase in the quantity of surface oxygen. It is also the case that treatment of the phosgene modified carbon with methanol does not result in

methanolysis, since the narrow scan O (1S) spectra for these samples are essentially the same (figure 8.12B). This is strong evidence in support of the view that methanol treatment does not result in any change in surface chemistry, and only effects the removal of adsorbed reagent and/ or reaction products (presumably from the pore structure). The O (1S) spectrum for control BPL carbon was very similar to those for the modified and modified/ treated carbon samples.

Analysis of the O (1S) spectra using peak deconvolution indicated that at least four different oxygen containing species were present on the control and the phosgene modified (and treated) carbon. This is clear from the raw spectral data (figure 8.12B).

The narrow scan Cl (2P) spectra for these carbons are at figure 8.12C. Again, no significant differences are apparent. In both cases, there are approximately five separate contributions to the total signal, suggesting that a number of chemically distinct surface carbon-chlorine species are present.

If methanol treatment resulted in, for example, the conversion of acid chloride groups to ester groups, obvious changes in both the O (1S) and Cl (2P) spectra would be anticipated.

XPS spectra for SCII carbon modified with phosgene or chlorine, and treated with methanol or water are illustrated at figures 8.12D-8.12K.

Phosgene

The C (1S) spectra for samples of control, phosgene modified, and phosgene modified/ methanol treated SCII carbons were similar to one another and also to the modified BPL samples (figure 8.12A, compare figure 8.12D). In

each case, the inflexions to higher binding energy values, which are smaller in comparison to those for the BPL samples, are attributed to carbon-oxygen bonds. The spectrum for the phosgene modified/ water treated sample was broader toward higher values of the binding energy, suggesting that more surface oxygen containing functional groups may be present. However, this broadening may also be due to carbon-chlorine bonds.

Analysis of the O (1S) regions (figure 8.12E) indicated that three principal types of oxygen containing functional groups probably contribute to the total signal. As a result of modification and treatment, the relative abundance of the groups giving rise to the two major peaks changed slightly in comparison to the control, but not markedly so. No extra peaks were present after modification/ treatment. That the O (1S) regions for these samples are different to those for the BPL samples may reflect the presence of surface (ash) impurities associated with oxygen in the case of BPL (the broad nature of the peaks for these carbons suggests that a more complex mixture of surface oxides are present).

Examination of the Cl (2P) spectra for the modified and modified/ treated samples (figure 8.12F) revealed that only two principal species contribute to the total signal, significantly fewer than for BPL. The ratio of the two peaks was found to change significantly after methanolysis, and a distinct doublet was evident (figure 8.12F). This difference may be due to the removal of weakly bound complexes from the surface of the phosgene modified sample (lower binding energy), with the consequent enhancement in the signal due to the more strongly bound chlorine containing species (quantification analysis indicates that methanolysis resulted in a reduction in the amount of surface "Cl": for BPL carbon, no change was observed). The phosgene modified sample treated with water was similar, in that no extra peaks were present: a significant difference in the relative abundance of the surface chlorides was apparent, however. This may be due the greater efficiency with which adsorbed reaction products were removed during solvolysis.

Chlorine

Modification resulted in a marked broadening of the C (1S) envelope (figure 8.12G), but treating the chlorinated carbon with water did not result in any further change. That this broadening is due to the presence of high concentrations of surface carbon-chlorine species, and not carbon-oxygen species, is apparent from a comparison of the O (1S) spectra for the control, modified, and modified/ treated samples (figures 8.12H-I). It is clear that treating the modified carbon with water does not result in the introduction of extra oxygen containing functional groups (that the envelope was wider for the control sample suggests that comparatively more oxygen containing groups were present on this sample).

The Cl (2P) spectra for the modified and treated samples were similar, but there were differences in the relative abundance of the surface groups (the modified and treated sample showed a well resolved doublet- figure 8.12J). This difference probably reflects the removal of less stable adsorbed species during solvolysis. None of the spectra indicated that treatment resulted in complete loss of any one peak (species). The spectra for the chlorine modified and methanol treated carbons were essentially the same as the spectra for the modified and water treated samples.

That the surface carbon-chlorine groups present on the phosgene or chlorine modified and treated samples are very similar is apparent from figure 8.12K. The only difference is the relative abundance of each species.

It is likely that the contribution at the higher binding energy values is due to chlorine species present within the more aromatic (graphitic) surface regions: the more weakly bound species may be present on aliphatic chains at the periphery of the basal planes (surface defects, and regions of unsaturation).

The XPS data therefore support the view that both modifications result in chlorination of the carbon surface to yield similar products, and that solvolysis does not result in any change to the nature of the chemibound species. Quantification analysis of the surface functional groups (by XPS, table 8.9) also supports the view that solvolysis merely serves to remove adsorbed reagent and/ or reaction products.

8.4.1 The Properties of Phosgene or Chlorine Modified and Treated Carbons

Nitrogen Adsorption

Examples of nitrogen isotherms for samples of control, modified, and treated carbons are at figures 8.13-8.15. Values of the external surface area and the micropore volume (α_s analysis), in addition to the values of the BET surface area, are recorded at table 8.10 for some of the samples.

Phosgene

Isotherms for samples of phosgene modified and methanol treated carbons are at figures 8.13 (BPL) and 8.14 (CECA). Treatment of the CECA carbon (or SCII) with methanol results in a decrease in nitrogen adsorption below a relative pressure of approximately 0.1 compared with the modified but untreated sample, indicating that a further proportion of the micropores are occluded after methanolysis. These effects were also observed for the phosgene modified nutshell carbons which were treated with water. The reason for this is unclear, since treatment of BPL carbon in the same way had little effect on the amount of nitrogen adsorbed. The observation is not, however, believed to arise from methanol- carbon reactions, because the adsorptive properties of the control samples were unaffected by methanol treatment alone.

Chlorine

The data at figure 8.15 suggest that treatment of the modified carbon with water or methanol enhances the accessibility of nitrogen to the micropore structure. In fact, treatment with water results in an isotherm which is almost identical to that of the control. The methanol treated sample was, in comparison, of reduced surface area. This may be because methanolysis did not result in complete removal of the adsorbed reagent and/or its reaction products (table 8.8).

8.4.2 Water Adsorption

Figure 8.16 shows the isotherms for samples of control CECA (nutshell) carbon, and CECA carbon which had been modified with phosgene and then treated with methanol. Both the first and second isotherms for the modified sample are at the figure. It is apparent that after modification and treatment with methanol, the carbon contains significantly fewer polar adsorption centres. The difference in the uptake of water below ca. RH50% in this case is principally due to the changes in hydrophobic character brought about by the modification process (that is, the isotherm is displaced to the right of the axis). The capacity of the modified carbon at saturation is probably unchanged, and the difference at ca. RH85% (the highest value of the RH used routinely in these studies) reflects the displacement of the pore filling region of the isotherm to higher values of the RH (due to the fewer number of polar adsorption centres).

The effect could not be brought about merely by heat treating control carbon: the water isotherm was unaffected by outgassing the sample at 180°C. It is notable that samples modified with phosgene or chlorine, and not treated with methanol or water, behaved in the same way as the example (they aged: SCII carbon, figure 8.6, 8.7) described above, indicating that the material

removed during treatment was responsible for the unstable nature of the modified carbon. It is also apparent that treatment with water is a more effective approach (figure 8.17).

Of more importance is the fact that the sample does not exhibit any significant ageing effects either as a result of exposure to RH80% air at 45°C for 45 days (figure 8.17), or during determination of the second isotherm (figure 8.16). The samples show no weight increase after outgassing on completion of both the first and second measurement, and only a marginal increase as a result of ageing. The implication is therefore that the modified and treated carbon is hydrolytically stable, and that the chlorinating reagent has reacted at the active sites on the carbon surface which would normally interact with oxygen and/ or moisture to give rise to polar surface oxides. In addition, XPS analysis indicated that little or no change in surface chemistry had taken place during ageing.

The effect on the water isotherm as a result of ageing a sample of control (SCII) carbon under the conditions described above was dramatic (figure 8.18), indicating that the chlorination technique does mask the surface sites which are normally susceptible to oxidation.

BPL carbon exhibited somewhat different water adsorption characteristics in comparison to the carbons derived from nutshell. As before, modification with phosgene or chlorine gave rise to an unstable product, but treatment with methanol or water did not produce a carbon of improved hydrophobic character. In fact, the hydrophobic character of the modified and treated carbons is largely unchanged in comparison to the control, although resistance to ageing effects was observed. This is illustrated at figure 8.19 for a sample of BPL carbon modified with chlorine and treated with water. It may be that the behaviour of BPL carbon is due to the presence of significantly greater quantities of ash impurity in comparison to the nutshell carbons (BPL contained ca. 7.5% ash; CECA carbon ca. 3%, and SCII ca. 2%. After modification using

either phosgene or chlorine, these values were typically reduced by 1-2%, although BPL carbons containing large quantities of chlorine were of approximately 50% lower ash content). Alternatively, BPL carbon contains few polar adsorption centres, which are not amenable to modification using these techniques.

8.4.3 Methanol Adsorption

Studies of the methanol adsorption characteristics of control and modified carbons largely support the conclusions drawn from analysis of the water isotherms described above.

Figure 8.20 shows methanol breakthrough curves for some of the CECA carbons whose water adsorption characteristics are described at figure 8.16. The quantity of methanol adsorbed at the low relative pressure used (0.03 p/p^0) reflects the differences in the polarities of the surfaces before and after modification. Similar measurements using BPL carbon (figure 8.21) support the view that modification has not resulted in a carbon of improved hydrophobic character.

That the shapes of these curves are essentially the same before and after modification suggests that the kinetics of adsorption are not significantly different, indicating that structural modification has not taken place to any obvious extent.

Figure 8.22 shows the breakthrough curves for samples of control CECA which had been aged at 45°C as described above. Samples treated with water or methanol alone prior to ageing behaved in an analogous manner. These results are consistent with the water adsorption properties of the aged and aged/ treated controls (chapter 6).

Figure 8.23 shows similar data but for a sample of CECA carbon which was modified with phosgene and treated with methanol prior to ageing. The amount of methanol adsorbed by the aged sample suggests that ageing has taken place, but to an extent that is small compared to that of the control samples (or indeed samples which had been modified with phosgene but not treated with methanol or water). This behaviour was exhibited by the three carbons used in the study.

BPL or nutshell carbons modified with chlorine and treated with methanol or water behaved in an analogous manner (figure 8.24 and 8.25).

8.4.4 Chloropicrin (PS) Adsorption

PS adsorption data for samples of control and modified carbons are at tables 8.11 and 8.12.

Phosgene

The data at table 8.11 illustrate that treatment of control carbon with methanol does not affect the filter breakthrough time, and that the effects of ageing this sample on filter performance are similar to those observed for the control. In both cases, the filter breakthrough time was reduced by approximately 25%. Treatment of control carbon with water, followed by ageing, lead to a more substantial reduction in performance: it is possible that the water treatment promotes the reaction between oxygen/ water vapour and the carbon.

Treatment of the modified BPL carbon with methanol or water has a marked effect upon the ageing characteristics. In each case, no significant change has taken place. The initial performance of the modified carbon is

somewhat less than that of the control (ca. 7%), however. These results are consistent with the water adsorption data described above.

Similar observations were made for both the nutshell carbons (table 8.11), except that the modified and treated carbons performed significantly better in comparison to the respective controls. Once again, no measurable ageing effects were observed.

The CECA carbon appears to be particularly amenable to modification, where an almost 50% improvement in filter performance was observed. On the basis of the present data, the use of nutshell based carbons is most promising.

Chlorine

Directly chlorinated carbons containing amounts of adsorbed chlorine similar to the quantities present on the samples modified with phosgene were found to behave in an analogous manner (table 8.12). It was observed that the performance of the modified and treated samples was improved, possibly due to the higher amounts of sorbed chlorine.

Treatment of the chlorinated carbons with water (or methanol) has a marked effect on filter performance, and supports the view that this technique merely serves to remove adsorbed reagent and/ or reaction products. This contention is further supported by the effect of the outgassing temperature on PS filter life- performance improves as the temperature is raised, but outgassing alone is clearly a less effective means of preparing the modified carbon (table 8.5).

Although the PS data are consistent with the water adsorption properties of the modified carbons, they appear inconsistent with the methanol data for the aged samples. Methanol adsorption indicated that ageing did occur, albeit to

a small degree. It must be the case that the distribution of the polar adsorption centres on the modified and aged samples was such that they did not significantly influence the adsorption of PS (chapter 6).

8.5 Modification of Aged and NO_2 Treated Carbons using Phosgene

Part of this research is intended to address the possibility of chemically modifying aged carbons (chapter 6). The rationale for selecting phosgene was that certain types of oxygen-containing functional groups may be present at the surface of such carbons (chapter 3,4), which may be reactive toward this reagent. A possible reaction sequence of such a functional group with phosgene is outlined at figure 8.26.

Thus samples of carbon which had been aged at 45°C were modified using phosgene in the manner described above. In addition, modification of carbons which had first been oxidised using NO_2 was attempted (chapter 6).

8.5.1 Aged Carbons

The weight increases observed after modification of aged carbons were consistently lower than those found for the unaged control samples (table 8.1, 8.13). This effect was independent of temperature across the range studied, and suggests that the surface oxygen containing functional groups mask a proportion of the sites which would otherwise be reactive toward phosgene.

The water adsorption isotherm for the modified and methanol treated aged sample does, however, suggest that the process is effective in reducing the polarity of the carbon surface (figure 8.27, 8.29), but the data at figure 8.28 indicates that the modification technique is more successful when unaged control carbon is used (because the pore filling region for the modified (unaged)

control sample is displaced to higher values of the RH compared with the sample which had been aged prior to modification). This was also apparent from PS adsorption (table 8.11; 8.13).

Because the treatment of aged carbon leads to a marked reduction in surface polarity, some reaction with surface oxides cannot be ruled out.

8.5.2 NO_2 Modified Carbons

Samples of control carbon were initially modified with dinitrogen tetroxide (700 mbar) as described at chapter 6. After outgassing to constant weight, the carbons were modified with phosgene and then treated with methanol.

The water adsorption isotherms at figures 8.30 and 8.31 indicate that the phosgene modified and methanol treated NO_2 oxidised carbons are of relatively high surface polarity: the isotherms for the NO_2 oxidised samples prior to modification were found to be similar. Treating the oxidised carbons with methanol alone did not significantly affect the water adsorption properties.

The PS adsorption data (table 8.13) reflect these observations, and indicate that such carbons are not amenable to modification using this approach. It may be that the functional introduced during modification sterically hinder PS adsorption in the presence of moisture.

The data at figures 8.1-8.11, and 8.13-8.31 are tabulated at the Appendix.

8.6 Summary

Modification of carbons with phosgene or chlorine results in the fixation of chlorine and a reduction in the carbon hydrogen content. Carbons modified in this manner are not suitable for vapour adsorption applications because the surface of the adsorbent is unstable in the presence of humid air (they age). This is due to the presence of adsorbed reagent or reaction products. The modification does not, however, result in any significant structural disruption when the amount of chlorine adsorbed is less than approximately 10% of the initial carbon weight.

Treatment of the modified nutshell samples with methanol or water yields carbons of similar adsorptive properties, which are of improved hydrophobic character compared to samples of control. XPS analysis also revealed that carbons modified using either technique were of similar surface chemistry. More importantly, the carbons afford significantly greater resistance to ageing effects compared to control samples.

Treatment of BPL carbon in this manner does not result in a carbon of improved hydrophobic character: the samples do, however, afford resistance to ageing effects.

Table 8.1 The Influence of Temperature on the Adsorption of Phosgene and Chlorine by BPL Activated Carbon

Sample	Amount of Phosgene Adsorbed at T°C (w/w %, initial carbon weight)				
	30	120	150	180	200
Control	0.0	3.4	3.9	4.8	4.9
Aged-Control*	0.1	2.6	3.1	4.2	4.3
	Amount of Chlorine Adsorbed				
Control	2.5	7.6	7.8	8.0	8.1
Aged-Control*	1.5	6.6	6.7	6.8	6.8

*Signifies the sample had been aged for 400 days at RH80% and 22°C prior to modification.

Table 8.2 Typical Gravimetric Changes Resulting from Carbon Modifications (at 180°C) using Phosgene and Chlorine

Sample	Weight Increase after Modification (w/w %, initial carbon weight)	
	Phosgene	Chlorine
BPL	6.3[1], 6.3	8.8, 8.5[2], 11.8[3]
SCII	7.4[4], 7.0	9.9[5], 12.5[6]
CECA	9.1[7], 9.0	16.5[8]

Samples modified using a single aliquot of reagent. Initial carbon weights were ca. 30g: the reactor contained two samples of carbon. Numbers ([superscript]) identify common samples for which other analyses are reported: the results are tabulated in this section.

Table 8.3 Elemental Analysis of Control and Phosgene and Chlorine Modified Carbons

Sample	Element (w/w %, Moisture Corrected)					
	C	H	N	O	S	Cl
Control and Phosgene Modified Carbons						
BPL Control	86.6	0.2	0.6	2.0	1.1	0.0
Phosgene[1]	81.5	0.1	0.45	1.3	1.0	5.8
SCII Control	92.4	0.3	0.2	1.1	0.0	0.0
Phosgene[4]	86.8	0.1	0.1	1.0	-	7.3
Control and Phosgene Modified Carbons- Element Molar Ratio (To Carbon= 100 moles)						
BPL Control	100	3.2	0.5	1.7	0.4	0.0
Phosgene[1]	100	1.5	0.5	1.2	0.4	2.4
SCII Control	100	3.2	0.1	1.0	-	0.0
Phosgene[4]	100	1.4	0.1	0.9	-	2.4
CECA Control	100	3.7	0.1	1.4	-	0.0
Phosgene	100	3.3	0.3	1.4	-	3.5
Chlorine Modified Carbons (Element, w/w %, Moisture Corrected)						
BPL Chlorine[2]	78.4	<0.1	0.4	1.9	0.9	8.0
SCII Chlorine[5]	84.4	<0.1	<0.1	-	-	9.7
Chlorine Modified Carbons- Element Molar Ratio (To Carbon= 100 moles)						
BPL Chlorine[2]	100	0.3	0.4	1.8	0.4	3.2
SCII Chlorine[5]	100	0.3	<0.1	-	-	3.9

The results are an average of at least two determinations.

Table 8.4 Nitrogen Adsorption and α_s analysis for Phosgene and Chlorine Modified Carbons

Sample	BET Surface Area (m^2g^{-1})	Micropore Volume (cm^3<STP>g^{-1})	External Surface Area (m^2g^{-1})
BPL			
Control	1208	0.53	53
Phosgene[1]	1050	0.45	45
Chlorine[3]	1080	0.47	46
SCII			
Control	1440	0.58	47
Phosgene[4]	1420	0.58	52
Chlorine (12.5%)	1285	0.52	34
CECA			
Control	1460	0.61	51
Phosgene[7]	1430	0.59	51
Chlorine[8]	1223	0.53	45

Results are for single determinations. Typical error on measurement of surface area is ±12 m^2g^{-1}: and ±0.01 cm^3<STP>g^{-1} for the total pore volume (per gram of carbon).

Table 8.5 Chloropicrin Adsorption for Phosgene and Chlorine Modified Carbons

Sample	Carbon Water Content (w/w %, RH80%, 22°C (Corrected)	Filter Breakthrough Time (minutes) 1st Break	1% Break
BPL			
Control	35.4	83	96
Control-Aged*	35.5	64	84
Phosgene	33.4	75	82
Phosgene-Aged*	33.2	65	85
Chlorine[2]	33.4	52	70
SCII			
Control	41.7	72	94
Control-Aged*	41.4	49	69
Phosgene[4]	39.5	71	96
Phosgene[4]-Aged*	39.1	59	77
Chlorine[5]	40.3	33	60
CECA			
Control	47.0	62	76
Control-Aged*	47.2	42	56
Chlorine (10.3 w/w%; 120°C[a])	41.0	51	66
Chlorine (9.4 w/w%; 250°C[a])	41.2	63	82
Chlorine (8.8% w/w%; 300°C[a])	41.9	69	91
Chlorine (8.8%) Aged*	42.2	47	61

2cm Diameter, 2cm Bed Depth Filters. Flow velocity 382 cm min^{-1}. Challenged in Equilibrium with RH80% Air at 22°C. PS Concentration 5000 mg m^3. 1st Break is 5-10 mg m^{-3}; 1% is 50 mg m^{-3}. *Signifies samples were aged at 45°C and RH80% for 45 days. [a]signifies that the sample was first outgassed to constant weight at 120°C, then 250°C, then 300°C.

Table 8.6 Gravimetric Changes Resulting from Carbon Modifications using Phosgene or Chlorine. The Effect of Post Treatment using Methanol or Water.

Sample	Weight Increase after Modification/ Treatment (w/w %, initial carbon weight)		
	Phosgene	Phosgene/ Methanol	Phosgene/ Water
BPL			
Control	Untreated	-0.04	-0.01
Phosgene[1]	6.3	5.5	3.4
Phosgene	6.3	5.1	-
Aged*-Phosgene	5.3	5.1	-
SCII			
Phosgene[4]	7.4	5.8	5.0
Phosgene	7.0	5.5	-
CECA			
Control	Untreated	-0.01	-0.02
Phosgene	9.0	6.3	-
Phosgene	9.1	6.9	-
Aged*Phosgene	7.0	4.4	-
	Chlorine	Chlorine/ Methanol	Chlorine/ Water
BPL			
Chlorine[2]	8.5	7.9	5.3
Chlorine	8.8	-	5.3
SCII			
Chlorine[5]	9.9	8.4	7.6
Chlorine[6]	12.5	-	9.3

*Samples were aged at 45°C and RH80% for 45 days prior to modification.

Table 8.7 Elemental Analysis of Phosgene Modified and Treated Carbons

Sample	Element (w/w %, Moisture Corrected)					
	C	H	N	O	S	Cl
Control, and Phosgene Modified and Treated Carbons						
BPL Control	86.6	0.2	0.6	2.0	1.1	0.0
Phosgene[1]	81.5	0.1	0.45	1.3	1.0	5.8
Phosgene[1]/Methanol	83.2	0.0	0.41	1.2	1.1	5.4
Phosgene[1]/Water	83.3	0.0	0.40	1.2	1.0	4.7
SCII Control	92.4	0.3	0.2	1.1	0.0	0.0
Phosgene[4]	86.8	0.1	0.1	1.0	-	7.3
Phosgene[4]/Methanol	88.5	0.1	0.1	0.9	-	6.5
Phosgene[4]/Water	88.8	<0.1	0.1	0.9	-	5.7
Element Molar Ratio (To Carbon= 100 moles)						
BPL Control	100	3.2	0.5	1.7	0.4	0.0
Phosgene[1]	100	1.5	0.5	1.2	0.4	2.4
Phosgene[1]/Methanol	100	0.1	0.4	1.1	0.5	2.3
Phosgene[1]/Water	100	0.1	0.4	1.1	0.5	2.0
SCII Control	100	3.2	0.1	1.0	-	0.0
Phosgene[4]	100	1.4	0.1	0.9	-	2.4
Phosgene[4]/Methanol	100	1.3	0.1	0.8	-	2.3
Phosgene[4]/Water	100	0.5	0.1	0.8	-	1.9
CECA Control	100	3.7	0.1	1.4	-	0.0
Phosgene	100	3.3	0.3	1.4	-	3.5
Phosgene/Methanol	100	1.0	0.3	1.2	-	3.6

The results are an average of at least two determinations.

Table 8.8 Elemental Analysis of Chlorine Modified and Treated Carbons

Sample	Element (w/w %, Moisture Corrected)					
	C	H	N	O	S	Cl
Control, and Chlorine Modified and Treated Carbons						
BPL Control	86.6	0.2	0.6	2.0	1.1	0.0
Chlorine[2]	78.4	<0.1	0.4	1.9	0.9	8.0
Chlorine[2]/Methanol	80.0	<0.1	0.4	1.9	0.9	7.4
Chlorine[2]/Water	81.3	0.0	0.4	1.8	0.9	6.0
SCII Control	92.4	0.3	0.2	1.1	0.0	0.0
Chlorine[5]	84.4	<0.1	<0.1	-	-	9.7
Chlorine[5]/Methanol	85.6	<0.1	<0.1	-	-	8.8
Chlorine[5]/Water	86.2	0.0	<0.1	-	-	8.1
Element Molar Ratio (To Carbon= 100 moles)						
BPL Control	100	3.2	0.5	1.7	0.4	0.0
Chlorine[2]	100	0.3	0.4	1.8	0.4	3.2
Chlorine[2]/Methanol	100	0.1	0.4	1.8	0.4	3.0
Chlorine[2]/Water	100	0.0	0.4	1.7	0.4	2.6
SCII Control	100	3.2	0.1	1.0	-	0.0
Chlorine[5]	100	0.3	<0.1	-	-	3.9
Chlorine[5]/Methanol	100	0.2	<0.1	-	-	3.6
Chlorine[5]/Water	100	0.1	<0.1	-	-	3.2

The results are an average of at least two determinations.

Table 8.9 Surface Quantification by XPS

Sample	Element	Atomic Concentration (%)	Mass Concentration (%)
SCII/Phosgene/Water	C	81.4	74.5
	O	16.7	20.5
	Cl	1.9	5.0
SCII/Chlorine	C	80.8	73.0
	O	16.6	20.0
	Cl	2.6	7.0
SCII/Chlorine/Water	C	81.7	75.0
	O	16.6	20.3
	Cl	1.7	4.7
SCII/Chlorine/Methanol	C	81.6	75.3
	O	15.8	19.2
	Cl	2.3	6.3

Table 8.10 Nitrogen Adsorption and α_s analysis for Phosgene and Chlorine Modified and Treated Carbons

Sample	BET Surface Area (m^2g^{-1})	Micropore Volume (cm^3<STP>g^{-1})	External Surface Area (m^2g^{-1})
BPL			
Control	1208	0.53	53
Phosgene[1]	1050	0.45	45
Phosgene[1]/Methanol	1068	0.45	51
Chlorine[3]	1080	0.47	46
Chlorine[3]/Water	1010	0.46	49
SCII			
Control	1440	0.58	47
Phosgene[4]	1420	0.58	52
Phosgene[4]/Methanol	1340	0.56	48
Chlorine/Methanol	1360	0.56	50
Chlorine/Water	1410	0.58	49
CECA			
Control	1460	0.61	51
Phosgene[7]	1430	0.59	51
Phosgene[7]/Methanol	1370	0.57	45
Aged*-Phosgene	1390	0.57	51
Aged*-Phosgene/Methanol	1330	0.55	43
Chlorine[8]	1223	0.53	45

*Signifies carbons aged at 45°C and RH80% for 45 days.

Results are for single determinations. Typical error on measurement of surface area is ±12 m^2g^{-1}: and ±0.01 cm^3<STP>g^{-1} for the total pore volume (per gram of carbon).

Table 8.11 Chloropicrin Adsorption for Phosgene Modified and Treated BPL, SCII and CECA Carbons

Sample	Carbon Water Content (w/w %) (RH80%, 22°C Corrected)	Filter Breakthrough Time (minutes) 1st Break	1% Break
BPL			
Control	35.4	83	96
Control-Methanol	35.5	84	97
Control-Methanol/Aged*	35.4	65	80
Control-Water/Aged*	35.4	55	72
Phosgene/Methanol	33.2	77	97
Phosgene/Methanol/Aged*	33.3	78	99
Phosgene/Water/Aged*	33.1	77	101
SCII			
Control	41.7	72	94
Control-Methanol	41.6	72	95
Control-Methanol/Aged*	41.5	52	70
Control-Water/Aged*	41.6	50	67
Phosgene/Methanol[4]	38.7	80	108
Phosgene/Methanol[4]/Aged	39.1	84	107
Phosgene/Water[4]/Aged	38.7	83	111
CECA			
Control	47.0	62	76
Control-Methanol	46.6	60	74
Control-Methanol/Aged*	47.0	46	59
Phosgene/Methanol	38.4	98	115
Phosgene/Methanol/Aged*	38.6	95	111

2cm Diameter, 2cm Bed Depth Filters. Flow velocity 382 cm min^{-1}. Challenged in Equilibrium with RH80% Air at 22°C. PS Concentration 5000 mg m^3. 1st Break is 5-10 mg m^{-3}; 1% is 50 mg m^{-3}. *Signifies samples were aged at 45°C and RH80% for 45 days.

Table 8.12 Chloropicrin Adsorption for Chlorine Modified and Treated BPL and SCII Carbons

Sample	Carbon Water Content (w/w %) (RH80%, 22°C Corrected)	Filter Breakthrough Time (minutes) 1st Break	1% Break
BPL			
Control	35.4	83	96
Chlorine[3]	33.4	52	70
Chlorine	34.2	58	78
Chlorine/Water	32.1	81	107
Chlorine/Water/Aged*	32.1	78	104
SCII			
Control	41.7	72	94
Chlorine[5]	40.3	33	60
Chlorine/Methanol	38.8	83	108
Chlorine/Water	39.3	80	112
Chlorine/Water/Aged*	38.9	78	109

2cm Diameter, 2cm Bed Depth Filters. Flow velocity 382 cm min^{-1}. Challenged in Equilibrium with RH80% Air at 22°C. PS Concentration 5000 mg m^3. 1st Break is 5-10 mg m^{-3}; 1% is 50 mg m^{-3}.

*Signifies samples were aged at 45°C and RH80% for 45 days.

Table 8.13 Chloropicrin Adsorption for Phosgene Modified NO_2 Oxidised BPL and CECA Carbons

Sample	Weight Change on Modification (w/w %)	Carbon Water Content (w/w %) (RH80%, 22°C Corrected)	Filter Breakthrough Time (minutes) 1st Break	1% Break
BPL				
NO_2 Oxidised	3.1	38.1	36	41
NO_2/ Methanol	3.0	38.2	39	53
NO_2/ Phosgene/ Methanol	6.4	38.7	45	61
CECA				
NO_2 Oxidised	4.5	47.8	8	21
NO_2/ Methanol	4.5	47.4	10	23
NO_2/ Phosgene/ Methanol	11.1	49.8	15	26
Phosgene/ Methanol	6.3	38.4	98	115
Aged*- Phosgene/ Methanol	3.2	41.7	55	75

*Signifies the sample was aged at 45°C and RH80% for 45 days prior to modification.

FIGURE 8.0 EDX SPECTRUM FOR CHLORINATED SCII CARBON

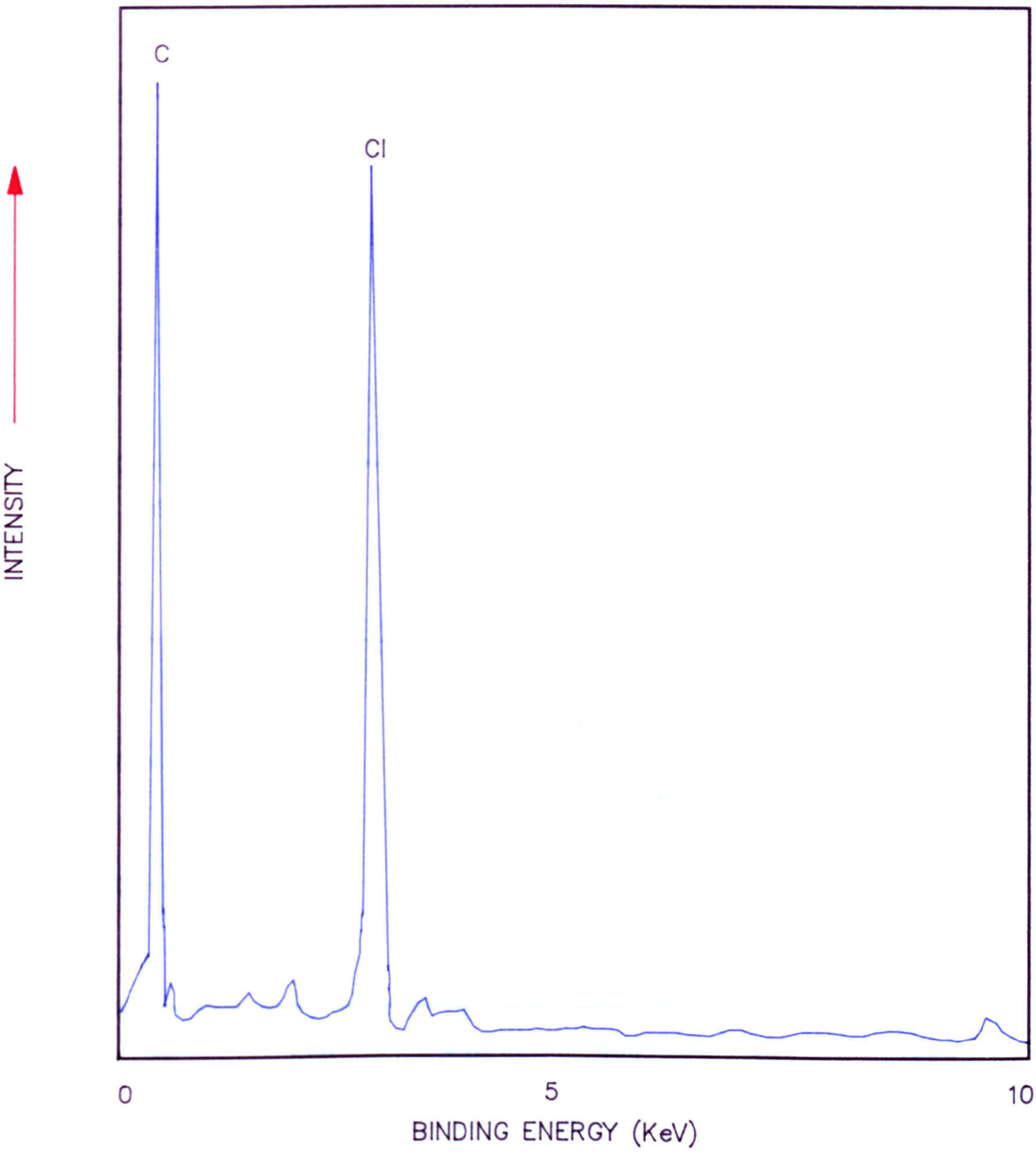

FIGURE 8.1 THERMAL ANALYSIS FOR SCII CARBONS

UPPER: ■ PHOSGENE MODIFIED

LOWER: ▲ CHLORINE MODIFIED

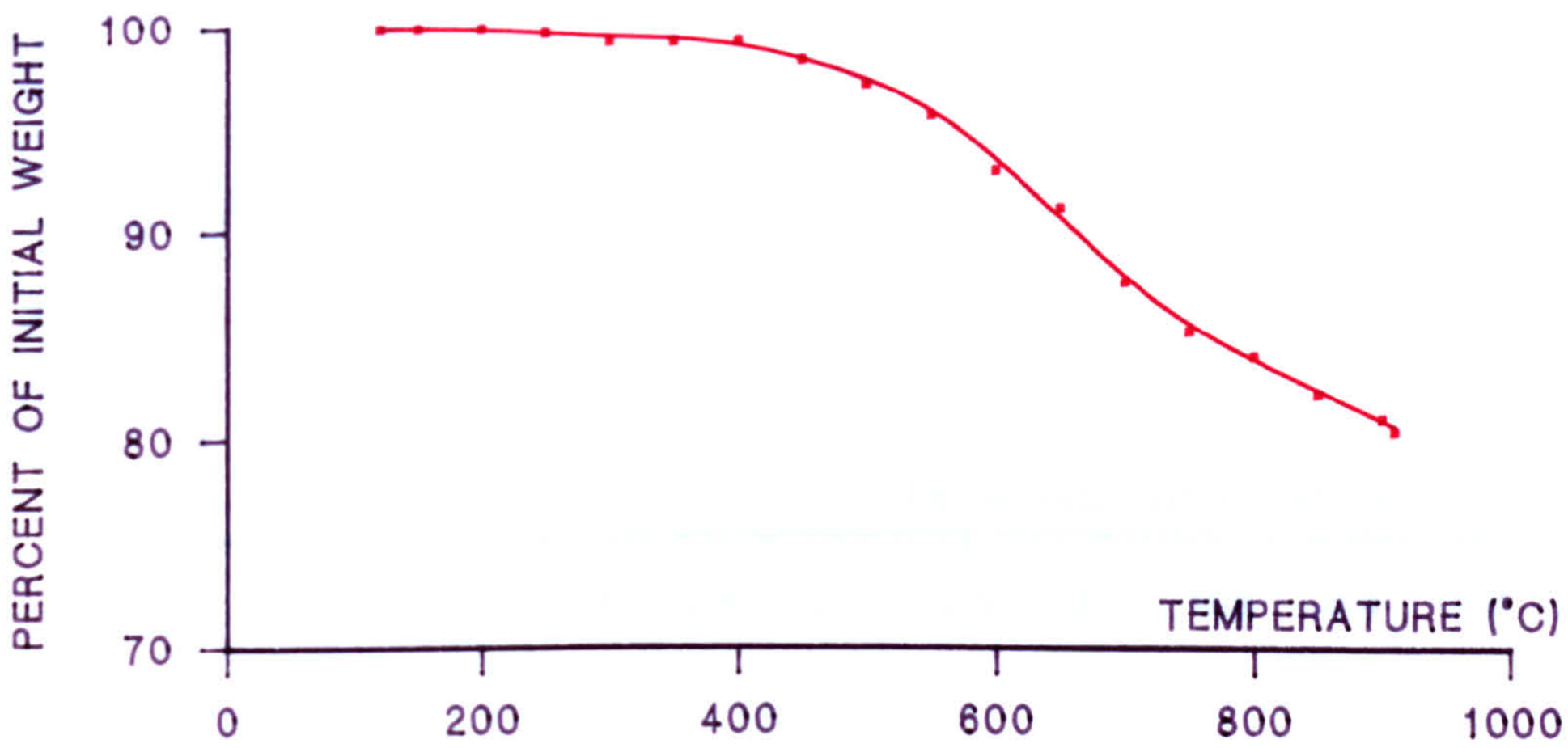

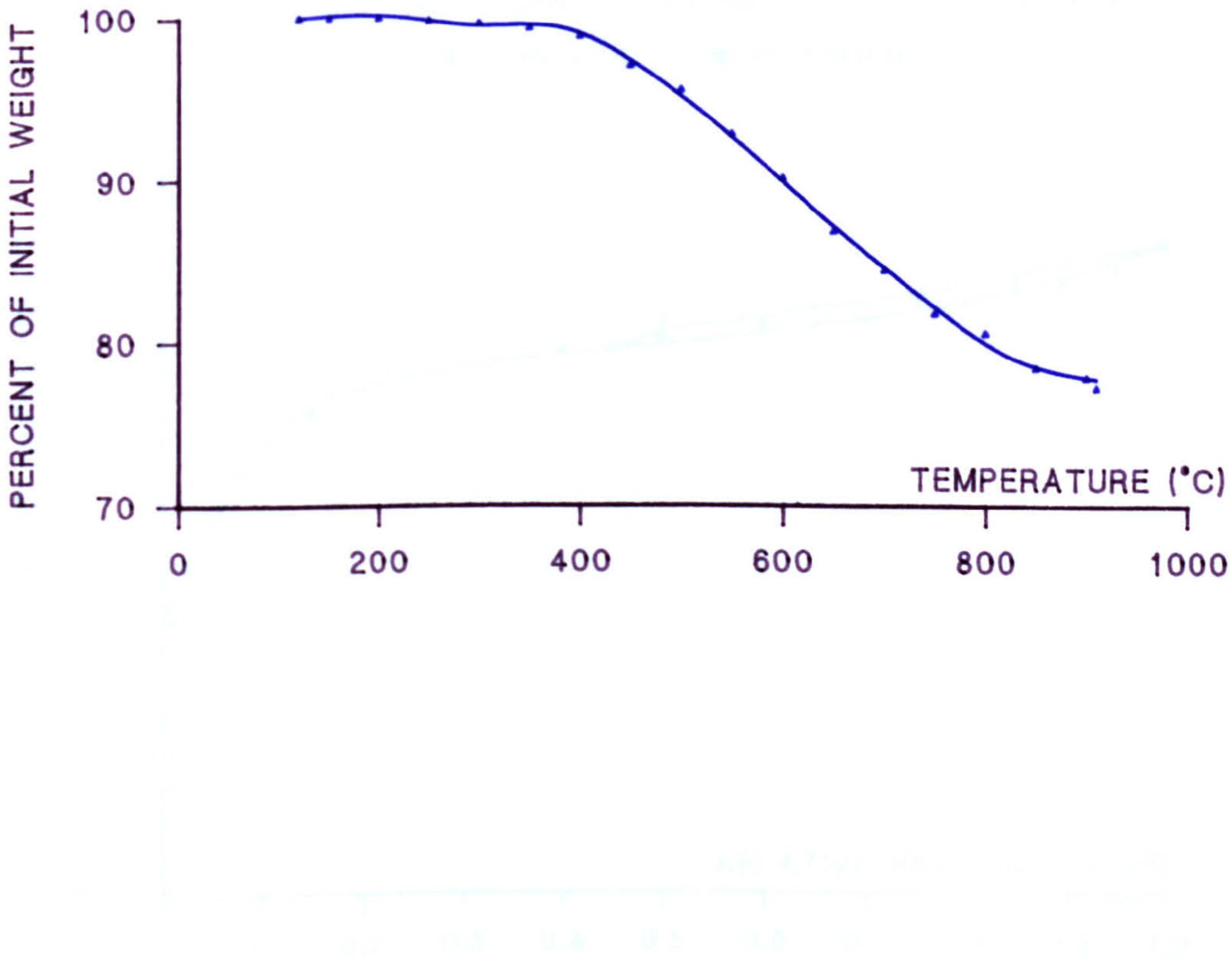

FIGURE 8.2 NITROGEN ISOTHERMS FOR BPL CARBON

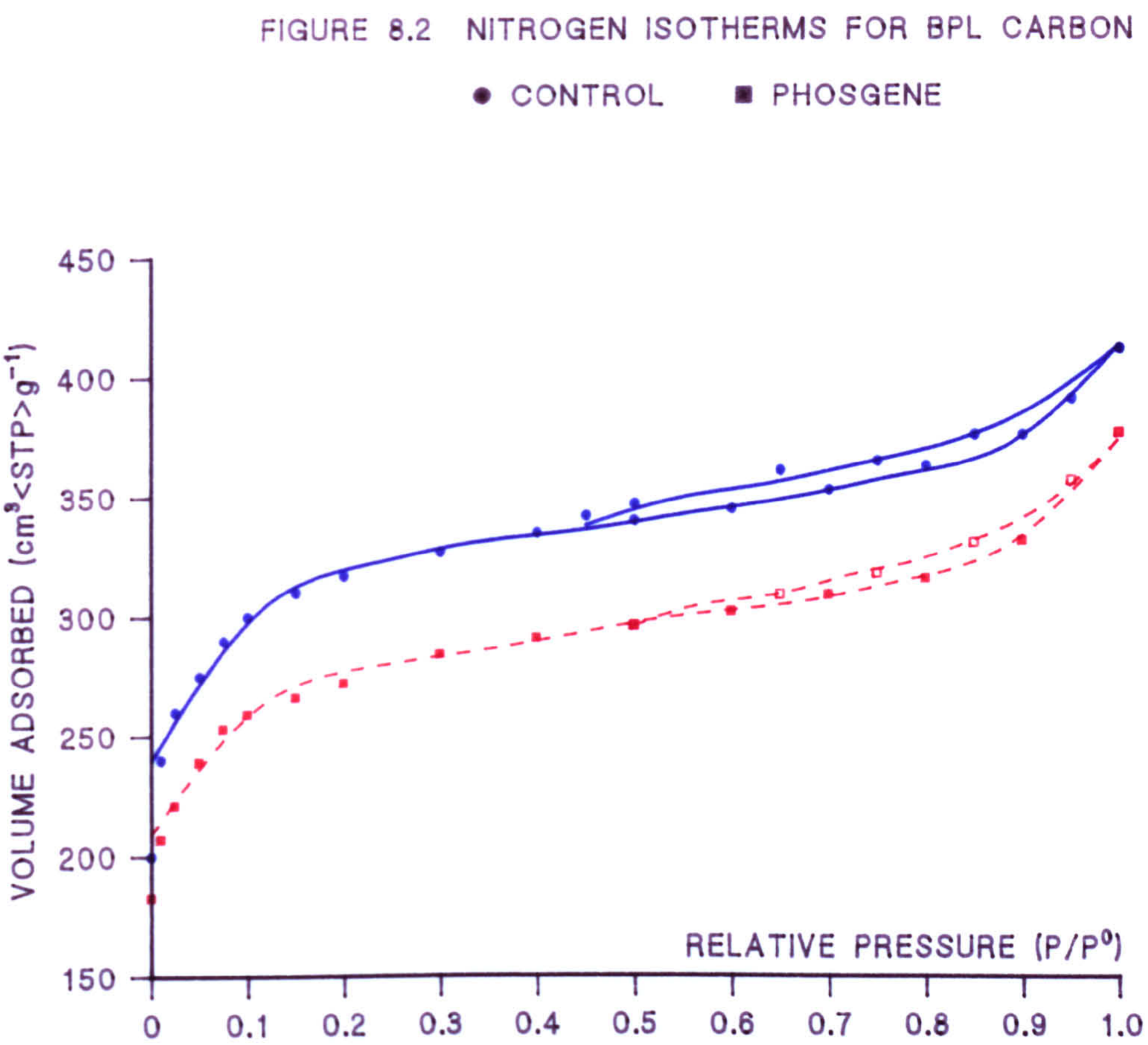

FIGURE 8.3 NITROGEN ISOTHERMS FOR CECA CARBONS

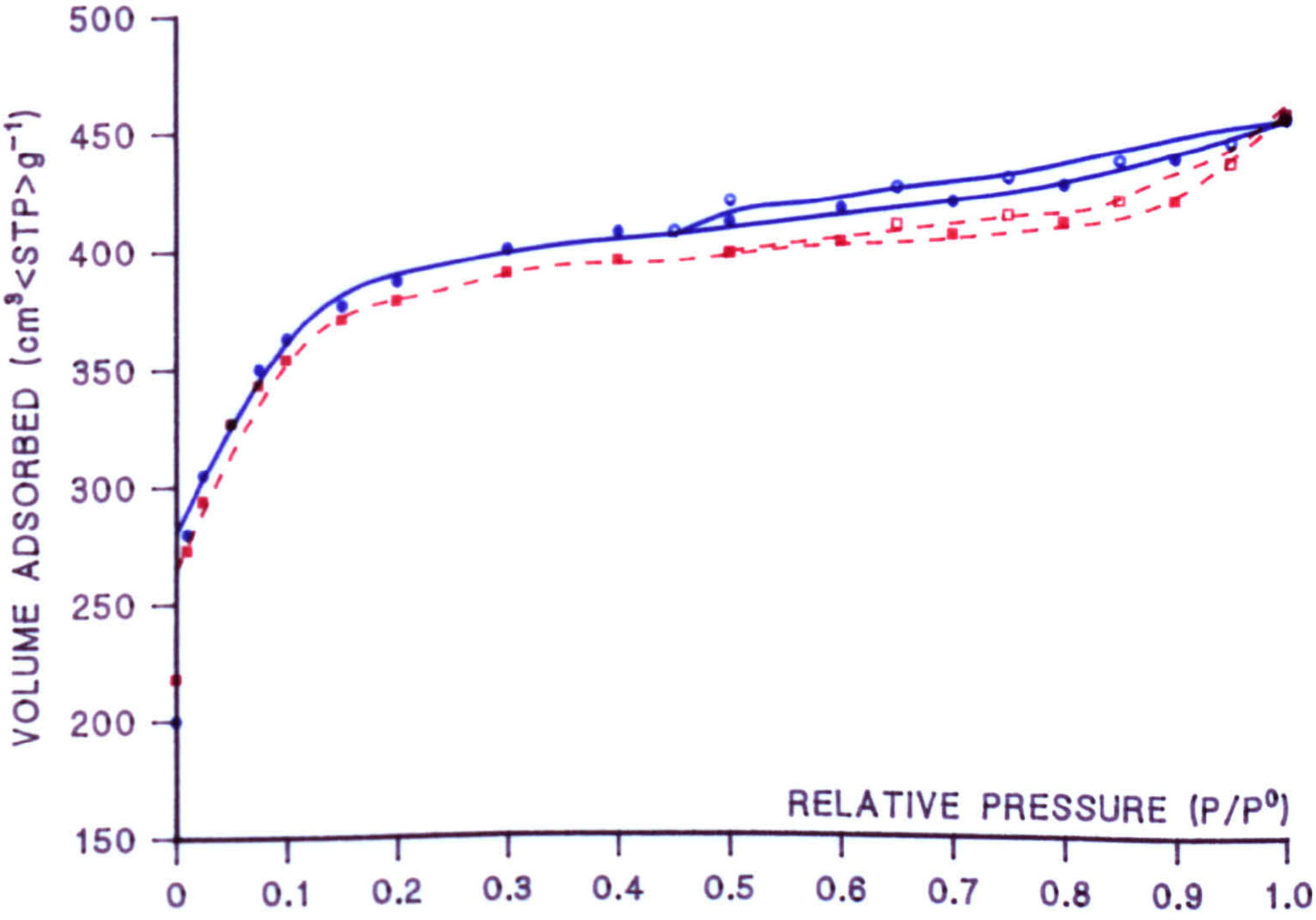

FIGURE 8.4 NITROGEN ISOTHERMS FOR CECA CARBON

● CONTROL ■ CHLORINATED

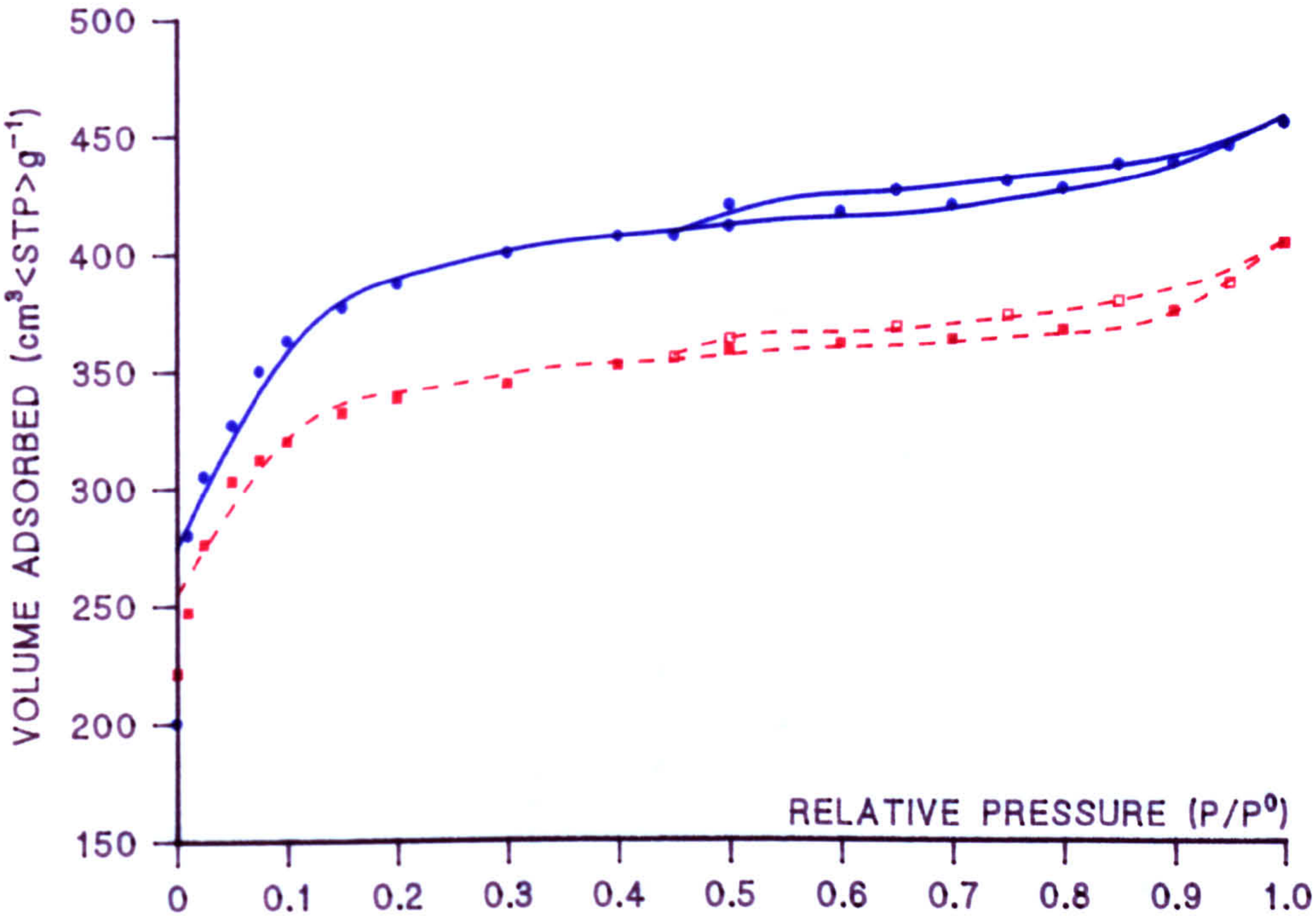

FIGURE 8.5 NITROGEN ISOTHERMS FOR SCII CARBON

● CONTROL ■ CHLORINE

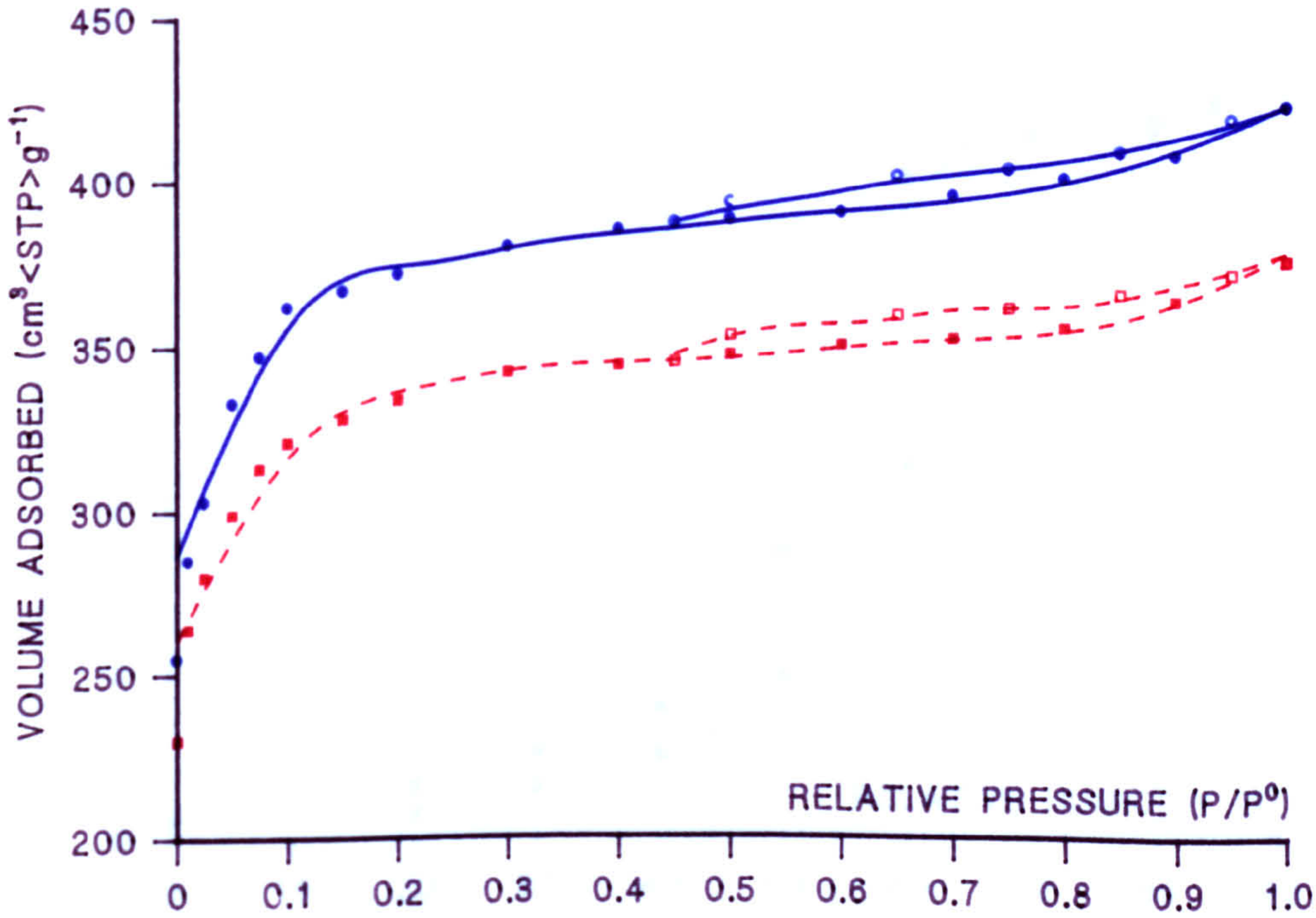

FIGURE 8.6 WATER ADSORPTION

▲ SCII CONTROL ● SCII PHOSGENE

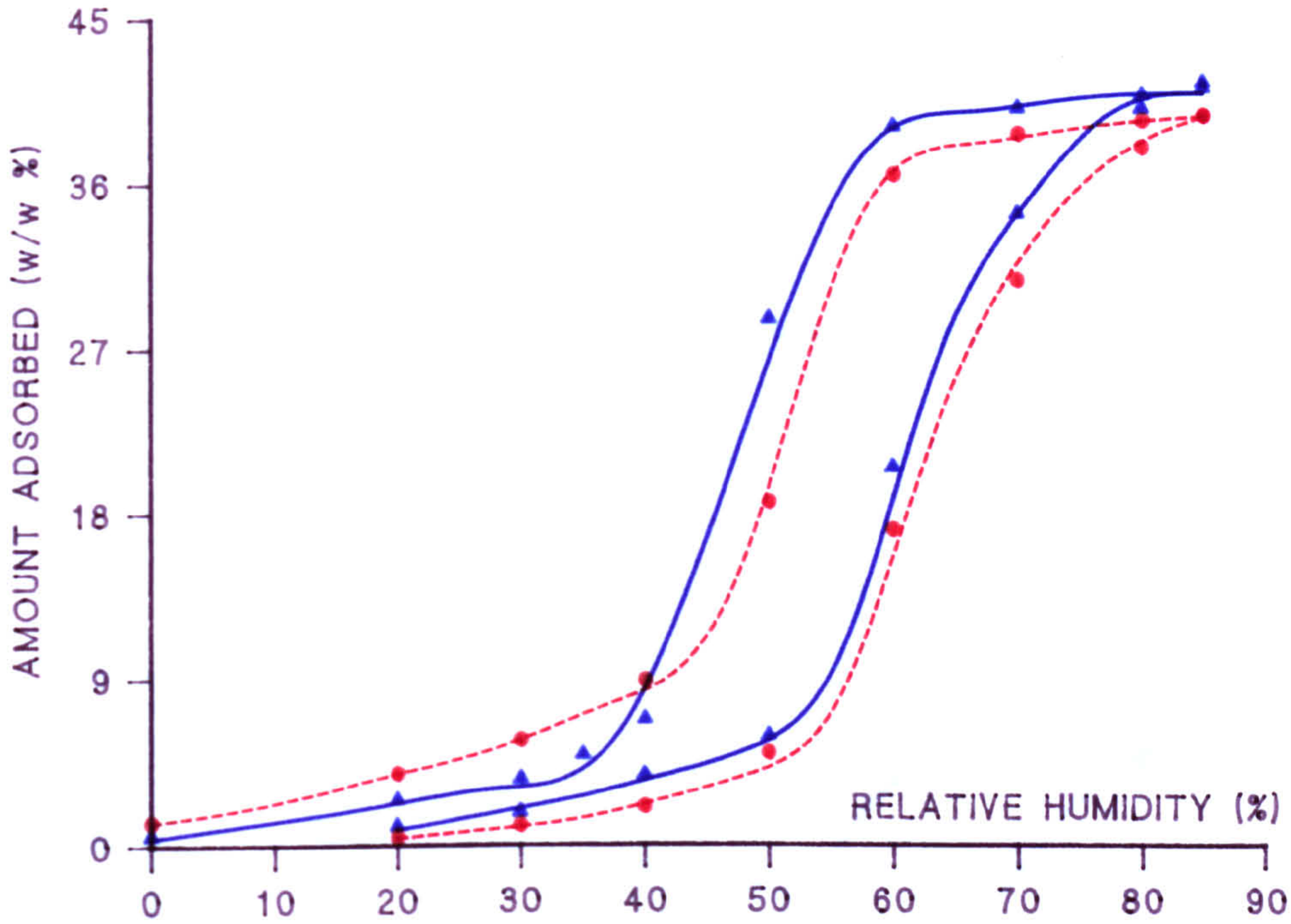

FIGURE 8.7 WATER ADSORPTION

▲ SCII PHOSGENE ● SCII PHOSGENE (SECOND ISOTHERM)

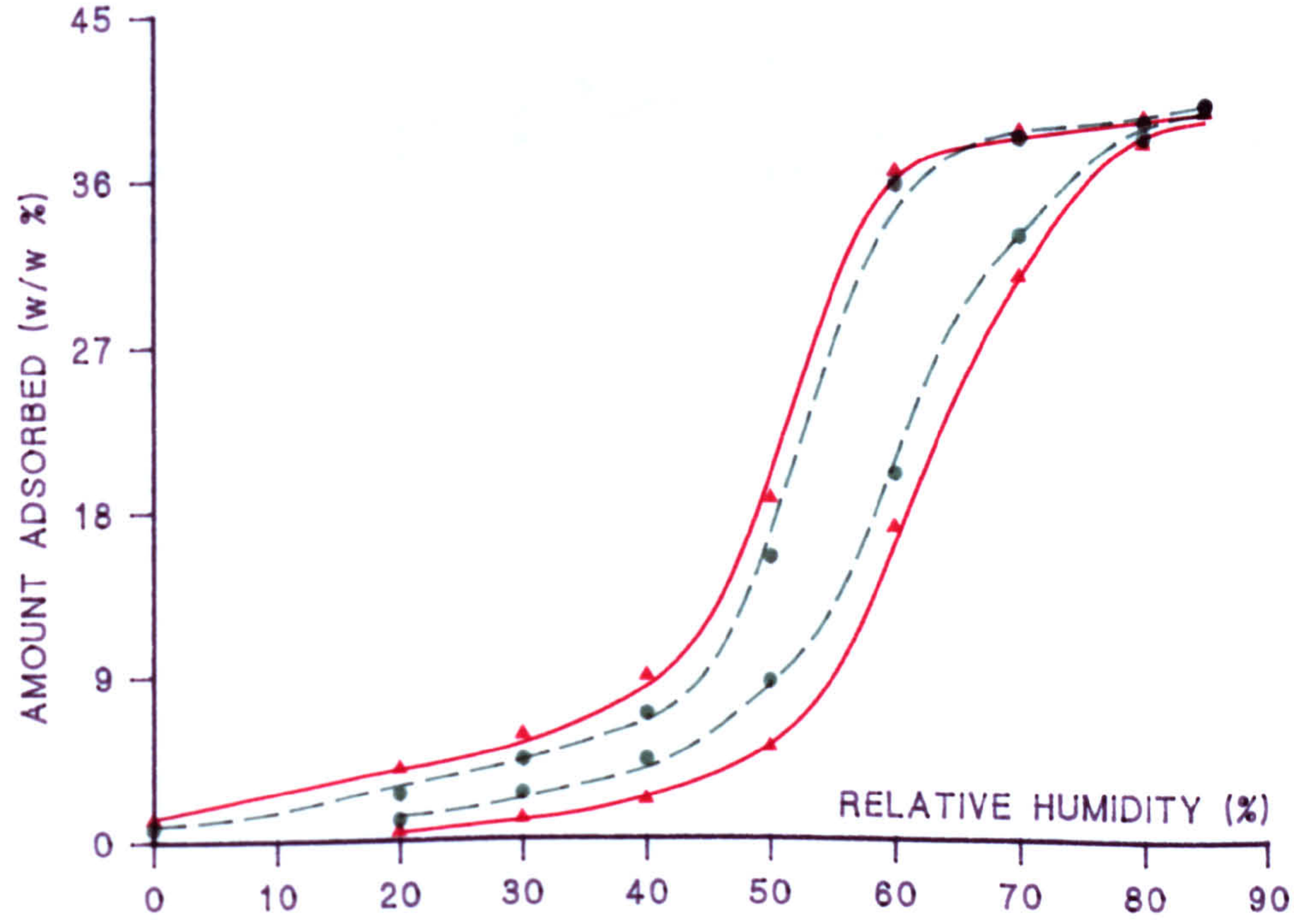

FIGURE 8.8 WATER ADSORPTION

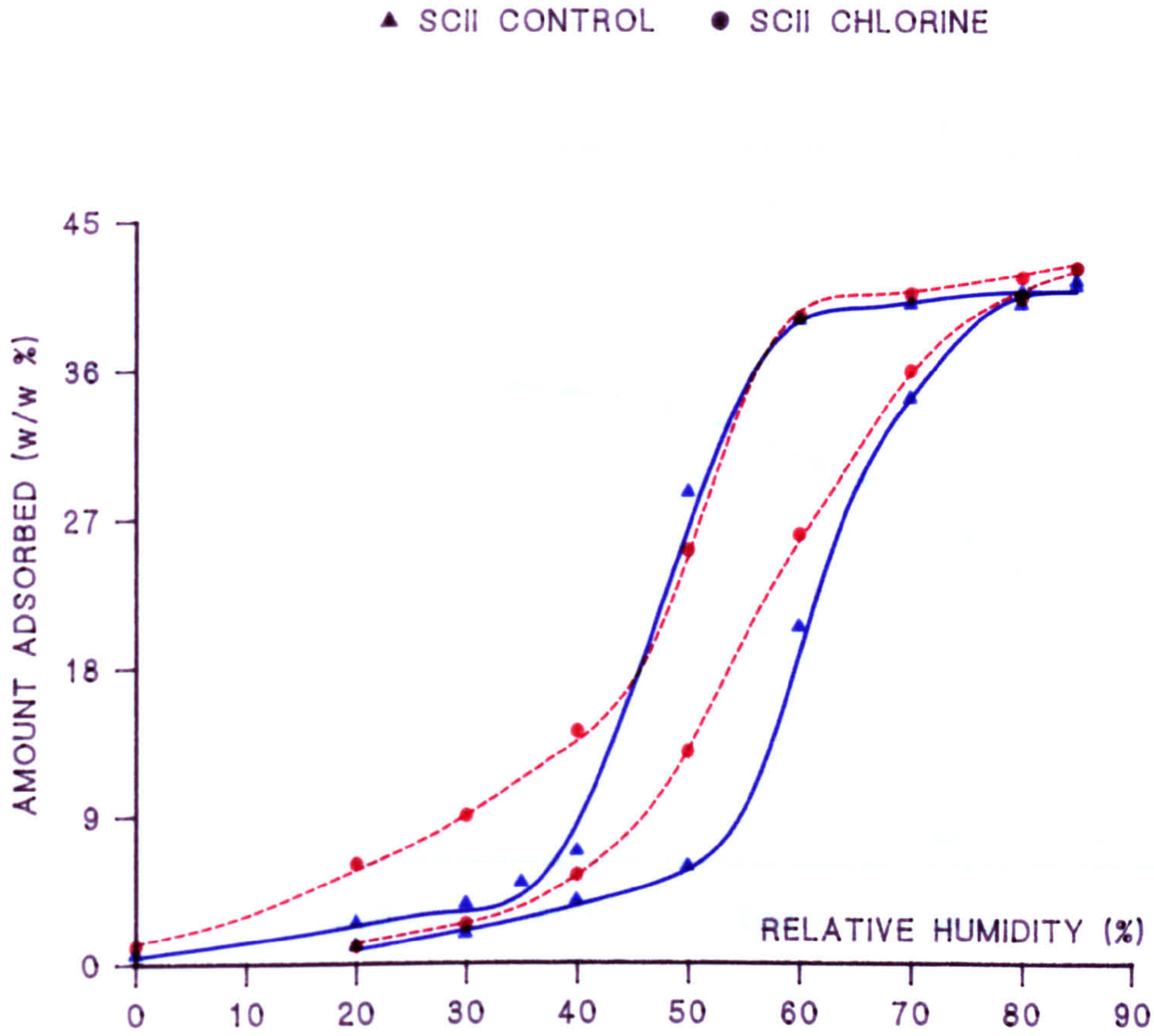

FIGURES 8.9 – 8.11 THERMAL ANALYSIS FOR SCII CARBONS
FIRST: ■ PHOSGENE ● PHOSGENE/WATER
SECOND: ■ CHLORINE ● CHLORINE/WATER
THIRD: ▲ CONTROL ■ PHOSGENE/WATER ● CHLORINE/WATER

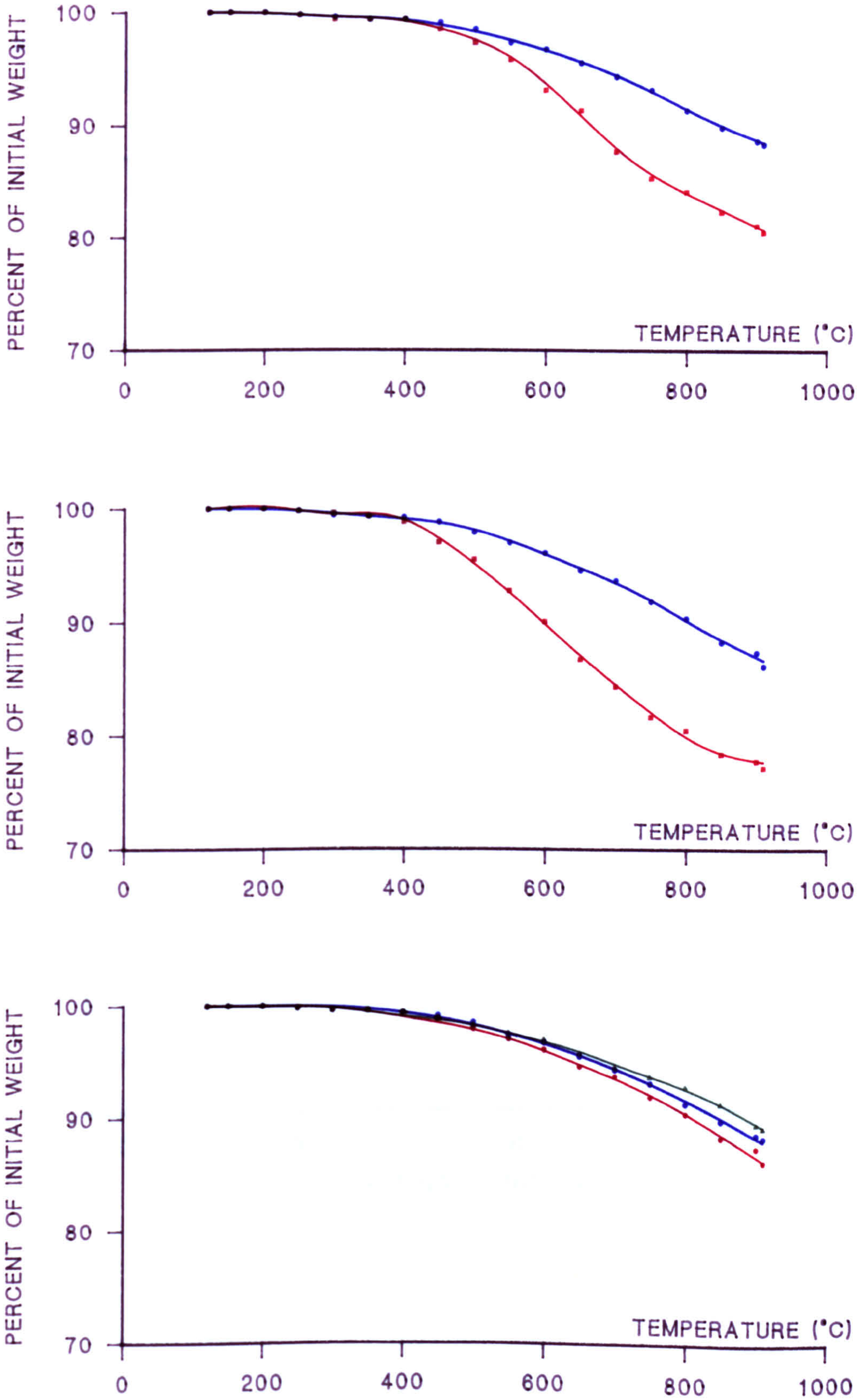

FIGURE 8.12A NARROW SCAN C (1S) XPS SPECTRUM FOR CONTROL BPL CARBON (BLUE) PHOSGENE MODIFIED: (RED) PHOSGENE MODIFIED, METHANOL TREATED

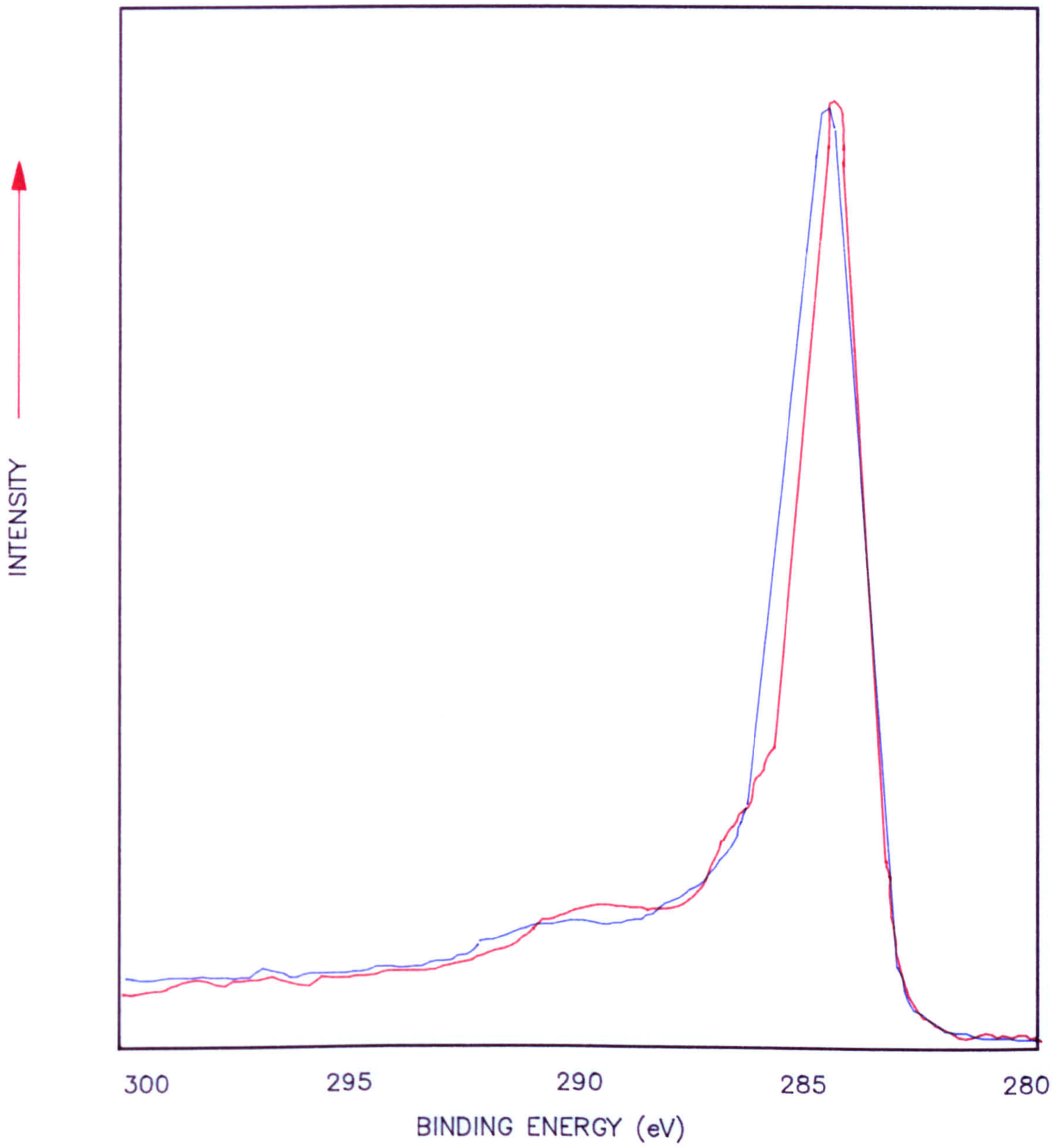

FIGURE 8.12B NARROW SCAN O (1S) XPS SPECTRUM FOR CONTROL BPL CARBON
(BLUE) PHOSGENE MODIFIED: (RED) PHOSGENE MODIFIED, METHANOL TREATED

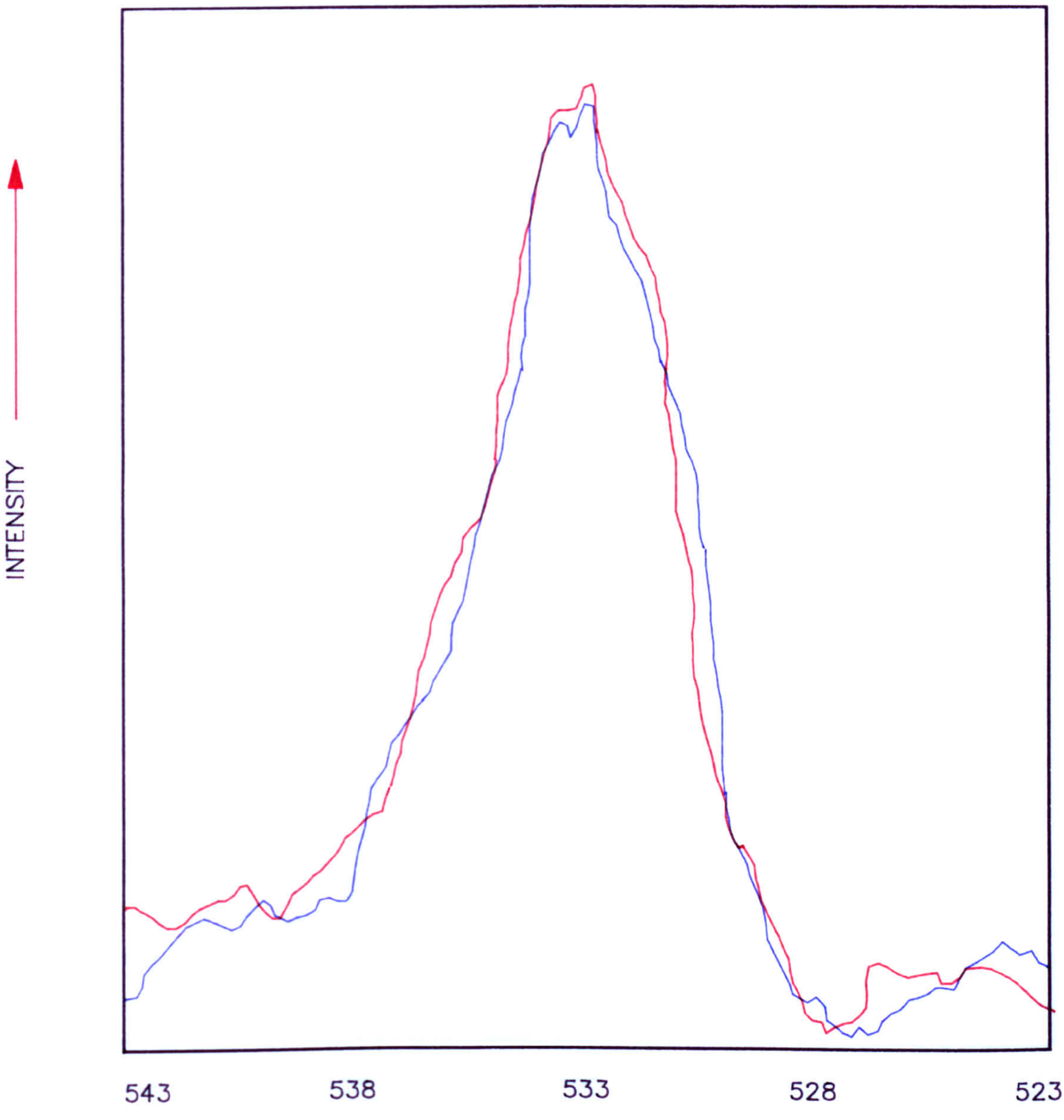

FIGURE 8.12C NARROW SCAN Cl (2P) XPS SPECTRUM FOR CONTROL BPL CARBON (BLUE) PHOSGENE MODIFIED: (RED) PHOSGENE MODIFIED, METHANOL TREATED

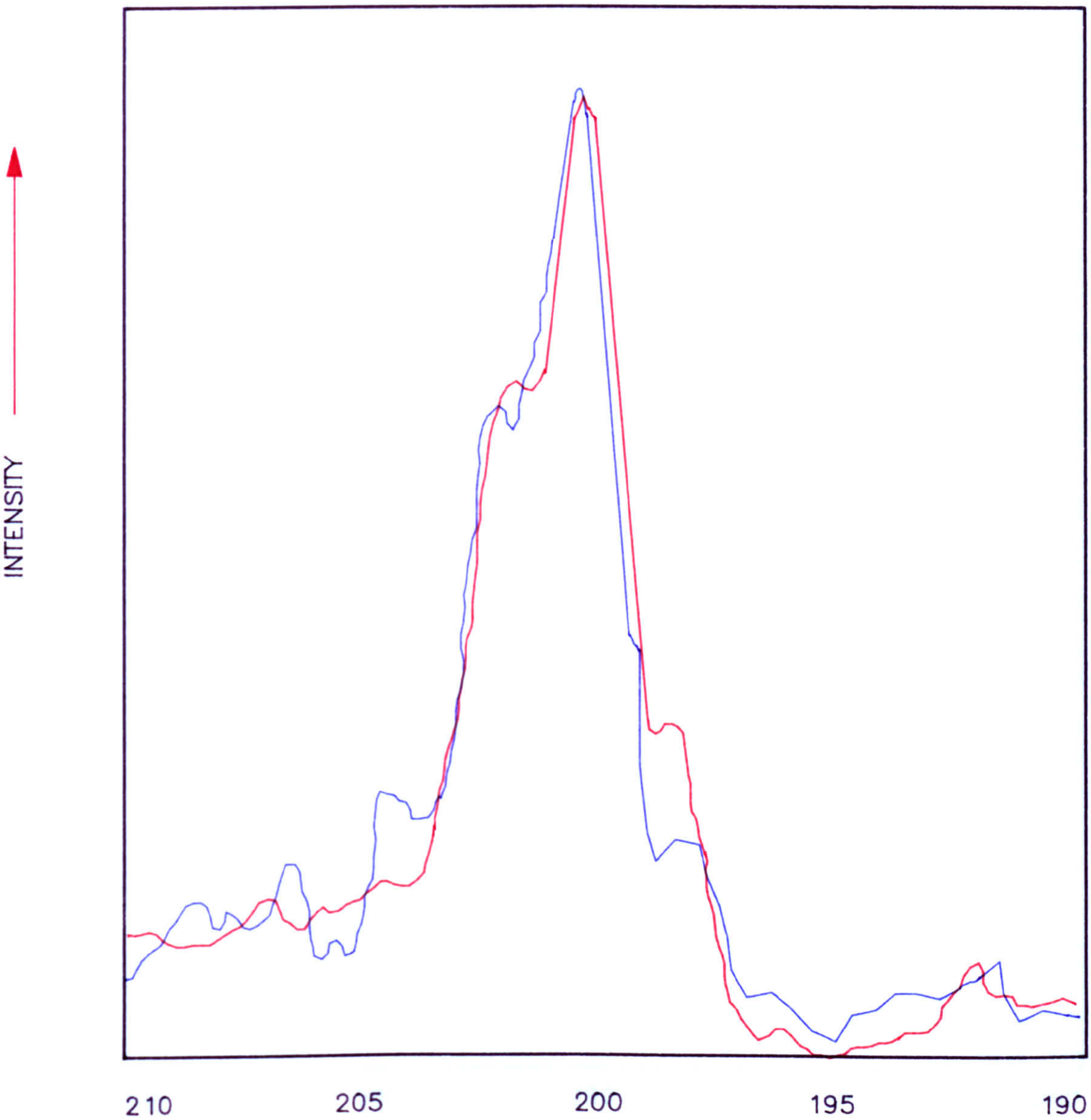

FIGURE 8.12D NARROW SCAN C (1S) XPS SPECTRUM FOR CONTROL SCII CARBON PHOSGENE MODIFIED, METHANOL TREATED

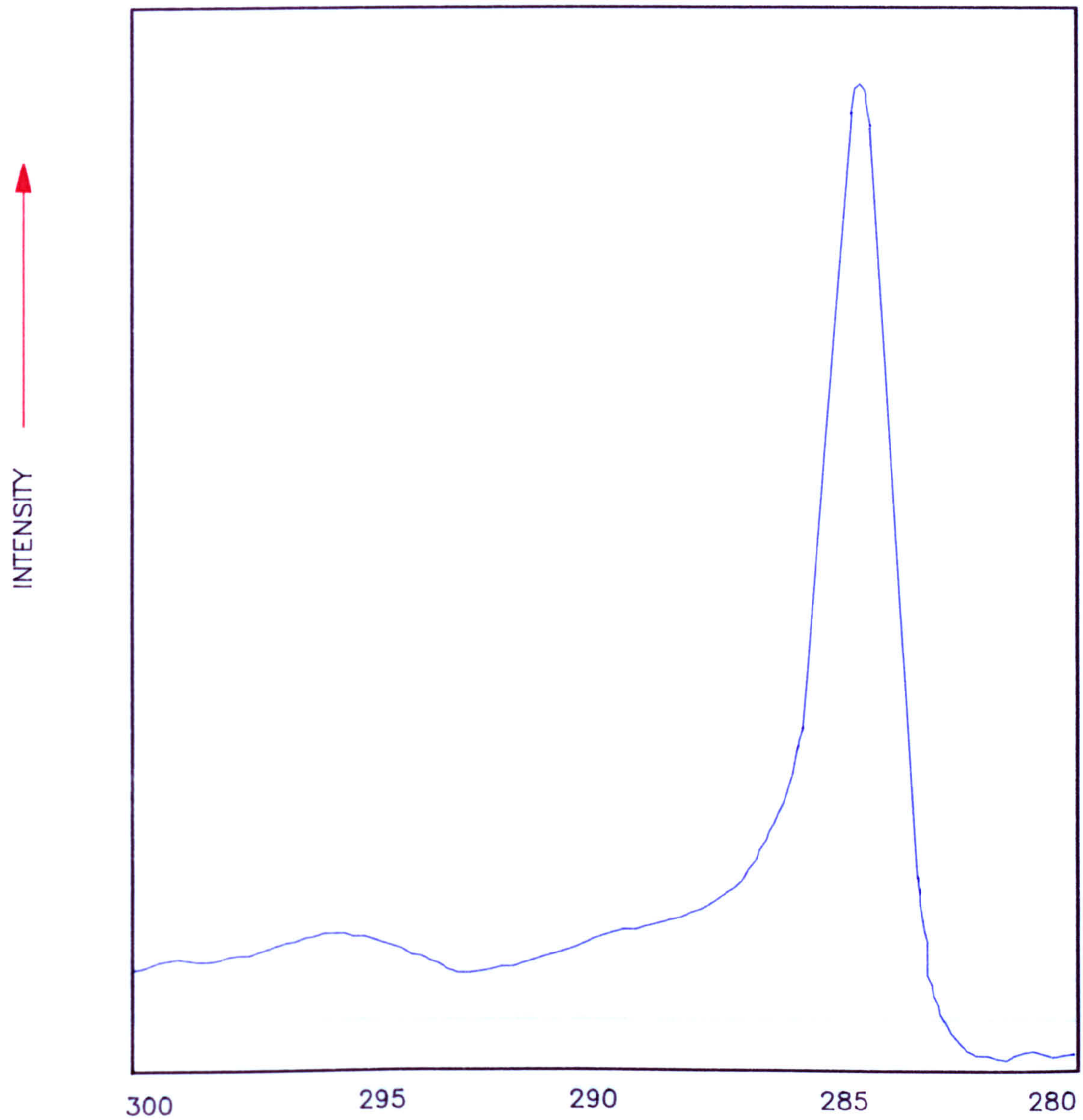

FIGURE 8.12E NARROW SCAN O (1S) XPS SPECTRUM FOR CONTROL SCII CARBON PHOSGENE MODIFIED: (BLUE) WATER TREATED; (RED) METHANOL TREATED

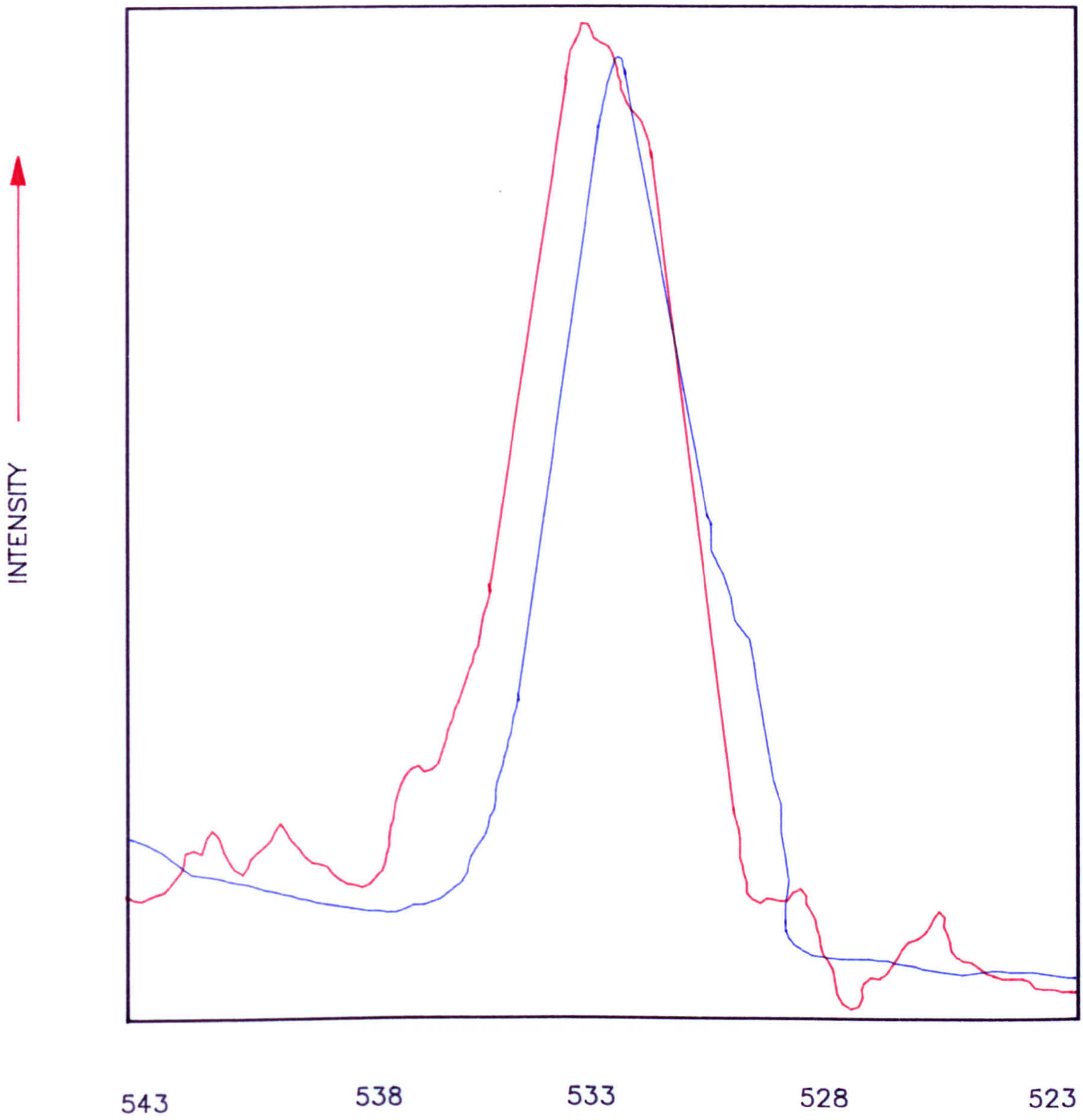

FIGURE 8.12F NARROW SCAN Cl (2P) XPS SPECTRUM FOR CONTROL SCII CARBON PHOSGENE MODIFIED: (BLUE) WATER TREATED; (RED) METHANOL TREATED

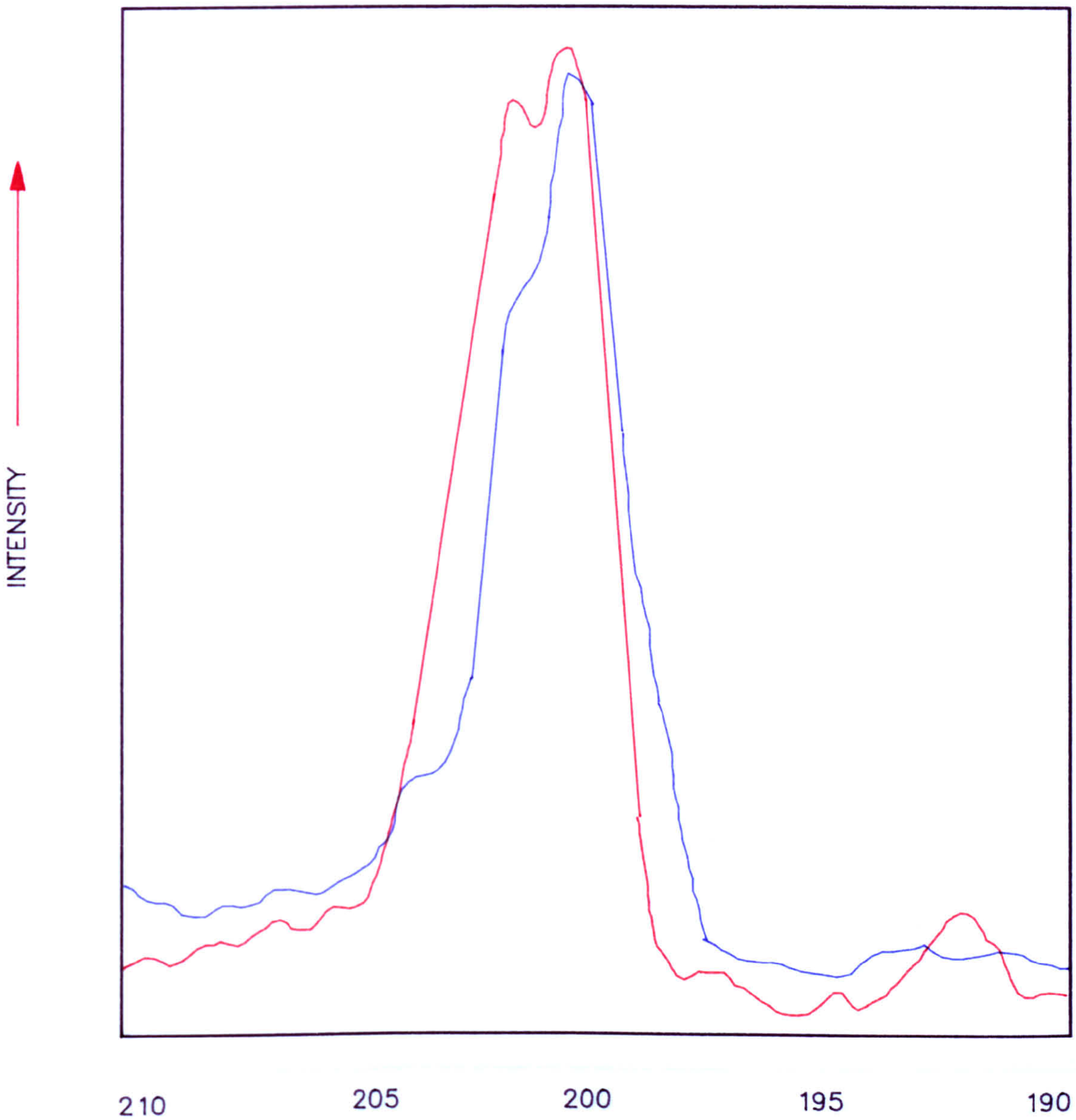

FIGURE 8.12G NARROW SCAN C (1S) XPS SPECTRUM FOR CONTROL SCII CARBON (BLUE) CHLORINE MODIFIED, WATER TREATED: (RED) CONTROL

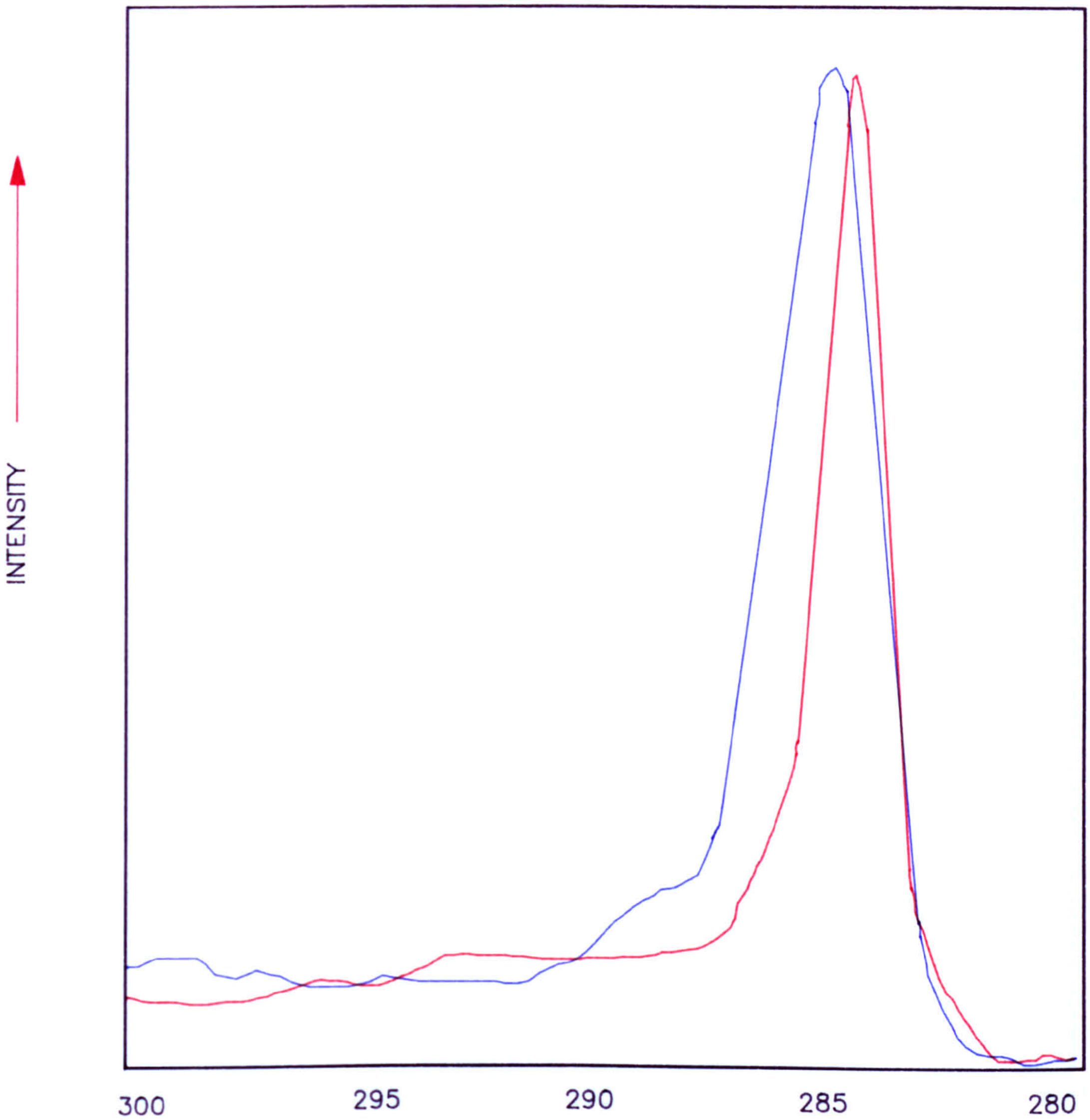

FIGURE 8.12H NARROW SCAN O (1S) XPS SPECTRUM FOR CONTROL SCII CARBON (BLUE) CHLORINE MODIFIED: (RED) CHLORINE MODIFIED, WATER TREATED

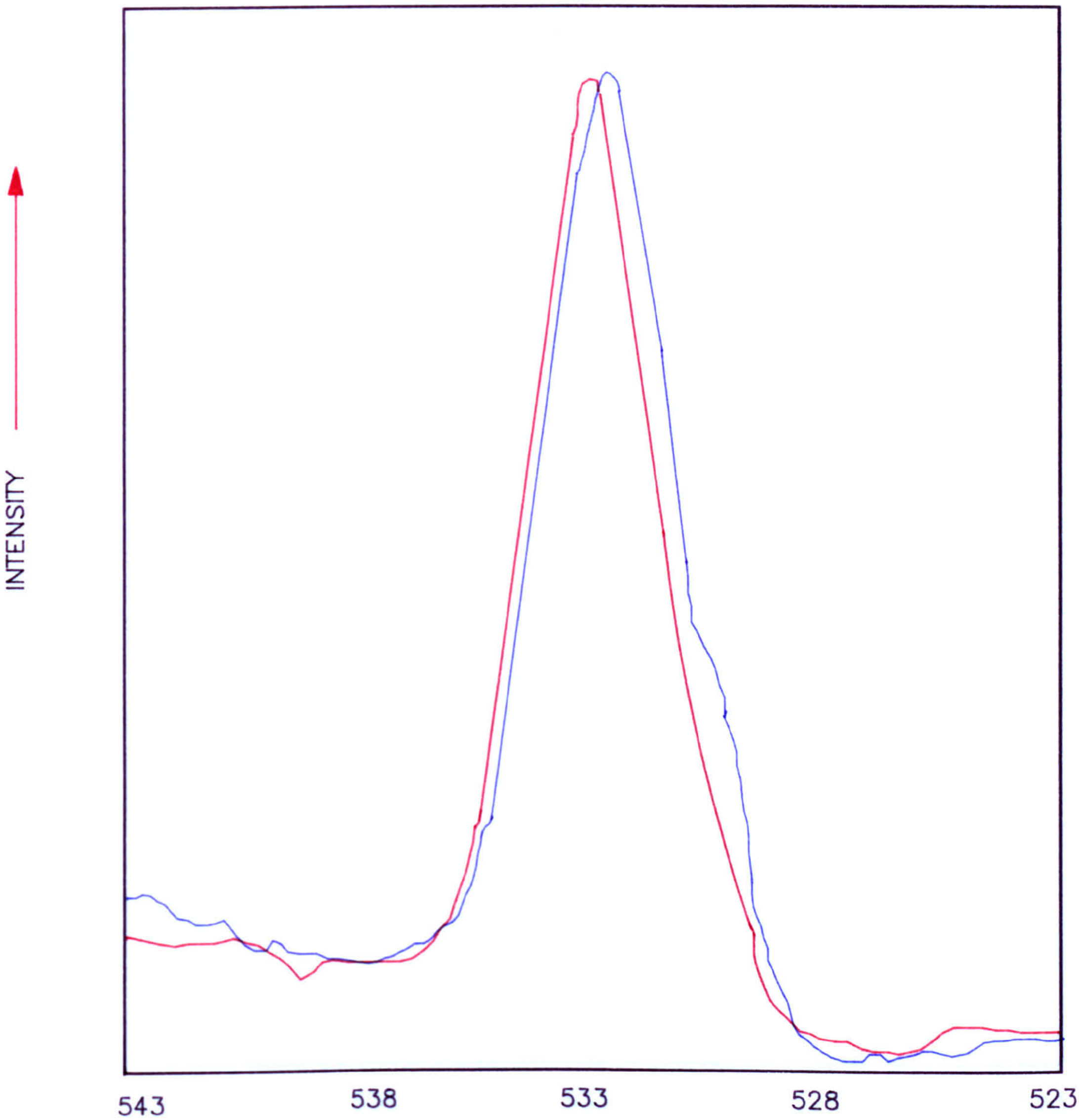

FIGURE 8.12I NARROW SCAN O (1S) XPS SPECTRUM FOR CONTROL SCII CARBON (BLUE) CHLORINE MODIFIED, WATER TREATED: (RED) CONTROL

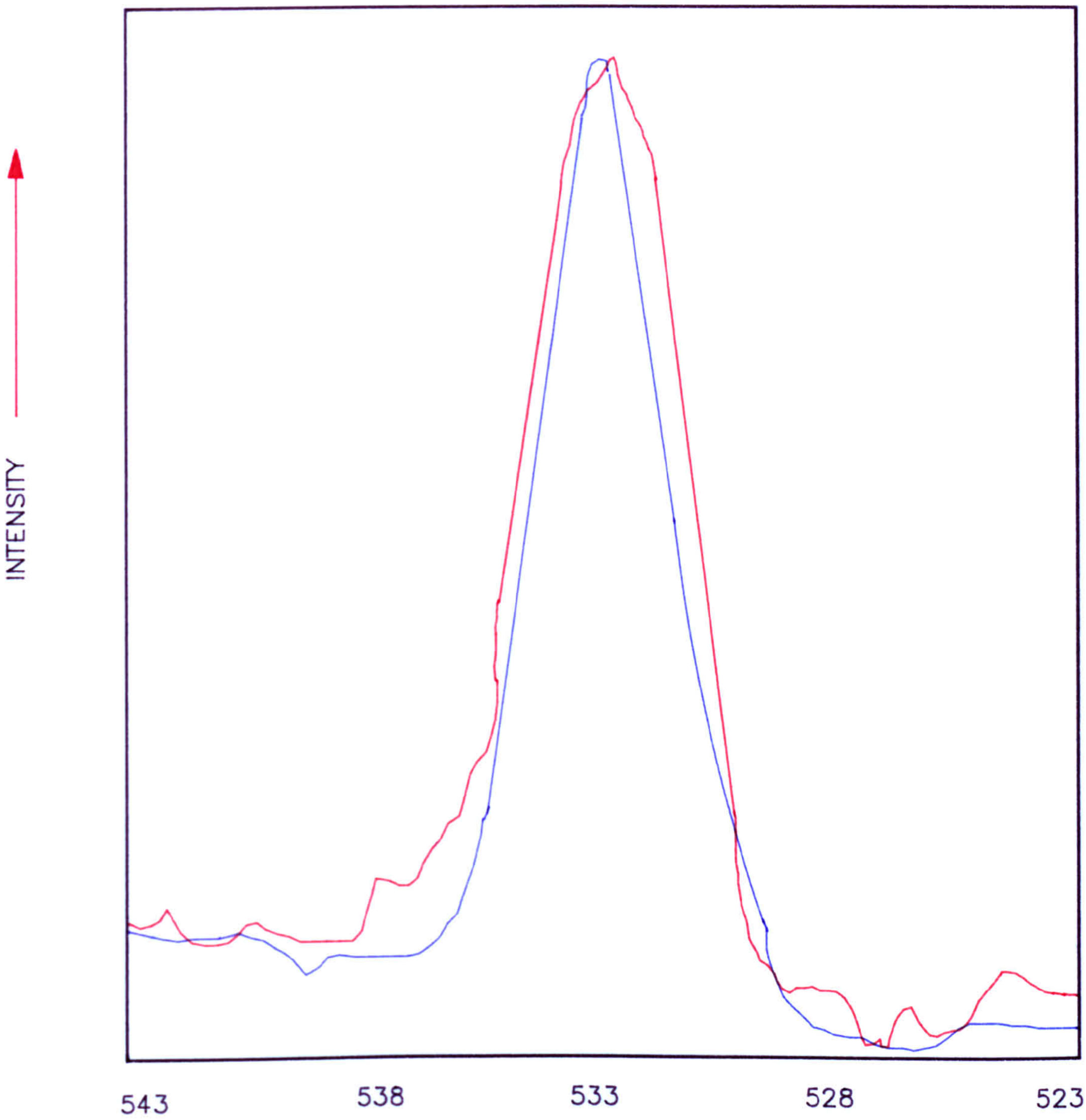

FIGURE 8.12J NARROW SCAN Cl (2P) XPS SPECTRUM FOR CONTROL SCII CARBON (BLUE) CHLORINE MODIFIED: (RED) CHLORINE MODIFIED, WATER TREATED

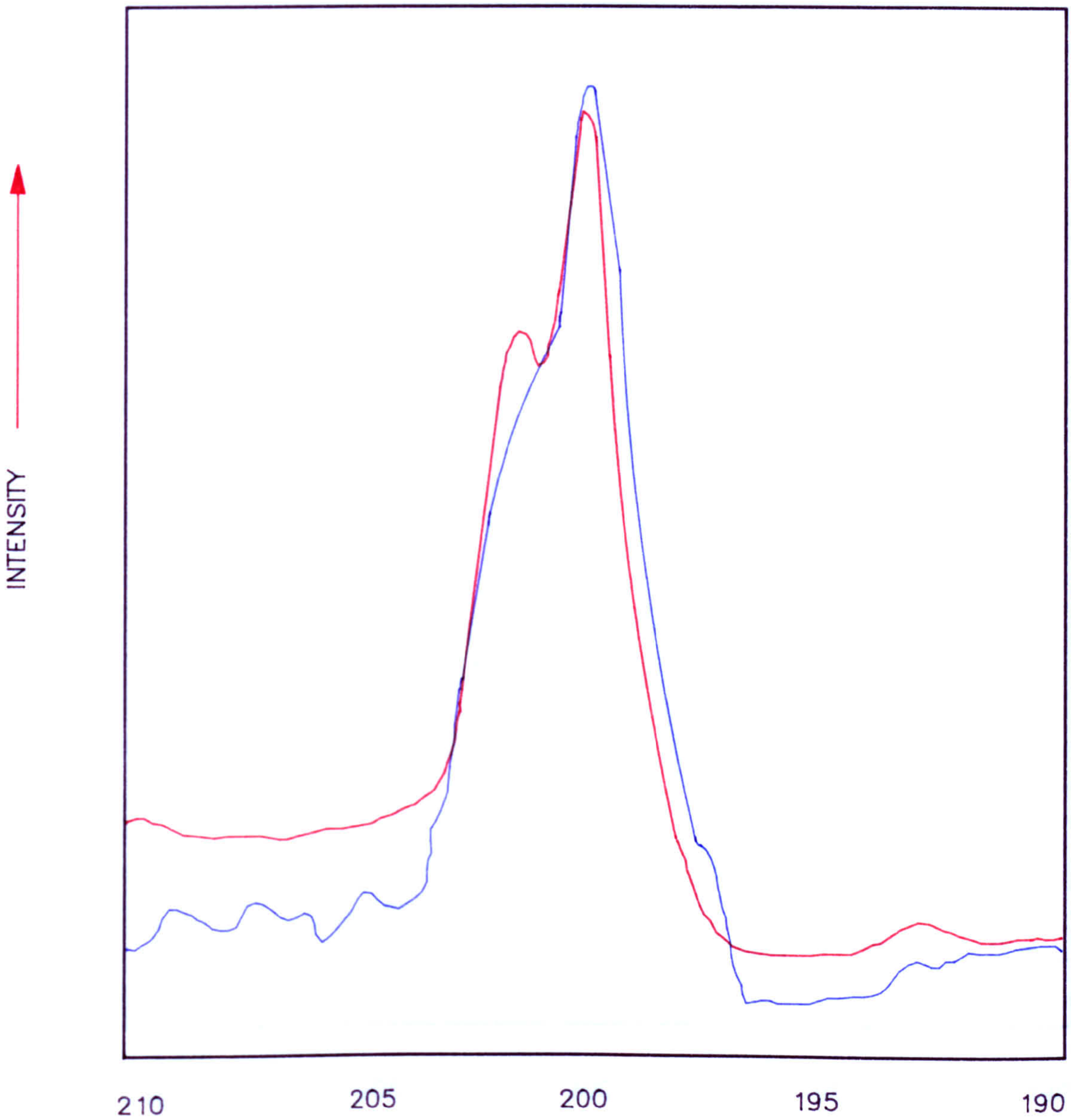

FIGURE 8.12K NARROW SCAN Cl (2P) XPS SPECTRUM FOR CONTROL SCII CARBON
(BLUE) PHOSGENE MODIFIED, WATER TREATED
(RED) CHLORINE MODIFIED, WATER TREATED

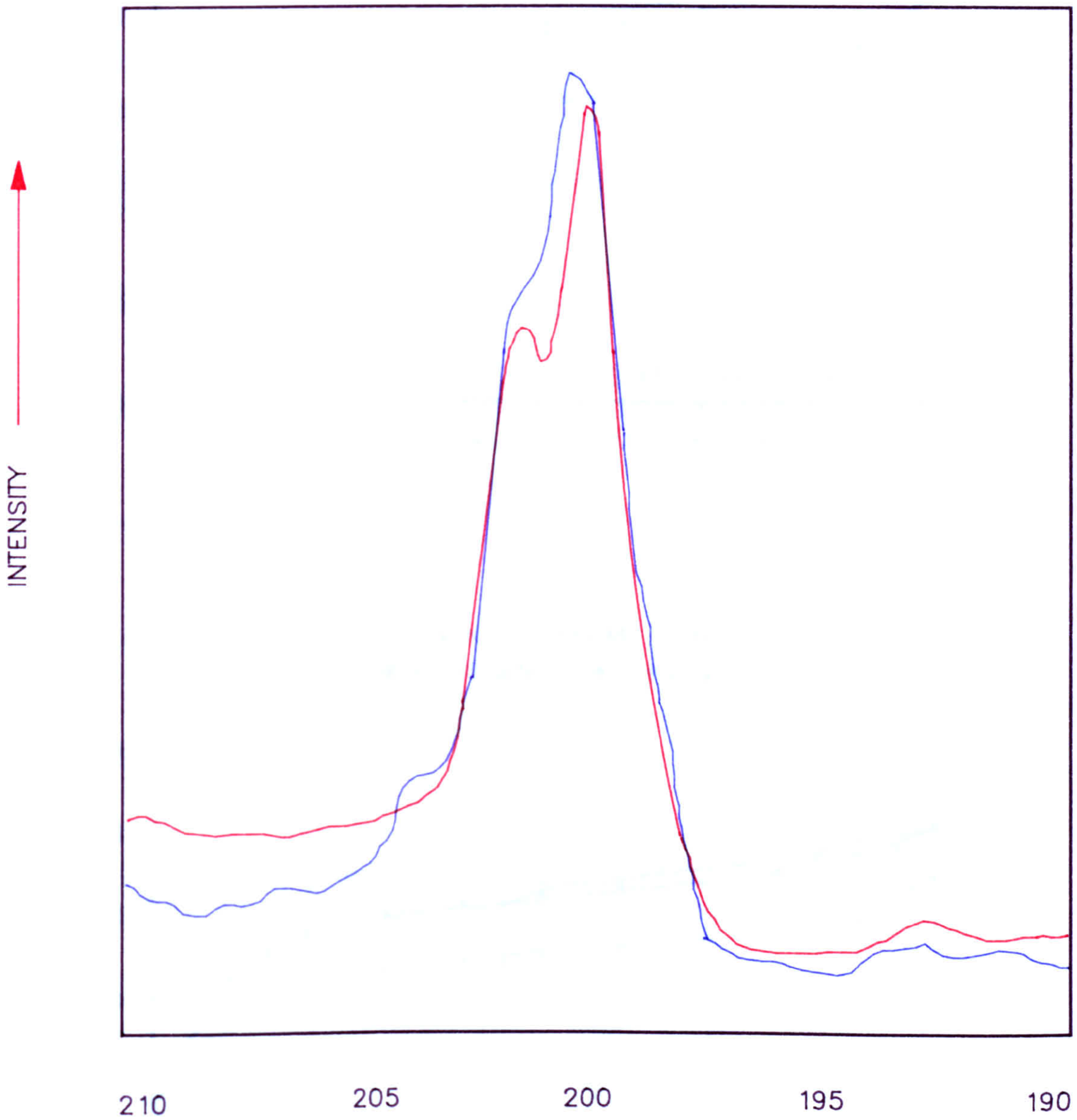

FIGURE 8.13 NITROGEN ISOTHERMS FOR BPL CARBON

● CONTROL ■ PHOSGENE ▲ PHOSGENE/METHANOL

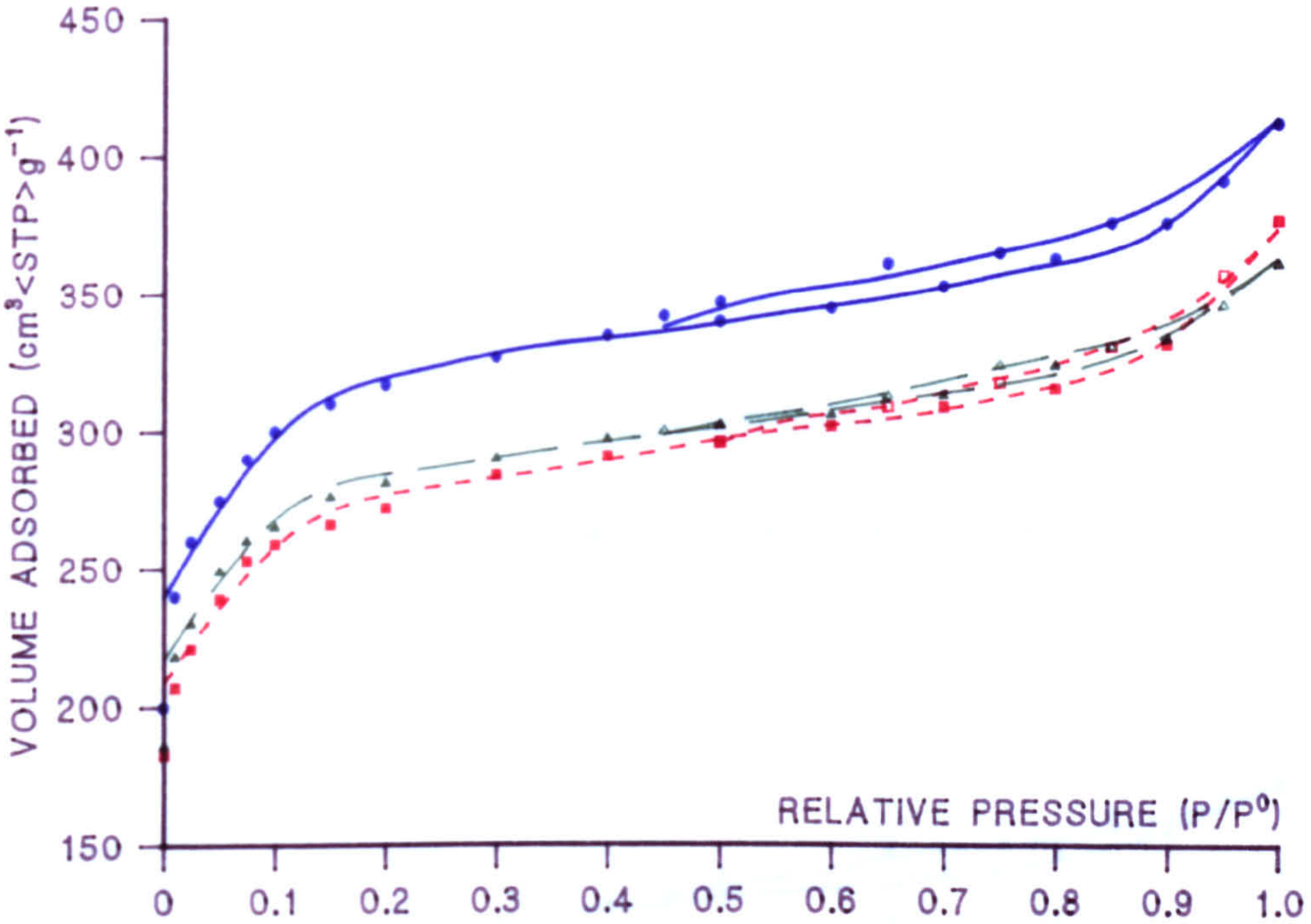

FIGURE 8.14 NITROGEN ISOTHERMS FOR CECA CARBONS

● CONTROL ■ PHOSGENE ▲ PHOSGENE/METHANOL

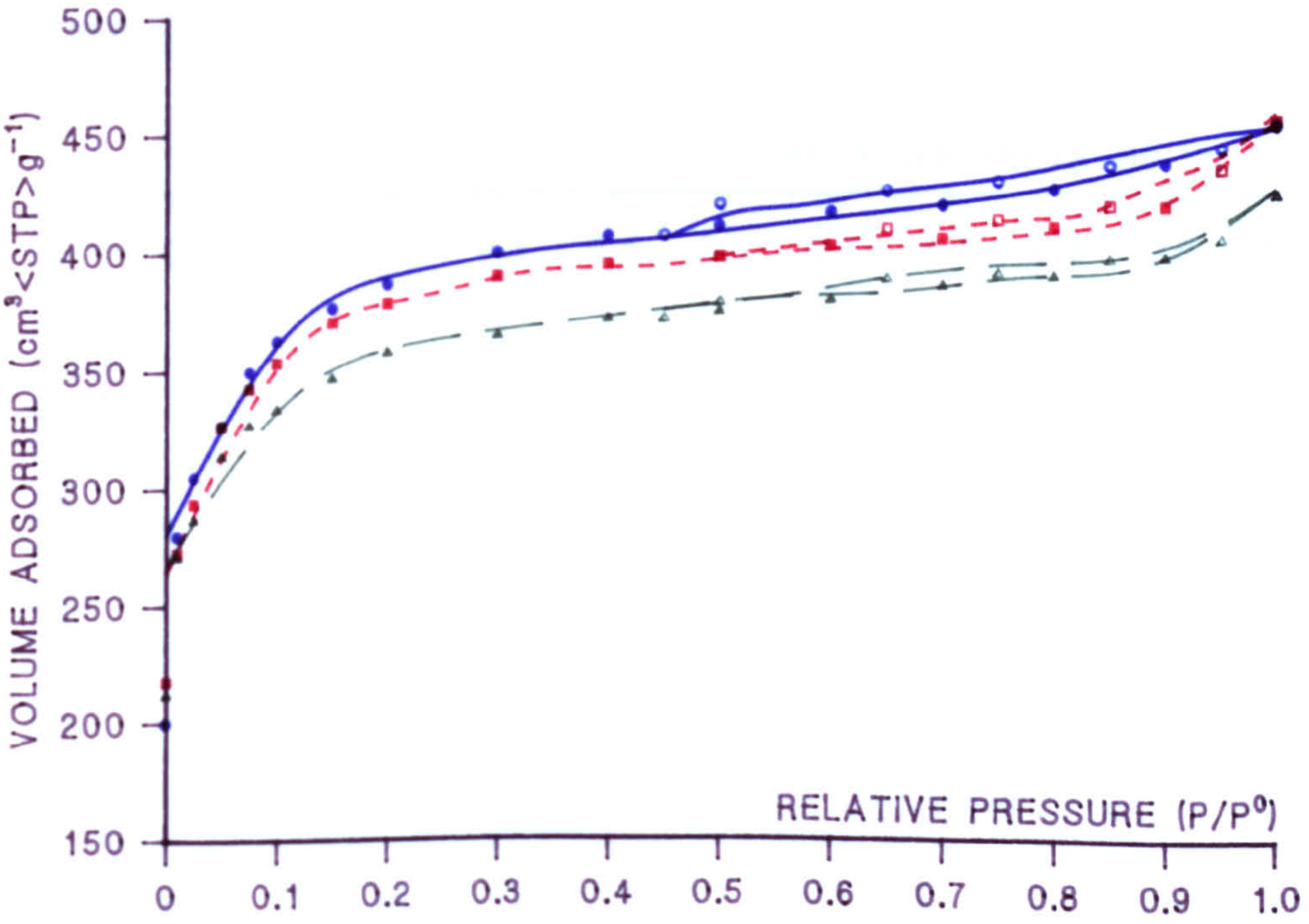

FIGURE 8.15 NITROGEN ISOTHERMS FOR SCII CARBON

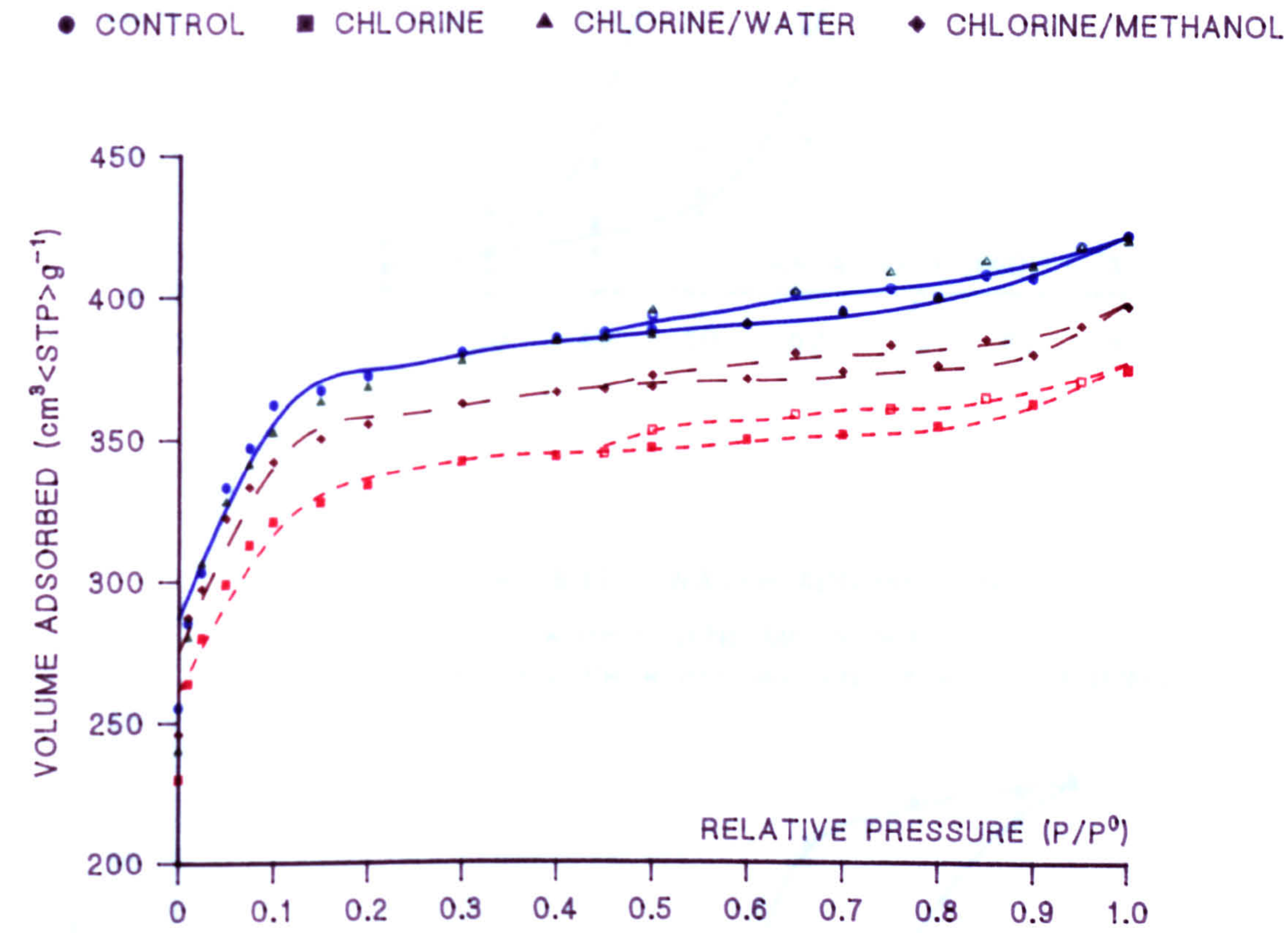

FIGURE 8.16 WATER ADSORPTION

▲ CECA CONTROL PHOSGENE/METHANOL ● FIRST AND ▬ SECOND ISOTHERMS

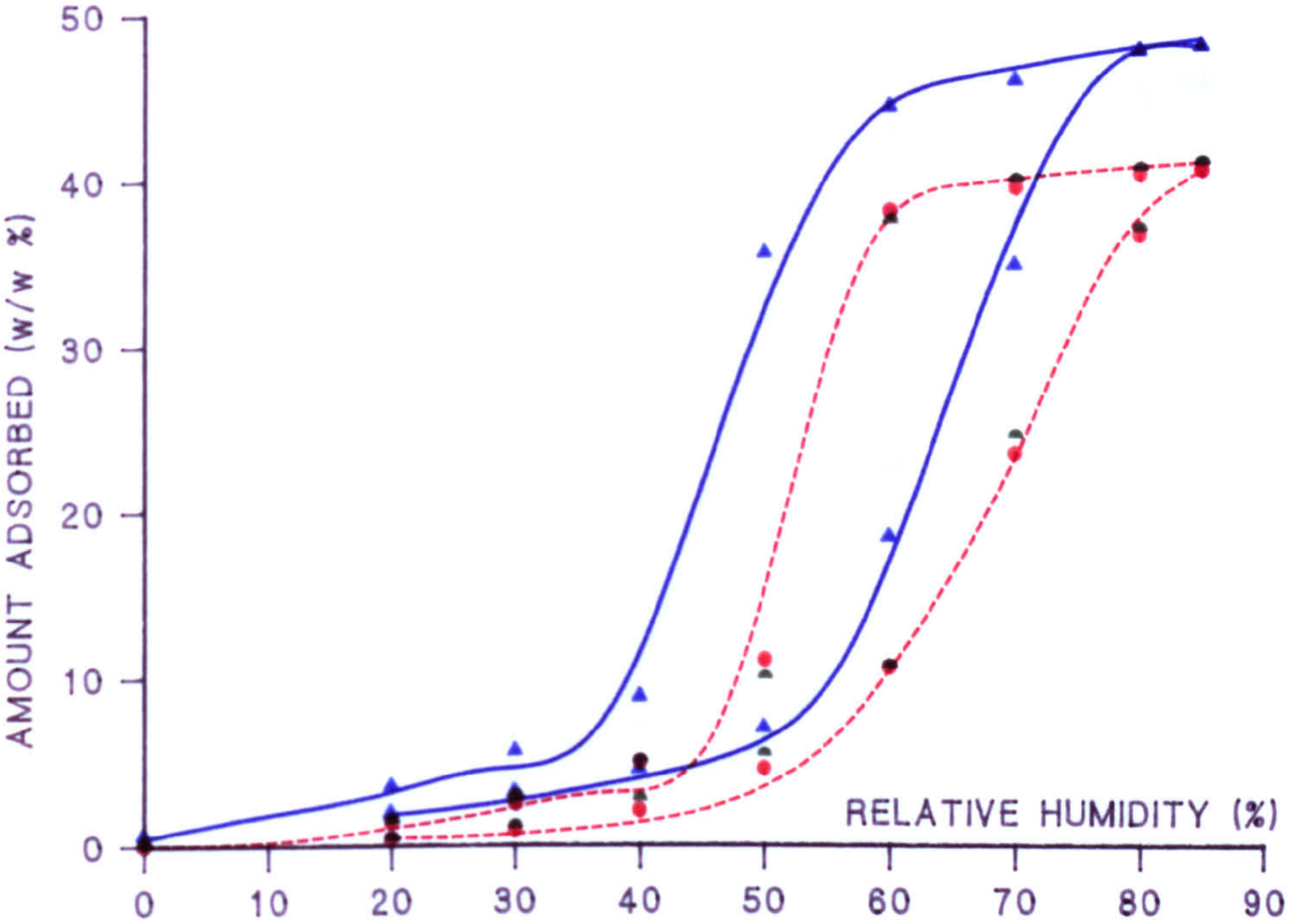

FIGURE 8.17 WATER ADSORPTION

SCII ▲ PHOSGENE/METHANOL

SCII PHOSGENE/WATER ● BEFORE AND ▬ AFTER AGEING

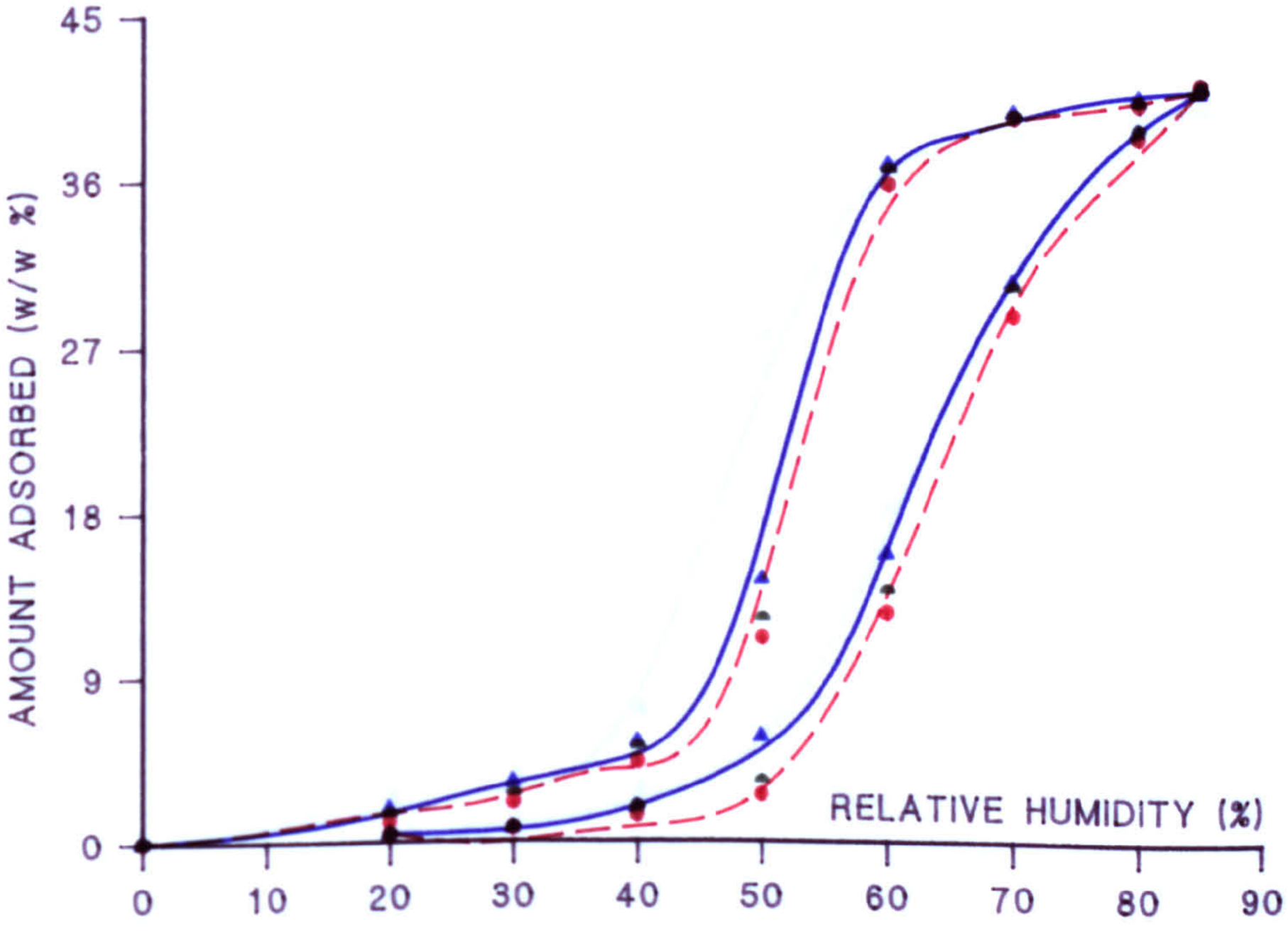

FIGURE 8.18 WATER ADSORPTION

▲ SCII CONTROL ● SCII AGED CONTROL

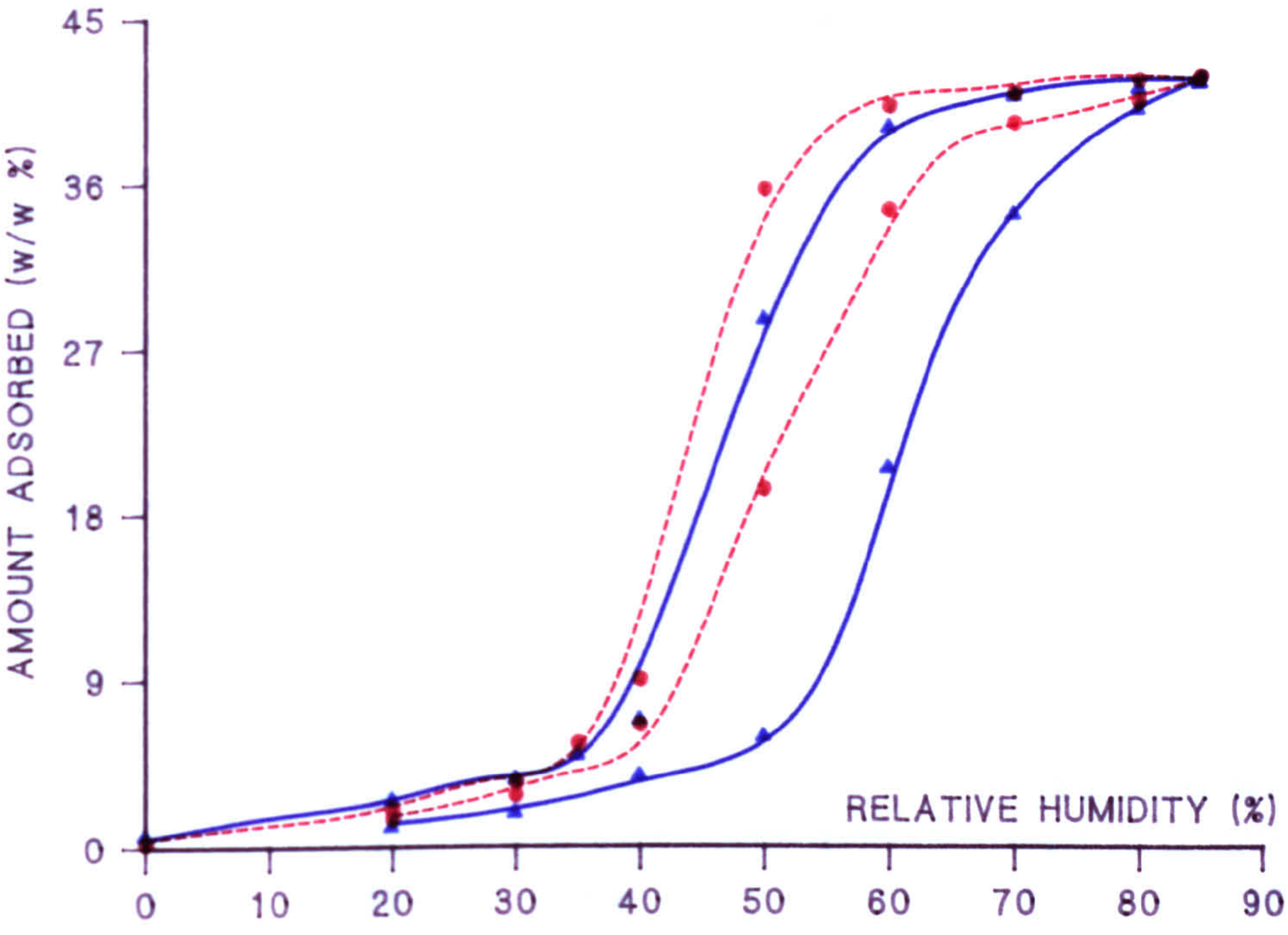

FIGURE 8.19 WATER ADSORPTION

▲ BPL CONTROL ● BPL CHLORINE/WATER

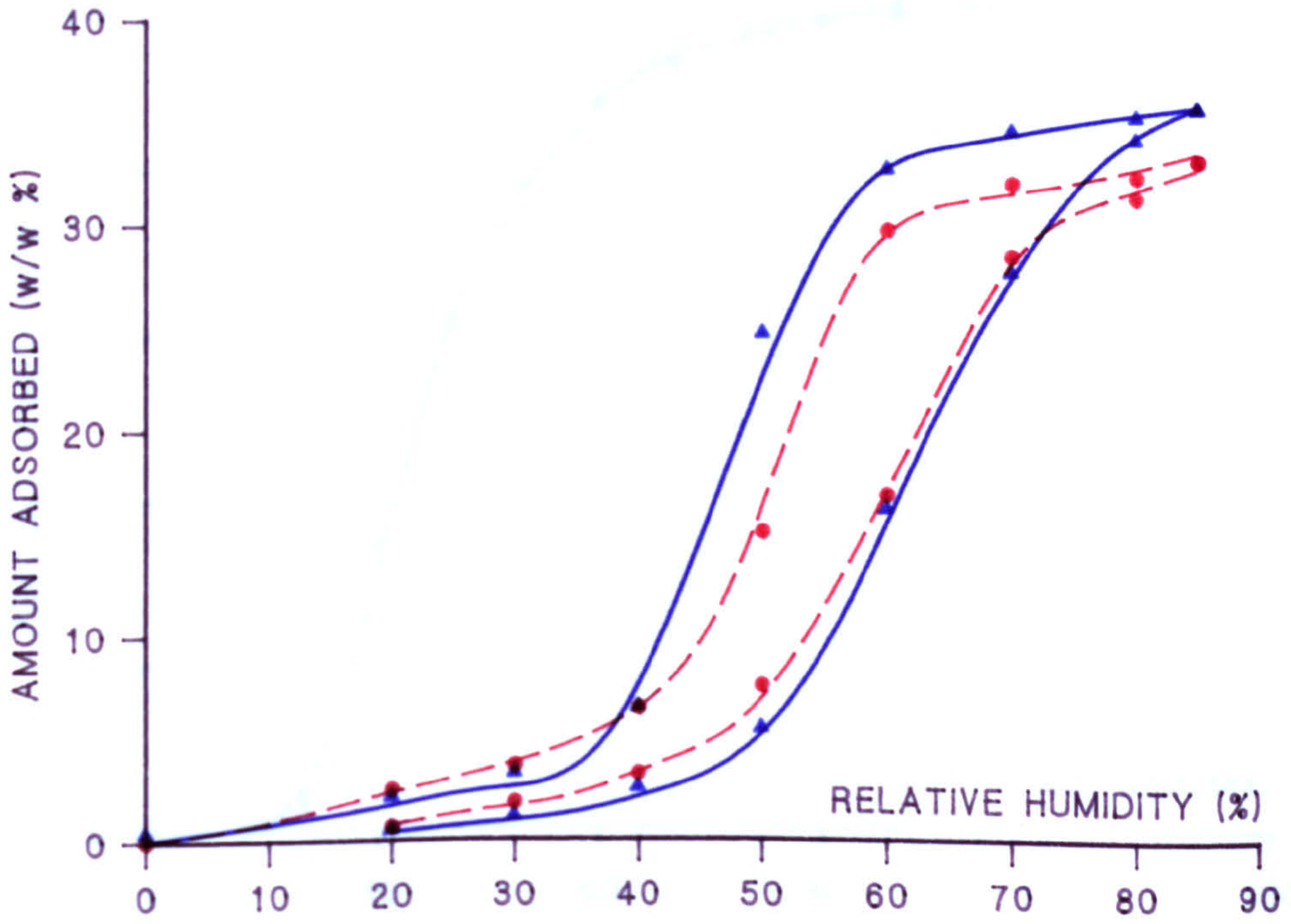

FIGURE 8.20 METHANOL BREAKTHROUGH CURVES

L-R: CECA PHOSGENE/METHANOL CECA PHOSGENE CECA CONTROL

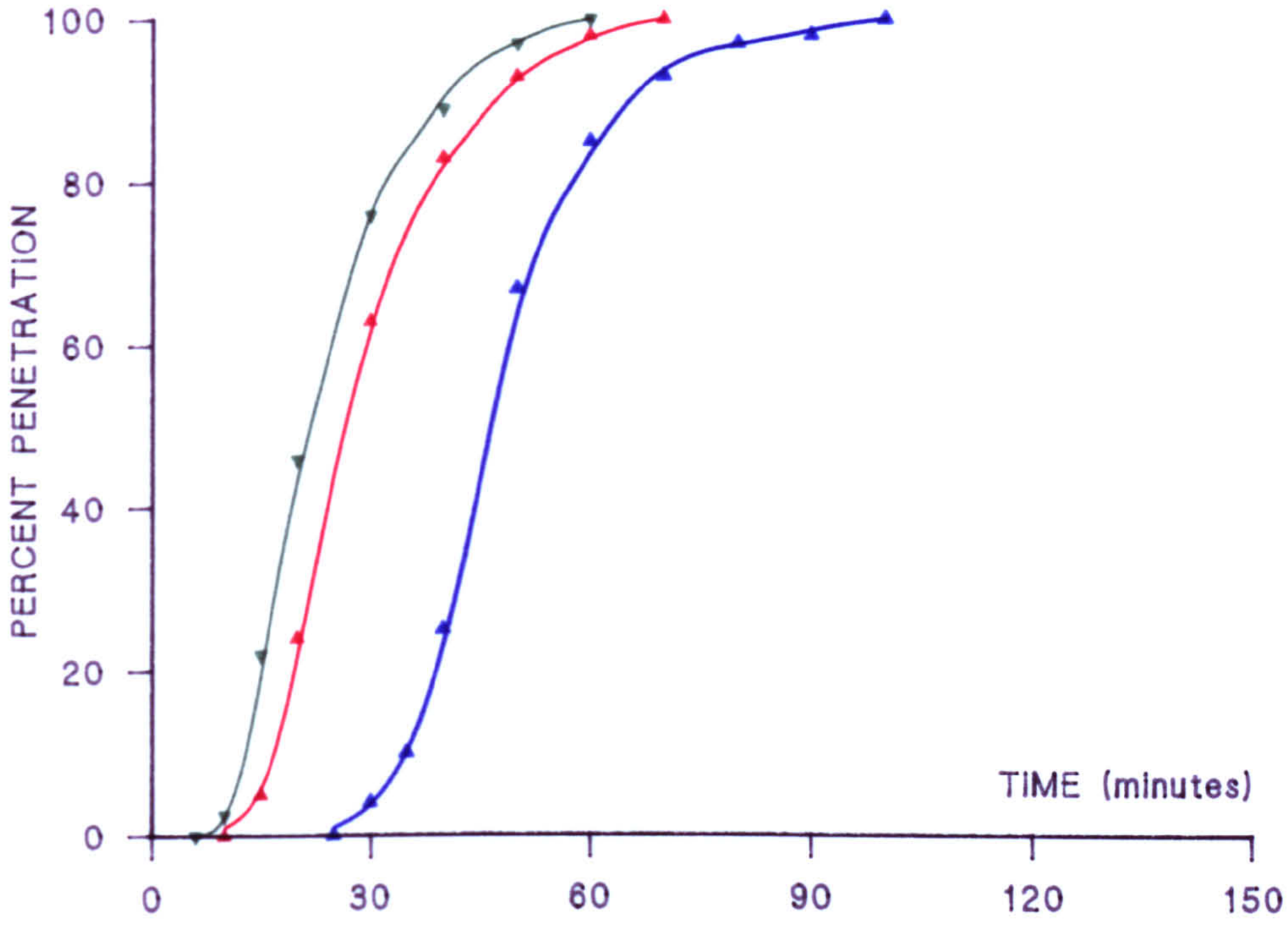

FIGURE 8.21 METHANOL BREAKTHROUGH CURVES

L-R: BPL PHOSGENE/METHANOL BPL CONTROL BPL PHOSGENE

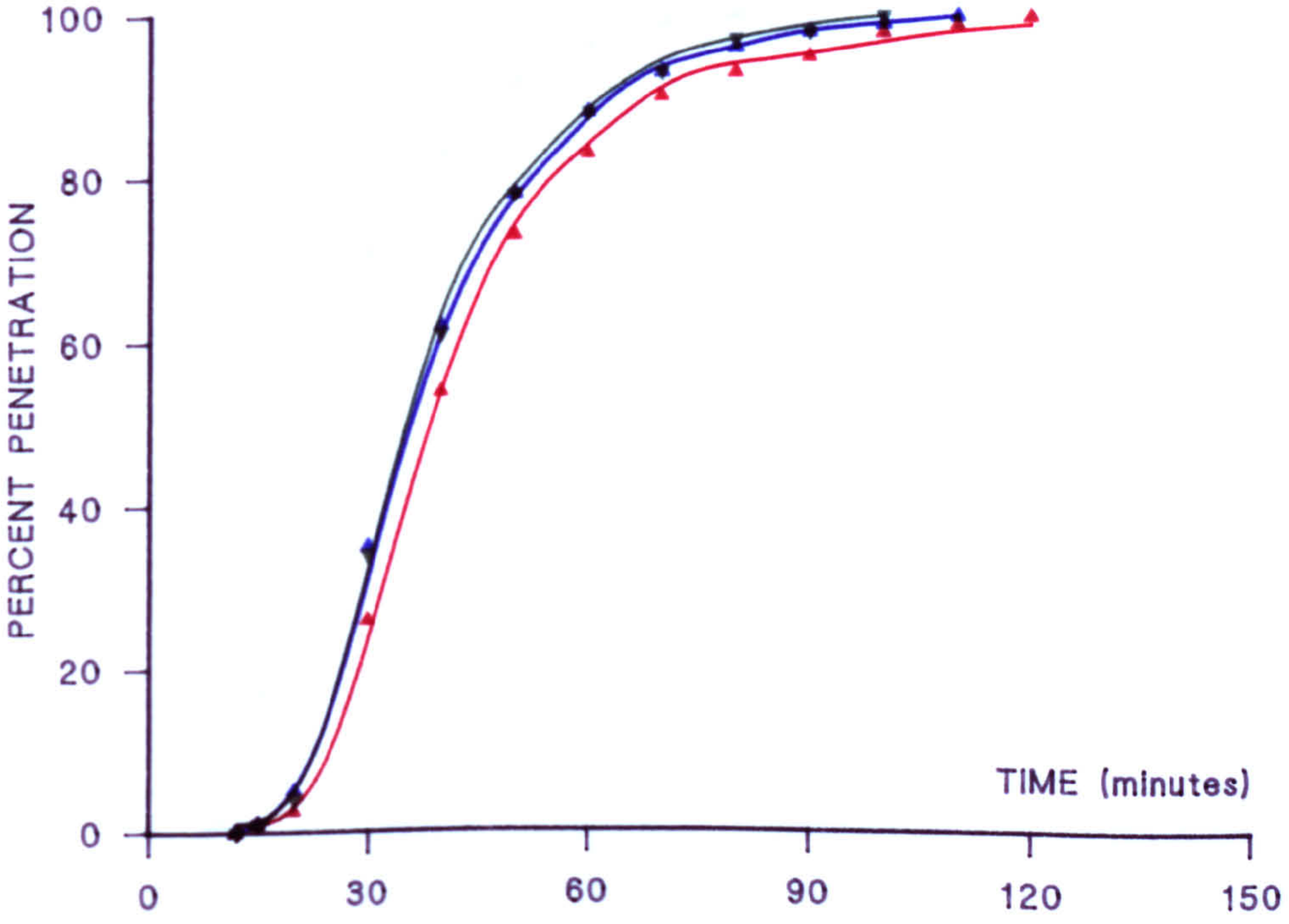

FIGURE 8.22 METHANOL BREAKTHROUGH CURVES

L-R: CECA CONTROL CECA AGED CONTROL

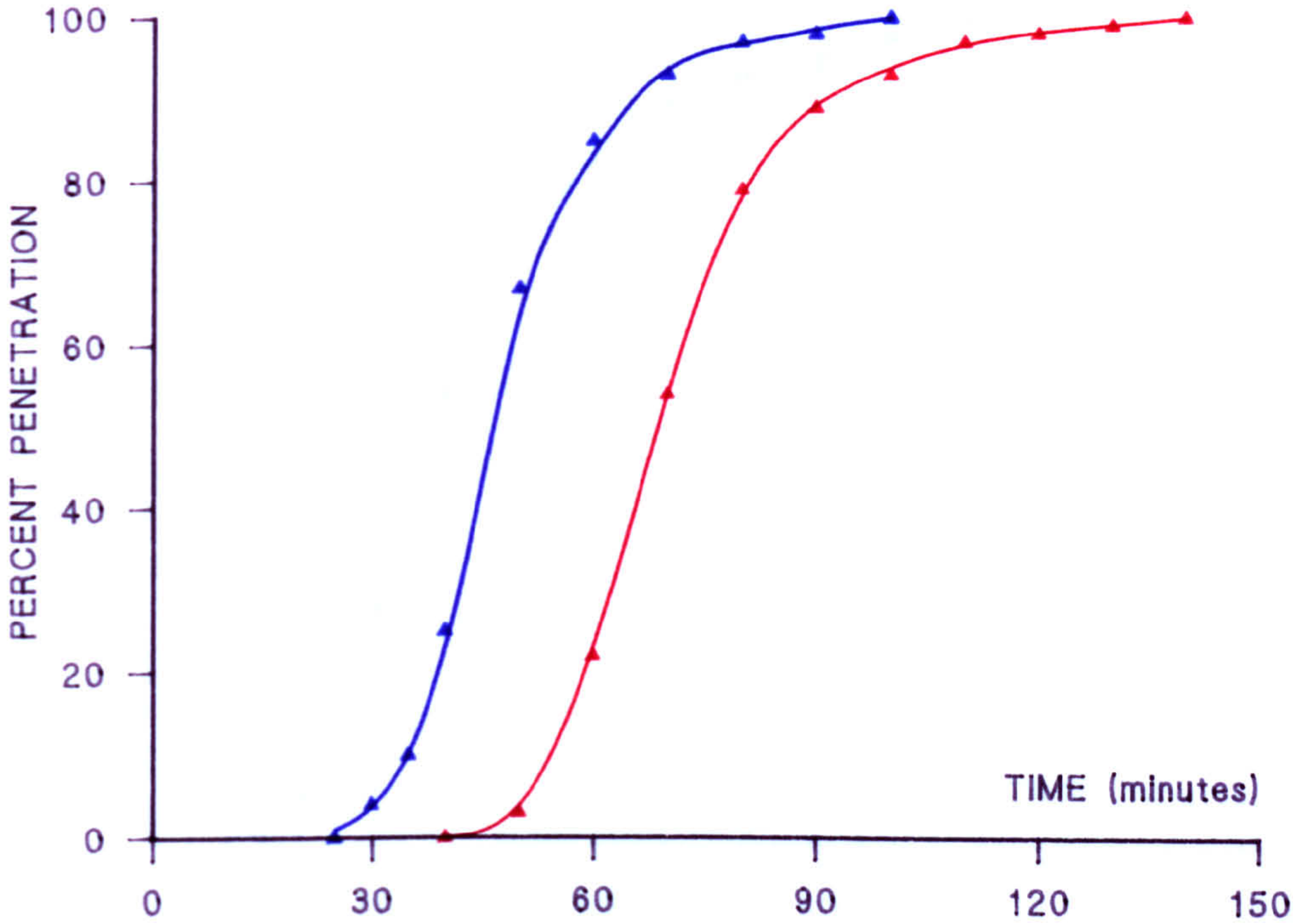

FIGURE 8.23 METHANOL BREAKTHROUGH CURVES

L-R: CECA PHOSGENE/METHANOL CECA PHOSGENE/METHANOL (AGED)

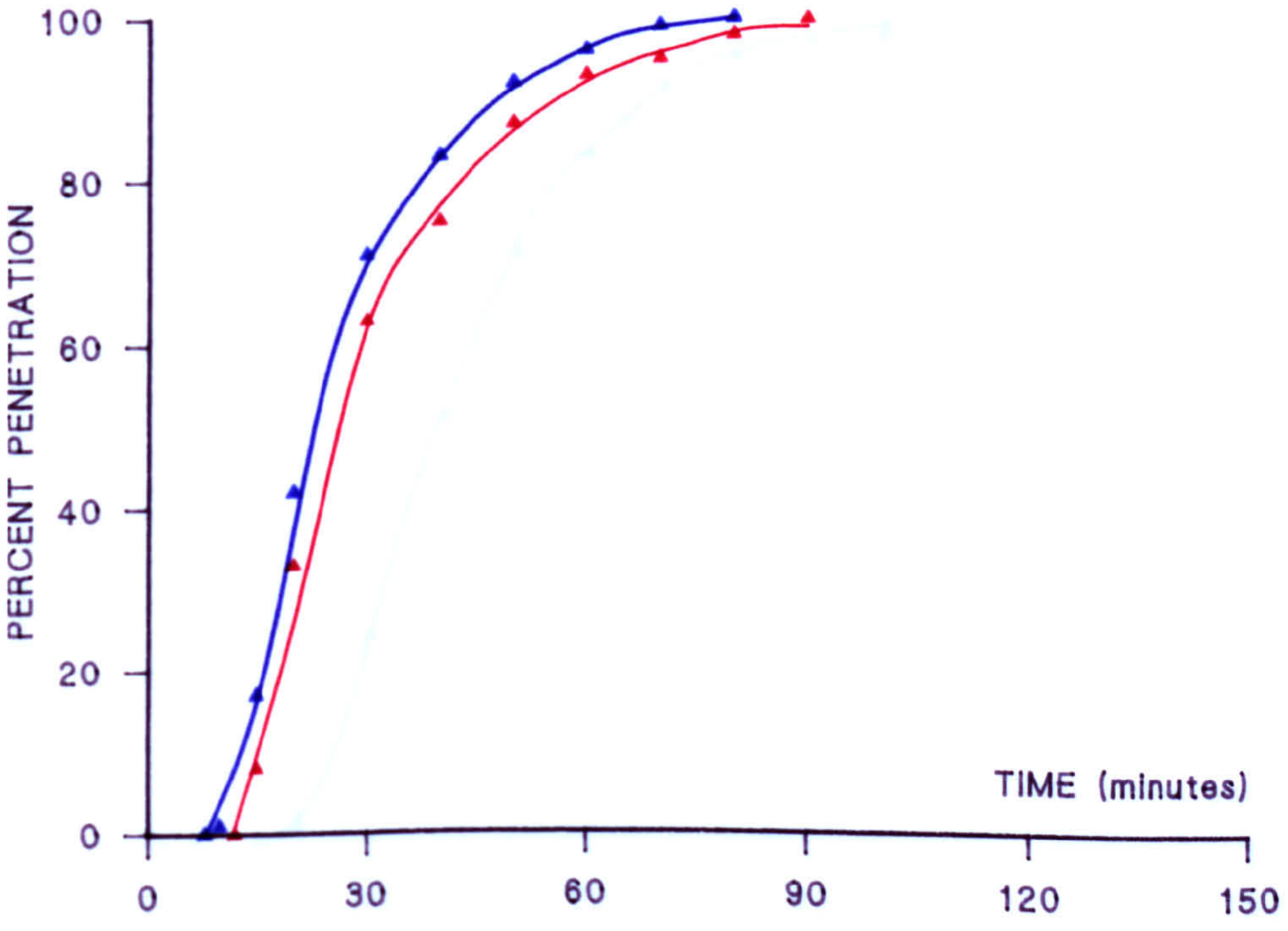

FIGURE 8.24 METHANOL BREAKTHROUGH CURVES

L-R: SCII CHLORINE/WATER SCII CHLORINE/WATER (AGED)

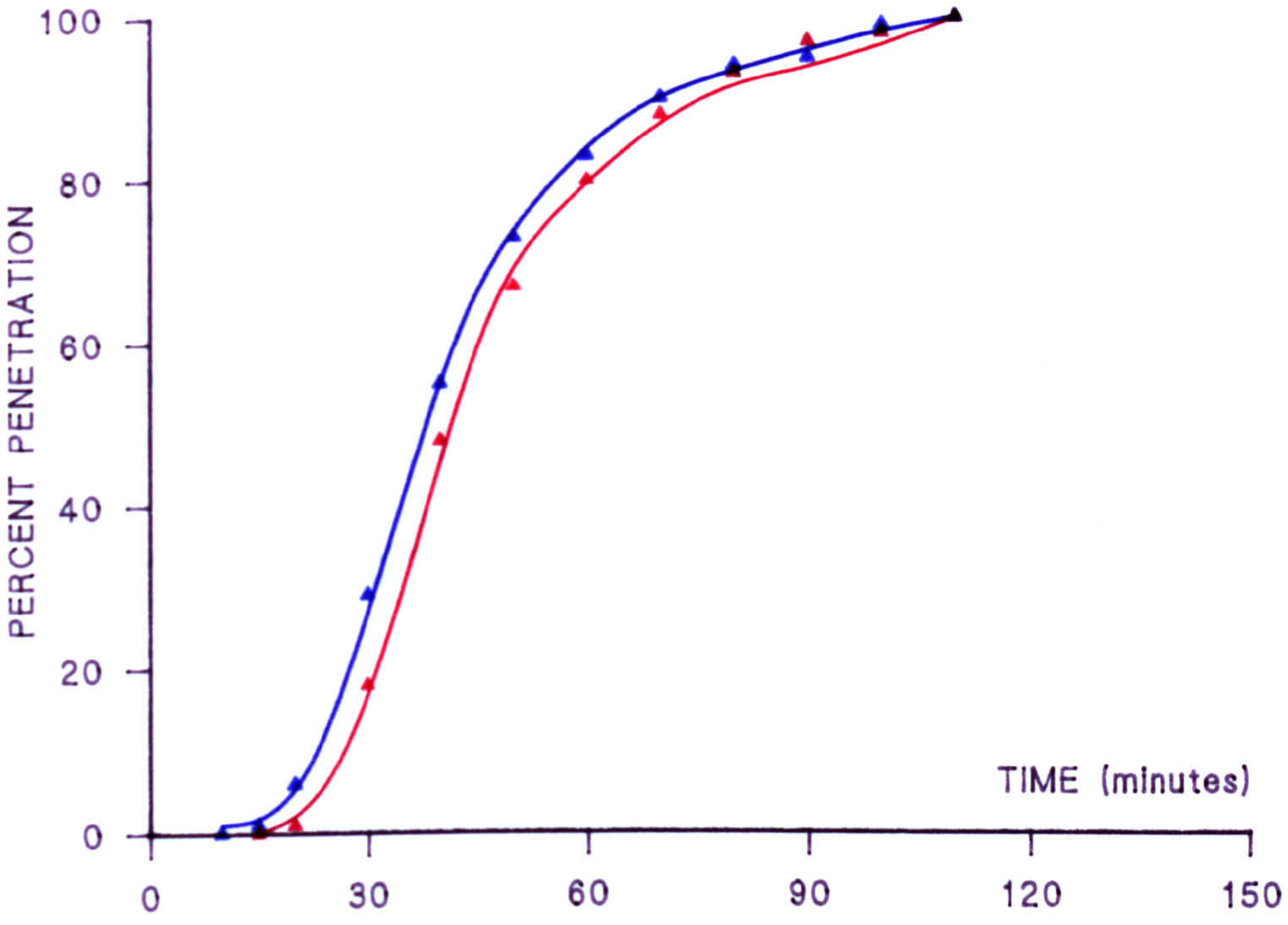

FIGURE 8.25 METHANOL BREAKTHROUGH CURVES

L-R: BPL CHLORINE/WATER BPL CHLORINE/WATER (AGED)

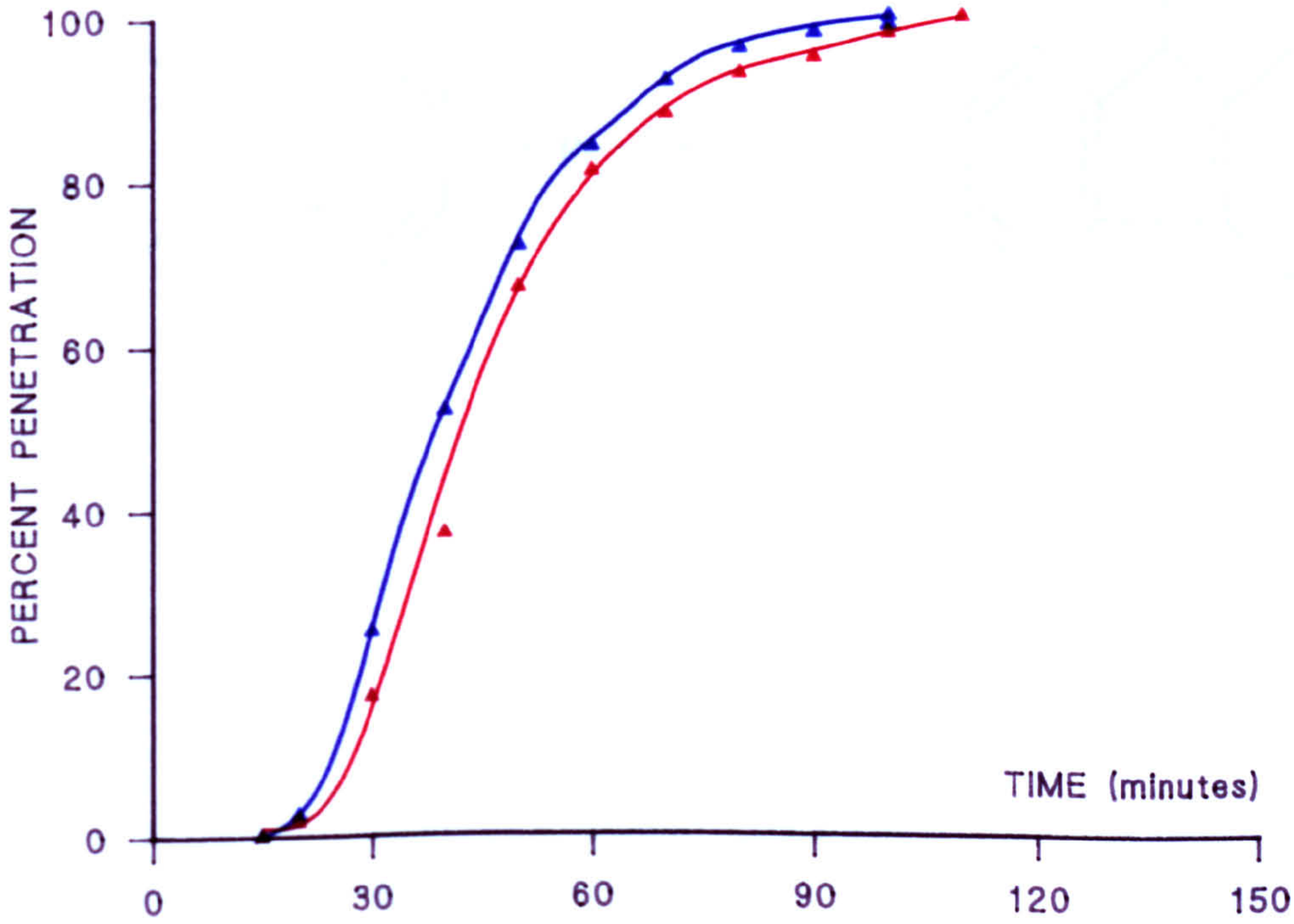

FIGURE 8.26 SURFACE CHEMICAL REACTIONS

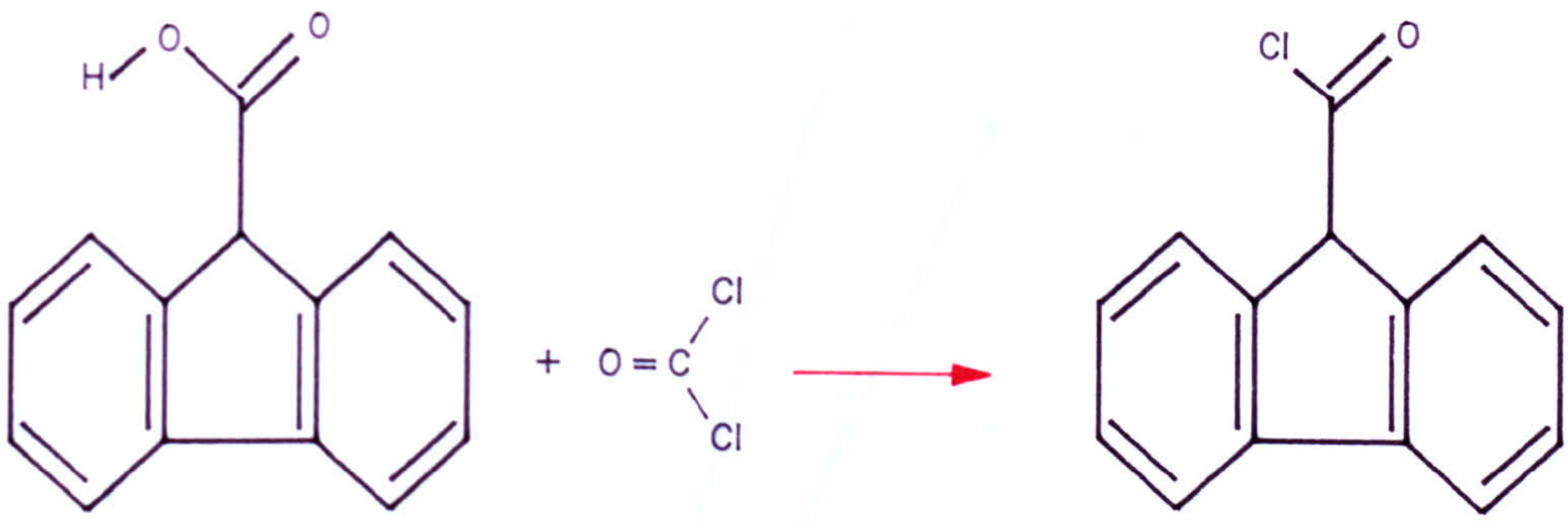

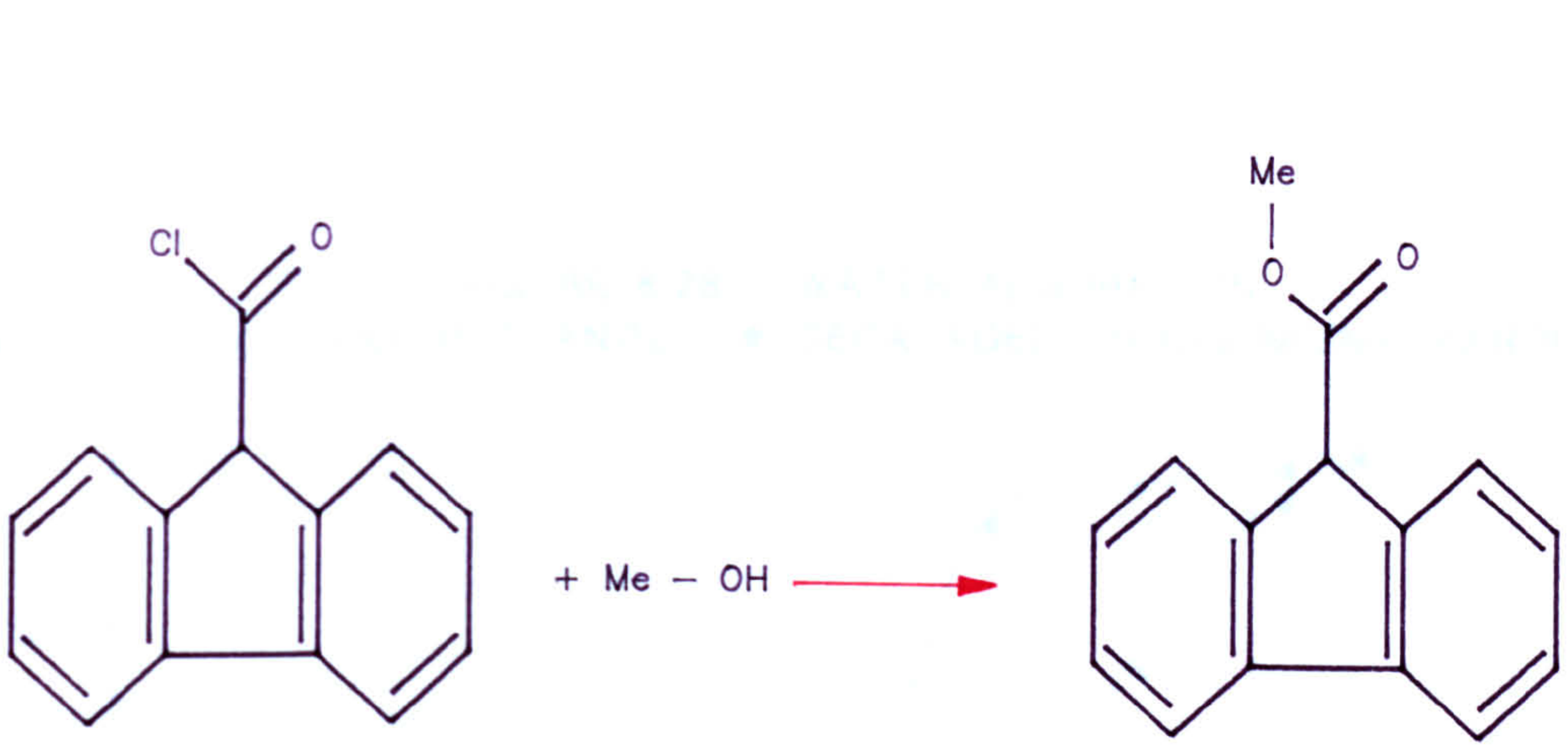

FIGURE 8.27 WATER ADSORPTION

▲ CECA AGED CONTROL PHOSGENE/METHANOL ● FIRST AND ▬ SECOND ISOTHERMS

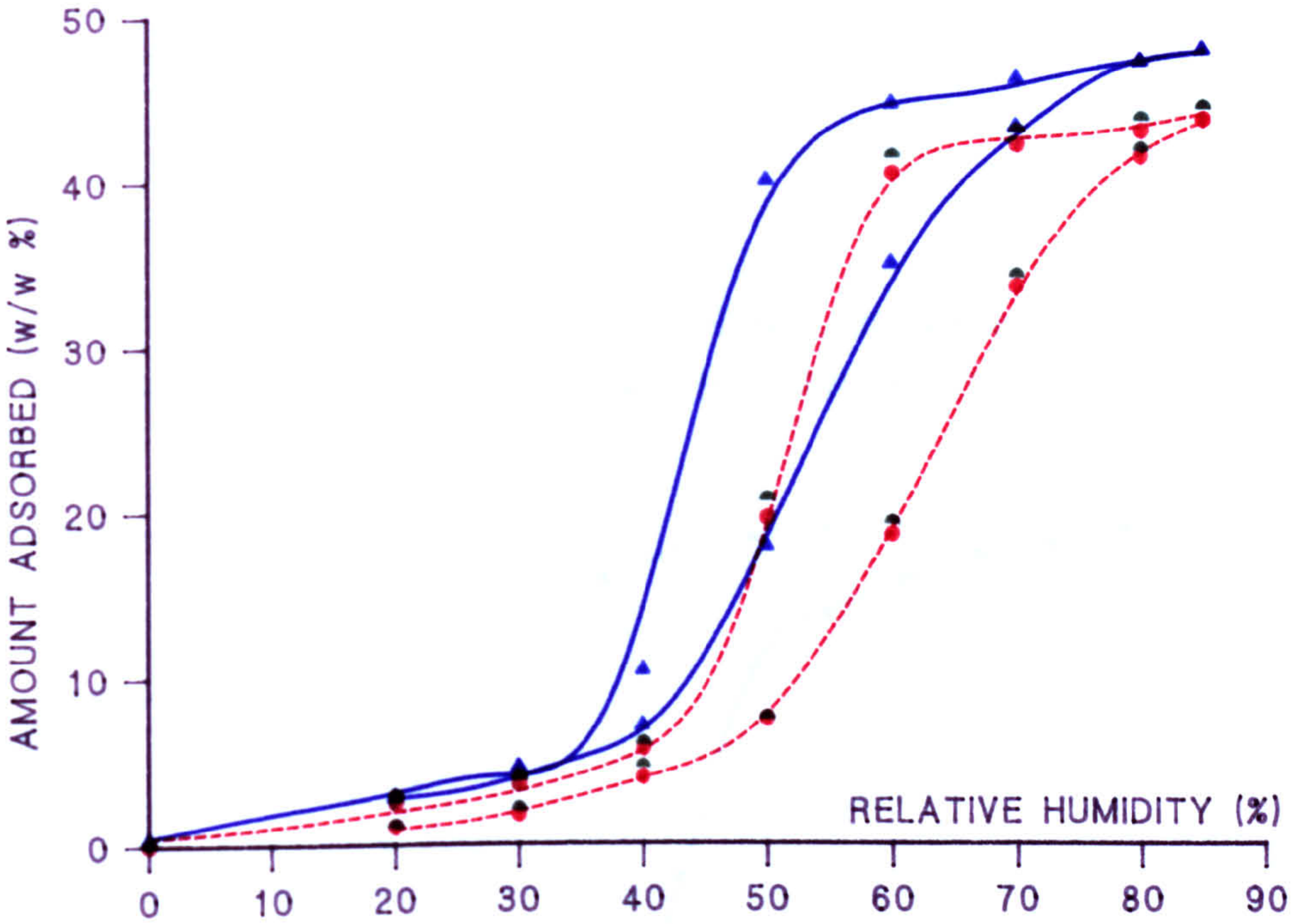

FIGURE 8.28 WATER ADSORPTION

▲ CECA PHOSGENE/METHANOL ● CECA AGED PHOSGENE/METHANOL

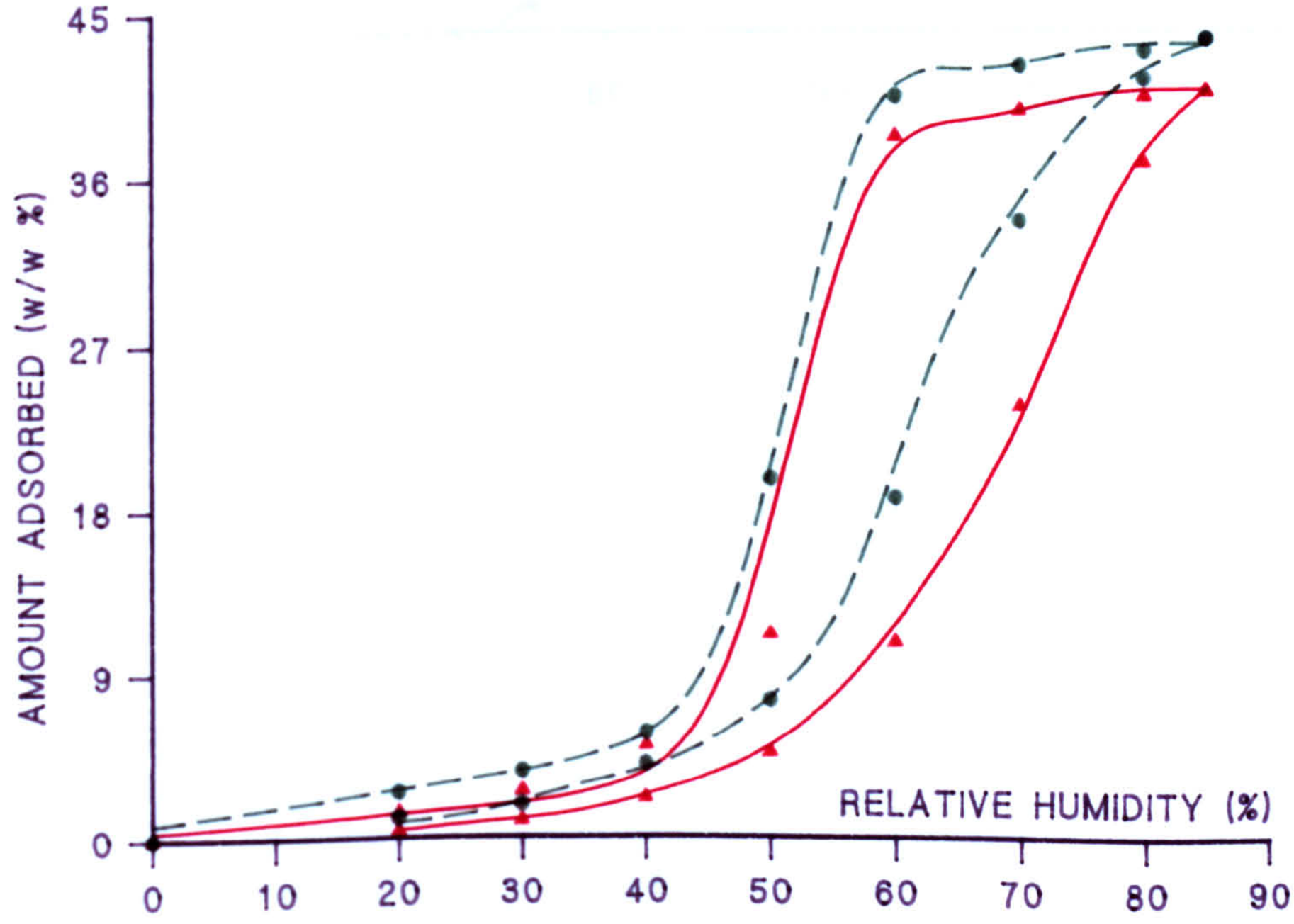

FIGURE 8.29 METHANOL BREAKTHROUGH CURVES

L-R: (AGED-CONTROL CECA) PHOSGENE/METHANOL PHOSGENE CONTROL

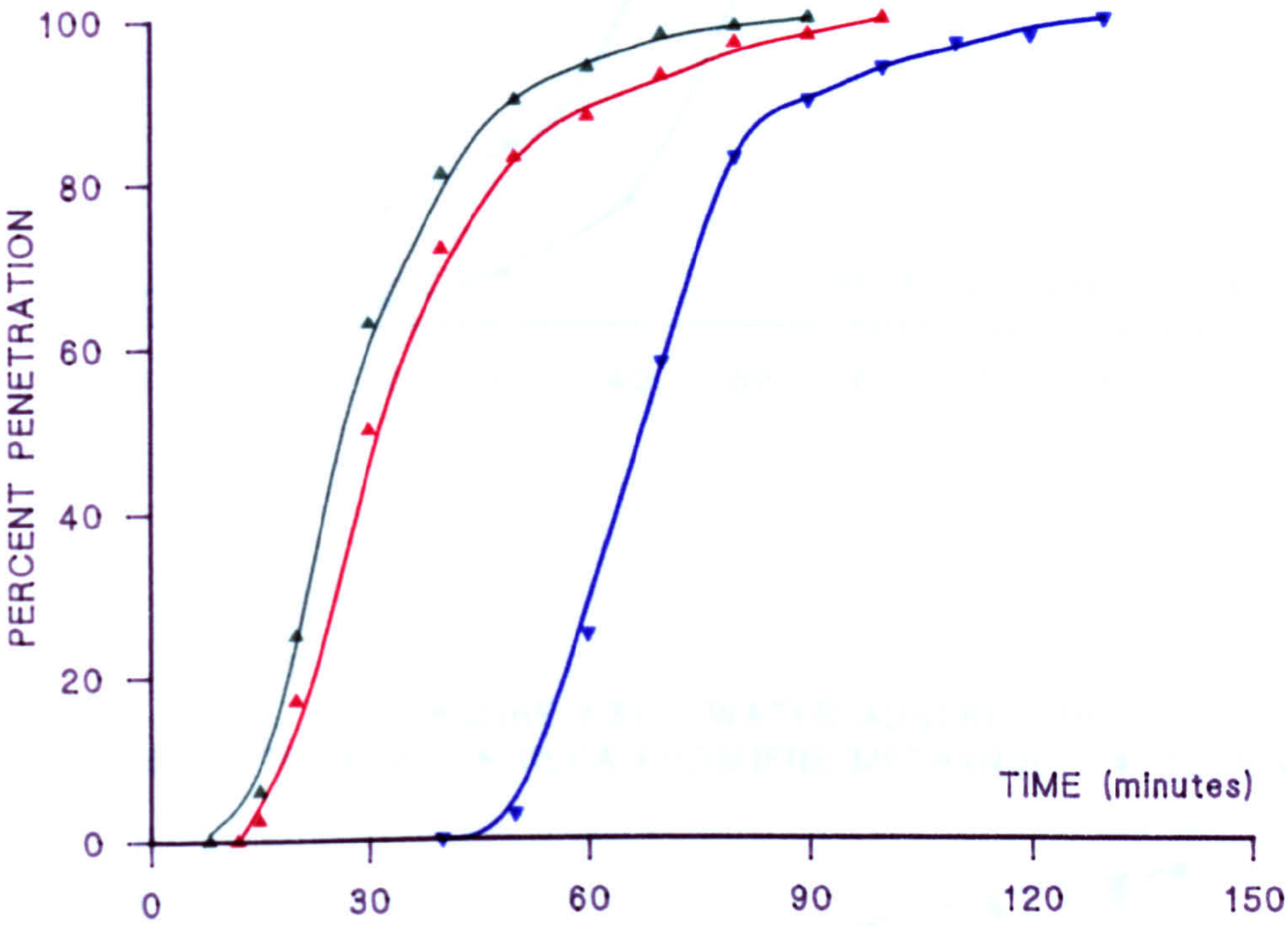

FIGURE 8.30 WATER ADSORPTION

DINITROGEN TETROXIDE ▲ BPL PHOSGENE/METHANOL ● BPL METHANOL

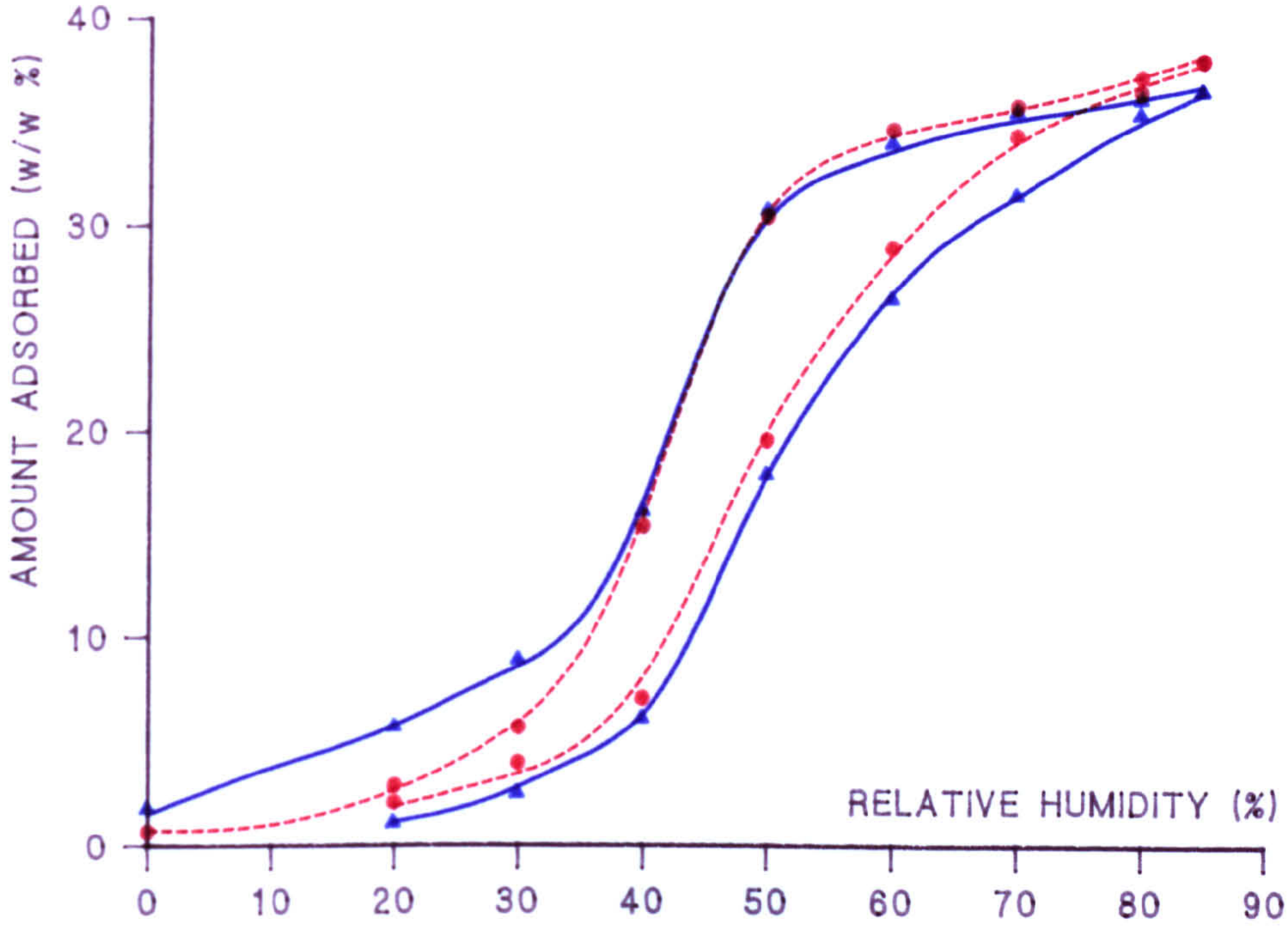

FIGURE 8.31 WATER ADSORPTION

DINITROGEN TETROXIDE ▲ CECA PHOSGENE/METHANOL ● CECA METHANOL

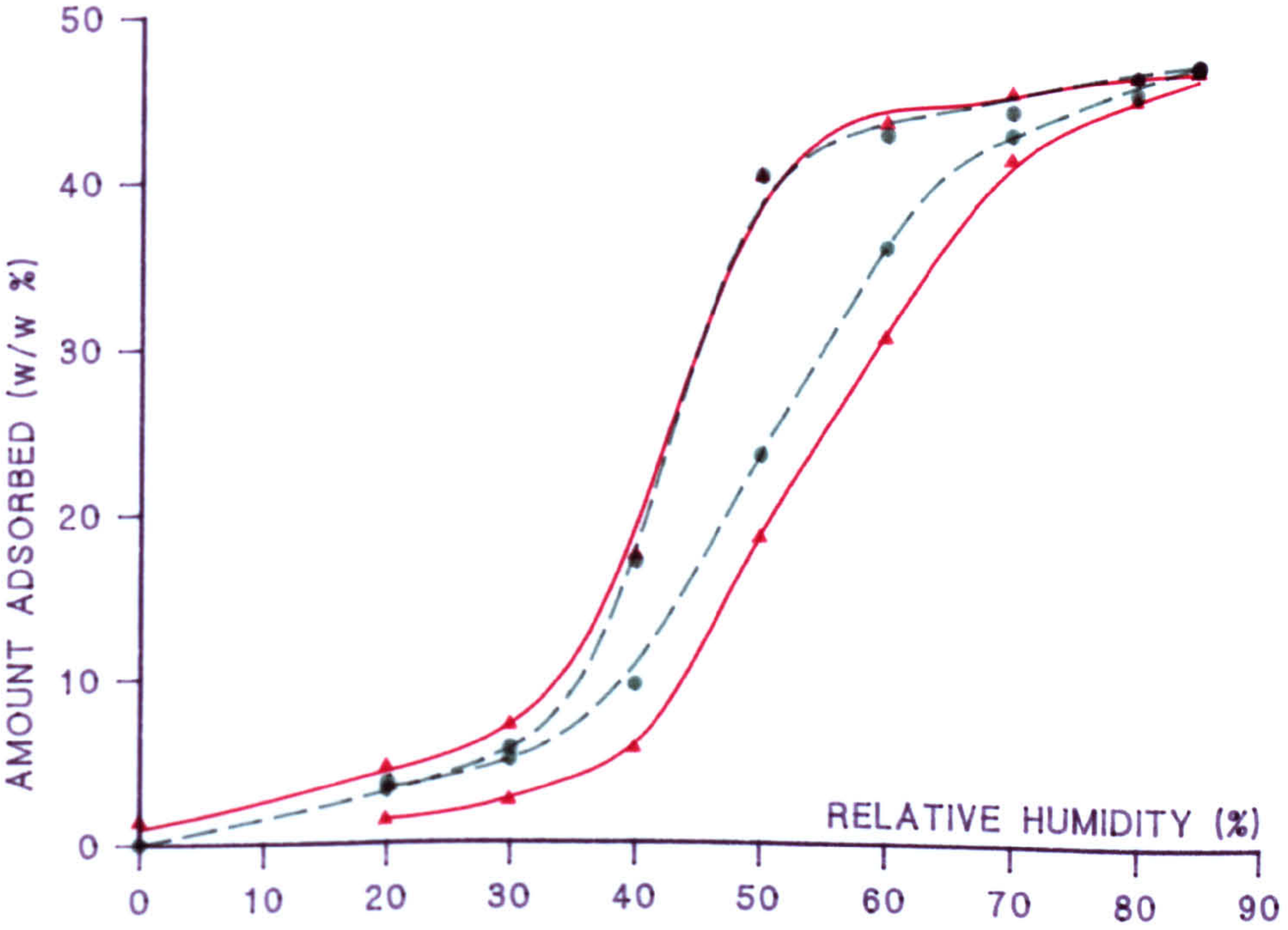

CHAPTER 9

Some Factors Controlling the Adsorption of a Model Hydrophobic Organic Vapour by Activated Carbon

Results and Discussion

Some Factors Controlling the Adsorption of a Model Hydrophobic Organic Vapour by Activated Carbon

9.0 Introduction

In a number of circumstances, activated carbon filters are required to remove volatile hydrophobic organic vapours from airstreams containing water vapour (chapter 4, 6). In general, and at equivalent partial pressures, the adsorption of the organic vapour will be favoured. However in many applications, both the atmospheric concentration of water vapour will be very much greater than that of the organic component, and the carbon filter will have been exposed to airflows containing water vapour for some time prior to use. The effect of storing the carbon in contact with water vapour on the efficiency with which volatile hydrophobic chemicals are adsorbed from humid air has been addressed (chapter 6).

The quantity of water vapour adsorbed by the filter is dependent on the relative humidity (RH) of the airstream (the adsorption isotherm, chapter 2, 4). In Europe, the RH is typically high (above RH60%): thus, the carbon may contain upwards of 30% by weight of adsorbed water at the time of use (eg. chapter 6). In such cases, it is likely that the kinetics of water displacement from the carbon pore structure will be important in determining filter performance.

This study involved the use of a volatile hydrophobic chemical, since the efficient filtration of these materials from humid airstreams represents one of the most demanding vapour adsorption applications (chapter 4).

Trichloronitromethane (CCl_3NO_2, PS) was selected as the adsorbate in this study as it is employed in many countries either to evaluate the

performance of vapour filters, or as part of a quality control regime for batch testing (chapter 4, references 65-67). PS has been used throughout this research programme as a way of monitoring the effect that surface modification has upon vapour adsorption efficiency in the presence of humid air (chapters 6-8).

PS is a colourless liquid: the melting and boiling points are -69°C and 112°C respectively, and the specific gravity (at 20°C) is 1.6 g cm^{-3}.

It is only sparingly soluble in water (0.17g $100g^{-1}$ at 20°C), and is not readily hydrolysed. The compound is stable at ambient temperatures in the dark, but decomposes slightly on exposure to strong light or as a result of heating to the boiling point. It is a volatile hydrophobic vapour (21mm Hg at 20°C, which is equivalent to a vapour concentration of approximately 200000 mg m^{-3}) and is of a similar toxicity to hydrogen cyanide. It is a potent lachrymator and pulmonary irritant, and inhalation often results in nausea and vomiting. For this reason, it was known as vomiting gas by British servicemen during World War 1. The TLV for PS is 0.7 mg m^{-3}.

Previous studies of chemically modified carbons did not include an adequate consideration of the adsorptive properties (chapter 3). Therefore, the importance of the surface chemistry on filter performance has not been fully demonstrated. More importantly, it is also apparent that the way in which carbon filters function, and the factors which limit their efficiency, is poorly understood (chapter 4).

In this chapter, the results of a study of the factors which control the efficiency of activated carbon filters will be presented. In addition, the use of chemically modified carbons in vapour adsorption applications will be considered.

Throughout the study, the internal diameter and bed depth of the filter was kept constant (2cm diameter, 1cm bed depth brass VA tube). Experiments were performed at 22 ±0.05°C, using a PS vapour concentration of 5000±25 mg m^{-3} and an airflow rate of apparent linear velocity 382 cm min^{-1} (which equates to 1.2 dm^3 min^{-1} through the filter bed) unless otherwise indicated. The pressure drop across the test line under the conditions employed was 225 Pa. The experimental conditions described reflect those in common usage (eg. references 65-67, chapter 4).

Dry carbon samples were filled into the filter using a snow storm device, and were pre-equilibrated at RH values between <2 and 95%. The samples were then transferred to the vapour adsorption apparatus for testing (because ageing effects are important at high values of the equilibration RH (chapter 6), testing was carried out within 24 hours after pre-equilibration). In each case, complete breakthrough measurements were made, and the influent and effluent temperatures, dewpoints, flowrates, and PS vapour concentrations were continuously monitored. The equipment, and the procedures used for filling, equilibrating, and testing the carbon samples are described in detail in the Appendix. All of the experiments described were reproduced at least once.

9.1 The Influence of the Relative Humidity and Carbon Water Content on Filter Performance

The quantity of water vapour adsorbed by an activated carbon is dependent upon the RH of the airflow, and at high values of the equilibration RH, significant amounts are adsorbed (chapter 4, 6). The results in this section address the impact of the RH on the efficiency with which carbon filters adsorb PS vapour from an airstream.

Figures 9.1.1-5 show the PS breakthrough and water displacement curves, the associated effluent temperature profiles, and the temperature corrected effluent RH values for samples of control BPL carbon challenged in equilibrium with dry (<RH2%), RH40%, RH65%, RH80%, and RH95% airflows (the temperature corrected effluent RH was calculated from measurements of the effluent dewpoint and temperature. The effluent temperature was measured using a thermocouple mounted in the centre of the gas flow in contact with the retaining mesh on the filter bed). Table 9.1.1 illustrates the net changes in carbon water content, and the amounts of PS adsorbed at equilibrium, for these samples. The filter breakthrough times (1%), and times to equilibrium (100% PS breakthrough), are at table 9.1.2.

Figure 9.1.1 shows the effluent PS concentration and temperature as a function of time for a sample of dry carbon. The PS breakthrough curve is sigmoidal in nature, and is approximately symmetrical at about the 50% breakthrough concentration. At breakthrough, the filter bed is at about 80-85% of capacity (that is, the bulk of the PS is adsorbed by the time penetration of the carbon takes place). The process is exothermic, and the effluent temperature remains at a maximum prior to, and shortly after, breakthrough (1.2^{o}C above the influent temperature). After this time, the effluent temperature decreases until the influent temperature is attained. Thereafter, no

further change was observed. Integration of the area under the temperature wave, and over the PS breakthrough curve, according to the equation, enabled an estimate of the average molar heat of adsorption for PS to be made. This was found to be 50 kJ mol^{-1}. Subsequent experiments using control, aged, and modified adsorbents revealed that the average heat of PS adsorption was in the range 50±1 kJ mol^{-1}.

$$\Delta Q = C_p . L . \int_{t0}^{t1} \Delta T dt$$

C_p = heat capacity of dry air ($Jg^{-1}K^{-1}$)
L = mass flow rate of air (gs^{-1})
T = temperature difference (K)
t = time (s)
ΔQ = heat change (J)

Attempts to measure the heat losses and gains during observations of the adsorption/ desorption phenomena were not successful, hence the calculations of adsorption (and vaporisation) heats are estimated values only. The measured heat changes, which are the sum of the various processes taking place on the filter bed, will be affected by the experimental parameters and the design and construction of the apparatus.

Figure 9.1.2 shows similar measurements for a filter challenged in equilibrium with RH40% air. From the beginning of the challenge, the absolute amount of water in the filter effluent increases: that the value of the temperature corrected effluent RH initially falls reflects the sharp increase in the effluent temperature. This effect was observed to a varying degree at each of the RH values studied. The reduction in breakthrough time under these

conditions was approximately 10% of that for the dry filter, and all of the preadsorbed water was displaced from the filter bed by PS (table 9.1.1). The differences between these effluent profiles and those for the dry carbon bed are not substantial, indicating that in low amounts (ie. 2.2% w/w), preadsorbed water does not markedly effect filter efficiency.

Throughout the experiment, the effluent temperature represents the sum of the heat liberating and consuming processes. Heat liberation is primarily due to the adsorption of PS, whereas the displacement of preadsorbed water consumes energy. However, it is probable that some of this heat energy is recovered during the early part of the experiment as a result of the re-adsorption of displaced water further down the filter bed, an effect which will influence the shape of the water displacement curve. Heat liberation is at a maximum during the early part of the experiment, when the amount of PS adsorbed as a function of time is a maximum, and where the amount of carbon available for re-adsorption of displaced water is significant. Once PS begins to penetrate the filter, the quantity adsorbed per minute is less because the capacity of the carbon is approached. It is also probable that, as a result of an increased local carbon water content, more water must be displaced per unit of PS adsorbed.

On the assumption that the heat of PS adsorption remains constant, the heat of vaporisation of water vapour was found to be ca. 33 kJ mol^{-1}. In all of the subsequent experiments, the average heat of water displacement (and adsorption, where measurements were made) was found to be 32±1 kJ mol^{-1}.

Increasing the equilibration and challenge RH to 65% resulted in a more marked change in the shapes of the effluent profiles (figure 9.1.3). The protection afforded by the filter is approximately 40% less compared to the dry carbon, and, as before, all of the preadsorbed water was displaced during filter challenge. The most notable differences are in the shape of the PS breakthrough curve, and the observation that the overall process of PS adsorption and water

displacement was endothermic. It is probable that the inflexion in the PS breakthrough curve (at ca. 220 minutes) represents the time after which readsorption of displaced water ceases to be significant. During the initial part of the experiment, the effluent water vapour concentration rises rapidly: as the effluent temperature stabilises, the slope of the water displacement curve decreases. During this period, it is likely that re-adsorption of water further along the filter is important. The steepening of the curve as the PS wavefront advances through the bed represents displacement of the water adsorbed during the earlier part of the challenge. In this example, a temperature depression of more than $2^{o}C$ was observed, reflecting the energy absorbed by the system during the vaporisation of the preadsorbed water (the maximum depression in temperature occurred at about the same time that the effluent water vapour concentration was greatest). The driving force for this process must reflect the most favourable thermodynamic situation.

An increase in the equilibration and challenge RH to 80% results in a further significant change to the shapes of the effluent profiles: the overall process of PS adsorption and water displacement was again endothermic, but not all of the preadsorbed water was displaced at the end of the experiment. It may be that adsorbed PS occludes some of the small micropores which contain adsorbed water: alternatively, it is possible that PS adsorption and water displacement continues after the experiment was terminated, but that the concentration changes are not significant enough to be measured using the techniques adopted in this present study. Thermodynamically, the adsorption of PS is most favoured. The most obvious effect of increasing the RH to 80% was on the shape of the PS breakthrough curve- it became distinctly biphasic (figure 9.1.4). It is also notable that unlike the situation at RH65%, the effluent RH reached 100%. The maximum depression in the effluent temperature was in comparison somewhat less, however ($1.6^{o}C$), reflecting the fact that at RH80% the airstream reached saturation, limiting the extent of bed cooling due to the vapourisation of adsorbed water. Most importantly, the capacity of the filter to breakthrough was only approximately 25% of that for the dry bed. Values

derived from the measurements are at tables 9.1.1-2.

Increasing the RH to 95% did not result in any marked changes compared with the results determined at RH80%. The breakthrough time was shorter, however (representing a capacity to breakthrough of about 15% of that for the dry filter), and the initial part of the PS breakthrough curve was steeper. The time to reach equilibrium was also somewhat greater (figure 9.1.5).

Figure 9.1.6 shows the PS breakthrough curves measured at each value of the equilibration and challenge RH described above.

On the basis of these measurements, it is apparent that the combined effects of the equilibration and challenge RH have a critical influence upon the degree of protection provided by carbon filters.

A further experiment was carried out to determine which of the two factors (the equilibration RH or the challenge RH) had the greatest impact upon filter performance.

Figure 9.1.7 shows the effluent curves measured for a dry bed of carbon challenged with PS vapour in RH80% air. The differences between these results, and those described at figure 9.1.4 are substantial, and suggest that the quantity of preadsorbed water is most critical in determining filter life (the breakthrough time was longer than that obtained at RH65%). The most notable effect was in the shape of the effluent water concentration profile, which initially rose to that of the influent concentration (equivalent to RH80% at 22^{o}C), but then continued to rise above this value: at the same time, a small depression in the effluent temperature was observed. This effect represents the displacement of the more weakly adsorbed component (water vapour) by PS toward the end of the experiment, which was retained by the carbon during the earlier part of the challenge (the filter bed was initially equilibrated with air of ca. RH2%). This observation suggests, therefore, that the reduced PS filter life

(compared to the dry filter) was due to a kinetic limitation (that is, a proportion of the micropore volume was probably occluded by adsorbed water: as the PS wavefront advanced through the bed, thermodynamic equilibrium was approached and some of the adsorbed water was displaced).

The results described at figures 9.1.4-7 provide evidence as to the reason why preadsorbed water is critical in determining filter performance.

Within a few minutes of initiating filter challenge at RH80% (figure 9.1.4), the effluent temperature approaches a maximum value (0.75°C above the influent temperature). The effluent RH then begins to rise, and at about the same time, the effluent temperature begins to fall, to values less than the temperature of the influent airstream as PS begins to penetrate the filter. The effluent temperature attains a minimum value at about the time that the effluent RH was observed to reach a maximum. The effluent temperature remains close to this minima for approximately 50 minutes before rising slowly to approach 22°C after about 450 minutes from the beginning of the experiment. The curves at figure 9.1.4 also suggest that the maximum effluent water concentration and minimum temperature are limited by the capacity of the airstream to carry away displaced water: that is, the effluent airstream reaches saturation (RH100%) after about 75 minutes from the start of the measurements.

Examination of the results suggests that the primary limitation on filter performance at RH80% is due to the occlusion of a significant proportion of the pore structure by saturated water vapour. That is, the water displaced from the favourable adsorption sites (micropores, polar surface sites) builds up in the less favourable areas (the transport pores- mesopores and macropores) and restricts the accessibility of the PS molecules to the micropores. This leads to a steepening of the PS breakthrough curve at about the same time that the effluent RH approaches saturation (that the two events do not coincide at precisely the same time probably reflects a difference in the relative velocities

of the PS adsorption and water displacement wavefronts within the bed). As the displaced water begins to be carried away from the bed (and the RH falls below 100%) the efficiency of PS adsorption improves (the slope of the PS breakthrough curve is reduced- ie., the rate of adsorption is increased). This hypothesis was tested by measuring breakthrough curves at RH95% (figure 9.1.5), where limitations on water transfer within, and displacement from, the filter bed would be expected to be even more critical. It was found that the PS breakthrough time was shorter; that the first part of the breakthrough curve was steeper, and that the final part of the curve was more shallow. In this case, the effluent RH remained at saturation for approximately 3.5 hours, reflecting the reduced capacity of the air for carrying away displaced water. These observations support the contention that filter performance at high values of the equilibration and challenge RH is limited by the build up of displaced water within the pore structure.

At the lower RH values used in this study (65, 40%) partial pore blockage by displaced water presumably results in the same limiting effect, but on a more localised scale (there is less water on the carbon, and the capacity of the airstream for carrying it away is substantially greater). The significantly deeper temperature depression observed at RH65% compared with the case at RH80% is a result of the greater capacity of the airflow for water vapour: thus, the concentration of water in the effluent is significantly greater at RH65%, and the impact of preadsorbed water on the breakthrough time less critical.

Further support for the view that the limitations on filter performance described above are due to kinetic, rather than thermodynamic, considerations was apparent from challenging a filter bed with PS in RH80% air after first equilibrating a dry bed with PS at the same concentration (5000 mg m^{-3}). Although some displacement of PS resulted, the quantity retained by the carbon was greater than that adsorbed by carrying out the experiment in reverse order (ie. challenging the filter bed with PS vapour after first equilibrating the carbon with RH80% air). A similar conclusion may be drawn from the experiment

described at figure 9.1.7, which was carried out to determine the efficiency with which PS was adsorbed by a dry carbon bed in competition with water vapour.

The observations described above probably represent a general situation for carbon filters which have been equilibrated with humid air and then challenged with a hydrophobic vapour (eg. reference 64, chapter 4).

It may be that this limitation on performance can be overcome, at least in part, by increasing the volume of meso- and macro- pores within the carbon. These pores could then act as a depot for the water displaced from the micropores which cannot be immediately carried away by the airstream (which will have reached saturation). This may then prevent the pore blocking effects which lead to the major decrement in filter performance observed at high RH. An alternative, and perhaps more elegant, solution, would be to provide an external heat source to the filter, which would prevent bed cooling during water displacement. This would limit the rise in the RH within the carbon bed, and prevent saturation of the airstream and hence pore blocking effects. Efficient filter performance could then be maintained.

Table 9.1.1 The Amounts of PS Adsorbed and Water Displaced by Samples of Control BPL Carbon as a Function of the Equilibration and Challenge RH

Carbon Weight (dry, g)	Test RH (%)	PS Adsorbed ($mg\ g^{-1}$)	Water Desorbed ($mg\ g^{-1}$)	Carbon Water Content ($mg\ g^{-1}$)	
				Initial	Final
1.754	95	344	78	414	336
1.755	80	438	219	352	133
1.758	65	593	203	206	3
1.743	40	584	19	22	3
1.742	<2	583	-	-	-

Table 9.1.2 PS Breakthrough Times, and Times to Equilibrium (Control BPL)

Test RH (%)	PS Breakthrough Time (min)	
	1% Breakthrough	100% Breakthrough
95	22	450
80	33	440
65	83	324
40	119	212
<2	134	201

{1% Breakthrough is 50 mg m^{-3}; 100% Breakthrough is 5000 mg m^{-3}}

FIGURE 9.1.1 CHLOROPICRIN BREAKTHROUGH FOR BPL CARBON

{CONTROL BPL CARBON CHALLENGED AT RH<2% AND 22°C}

[▵ PS; o TEMPERATURE]

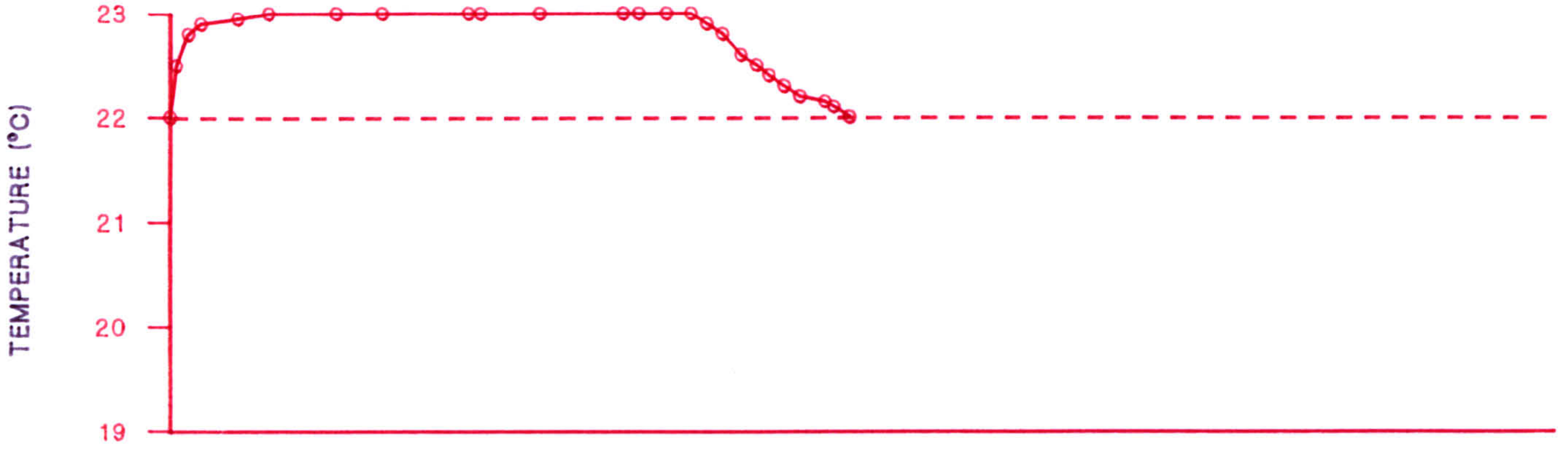

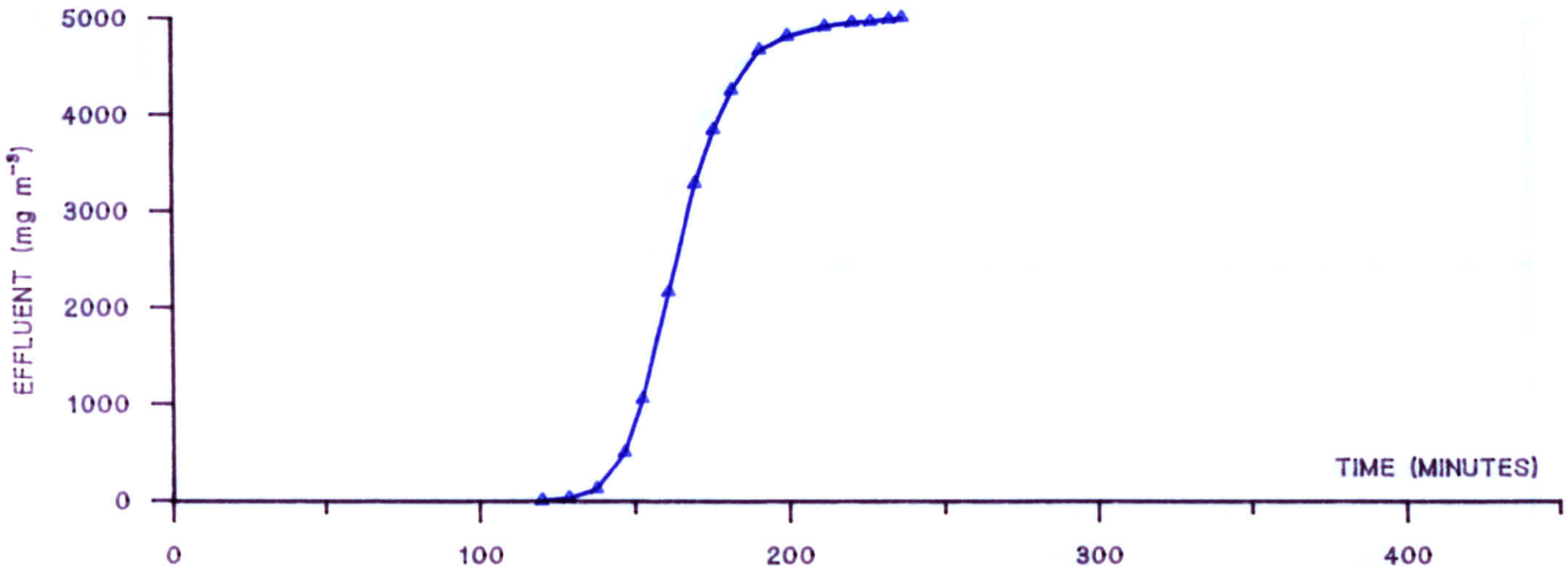

FIGURE 9.1.2 CHLOROPICRIN BREAKTHROUGH AND WATER DISPLACEMENT CURVES
(CONTROL BPL CARBON CHALLENGED AT RH40% AND 22°C)

[△ PS; ○ TEMPERATURE; □ WATER (mg m^{-3}); ◇ TEMPERATURE CORRECTED RH]

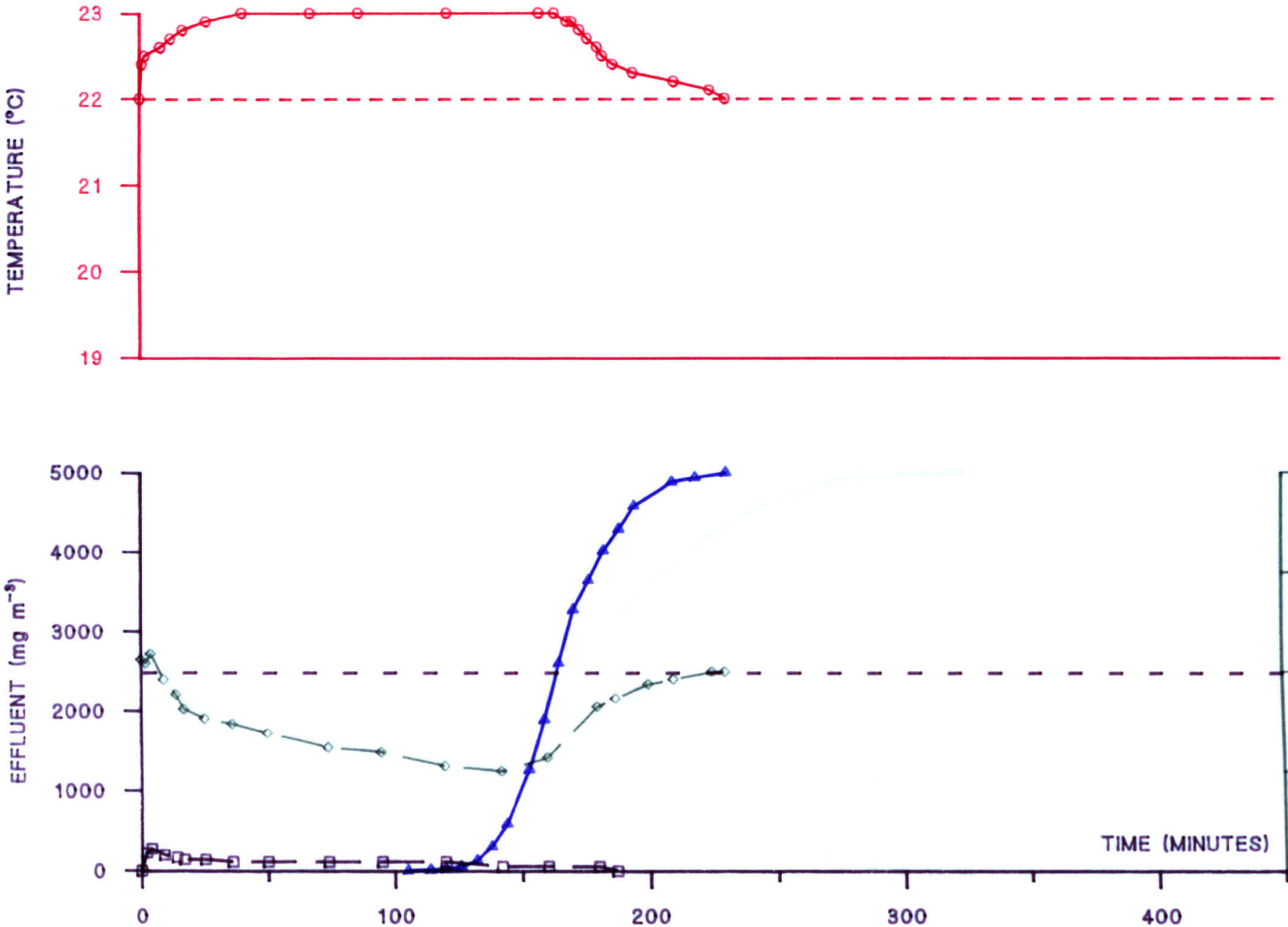

FIGURE 9.1.3 CHLOROPICRIN BREAKTHROUGH AND WATER DISPLACEMENT CURVES
(CONTROL BPL CARBON CHALLENGED AT RH65% AND 22°C)

[△ PS; ○ TEMPERATURE; □ WATER (mg m^{-3}); ◇ TEMPERATURE CORRECTED RH]

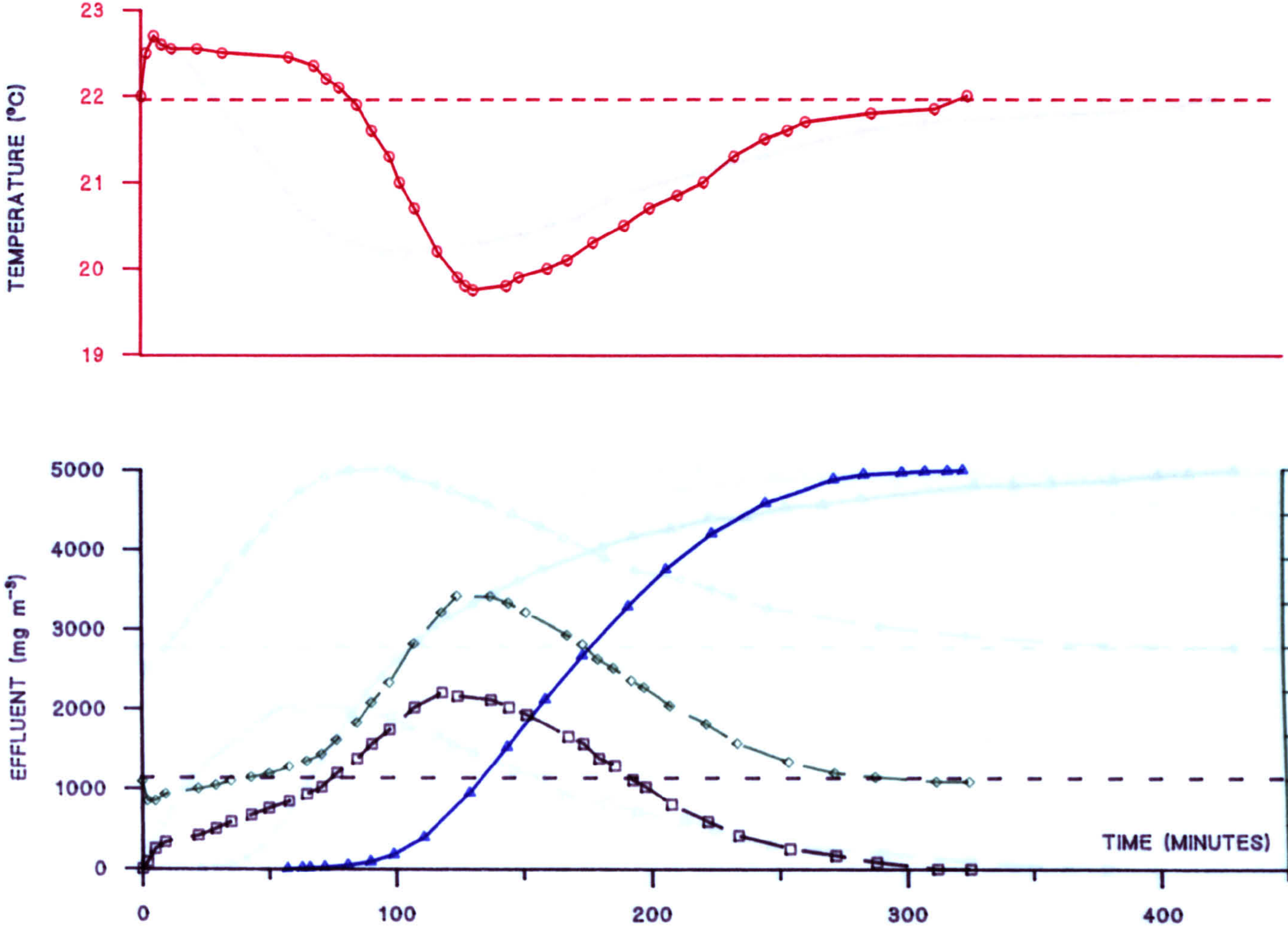

FIGURE 9.1.4 CHLOROPICRIN BREAKTHROUGH AND WATER DISPLACEMENT CURVES
(CONTROL BPL CARBON CHALLENGED AT RH80% AND 22°C)

[△ PS; ○ TEMPERATURE; □ WATER (mg m^{-3}); ◇ TEMPERATURE CORRECTED RH]

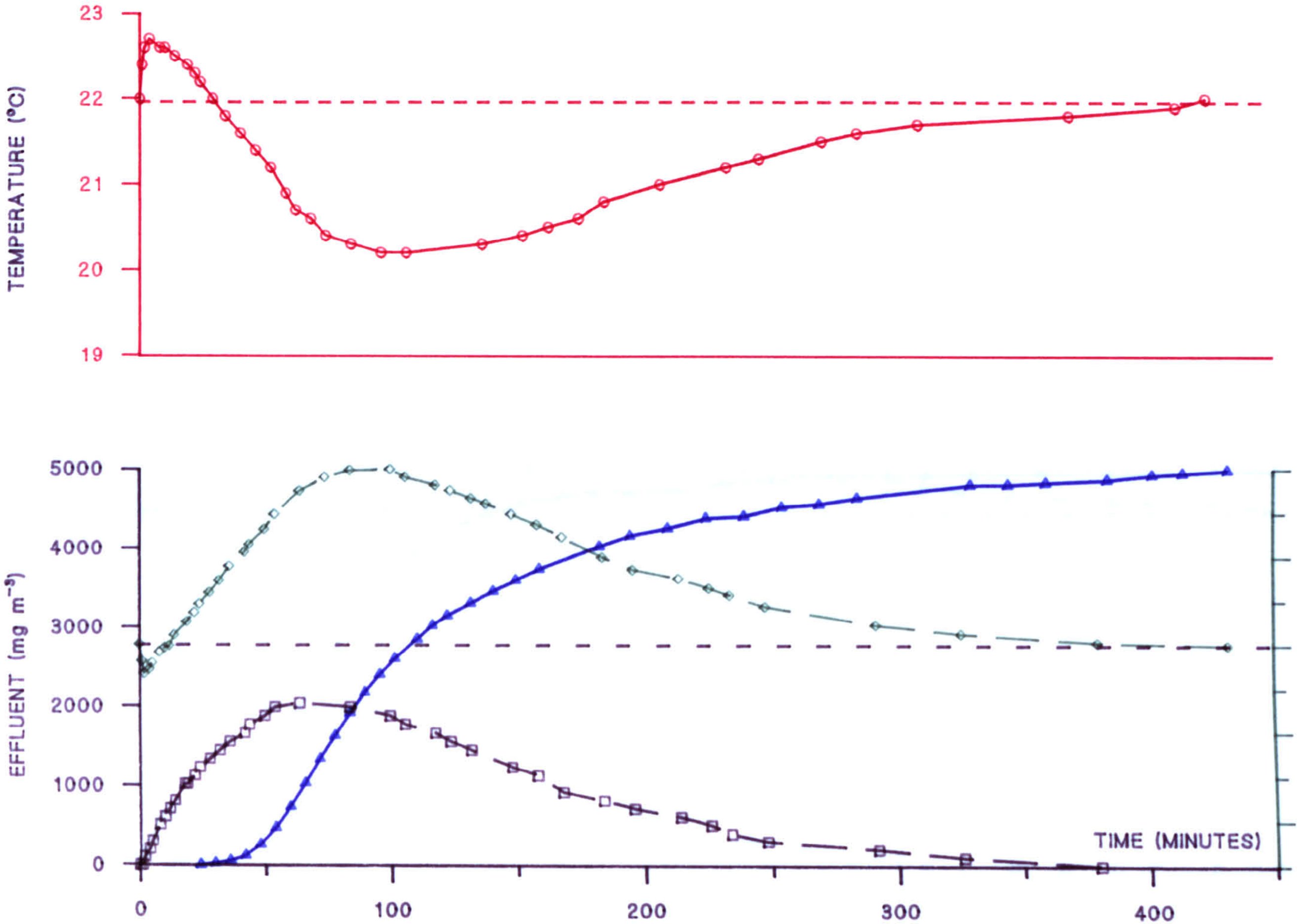

FIGURE 9.1.5 CHLOROPICRIN BREAKTHROUGH AND WATER DISPLACEMENT CURVES
(CONTROL BPL CARBON CHALLENGED AT RH95% AND 22°C)

[△ PS; ○ TEMPERATURE; □ WATER (mg m^{-3}); ◇ TEMPERATURE CORRECTED RH]

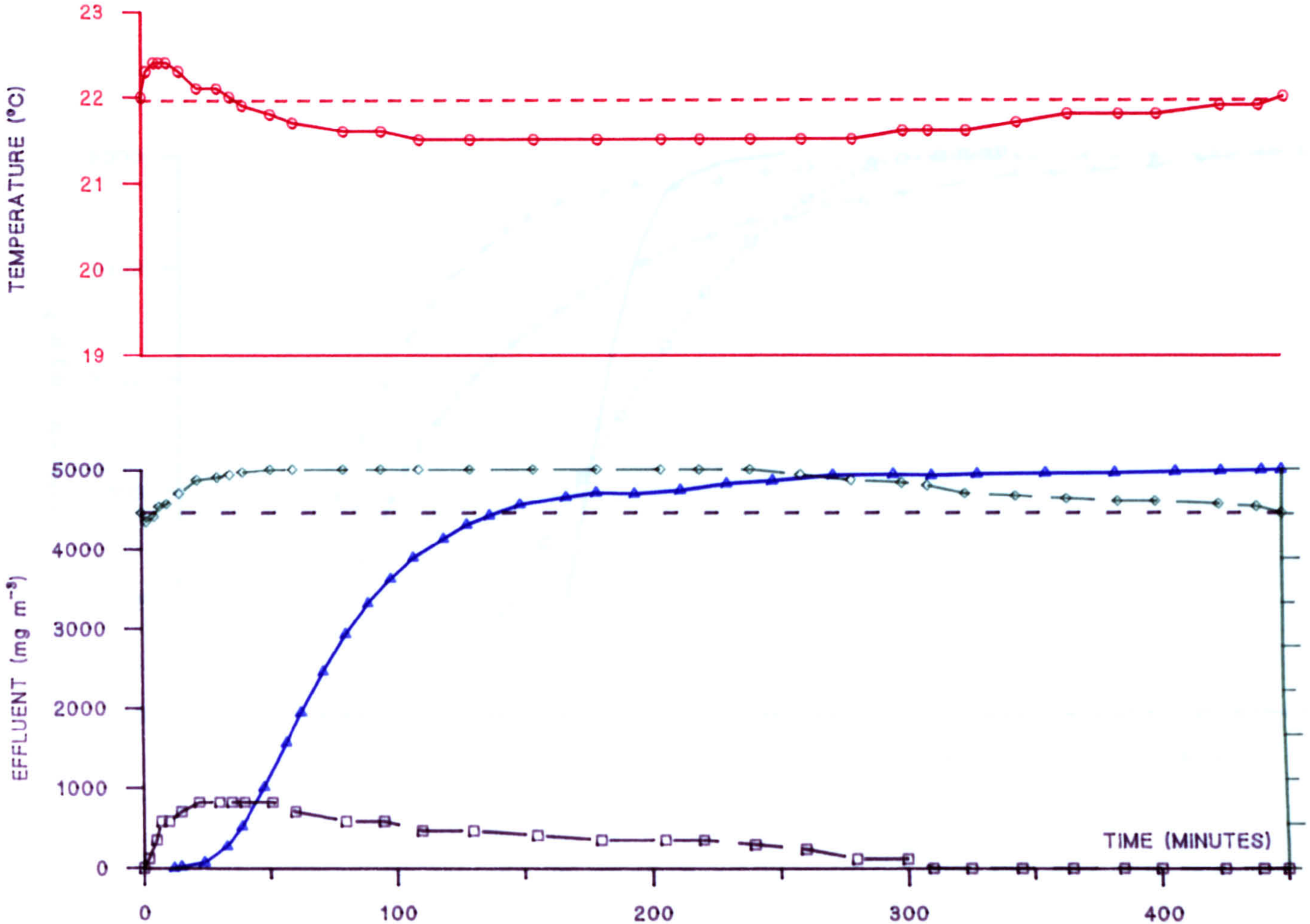

FIGURE 9.1.6 CHLOROPICRIN BREAKTHROUGH CURVES AS A FUNCTION OF THE RH

(L -> R: RH95%; RH80%; RH65%; RH40%; RH<2%)

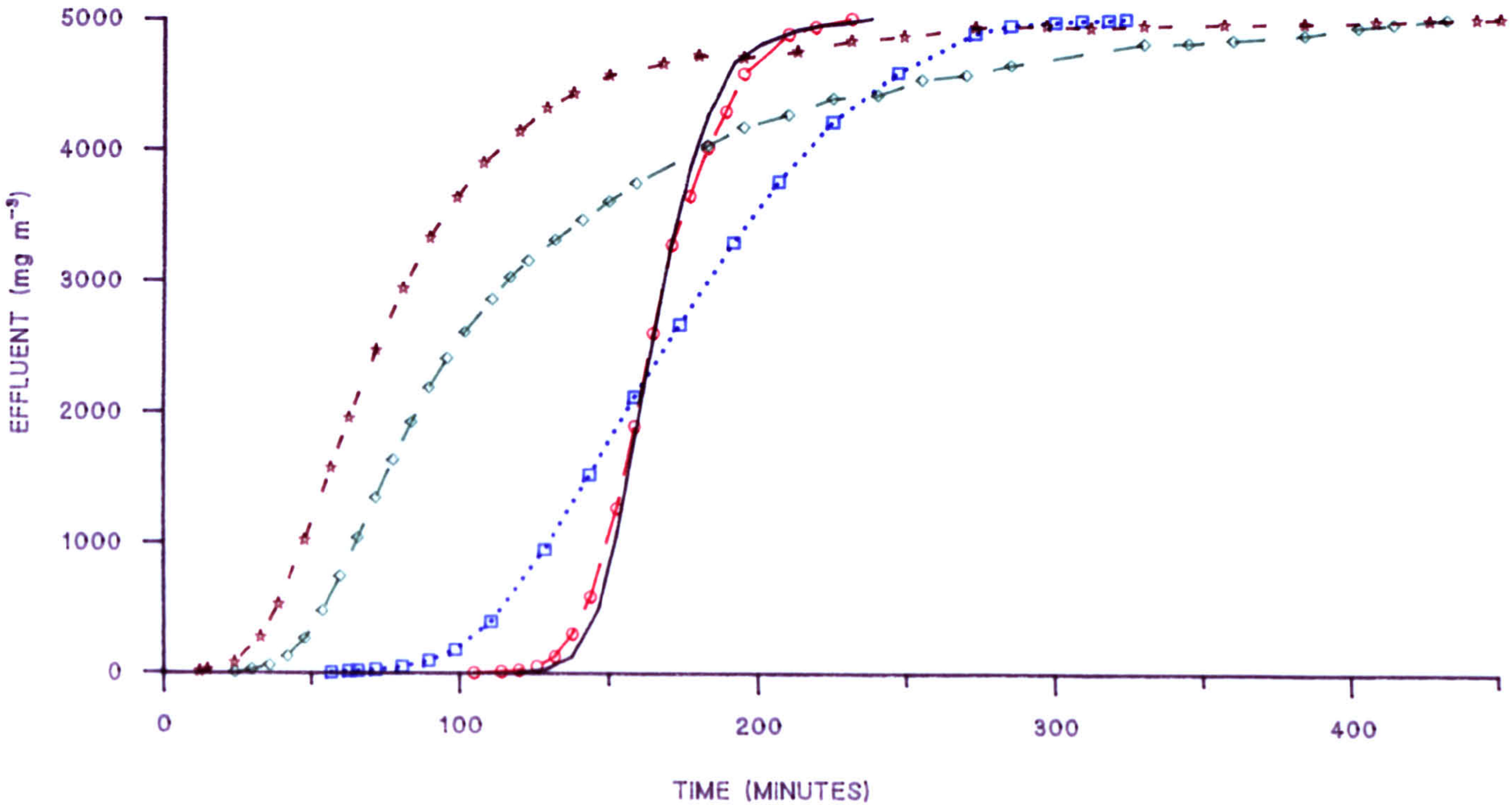

FIGURE 9.1.7 CHLOROPICRIN AND WATER BREAKTHROUGH CURVES

(DRY CONTROL BPL CARBON CHALLENGED AT RH80% AND 22°C)

[△ PS; ○ TEMPERATURE; □ WATER (mg m^{-3})]

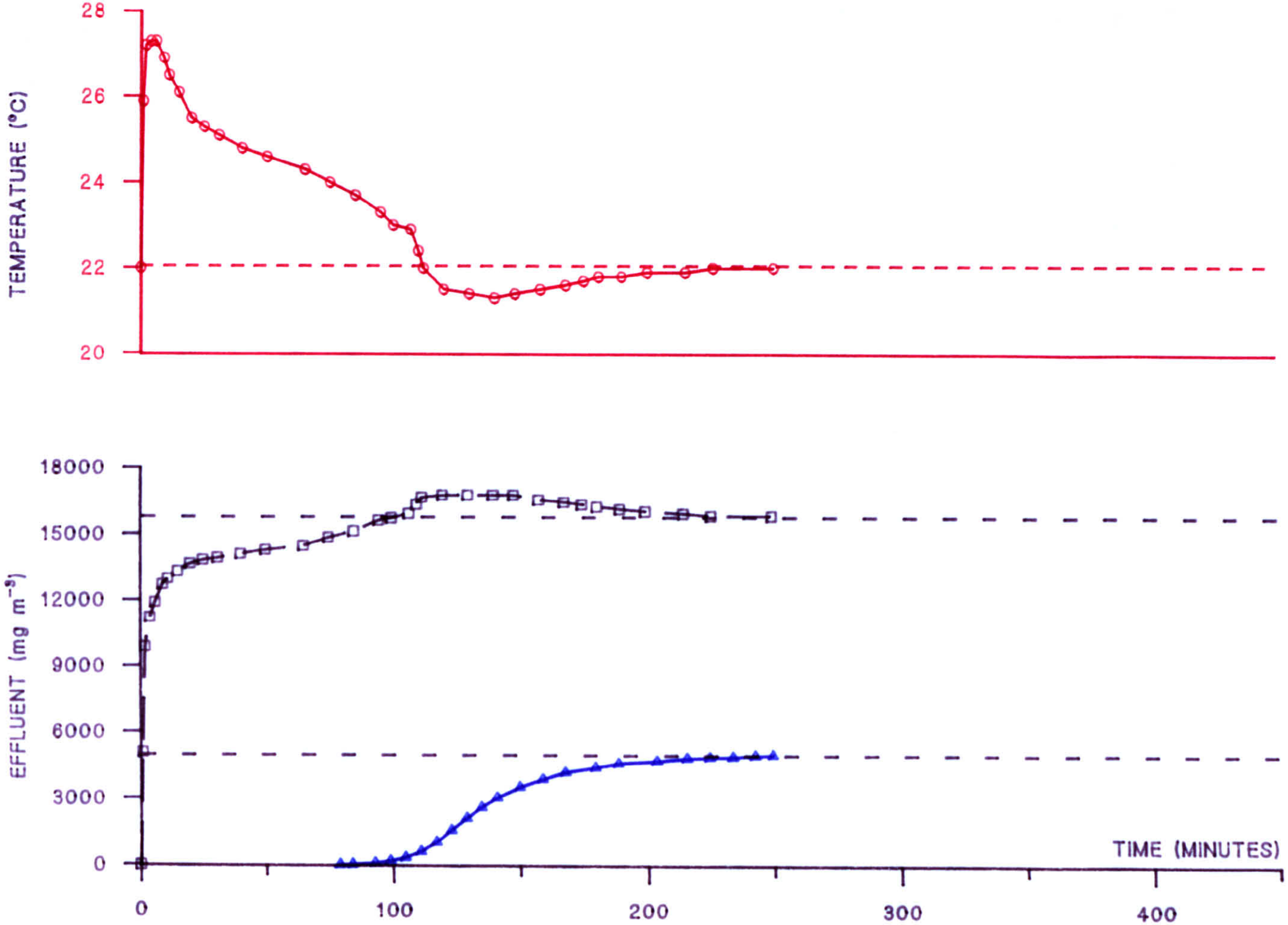

9.2 The Influence of Temperature on Filter Performance

Filter performance is usually measured at a single temperature. As part of this investigation, temperature effects were studied by challenging filters (BPL carbon) at RH80% at 22, 3, and -3°C. The other experimental parameters were the same as those described above (9.1).

If it is the process of water displacement that controls filter efficiency (9.1), then at first consideration, performance must degrade as the temperature is reduced, because the capacity of the air for displaced water will be lowered. However, the precise effect will also depend on the PS adsorption isotherm, and the water adsorption characteristics of the carbon. Accurate predictions are therefore difficult.

The effect of the temperature on the equilibrium water adsorption isotherm for activated carbon has received little attention (only a single article has been found: chapter 2, reference 30). This study revealed that the adsorption characteristics were independent of temperature between 15 and 40°C. On this basis, it may be that the water isotherm will be unaffected by temperature in the range used in this present study.

Figure 9.2.1 shows the equilibrium water adsorption isotherms measured for samples of BPL carbon at 22°C and 3°C. The equilibration times determined for each value of the RH, and the amounts of water adsorbed, are at table 9.2.1.

The results show that the adsorption- desorption water isotherms are very similar at the RH values studied (RH20-95%): it is apparent, however, that the equilibration times are significantly longer at the lower temperature (table 9.2.1). This is probably a consequence of the lower absolute water vapour concentratio

The present results indicate that the temperature range over which the water isotherm is invariant is at least +3°C to +40°C (including the data described at chapter 2, reference 30). In addition, single point adsorption at -3°C and RH80% suggests that this range is greater still (the value was the same as those shown at table 9.2.1).

The effect of temperature on the PS adsorption isotherm was determined in much the same way as for the water isotherms (that is, dry filter beds were challenged in flowing air using a known concentration of PS until equilibrium was attained (ie. 100% filter penetration occurred). The quantities of PS adsorbed per gram of carbon were determined gravimetrically, and by integration. The values were in close agreement. The results (figure 9.2.2) typify the behaviour of organic compounds, where it is found that physical adsorption increases as the temperature is reduced.

Although the PS adsorption isotherm changes considerably between 22°C and -3°C, it is probable that the change in the capacity of the airstream for displaced water vapour over this range will be most important because this will affect the extent to which occlusion of the micropores by saturated water vapour (and hence the accessibility of these pores to the PS molecules) will take place (the difference between RH80% and RH100% is 4060 mg m^{-3} at 22°C: 1200 mg m^{-3} at 3°C, and 790 mg m^{-3} at -3°C).

Figures 9.2.3, 9.2.4, and 9.2.5 compare the effluent profiles for samples of BPL carbon challenged at 80% and 22°C, 3°C, and -3°C. The first parts of the PS breakthrough curves are at figure 9.2.6, and the breakthrough times, and quantities of PS adsorbed, and water displaced are at table 9.2.2. It is apparent from these results that PS filter performance improves significantly as the temperature is reduced. It is also notable that at +3°C and -3°C, essentially all of the preadsorbed water was displaced at the end of the experiment, and that there is no discontinuity in performance below the freezing point of water.

As the temperature is reduced, the slope of the PS breakthrough curve becomes progressively more shallow. At each temperature studied, the curves are distinctly biphasic, suggesting that the overall limitation on performance remains the transport and vapourisation of displaced water from the filter bed (9.1).

The improvement in performance (time to initial filter breakthrough) appears to be related to the exotherm observed during the initial part of the experiment (figures 9.2.3-5). The size of the exotherm increased as the temperature was reduced, presumably due to the change to the PS adsorption isotherm. Although the rate at which water is displaced will be lower at reduced temperatures, the increased localised heating of the filter bed due to PS adsorption may enhance water displacement, with the result that PS adsorption occurs more efficiently. It is also evident that this heating effect reduces the RH of the air thus delaying its saturation. These effects are reflected in the increasingly shallow nature of the PS breakthrough curves as the temperature was reduced (figure 9.2.6). At -3^{o}C, examination of a filter bed removed after the effluent airstream had reached saturation revealed that ice formation within the bed had taken place (the carbon was held rigidly within the filter until the temperature rose sufficiently for it to flow freely). Because PS adsorption was taking place at the time the filter was removed, it is likely that the displaced water accumulated within the intergranular spaces. Indeed, the improvement in performance with decreasing temperature could be explained equally well on the basis that as the temperature was reduced, displaced water accumulated preferentially within the intergranular spaces, where it initially had only a limited effect on the adsorption of PS, rather than within the transport pore structure, where the effect on the ease with which the PS molecules could access the micropore structure would be more marked. This contention is supported by the observation that at 3^{o}C and -3^{o}C, essentially all of the preadsorbed water was displaced from the filter bed at the end of the experiment (the most thermodynamically favourable position; table 9.2.2).

The results therefore suggest that the observed improvement in filter efficiency is a consequence of the change in the PS adsorption isotherm which gives rise to an increased local heat liberation, but also to the location of the displaced water (that is, whether pore occlusion results, preventing thermodynamic equilibrium being attained, or whether the water accumulates principally within the intergranular spaces where it has a more limited effect upon the overall behaviour of the filter).

It should be noted that the vapour adsorption apparatus was constructed such that cooling, or heating, of the influent air to the filter bed took place immediately prior to impingement of the flow onto the carbon. That is, air at 22°C was cooled to 3°C or -3°C. This process of adiabatic cooling therefore resulted in a volume (air) and hence concentration (PS) change. At -3°C, these effects equate to a 7% decrease in volume, and a 7% increase in PS vapour concentration. To ensure that these effects did not influence the behaviour of the filter, experiments were carried out where the volume flow rate (measured at a rotameter at ca. 22°C) was increased by 7%, and the PS concentration decreased by this amount. The results were found to be identical to those described above, indicating that under the experimental conditions employed in this study, the two effects balance.

Because the improvement in filter performance is clearly related to the nature of the PS isotherm, an alternative means of assessing the effect of temperature was investigated, whereby filters were challenged using a PS concentration that for dry carbon resulted in equivalent uptakes at each temperature (figure 9.2.2). Thus, filters were challenged at the same point on the PS isotherm. Figure 9.2.7 shows the effluent profiles measured using a PS concentration of 910 mg m^{-3} at +3°C (the comparable experiment, measured at the same point on the PS isotherm (at 22°C, using a PS concentration of 5000 mg m^{-3}) is at figure 9.2.3). Comparison of the results indicates that at +3°C, the breakthrough time is very much greater than at 22°C. This effect presumably results from the observation that the airstream failed to reach

saturation: that is, performance was not limited by the mechanism described above (9.1). That this mechanism was not operable at the lower temperature reflects the reduction in the amount of PS adsorbed per minute at the lower vapour concentration: the consequence of this was that the lower amount of displaced water could be carried away by the airstream more efficiently. The results of challenging filters at the same point on the PS adsorption isotherm are at table 9.2.3.

The above results probably represent the general case for filter beds challenged with volatile hydrophobic chemicals, and illustrate the complex relationship which exists between the kinetic adsorption performance of activated carbon filters and environmental parameters. It is apparent that there exists a fine balance as to whether the accumulation of displaced water results in pore blockage thus preventing the attainment of thermodynamic equilibrium, or whether the water accumulates in the intergranular spaces, where it has a more limited effect.

Table 9.2.1 Water Adsorption at 22°C and 3°C for Control BPL Carbon

Relative Humidity (%)	22°C Amount Adsorbed(w/w%)	22°C Eqm. Time (hours)	3°C Amount Adsorbed(w/w%)	3°C Eqm. Time (hours)
Adsorption				
30	1.7	5	2.2	5
40	3.0	6	3.7	13
50	7.1	16	7.5	27
60	16.7	13	16.2	27
70	29.0	16	27.7	26
80	35.8	13	35.4	16
85	38.2	5	37.8	9
90	40.0	5	39.6	7
95	41.5	5	41.4	8
Desorption				
90	41.1	4	41.0	5
85	40.9	2	40.1	3
80	40.2	7	39.7	7
70	37.8	4	38	5
60	35.8	4	36.1	6
50	26.5	25	28.5	41
40	6.7	24	9.6	60
30	3.6	13	5.1	31
0 (Dried)	0.3	-	0.2	-

Table 9.2.2 PS Adsorption and Water Displacement as a Function of Temperature (BPL Carbon)

Temp (°C)	PS Breakthrough Time (min)		Total PS Adsorbed (mg g^{-1})	Carbon Water Content (mg g^{-1})	
	1%	100%		Initial	Final
22	33	440	438	352	133
+3	76	690	643	354	12
-3	90	800	656	355	17

{5000 mg m^{-3} challenge, RH80%. The amounts of PS adsorbed by dry carbon at 22, 3, and -3°C were 583, 646 and 662 mg g^{-1} respectively}

Table 9.2.3 PS Breakthrough for BPL Carbon at 22°C and +3°C. Challenge at the Same Point on the PS Adsorption Isotherm

Relative Humidity (%)	Temperature (°C)	PS Challenge (mg m^{-3})	Breakthrough Time (1%, min)	Total PS Adsorbed (mg g^{-1})
95	22	5000	21	344
80	22	5000	33	438
<2	22	5000	134	583
95	+3	910	132	*
80	+3	910	312	*
<2	+3	910	609	581

*Experiments were not complete after 950 minutes challenge

FIGURE 9.2.1 WATER ADSORPTION FOR BPL CARBON
ISOTHERM DETERMINED AT ▲ 22°C AND ● 3°C

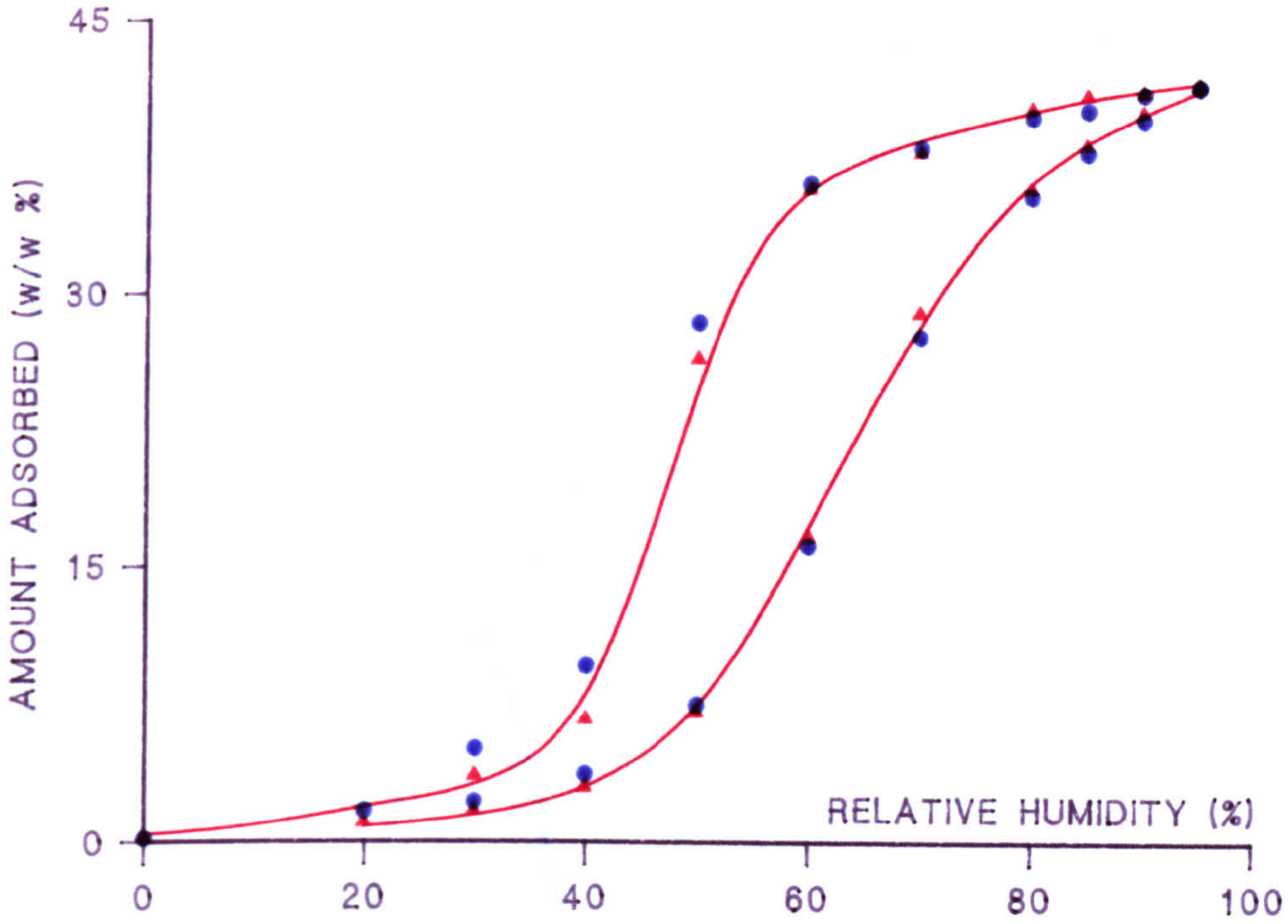

FIGURE 9.2.2 PS ADSORPTION ISOTHERMS
● −3°C ■ +3°C ▲ +22°C

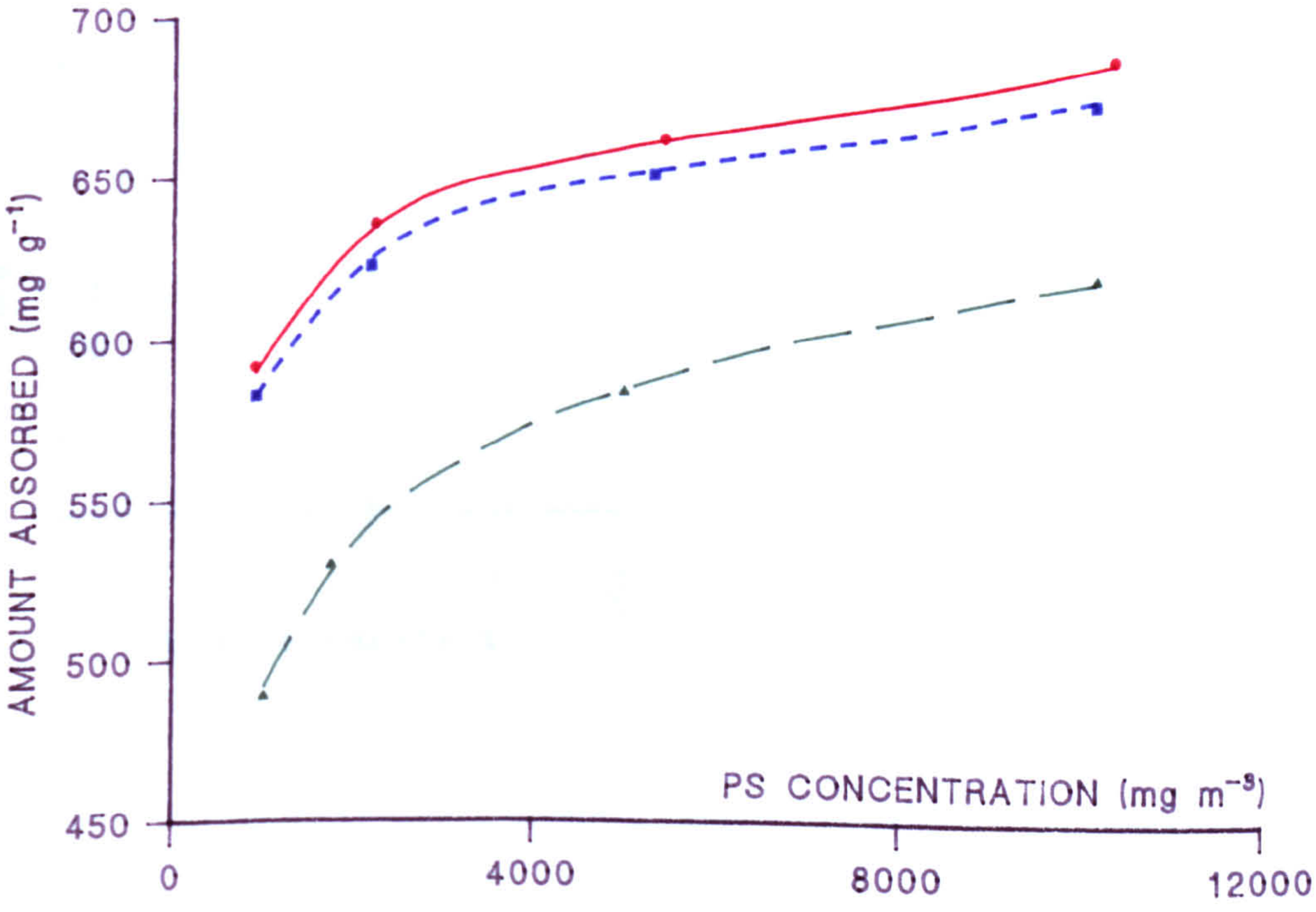

FIGURE 9.2.3 CHLOROPICRIN BREAKTHROUGH AND WATER DISPLACEMENT CURVES
(CONTROL BPL CARBON CHALLENGED AT RH80% AND 22°C)

[▵ PS; ○ TEMPERATURE; □ WATER (mg m^{-3}); ◇ TEMPERATURE CORRECTED RH]

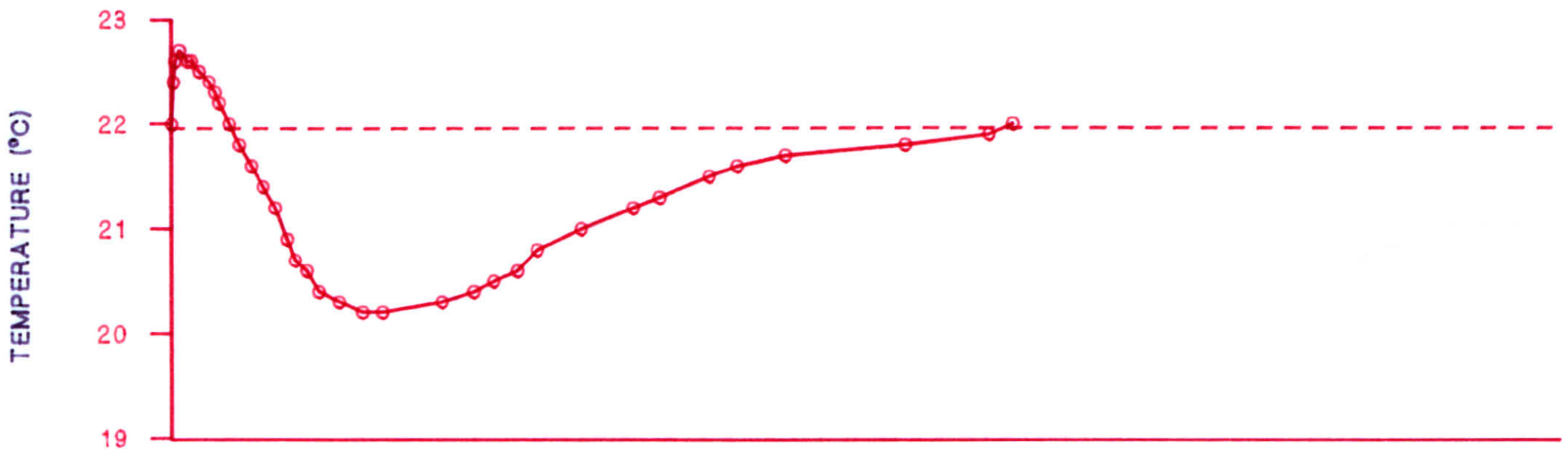

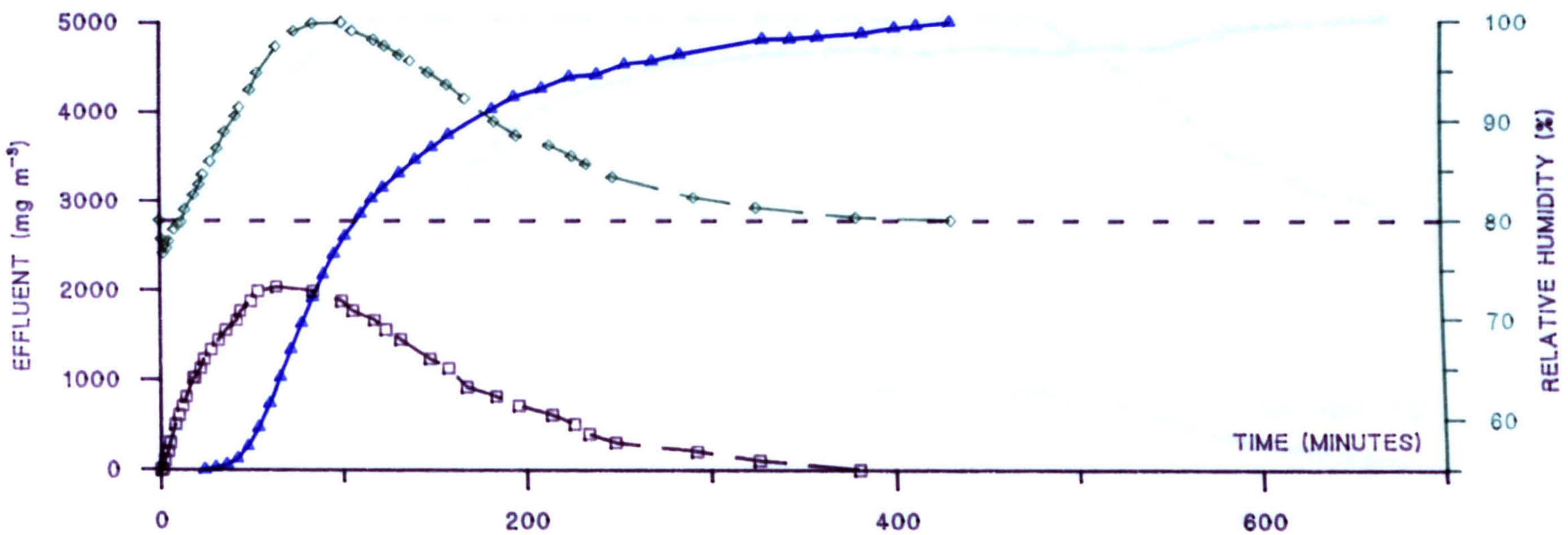

FIGURE 9.2.4 CHLOROPICRIN BREAKTHROUGH AND WATER DISPLACEMENT CURVES
{CONTROL BPL CARBON CHALLENGED AT RH80% AND 3°C}

[△ PS; ○ TEMPERATURE; □ WATER (mg m^{-3}); ◇ TEMPERATURE CORRECTED RH]

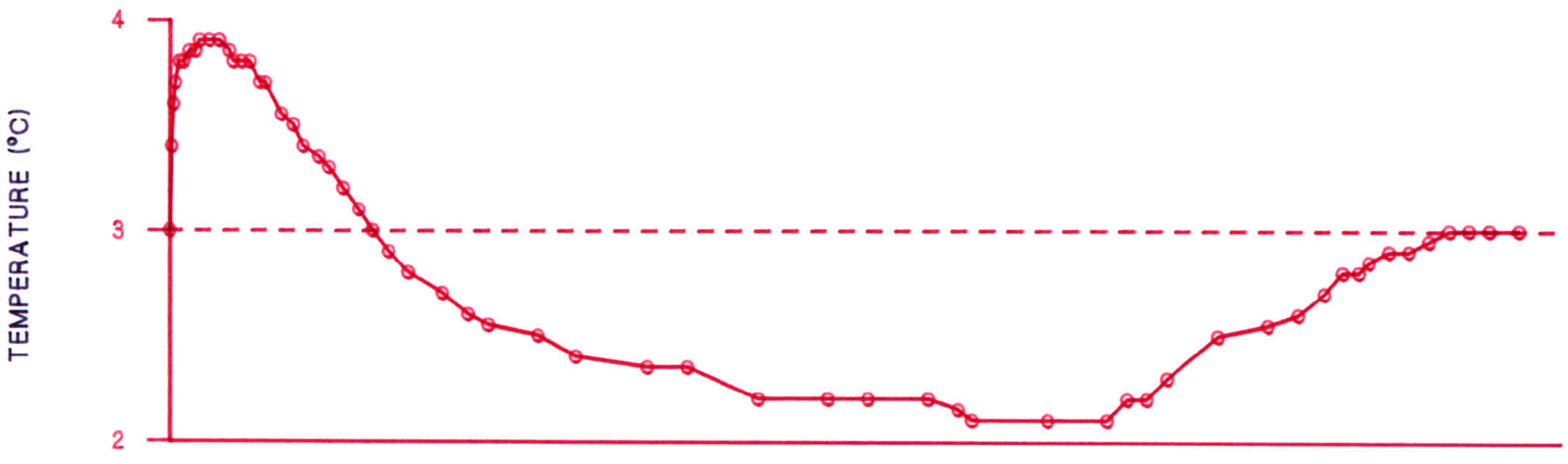

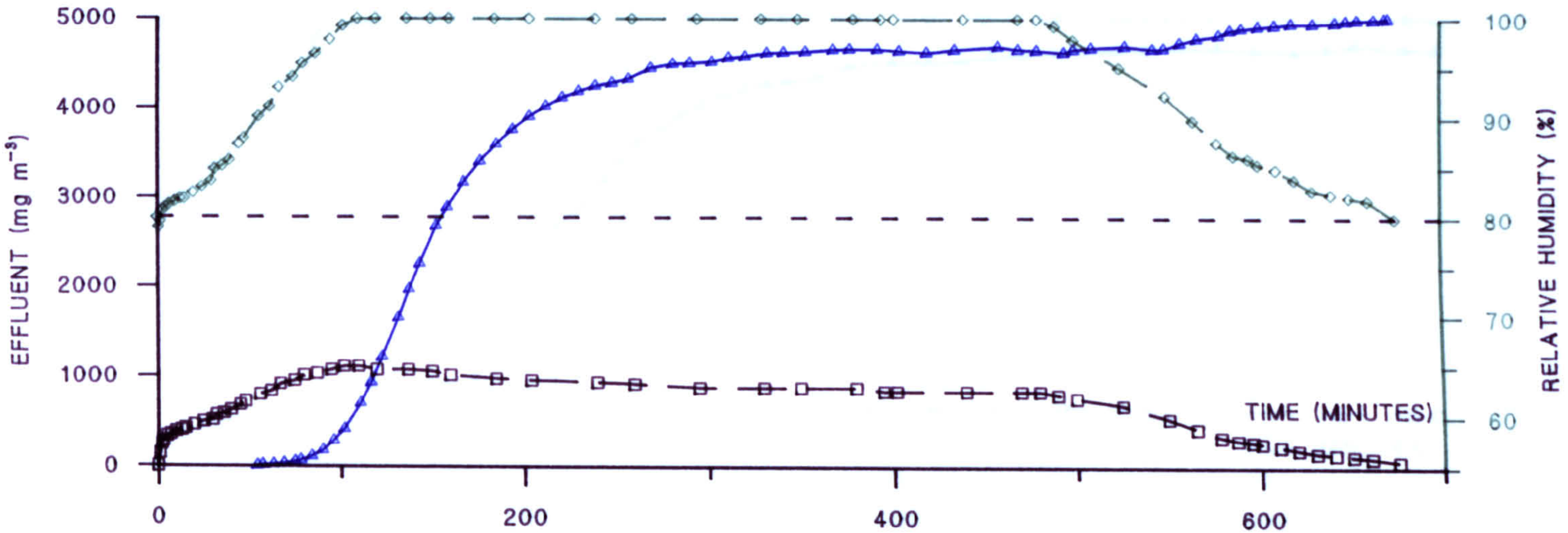

FIGURE 9.2.5 CHLOROPICRIN BREAKTHROUGH AND WATER DISPLACEMENT CURVES
{CONTROL BPL CARBON CHALLENGED AT RH80% AND −3°C}

[△ PS; ○ TEMPERATURE; □ WATER (mg m^{-3}); ◇ TEMPERATURE CORRECTED RH]

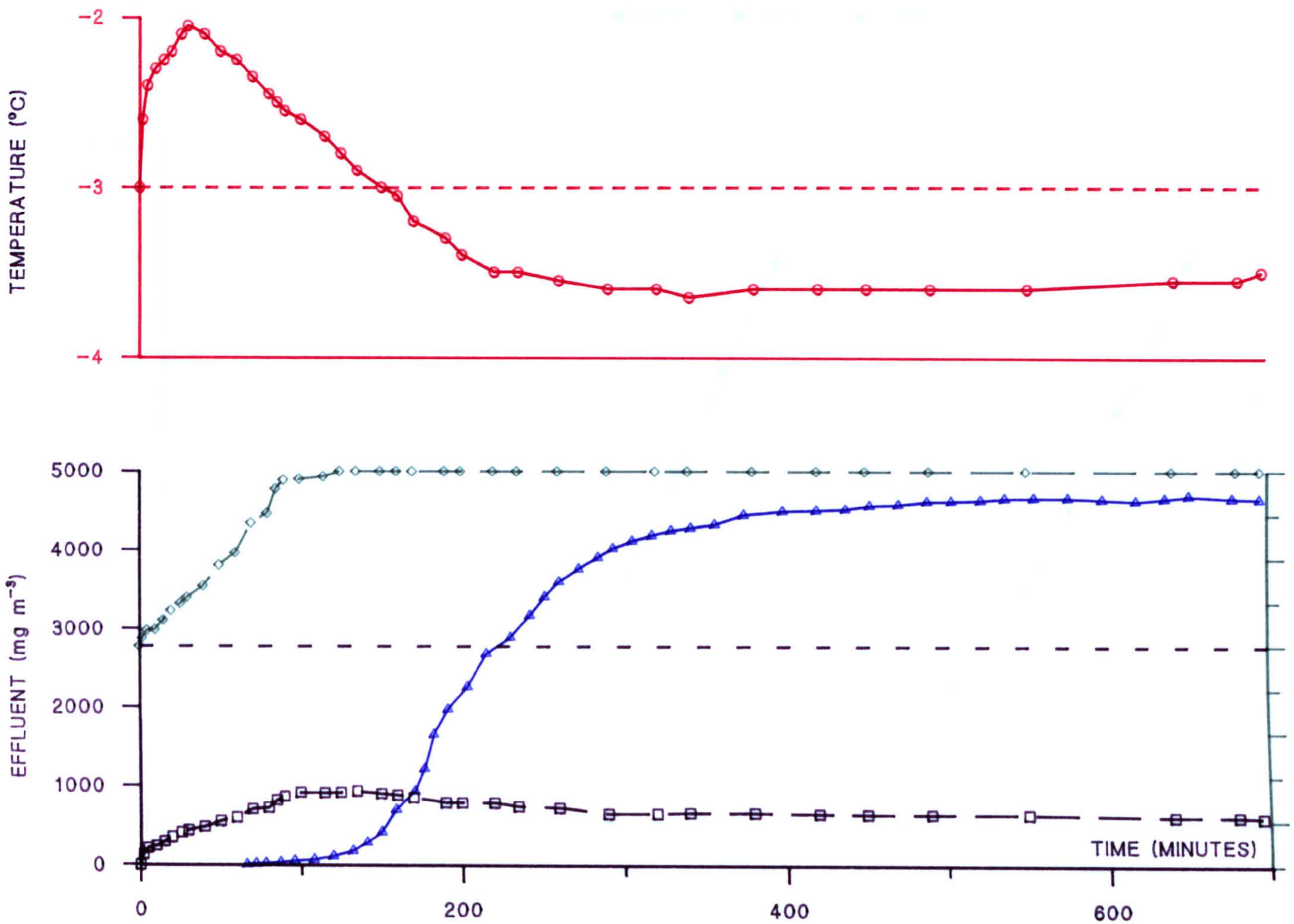

FIGURE 9.2.6 INITIAL BREAKTHROUGH OF PS AS A FUNCTION OF TEMPERATURE

■ 22°C ● +3°C ▲ −3°C

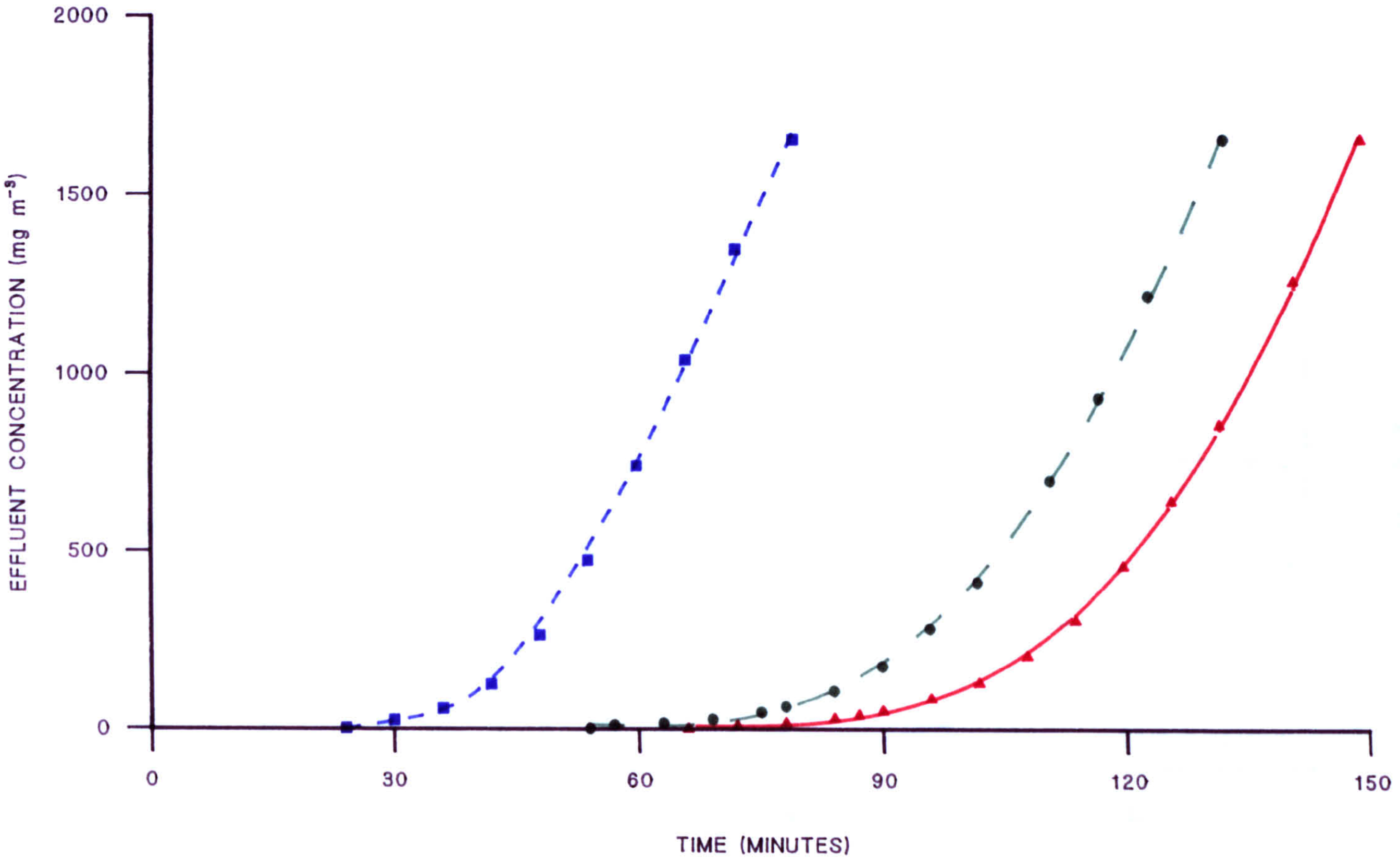

FIGURE 9.2.7 CHLOROPICRIN BREAKTHROUGH AND WATER DISPLACEMENT CURVES

{CONTROL BPL CARBON CHALLENGED AT RH80%, 3°C: PS CONCENTRATION= 910 mg m^{-3}}

[△ PS; ○ TEMPERATURE; □ WATER (mg m^{-3}); ◇ TEMPERATURE CORRECTED RH]

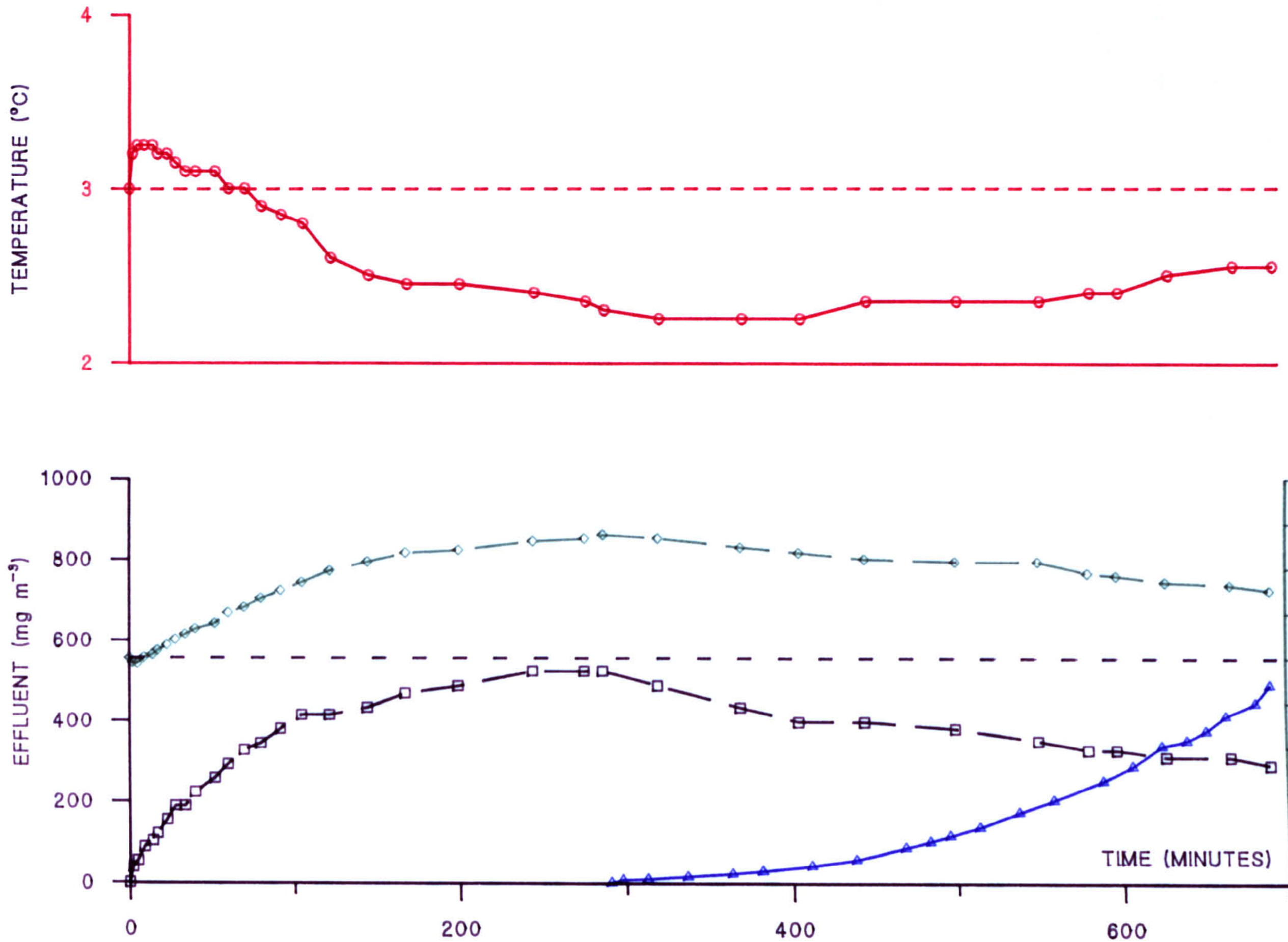

9.3 The Effect of the Carbon Pore Structure

During the course of this research, it was apparent that activated carbons derived from nutshells (control SCII and CECA), which were of a higher surface area (nitrogen adsorption- chapter 8, table 8.10) than the BPL carbon, performed comparatively less well against PS at high RH values. Under dry conditions, the efficiency of the nutshell carbons was, as expected, greater (table 9.3.1). This observation suggests that at high values of the equilibration and challenge RH, pore occlusion effects are more significant for the nutshell carbons. Indeed, α_s analysis (chapter 8, table 8.10) revealed that all the carbons used in this study were of very similar meso- and macro- pore volume (ca. 50 m^2g^{-1} external surface area), indicating that if the factor limiting filter performance is (micro) pore occlusion by displaced water vapour (9.1), then the nutshell carbons must perform proportionally worse compared with BPL carbon. That this is the case indicates the importance of the transport pore structure in controlling filtration efficiency.

The observations also suggest that enlargement of some of the pores (that is, increasing the meso- and macro- pore volume) may result in improved filter performance (9.1).

An alternative interpretation is that the nutshell based carbons do not contain predominantly slit shaped pores (as is believed to be the case with BPL carbon): rather, that they contain pores with constricted entrances (eg. ink bottle pores). It would be expected that such pores would be more readily occluded by displaced water than those of the slit shaped type.

On the presumption that the limitation on filter efficiency is due to a less efficient transport pore network, attempts were made to enlarge the meso- and macro- pore structure by use of a mild oxidant.

Carbon samples (BPL and SCII) were treated with NO_2 at a pressure of 900 mbar (as described at chapter 6), before, or after, preadsorption of nonane (Appendix). Nonane was used in an attempt to occlude the micropores from the oxidant, such that reaction occurred preferentially in the larger pores.

After exposure to NO_2 for approximately 22 hours, the carbons were outgassed at ca. 950°C (1 mbar). High temperature outgassing was employed to remove the preadsorbed nonane, and to decompose the surface oxygen containing groups generated during oxidation. It was presumed that the decomposition of these groups would result in some gasification of the carbon. Gasification of carbon from within the pore structure may then result in pore enlargement. The control experiment (without nonane preadsorption) was carried out in the same way.

Table 9.3.2 shows the weight changes associated with the treatment stages described above. It is apparent that significant gasification occurred when either carbon was used, but that the loss was more substantial for BPL. Nitrogen adsorption (table 9.3.3, figures 9.3.1-2) indicates that oxidation resulted in a reduction in BET surface area. This was due to a loss of microporosity. The proportion of meso- and macro- pores remained essentially unchanged, suggesting that the oxidation mechanism involved a loss of these pores by gasification, followed by enlargement of some of the micropores. It may be that the proportion of meso- and macro- pores represents the maximum value for the carbons used in this study. The results also indicate that nonane did not effectively mask the micropores during oxidation. Examination of the PS adsorption data supports the contention that the volume of the transport pores has a critical impact on the performance of activated carbon filters (table 9.3.3). That is, the significant reductions in the micropore volume (table 9.3.3) resulted in only a small change in performance.

Analysis of the carbons using mercury porosimetry supports the view that the control and modified carbons contained a very similar meso- and macro-pore size distribution in the range that could be studied. Examination of the porosimetry data did, however, reveal that the BPL carbon contained proportionally more smaller macropores, and the SCII carbon proportionally more larger macropores (figure 9.3.3). Thus it may be that the smaller macropores are most important for the storage and transport of displaced water vapour.

Previous studies using a combination of vapour adsorption measurements and mercury porosimetry (chapter 4, reference 46) indicated that carbons with a small and unevenly distributed mesopore structure offered less protection under humid conditions than those carbons possessing a broad and even meso- and macro- porosity in the range 5 to 100 nm. Both of the carbons used in this part of the study contained a similar, and relatively even, pore size distribution in this range (figure 9.3.3).

It may also be the case that the method used to oxidise the carbons was too severe. Alternatively, it is possible that during outgassing, the desorbing oxygen containing complexes had a catalytic action, resulting in non-localised gasification.

A more promising approach may involve study of the possibility of modifying pore shape. It has been demonstrated (chapter 4, reference 71) that this can have a dramatic influence on the water adsorption properties of an adsorbent. In this example, the adsorbent (Silicalite) was shown to possess a tubular, rather than slit shaped, pore network. Packing limitations of water molecules within the tubular pores were such that only small quantities were adsorbed, even at saturation. This would presumably place little or no limitation on filtration efficiency, because the complete pore space would be available for the adsorption of the organic vapour.

Table 9.3.1 PS Adsorption for BPL (Coal Based) and CECA (Nutshell) Carbons

Sample	Relative Humidity (%)	Carbon Water Content (%)	Nitrogen BET $m^2 g^{-1}$ (STP)	Breakthrough Time (1%)
BPL	80	35.4	1208	33
CECA	80	47.6	1460	24
BPL	<2	-	-	134
CECA	<2	-	-	154

{The same trend was observed for SCII carbon}

Table 9.3.2 Pore Modification of BPL and SCII Carbons

Treatment	BPL (%w/w, initial carbon weight)	SCII (%w/w, initial carbon weight)
1] Outgas, 950°C, 4 hours, vacuum	-2.1	-1.6
2] Preadsorb nonane	+22.2	+28.3
3] Preadsorb nonane, outgas 950°C, 4 hours, vacuum	-24.4	-
4] Treat NO_2 (900 mbar), outgas 30°C	+36.8	+36.1
5] Preadsorb nonane, treat NO_2, outgas 30°C	+30.6	+38.3
6] 4] + 1]	-7.1	-2.5
7] 5] + 1]	-8.4	-2.1

Table 9.3.3 PS and Nitrogen Adsorption for Pore Modified BPL and SCII Carbons

Sample and Treatment	Nitrogen Adsorption			PS (1st break, min)
	BET Area (m^2g^{-1})	Pore Vol. ($cm^3<STP>g^{-1}$)	Meso/Macro porosity (%)	
SCII Control	1440	0.58	7	72
BPL Control	1208	0.53	15	83
SCII 4] + 1]*	1340	0.55	8	63
BPL 4] + 1]*	964	0.48	14	90
SCII 5] + 1]*	1350	0.55	9	66
BPL 5] + 1]*	1050	0.50	14	84

{*Refer to table 9.3.2. 1st break is 5-10 mg m^{-3}. 2cm carbon beds were used for these determinations. The other experimental parameters were as described above (9.1). The nitrogen adsorption data is tabulated at the Appendix.}

FIGURE 9.3.1 NITROGEN ISOTHERMS FOR BPL CARBON

● CONTROL ▲ NONANE PREADSORBED, NO_2 MODIFIED AND OUTGASSED

■ NO_2 MODIFIED AND OUTGASSED

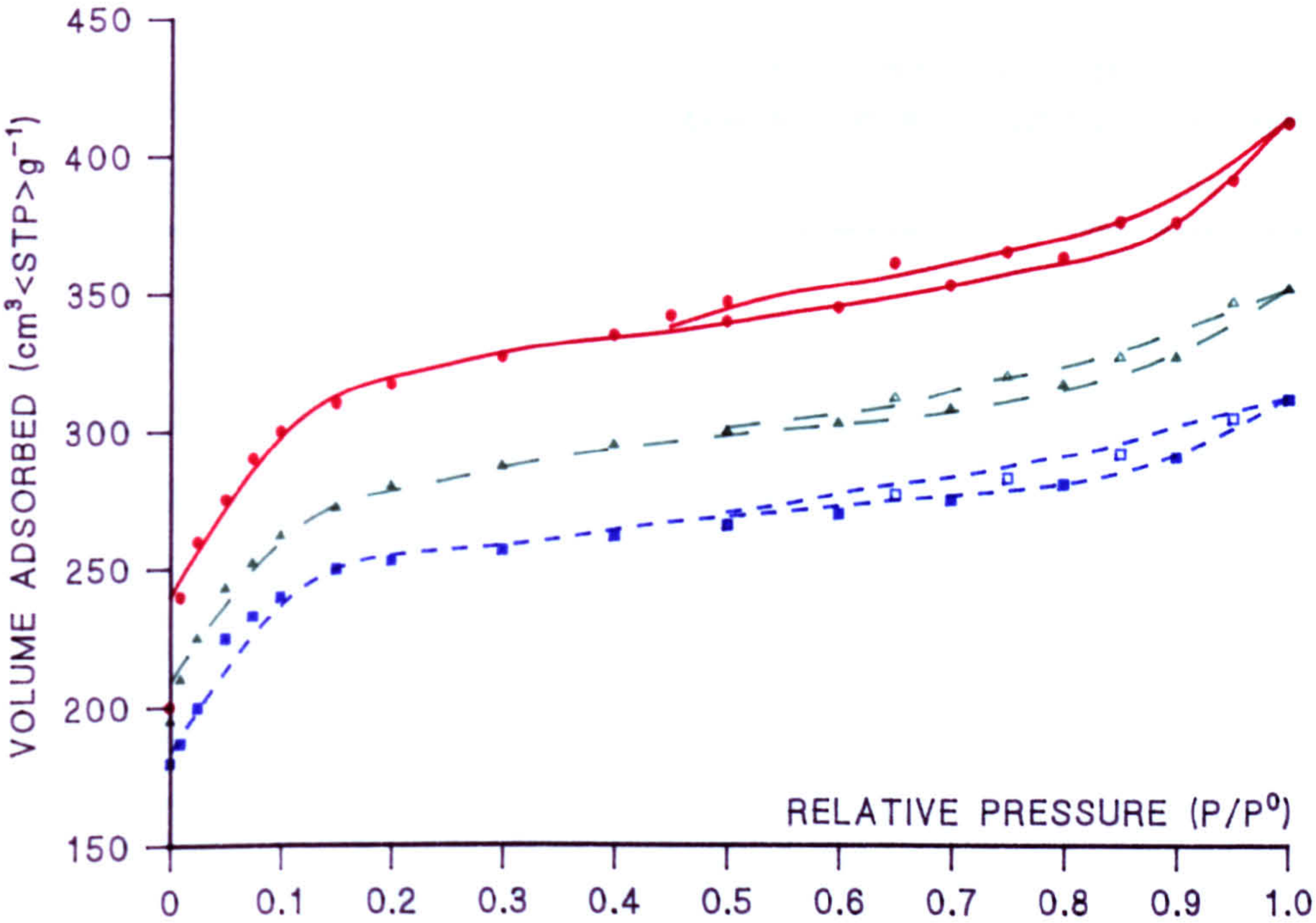

FIGURE 9.3.2 NITROGEN ISOTHERMS FOR SCII CARBON

● CONTROL ▲ NONANE PREADSORBED, NO_2 MODIFIED AND OUTGASSED

■ NO_2 MODIFIED AND OUTGASSED

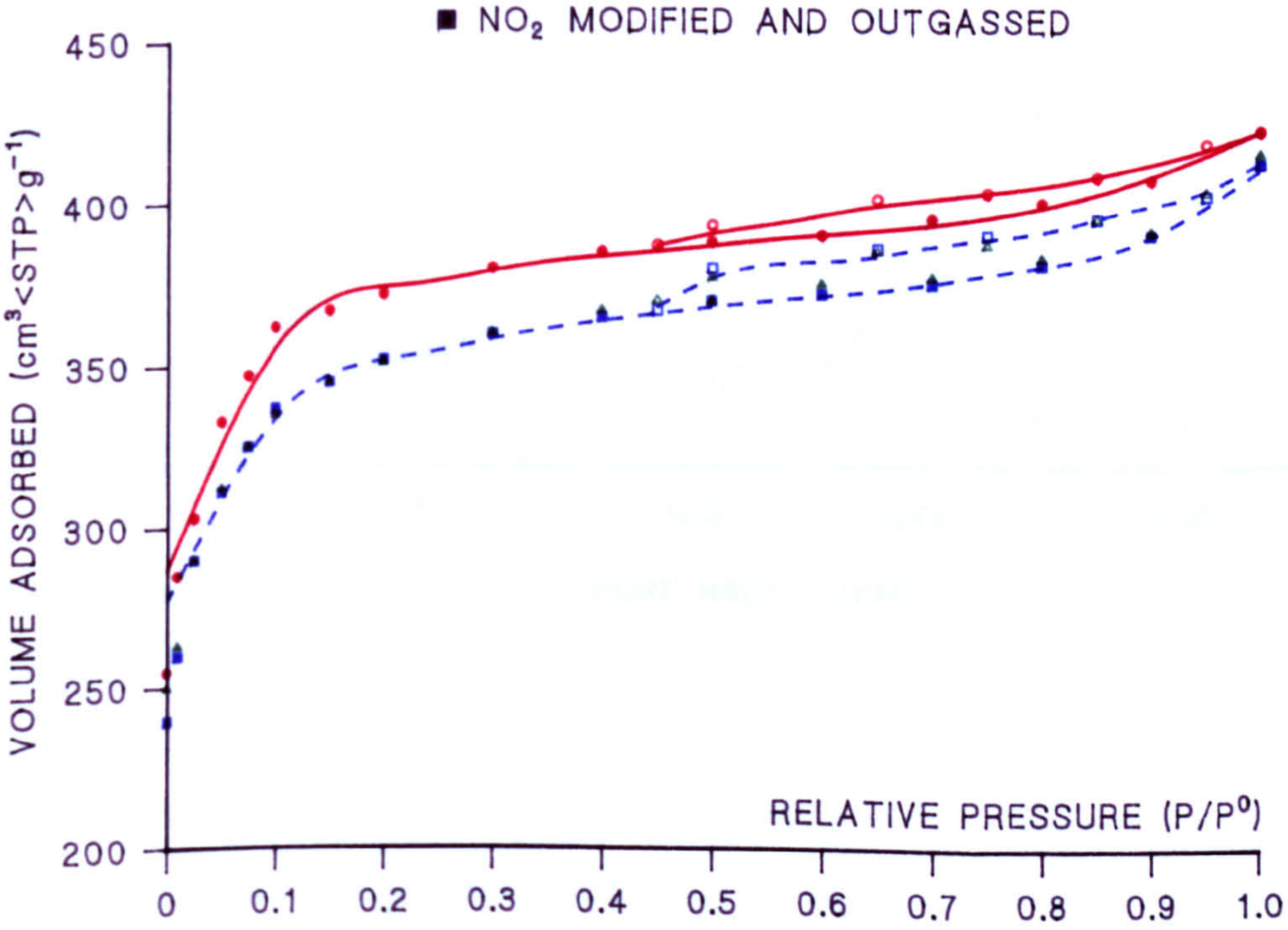

FIGURE 9.3.3 MERCURY POROSIMETRY
(RED) CONTROL BPL CARBON; (BLUE) CONTROL SCII CARBON

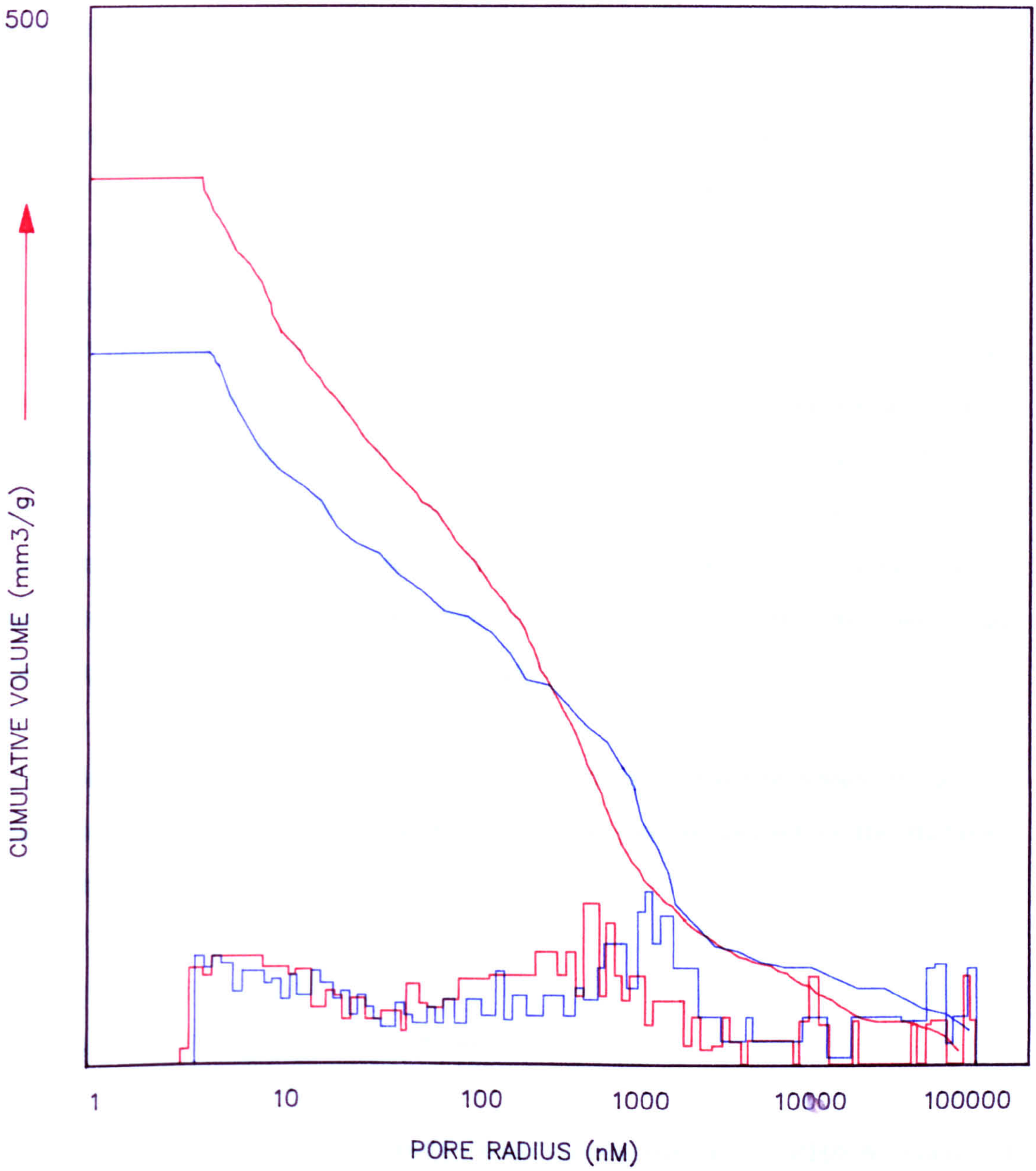

9.4 The Effect of the Surface Chemistry on Adsorption

Because the adsorption of PS at high RH depends to some extent on the rate at which preadsorbed water is displaced from the carbon, the surface chemistry of the adsorbent must inter alia also have some impact upon filter performance. This has been shown to be the case for BPL carbon which had been aged by exposure to RH80% air at 22°C or to dinitrogen tetroxide (NO_2) at ambient temperatures (chapter 6). In these examples, the polarity of the carbon surface was increased in comparison to control samples, as shown by methanol and water adsorption. In both cases, little or no structural modification occurred (nitrogen and hexane adsorption). The reduction in filter efficiency at high RH must therefore be a consequence of the presence of additional polar surface oxygen containing functional groups. Conversely, modification of carbons using some fluorinating and chlorinating reagents (chapter 7, fluorination; chapter 8, chlorination) results in an increase in the hydrophobic character of the surface. In these examples, PS adsorption efficiency was found to be improved in comparison to the respective controls.

Based upon the observations described above, complete breakthrough measurements have been made to determine the overall impact of the surface chemistry on the behaviour of carbon filters.

9.4.1 Aged and NO_2 Modified Carbons

Figure 9.4.1 shows the breakthrough measurements (at RH80%) made for a sample of BPL carbon which had been aged by exposure to RH80% air at 22°C for 800 days. The quantity of water adsorbed at equilibrium was essentially the same as that for the control (figure 9.1.4, table 9.4.1). The effluent profiles for the aged carbon were found to be similar to those described in 9.1 (the maxima

and minima in the curves were the same), except that the initial breakthrough of PS, the point where the effluent temperature intersects 22°C and where it attains a minimum value, are all displaced to shorter times (by approximately 18 minutes). It was also found that the aged carbon adsorbed about 15% less PS at equilibrium, but that the quantity of water displaced was the same as that for the control (table 9.4.1). These differences are interpreted in terms of the difficulty with which preadsorbed water is displaced from the aged carbon by PS, although this may not appear to be valid at first sight. That is, if as is likely, the adsorption of a fixed amount of PS requires the displacement of the same quantity of water from both control and aged samples, and if water displacement from the surface of the aged carbon is less energetically favourable (because the adsorption energy of water is greater), then PS will, as is found, break through the bed of aged carbon comparatively more quickly. This indicates that the PS adsorption wave traverses the bed of aged carbon more rapidly, suggesting that, because in a given time (and before PS breakthrough) both the control and aged carbons will have adsorbed the same quantity of PS resulting in the displacement of the same amounts of water, there will be less scope for displaced water to be readsorbed on the aged carbon, with the consequence that the effluent water vapour concentration will rise more rapidly (as is observed). For both carbons, the maximum effluent water concentration is the same (the effluent RH reaches saturation) indicating that the same mechanism (9.1) limits the overall performance of both carbons. That proportionally more water is ultimately displaced from the aged carbon (table 9.4.1) reflects the reduced scope for its readsorption, and the fact that control carbon pre-equilibrated at RH80% can adsorb water more quickly (and to a greater extent) from air of a higher humidity. This is apparent from figure 9.4.2, which shows the first parts of the water breakthrough curves for control and aged carbons which had been equilibrated at RH80% and 22°C, then challenged with RH90% air at 22°C.

Comparison of the results of challenging samples of control and aged carbons at RH65% (figure 9.4.3 compare figure 9.1.3) illustrates that the polar

surface functional groups have a considerable impact on filter performance at lower RH values. The general pattern at RH65% is similar to the experiment at RH80%, except that the air has a greater capacity to carry away the displaced water. As a consequence, the water displacement curve reaches a greater maximum (ca. 2900 mg m^{-3}) and the effluent temperature a greater minimum (about $3^{o}C$ below influent). For the aged carbon, not all of the preadsorbed water had been displaced by the end of the experiment (table 9.4.1). It should be noted, however, that the aged carbon contained significantly more preadsorbed water at RH65% compared to the control sample. This is a consequence of the change to the water adsorption isotherm which results from ageing (chapter 6). Figure 9.4.4 shows the effluent profiles measured for a sample of the aged carbon at RH40%. In this example, all of the preadsorbed water was displaced, and the energy balance was such that a small depression in the effluent temperature was observed. This effect was not found for a sample of control carbon (figure 9.1.2), although in this case, the equilibrium carbon water content was lower (table 9.4.1; and chapter 6).

In the examples described above, the presence of polar functional groups on the carbon surface are shown to have a major impact on filter performance, presumably as a result of kinetic limitations on water displacement (and hence PS adsorption). The overall filter performance at high RH (eg. 80%) is controlled by the same limiting mechanism found for the control sample (9.1). On this basis, it would be anticipated that a further significant reduction in filter efficiency would be observed by increasing the number of polar functional groups. Thus, carbons modified using NO_2 were challenged at RH80% as described above (9.1). The results (NO_2 treated, 900 mbar pressure; figure 9.4.5, table 9.4.2) confirm the critical effect that polar surface functional groups have on the adsorption of volatile hydrophobic compounds from high humidity air. As before, the differences are attributed only to the number of polar groups, because little or no structural disruption resulted from modification (chapter 6).

9.4.2 1,1-Difluoroethene (DFE) Modified Carbons

Modification of BPL or nutshell carbons using DFE resulted in an increase in hydrophobic character compared to control samples (ie. the surface contained fewer polar adsorption centres). This was shown to be the case from methanol and water adsorption measurements (chapter 7). As before, the modification was not found to result in significant disruption of the carbon pore structure. The quantity of water on the filter bed at RH80% was reduced compared to the control carbon and the carbon modified with NO_2 (table 9.4.2). This was a consequence of the displacement of the pore filling region of the water isotherm to higher values of the RH because of the reduction in the number of polar adsorption centres (chapter 7).

On the basis that the initial breakthrough of PS through the filter at high RH is controlled by the surface chemistry of the carbon, the observed improvement in performance for the DFE carbon is predictable (figure 9.4.6). The effect of modification is to displace the various events taking place on the filter bed during adsorption to longer times (9.1, 9.4). The improvement probably reflects a combination of the ease with which the preadsorbed water is displaced, and the fact that the displaced water can be readsorbed further along the filter bed during the initial part of the experiment. As before, the overall process of PS adsorption is controlled by the limitation on the displacement and vaporisation of preadsorbed water from the filter bed.

The effects described above for the DFE modified carbon were also observed for samples of chlorinated and washed carbons (chapter 8) to a lesser or greater degree, depending upon the precise effect that the modification had on the hydrophobic character of the carbon surface.

The observations therefore illustrate the importance of the surface chemistry on filter efficiency, and the measurement of complete breakthrough curves at high RH indicates that it is the displacement and vaporisation of preadsorbed water from the carbon, and not the surface chemistry, that limits filter performance. The surface chemistry is shown to be important, however, in controlling, to some extent, the initial breakthrough of PS through the filter.

Table 9.4.1 The Amounts of PS Adsorbed and Water Displaced by Samples of Control and Aged BPL Carbons as a Function of the Equilibration and Challenge RH

Carbon Weight (dry, g)	Test RH (%)	PS Adsorbed (mg g^{-1})	Water Desorbed (mg g^{-1})	Carbon Water Content (mg g^{-1})	
				Initial	Final
1.754 (C)	95	344	78	414	336
1.755 (C)	80	438	219	352	133
1.746 (A)	80	372	225	354	128
1.758 (C)	65	593	203	206	3
1.754 (A)	65	447	262	294	32
1.743 (C)	40	584	19	22	3
1.726 (A)	40	546	64	62	2
1.742 (C)	<2	583	-	-	-
1.734 (A)	<2	544	-	-	-

{C= Control carbon; A= Aged Carbon (800 days; RH80%; 22°C)}

Table 9.4.2 PS Adsorption for DFE and NO_2 Modified Carbons at RH80% and 22°C

	DFE Carbon	NO_2 Carbon	Control
Sample Weight	1.759	1.746	1.755
PS Adsorbed (mg g^{-1})	392	384	438
Water Displaced (mg g^{-1})	196	251	219
Carbon Water Content (mg g^{-1})			
Initial	319	362	352
Final	123	111	133
PS Breakthrough (1% Break, min.)	41	14	33
PS Breakthrough (100%, min.)	320	530	440

FIGURE 9.4.1 CHLOROPICRIN BREAKTHROUGH AND WATER DISPLACEMENT CURVES
{AGED BPL CARBON CHALLENGED AT RH80% AND 22°C}

[△ PS; ○ TEMPERATURE; □ WATER (mg m^{-3}); ◇ TEMPERATURE CORRECTED RH]

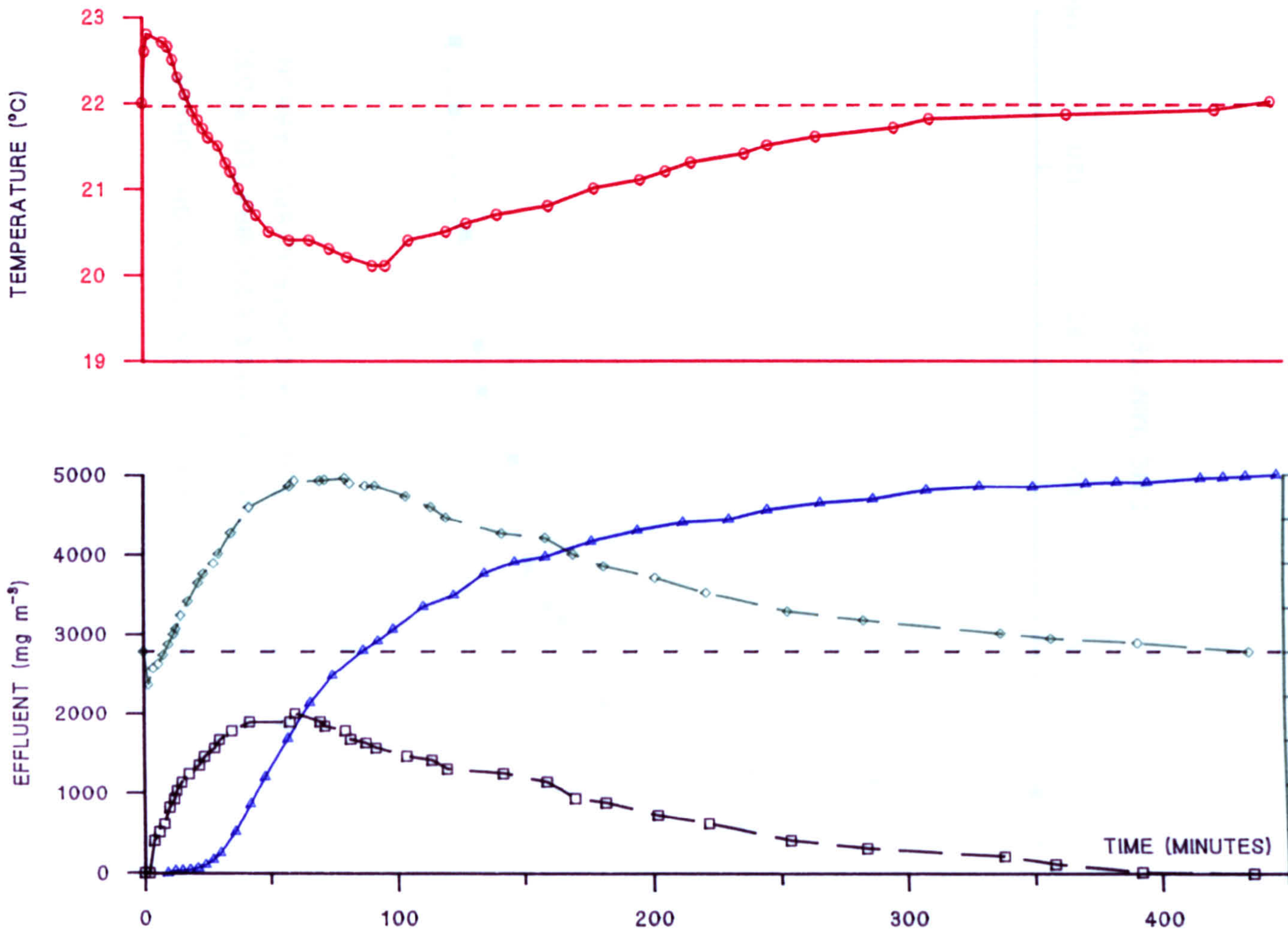

FIGURE 9.4.2 WATER BREAKTHROUGH CURVES

{RH90% CHALLENGE ON RH80% EQUILIBRATED BEDS}

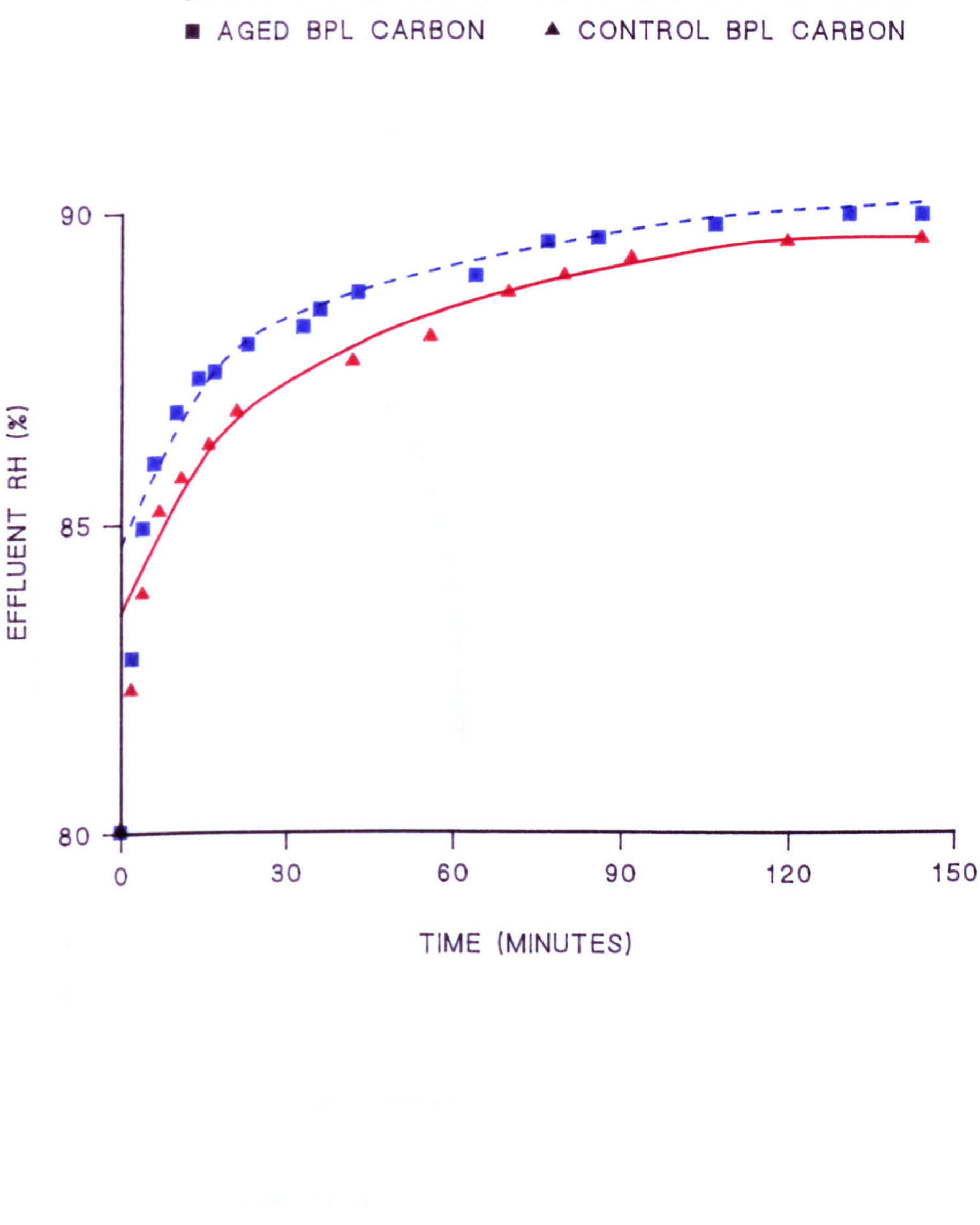

FIGURE 9.4.3 CHLOROPICRIN BREAKTHROUGH AND WATER DISPLACEMENT CURVES
{AGED BPL CARBON CHALLENGED AT RH65% AND 22°C}

[△ PS; ○ TEMPERATURE; □ WATER (mg m^{-3}); ◇ TEMPERATURE CORRECTED RH]

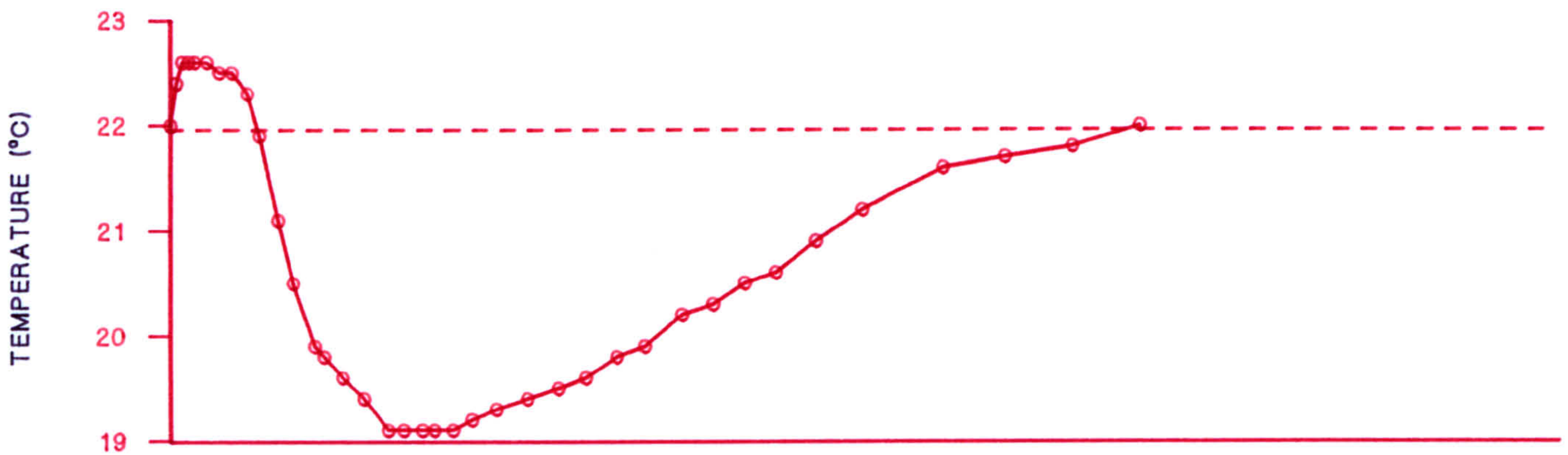

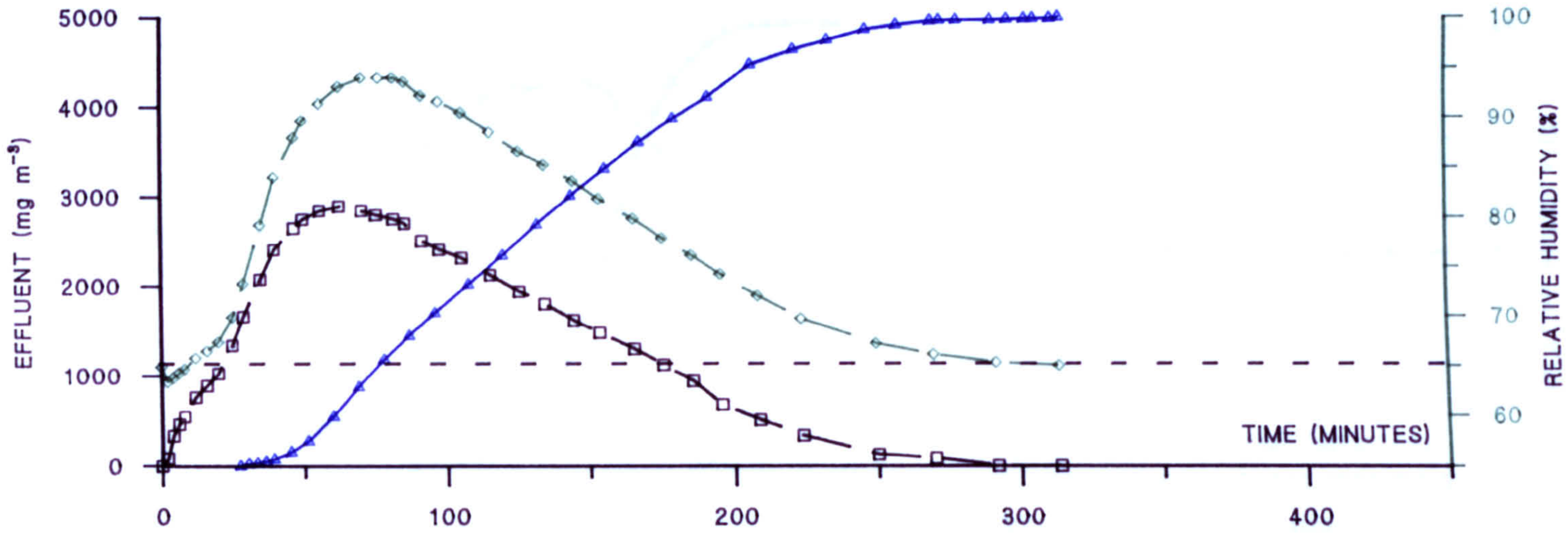

FIGURE 9.4.4 CHLOROPICRIN BREAKTHROUGH AND WATER DISPLACEMENT CURVES
{AGED BPL CARBON CHALLENGED AT RH40% AND 22°C}

[△ PS; ○ TEMPERATURE; □ WATER (mg m^{-3}); ◇ TEMPERATURE CORRECTED RH]

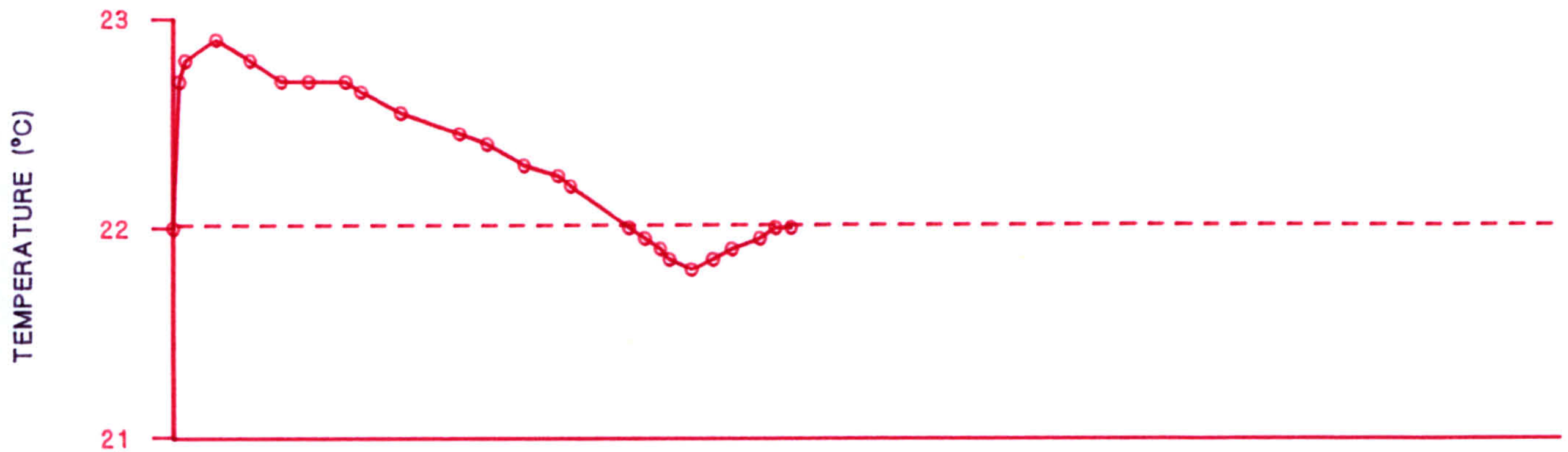

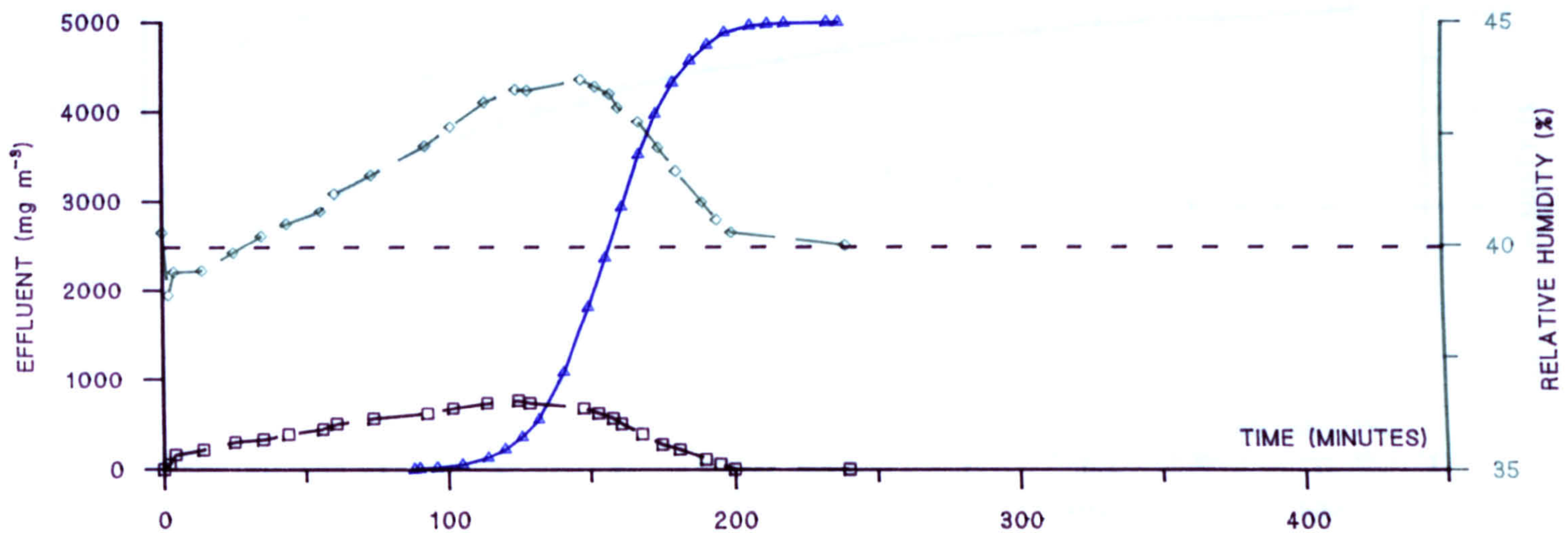

FIGURE 9.4.5 CHLOROPICRIN BREAKTHROUGH AND WATER DISPLACEMENT CURVES

{NO_2 MODIFIED BPL CARBON CHALLENGED AT RH80% AND 22°C}

[△ PS; ○ TEMPERATURE; □ WATER (mg m^{-3}); ◇ TEMPERATURE CORRECTED RH]

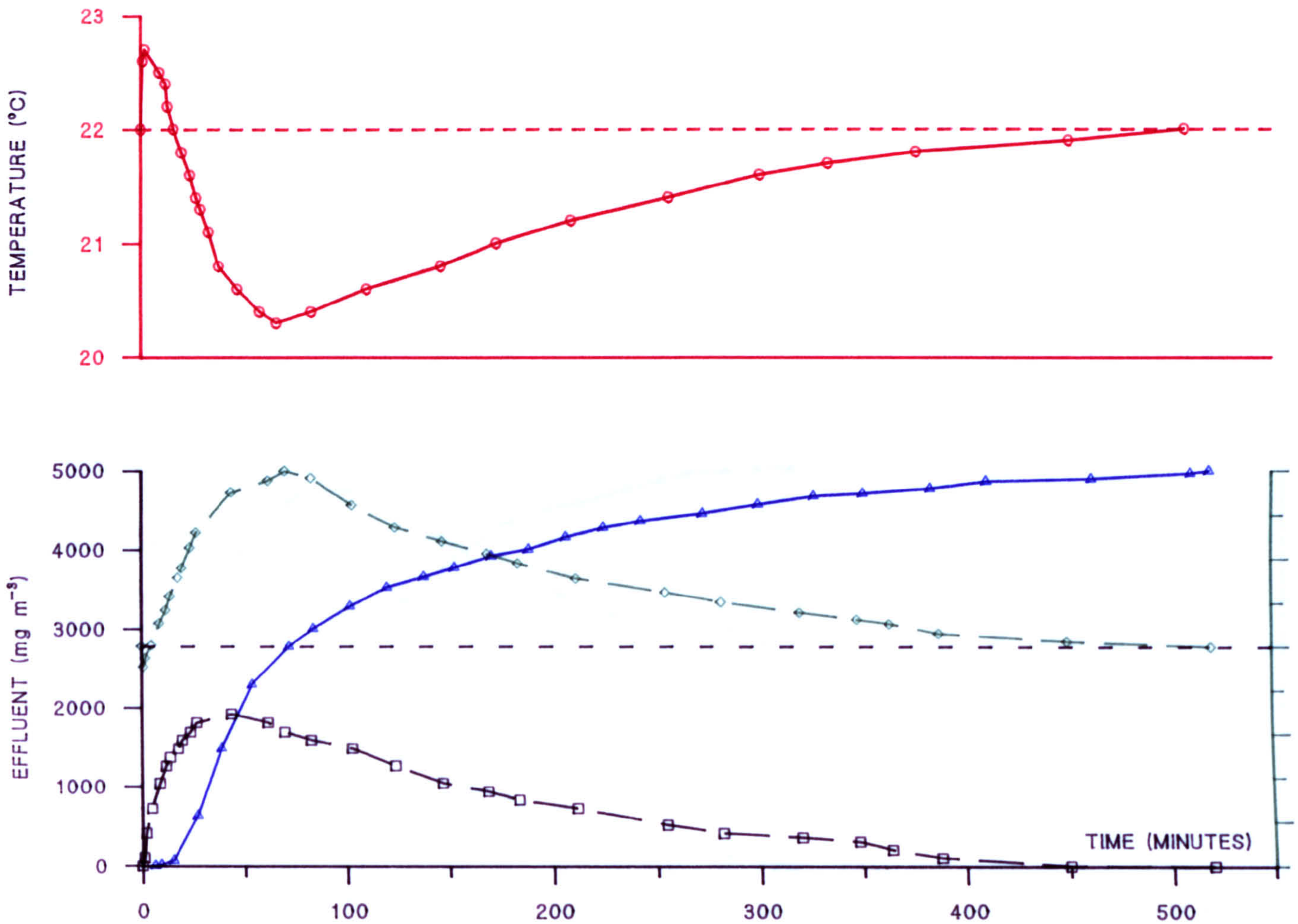

FIGURE 9.4.6 CHLOROPICRIN BREAKTHROUGH AND WATER DISPLACEMENT CURVES
{DFE MODIFIED BPL CARBON CHALLENGED AT RH80% AND 22°C}

[△ PS; ○ TEMPERATURE; □ WATER (mg m^{-3}); ◇ TEMPERATURE CORRECTED RH]

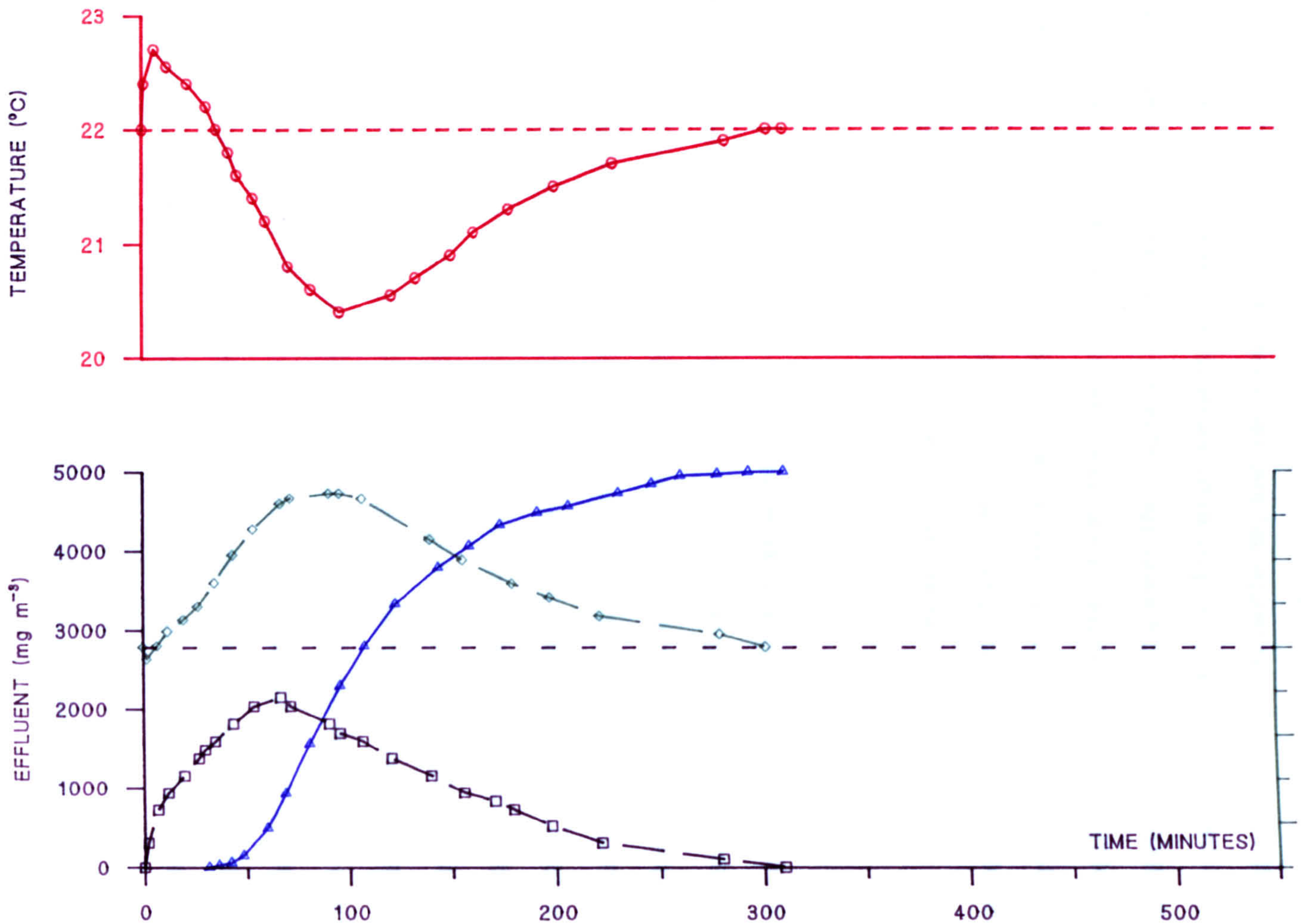

9.5 Summary

The efficiency of chloropicrin (PS) adsorption from a flowing airstream by beds of control BPL activated carbon decreases as the equilibration and challenge RH is increased. This loss of performance is due to limitations on the transfer of preadsorbed water from the pore structure, and the efficiency with which it is carried away by the airstream. At high values of the RH (eg. 80% and above) the overall process of PS adsorption and water displacement is notably endothermic, and the displaced water that cannot be carried away immediately by the airflow (it reaches saturation) occludes the micropore structure, limiting the rate at which PS is adsorbed. At the end of the experiments performed at high RH values, significant quantities of preadsorbed water remained on the filter beds. The adsorption process is therefore limited by kinetic, rather than thermodynamic aspects. It was also apparent that the quantity of preadsorbed water on the filter bed is more critical in this respect than the RH of the challenge airstream.

Reducing the temperature does not affect the equilibrium water adsorption properties of BPL activated carbon, but the quantity of PS adsorbed increased. Challenging filters using the same concentration of PS at RH80% revealed that the performance improved, even though the capacity of the airstream for carrying away the displaced water was significantly reduced at the lower temperatures. The improvement is interpreted in terms of the change in the PS adsorption isotherm, and the location of the displaced water. That is, because the amount of PS adsorbed is increased at reduced temperature, increased local heat liberation during the initial part of the experiment occurs, which delays saturation of the airstream. In addition, at the lower temperatures, essentially all of the preadsorbed water was displaced by PS, indicating that the water did not occlude the micropores as significantly than at

22°C: rather, the water probably remained in the intergranular spaces until it could be carried away by the airstream, and where it had a smaller impact on the efficiency of PS adsorption.

Challenging filters at the same point on the PS isotherm (such that the uptake by dry carbon beds was the same at each temperature) did not result in similar breakthrough curves, because the limiting case (pore occlusion by displaced water) was not observed at the lower temperatures. Although the capacity of the airstream for displaced water was reduced as the temperature was decreased, less water was displaced per minute because a lower PS concentration was used. Thus the breakthrough times under these conditions increased substantially. The results show that there is a complex relationship between the kinetic adsorption performance of activated carbon filter beds and environmental parameters. In particular, the displacement of preadsorbed water is critical. In such cases, there is a fine balance as to whether the build up of displaced water results in pore blockage thus preventing the system reaching thermodynamic equilibrium, or whether build up occurs in the intergranular spaces where it has a more limited effect on filter performance.

The structure (porosity) of the carbon also affects the efficiency with which filters function at high RH. Nutshell carbons were found to adsorb PS more efficiently than coal based BPL carbon under dry conditions because they were more microporous (higher BET surface area). Under humid conditions, the nutshell carbons performed proportionally less well than the coal based carbon. This effect is probably due to the fact that more significant pore occlusion occurred for the nutshell carbons, which were of a similar meso- and macro-pore volume (transport pore volume) to the BPL carbon. It may also be the case that the nutshell carbons contained different shaped micropores (eg "ink bottle" types) which were blocked more readily by displaced water. Attempts to enlarge the volume of the transport pores by selective oxidation were not successful, suggesting that the either the oxidation conditions were too severe, or that the

volume of these pores originally present represents a maximum value. It is probable that further improvements in the efficiency of carbon filters could be achieved through modification of pore shape.

The surface chemistry of the carbon is also important in controlling the efficiency of activated carbon filters. Increasing the number of polar surface functional groups through intentional (NO_2 oxidation) or unintentional (ageing by storing the carbon in humid air) modification results in a decrease in filter performance at high values of the equilibration and challenge RH because of the difficulty with which preadsorbed water is displaced from the polar surface by the non-polar adsorbate. Intentional chemical modification as a means of improving the hydrophobic character of the carbon surface results in an improvement in filter performance, because the preadsorbed water can be displaced more readily from the carbon surface. Although the surface chemistry is important, at high RH values it is the transport of the preadsorbed water from the pore structure, and the efficiency with which it is carried away by the airstream that limits overall filter performance (the airstream reaches saturation).

CHAPTER 10

Concluding Remarks

10.1 General Discussion

The Effect of Storage Conditions

The surface of activated carbon can be regarded as being chemically reactive due to the presence of active sites, impurities, and centres of unsaturation. Under certain conditions of storage and use, this reactivity can result in changes to the surface chemistry. For many years, carbon adsorbents have been used in vapour adsorption applications, and whilst in some cases, the limitations on their useful service life have been considered (chapter 4), the parameters affecting this aspect are not generally appreciated.

In many vapour adsorption applications, the limitation on service life is due to a degradation in filtration efficiency that results from storage and use in the presence of air of high relative humidity (RH). Loosely termed "ageing", this degradation is particularly important in critical processing applications and in hazardous operations, such as in the nuclear industry, and in situations where the use of respiratory protection is necessary: in general, the degradation process is important when the hazard is posed by volatile hydrophobic vapours (chapter 4).

The studies reported herein illustrate that on exposure to air of high RH (above ca. 50%), some of the adsorptive properties of activated carbon are permanently changed (chapter 6). The most important change observed during storage under these conditions is that the carbon surface becomes increasingly polar as revealed by the enhancement in the quantity of methanol vapour adsorbed by the (moisture free) material. Monitoring the change in surface chemistry using this probe molecule was found to be a rapid technique, which relies on the presence of specific adsorbent- adsorbate interactions. The increasingly polar nature of the carbon surface also resulted in changes to the water adsorption properties of the carbon, in that the quantity of water vapour

adsorbed at low values of the RH (below ca. RH60%) was enhanced. This enhancement in surface polarity resulted in the promotion of pore filling at lower values of the RH in comparison to control carbon, and can be explained on the basis of the change in the number of polar adsorption centres. At low RH, these centres act as a focus for the adsorption of water vapour such that the surface of the carbon may be visualised as possessing discreet islands or clusters of adsorbed water. As the number of these sites is increased, the number and proximity of the clusters rise, until they merge to form a continuous surface film. The formation of this film, followed by further adsorption of water vapour, can then be envisaged as the process of pore filling (the steep region of the isotherm). This mechanism, which has been proposed to describe the nature of the interaction between activated carbon and water vapour (chapter 4) therefore appears to adequately explain the change in the water adsorption properties due to ageing effects. The ageing process was not, however, found to result in a significant change to the porosity of the carbon, although a small reduction in the quantity of nitrogen adsorbed at -196^{o}C was found: this may be due to pore constrictions associated with the presence of the surface oxygen containing functional groups (elemental analysis indicated that ageing resulted only in an increase in the carbon oxygen content). Hexane adsorption by dry carbon was also found to be a useful technique for monitoring structural changes. The adsorption of hexane by dry carbons was not found to be directly affected by the presence of polar adsorption sites because hexane is non polar: the extent of adsorption is therefore controlled by the available pore volume. The small reduction in the amount adsorbed by the aged carbons is explained on the same basis as the nitrogen adsorption data. That the shapes of the hexane breakthrough curves were unchanged indicates that the adsorption kinetics are unaffected by the presence of the additional surface functional groups.

Because the change in surface chemistry results in an increase in the selectivity of the adsorbent for polar vapours, a reduction in the efficiency with which volatile hydrophobic chemicals are adsorbed by aged carbons from an

airstream in the presence of polar vapours might be predicted, because the polar adsorption centres will act as a focus for the adsorption of the polar vapour. The most relevant example in the context of this present research is when a filter has been exposed to air of high RH (eg. RH80%) for some time prior to exposure to a contaminant vapour. In this situation, the carbon will be of enhanced polarity (due to ageing effects), but will also contain a substantial quantity of preadsorbed water (chapter 2, 3, 6). For the adsorption of the contaminant to proceed, some displacement of preadsorbed water must take place and because the carbon surface is more polar, the ease with which preadsorbed water can be displaced will be reduced: the result of this is then that the contaminant vapour penetrates the filter bed more rapidly compared to a sample of fresh (control) carbon (it is notable that at RH80%, the equilibrium water content of control and aged carbon was the same: the reduction in filter efficiency cannot therefore be a consequence of the amount of preadsorbed water vapour present on the filter bed). Thus, the efficiency of adsorption of hexane and chloropicrin (PS) under humid conditions by samples of aged carbons was poor compared to control samples. The extent of degradation depended on the length of time for which the carbon had been stored in humid air. The most significant changes were observed within the first 50-100 days of storage, over which time the rate of ageing (as revealed by methanol and water adsorption at low RH) was a maximum.

Storing carbon in RH60% also resulted in significant ageing effects, but the degradation in PS adsorption efficiency was less than at RH80%. That the methanol adsorption properties of carbons aged at RH60 and 80% were similar presumably reflects a difference in the distribution of the oxygen containing functional groups, because thermal desorption indicated that more of these groups were present on the surface of the RH80% aged sample. This apparent discontinuity can be explained on the basis that the polar groups are in closer proximity on the surface of the RH80% aged sample: a number of these groups could then act as a focus for the adsorption of a single molecule of methanol.

That the efficiency of PS adsorption was poorer for the RH80% aged sample is then due to the fact that additional polar sites more effectively inhibit the vaporisation of preadsorbed water.

In addition to the RH, the storage temperature was also found to be important, and carbon ageing was found to be more rapid at 45°C and RH80% than at 22°C and RH80%. It is also probable that the extent of ageing is grater at the higher temperature.

That ageing is strongly dependent on the RH of the air (and hence the carbon water content, chapter 2, 4) was evident from the results of storing carbon at RH40% and 34°C. Under these conditions, no measurable change in surface polarity (and hence PS adsorption efficiency) was found even though the air contained the same concentration of water vapour as at RH80% and 22°C. It is probable that under these conditions, water adsorption only occurred on the polar sites present on the carbon after manufacture and not on the less favourable surface sites prone to oxidation which are occupied by water molecules at higher RH values.

Ageing at high RH (and at 22°C or 45°C) generally takes a period of months to approach completion. Although the precise timescale over which this oxidative process continues is not known, it is at least one year. In practice, a technique for producing aged carbons more rapidly for further experimental study would be desirable. Thus the use of a mild oxidation technique was investigated which would not result in any significant modification to the carbon pore structure (as a result of, for example, carbon burnoff). Dinitrogen tetroxide (N_2O_4, abbreviated here as NO_2) was selected, and the properties of carbons modified using this oxidant were found to be similar to those of carbons aged at high RH. The changes in surface chemistry were therefore consistent with their being a greater number of polar adsorption centres at the surface, and elemental analysis confirmed that the reaction (which was complete in ca. 60 minutes at 25°C) primarily resulted in an increase in the oxygen content of

the carbon. As the nitrogen content of the modified carbon was slightly greater, the technique may also be useful for introducing nitrogen containing functional groups onto the surface. Modification using high NO_2 treatment pressures resulted in a more significant change in surface chemistry compared to carbons aged by exposure to humid air. It is possible that this effect represents the limit to which surface oxidation may proceed (at least at low temperatures: 22-25°C), although an equally valid interpretation is that the NO_2 reaction results in more extensive oxidation. It may also be that the functional groups present on the surface of NO_2 oxidised carbon are not the same as those produced through exposure to air of high RH, and that this difference is manifested through a comparison of the adsorptive properties of the carbons. Thus, NO_2 oxidised carbons may not be a good model for aged carbons, but they may be suitable for further chemical transformations.

The results of this part of the research therefore highlight the importance of surface chemistry on some of the adsorptive properties of activated carbon, and indicate that in some situations, a significant degradation in filter efficiency can occur over a relatively short timescale. It is also apparent that the impact of ageing on filtration efficiency can be minimised by conditioning the airflow such that the RH does not exceed ca. 40% (ie. by preheating or dehumidifying the airstream). Such an approach may be a realistic option for fixed filter assemblies where space and weight constraints are less likely to be a limitation, but this option would not be viable, for example, in the case of individual respiratory protection.

Surface Chemical Modification

The majority of research concerned with activated carbons to date has concentrated largely on techniques for optimising porosity (ie. the pore size and distribution, and the pore volume). Much less attention has been paid to the importance of surface chemistry. However, because the carbon is shown to be

reactive, the possibility exists for altering the chemistry of the surface as a means of optimising specific adsorptive properties. For example, by appropriate chemical modification, resistance to the ageing effects at high RH described above could be improved, and the hydrophobic character of the surface could be enhanced (an increase in surface polarity results in a reduction in the efficiency with which volatile hydrophobic vapours are adsorbed from high RH air (eg. ageing, NO_2 modification): conversely, it follows that a reduction in the number of polar adsorption sites on the carbon surface should lead to an improvement in the efficiency with which such vapours are adsorbed. Although this contention is somewhat simplistic (activated carbon would, for example, still adsorb water vapour due to the presence of the pore structure, which is of a size distribution favourable for molecular sorption) some enhancement in hydrophobic character is possible by, for example, masking the polar sites which are present on freshly manufactured carbon). In addition, it is also probable that specific functional groups could be introduced onto the carbon surface.

Thus activated carbons (BPL which is derived from coal, and CECA and SCII, which are derived from coconut shells) have been modified using a range of reactive chemicals with the intention of achieving the changes described above. Because the aim of this part of the research was to manipulate the surface chemistry of the carbon, it was the intention that chemical modification would not result in significant disruption of the underlying pore structure. Any significant loss of porosity would complicate analysis of the modified adsorbents because of the difficulty of distinguishing between simultaneous changes in both surface chemistry and porosity.

Fluorination

Of the candidate modifiers, the use of a direct fluorination technique appeared to offer some promise because fluorinated surfaces are generally hydrophobic and chemically inert. Such an approach could therefore result in a carbon of improved hydrophobic character which would also afford resistance to

ageing effects. Previous studies using fluorine (chapter 3) were not conclusive, since the stability of the modified carbons was not established. In addition, their utility for vapour adsorption applications had not received attention. In this present research, carbon modifications were studied initially at low temperatures (30-180°C; chapter 7). Irrespective of the carbon type (coal or coconut shell), substantial quantities of fluorine were absorbed with only minimal carbon gasification. However, a significant loss of microporosity resulted when the amount of adsorbed fluorine exceeded approximately 10 weight percent (w/w %). The products were found to be unstable, in that they formed acidic aqueous suspensions, and liberated iodine from iodide. Water adsorption indicated that the samples aged in flowing air, presumably as a result of hydrolysis of weak carbon- fluorine bonds. DSC and thermal desorption analysis suggested that the unstable nature of the fluorinated carbons was due to the desorption of weakly adsorbed (or absorbed) fluorine, indicating that the carbons are not suitable for vapour adsorption applications. Indeed, the efficiency of PS adsorption from humid air by the samples was poor in comparison to control samples. Attempts to stabilise the carbons by high temperature outgassing were not successful, because the bulk of the fluorine was removed, and the modified adsorbents were unstable in humid air. Because carbons fluorinated at low temperatures contained thermally unstable fluorine and/or surface fluorine containing functional groups, treatments were carried out above 300°C in an attempt to generate stable surface functional groups. However, under these conditions the principal reaction was one of carbon gasification, and only small quantities (ca. 1-2%) of fluorine were fixed.

Because the modified adsorbents were reactive, the possibility of further chemical transformation to yield stable functional groups (by substitution of, for example, weak carbon- fluorine bonds) was investigated by treatment with water, methanol, and dipropylamine. The changes in the adsorptive properties of the modified carbons treated with methanol or water were consistent with their being hydroxy or methoxy functional groups at the surface, since the water

treated sample was of increased, and the methanol treated sample decreased, surface polarity. DSC examination revealed that the methanol treated sample contained adsorbed/ absorbed fluorine, suggesting that reaction was incomplete (outgassing the carbon at elevated temperature did not result in complete fluorine desorption). A DSC and TG examination of fluorinated and dipropylamine modified carbons suggested that amine functional groups had been successfully grafted onto the surface. It is apparent from these results that direct fluorination offers a potential route to producing carbon adsorbents containing specific types of functional groups at the surface.

Since the carbon- fluorine interaction may be anomalous, indirect fluorination was therefore considered, and the reaction between activated carbon and hexafluoropropene (HFP) was investigated. The reaction proceeded readily at 180°C, but did not result in significant structural disruption, although a small loss of microporosity was apparent from examination of the nitrogen adsorption isotherms. TG analysis indicated that the carbons were thermally stable.

The modified carbons were, however, found to be more hydrophobic compared to control samples, suggesting that the technique was successful in masking some of the polar adsorption centres on the surface of both control and aged carbons. The improved hydrophobic character (revealed by water and methanol adsorption) was not reflected in the efficiency with which the modified carbons adsorbed PS from humid air. That is, only a small improvement in filtration efficiency was found, suggesting that the surface functional groups may be of sufficient bulk to hinder vapour adsorption from an airflow. These effects were also found for samples which had been aged prior to modification.

Although the results confirm that the rationale for selecting fluoroolefins was correct, it is probable that the molecular size of the modifier is equally

important. Thus 1,1-difluoroethene (DFE) was selected. Exploratory studies indicated that significant reaction did not take place until approximately 450°C, at which temperature weight increases of the order of 3.5 w/w % were observed. EDX and elemental analysis revealed that reaction resulted in fluorine fixation: that the nitrogen and hexane adsorption characteristics of the carbons were essentially the same as those of the control indicated that the interaction did not result in significant pore occlusion effects. This suggests that under these conditions, the DFE- carbon reaction was selective, a contention supported by the observation that at higher temperatures large increases in sample weight occurred (>10 w/w%), which were associated with a significant loss of microporosity. This indicates that above 450°C, the reaction is not selective, and that polymerisation of DFE at the carbon surface was the primary reaction sequence. That the carbons treated at 450°C were of greater hydrophobic character than samples modified using HFP indicated that the use of DFE is a more effective approach. More importantly, the DFE modified carbons were found to adsorb PS (or hexane) from humid air with a significantly greater efficiency compared to the control (that the difference was due to a change in surface chemistry, rather than a thermal effect, was apparent from the observation that the properties of carbon outgassed at 450°C were the same as the control). This observation establishes a clear link between the hydrophobic character of the surface and the efficiency with which volatile hydrophobic chemicals are adsorbed. It is probable that the improvement in vapour adsorption efficiency at high RH is a consequence of an increase in the ease with which preadsorbed water is displaced from the surface. However, because the underlying porosity remains largely intact (as it must if vapour adsorption is to occur) the carbon will still adsorb significant quantities of water vapour: thus there will be a limit to which the hydrophobic character of the surface can be enhanced to promote vapour adsorption under these conditions. The DFE modified carbons were found to age in humid air, however, but at a reduced rate compared to the control. This suggests either that the reaction does not successfully mask all of the active sites at the surface, or that the functional groups introduced are not hydrolytically stable.

XPS analysis suggested that the DFE- carbon reaction resulted primarily in the generation of surface CF_2 groups, indicating that reaction may proceed via difluorocarbene: conversely, direct fluorination resulted in the formation of predominantly CF species. One explanation for the difference between carbons modified using these techniques is that the CF groups are less hydrolytically stable than CF_2 groups. However, it is equally possible that the unstable nature of directly fluorinated carbon is due to weakly sorbed fluorine present within the pore structure, which cannot be studied using XPS techniques.

The results illustrate that treatment with fluoroolefins results in a significant enhancement in the hydrophobic character of carbon surfaces, but that carbons modified using HFP or DFE are not resistant to ageing effects. It is also apparent that careful selection of the modifier is necessary.

Chlorination

Since one of the principal aims of this research was to improve resistance to ageing effects, an alternative rationale was considered. In this case, carbon surfaces were assumed to possess at least some surface oxygen containing functional groups (eg. control BPL carbon contained ca. 2 w/w% oxygen) which would be chemically reactive (eg. hydroxyl and carboxyl groups). Thus carbons were modified using a reagent with which such groups might react specifically. Phosgene was selected because it might *inter alia* chemically transform surface hydroxyl groups to carbon- chlorine species, and any carboxyl groups to acid chlorides: treatment with, for example, methanol would then convert the acid chlorides into stable esters (chapter 8). The resulting carbon should then be more hydrophobic in comparison to the control. In addition, because aged and NO_2 modified carbons contain significant quantities of chemisorbed oxygen, this approach could provide a synthetic route for producing a relatively hydrophobic material which may be resistant to further ageing.

Exploratory experiments revealed that the carbon phosgene reaction was

temperature dependent. A reaction temperature of 180°C was selected, which resulted in significant reaction but without substantial structural modification (the sample handling procedures were also simplified by treating the carbons at low temperatures). Gas analysis did not suggest that the reaction resulted in significant carbon burnoff.

Carbons modified with phosgene were found to be unstable, in that they formed acidic aqueous suspensions, and aged rapidly in humid air. This behaviour is consistent with, for example, their being acid chloride functional groups at the surface (elemental analysis showed that reaction primarily resulted in chlorine fixation, but also in a small decrease in the hydrogen content of the carbon). Although methanolysis resulted in a significant weight loss, the carbon was then found to be at least as hydrophobic as the control material, and adsorbed PS from humid air at least as efficiently as control material (the nutshell carbons were more hydrophobic than the control, whereas little change in hydrophobic character was apparent for BPL carbon. This difference may be due to the presence of greater quantities of ash impurity in BPL carbon (ca. 7.5 w/w% cf. 2 w/w%)). Nitrogen adsorption indicated that little change in porosity resulted from modification and treatment. The most important observation was that the phosgene modified and methanol treated carbons were resistant to the ageing effects normally observed after exposure to air of high RH. However, elemental analysis revealed that methanolysis only resulted in a reduction in the chlorine content of the carbon. Thus the initial rationale for selecting phosgene was incorrect, because comparison of the oxygen content of the carbons after modification and then after methanolysis were not consistent with their being ester functional groups at the surface (in fact, the molar ratio of chlorine to oxygen for the phosgene modified carbon was approximately 2:1, indicating that the reaction cannot be due principally to the formation of acid chloride groups). It was more likely, therefore, that methanolysis resulted in the removal of strongly adsorbed reagent and/ or reaction products, and that the phosgene-carbon reaction proceeded by substitution of surface hydrogen by chlorine, and by incorporation of chlorine at the active sites. This is then consistent with the

elemental analysis data, and is supported by the observation that the methylated carbons did not form acidic suspensions, and were more thermally stable compared to the samples modified with phosgene but not treated with methanol. On this basis, the unstable nature of the phosgene modified carbons in the presence of humid air is then due to the presence of adsorbed chlorine or chlorine containing species which promote a moisture- carbon reaction.

Further support for this contention was that the adsorptive properties of phosgene modified carbons treated with water were the same: if the phosgene-carbon reaction proceeded via the acid chloride, this could not be the case. XPS analysis provided further evidence to substantiate this, because the spectra for the modified and water or methanol treated samples were essentially the same. That the properties of directly chlorinated and methanol or water treated carbons were the same as the phosgene modified and treated samples further supports the contention that the reaction involves surface chlorination.

For aged and NO_2 modified carbons, it is possible that reaction with phosgene may proceed via the acid chloride. This was investigated by treating the carbons as described above, and although some reduction in the polarity of the surface resulted, the changes were not substantial. This suggests that the majority of the oxygen containing functional groups on the surface were not amenable to modification using this technique. It is also possible that the functional groups introduced by NO_2 modification are different to those present on the surface of aged carbon.

Vapour Adsorption from Humid Air

Although the modification techniques described above (indirect fluorination, chlorination) do result in an improvement in the efficiency with which volatile hydrophobic chemicals are adsorbed in the presence of high humidity air, it is apparent that surface chemistry is not the most important factor controlling the adsorption process. This is evident from comparing the

efficiency of chloropicrin (PS) vapour adsorption by dry and humidified filter beds (chapter 9). Measurement of complete breakthrough curves indicates that under typical conditions of storage and use (ie. high RH) vapour adsorption efficiency is limited by the ease of displacement of preadsorbed water from the carbon surface, and the rate at which it is transported away from the filter bed. In many cases, it is the transport of displaced water from the bed that is most important because the airstream reaches saturation: vapour penetration through the filter then takes place more rapidly because the micropores are temporarily occluded by condensed water vapour. It is also shown that the ease with which the preadsorbed water is displaced from the surface has a significant impact on the overall process of vapour adsorption and water displacement, and that this is controlled by the polarity of the carbon surface.

Conclusions

The results described herein therefore illustrate that the surface chemistry of activated carbon can be manipulated without significantly altering the underlying porosity. Depending upon the modification technique employed, the surface of the carbon is shown to be of greater hydrophobic or hydrophilic character. Resistance to the ageing effects normally observed in humid air can also be significantly enhanced. It is also apparent that some surface modified carbons are suitable precursors for the introduction of specific types of functional groups. Measurement of the adsorption of volatile hydrophobic vapours from air of high RH (eg. chloropicrin, PS) illustrates that, although the polarity of the adsorbent surface is important, the efficiency of activated carbon filters is limited both by the ease with which preadsorbed water can be displaced from the surface, and, more importantly, under typical conditions of storage and use, the rate at which it can be transported away by the airstream.

10.2 Recommendations for Further Research

1] Carbons modified with fluoroolefins are more hydrophobic than control carbons and adsorb volatile hydrophobic vapours from humid air more efficiently. Further study of the preparation and properties of carbons modified using these chemicals may result in an adsorbent which would be more resistant to the ageing effects observed at high RH.

2] Directly fluorinated carbons are reactive and amenable to further chemical transformation, and the potential for introducing specific types of functional groups onto the surface has been demonstrated. Further study may reveal that the technique is suitable for engineering selective adsorbents for specific applications, and for the preparation of catalytically active carbons.

3] Chlorinated carbons are resistant to ageing effects, indicating that the surface is relatively inert to mild oxidation. The use of such carbons as supports for reactive impregnants (such as copper and chromium) which degrade in the presence of humid air may allow impregnated adsorbents of improved service life to be prepared.

4] The vapour adsorption efficiency of activated carbon at high RH is limited, at least in part, by the inability of the airstream to carry away displaced water vapour. One way in which this effect could be addressed would be by increasing the volume of the transport pore structure to provide regions where the displaced water could reside prior to transport away from the filter bed by the airstream. In this way, temporary blockage of the micropores by condensed water should not occur, resulting in an improvement in vapour adsorption efficiency.

5] Ultimately, a combination of chemical modification, and the modification of pore shape, could provide an adsorbent which would not adsorb significant quantities of moisture, but would adsorb organic vapours efficiently.

APPENDIX

Index

Appendix 1. Experimental Methods

Appendix 2. Tabulated Data

Appendix 3. List of Publications, Acknowledgements

1 Experimental Methods

1.1 Water Adsorption

The water adsorption properties of control and modified samples were determined using the apparatus shown at figure 1.1. This consisted of a large perspex cabinet, maintained at constant temperature (±0.1°C) by use of a radiator through which water was circulated, and a fan, mounted within the cabinet. The fan motor was mounted outside the cabinet. The temperature of the external water supply was controlled using a Grant instruments Barrington digital immersion heater and a Haake model EK12 immersion cooler.

A supply of clean (activated carbon filter) humidified air was passed from a Miller Nelson flow-temperature-humidity control system (model HCS-301) fitted with a dry air balance to a perspex reservoir mounted inside the cabinet. The dewpoint of the air in the reservoir was constantly monitored using a Michell Instruments series 3000 dew point hygrometer (calibration traceable to the NPL and NBS standard). Careful control of the dry and wet airflows enabled the dewpoint to be controlled to within 0.1°C.

Air from the reservoir was drawn via a number of glass sample holders (figure 1.2), and the airflow rate through each was measured using a calibrated rotameter fitted with a flow controller. Effluent air was exhausted from the system via a manifold and pump.

Samples

Dry (3 hours, 120°C, 3 mbar) carbon samples were snow storm filled* into 2cm diameter, 2cm depth VA tubes (cylindrical brass base and lid units fitted with fine stainless steel retaining meshes). The packed tubes were mounted in the glass sample holders (figure 1.2), and air of the appropriate RH was drawn through them at a flow rate of 1.0 dm^{-3} min^{-1} until equilibrium was attained (less than 0.1% change in weight per hour (based on the initial dry weight of carbon)). By this technique, both water adsorption and desorption was determined.

In addition to the water adsorption apparatus at figure 1.1, a large volume climatic chamber was used for equilibrating carbon samples with air of high RH. The chamber was maintained at RH 80±1% at 22±0.1°C.

The apparatus was also used for preconditioning carbon samples with humid air prior to measurements of vapour adsorption.

*The snow storm filling device consisted of three cross wires mounted within a brass funnel. The device ensured that the granular carbon samples were packed with the optimum density into the sample holder (VA tube).

1.2 Methanol Adsorption

Methanol adsorption was determined using the apparatus shown at figure 1.3. Dry air (1.2 dm^{-3} min^{-1}, <2% RH) was drawn from a reservoir via a carbon filter to a glass T. The bulk of the flow passed directly to a calibrated rotameter via the T joint, and the remainder (ca. 100 cm^3 min^{-1}) passed via a needle valve and vapour generator (1.4) containing dry methanol. The vapour/ air mixture from the generator was mixed with the bulk airflow during passage through the rotameter and a stainless steel heat exchanger which was mounted within a water bath maintained at 22±0.05°C (Grant Instruments immersion heater balanced against a Haake model EK12 immersion cooler). The airflow was then directed through a glass sample holder (figure 1.2). Effluent air from the glass holder was sampled using a Chrompack 437A gas chromatograph fitted with an FID detector (2m, 2mm diameter glass column, Poropak QS. An oven temperature of 160°C was used, and the carrier gas was nitrogen (17 cm^3 min^{-1}, high purity)). Effluent air not sampled by the GC was passed to a carbon filter prior to being exhausted into a fume cupboard. Data from the GC was collected using a Chrompack PCI four channel computer integrator fitted with an analogue/digital converter.

The GC was calibrated using the procedure outlined below (1.5). The airflow through the vapour generator was adjusted such that the concentration of methanol vapour was 1300±25 mg m^{-3}.

Samples

Dry (3 hours, 120°C, 3mbar) carbon samples were snow storm filled into 2cm diameter brass tubes (VA tubes) of bed depth 2cm. The VA tubes were placed into the glass holder when the vapour concentration was of an appropriate value, and data acquisition was continued until the influent and effluent vapour concentrations were equal. Samples were removed and weighed.

1.3 Vapour Adsorption Apparatus

The efficiency with which samples of control and modified carbons adsorbed vapour from a flowing airstream was determined using the apparatus shown in schematic form at figure 1.4. The apparatus was designed such that filter challenge experiments could be carried out under conditions of controlled temperature and RH by one operator, and all wetted components were constructed from glass, PTFE, or stainless steel. Connecting tubing was contained in an insulating jacket.

The apparatus consisted of two independent parts, both of which were constructed within a fume cupboard: the front section (black), containing the carbon sample, and the rear section (brown), to allow the vapour challenge to be set.

Prior to, and during, filter challenge, clean humidified air was passed from a Miller Nelson flow-temperature-humidity control system (model HCS-301) fitted with a dry air balance to a perspex reservoir. The dewpoint of the air in the reservoir was constantly monitored using a Michell Instruments series

3000 dew point hygrometer (calibration traceable to the NPL and NBS standard). Air from the reservoir passed to both parts of the test apparatus, and careful monitoring of the dry and wet airflows enabled the dewpoint to be controlled to within 0.1°C.

Air to the front section was drawn via a rotameter and mixer to a stainless steel heat exchanger immersed in a water bath at the test temperature. The airflow then passed through a valve (1) (Swagelok SS43XS4 air actuated 3-way Ball valve) to the sample. The airflow from the sample was divided, such that measurements of dewpoint (2), and the concentration of any vapour in the filter effluent, could be made. The effluent humidity was determined using a second Michell Instruments dewpoint hygrometer, which was encased in a water jacket at the test temperature. The output of both hygrometers was periodically checked against a standard instrument (Michell Instruments series 3020 dewpoint hygrometer). Vapour concentration was measured routinely using a dual channel Chrompack Gas Chromatograph equipped for automatic gas sampling (1 ml).

The GC was fitted with two 2 metre glass columns of 4 mm diameter packed with (for Chloropicrin (PS) determination) 5% OV101 on DMCS (oven temperature 160°C, nitrogen carrier gas flow 15 cm^3 min^{-1}). The GC conditions for n-hexane determination were the same, except that an oven temperature of 140°C was used.

Output from the GC was passed to a Chrompack PCI four channel computer integrator fitted with an analogue/digital converter. A mass spectrometer could also be used for gas sampling (VG instruments PETRA quadrupole spectrometer). All effluent air was passed to a carbon filter prior to discharge within the fume cupboard via the analytical instruments or a rotameter, flow controller (Swagelok SS31RS4 stainless steel needle valve) and a pump.

At the same time, air passed via the vapour generator (3) (1.4) through an isolating valve, rotameter and mixer, to the rear section of the test apparatus. The temperature of the air was controlled by passage through a second stainless steel heat exchanger immersed in the water bath. A small quantity (ca. 100 cm^3 min^{-1}) of the vapour/ air mixture passed to the second channel of the GC; the remaining mixture was discharged via a rotameter, flow controller, pump and carbon filter to the fume cupboard. Adjustment of the vapour concentration was made by a needle valve (Swagelok SS31RS4) with reference to a calibration standard (1.5). By this method, the vapour concentration could be set without disturbing the carbon sample.

Samples

Carbon samples were, after pre conditioning (1.1), mounted in a glass VA tube holder (figure 1.2) to which thermocouples (Comark Electronics NiCr/NiAl) were fitted such that the temperature of the influent and effluent air could be monitored. The assembly was lowered into a water bath to improve thermal stability, and was attached to the test apparatus via PTFE tubing. No air was drawn through the sample until its temperature stabilised to that of the water bath (sample handling resulted in a temperature increase). After thermal equilibrium was attained, clean air was drawn through the sample until the influent and effluent temperatures and humidities were equal (to within 0.1^{o}C of temperature and dewpoint). Once equilibrium was attained, and the vapour concentration in the rear section of the test apparatus was of an appropriate value, the filter challenge was begun.

Filter challenge was initiated by simultaneously switching a number of valves (1,4) (Swagelok air actuated Ball valves), such that the vapour/ air mixture passed from the rear section of the apparatus to the front sample containing section. At the same time, a valve (5) was actuated to enable the influent vapour concentration to the filter to be monitored. An additional valve (6) was actuated to enable a flow of air from the reservoir to be passed along

the rear section of the line during filter challenge. This prevented the formation of a partial vacuum, which would lead to liquid agent being drawn into the apparatus at the end of the experiment when the valves were switched off.

Data acquisition (influent and effluent dewpoint, temperature, and vapour concentration) was continued until the end of the experiment (see main body of text). The test apparatus was used for all vapours other than methanol.

1.4 Vapour Generation

To carry out the vapour adsorption studies, it was necessary to develop equipment to enable a stable vapour concentration to be generated over long periods (1-12 hours). The use of a syringe drive and hot finger device was not found to be appropriate, since large variations in the challenge concentration about the mean were observed (ca. ±10-15%). This variation was due to the stepper motor in the syringe drive, which gave rise to a frequent fluctuation in the quantity of liquid impinging on the hot finger. Other techniques were studied, including the use of bubbler devices, but these were also found to be unsuitable because of significant instabilities in the resultant vapour concentration.

The equipment used in the vapour adsorption studies is detailed at figure 1.5. It consisted of a conical flask (placed within a water bath) fitted with a side arm, within which the liquid agent was contained. Tubing from the side arm passed to the reservoir shown at figure 1.4. An outer open tube, one end of which was submerged below the liquid surface, was sealed to the neck of the flask by means of a quickfit joint. A narrow tube was placed within the outer tube, and was sealed into an adaptor by means of a septum and cap. A controlled flow of air (Swagelok SS31RS4 needle valve) was drawn through the narrow tube to the test apparatus via the adaptor. Air passing down the narrow tube mixed with vapour above the liquid, and carried it into the test apparatus via PTFE tubing.

The outer tube presents a small surface area of liquid to the airflow. The level of liquid in the tube remained constant over relatively long time periods (dependent upon a combination of the required vapour concentration and volumetric airflow rate in the test apparatus) since the diameter of the flask was very large in comparison to that of the tube (> 50 x). It was this aspect of the design which ensured a consistent vapour concentration.

The concentration of vapour in the airstream was thus set by control of the liquid temperature via that of the water bath, the airflow rate through the narrow tube (and its height above the liquid surface), and the diameter of the outer tube.

Measurement of typical output (5000 mg m^{-3} of PS) using either a GC or Mass Spectrometer indicated that the variation in the vapour concentration was no more than ±0.5%; and at best ±0.25%. The concentration remained stable for a period of hours, although slight adjustment of the airflow rate was necessary during extended data acquisitions (for example, >4-5 hours, using a volumetric flow rate of 1.2 dm^3 min^{-1} through the test apparatus and a (PS) vapour concentration of 5000 mg m^{-3}). The generator was used for all vapour adsorption studies (PS, methanol, hexane).

1.5 Calibration

Calibration of the analytical instruments used in the measurement of vapour concentration was achieved using vapour/ air mixtures made up in Lamofoil (polythene lined aluminium) M12/12/75 sample bags fitted with an inlet valve and septum.

For liquids, a volume calculated to produce the desired vapour concentration was injected via a septum into a three neck round bottom flask

through which dry air (the FID detector on the GC was insensitive to moisture: for the mass spectrometer, it was necessary to calibrate using air of the test RH since vapour transport across the membrane was affected by the presence of moisture) of a known flow rate was passed. The airflow was passed from the flask via PTFE tubing and the inlet valve of a Lamofoil bag. The airflow was continued until the desired vapour concentration was produced (at which time all the liquid had evaporated from the flask). The calibration bag was attached to the test apparatus via a glass/PTFE stopcock (eg. Figure 4), and the vapour/ air mixture was drawn through the analytical instruments (auto sampling GC valve, or membrane inlet to a VG quadrupole mass spectrometer). For the GC, the vapour concentration was measured using a Chrompack PCI four channel integrator fitted with an analogue/digital converter. For the mass spectrometer, the output was measured using a chart recorder.

The validity of this approach was verified by two techniques.

The first involved making up vapour/ air mixtures in a glass bottle, of known volume, fitted with a septum, and then manually injecting a known quantity of the mixture onto a GC column (to establish that adsorption of vapour onto the walls of the Lamofoil bag was not taking place). The GC sample loop was calibrated by comparing the integrated peak area obtained by automatic injection as described above, with that peak area obtained by manually injecting a known quantity of the mixture from the same Lamofoil bag onto the GC column.

The second approach involved placing a sample of dry carbon into the test apparatus and then flowing the dry air/ vapour mixture through the bed at a known volumetric flow rate and for a known time, (which was less than the filter breakthrough time) and then removing and weighing the carbon sample. Comparison of the gravimetric and calculated* weight increases were made.

*Amount adsorbed (mg) = F.Co.t

F = volumetric flow rate ($m^3 s^{-1}$)

Co= vapour concentration (mg m^3)

t = time (s)

For gases, an amount calculated to produce the desired concentration was injected via a septum directly into a Lamofoil bag containing an appropriate volume of air.

1.6 Preparation of Modified Carbons

Chemically modified carbon samples were prepared using the equipment shown at figures 1.6 and 1.7. The apparatus at figure 1.6 was used for low temperature modifications (up to 200°C), and that shown at figure 1.7 for high temperature modifications (maximum 850°C).

1.6.1 Low Temperature Modifications

Dry carbon (3 hours, 120°C, 3 mbar (approximately 30g) was placed into each of two stainless steel dishes fitted with retaining meshes. The dishes were transferred into a 316 stainless steel reactor vessel (8.0 litre) fitted with a PTFE seal. The lid of the reactor was held in place by means of eight bolts. The vessel was placed into an air oven fitted with an overtemperature safety cutout, and was attached to the gas handling apparatus via a Cajon SS4VCR face seal gasket. The reactor was evacuated by means of a Genevac chemical vapour pump model CVP 100/2 (ultimate vacuum 0.5 mbar (Edwards high vacuum pressure transducer model EMV251)), and was heated to the reaction temperature. The vessel was maintained at the reaction temperature for three hours prior to the introduction of gaseous reagent, which was introduced via a Swagelok high integrity bellows valve (model SS4BG) such that the system pressure was approximately 1200 mbar. During reaction, the pressure and

temperature were monitored. Balance gas (high purity nitrogen or helium) could be introduced into the system via a second bellows valve. Gaseous reaction products could also be sampled directly into a Lamofoil bag, and the products were analysed using either a VG Instruments PETRA quadrupole mass spectrometer, or a Finnegan MAT GC-ITD (Ion Trap Detector) system. At the end of the reaction (the vessel was left to stand typically for 22 hours), the system was either evacuated and cooled to room temperature, or further aliquots of reagent gas were introduced to the vessel. After cooling, the vessel was pressurised to one atmosphere using high purity nitrogen gas prior to removal of the modified carbon samples. The samples were weighed prior to further outgassing and/or analysis (see main body of text).

1.6.2 High Temperature Modifications

Approximately 30g of dry carbon (3 hours, 120°C, 3 mbar) was placed within an Inconel lined 316 stainless steel tube. The sample was retained by means of a metal grid positioned midway down the tube. The lid of the reactor tube was fitted with a PTFE seal, and was retained using three bolts. The vessel and carbon sample were placed into a three zone tube furnace contained within a fume cupboard, and positioned such that the sample was at the mid point of the centre zone. The temperature of the sample was monitored using NiCr/NiAl thermocouples which were placed in contact with the outer wall of the vessel prior to closure of the furnace doors. Connections were made to the base of the tube to enable reagent or balance gas (high purity nitrogen or helium) to be introduced. The gas supplies were isolated by means of glass/PTFE stopcocks. A cooling water supply was attached to the tube, and the system was evacuated using an Edwards two stage rotary oil pump to an ultimate vacuum of 0.5 mbar (Edwards EMV251 pressure transducer). The tube was heated under vacuum to the reaction temperature, and reagent gas was introduced to a pressure of approximately 1200 mbar after first degassing the sample for approximately 1 hour. During reaction, both the system pressure and temperature was

monitored. After completion of reaction (typically 0.5-1 hour), the tube was evacuated prior to the introduction of further aliquots of reagent, or cooled under vacuum. After cooling, the system was pressurised to one atmosphere using a supply of balance gas, and the modified carbon sample was removed and weighed. During reaction, gas samples could be removed from the system for analysis using a mass spectrometer.

1.7 Thermal Analysis

The thermal stability of control and modified carbons was investigated using a Stanton Redcroft TG770 system, and a Stanton Redcroft DSC 1500 differential scanning calorimeter. For both analyses, granular samples (approximately 20mg) were heated in a platinum crucible to 120°C. The sample temperature was maintained at this value until a constant signal was attained from the instrument (ie. after loss of moisture). Thereafter, (TG analyses) the sample was heated to 900 or 950°C at 5°C min^{-1}. For DSC analyses, samples were heated to 700°C at a rate of 5 or 10°C min^{-1}. Both analyses were performed under an atmosphere of high purity argon. Weight losses recorded below 120°C were due to adsorbed moisture, since all the samples studied were outgassed at or above this temperature. The analytical results presented at the main body of the text reflect this.

1.8 Nonane Preadsorption

Carbon samples (approximately 30g) were outgassed in a glass-PTFE high vacuum system at 300°C using a silicon oil diffusion pump and rotary oil backing pump. The samples were outgassed to a residual pressure of 10^{-6} mbar (Edwards Penning gauge). After cooling, the carbons were exposed to nonane vapour at 25°C until constant weight was attained (the nonane was first degassed using the freeze- thaw technique). The samples were then outgassed at 25°C to a residual pressure of ca. 10^{-5} mbar prior to removal.

1.9 Nitrogen Adsorption

A Carlo Erba semi-automatic volumetric instrument was used in determining all of the nitrogen adsorption data. Carbon samples (ca. 0.5g) were outgassed in situ at 110°C to an ultimate vacuum of 1×10^{-4} mbar. High purity nitrogen (99.99%, Gas and Equipment) was used, and the measurements were made at liquid nitrogen temperature (-196°C). In each case, the adsorption and desorption branches of the isotherms were determined.

Correction for the sample volume was made using a volume compensator supplied with the instrument. Calibration of the dead space was made using a series of nitrogen gas doses, which were admitted to the empty sample burette immersed in liquid nitrogen. A diagram of the instrument, and full details of its operation and use, are contained in the instrument manual.

Adsorption data were compared on the basis of equal carbon weights: that is, the data for modified samples were corrected using the change in weight resulting from chemical treatment. This procedure enabled adsorption data for control and modified samples to be compared. In the present study, micropore filling (primary and secondary) was presumed to be complete at $p/p^{o}=0.4$.

The validity of this approach is dependent on there being no carbon gasification during the modification process (chapters 6-8).

1.10 Mercury Porosimetry

A Carlo Erba porosimeter 2000 automatic instrument was used in determining all of the porosimetry data. The instrument was capable of measuring pore size distribution in the range 3.7 to 7,500 nm using a capacitance monitoring device.

Carbon samples (ca. 0.5g) were, after outgassing (90 minutes, 110°C, air oven), placed in a dilatometer and attached to the pressurising system and the capacitance monitoring device. Measurements of mercury intrusion and extrusion were made for each sample. A diagram of the instrument, and full details of its operation and use, are contained in the instrument manual.

1.11 X ray Photoelectron Spectroscopy (XPS) and Energy Dispersive X ray Analysis (EDX) Measurements

XPS spectra were determined using a Kratos Analytical XSAM800 instrument, using an unmonochromated Mg K_α X ray source (hυ=1253.6ev) at a total power output of 300W. The working pressure was better than 10^{-9} mbar. The instrument was also fitted with a quadrupole mass analyser.

Wide scan spectra were recorded over the range 1100-0ev, and the analyser was operated in fixed transmission mode with a pass energy of 80ev for wide survey scans and 20ev for narrow region scans (C(1S) and F(1S)). Deconvolution techniques have not been applied to complex regions. The instrument was calibrated such that the Cu($2P^{3/2}$) peak was at a binding energy of 332.7ev, and that the separation of the Cu(2P) doublet was 19.8ev.

Granular carbon samples were mounted in a small flat bottom stainless steel cup approximately 8mm in diameter and 3mm deep. Sample charging effects, which give rise to peak broadening, were corrected by reference to the C-C/ C-H peak at 285.0ev in the C(1S) envelope. Binding energy values are accurate to 0.2ev.

Energy dispersive X- ray analyses were performed on selected samples to confirm experimental observations and to study the surface texture of the modified carbons, and were carried out using a Hitachi S800 Scanning Electron Microscope equipped with an energy dispersive X ray analyser (Link Systems thin window/ windowless detector).

1.12 X ray Diffraction Analysis

X ray diffraction measurements were performed using an instrument fitted with a 40kV 50mA copper anode and graphite monochromator. The scanning speed was 0.5° two theta per minute, and the range scanned was 5 - 50° two theta. The full scale deflection was 2K counts per second. Samples were ground prior to each measurement, under air, or high purity nitrogen.

1.13 Thermal Desorption- Mass Spectrometry

Measurements of the species desorbed during thermal treatment of the modified carbons was made using a VG 7070H double focusing mass spectrometer fitted with a temperature controlled solids probe. In each case, three grains of carbon were placed in a stainless steel boat, which was inserted directly into the ion source via the solids probe. The sample was heated at 13°C min^{-1}, to a maximum temperature of 700°C. Mass spectra were recorded using the electron impact technique (70 eV), over the range 650-10 amu, at a scan rate of 3 seconds per mass decade.

1.14 Elemental Analysis

1.14.1 Carbon, Hydrogen and Nitrogen Analysis

These analyses were performed using a Carlo Erba model 1106 elemental analyser under the following conditions:

combustion zone	1030°C
reduction zone	650°C
carrier gas flow rate	30 cm^3 min^{-1} (Helium)
Sample weight	0.5 - 1.5 mg

Ground samples were weighed into tin crucibles and placed into the instrument. Standards (acetanilide) and blanks were determined between each analysis to ensure that instrumental drift was not taking place.

1.14.2 Oxygen Analysis

This was performed using the same instrument, and under the following conditions:

pyrolysis zone	1030°C
carrier gas flow rate	30 cm^3 min^{-1} (Helium) passed over chloropentane vapour
sample weight	0.5 - 1.5 mg (silver crucible)

Standards (benzoic acid) and blanks were determined between each analysis.

1.14.3 Chlorine and Fluorine

A combustion technique was employed for both determinations. Approximately 0.5g of sample was placed into an inconel crucible and burnt in oxygen (30 atmospheres) within a Gallenkamp adiabatic bomb calorimeter containing 5 ml of 1N sodium hydroxide solution. The sodium hydroxide absorbed the chloride and fluoride ions, and also served to minimise corrosive attack of the metal surfaces of the bomb. Residues in the bomb were washed into a beaker using dilute nitric acid, and were made up to 500 ml in distilled water after filtration. Chloride and fluoride ion concentrations were determined using a Dionex 2010i ion chromatograph fitted with an AS2 column and the following eluents:

Chloride:

5% acetonitrile; 0.00071 M 4-cyanophenol; 0.002 M sodium hydroxide; 0.0045 M sodium carbonate.

Fluoride:

0.0025 M borax

The eluent flow rates were 2 cm^3 min^{-1}, and chloride and fluoride ions were measured using a conductivity detector after passing the solvent through an anion micromembrane suppressor carrying 0.0125 M sulphuric acid as the regenerant.

Chlorine and fluorine content in selected samples was also determined using a fusion technique.

Approximately 0.1g was mixed with anhydrous sodium carbonate. The mixture was sintered in a platinum crucible at 600°C, then 800°C, and was held at 1000°C for approximately 30 minutes. After cooling, the mixture was digested using hot water and 30% nitric acid. The solutions were made up to 100 ml with distilled water and filtered. Chloride and fluoride was determined as above.

1.15 Ash Determination

Approximately 1g of carbon was dried at 100°C for 4 hours, and after cooling and weighing, was transferred to a porcelain crucible and heated in a muffle furnace at 800°C until constant weight residues remained.

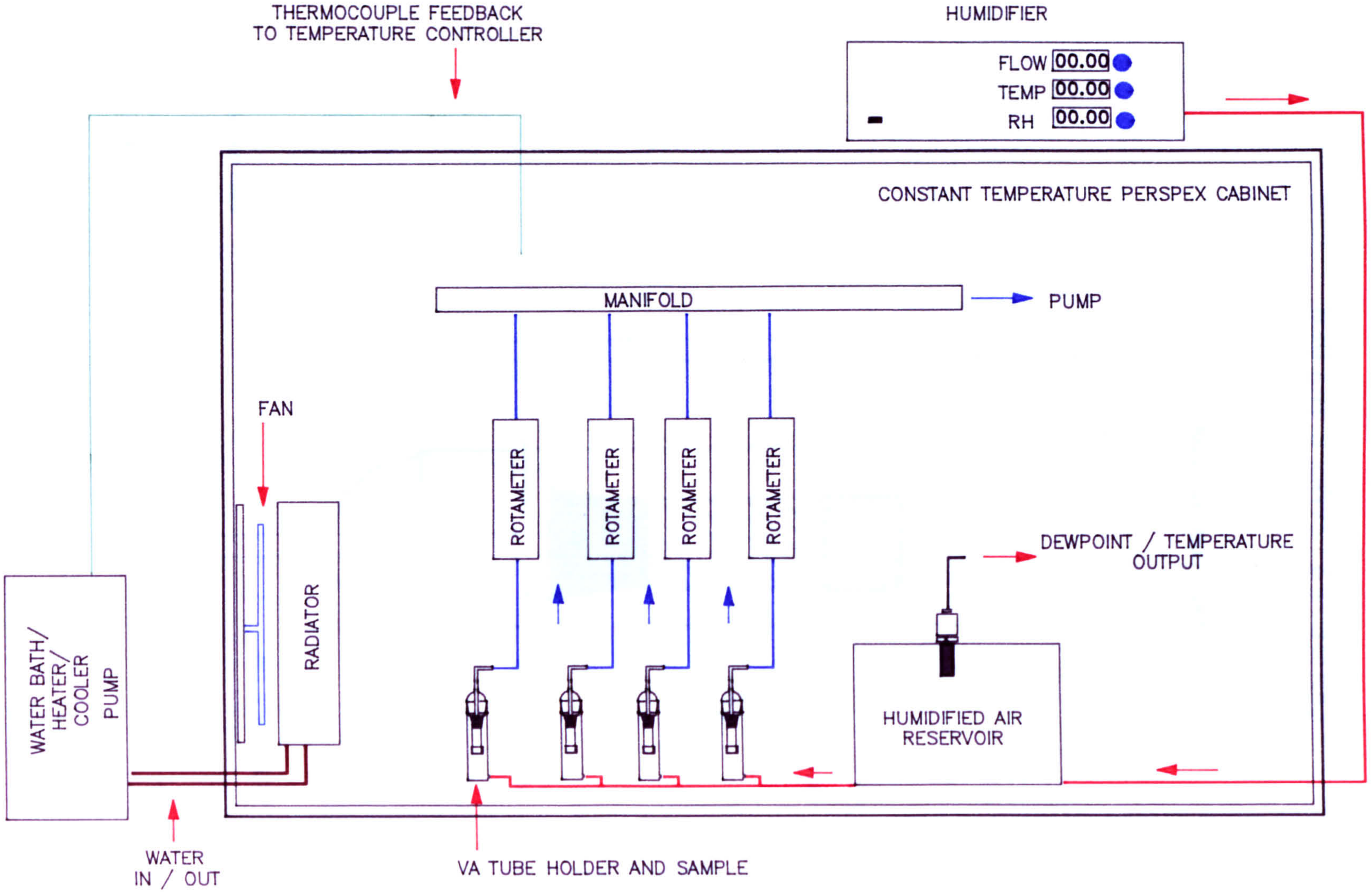

FIGURE 1.1. WATER ADSORPTION APPARATUS

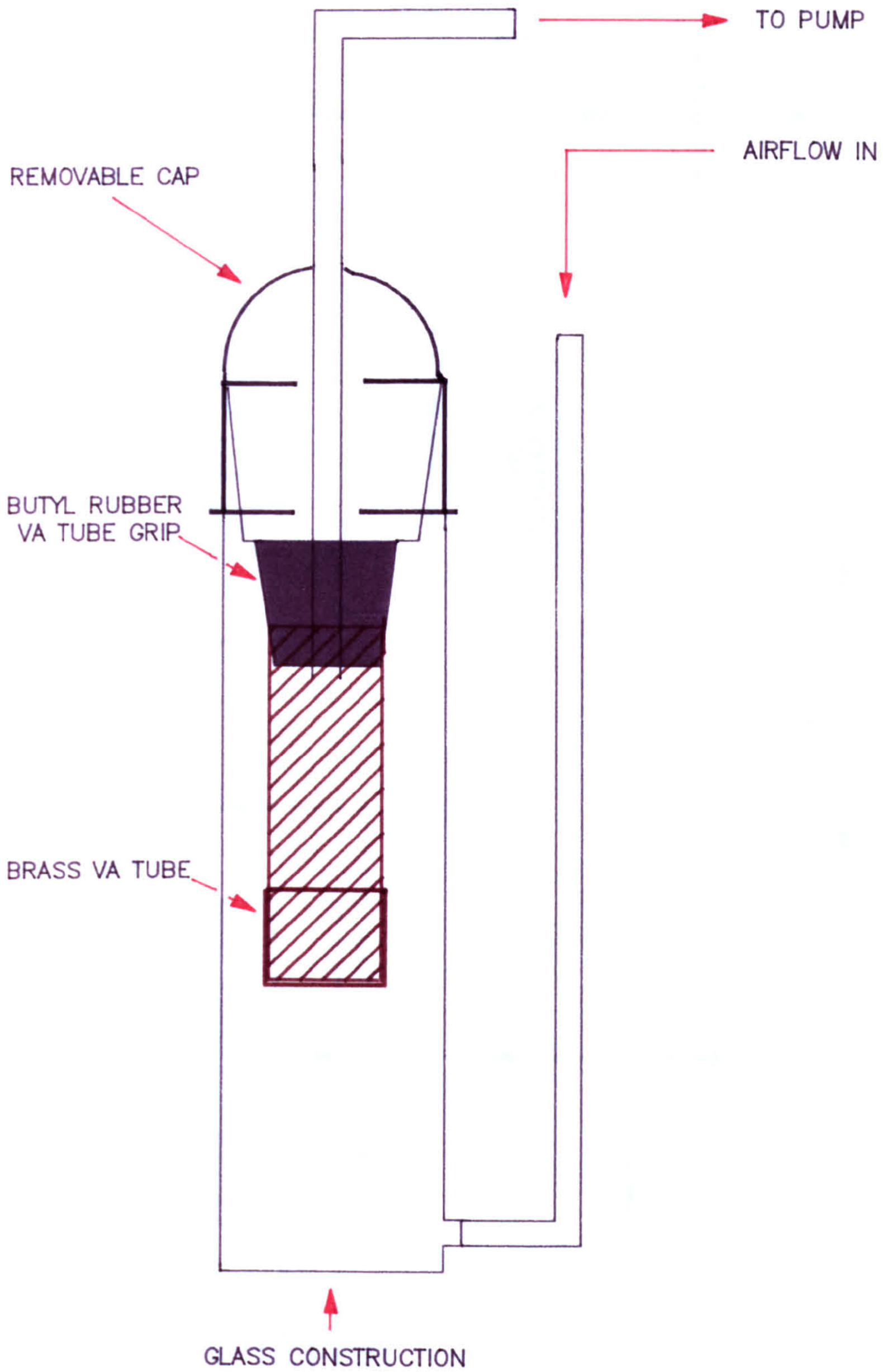

FIGURE 1.2. SAMPLE HOLDER

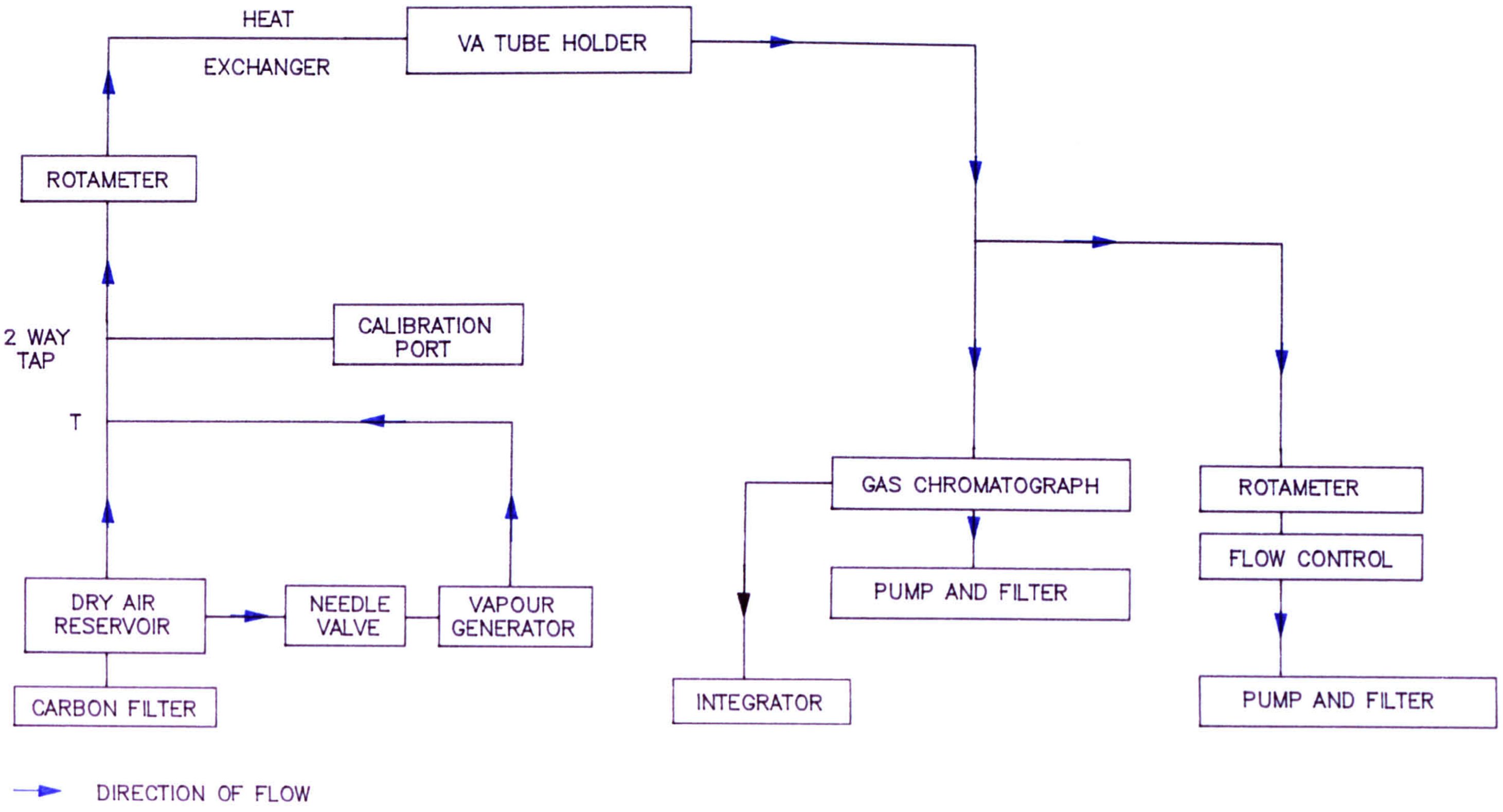

FIGURE 1.3. METHANOL ADSORPTION APPARATUS

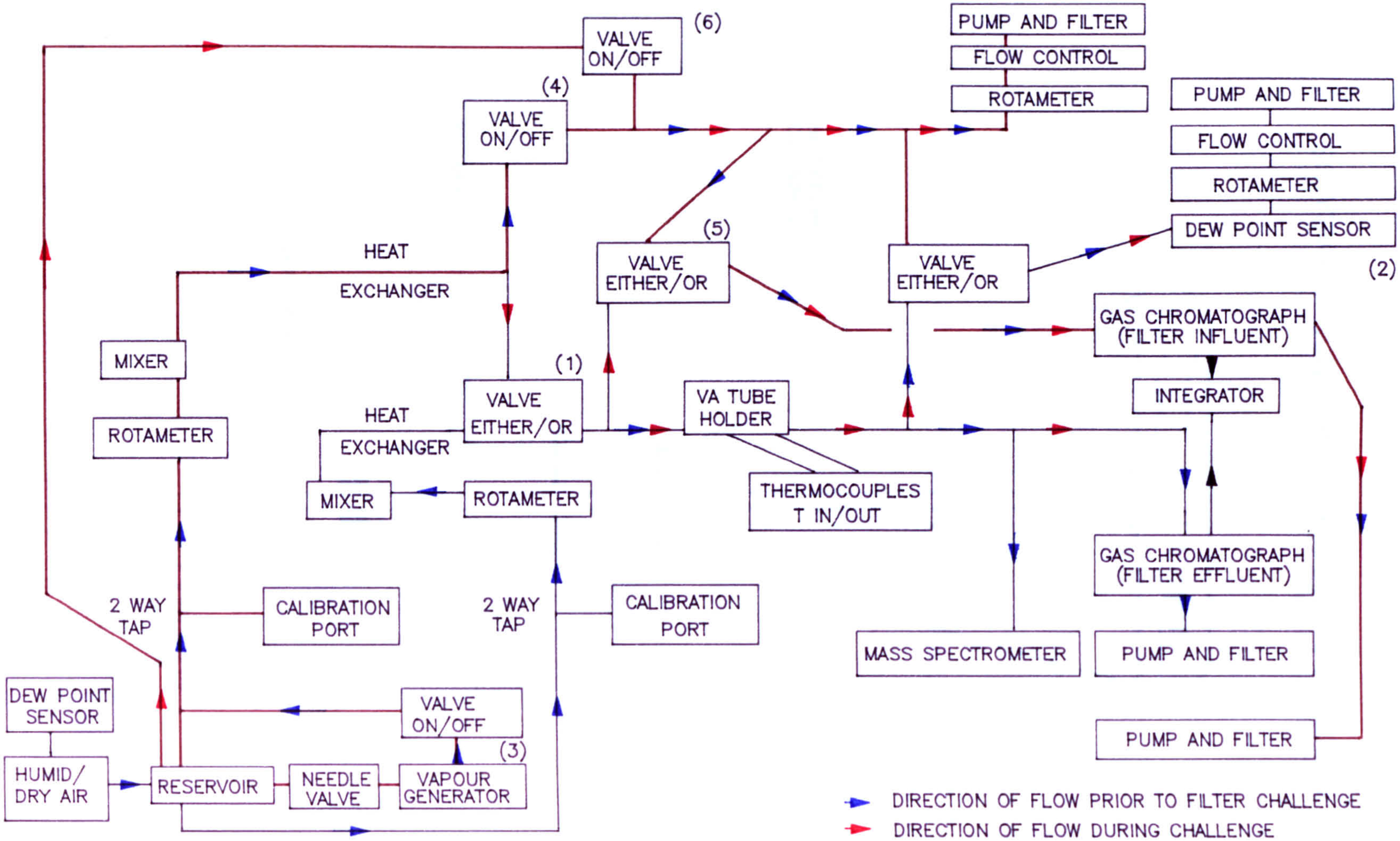

FIGURE 1.4. VAPOUR ADSORPTION APPARATUS

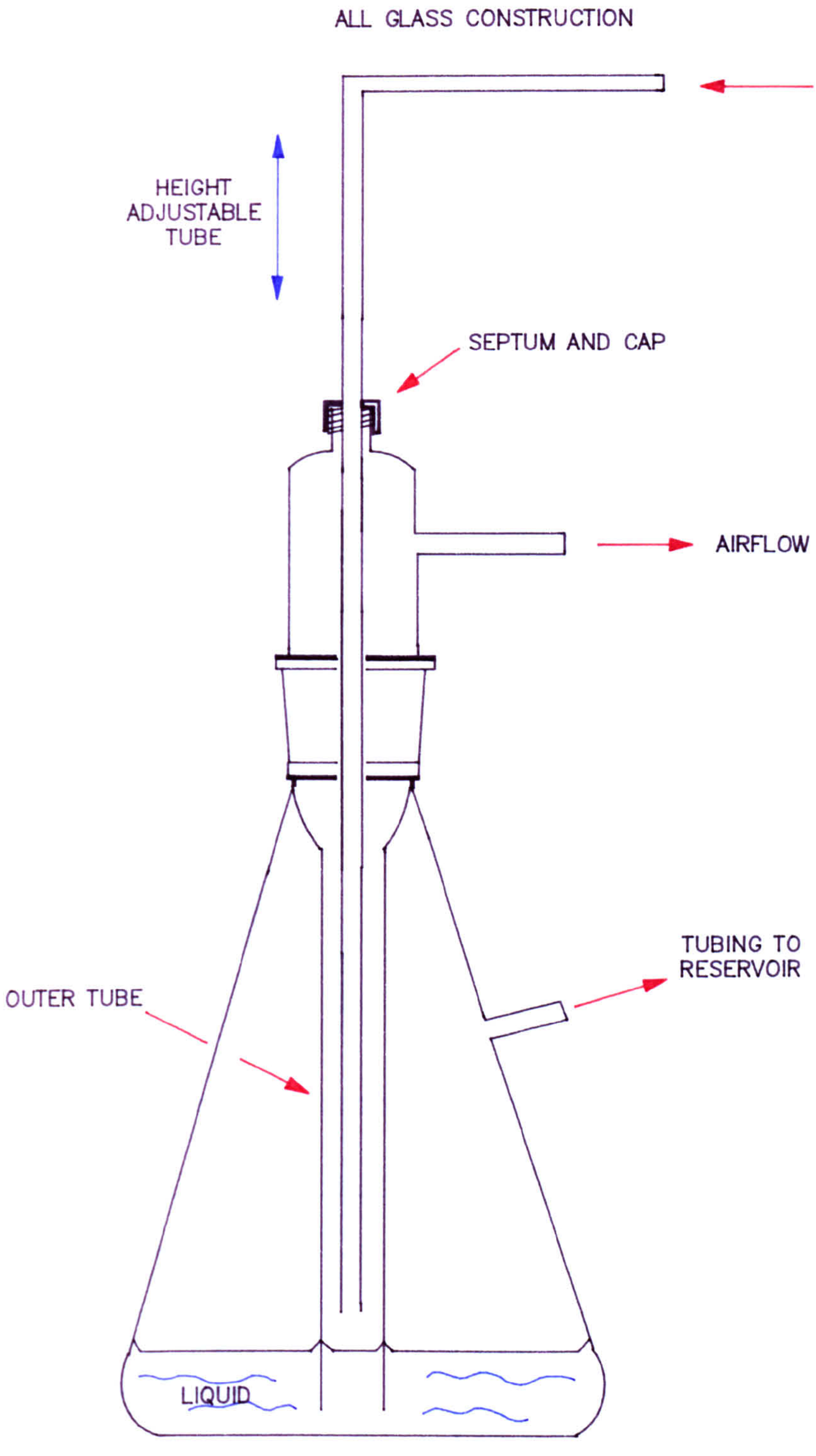

FIGURE 1.5. VAPOUR GENERATION APPARATUS

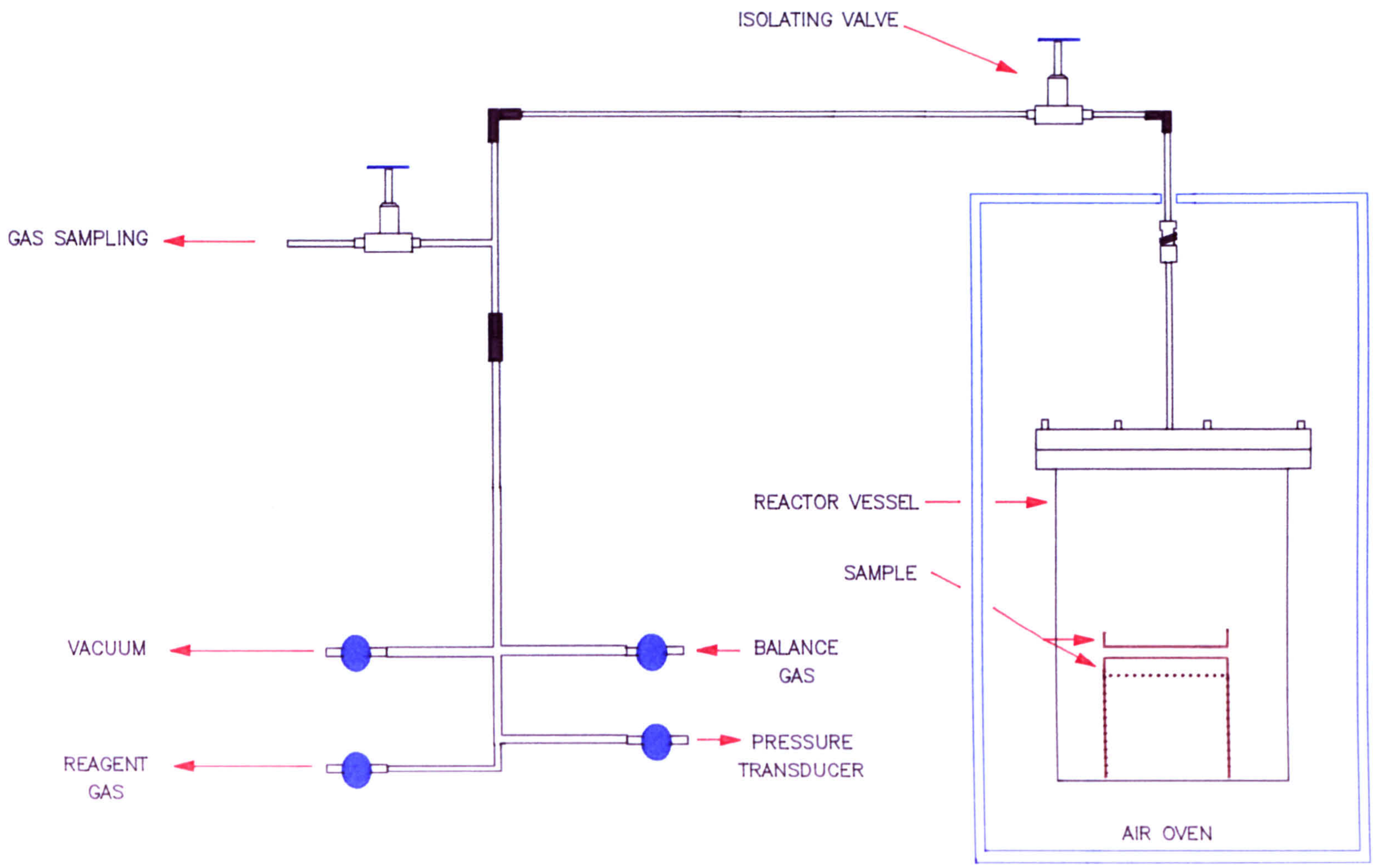

FIGURE 1.6. LOW TEMPERATURE CARBON MODIFICATION APPARATUS

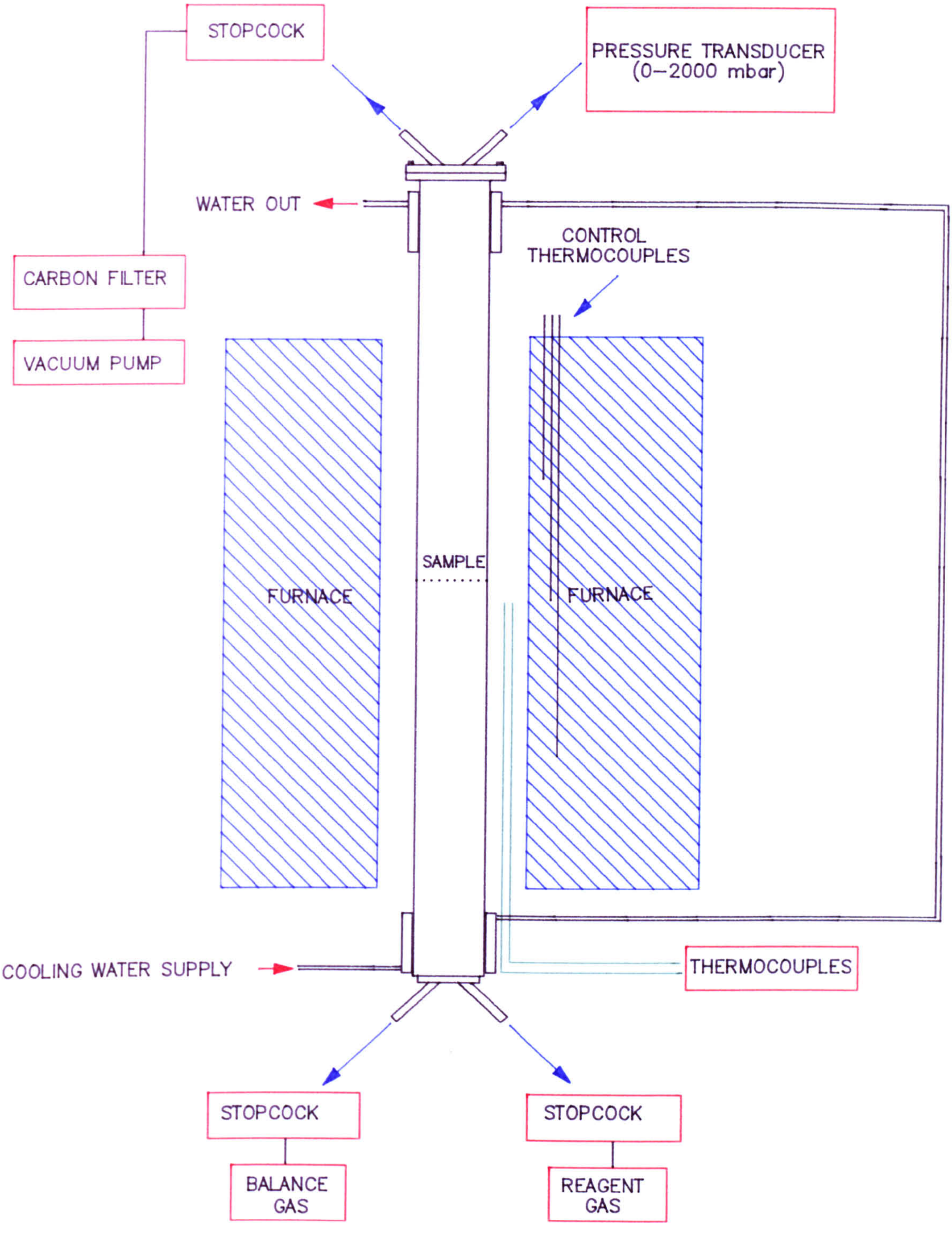

FIGURE 1.7. HIGH TEMPERATURE CARBON MODIFICATION APPARATUS

2 Tabulated Data

2.1 Chapter 6

Methanol Adsorption (BPL Carbons, Figures 6.2.1, 6.3.9)

Time (minutes)	Sample: Percentage Penetration						
	Control	Aged, RH80%, 22°C (days)			Aged, RH80%, 400 Days		
		7	35	250	Control	NO_2 500 mbar	NO_2 900 mbar
First Break	12	16	16	20	25	40	50
5	-	-	-	-	-	-	-
10	-	-	-	-	-	-	-
15	1	-	-	-	-	-	-
20	5	1	1	-	-	-	-
30	35	21	11	2	2	-	-
40	62	49	38	25	17	-	-
50	78	71	61	53	42	2	-
60	88	83	77	73	62	8	5
70	93	90	84	82	76	22	18
80	96	95	91	88	85	45	37
90	98	96	95	93	91	65	60
100	99	97	97	94	93	81	76
110	100	98	97	95	94	88	83
120	-	99	98	97	96	92	90
130	-	99	99	98	97	96	92
140	-	99	99	98	98	97	95
150	-	100	99	99	99	98	97
160	-	-	100	99	99	99	98
170	-	-	-	99	99	100	99
180	-	-	-	100	100	100	100

Methanol Adsorption (BPL Carbons, Figures 6.2.2, 6.2.7-6.28)

Ageing Period (days @ RH%)	Time to 50% Filter Breakthrough (min)		
	RH80%, 22°C	RH60%, 22°C	RH40%, 34°C
0	32.0	31.0	32.0
7	35.0	33.0	32.0
12	38.0	37.0	32.5
35	43.0	44.5	32.0
50	45.0	46.5	32.0
72	46.0	47.0	32.5
120	48.0	49.0	32.0
150	48.5	50.0	32.5
196	49.0	50.0	32.0
220	49.0	-	-
270	49.5	-	-
300	50.0	-	-

Methanol Adsorption (BPL Carbons, Figure 6.2.9)

Ageing Period (days @ RH80%)	Amount Adsorbed (equilibrium, mg g^{-1})	
	22°C	45°C
0	16.0	16.0
7	20.1	23.6
21	26.1	29.2
42	27.9	32.0
56	28.0	33.4
70	29.0	34.4
98	28.9	35.1
154	29.5	34.4

Water Adsorption (Figures 6.2.3, 6.2.10-6.2.14)

	Amount Adsorbed (w/w %)					
RH (%)	Sample					
Adsorption	Control BPL	Aged 860 days, RH80%, 22°C	Ageing Period (days) at RH80% @ °C			
			56 22°C	56 45°C	100 22°C	100 45°C
20	0.5	0.5	0.8	1.0	1.0	1.3
30	1.1	2.4	2.0	2.5	2.5	3.3
40	2.8	7.4	4.9	6.3	5.6	7.8
50	5.4	17.5	13.2	16.3	12.6	15.6
60	16.1	27.6	24.2	26.6	25.9	27.5
70	27.3	32.9	32.3	33.0	32.3	32.2
80	35.4	35.4	35.3	35.3	35.4	35.2
85	36.2	36.3	36.5	36.5	36.2	35.8
Desorption						
80	36.1	36.1	36.3	36.3	35.8	35.4
70	35.2	35.0	35.1	35.2	34.6	33.8
60	32.8	33.6	33.8	34.1	33.2	32.4
50	21.9	29.1	28.6	30.2	28.3	29.2
40	6.1	13.3	9.7	12.6	11.2	13.5
30	3.2	4.7	4.2	5.1	4.4	5.3
20	0.8	2.0	2.0	2.4	2.2	2.5
0*	0.3	0.0	0.1	0.2	0.1	0.0

*These values were obtained after outgassing the carbon at the end of the measurement (120°C; 3 hours; 3 mbar).

Hexane Adsorption (BPL Carbons, Dry, Humid Air- Figures 6.2.4-6.2.5)

Time (min)	Percent Penetration (dry, min)		Time (min)	Percent Penetration (Control, RH80%)	Time (min)	Percent Penetration (Aged, RH80%)
	Aged	Control				
25	0.0	-	71	0.0	39	0.0
30	2.0	0.0	81	3.0	44	2.2
40	5.0	1.0	86	4.8	49	4.8
45	11.0	6.1	91	7.2	54	9.1
50	28.2	18.2	96	10.3	59	15.4
55	56.0	43.1	101	14.0	64	23.6
60	70.3	61.0	106	18.6	69	32.8
65	93.1	84.0	111	23.5	74	42.0
70	98.0	95.2	116	28.7	79	50.0
75	100.0	97.5	121	34.0	84	57.0
80	-	99.0	126	39.0	89	63.0
85	-	100.0	131	44.0	94	68.0
-	-	-	136	48.4	99	72.0
-	-	-	141	52.5	104	74.5
-	-	-	146	56.3	114	79.2
-	-	-	151	59.7	124	83.6
-	-	-	156	62.6	134	86.3
-	-	-	161	65.4	144	87.5
-	-	-	171	69.7	-	-
-	-	-	181	72.7	-	-
-	-	-	191	74.8	-	-

{Humid challenge conditions were: RH80-80%, 22°C. 2cm diameter, 2cm bed depth filters, challenged at an apparent linear flow velocity of 382 cm min^{-1}. The hexane influent concentration was 240 ppm}

Chloropicrin Adsorption (BPL Carbons, Humid Air- Figures 6.2.6, 6.2.9)

Ageing Period (days) (RH80%, 22°C)	TTB (min)	Ageing Period (days, RH80%)	TTB (min) @ °C	
			22°C	45°C
0	81	0	81	81
46	73	7	73	68
197	60	21	67	64
289	57	42	63	54
408	55	56	58	53
570	52	70	55	48
1220	48	98	47	43
-	-	154	46	44

{TTB is the First Break (10-12 mg m^{-3}). 2cm bed, 2cm diameter filters, flow velocity 382 cm min^{-1}, challenged in equilibrium with RH80% air at 22°C: influent PS concentration 5000 mg m^{-3}}

Nitrogen Adsorption (BPL Carbons, Figures 6.3.1-6.3.3; Corrected Data)

Volume Adsorbed (cm^3<STP>g^{-1})						
P/P^0	Sample					
	Control	Aged (RH80%, 400 days)	Aged, NO_2 500 mbar	Control NO_2 Modified (@ mbar Pressure) 500	700	900
Adsorption						
<0.001	200	182	182	200	220	230
0.001	240	205	205	244	250	260
0.025	260	218	218	265	267	277
0.050	275	250	250	280	287	297
0.075	290	264	264	296	301	311
0.100	300	272	272	308	312	322
0.150	310	282	282	320	315	325
0.200	317	291	300	327	325	335
0.300	327	300	310	338	327	337
0.400	335	305	323	343	336	347
0.500	340	313	332	356	342	352
0.600	345	323	341	359	347	357
0.700	353	327	354	367	356	366
0.800	363	336	364	378	365	375
0.900	376	345	382	391	378	388
1.000	412	386	441	428	435	445
Desorption						
0.950	391	363	420	420	410	420
0.850	376	350	390	405	384	394
0.750	365	336	365	391	363	373
0.650	361	332	341 (0.5)	365 (0.5)	354	364
0.500	347	322	332 (0.4)	358 (0.4)	347	357
0.450	342	310	309 (0.2)	352 (0.3)	-	-

Water Adsorption (Figures 6.3.4-6.3.8; Corrected Data)

	Amount Adsorbed (w/w %)					
RH (%)	Sample					
Adsorption	Aged (RH80%, 400 days)		Control, NO_2 @ mbar			
	Aged	NO_2 900 mbar	120	500	700	900
20	1.2	4.0	2.3	3.4	3.9	3.0
30	2.1	6.1	3.1	4.8	5.4	5.8
40	5.6	13.5	7.6	11.9	13.1	12.8
50	15.8	22.0	15.4	22.5	22.1	21.5
60	24.1	29.0	24.5	30.1	29.6	29.2
70	31.3	33.8	32.3	34.5	35.0	34.5
80	34.2	35.3	35.6	37.0	36.8	36.4
85	36.0	36.5	37.2	37.7	38.4	37.7
Desorption						
80	35.5	36.0	36.5	37.4	37.7	37.1
70	34.6	34.5	35.5	36.1	36.3	35.5
60	33.2	33.2	33.4	34.6	34.7	34.2
50	26.3	31.2	26.8	31.3	32.3	32.1
40	9.7	21.4	10.2	18.2	19.8	20.2
30	4.4	7.1	4.8	6.7	7.2	7.1
20	2.4	3.7	2.6	3.0	3.6	3.5
0*	0.1	0.0	0.1	0.0	0.0	0.0

*These values were obtained after outgassing the carbon at the end of the measurement (120°C; 3 hours; 3 mbar).

2.2 Chapter 7

X Ray Diffraction Analysis (Figure 7.1.3; BPL Carbons)

Scanning Angle (Two θ,°)	Counts Second^{-1}/10^3 (BPL Control)	Counts Second^{-1}/10^3 (BPL, 30% F)
5	100	100
6	100	95
7	100	75
8	91	64
9	78	55
10	65	50
11	57	45
12	52	40
13	50	35
14	42	33
16	38	30
18	37	27
20	40	27
22	44	28
24	45	27
26	42	26
28	31	18
30	26	13
32	17	11
34	12	9
36	9	10
38	9	11
40	8	11
42	9	14
44	16	15
46	15	10

Thermal Analysis (Figures 7.1.4; BPL Carbon)

BPL Control			BPL Fluorinated (16.7% F)		
Temp (°C)	TG (As % Weight Change)	DTA	Temp (°C)	TG (As % Weight Change)	DTA
120	100	20	120	100	20
147	100	21.5	148	100	22.5
210	100	21.5	183	99.7	20.8
335	99.7	22	200	99.4	16.6
417	99.7	21	220	98.8	14.8
554	99.4	21	238	98.1	13.3
690	98.9	23	260	97.5	11.8
790	98.4	25	278	96.6	10.0
878	97.8	28	298	95.7	6.8
914	97.3	29	318	94.4	5.9
960	96.3	32.5	338	93.5	6.8
960	95.2	-	370	91.0	13.3
960	94.1	-	390	90.1	15.8
960	92.5	-	425	88.6	18.8
960	89.9	-	442	88.0	19.8
960	87.8	-	490	86.4	20.8
			540	85.5	20.8
			613	83.6	21
			696	81.5	21.8
			770	79.3	22.8
			845	76.5	23
			920	74.4	26
			960	73.2	31
			960	71.3	31
			960	68.2	31

Nitrogen Adsorption (Figures 7.1.5-7.1.6; Corrected Data)

Volume Adsorbed (cm^3<STP>g^{-1})						
P/P^0	Sample					
	BPL Control	BPL Fluorine 16.7% F	BPL Fluorine 13.7% F	CECA Control	CECA Fluorine 6% F	CECA Fluorine 30% F
Adsorption						
<0.001	200	140	79	200	233	162
0.001	240	181	199	280	272	217
0.025	260	204	227	305	299	250
0.050	275	227	244	327	325	276
0.075	290	239	257	350	341	292
0.100	300	245	267	363	355	303
0.150	310	257	277	377	371	318
0.200	317	262	281	387	378	325
0.300	327	268	286	400	389	334
0.400	335	276	296	407	397	341
0.500	340	282	303	411	403	343
0.600	345	289	308	417	410	347
0.700	353	300	318	420	413	352
0.800	363	309	330	427	419	357
0.900	376	321	343	438	426	364
1.000	412	373	381	455	462	383
Desorption						
0.950	391	340	360	445	437	373
0.850	376	321	341	437	421	365
0.750	365	307	330	430	415	360
0.650	361	299	316	426	410	357
0.500	347	288	303	420	403	347
0.450	342	279	-	407	400	342

Methanol Adsorption (Figures 7.1.7-7.1.8)

Time (minutes)	Sample: Percentage Penetration					
	CECA Control	CECA Fluorine 6% F	CECA Fluorine 18.8% F	CECA Fluorine 30% F	BPL Control	BPL Fluorine 6% F
First Break	25	18	8	6	12	14
5	-	-	-	-	-	-
10	-	-	2	3	-	-
15	-	-	5	13	1	1
20	-	4	18	42	5	3
30	4	42	57	71	35	25
40	25	65	75	82	62	50
50	67	84	88	92	78	75
60	85	90	92	95	88	83
70	93	94	97	98	93	90
80	97	98	98	99	96	92
90	98	99	100	100	98	94
100	100	100	-	-	99	98
110	-	-	-	-	100	98
120	-	-	-	-	-	99
130	-	-	-	-	-	100
140	-	-	-	-	-	-
150	-	-	-	-	-	-
Amount Adsorbed (mg g^{-1})	24.0	14.0	11.9	8.3	16.2	19.2

Water Adsorption (Figures 7.1.9-7.1.11)

	Amount Adsorbed (w/w %)					
RH (%)	Sample					
Adsorption	Control BPL	BPL Fluorine (10% F)	CECA Control	CECA Fluorine (6% F)	CECA Fluorine (18.8% F) First Isotherm	CECA Fluorine (18.8% F) Second Isotherm
20	0.5	1.0	2.2	3	3.8	4.6
30	1.1	2.3	3.6	4.5	5.2	7.4
40	2.5	6.2	5.5	6.3	6.4	10.1
50	5.4	15.1	6.1	15.0	14.6	20.7
60	16.1	24.3	19.8	32.2	25.5	32.2
70	27.5	31.5	38.6	43.2	31.4	39.0
80	33.9	35.2	47.4	46.8	35.9	41.9
85	35.4	37.4	48.6	47.8	37.7	43.2
Desorption						
80	35.0	37.0	48.0	47.5	37.2	42.6
70	34.3	35.8	47.1	46.3	35.6	41.3
60	32.5	34.3	45.7	45.0	34.0	39.7
50	24.6	32.0	38.2	42.1	30.7	35.9
40	6.4	26.2	8.7	15.6	14.0	16.4
30	3.2	15.5	5.2	2.3	3.0	10.6
20	2.1	7.8	3.2	1.1	-0.1	2.7
0*	0.4	-3.6	0.0	-3.1	-5.1	-2.1

*These values were obtained after outgassing the carbon at the end of the measurement (120°C; 3 hours; 3 mbar).

Chloropicrin Adsorption (Figure 7.1.12)

CECA Fluorine (6% F)		CECA Control	
Time (minutes)	Percent Penetration	Time (minutes)	Percent Penetration
102	0	138	0
111	0.3	156	1.1
126	1.1	168	3.9
141	3.6	183	12.6
154	7.3	192	21.3
165	13.6	204	36.9
177	22.2	213	50.1
192	37.4	225	68.6
207	55.9	240	87.4
219	72.4	249	94.3
233	87.8	258	97.9
246	94.7	267	98.9
261	98.1	273	99.3
276	99.6	282	99.8
288	100	288	100
102,123[1]	-	138,156[1]	-
680[2]	-	761[2]	-

[1]First Break (10-12 mg m^{-3}), 1% break (50 mg m^{-3}) (minutes). [2]Equilibrium PS adsorption (mg g^{-1}).

{2cm bed, 2cm diameter filters, flow velocity 382 cm min^{-1}, challenged in equilibrium with dry (<RH2%) air at 22°C: PS concentration 5000 mg m^{-3}}

Hexane and Methanol Adsorption (Figures 7.2.1-7.2.2)

	Sample				
Time (minutes)	Percentage Penetration				
	Hexane Adsorption		Methanol Adsorption		
	BPL Control	BPL HFP	BPL Control	BPL HFP	BPL (Aged) HFP
First Break	30	20	12	4	6
5	-	-	-	2	-
10	-	-	-	13	8
15	-	-	1	26	22
20	-	0	5	58	54
30	0	1	35	79	76
40	1	19	62	92	87
45	6	46	-	-	-
50	18	71	78	94	90
55	43	90	-	-	-
60	61	96	88	97	93
65	84	97	-	-	-
70	95	98	93	99	95
80	99	99	96	100	98
85	100	100	-	-	-
90	-	-	98	-	99
100	-	-	99	-	100
110			100		-
120	-	-	-	-	-
Amount Adsorbed (mg g^{-1})	247	201	18.0	12.0	13.0

Water Adsorption (Figures 7.2.3-7.2.4)

	Amount Adsorbed (w/w %)			
RH (%)	Sample			
Adsorption	Control BPL	BPL HFP Modified	BPL (Aged) Control	BPL (Aged) HFP Modified
20	0.5	0.4	0.9	0.5
30	1.2	0.8	1.7	1.0
40	2.8	1.5	5.0	1.9
50	5.4	3.4	12.5	4.8
60	15.9	7.8	22.5	11.7
70	27.2	17.8	30.5	21.6
80	35.4	28.5	34.3	27.7
85	36.2	31.1	35.1	29.9
Desorption				
80	36.1	30.8	34.6	29.6
70	35.2	29.7	33.5	28.7
60	32.8	26.8	31.6	26.6
50	21.9	15.3	25.3	18.0
40	6.1	6.8	8.4	7.8
30	3.1	3.4	3.1	3.9
20	0.7	2.2	0.7	2.3
0*	0.3	0.4	0.0	0.5

*These values were obtained after outgassing the carbon at the end of the measurement (120°C; 3 hours; 3 mbar).

Nitrogen Adsorption (Figure 7.3.1; Corrected Data)

Volume Adsorbed (cm^3<STP>g^{-1})				
P/P^0	Sample			
	BPL Control	BPL Difluoroethene (1 Cycle)	BPL Difluoroethene (3 Cycles)	BPL Difluoroethene (6 Cycles)
Adsorption				
<0.001	200	194	189	186
0.001	240	211	205	205
0.025	260	242	230	227
0.050	275	265	246	248
0.075	290	273	258	264
0.100	300	286	266	274
0.150	310	296	276	287
0.200	317	306	283	296
0.300	327	314	294	310
0.400	335	323	302	321
0.500	340	332	307	326
0.600	345	337	314	329
0.700	353	341	322	341
0.800	363	357	332	358
0.900	376	367	345	372
1.000	412	418	404	414
Desorption				
0.950	391	388	373	393
0.850	376	372	348	368
0.750	365	359	338	348
0.650	361	352	327	341
0.500	347	341	314	331
0.450	342	327	305	323

Hexane Adsorption (Figure 7.3.2)

Sample			
Time (minutes)	Percentage Penetration		
	BPL Control	BPL Difluoroethene (1 Cycle)	BPL Difluoroethene (6 Cycles)
First Break	30	25	25
20	-	-	-
25	-	0	0
30	0	1	1
35	1	2	2
40	1	3	7
45	6	11	28
50	18	33	50
55	43	66	78
60	61	86	92
65	84	96	98
70	95	99	99
80	99	100	100
85	100	-	-
Amount Adsorbed (mg g^{-1})	255	232	216

Water Adsorption (Figures 7.3.3-7.3.7; corrected data)

	Amount Adsorbed (w/w %)						
RH (%)	Sample (BPL Carbons)						
Ads.	Control (120°C)	Control (450°C)	DFE 3 Cycles	DFE 6 Cycles	DFE 12 Cycles	DFE 6 Cycles (Aged)	DFE 6 Cycles (600°C)
20	0.5	0.4	0.2	0.1	0.2	0.3	0.2
30	1.2	0.8	0.3	0.2	0.4	0.8	0.3
40	2.8	2.3	1.0	0.6	0.7	2.0	0.7
50	5.4	6.1	2.6	2.0	2.4	5.9	1.7
60	15.9	14.6	8.4	7.5	6.8	13.3	4.2
70	27.2	27.3	21.0	19.7	17.3	22.9	8.9
80	35.4	34.8	30.7	28.5	27.3	28.4	12.8
85	36.2	37.3	33.4	31.0	29.3	30.7	16.2
Des.							
80	36.1	37.0	33.3	30.8	28.8	30.3	16.1
70	35.2	35.8	32.1	29.8	28.0	29.2	15.8
60	32.8	33.7	30.1	27.8	25.7	27.3	15.2
50	21.9	23.2	16.9	15.2	12.6	15.8	11.8
40	6.1	7.5	4.6	4.1	4.2	4.6	6.5
30	3.1	3.6	2.5	2.2	1.9	2.2	3.7
20	0.7	2.2	1.3	1.1	1.2	1.4	2.1
0*	0.3	0.7	0.6	0.4	0.6	0.1	0.5

Hexane Adsorption at High RH (Figure 7.3.8)

BPL Control		BPL Aged		BPL Difluoroethene (6 Cycles)	
Time (minutes)	Effluent (mg m^{-3})	Time (minutes)	Effluent (mg m^{-3})	Time (minutes)	Effluent (mg m^{-3})
0	0	0	0	0	0
0.5	0	0.5	0	0.5	0
1	0	1	58	1	0
1.5	8	1.5	250	1.5	0
2	40	2	673	2	2
2.5	40	2.5	962	2.5	2
3	38	3	865	3	3
4	38	4	827	4	3
6	37	6	692	6	4
8	36	8	558	8	4
10	35	10	442	10	5
15	31	15	308	15	4
20	29	20	250	20	3
30	29	30	192	30	3
40	29	40	173	40	3
50	28	50	154	50	3
60	28	60	135	60	3
80	20	64	125	80	2
100	15	80	100	100	2
120	10	100	72	120	0
140	5	120	60	-	-
180	0	140	29	-	-
-	-	190	0	-	-

{2cm diameter, 2cm bed depth filters: flow velocity 382 cm min^{-1}: challenged in equilibrium with RH80% air at 22°C: 2 minute x 15000 mg m^{-3} challenge of hexane vapour}

2.3 Chapter 8

Thermal Analysis (Figures 8.1; 8.9 - 8.11; SCII Carbons)

Sample	Phosgene	Phosgene/ Water	Control	Chlorine	Chlorine/ Water
Temperature (°C)	Percent of Initial Sample Weight				
120	100	100	100	100	100
150	100	100	100	100	100
200	100	100	100	100	100
250	99.8	99.8	99.8	99.8	99.8
300	99.6	99.6	99.6	99.6	99.6
350	99.6	99.6	99.5	99.3	99.6
400	99.4	99.4	99.4	98.8	99.4
450	98.5	99.1	98.8	97.0	98.8
500	97.3	98.5	98.2	95.5	97.9
550	95.8	97.3	97.6	92.8	97.0
600	93.1	96.7	97.0	90.1	96.1
650	91.3	95.5	95.8	86.8	94.6
700	87.7	94.3	94.6	84.4	93.7
750	85.3	93.1	93.7	81.7	91.9
800	84.1	91.3	92.8	80.5	90.4
850	82.3	89.8	91.3	78.4	88.3
900	81.1	88.6	89.5	77.8	87.4
910	80.5	88.3	89.2	77.2	86.2
910*	78.1	86.2	85.6	73.3	82.3
Initial Sample Weight (mg)	22.5	23.2	22.6	25.0	23.1

*Samples maintained at 910°C until constant weight attained.

Nitrogen Adsorption (Figures 8.2-8.5; 8.13-8.15 Corrected Data)

Volume Adsorbed (cm^3<STP>g^{-1})						
P/P^0	Sample					
	SCII Control	SCII Chlorine	SCII Chlorine/ Methanol	SCII Chlorine/ Water	CECA Control	CECA Phosgene
Adsorption						
<0.001	255	230	246	240	200	218
0.001	285	264	287	280	280	273
0.025	303	280	297	306	305	294
0.050	333	299	322	328	327	327
0.075	347	313	333	341	350	343
0.100	362	321	342	352	363	354
0.150	367	328	350	363	377	371
0.200	372	334	355	368	387	379
0.300	380	342	362	377	400	390
0.400	385	344	366	384	407	395
0.500	388	347	368	386	411	398
0.600	390	350	371	391	417	403
0.700	395	352	374	395	420	406
0.800	400	355	376	400	427	411
0.900	407	363	380	411	438	420
1.000	422	375	397	420	455	457
Desorption						
0.950	418	371	390	418	445	436
0.850	408	365	385	413	437	420
0.750	403	361	383	409	430	414
0.650	401	359	380	402	426	410
0.500	393	353	372	395	420	398
0.450	387	345	367	385	407	-
*	0.0	12.5	9.3	6.7	0.0	9.0

Volume Adsorbed (cm^3<STP>g^{-1})					
P/P^0	Sample				
	CECA Phosgene/ Methanol	CECA Chlorine	BPL Control	BPL Phosgene	BPL Phosgene/ Methanol
Adsorption					
<0.001	212	221	200	183	186
0.001	271	247	240	207	218
0.025	287	276	260	221	230
0.050	314	303	275	239	249
0.075	327	312	290	253	260
0.100	334	320	300	259	265
0.150	347	332	310	266	276
0.200	358	338	317	272	281
0.300	365	344	327	284	290
0.400	372	352	335	291	297
0.500	375	358	340	296	302
0.600	380	361	345	302	306
0.700	386	363	353	309	313
0.800	390	367	363	316	324
0.900	398	375	376	332	334
1.000	425	404	412	377	361
Desorption					
0.950	406	387	391	357	346
0.850	397	379	376	331	331
0.750	391	373	365	318	324
0.650	389	368	361	309	313
0.500	379	363	347	296	302
0.450	372	355	342	-	300
*	6.2	16.6	0.0	7.8	6.1

*Weight change resulting from modification/ treatment.

Water Adsorption (Figures 8.6-8.8; 8.16-8.19; 8.27-8.28; 8.30-8.31: (corrected)

	Amount Adsorbed (w/w %)						
RH (%)	Sample (SCII Carbons)						
Ads.	Control	CG[1]	CG[2]	CG Methanol	CG Water[1]	CG Water[a]	Chlorine (12.5%)
20	1.1	0.5	1.1	0.4	0.4	0.4	1.1
30	1.8	1.1	2.5	0.7	0.7	0.7	2.4
40	3.8	2.1	4.3	1.8	1.4	1.7	5.4
50	5.9	5.0	8.6	5.7	2.5	2.8	12.9
60	20.5	17.1	20.0	15.7	12.5	13.3	26.1
70	34.3	30.7	32.9	30.4	28.6	30.0	36.0
80	40.0	37.9	38.2	38.6	38.2	38.5	40.4
85	41.4	39.6	40.0	40.7	41.1	40.7	42.2
Des.							
80	40.7	39.3	39.0	40.4	40.0	40.0	41.6
70	40.0	38.6	38.2	39.6	39.3	39.3	40.6
60	39.0	36.4	35.7	36.8	35.7	36.4	39.2
50	28.6	18.6	15.4	14.3	11.1	12.0	25.1
40	6.8	8.9	6.8	5.4	4.3	5.0	14.1
30	3.6	5.7	4.3	3.2	2.1	2.4	9.0
20	2.5	3.9	2.5	1.8	1.1	1.3	6.1
0*	0.7	1.4	0.7	0.0	0.0	0.0	1.1

CG is Phosgene. superscript numbers designate first and second isotherms measured for the same samples. [a]Signifies the sample was aged at 45°C and RH80% for 45 days prior to measurement of the isotherm. *These values were obtained after outgassing the carbon at the end of the measurement (120°C; 3 hours; 3 mbar).

	Amount Adsorbed (w/w %)							
R H	Sample (CECA Carbons)							
A	Control	Control Aged	CG^1 Meoh	CG^2 Meoh	Aged-CG^1 Meoh	Aged-CG^2 Meoh	NO_2-Meoh	NO_2-CG Meoh
20	2.0	2.9	0.4	0.4	1.1	1.1	3.2	1.4
30	3.2	4.6	0.9	1.1	1.8	2.1	5.0	2.5
40	4.6	7.1	2.1	2.6	4.0	4.4	9.6	5.7
50	7.1	17.9	4.6	5.2	7.5	7.5	23.6	18.6
60	18.6	35.0	10.7	10.7	18.6	19.1	36.1	30.7
70	35.0	43.2	23.6	24.2	33.6	34.1	42.9	41.4
80	47.9	47.1	36.8	37.1	41.4	41.8	45.4	45.0
85	48.2	47.8	40.7	40.9	43.6	44.0	47.1	46.8
D								
80	47.9	47.1	40.4	40.7	42.9	43.6	46.4	46.4
70	46.1	46.1	39.6	40.0	42.1	42.9	44.3	45.4
60	44.5	44.6	38.2	37.5	40.4	41.4	42.9	43.6
50	35.7	40.0	11.1	10.0	19.6	20.7	40.4	40.4
40	8.9	10.4	5.0	5.0	5.7	6.0	17.1	17.5
30	5.7	4.6	2.5	2.8	3.6	3.9	5.7	7.1
20	3.6	2.9	1.4	1.4	2.5	2.9	3.6	4.6
0*	0.7	0.4	0.0	0.0	0.0	0.0	1.2	1.4

NO_2: Carbons were first modified with dinitrogen tetroxide

	Amount Adsorbed (w/w %)					
RH (%)	Sample (SCII and BPL Carbons)					
Adsorption	SCII Control	SCII Aged[a] Control	BPL Control	BPL Chlorine/ Water	BPL NO_2/ Methanol	BPL NO_2/ Phosgene/ Methanol
20	1.1	1.6	0.5	0.7	2.1	1.1
30	1.8	2.8	1.1	1.8	4.6	2.5
40	3.8	6.6	2.5	3.2	7.1	6.1
50	5.9	19.4	5.4	7.5	19.6	17.9
60	20.5	34.6	16.1	16.8	28.9	26.4
70	34.3	39.3	27.5	28.3	34.3	31.4
80	40.0	40.5	33.9	31.1	36.4	35.3
85	41.4	41.8	35.4	32.9	37.4	36.9
Desorption						
80	41.1	41.6	35.0	32.1	37.1	36.0
70	40.7	40.9	34.3	31.8	35.7	35.4
60	39.0	40.2	32.5	29.6	34.6	33.9
50	28.6	35.7	24.6	15.0	30.4	30.7
40	6.8	9.0	6.4	6.4	15.4	16.1
30	3.6	3.5	3.2	3.6	5.7	8.9
20	2.5	2.0	2.1	2.5	2.9	5.7
0*	0.6	0.2	0.4	0.0	0.7	1.4

NO_2: Carbons were first modified with dinitrogen tetroxide
[a]Aged at 45°C and RH80% for 45 days

Methanol Adsorption (Figures 8.20-8.25; 8.29)

Time (minutes)	Sample: Percentage Penetration				
	CECA Control	CECA Phosgene	CECA Phosgene/ Methanol	CECA Aged Control*	CECA Aged Phosgene*
First Break	25	10	6	40	12
5	-	-	-	-	-
10	-	-	2.5	-	-
15	-	5	22	-	2.5
20	-	24	46	-	17
30	4	63	76	-	50
40	25	83	89	-	72
50	67	93	97	3	83
60	85	98	100	22	88
70	93	100	-	54	93
80	97	-	-	79	97
90	98	-	-	89	98
100	100	-	-	93	100
110	-	-	-	97	-
120	-	-	-	98	-
130	-	-	-	99	-
140	-	-	-	100	-
150	-	-	-	-	-
Amount Adsorbed (mg g^{-1})	24.0	15.2	9.9	36.0	18.0

*Samples were aged at 45°C and RH80% for 45 days.

Sample					
Time (minutes)	Percentage Penetration				
	CECA Aged* Phosgene/ Methanol	CECA Phosgene/ Methanol	CECA Phosgene/ Methanol Aged*	SCII Chlorine/ Water	SCII Chlorine/ Water- Aged*
First Break	8	10	12	10	15
5	-	-	-	-	-
10	-	-	-	-	-
15	6	17	8	1	-
20	25	42	33	6	2
30	63	71	63	29	18
40	81	83	75	55	48
50	90	92	87	73	67
60	94	96	93	83	80
70	98	99	95	90	88
80	99	100	98	94	93
90	100	-	100	98	97
100	-	-	-	99	98
110	-	-	-	100	100
120	-	-	-	-	-
130	-	-	-	-	-
140	-	-	-	-	-
150	-	-	-	-	-
Amount Adsorbed (mg g^{-1})	11.7	10.7	13.0	21.2	23.0

Sample					
Time (minutes)	Percentage Penetration				
	BPL Control	BPL Phosgene	BPL Phosgene/ Methanol	BPL Chlorine/ Water	BPL Chlorine/ Water Aged*
First Break	12	12	12	15	15
5	-	-	-	-	-
10	-	-	-	-	-
15	1	1	1	2.5	1.7
20	5	2.5	4	25	17
30	35	26	34	52	37
40	62	54	61	72	67
50	78	73	78	84	81
60	88	83	88	92	88
70	93	90	93	96	93
80	96	93	97	98	95
90	98	95	98	99	98
100	99	98	100	100	100
110	100	99	-	-	-
120	-	100	-	-	-
130	-	-	-	-	-
140	-	-	-	-	-
150	-	-	-	-	-
Amount Adsorbed (mg g^{-1})	16.2	18.0	15.0	19.0	21.6

2.4 Chapter 9

PS ADSORPTION AND WATER DISPLACEMENT (Figure 9.1.1- Control, RH<2%)

Time (minutes)	Effluent Temperature (^{o}C)	Time (minutes)	Effluent PS Concentration (mg m^{-3})
0	22.0	120	0
2	22.5	129	25
6	22.8	138	120
10	22.9	147	500
22	22.9	153	1055
32	23.0	162	2160
54	23.0	171	3290
69	23.0	177	3845
97	23.0	183	4255
101	23.1	192	4670
120	23.1	201	4808
147	23.1	213	4910
152	23.2	222	4950
161	23.0	228	4960
169	23.0	234	4985
174	22.9	238	5000
179	22.8	-	-
185	22.6	-	-
190	22.5	-	-
194	22.4	-	-
199	22.3	-	-
204	22.2	-	-
212	22.2	-	-
215	22.1	-	-
220	22.0	-	-

PS ADSORPTION AND WATER DISPLACEMENT (Figure 9.1.2- Control, RH40%)

Time (min)	Temp (^{o}C)	Time (min)	PS (mg m^{-3})	Time (min)	RH% (Corrected)	Time (min)	Water (mg m^{-3})
0	22	105	0	0	40.3	0	0
1	22.4	114	10	2	40.2	2	221
2	22.5	120	21	4	40.5	4	276
8	22.6	126	49	9	39.8	9	193
12	22.7	132	124	14	39.4	14	165
17	22.8	138	302	17	39.0	17	138
26	22.9	144	586	25	38.8	25	138
40	23.0	153	1268	36	38.7	36	110
67	23.0	159	1894	50	38.5	50	110
86	23.0	165	2605	74	38.1	74	110
121	23.0	171	3280	95	37.9	95	110
157	23.0	177	3650	120	37.6	120	110
163	23.0	183	4020	142	37.5	142	55
168	22.9	189	4290	160	37.8	160	55
170	22.9	195	4580	180	39.1	180	55
173	22.8	210	4880	187	39.3	187	0
176	22.7	219	4935	200	39.7	-	-
180	22.6	231	5000	210	39.8	-	-
182	22.5	-	-	225	40.0	-	-
186	22.4	-	-	230	40.0	-	-
194	22.3	-	-	-	-	-	-
210	22.2	-	-	-	-	-	-
224	22.1	-	-	-	-	-	-
230	22.0	-	-	-	-	-	-

{Values are for effluent amounts}

PS ADSORPTION AND WATER DISPLACEMENT (Figure 9.1.3- Control, RH65%)

Time (min)	Temp (^{o}C)	Time (min)	PS (mg m^{-3})	Time (min)	RH% (Corrected)	Time (min)	Water (mg m^{-3})
0	22.0	57	0	0	64.8	0	0
2	22.5	63	9	2	62.6	2	83
5	22.7	66	12	5	62.6	5	249
8	22.6	72	20	9	63.4	9	332
12	22.5	81	44	22	64	22	417
22	22.5	90	89	29	64.4	29	503
32	22.5	99	177	35	64.9	35	588
58	22.4	111	392	43	65.3	43	673
68	22.3	129	950	50	65.7	50	758
73	22.2	144	1522	58	66.5	58	845
78	22.1	159	2118	65	67.1	65	932
85	21.9	174	2669	71	67.9	71	1022
91	21.6	192	3294	77	69.5	77	1198
98	21.3	207	3757	85	71.5	85	1376
102	21.0	225	4209	91	73.7	91	1558
108	20.7	246	4587	98	76.0	98	1740
117	20.2	273	4886	108	80.4	108	2020
125	19.9	285	4946	119	83.9	119	2208
128	19.8	300	4971	125	85.8	125	2160
131	19.7	309	4985	138	85.8	138	2113
144	19.8	318	4990	145	85.0	145	2020
149	19.9	324	5000	152	83.9	152	1924
160	20.0	-		168	81.3	168	1649
168	20.1	-	-	174	80.3	174	1558
178	20.3	-	-	180	78.6	180	1376
190	20.5	-	-	186	77.6	186	1287
200	20.7	-	-	193	76.2	193	1109

211	20.9	-	-	198	75.4	198	1021
221	21.0	-	-	208	73.3	208	802
233	21.3	-	-	222	71.3	222	588
245	21.5	-	-	234	69.1	234	417
254	21.6	-	-	254	67.0	254	249
261	21.7	-	-	272	65.7	272	166
287	21.8	-	-	288	65.3	288	83
312	21.9	-	-	312	64.8	312	0
325	22.0	-	-	325	64.8	325	0

<u>PS ADSORPTION AND WATER DISPLACEMENT</u> (Figures 9.1.4, 9.2.3- Control, RH80%)

Time (min)	Temp (°C)	Time (min)	PS (mg m^{-3})	Time (min)	RH% (Corrected)	Time (min)	Water (mg m^{-3})
0	22.0	24	0	0	80.1	0	0
1	22.4	30	23	1	78.1	1	0
2	22.6	36	55	2	76.7	2	99
4	22.7	42	123	4	77.2	4	200
8	22.6	48	261	5	77.9	5	301
10	22.6	54	473	8	79.2	8	503
14	22.5	60	740	10	79.7	10	606
19	22.4	66	1037	12	79.9	12	709
22	22.3	72	1345	14	81.1	14	811
24	22.2	78	1635	19	82.7	18	1021
29	22.0	84	1921	22	83.7	19	1021
34	21.8	90	2186	24	84.7	22	1126
40	21.6	96	2410	28	86.0	24	1231
46	21.4	102	2610	32	87.4	28	1338
52	21.2	111	2860	36	89.0	32	1445

58	20.9	117	3030	42	90.6	36	1552
62	20.7	123	3155	44	91.5	42	1661
68	20.6	132	3315	50	93.2	44	1770
74	20.4	141	3465	54	94.9	50	1879
84	20.3	150	3605	64	97.6	54	1990
96	20.2	159	3745	74	99.1	64	2039
106	20.2	183	4035	84	99.9	84	1990
136	20.3	195	4170	100	100.0	100	1879
152	20.4	210	4263	106	99.1	106	1770
162	20.5	225	4390	118	98.2	118	1661
174	20.6	240	4415	124	97.6	124	1552
184	20.8	255	4532	132	96.7	132	1445
206	21.0	270	4568	138	96.1	148	1231
232	21.2	285	4645	148	94.9	158	1128
245	21.3	330	4810	158	93.7	168	916
270	21.5	345	4815	168	92.3	184	811
284	21.6	360	4838	184	90.0	196	708
308	21.7	384	4875	196	88.6	214	606
368	21.8	402	4935	214	87.6	226	503
410	21.9	414	4960	226	86.5	234	396
422	22.0	432	5000	234	85.7	248	301
-	-	-	-	248	84.4	292	200
-	-	-	-	292	82.3	326	99
-	-	-	-	326	81.3	380	0
-	-	-	-	380	80.3	-	-
-	-	-	-	432	80.0	-	-

PS ADSORPTION AND WATER DISPLACEMENT (Figure 9.1.5- Control, RH95%)

Time (min)	Temp (°C)	Time (min)	PS (mg m^{-3})	Time (min)	RH% (Corrected)	Time (min)	Water (mg m^{-3})
0	22.0	12	0	0	95.1	0	0
2	22.3	15	15	2	94.1	2	116
5	22.4	24	70	5	94.7	5	349
7	22.4	33	270	7	95.8	7	585
10	22.4	39	520	10	96.1	10	585
15	22.3	48	1015	15	97.3	15	703
22	22.1	57	1570	22	98.8	22	823
30	22.1	63	1950	30	99.1	30	823
35	22.0	72	2465	35	99.4	35	823
40	21.9	81	2935	40	99.7	40	823
51	21.8	90	3325	51	100.0	51	823
60	21.7	99	3630	60	100.0	60	703
80	21.6	108	3895	80	100.0	80	585
95	21.6	120	4135	95	100.0	95	585
110	21.5	129	4310	110	100.0	110	466
130	21.5	138	4425	130	100.0	130	466
155	21.5	150	4560	155	100.0	155	408
180	21.5	168	4655	180	100.0	180	349
205	21.5	180	4715	205	100.0	205	349
220	21.5	195	4720	220	100.0	220	349
240	21.5	213	4745	240	100.0	240	291
260	21.5	231	4825	260	99.4	260	233
280	21.5	249	4860	280	98.8	280	116
300	21.6	273	4930	300	98.5	300	116
310	21.6	297	4940	310	98.2	310	0
325	21.6	312	4925	325	97.3	-	-
345	21.7	330	4945	345	97.0	-	-
365	21.8	357	4955	365	96.7	-	-

385	21.8	384	4960	385	96.4	-	-
400	21.8	408	4975	400	96.4	-	-
425	21.9	426	4985	425	96.1	-	-
440	21.9	442	4995	440	95.8	-	-
450	22.0	450	5000	450	95.1	-	-

PS ADSORPTION AND WATER DISPLACEMENT (Figure 9.1.7-Dry Control,RH80%)

Time (min)	Temp (°C)	Water (mg m^{-3})	Time (min) (Contd)	Temp (°C) (Contd)	Water (mg m^{-3}) (Contd)	Time (min)	PS (mg m^{-3})
0	22.0	0	130	21.4	16791	79	0
1	25.9	5100	140	21.3	16791	84	20
2	27.2	9886	148	21.4	16791	93	80
4	27.3	11224	158	21.5	16578	99	175
6	27.3	11912	168	21.6	16472	105	340
9	26.9	12721	175	21.7	16368	111	610
11	26.5	12973	181	21.8	16264	117	1035
15	26.1	13317	190	21.8	16160	123	1575
20	25.5	13667	200	21.9	16057	129	2125
25	25.3	13847	215	21.9	15955	135	2615
31	25.1	13936	226	22.0	15853	141	3045
40	24.8	14118	250	22.0	15853	150	3530
50	24.6	14302	-	-	-	159	3890
65	24.3	14488	-	-	-	168	4200
75	24.0	14867	-	-	-	180	4420
85	23.7	15157	-	-	-	189	4610
95	23.3	15652	-	-	-	204	4715
100	23.0	15752	-	-	-	216	4845
107	22.9	15955	-	-	-	225	4885
110	22.4	16368	-	-	-	234	4905
112	22.0	16685	-	-	-	243	4965
120	21.5	16791	-	-	-	250	5000

PS ADSORPTION AND WATER DISPLACEMENT Figure 9.2.4- Control RH80% 3°C

Time (min)	Temp (°C)	Water (mg m^{-3})	RH% (Corrected)	Time (min)	PS (mg m^{-3})
0	3.0	0	80.0	54	0
1	3.4	139	79.0	57	9
2	3.6	244	79.6	63	15
3	3.7	278	80.7	69	26
5	3.8	331	81.0	75	46
7	3.8	349	81.3	78	62
10	3.8	385	81.6	84	106
13	3.9	402	81.9	90	175
15	3.9	421	81.9	96	281
20	3.9	456	82.5	102	412
25	3.9	493	83.1	111	698
30	3.9	511	83.7	117	930
32	3.8	566	84.9	123	1215
36	3.8	585	85.2	132	1650
40	3.8	622	85.8	138	1970
45	3.7	678	87.4	144	2260
48	3.7	717	88.0	153	2680
56	3.6	793	90.2	159	2890
62	3.5	832	91.2	168	3170
67	3.4	910	93.1	177	3405
75	3.4	949	94.1	186	3595
80	3.3	1008	95.5	195	3760
87	3.2	1029	96.5	204	3905
95	3.1	1069	97.9	213	4020
102	3.0	1108	99.3	222	4115
110	2.9	1108	100.0	231	4185
120	2.8	1068	100.0	240	4245
137	2.7	1068	100.0	249	4280

150	2.6	1048	100.0	258	4325
160	2.6	1008	100.0	270	4445
185	2.5	969	100.0	282	4490
204	2.4	950	100.0	291	4500
240	2.4	929	100.0	303	4515
260	2.3	910	100.0	312	4560
295	2.2	870	100.0	321	4575
330	2.2	870	100.0	333	4615
350	2.2	870	100.0	342	4620
380	2.2	870	100.0	354	4630
395	2.2	832	100.0	369	4655
402	2.1	832	100.0	378	4660
440	2.1	832	100.0	393	4660
470	2.1	832	100.0	405	4640
480	2.2	832	100.0	420	4620
490	2.2	793	99.3	435	4655
500	2.3	755	97.9	459	4690
525	2.5	678	95.1	470	4655
550	2.6	530	92.3	480	4645
565	2.6	420	89.8	495	4620
578	2.7	331	87.6	500	4655
587	2.8	296	86.3	510	4675
595	2.8	278	86.0	528	4695
600	2.8	261	85.4	543	4660
610	2.9	226	84.9	549	4665
620	2.9	191	83.9	558	4730
630	2.9	156	82.8	567	4780
640	3.0	139	82.4	579	4817
650	3.0	123	82.1	585	4870
660	3.0	103	81.8	591	4890
675	3.0	64	80.0	598	4950

PS ADSORPTION AND WATER DISPLACEMENT Figure 9.2.5-Control RH80% -3°C

Time (min)	Temp (°C)	Water (mg m^{-3})	RH% (Corrected)	Time (min)	PS (mg m^{-3})
0	-3.0	0	80.0	66	0
2	-2.6	131	80.9	72	9
5	-2.4	212	81.8	78	15
10	-2.3	239	81.9	87	26
15	-2.3	294	83.0	96	46
20	-2.2	351	84.1	108	62
26	-2.1	408	84.9	120	106
30	-2.1	438	85.6	132	175
40	-2.1	481	86.9	141	281
50	-2.2	555	89.3	150	412
60	-2.3	600	90.7	159	698
70	-2.4	707	94.1	171	930
80	-2.5	723	95.2	177	1215
85	-2.5	818	98.0	183	1650
90	-2.6	866	99.0	192	1970
100	-2.6	915	99.1	204	2260
115	-2.7	911	99.4	216	2680
125	-2.8	915	100.0	231	2890
135	-2.9	932	100.0	243	3170
150	-3.0	899	100.0	252	3405
160	-3.1	882	100.0	261	3595
170	-3.2	850	100.0	273	3760
190	-3.3	786	100.0	285	3905
200	-3.4	786	100.0	294	4020
220	-3.5	786	100.0	306	4115
235	-3.5	739	100.0	318	4185

260	-3.6	723	100.0	330	4245
290	-3.6	646	100.0	342	4280
320	-3.6	650	100.0	357	4325
340	-3.7	660	100.0	375	4445
380	-3.6	660	100.0	399	4490
420	-3.6	646	100.0	420	4500
450	-3.6	640	100.0	438	4515
490	-3.6	640	100.0	453	4560
550	-3.6	640	100.0	471	4575
640	-3.6	615	100.0	489	4615
680	-3.5	615	100.0	504	4620
695	-3.5	600	100.0	522	4630
-	-	-	-	537	4655
-	-	-	-	555	4660
-	-	-	-	576	4660
-	-	-	-	597	4640
-	-	-	-	618	4620
-	-	-	-	636	4655
-	-	-	-	651	4690
-	-	-	-	678	4655
-	-	-	-	695	4645

PS ADSORPTION AND WATER DISPLACEMENT Figure 9.2.7- Control, RH80%
3°C: 910 mg m^{-3} PS Challenge

Time (min)	Temp (°C)	Water (mg m^{-3})	RH% (Corrected)	Time (min)	PS (mg m^{-3})
0	3.0	0	80.0	290	0
2	3.2	38	79.5	297	7
5	3.25	54	79.4	312	9
9	3.25	88	80.1	336	16
14	3.25	103	80.4	363	23

17	3.2	121	80.9	381	29
23	3.2	155	81.5	411	42
28	3.1	189	82.1	438	57
34	3.1	189	82.7	468	87
40	3.1	223	83.3	483	102
52	3.1	258	83.9	495	116
60	3.0	292	85.1	513	137
70	3.0	327	85.7	537	174
80	2.9	344	86.7	558	204
92	2.9	380	87.6	588	252
105	2.8	415	88.5	606	288
122	2.6	415	89.8	624	338
145	2.5	433	90.8	639	352
168	2.4	469	91.8	651	376
200	2.4	487	92.1	663	413
245	2.4	524	93.1	681	445
276	2.3	524	93.4	690	490
287	2.3	524	93.8	-	-
320	2.3	487	93.4	-	-
370	2.3	433	92.4	-	-
405	2.3	397	91.8	-	-
445	2.4	397	91.1	-	-
500	2.4	380	90.8	-	-
550	2.4	350	90.8	-	-
580	2.4	327	89.5	-	-
597	2.4	327	89.2	-	-
627	2.5	310	88.5	-	-
666	2.5	310	88.2	-	-
690	2.5	290	87.6	-	-

Nitrogen Adsorption (Figures 9.3.1-9.3.2)

Volume Adsorbed (cm^3<STP>g^{-1})						
P/P^0	Sample					
	SCII	SCII NO_2 O/G 950°C	SCII nonane/NO_2 O/G 950°C	BPL	BPL NO_2 O/G 950°C	BPL nonane/NO_2 O/G 950°C
Adsorption						
<0.001	255	240	250	200	180	195
0.001	285	260	263	240	187	210
0.025	303	290	290	260	200	225
0.050	333	311	312	275	225	243
0.075	347	325	325	290	233	252
0.100	362	337	335	300	240	262
0.150	367	345	345	310	250	272
0.200	372	352	351	317	253	280
0.300	380	360	360	327	257	287
0.400	385	365	367	335	262	295
0.500	388	370	370	340	266	300
0.600	390	372	375	345	270	303
0.700	395	375	377	353	275	308
0.800	400	381	383	363	281	317
0.900	407	390	391	376	291	327
1.000	422	412	415	412	312	352
Desorption						
0.950	418	402	403	391	305	347
0.850	408	395	395	376	292	327
0.750	403	390	387	365	283	320
0.650	401	386	385	361	277	312
0.500	393	380	377	347	266	300
0.450	387	367	370	342	-	-
Wt. Ch. %	0.0	-2.5	-2.1	0.0	-7.1	-8.4

PS ADSORPTION AND WATER DISPLACEMENT (Figure 9.4.1- Aged, RH80%)

Time (min)	Temp (°C)	Time (min)	PS (mg m^{-3})	Time (min)	RH% (Corrected)	Time (min)	Water (mg m^{-3})
0	22.0	9	0	0	80.0	0	0
1	22.6	12	28	2	76.3	2	0
2	22.8	15	31	4	78.2	4	406
8	22.7	18	41	6	78.7	6	513
10	22.6	21	63	8	79.7	8	616
12	22.5	24	105	10	80.9	10	822
14	22.3	27	171	12	82.1	12	926
17	22.1	30	257	13	82.7	13	1032
20	21.9	36	519	15	84.2	15	1136
22	21.8	42	866	18	85.8	18	1241
24	21.7	48	1205	22	87.9	22	1348
26	21.6	57	1685	24	88.9	24	1455
30	21.5	66	2141	28	90.1	28	1562
33	21.3	75	2483	30	91.2	30	1671
35	21.2	87	2795	35	93.5	35	1780
38	21.0	93	2915	42	96.4	42	1889
42	20.8	99	3062	58	98.8	58	1889
45	20.7	111	3345	60	99.4	60	2000
50	20.5	123	3490	70	99.8	70	1889
58	20.4	135	3765	72	100.0	72	1833
66	20.4	147	3910	80	100.0	80	1781
74	20.3	159	3976	82	99.1	82	1671
81	20.2	177	4170	88	98.8	88	1623
91	20.1	195	4305	92	98.8	92	1558
96	20.1	213	4406	104	97.6	104	1455
105	20.4	231	4442	114	96.4	114	1406
120	20.5	246	4561	120	95.2	120	1295
128	20.6	267	4650	142	93.4	142	1241
140	20.7	288	4698	159	92.9	159	1137

160	20.8	309	4809	170	91.1	170	927
178	21.0	330	4855	182	89.7	182	875
196	21.1	351	4845	202	88.4	202	719
206	21.2	372	4887	222	86.7	222	616
216	21.3	384	4907	254	84.6	254	406
237	21.4	396	4903	284	83.6	284	310
246	21.5	417	4958	338	82.1	338	210
265	21.6	426	4966	358	81.5	358	109
296	21.7	435	4980	392	81.0	392	10
310	21.8	447	5000	436	80.0	436	0
364	21.9	-	-	-	-	-	-
422	21.9	-	-	-	-	-	-
444	22.0	-	-	-	-	-	-

PS ADSORPTION AND WATER DISPLACEMENT (Figure 9.4.3- Aged, RH65%)

Time (min)	Temp (^{o}C)	Water (mg m^{-3})	RH% (Corrected)	Time (min)	PS (mg m^{-3})
0	22.0	0	64.9	27	0
2	22.4	83	63.4	30	22
4	22.6	335	63.8	33	32
6	22.6	461	64.3	36	50
8	22.6	546	64.7	39	76
12	22.6	763	65.8	45	155
16	22.5	893	66.5	51	275
20	22.5	1025	67.4	60	547
25	22.3	1339	69.9	69	877
29	21.9	1658	73.3	78	1180
35	21.1	2077	79.2	87	1447
40	20.5	2410	84.0	96	1700
47	19.9	2651	88.0	108	2022
50	19.8	2750	89.7	120	2346
56	19.6	2848	91.4	132	2693
63	19.4	2897	93.1	144	3013

71	19.1	2847	94.0	156	3315
76	19.1	2798	94.0	168	3616
82	19.1	2751	94.0	180	3878
86	19.1	2701	93.6	192	4117
92	19.1	2507	92.2	207	4476
98	19.2	2410	91.6	222	4644
106	19.3	2315	90.5	234	4749
116	19.4	2125	88.5	247	4865
126	19.5	1937	86.6	258	4918
135	19.6	1796	85.2	270	4962
145	19.8	1612	83.6	273	4968
154	19.9	1475	81.8	279	4970
166	20.2	1294	79.8	291	4972
176	20.3	1115	77.8	297	4978
186	20.5	939	76.1	303	4983
196	20.6	675	74.2	306	4985
209	20.9	505	72.0	312	4987
224	21.2	335	69.7	315	5000
250	21.6	125	67.2	-	-
270	21.7	83	66.1	-	-
292	21.8	0	65.3	-	-
314	22.0	0	65.0	-	-

PS ADSORPTION AND WATER DISPLACEMENT (Figure 9.4.4- Aged, RH40%)

Time (min)	Water (mg m^{-3})	RH% (Corrected)	Time (min)	Temp (^{o}C)	Time (min)	PS (mg m^{-3})
0	0	40.3	0	22.0	88	0
2	55	38.9	2	22.7	90	10
4	165	39.4	4	22.8	96	19

14	221	39.5	14	22.9	105	53
25	305	39.9	25	22.8	114	135
35	333	40.2	35	22.7	120	228
44	390	40.5	44	22.7	126	363
56	446	40.8	56	22.7	132	557
61	503	41.2	61	22.7	141	1086
74	561	41.6	74	22.6	150	1812
93	619	42.3	93	22.5	156	2365
102	678	42.7	102	22.4	162	2937
114	737	43.2	114	22.3	168	3527
125	766	43.5	125	22.3	174	3983
129	737	43.5	129	22.2	180	4326
148	678	43.7	148	22.0	186	4576
153	619	43.6	153	21.9	192	4745
158	561	43.4	158	21.9	198	4885
161	503	43.1	161	21.8	207	4963
168	390	42.8	168	21.8	213	4981
175	277	42.2	175	21.9	219	4991
181	221	41.7	181	21.9	234	5000
190	110	40.9	190	22.0	238	5000
195	55	40.6	195	22.0	-	-
200	0	40.3	200	22.0	-	-
240	0	40.0	-	-	-	-

PS ADSORPTION AND WATER DISPLACEMENT Figure 9.4.5 NO_2 Modified RH80%

Time (min)	Water (mg m^{-3})	RH% (Corrected)	Time (min)	Temp (^oC)	Time (min)	PS (mg m^{-3})
0	0	80.0	0	22.0	6	0
1	102	77.7	1	22.6	9	15
2	410	78.7	2	22.7	15	70
5	724	80.2	9	22.5	27	635
9	1042	82.7	12	22.4	39	1485
12	1260	84.2	13	22.2	54	2300
14	1369	85.8	16	22.0	72	2780
18	1479	87.9	20	21.8	84	3008
20	1588	89.0	24	21.6	102	3290
24	1692	91.3	27	21.4	120	3530
27	1811	93.0	29	21.3	138	3665
44	1923	97.6	33	21.1	153	3780
62	1811	98.9	38	20.8	171	3926
70	1692	100.0	47	20.6	189	4012
83	1588	99.2	58	20.4	207	4165
103	1479	96.1	66	20.3	225	4286
124	1260	93.6	83	20.4	243	4371
147	1042	92.0	110	20.6	273	4465

169	937	90.6	146	20.8	300	4580
184	829	89.5	173	21.0	327	4685
212	724	87.8	209	21.2	351	4718
255	516	86.2	256	21.4	384	4780
282	410	85.1	300	21.6	411	4870
320	359	83.9	333	21.7	462	4901
348	307	83.1	376	21.8	510	4971
364	204	82.6	450	21.9	519	5000
388	102	81.5	506	22.0	-	-
450	0	80.6	-	-	-	-
520	0	80.0	-	-	-	-

PS ADSORPTION AND WATER DISPLACEMENT Figure 9.4.6 DFE Treated RH80%

Time (min)	Temp (^{o}C)	Time (min)	RH% (Corrected)	Time (min)	PS (mg m^{-3})	Time (min)	Water (mg m^{-3})
0	22.0	0	80.0	31	0	0	0
1	22.4	2	78.8	36	27	2	307
6	22.7	7	80.2	42	58	7	724
12	22.6	12	81.9	48	148	12	937
22	22.4	20	83.2	60	489	20	1152
31	22.2	27	84.7	69	930	27	1369
36	22.0	35	87.4	81	1560	30	1479

42	21.8	44	90.6	96	2295	35	1588
46	21.6	54	93.5	108	2800	44	1811
54	21.4	67	96.4	123	3330	54	2036
60	21.2	72	97.0	144	3795	67	2150
71	20.8	91	97.6	159	4065	72	2036
82	20.6	96	97.6	174	4330	91	1811
96	20.4	107	96.9	192	4487	96	1692
121	20.6	140	92.3	207	4565	107	1588
133	20.7	156	90.0	231	4730	121	1369
150	20.9	180	87.3	247	4849	140	1152
161	21.1	198	87.5	261	4949	156	937
178	21.3	222	85.7	279	4968	171	829
200	21.5	280	81.6	294	4995	180	724
228	21.7	302	80.0	311	5000	198	516
282	21.9	-	-	-	-	222	307
302	22.0	-	-	-	-	280	102
310	22.0	-	-	-	-	310	0

3 Publications, Acknowledgements

Publications

1 An Examination of how Exposure to Humid Air can Result in Changes in the Adsorption Properties of Activated Carbons.
L.B. Adams, C.R. Hall, R.J. Holmes and R.A. Newton, Carbon 26 1988 451-459.

2 An Investigation into the Way in which Exposure to Humid Air can Modify the Adsorption Properties of Activated Carbon. C.R. Hall, L.B. Adams and R.J. Holmes, Carbon '88 (5^{th} International Conference on Carbon, Sept. 18-23, Newcastle, UK), 140.
B. McEnaney and T.J. Mays, Eds., Institute of Physics, London.

3 Observations and Comments on the Displacement of Pre-Adsorbed Water from BPL Activated Carbon by Chloropicrin Vapour.
C.R. Hall and R.J. Holmes, Adsorption Science and Technology 6 1989 83-92.

4 The Adsorption Properties of Chemically Modified Activated Carbons.
C.R. Hall and R.J. Holmes, Gas Separation Technology, 231-237. E.F. Vansant and R. Dewolfs, Eds., Elsevier Process Technology Proceedings 8, 1990.

5 The Influence of Pore Structure, Surface Chemistry and Temperature on the Displacement of Pre-Adsorbed Water from Activated Carbon.
C.R. Hall and R.J. Holmes, Carbon '90 (7^{th} International Conference on Carbon, July 16-20, 1990, Paris, France), 66.

6 The Preparation and Properties of some Fluorinated Activated Carbons. C.R. Hall and R.J. Holmes, Colloids and Surfaces, in press.

7 The Preparation and Properties of Some Activated Carbons Modified with Phosgene or Chlorine. C.R. Hall and R.J. Holmes. Accepted for Publication in Carbon.

8 Further Observations on the Displacement of Pre-Adsorbed Water from BPL Activated Carbon by Chloropicrin Vapour. C.R. Hall, R.J. Holmes, and I.W. Lawston. Submitted for Publication in Adsorption Science and Technology.

9 Degradation in the Performance of Activated Carbon Filters and How to Overcome the Problem. C.R. Hall and R.J. Holmes, ISRP Conference Proceedings, 4-7 November 1991, Winchester, UK

Acknowledgements

I am most grateful to Dr. C.R. Hall of CBDE Porton, and Dr. C.R. Theocharis of Brunel University, for supervising this research, and also to Professor K.S.W. Sing of Brunel University, for helpful discussions and encouragement. I also wish to thank Dr. C.R. Hall and the senior management at CBDE for allowing this research to be submitted for a Phd degree.

Dr. Mike Rutter, Dr. Simon Elwell, and Simon Mundy, all of DQA/TS Woolwich, are thanked for their involvement with surface analysis studies (XPS, and Thermal Desorption Mass Spectrometry). Mr. J.M. Creasey, and Mrs. Judy Parkes, of CBDE, are thanked for SEM and EDX analysis. Dr. Colin Hutchinson and Staff at DQA/TS Chorley are thanked for carrying out elemental analyses.

The careful and timely provision of nitrogen adsorption and mercury porosimetry data by Dr. Malcolm Yates of Brunel University as part of a CBDE Extra Mural research contract is gratefully acknowledged.

Some of the experimental work described in this document was produced with the assistance of Mrs. J.R.M. Rollins and Mrs. L. Slater, both of CBDE Porton. Their help is warmly acknowledged. Dr. L.B. Adams of CBDE is also thanked for reviewing this thesis.

This thesis was produced entirely on an IBM compatible Personal Computer. The text and tables were produced using Wordperfect version 5.1 (Wordperfect Corporation). The figures were produced using Fig. P version 5.1 (Biosoft Ltd.), and Lotus Freelance Plus version 4.0 (Lotus Development Corporation).